DYNAMICS, SELF-ASSEMBLY, AND FUNCTION OF MULTICOMPONENT COORDINATION SUPRAMOLECULAR SYSTEMS

by

Yaorong Zheng

A dissertation submitted to the faculty of
The University of Utah
in partial fulfillment of the requirements for the degree of

Doctor of Philosophy

Department of Chemistry

The University of Utah

August 2011

The University of Utah Graduate School

STATEMENT OF DISSERTATION APPROVAL

The dissertation of **Yaorong Zheng**

has been approved by the following supervisory committee members:

Peter J. Stang	, Chair	**6/6/2011** Date Approved
Matthew S. Sigman	, Member	**6/6/2011** Date Approved
Ilya Zharov	, Member	**6/6/2011** Date Approved
Haitao Ji	, Member	**6/6/2011** Date Approved
Nelson H.F. Beebe	, Member	**6/6/2011** Date Approved

and by **Henry S. White** , Chair of the Department of **Chemistry**

and by Charles A. Wight, Dean of The Graduate School.

ABSTRACT

Self-assembly allows for the preparation of highly complex molecular and supramolecular systems from relatively simple starting materials. Self-assembled supramolecules are typically constructed by combining complementary pairs of highly symmetric molecular components, thus limiting the formation of unwanted side products. In the subset of self-assembly which uses metal-ligand bonding interactions– coordination-driven self-assembly, syntheses are achieved by mixing two molecular components: one metal acceptor and one organic donor. Two-component coordination-driven self-assembly simplifies design principles at the cost of the complexity and diversity of the supramolecular products, limiting further applications. Combining more than two complementary sets of molecular components in one mixture can result in a myriad of different ordered two-component and/or multicomponent supramolecular assemblies. This dissertation describes our investigations of multicomponent Pt(II)-based supramolecular systems, in particular, to understand the fundamental dynamic feature of coordination supramolecular systems, discover information that controls multicomponent self-assembly, and explore potential applications of such complex supramolecular structures.

CONTENTS

LIST OF ABBREVIATIONS

1D – one-dimensional

2D – two-dimensional

3D – three-dimensional

Å– angstrom

anal. – analysis

conc. – concerntrated

d – doublet

deg – degree

Da – Dalton

DNA – deoxylribonucleic acid

equiv. – equivalent

ESI – electro spray ionization

Et – ethyl

FRET – fluorescent resonance energy transfer

g – gram

G – generation

h – hour

J – coupling constant

M – metal

m – multiplet

MeCN – acetonitrile

mg – milligram

MS – mass spectrometry

n – normal

n-Bu – *normal*-butyl

nm - nanometer

NMR – nuclear magnetic resonance

ORTEP – Oak Ridge Thermal Ellipsoid

p – para

Pd – palladium

PEt_3 – triethylphosphine

PGSE – pulsed field gradient spin echo

Ph – phenyl

PMe_3 – trimethylphosphine

PPh_3 – triphenylphosphine

Pt – platinum

Py - pyridine

r.t. – room temperature

s – singlet

THF – tetrahydrofuran

LIST OF SCHEMES

Scheme Page

ACKNOWLEDGEMENTS

Foremost, I would like to thank my supervisor Professor Peter J. Stang for his guidance and the continuous support of my Ph.D. study and research. Learning how to be a scientist from him has been a real pleasure. I am very grateful for the freedom he gave me to explore my ideas and the guidance he gave when I needed it.

Deepest gratitude are also due to the members of my supervisory committee, Professors Matthew S. Sigman, Ilya Zharov, Haitao Ji, and Nelson H. F. Beebe, without whose knowledge and assistance this study would not have been successful.

I am deeply indebted to my colleagues who supported me during my graduate research and preparation of this dissertation. They have been a great source of support, friendship, and encouragement. Dr. Haibo Yang and Dr. Brian H. Northrop offered me tremendous guidance and support in the beginning of my research. Dr. Liang Zhao, Dr. Koushik Ghosh, Dr. Ming Wang, Dr. Greg Molve, and Dr. Rajesh Chakrabarty are great friends who were always present with help and advice. I would also like to thank J. Bryant Pollock for proof-reading this document. My sincere thanks also go to Dr. Timothy R. Cook, a friend always providing me useful suggestions and kind help.

I would also like to express my gratitude to staff members Dr. Jim Muller for mass spect, Dr. Atta Arif for X-ray, and Margaret Beebe for their friendship and support.

Lastly, but most importantly, my special thanks go to my wife, Xiaomu Guan, and my parents for their support and encouragement.

CHAPTER 1

INTRODUCTION

1.1 Supramolecular Self-assembly

Chemists in general, and synthetic chemists in particular, have developed an extensive collection of protocols for making compounds with desirable properties and/or functions. It is often the case, however, that complex molecules require equally complex syntheses, which can be costly in terms of time, materials, atom economy, and yield. Natural systems, on the other hand, are capable of synthesizing molecular and supramolecular systems of impressive complexity and functionality in high yield with relative ease. For example, while it may take a biochemist a few days to prepare a polypeptide with 100 amino acids, a bacterial cell can carry out the same feat in the order of seconds.[1] Some enzymes have evolved to be so efficient that their catalysis[2] is limited only by the rate of diffusion, a target so far unattained in synthetic systems. More often than not, biological systems are able to perform complex tasks by taking advantage of a range of reversible noncovalent interactions to dictate their structural, physical, and functional properties. For instance, DNA is the genetic material responsible for the storage of genetic information in most living organisms. The main reason DNA is a safe storage medium is its stability. DNA is a supramolecular double helical structure self-assembled by two encoded nucleotides and its high stability is mainly attributed to noncovalent interactions–hydrogen bonding[3] and π-π interactions[4]–between the

nucleotides. Taking inspiration from nature, chemists have developed a myriad of ways to utilize noncovalent interactions to direct the spontaneous self-assembly of supramolecular systems[5] in manners similar to the same phenomena that occur throughout nature. Self-assembly protocols can considerably reduce synthetic costs and often lead to the formation of a single thermodynamic product in high yield.

Supramolecular chemistry[6] takes advantage of the fact that complementary molecular subunits – e.g., hydrogen bond donors and acceptors, Lewis acidic metals and Lewis basic ligands, electron-poor π-acceptors and electron-rich π-donors, etc. – can be specifically designed such that they selectively recognize each other and spontaneously assemble into well-defined supramolecular structures. In the 1960s, Lehn,[7] Cram,[8] and Pederson[9] provided early examples of self-assembly in supramolecular systems in their studies, for example, cation-binding cryptand[7] and crown ether compounds.[9] In the intervening years, researchers designed and synthesized complementary pairs of molecular subunits that are capable of utilizing the noncovalent information stored within their structural and electronic properties to spontaneously self-assemble into preferred supramolecule(s).[10] It is often advantageous to limit the number of potential supramolecular products by combining, for example, only one hydrogen bond donor with one hydrogen bond acceptor or one metal acceptor with one organic donor, etc. Such a protocol has the clear advantage of reducing the complexity of the system and promoting the efficient, high-yielding assembly of a singular product.

1.2 Coordination-driven Self-assembly

A particularly powerful method for constructing large, rigid metal–organic supramolecules with well-defined shapes and sizes is coordination-driven self-assembly,

a self-assembly approach developed relying on metal-ligand coordination bonding. Many noncovalent interactions employed in natural systems have been well-studied in analogous abiological systems. Of these, metal-ligand coordination bonding interactions are relatively strong and highly directional. The energies of metal-ligand bonds (15-60 kcal/mol) are intermediate between the energies of organic covalent bonds (ca. 60-120 kcal/mol) and the weak noncovalent interactions—e.g., hydrogen-bonding, van der Waals, and solvophobic—(ca. 0.5-10 kcal/mol). Thus, coordination offers a suitable balance between providing sufficient stability for resulted products and modulating the coordination kinetics of the self-assembly process by introducing reversibility. The kinetic reversibility between complementary molecular components, reaction intermediates, and self-assembled products provide self-correction for supramolecular systems, leading to a product that is under thermodynamic control. Moreover, based on the preferred coordination geometries of transition metal cations and directionality of metal-ligand bonds, logical design allows for self-assembly with various organic ligands into predictable supramolecular architectures.

By virtue of the advantages afforded by metal-ligand bonds, coordination-driven self-assembly has attracted much attention. Over the last two decades, Stang,[11] Fujita,[12] Raymond,[13] Mirkin,[14] Lehn,[15] and others[16] have pioneered the use of the coordination-driven approach to self-assemble abiological supramolecular architectures. The approach allows for the predictable self-assembly of electron-poor metal centers and complementary, electron-rich organic donors to produce metal-organic supramolecules of high complexity in a simple, efficient manner. As shown in Figure 1.1, an early example reported by Lehn and coworkers demonstrates the use of a coordination-driven self-

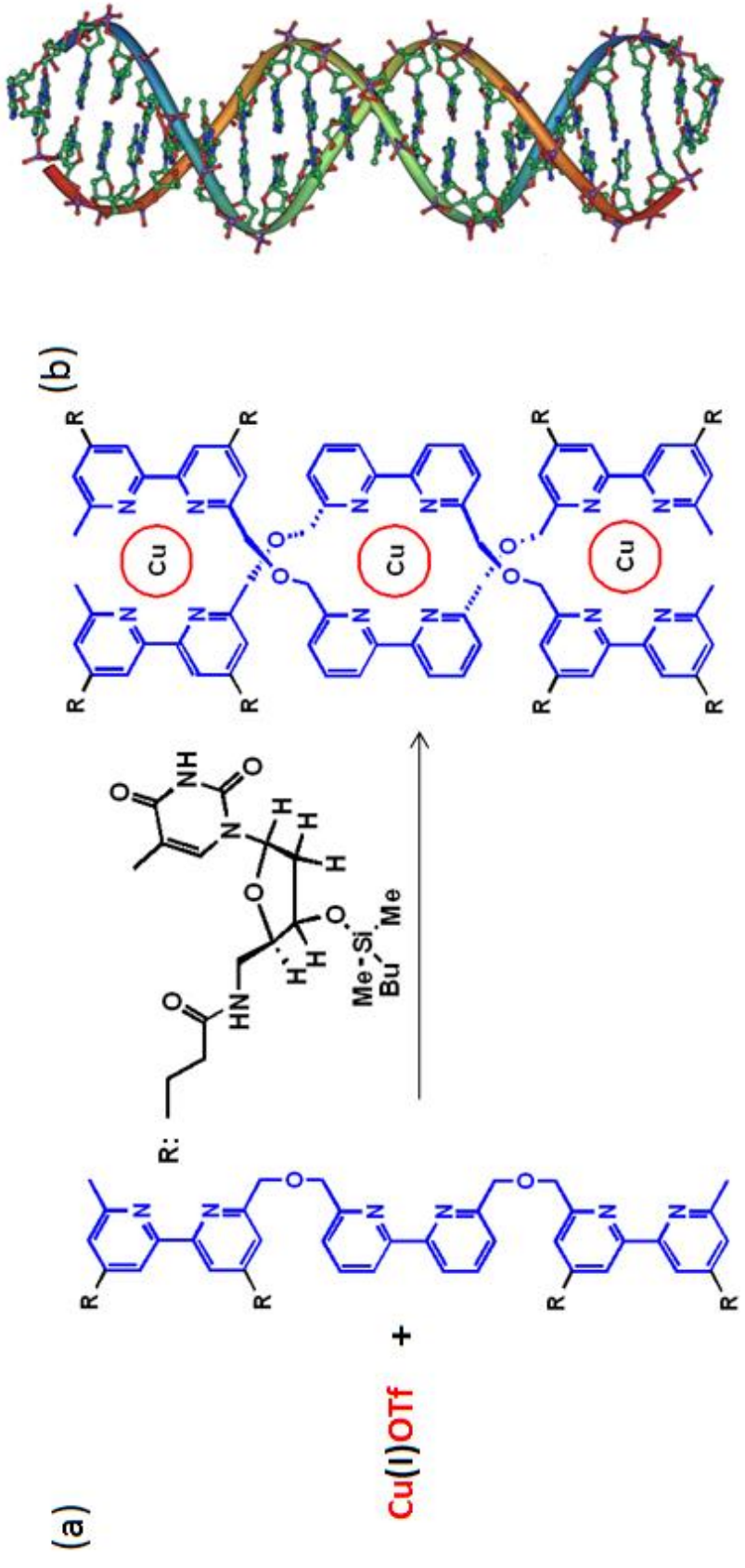

Figure 1.1. Self-assembly: (a) Coordination-driven self-assembly of copper (I) and the oligobipyridyl ligand to form a metal-organic supramolecular double helix; (b) Schematic representation of natural DNA double helix.

assembly of copper (I) and an oligobipyridyl ligand to form a metal-organic supramolecular double helicate,[17] mimicking the natural assembly of DNA.

In the past two decades, a significant increase of knowledge about the synthesis and characterization of large complex molecules and supramolecules resulted in a tremendous proliferation of strategies for building complex supramolecular architectures using coordination-driven self-assembly. Of the various strategies, directional bonding,[11] symmetry interaction,[13] and molecular paneling[12] approaches have been the most widely used and adopted and have led to a wide variety of supramolecular architectures.

1.3 Self-assembly of Two-component Supramolecular Structures

All the approaches developed in the past two decades share a common design, which is the use of only two molecular components: one metal acceptor and one organic donor, because of its advantages of limiting the number of potential supramolecular products and simplifying the design of supramolecular architectures.

As shown in Scheme 1.1 and 1.2, directional bonding approach[11] allows for a combinatorial molecular library consisting of complementary building blocks (metal acceptors and organic donors) that allow one to think retrosynthetically on how best to achieve the geometry of a particular discrete assembly. This approach relies on the square planar coordination geometry of Pt(II) and Pd(II) and the highly directional coordination bond formed upon the metal center and rigid organic ligands. The two most important structural factors dictating a self-assembled supramolecular structure are the shapes and sizes of the individual molecular building blocks. The shape of donor and/or acceptor building blocks is dominated by the turning angle defined as the angle formed between the two open valencies of a ditopic donor or acceptor. For example, as shown in

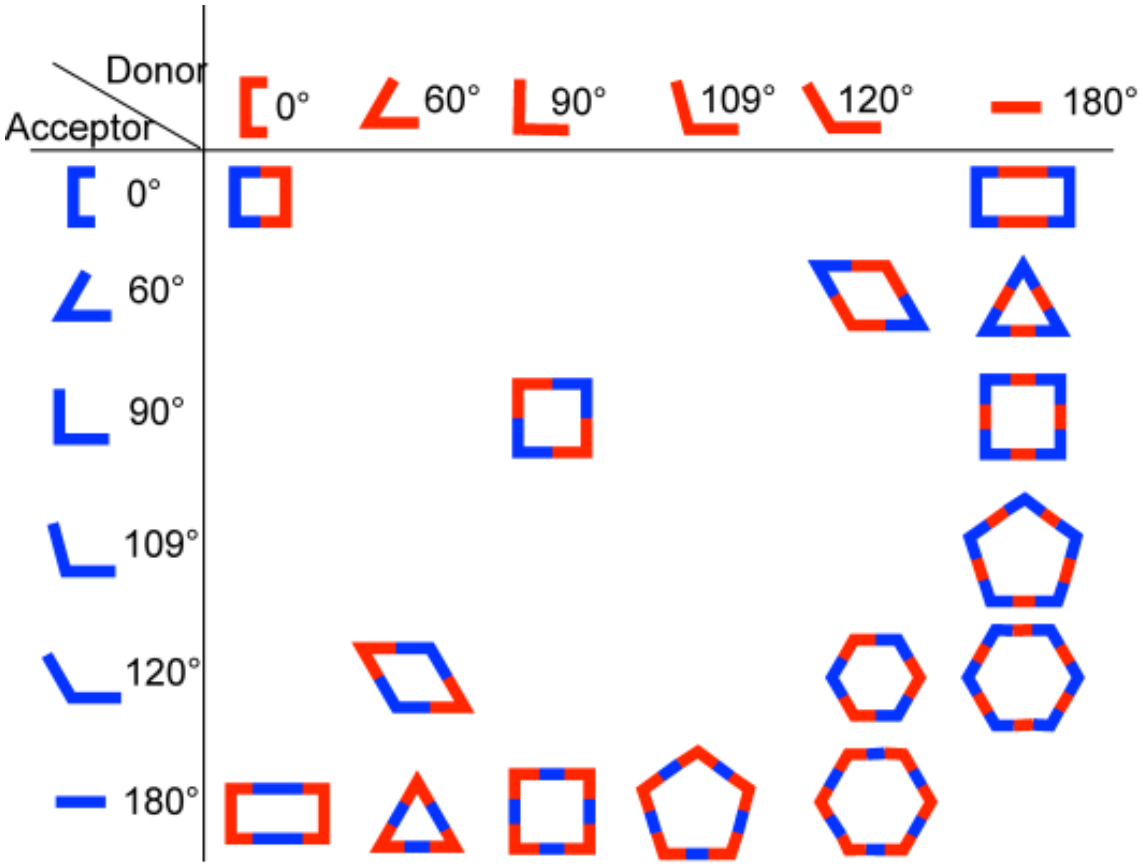

Scheme 1.1. Schematic representation of the combination of various building units for accessing convex polygons by the directional bonding approach.

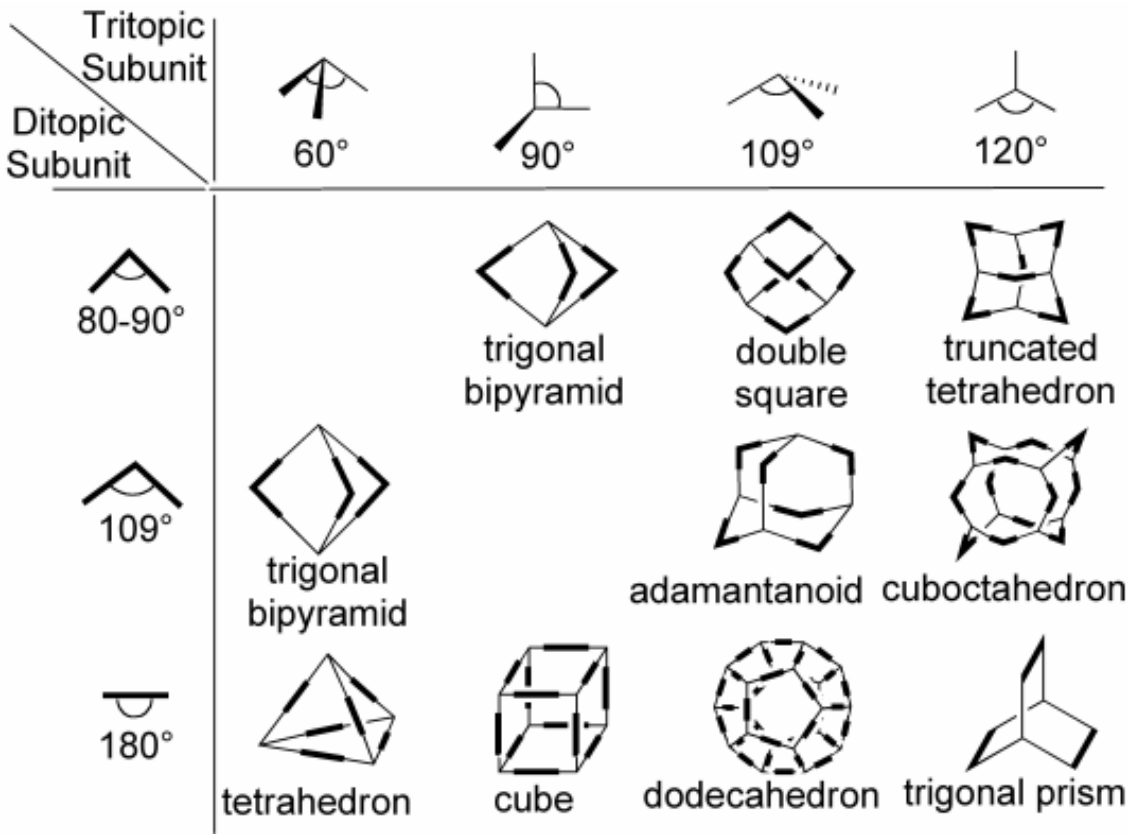

Scheme 1.2. Schematic representation of 3D architectures formed by the combination of ditopic and tritopic subunits by the directional bonding approach.

Figure 1.2, a ditopic organoplatinum acceptor will have its two sites of free valence oriented 60 ° from each other while a ditopic donor such as 1,4-bispyridine has a turning angle of 180 ° between its two pyridyl donor sites. Scheme 1.1 and 1.2 demonstrate how the directional bonding approach directs coordination-driven self-assembly to synthesize 2D metallacyclic polygons such as squares, rectangles, rhomboids, triangles, and hexagons, as well as highly complicated 3-D supramolecular cages and polyhedra. A triangle,[18] for example, is self-assembled by three organoplatinum acceptors and three pyridyl donors, as shown in Figure 1.2.

Symmetry interaction approach[13] is based on the geometric relationship between chelating ligands and metal acceptors. The strong binding affinity of chelating ligands towards metals acts as the driving force for the assembly process. The specific binding mode of chelating ligands and the inherent symmetry of the coordination sites on the 'naked' metal center allow for a predictive self-assembly design. The requisites of this design principle are based on symmetry considerations. A coordinate vector represents the interaction between a ligand and metal. For chelating ligands, the plane orthogonal to the major symmetry axis of a metal complex is the chelate plane (Scheme 1.3a), which in the case of bidentate chelators holds all chelate vectors. Thus, depending on the orientation of the chelate planes, the construction of highly symmetrical coordination clusters can be realized. For example, to prepare a M_2L_3 triple helicate with an idealized D3 symmetry, it is required that both the C2 and C3 axes are orthogonal and are encoded into the chelating ligands and metal centers. As demonstrated in Scheme 1.3b, since the two pseudo-octahedral metal centers share the same C3 axis, the two chelating planes must be parallel to achieve C2 axis to result in a triple helicate.[19]

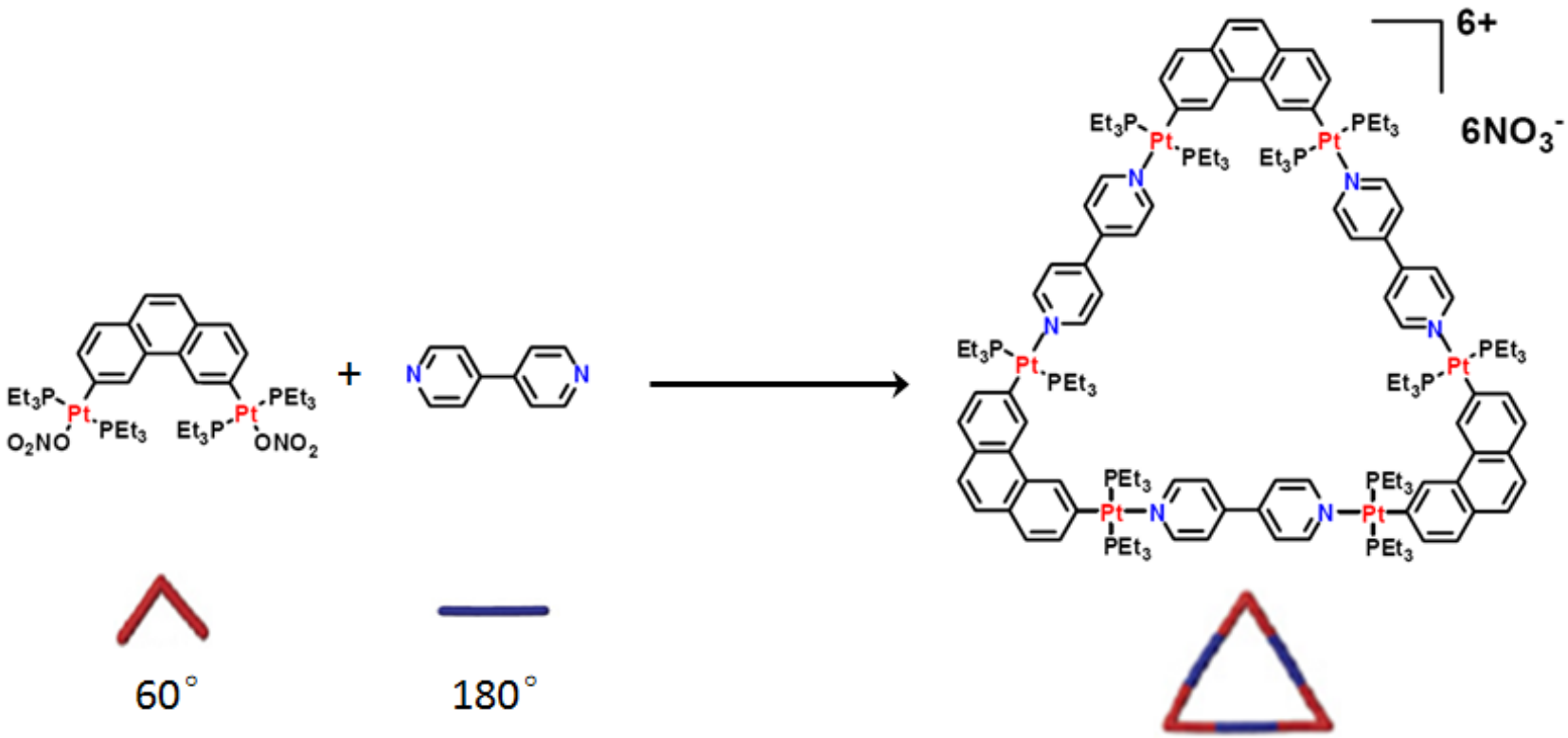

Figure 1.2. Coordination-driven self-assembly of a supramolecular triangle by the directional bonding approach.

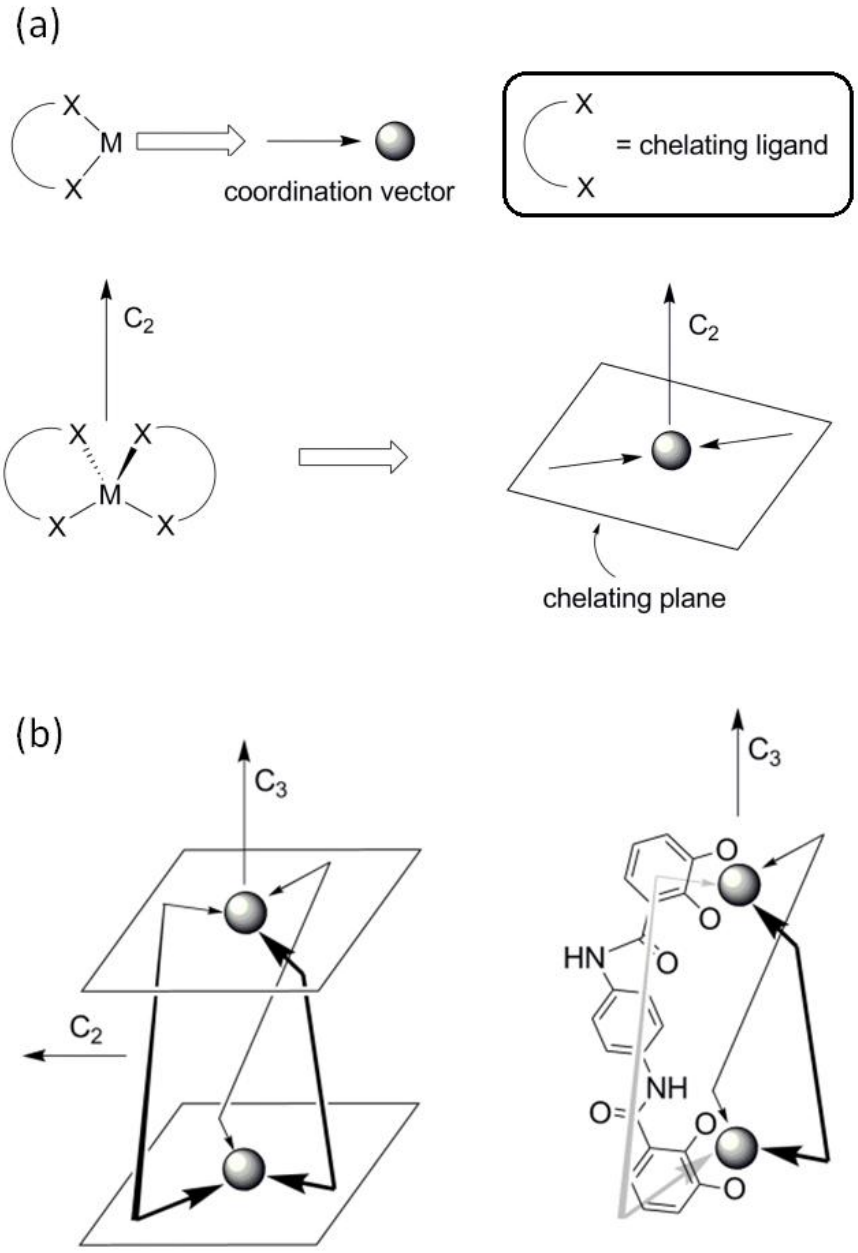

Scheme 1.3. Symmetry interaction approach: (a) Coordinate vector and chelate plane; (b) Design of a D3-symmetrical triple helicate using the symmetry interaction approach.

Molecular paneling approach[12] is mainly used in the formation of various 3D supramolecular architectures that resemble platonic solids. Since platonic solids, in general, are comprised of equilateral triangles, squares, and pentagons, 3D supramolecular architectures can, in principle, be designed by deducing the molecular components of these polyhedra. An octahedron, for example, can be designed by stitching together six triangular panels (Scheme 1.4a). The corner units employed to hold the panels together are usually cis-protected square planar Pt(II) or Pd(II) ions. In contrast to the naked metal centers used in the symmetry interaction approach, cis-protection makes the coordination geometry around the metal center convergent, and therefore, it is relatively simple to design the self-assemblies. This approach has led to varied supramolecular architectures such as the M_6L_4 truncated tetrahedral cage[20] (Scheme 1.4b), M_8L_4 tetrahedra.[21]

The directional bonding, symmetry interaction, and paneling approaches, as well as other strategies developed in the last dozen years, have proven to be successful methodologies for supramolecular construction by taking advantage of the simplicity of two-component self-assembly. As a result, an extensive collection of both 2D and 3D metal-organic supramolecular architectures have been obtained. However, due to the limited number of components employed in these strategies, coordination supramolecular systems developed and investigated in the past decades have been mostly constrained to two-component systems.

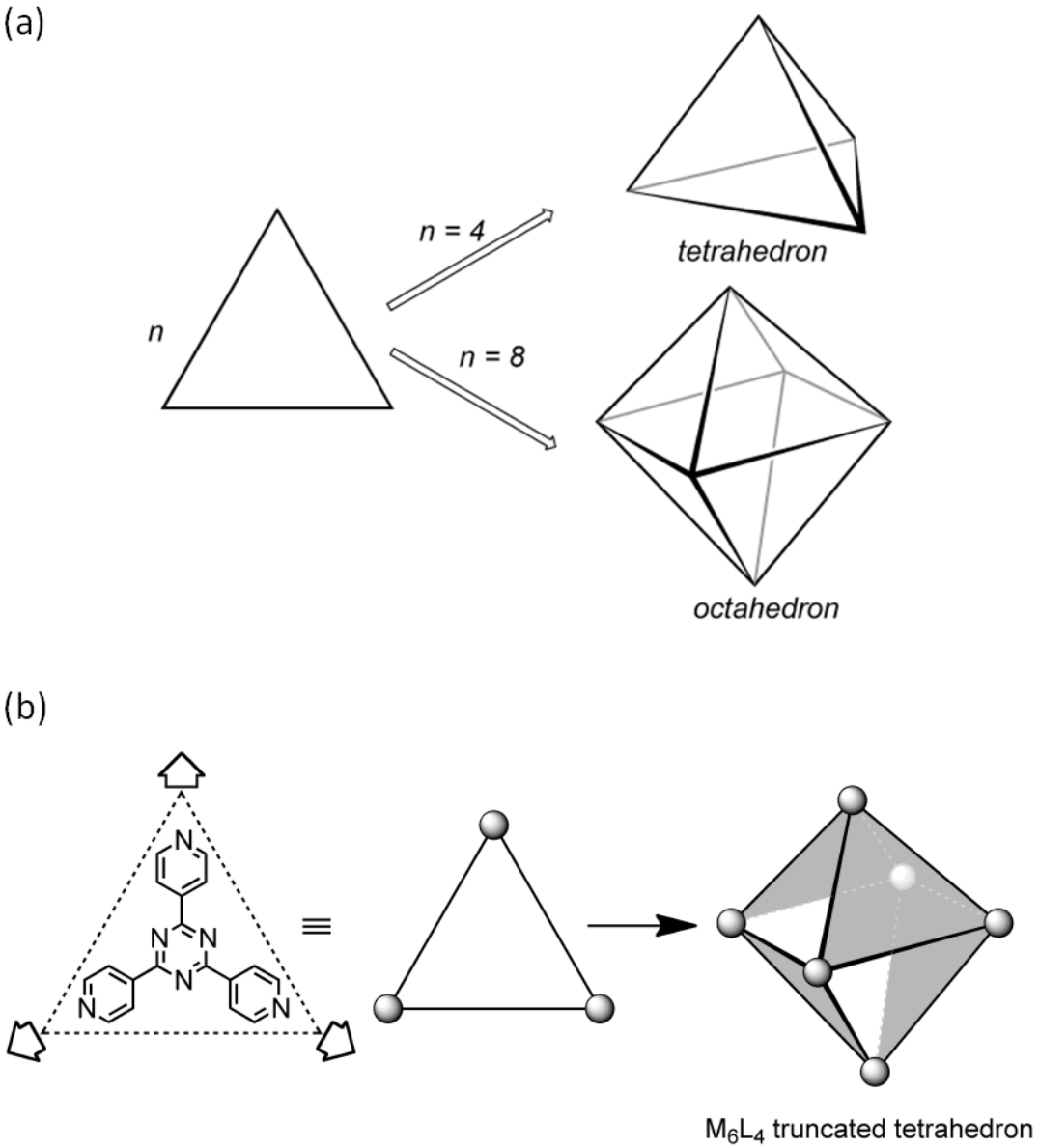

Scheme 1.4. Paneling approach: (a) Schematic representation for assembling a tetrahedron and an octahedron using triangular panels; (b) Design of a truncated tetrahedron.

1.4 From Two-component to Multicomponent Systems

Chemists are always pursuing the capability of building and controlling chemical systems of high complexity. For synthetic chemists concerned with covalent bonds, organic synthesis allows for the preparation of molecules of high complexity via step-by-step methods, because of the kinetic stability of covalent bonds in organic structures. The total synthesis of, e.g., vitamin B_{12},[22] Taxol,[23] and Trabectedin[24] are marvelous examples of synthetic chemists manipulating covalent bonds to approach nature's own complexity. For chemical systems employing noncovalent interactions, nature represent the ultimate form of complex supramolecular systems. In biological systems, self-assembly allows for the controlled combination of multiple different molecular components to aggregate into supramolecular systems of high complexity with well-defined structures. For example, mammalian cells can be considered highly complex supramolecular systems composed of multiple biomolecules brought together by noncovalent self-assembly. Viral capsids such as *Tomato Bushy Stunt Virus*[25] and *Rhinovirus*[26] are self-assembled results of three and four different protein subunits. Comparing biological self-assembly with recently developed abiological supramolecular self-assembly, such as the coordination-driven self-assembly discussed previously, a significant difference is apparent: abiological self-assembly is mostly limited to two components, while nature is able to control multiple components. Thus, to construct supramolecular systems toward nature's complexity, progress in understanding and controlling supramolecular systems of multiple molecular components is essential.

Supramolecular systems containing multiple, different molecular components are more complex and thus more difficult to control than two-component ones.[27] In recent

years, much of effort has been made to investigate multicomponent supramolecular systems.[28] Scheme 1.5 demonstrates a simplified model of a supramolecular system comprised of three molecular components. In such a multicomponent system, not only two-component self-assembled species but also complicated structures formed by aggregation of three components can be produced. An increase in the number of components in the mixture results in an increase of complexity of the multicomponent supramolecular system. When a system forms only two-component species as a result of molecular recognition by pairs of complementary building blocks, it is called *self-sorting*,[29] shown by the right side of Scheme 1.5. If multiple molecular components can recognize each other and selectively aggregate into one discrete well-defined supramolecular entity in the mixture, it is dubbed *selective self-assembly*,[28a] shown by the left side of Scheme 1.5. This thesis is mainly focused on self-sorting and selective self-assembly in a coordination-driven multicomponent supramolecular system.

1.5 Self-sorting in Multicomponent Systems

Self-sorting[30] requires high-fidelity molecular recognition and is a fundamental property of biological systems. By utilizing specific recognition motifs encoded within the geometric and/or electronic properties of molecular subunits, self-sorting enables the self-assembly of multiple different supramolecular structures from a mixture of molecular components. In the last decade, various synthetic self-sorting systems have been developed based on metal ligand coordination bonding,[29d,31] hydrogen bonding,[16k,30l,32] solvophobic effects,[33] and dynamic covalent interactions.[34]

In the late 1990s, the research groups of Lehn, Raymond, and Albrecht developed and explored the self-sorting of supramolecular helicates. Lehn et al., for example,

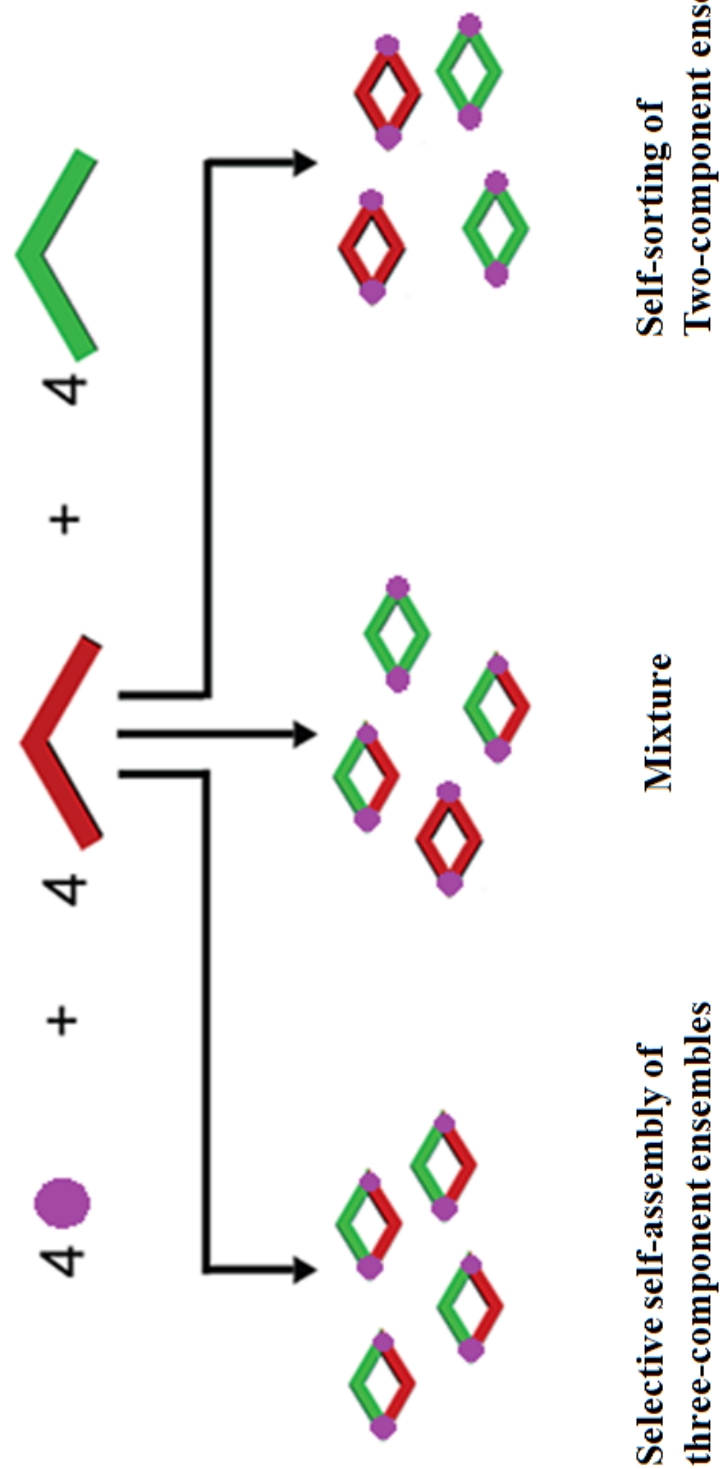

Scheme 1.5. Schematic representation of a model supramolecular system comprised of three molecular components.

demonstrated that mixtures of oligobipyridine strands containing 2–5 bipyridine units will, in the presence of Cu(I) ions, self-sort into double helicates that are exclusively composed of oligobipyridine strands of the same length (i.e., 2:2, 3:3, 4:4, 5:5).[31i] By preparing a number of biscatecolamide ligands separated by *o*-C_6H_4, *p*-C_6H_4, and 4,4′-biphenyl spacers, Raymond and coworkers showed that the addition of Ga(III) ions prompted the facile self-sorting of triple helicies composed exclusively of identical ligands (Figure 1.3).[31f] Albrecht and coworkers observed that the extent of self-sorting of alkyl-bridged bis-catechol ligands into discrete triple helicates in the presence of Ti(IV) and alkali metal carbonate could be controlled by the nature of the alkali metal (Li^+, Na^+, or K^+).[31e] In the presence of Na^+ in mixed alkali systems, the different bis-catechol ligands selectively self-organized into triple helicates containing identical ligands. In each of these helicate self-organizing systems, metal cations were utilized as "external effectors" to trigger the spontaneous ordering of individual components. The use of reversible metal-ligand coordination interactions allows for a dynamic self-assembly process to take place: supramolecular complexes can be assembled and disassembled repeatedly until the most favorable collection of supramolecules is obtained.

Recent studies by Nistchke,[29d] Severin,[35] Isaacs,[30k] and Barboiu[31c] have explored a wide range of complex synthetic mixtures that undergo varying degrees of self-sorting. Isaacs et al., for example, have performed an extensive exploration of multiple different complementary hydrogen bond donors and acceptors and showed that the temperature, concentration, association constants, and the presence of competitors all play a part in determining the extent of self-sorting.

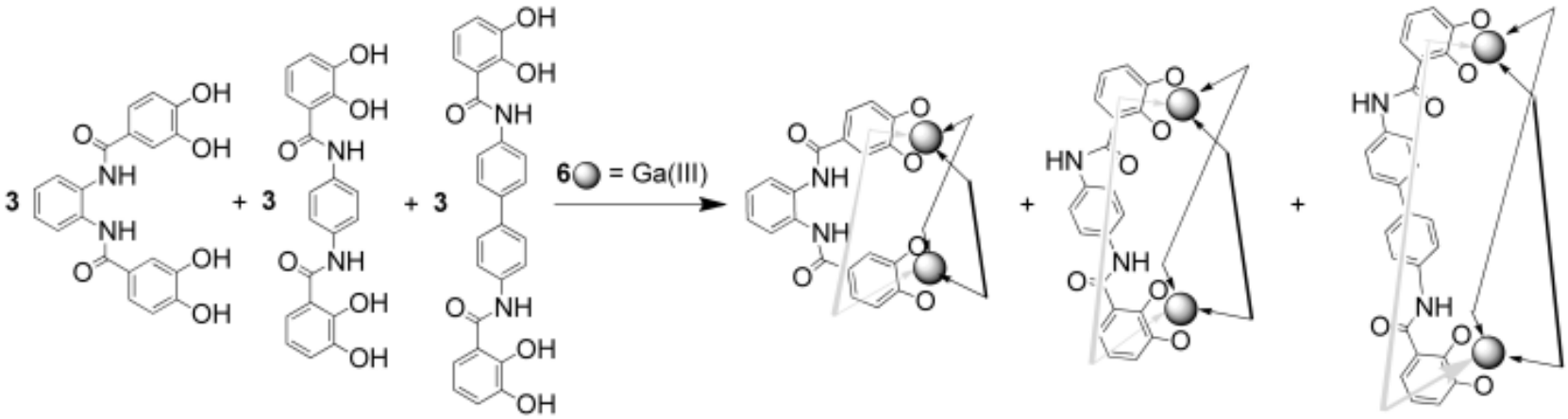

Figure 1.3. Self-sorting of triple helicies composed exclusively of identical ligands.

1.6 Selective Self-assembly of Multicomponent Structures

Multicomponent selective self-assembly represents a unique self-assembly process, by which multiple varying components can selectively recognize and combine with each other to generate only one discrete structure within a mixture.[28a] Multicomponent selective self-assembly is a critical phenomenon in many biological systems. For example, the proteasome of yeast *Saccharomyces Cerevisiae* is constructed from pairs of seven different proteins. However, obtaining multicomponent selective self-assembly in an abiological system is a formidable challenge. While mixing various molecular components that lack sufficient complementary electronic and/or structural information, a self-organized mixture or even disordered oligomeric species can be formed instead of one finite discrete supramolecule. How to provide sufficient molecular information to control selective self-assembly in a multicomponent system remains a demanding issue in modern supramolecular chemistry.

In the area of coordination-driven self-assembly, several methods have been developed to achieve multicomponent selective self-assembly by taking advantage of the predictable coordination of transition metal acceptors and tunable organic donors.

Sauvage[36] and Lehn[31i,37] explored the approach of using the topological information of molecular components to guide selective self-assembly of multicomponent supramolecular pseudorotaxanes in pioneering studies. As shown in Figure 1.4a, the combination of an endotopic phenanthroline ligand and an open chain phenanthroline in presence of copper (I) produced only the three-component complex due to the endotopic ligand site.[38] This selective coordination motif was successfully utilized to achieve a wide variety of discrete supramolecular assemblies, such as catenanes,

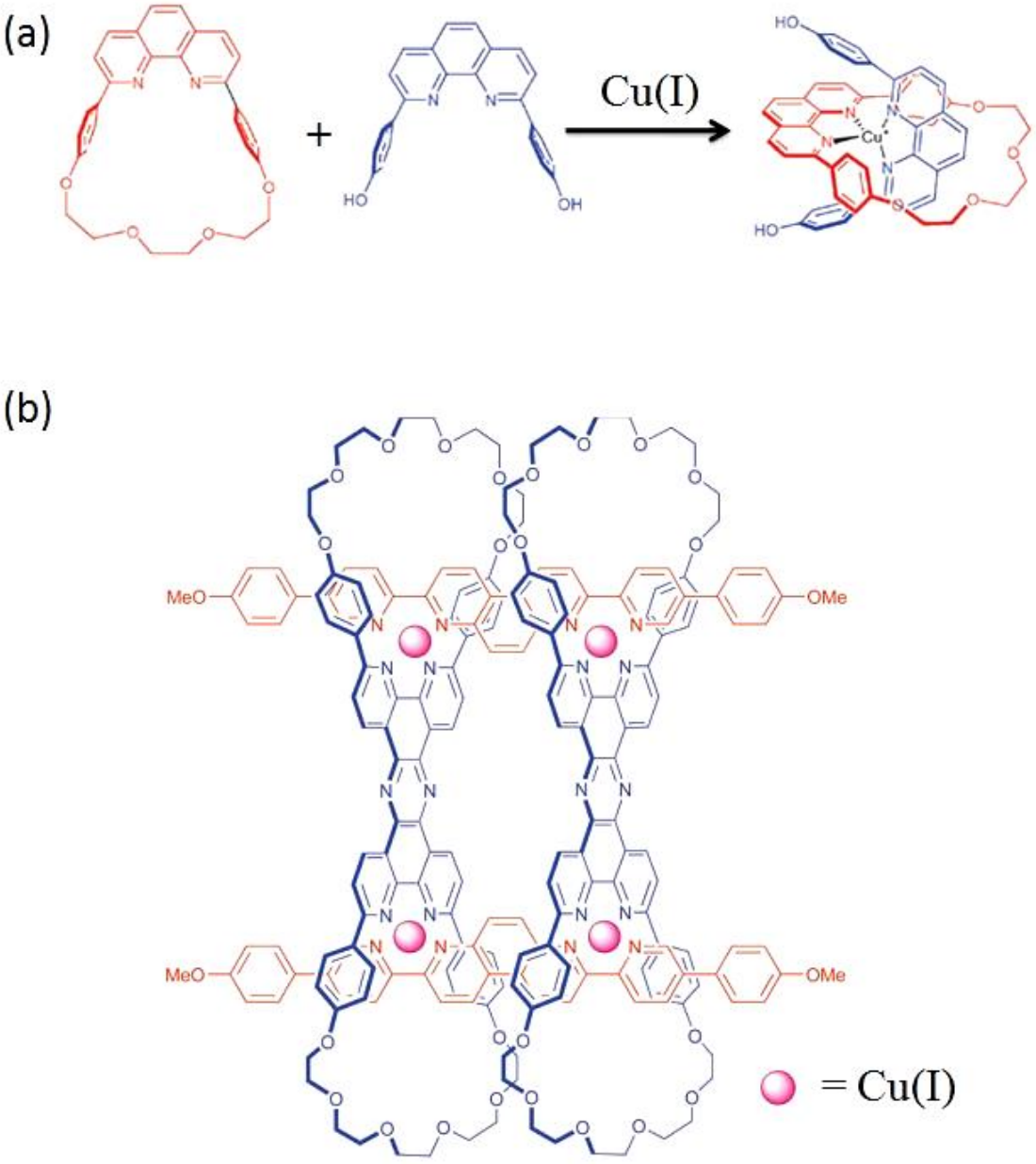

Figure 1.4. Topological constraints lead to a preferential formation of the three-component complex. (a) Basic design and (b) Formation of three-component supramolecular pseudorotaxanes is guided by topological constraints.

rotaxanes, pseudorotaxanes, etc. For example, as shown in Figure 1.4b, a three-component cyclic [2]pseudorotaxane tetramer can be synthesized in one pot based on this selective self-assembly.[36d] Using a similar design, Lehn et al. reported the fabrication of rigid rack-pseudorotaxanes.[37e]

Recently, it was found that steric constraints could be exploited to control multicomponent selective self-assembly and interesting examples have been reported by Schmittel,[39] Fujita,[40] and Kobayashi.[41] Schmittel et al. described the selective self-assembly of three-component complexes using both bulky and regular 2,9-diarylphenanthrolines as ligands to coordinate transition metals such as Zn(II), Cu(I), and Ag(I) bearing tetrahedral coordination geometries (Figure 1.5a). This strategy is known as the HETPHEN approach.[39a] The generality of the HETPHEN approach allows for the fabrication of various interesting multicomponent supramolecular architectures, such as ring-in-ring structures, nanoboxes, grids, nanobaskets, racks, rectangles, tweezers, etc. For example, based on the HETPHEN approach, the combination of two exotopic phenanthroline binding sites in combination with linear bis- or trisphenanthrolines and Cu(I) ions results in selective self-assembly of nanoscale double and triple deckers (Figure 1.5b).[39k] Recently, another similar approach–the HETTAP[39f,39i,j,39m] concept–using Zn(II) and Hg(II) bearing an octahedral coordination configuration was also developed in Schmittel's group. Fujita[40] and Kobayashi[41] used cis-protected square planar Pd(II) to self-assemble with a pyridyl ligand bearing bulky groups to direct the selective formation of three-component squares and cages.

Incorporating topological or steric information onto molecular components requires a significant synthetic effort. To reduce synthetic labor, facile approaches were

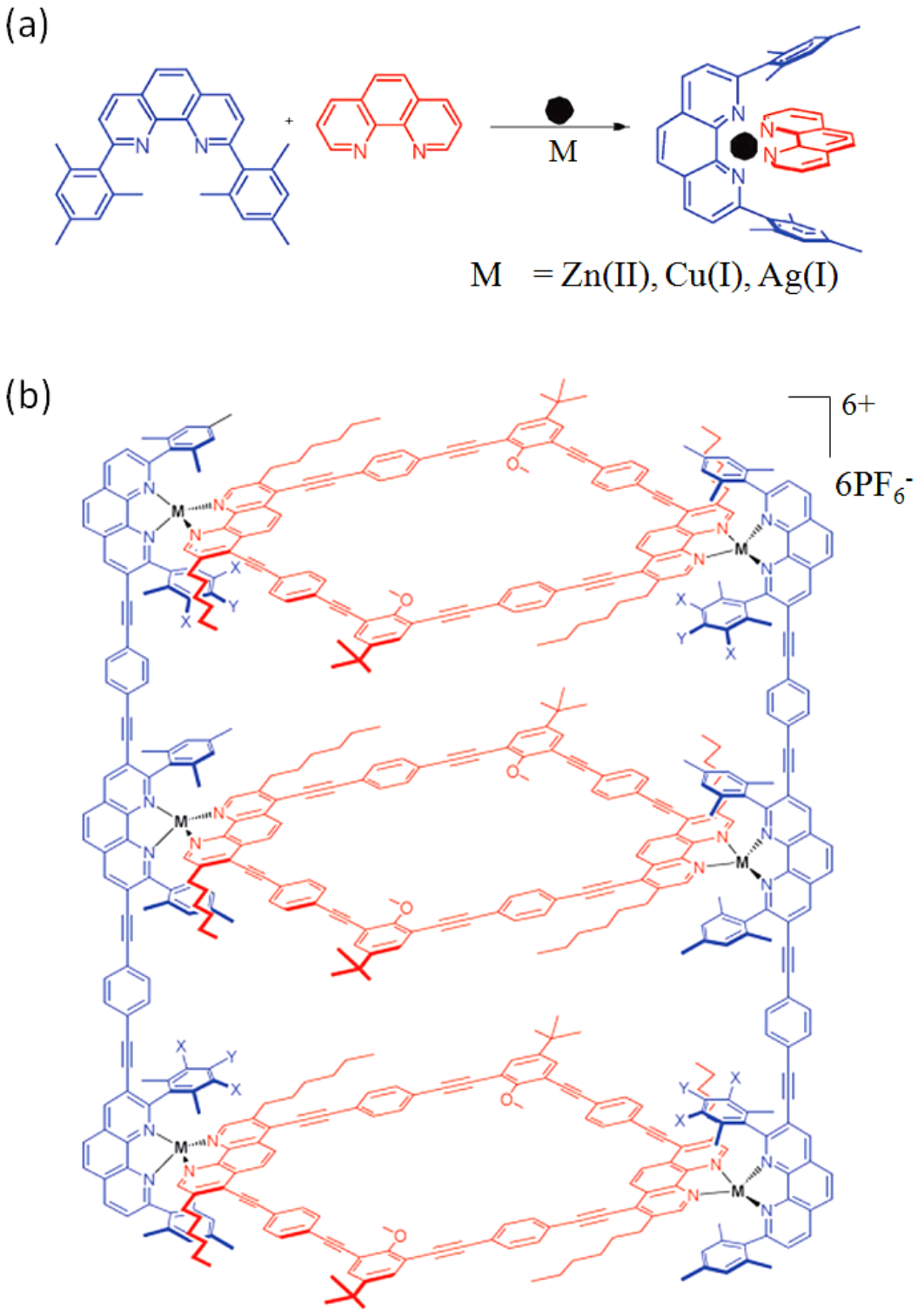

Figure 1.5. HETPHEN approach for quantitative three-component self-assembly. (a) Basic design and (b) A nanotubular structure constructed based on the HETPHEN approach.

recently developed based on the template effect and stoichiometry control. Fujita and coworkers[42] demonstrated that cis-protected Pd(II) acceptors with di- and trioptic pyridyl ligands could easily and selectively self-assemble into 3D trigonal prisms (Figure 1.6). Recently, Stang et al. demonstrated the facile selective self-assembly of multicomponent 2D fused polygons (Figure 1.7)[43] and 3D tetragonal prisms,[44] achieved by mixing suitable directional organoplatinum acceptors and different pyridyl donors in specific stoichiometries. These assemblies rely mainly on the directionality of the molecular components and are controlled by maximum site occupancy and entropy.

1.7 Functions of Coordination Supramolecular Systems

Supramolecules constructed by coordination-driven self-assembly have proven to be useful in a variety of applications, such as catalyst for organic reactions, molecular flasks, the synthesis of dendrimers and nanoparticles, and molecular devices. Most of the applications rely on two major features of these supramolecules: host-guest chemistry[45] and functionalization.[46]

By virtue of the directionality and rigidity of metal-ligand coordination bonds, coordination-driven self-assembly leads to the formation of supramolecules, which bear robust structural backbones and cavities of well-defined shapes and sizes. Supramolecules with cavities can act as containers to encapsulate suitable guest molecules under appropriate conditions. In the past decades, the great progress of coordination-driven self-assembly has enabled construction of versatile supramolecular containers with large cavities and the host-guest chemistry of these coordination supramolecules has been extensively studied. Systematic investigations carried out by

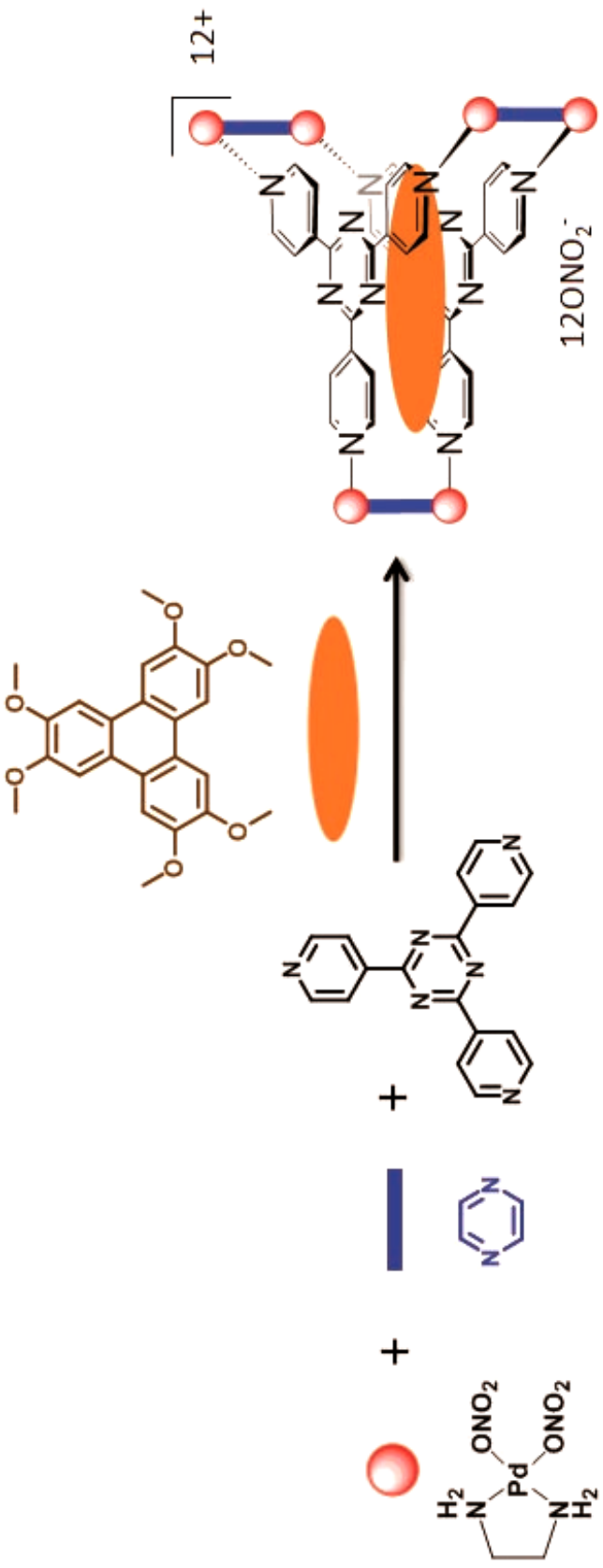

Figure 1.6. Self-assembly of a trigonal prism in presence of a template.

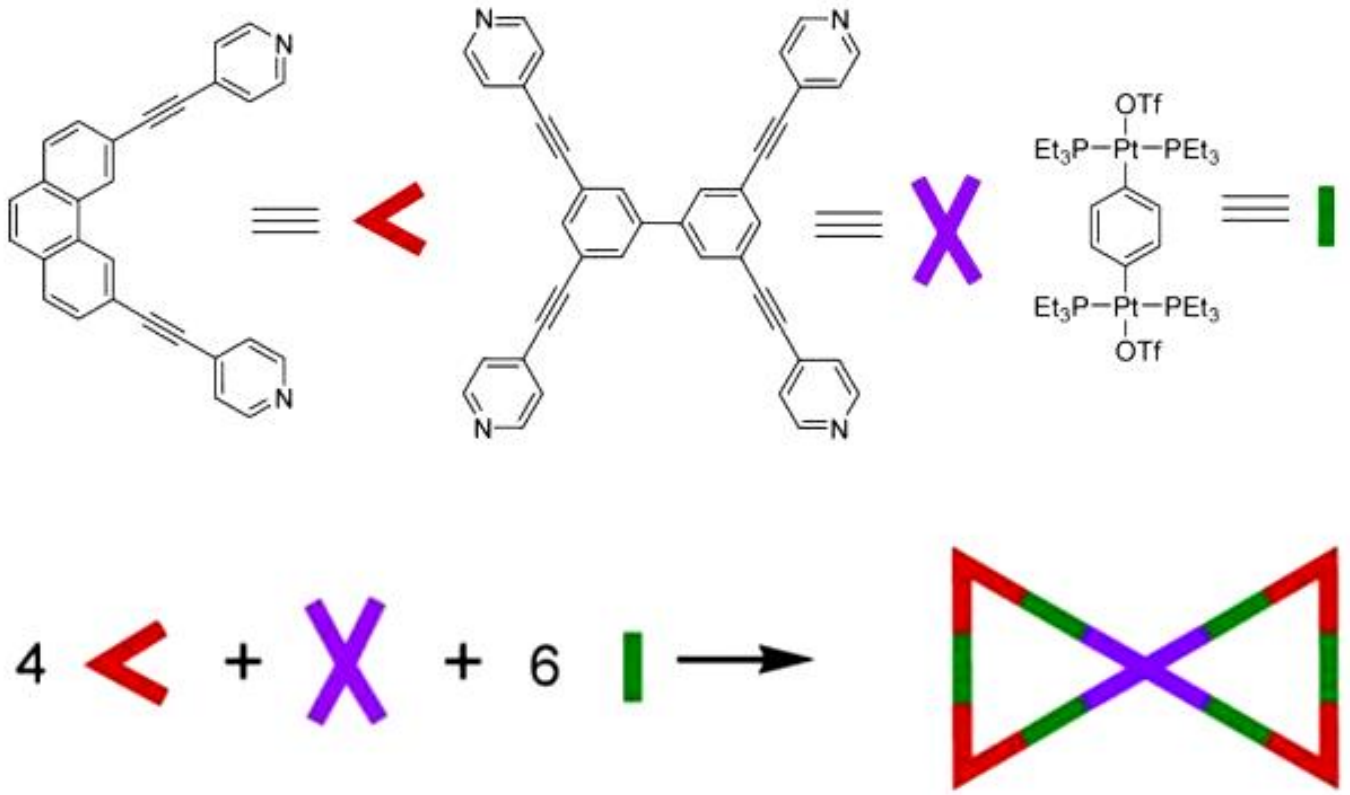

Figure 1.7. Synthesis of double triangle under stoichiometry control.

Raymond and Fujita are impressive studies in the field. Raymond and co-workers developed M_4L_6 tetrahedral supramolecular cages consisting of four octahedral metal ions, e.g., Fe(III) or Ga(III), and six naphthalene-based catechol amide ligands (Figure 1.8).[45a-c] The highly anionic nature of the cage allows for exclusive encapsulation of monocationic guests such as alkylammonium ions and organometallic complexes, e.g., $[CpRu(C_6H_6)]^+$ and $Rh(PMe_3)_2(H_2O)_2^+$. Fujita and coworkers have designed an octahedral M_6L_4 coordination cage self-assembled by six cis-protected square planar Pd(II) or Pt(II) metal accceptors and four panel-like triangular pyridyl donors (2,4,6-tris(4- pyridyl)-1,3,5-triazine; Figure 1.9).[45e,45i] This cage can accommodate a variety of anionic and neutral guest molecules, e.g., adamantane and ferrocene. Recently, the host-guest properties of coordination supramolecular cages have been successfully applied to develop catalysts for organic reactions and molecular flasks.

To design advanced materials that incorporate multiple functionalities, it becomes highly desirable to control the precise location, orientation, and stoichiometry of functional groups. The structural aspects of rigid, well-defined, supramolecular metal–organic assemblies present unique opportunities for incorporating various functionalities into their architectures. Functionalized coordination-driven self-assembled supramolecules can be used in a variety of applications, e.g., the synthesis of dendrimers and nanoparticles, and molecular devices. In one recent example (Figure 1.10), Stang and coworkers incorporated Fréchet-type[47] dendrons onto molecular building blocks and via coordination-driven self-assembly, 2D metal-organic supramolecular dendrimers from the first to the third generation were synthesized in high yields.[48] A similar strategy was also applied to functionalize with pseudorotaxanes[49] and electrochemically active

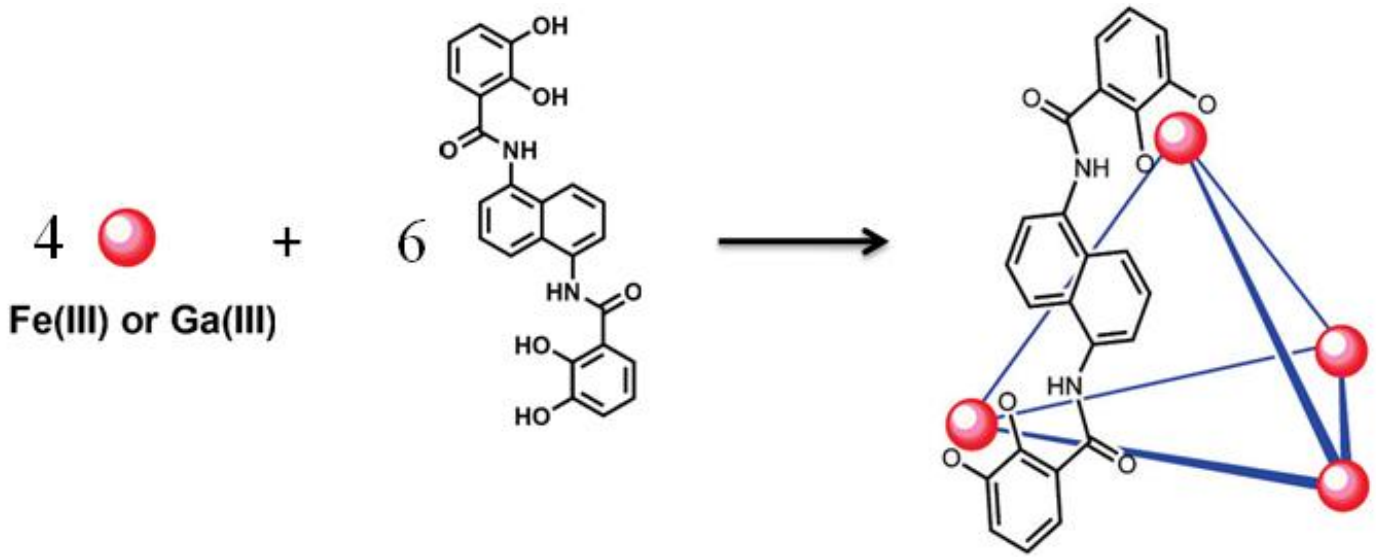

Figure 1.8. An M_4L_6 tetrahedral supramolecular cage consisting of four octahedral metal ions, e.g. Fe(III) or Ga(III), and six naphthalene-based catechol amide ligands.

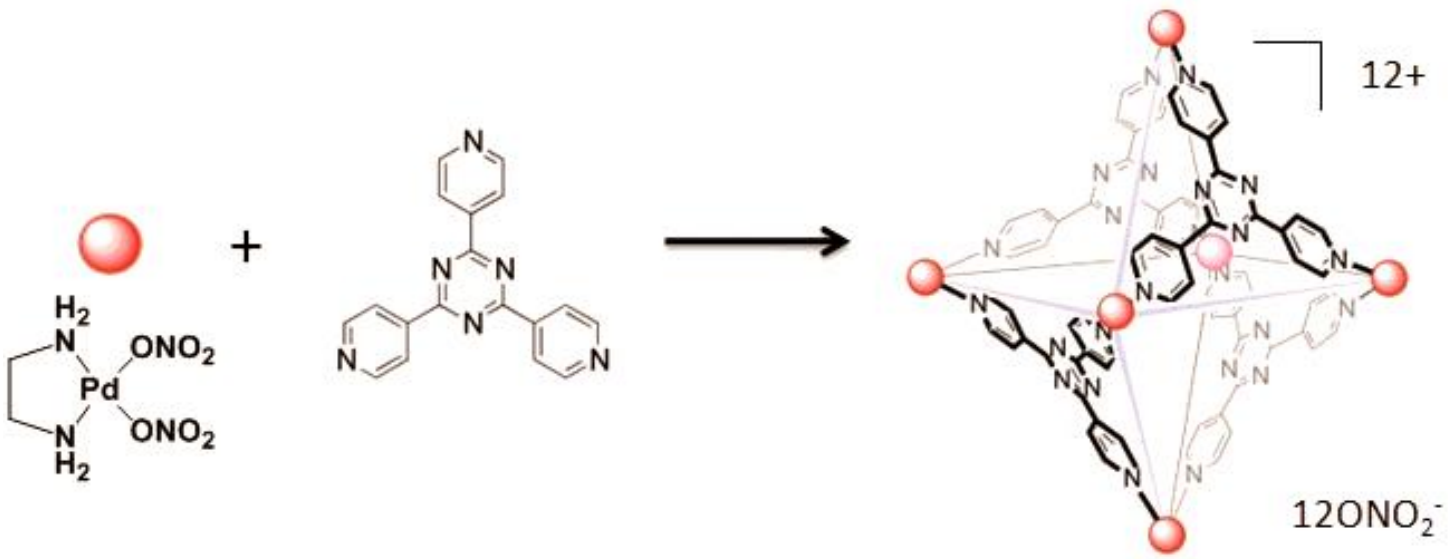

Figure 1.9. An octahedral M_6L_4 coordination cage self-assembled from six cis-protected square planar Pd(II) or Pt(II) metal acceptors and four panel-like triangular pyridyl donors (2,4,6-tris(4- pyridyl)-1,3,5-triazine).

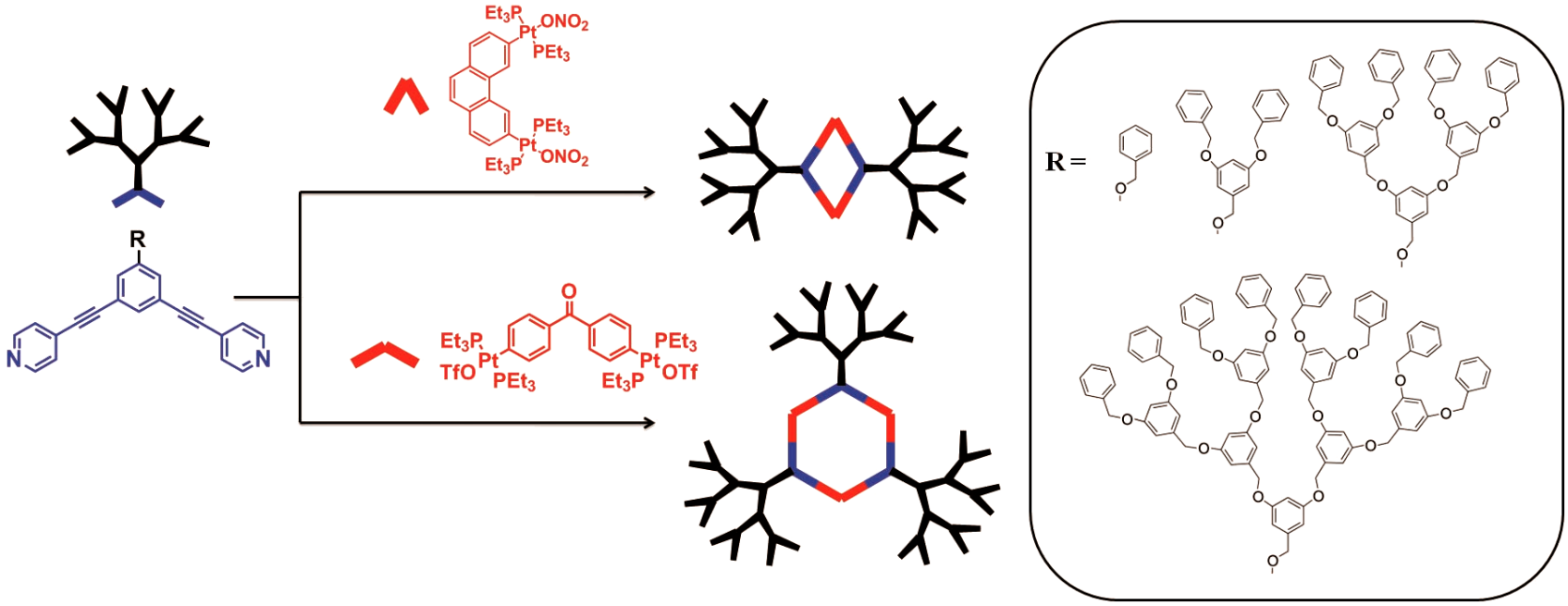

Figure 1.10. Self-assembly of 2D metal-organic supramolecular dendrimers.

metal-organic supramolecules.[50] Recent examples (Figure 1.11) reported by Fujita et al.[51] demonstrated that functionalization of the interior and/or exterior of a $M_{12}L_{24}$ Pd-based supramolecular sphere can result in applications such as saccharide clusters, nanoscale fluoro-droplets, confined polymerization, and confined formation of nanoparticles.

1.8 Summary

Recent years have seen rapid developments in supramolecular chemistry and coordination-driven self-assembly. While modern chemical laboratories allow for self-assembly to be carried out in exceedingly simple conditions, biological systems are forced to develop, survive, and reproduce in the significantly more chaotic natural world, yet they do so with aplomb. Systematic investigations of the factors that influence and control self-sorting and selective self-assembly in abiological systems containing multiple molecular components contribute to an increased understanding of analogous processes in nature. By merging the host-guest properties and functionalization of coordination-driven self-assembled supramolecules, multicomponent supramolecular systems may provide novel pathways towards interesting supramolecular phenomena and advanced functional materials. The following chapters demonstrate our systematic investigations of Pt(II)-based multicomponent supramolecular systems from understanding the fundamental dynamic properties, to developing approaches of controlling multicomponent self-assembly and searching for potential applications based on host-guest chemistry and functionalizations.

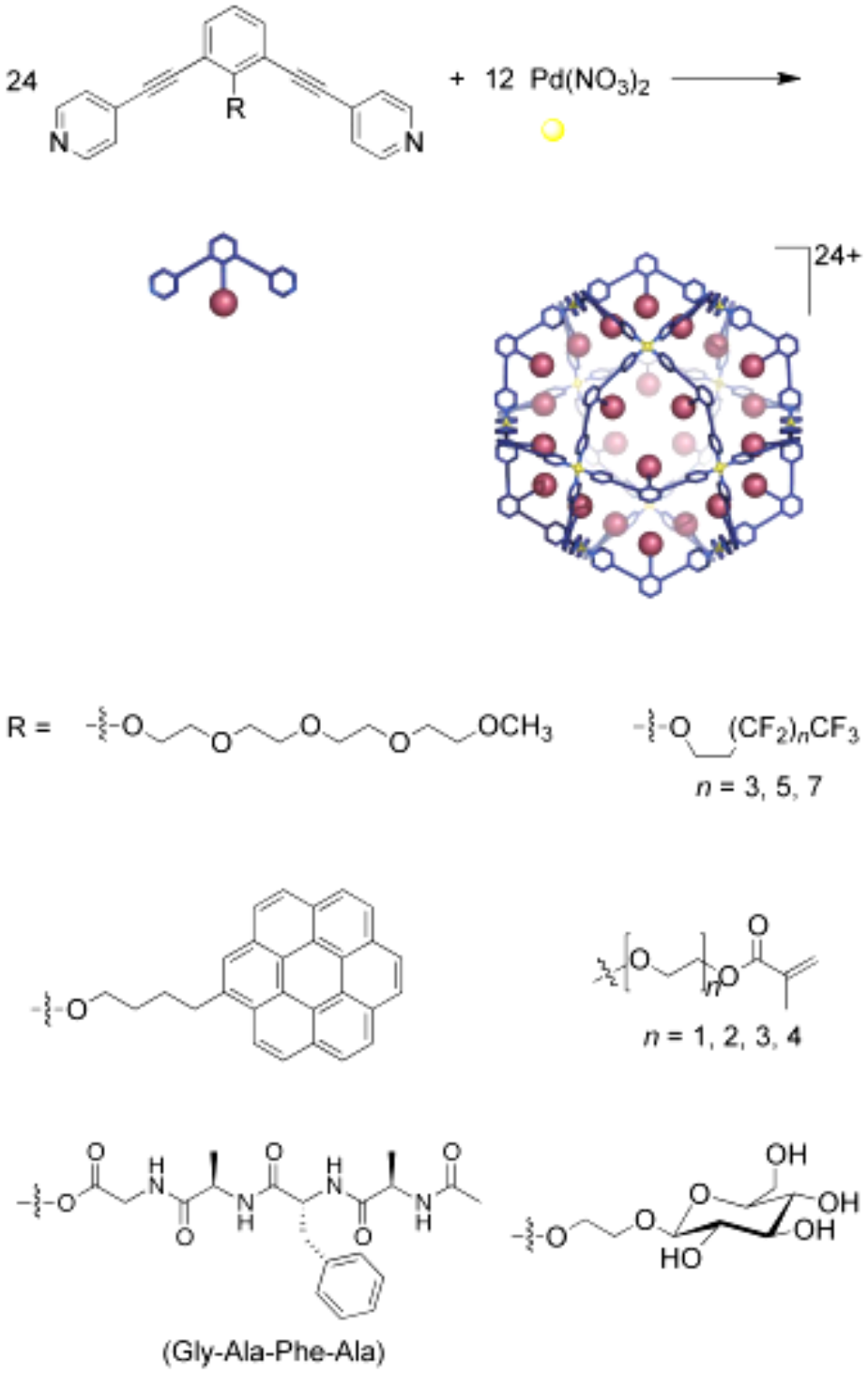

Figure 1.11. Various functionalizations in the interior of a $M_{12}L_{24}$ Pd-based supramolecular sphere.

1.9 References

(1) Chen, C. P.; Park, Y.; Rice, K. G. *J. Pept. Res.* **2004**, *64*, 237.

(2) Zhang, X.; Houk, K. N. *Acc. Chem. Res.* **2005**, *38*, 379.

(3) (a) Every, A. E.; Russu, I. M. *Biopolymers* **2007**, *87*, 165 (b) Mo, Y. *J. Mol .Model.* **2006**, *12*, 665.

(4) (a) Aida, M. *J. Theor. Biol.* **1988**, *130*, 327 (b) Huang, Y. T.; Rusinova, E.; Ross, J. B.; Senear, D. F. *J. Mol. Biol.* **1997**, *267*, 403.

(5) (a) Whitesides, G. M.; Boncheva, M. *Proc. Natl. Acad. Sci. U S A* **2002**, *99*, 4769 (b) Whitesides, G. M.; Grzybowski, B. *Science* **2002**, *295*, 2418 (c) Whitesides, G. M.; Mathias, J. P.; Seto, C. T. *Science* **1991**, *254*, 1312.

(6) (a) Lehn, J. M. *Science* **1993**, *260*, 1762 (b) Lehn, J. M. *Science* **1985**, *227*, 849 (c) Menger, F. M. *Proc Natl Acad Sci U S A* **2002**, *99*, 4818 (d) Jorgensen, W. L. *Proc. Natl. Acad. Sci. U S A* **1993**, *90*, 1635 (e) Diederich, F.; Felber, B. *Proc. Natl .Acad. Sci. U S A* **2002**, *99*, 4778 (f) van Esch, J. H. *Nature* **2010**, *466*, 193 (g) Schmidbaur, H. *Nature* **2001**, *413*, 31 (h) Lindoy, L. F. *Nature* **1992**, *356*, 197(i) Hunter, C. *Nature* **2011**, *469*, 39 (j) Helmer, M. *Nature* **2004**, *427*, 597 (k) Davis, A. P. *Nature* **2010**, *464*, 169 (l) Cohen, S. M. *Nature* **2009**, *461*, 602 (m) Bethell, D.; Schiffrin, D. J. *Nature* **1996**, *382*, 581 (n) Tomalia, D. A. *Nat. Mater.* **2003**, *2*, 711 (o) Purrello, R. *Nat. Mater.* **2003**, *2*, 216 (p) Thomas, J. A. *Nat. Chem.* **2009**, *1*, 25 (q) Stoddart, J. F. *Nat Chem* **2009**, *1*, 14 (r) Shimizu, K. D. *Nat Chem* **2010**, *2*, 612

(7) Lehn, J. M. *Acc. Chem. Res.* **1978**, *11*, 49.

(8) Cram, D. J.; Cram, J. M. *Science* **1974**, *183*, 803.

(9) Pederson, C. J. *Ger. Offen.* **1970**

(10) Badjic, J. D.; Nelson, A.; Cantrill, S. J.; Turnbull, W. B.; Stoddart, J. F. *Acc. Chem. Res.* **2005**, *38*, 723.

(11) (a) Seidel, S. R.; Stang, P. J. *Acc. Chem. Res.* **2002**, *35*, 972 (b) Leininger, S. O., Bogdan; Stang, Peter J. *Chem. Rev.* **2000**, 167.

(12) (a) Fujita, M.; Tominaga, M.; Hori, A.; Therrien, B. *Acc. Chem. Res.* **2005**, *38*, 369 (b) Fujita, M. U., Kazuhiko; Yoshizawa, Michito; Fujita, Norifumi; Kusukawa, Takahiro; Biradha, Kumar *Chem. Commun.* **2001**, 509.

(13) (a) Caulder, D. L.; Raymond, K. N. *Acc. Chem. Res.* **1999**, *32*, 975 (b) Caulder, D. L.; Raymond, K. N. *J. Chem. Soc., Dalton Trans.* **1999**, 1185.

(14) (a) Holliday, B. J.; Mirkin, C. A. *Angew. Chem., Int. Ed.* **2001**, *40*, 2022 (b) Oliveri, C. G.; Ulmann, P. A.; Wiester, M. J.; Mirkin, C. A. *Acc. Chem. Res.* **2008**, *41*, 1618.

(15) (a) Ruben, M.; Rojo, J.; Romero-Salguero, F. J.; Uppadine, L. H.; Lehn, J.-M. *Angew. Chem., Int. Ed.* **2004**, *43*, 3644 (b) Ruben, M.; Lehn, J.-M.; Mueller, P. *Chem. Soc. Rev.* **2006**, *35*, 1056.

(16) (a) Albrecht, M. *Chem. Soc. Rev.* **1998**, *27*, 281 (b) Albrecht, M. *Angew. Chem., Int. Ed.* **1999**, *38*, 3463 (c) Albrecht, M. *Chem. Rev.* **2001**, *101*, 3457 (d) Ward, M. D.; McCleverty, J. A.; Jeffery, J. C. *Coord. Chem. Rev.* **2001**, *222*, 251 (e) Kim, K. *Chem. Soc. Rev.* **2002**, *31*, 96 (f) Piguet, C.; Borkovec, M.; Hamacek, J.; Zeckert, K. *Coord. Chem. Rev.* **2005**, *249*, 705 (g) Steel, P. J. *Acc. Chem. Res.* **2005**, *38*, 243 (h) Hamacek, J.; Borkovec, M.; Piguet, C. *Dalton Trans* **2006**, 1473 (i) Albrecht, M.; Fiege, M.; Osetska, O. *Coord. Chem. Rev.* **2008**, *252*, 812(j) Friese, V. A.; Kurth, D. G. *Coord. Chem. Rev.* **2008**, *252*, 199 (k) Miyashita, N.; Kurth, D. G. *J. Mater. Chem.* **2008**, *18*, 2636 (l) Friese, V. A.; Kurth, D. G. *Curr. Opin. Colloid Interface Sci.* **2009**, *14*, 81 (m) Ward, M. D. *Chem. Commun.* **2009**, 4487.

(17) (a) Koert, U. H., Margaret M.; Lehn, J. M. *Nature* **1990**, 339 (b) Lehn, J. M. R., A.; Siegel, J.; Harrowfield, J.; Chevrier, B.; Moras, D. *Proc. Natl. Acad. Sci. USA* **1987**, 2565.

(18) (a) Jude, H.; Disteldorf, H.; Fischer, S.; Wedge, T.; Hawkridge, A. M.; Arif, A. M.; Hawthorne, M. F.; Muddiman, D. C.; Stang, P. J. *J. Am. Chem. Soc.* **2005**, *127*, 12131 (b) Kryschenko, Y. K.; Seidel, S. R.; Arif, A. M.; Stang, P. J. *J. Am. Chem. Soc.* **2003**, *125*, 5193 (c) Mukherjee, P. S.; Das, N.; Kryschenko, Y. K.; Arif, A. M.; Stang, P. J. *J. Am. Chem. Soc.* **2004**, *126*, 2464 (d) Jude, H.; Sinclair, D. J.; Das, N.; Sherburn, M. S.; Stang, P. J. *J. Org. Chem.* **2006**, *71*, 4155 (e) Northrop, B. H.; Chercka, D.; Stang, P. J. *Tetrahedron* **2008**, *64*, 11495.

(19) (a) Hou, Z.; Raymond, K. N.; O'Sullivan, B.; Esker, T. W.; Nishio, T. *Inorg Chem* **1998**, *37*, 6630 (b) Xu, J.; Parac, T. N.; Raymond, K. N. *Angew. Chem. Int. Ed. Engl.* **1999**, *38*, 2878 (c) Yeh, R. M.; Raymond, K. N. *Inorg. Chem.* **2006**, *45*, 1130 (d) Yeh, R. M.; Ziegler, M.; Johnson, D. W.; Terpin, A. J.; Raymond, K. N. *Inorg. Chem.* **2001**, *40*, 2216.

(20) Hong, M. Z., Y.; Su, W.; Cao, R.; Fujita, M.; Zhou, Z.; Chan, Albert S. C. *J. Am. Chem. Soc.* **2000**, 4819.

(21) Umemoto, K. Y., K.; Fujita, M. *J. Am. Chem. Soc.* **2000**, 7150.

(22) Woodward, R. B. *Pure Appl. Chem.* **1973**, 145.

(23) (a) Nicolaou, K. C.; Liu, J. J.; Yang, Z.; Ueno, H.; Sorensen, E. J.; Claiborne, C. F.; Guy, R. K.; Hwang, C. K.; Nakada, M.; Nantermet, P. G. *J. Am. Chem. Soc.*

1995, *117*, 8690 (b) Nicolaou, K. C.; Liu, J. J.; Yang, Z.; Ueno, H.; Sorensen, E. J.; Claiborne, C. F.; Guy, R. K.; Hwang, C. K.; Nakada, M.; Nantermet, P. G. *J. Am. Chem. Soc.* **1995**, *117*, 634 (c) Nicolaou, K. C.; Ueno, H.; Liu, J. J.; Nantermet, P. G.; Yang, Z.; Renaud, J.; Paulvannan, K.; Chadha, R. *J. Am. Chem. Soc.* **1995**, *117*, 653 (d) Nicolaou, K. C.; Yang, Z.; Liu, J. J.; Nantermet, P. G.; Claiborne, C. F.; Renaud, J.; Guy, R. K.; Shibayama, K. *J. Am. Chem. Soc.* **1995**, *117*, 645 (e) Nicolaou, K. C.; Nantermet, P. G.; Ueno, H.; Guy, R. K.; Couladouros, E. A.; Sorensen, E. J. *J. Am. Chem. Soc.* **1995**, *117*, 624 (f) Nicolaou, K. C.; Yang, Z.; Liu, J. J.; Ueno, H.; Nantermet, P. G.; Guy, R. K.; Claiborne, C. F.; Renaud, J.; Couladouros, E. A. *Nature* **1994**, *367*, 630 (g) Holton, R. A.; Kim, H. B.; Somoza, C.; Liang, F.; Biediger, R. J.; Boatman, P. D.; Shindo, M.; Smith, C. C.; Kim, S. *J. Am. Chem. Soc.* **1994**, *116*, 1599 (h) Holton, R. A.; Somoza, C.; Kim, H. B.; Liang, F.; Biediger, R. J.; Boatman, P. D.; Shindo, M.; Smith, C. C.; Kim, S. *J. Am. Chem. Soc.* **1994**, *116*, 1597.

(24) (a) Endo, A.; Yanagisawa, A.; Abe, M.; Tohma, S.; Kan, T.; Fukuyama, T. *J. Am. Chem. Soc.* **2002**, *124*, 6552 (b) Corey, E. J.; Gin, D. Y.; Kania, R. S. *J. Am. Chem. Soc.* **1996**, *118*, 9202 (c) Chen, J.; Chen, X.; Bois-Choussy, M.; Zhu, J. *J. Am. Chem. Soc.* **2006**, *128*, 87.

(25) (a) Timmins, P. A.; Wild, D.; Witz, J. *Structure* **1994**, *2*, 1191 (b) Robinson, I. K.; Harrison, S. C. *Nature* **1982**, *297*, 563 (c) Harrison, S. C.; Olson, A. J.; Schutt, C. E.; Winkler, F. K.; Bricogne, G. *Nature* **1978**, *276*, 368 (d) Bernal, J. D.; Fankuchen, I.; Riley, D. P. *Nature* **1938**, *142*, 1075.

(26) (a) Appleby, T. C.; Luecke, H.; Shim, J. H.; Wu, J. Z.; Cheney, I. W.; Zhong, W.; Vogeley, L.; Hong, Z.; Yao, N. *J. Virol.* **2005**, *79*, 277 (b) Love, R. A.; Maegley, K. A.; Yu, X.; Ferre, R. A.; Lingardo, L. K.; Diehl, W.; Parge, H. E.; Dragovich, P. S.; Fuhrman, S. A. *Structure* **2004**, *12*, 1533 (c) Ding, J.; Smith, A. D.; Geisler, S. C.; Ma, X.; Arnold, G. F.; Arnold, E. *Structure* **2002**, *10*, 999 (d) Oren, D. A.; Zhang, A.; Nesvadba, H.; Rosenwirth, B.; Arnold, E. *J Mol Biol* **1996**, *259*, 120 (e) Tormo, J.; Blaas, D.; Parry, N. R.; Rowlands, D.; Stuart, D.; Fita, I. *EMBO J* **1994**, *13*, 2247 (f) Kim, S. S.; Smith, T. J.; Chapman, M. S.; Rossmann, M. C.; Pevear, D. C.; Dutko, F. J.; Felock, P. J.; Diana, G. D.; McKinlay, M. A. *J. Mol. Biol.* **1989**, *210*, 91.

(27) (a) Lehn, J.-M. *Proc. Natl. Acad. Sci. U. S. A.* **2002**, *99*, 4763 (b) Lehn, J.-M. *Science* **2002**, *295*, 2400.

(28) (a) De, S.; Mahata, K.; Schmittel, M. *Chem. Soc. Rev.* **2010**, *39*, 1555 (b) Northrop, B. H.; Zheng, Y.-R.; Chi, K.-W.; Stang, P. J. *Acc. Chem. Res.* **2009**, *42*, 1554.

(29) (a) Ghosh, S.; Isaacs, L., J. Am. Chem. Soc. **2010**, 118 (b) Rudzevich, V.; Rudzevich, Y.; Boehmer, V. *Synlett* **2009**, 1887(c) Legrand, Y.-M.; Dumitru, F.; Arnal-Herault, C.; Michau, M.; Barboiu, M. D. *Rev. Roum. Chim.* **2009**, *54*, 421(d)

Nitschke, J. R. *Acc. Chem. Res.* **2007**, *40*, 103(e) Maeda, C.; Kamada, T.; Aratani, N.; Osuka, A. *Coord. Chem. Rev.* **2007**, *251*, 2743.

(30) (a) Jiang, W.; Schalley, C. A. *J. Mass Spectrom.* **2010**, *45*, 788 (b) Ulrich, S.; Petitjean, A.; Lehn, J.-M. *Eur. J. Inorg. Chem.* **2010**, 1913 (c) Jiang, W.; Schalley, C. A. *Proc. Natl. Acad. Sci. U. S. A.* **2009**, *106*, 10425 (d) Ulrich, S.; Lehn, J.-M. *Chem.--Eur. J.* **2009**, *15*, 5640 (e) Rudzevich, Y.; Rudzevich, V.; Klautzsch, F.; Schalley, C. A.; Boehmer, V. *Angew. Chem., Int. Ed.* **2009**, *48*, 3867 (f) Jiang, W.; Schalley, C. A. *Proc. Natl. Acad. Sci. U. S. A., Early Ed.* **2009**, 1 (g) Ajami, D.; Hou, J.-L.; Dale, T. J.; Barrett, E.; Rebek, J., Jr. *Proc. Natl. Acad. Sci. U. S. A., Early Ed.* **2009**, 1 (h) Ulrich, S.; Lehn, J.-M. *J. Am. Chem. Soc.* **2009**, *131*, 5546 (i) Rang, A.; Nieger, M.; Engeser, M.; Luetzen, A.; Schalley, C. A. *Chem. Commun.* **2008**, 4789 (j) Jiang, W.; Winkler, H. D. F.; Schalley, C. A. *J. Am. Chem. Soc.* **2008**, *130*, 13852 (k) Wu, A.; Isaacs, L. *J. Am. Chem. Soc.* **2003**, *125*, 4831(l) Wu, A.; Chakraborty, A.; Fettinger, J. C.; Flowers, R. A., II; Isaacs, L. *Angew. Chem., Int. Ed.* **2002**, *41*, 4028.

(31) (a) Addicott, C.; Das, N.; Stang, P. J. *Inorg. Chem.* **2004**, *43*, 5335 (b) Albrecht, M.; Schneider, M. *Eur. J. Inorg. Chem.* **2002**, 1301 (c) Barboiu, M.; Petit, E.; van, d. L. A.; Vaughan, G. *Inorg. Chem.* **2006**, *45*, 484(d) Zheng, Y.-R.; Yang, H.-B.; Northrop, B. H.; Ghosh, K.; Stang, P. J. *Inorg. Chem.* **2008**, *47*, 4706 (e) Albrecht, M.; Schneider, M.; Rottele, H. *Angew. Chem., Int. Ed.* **1999**, *38*, 557 (f) Caulder, D. L.; Raymond, K. N. *Angew. Chem., Int. Ed. Engl.* **1997**, *36*, 1440 (g) Mukhopadhyay, P.; Zavalij, P. Y.; Isaacs, L. *J. Am. Chem. Soc.* **2006**, *128*, 14093 (h) Yang, H.-B.; Ghosh, K.; Northrop, B. H.; Stang, P. J. *Org. Lett.* **2007**, *9*, 1561 (i) Kramer, R.; Lehn, J. M.; Marquis-Rigault, A. *Proc. Natl. Acad. Sci. U. S. A.* **1993**, *90*, 5394.

(32) (a) Cooks, R. G.; Zhang, D.; Koch, K. J.; Gozzo, F. C.; Eberlin, M. N. *Anal. Chem.* **2001**, *73*, 3646 (b) Shi, X.; Fettinger, J. C.; Cai, M.; Davis, J. T. *Angew. Chem., Int. Ed.* **2000**, *39*, 3124 (c) Barrett, E. S.; Dale, T. J.; Rebek, J., Jr. *J. Am. Chem. Soc.* **2008**, *130*, 2344 (d) Castellano, R. K.; Nuckolls, C.; Rebek, J., Jr. *J. Am. Chem. Soc.* **1999**, *121*, 11156 (e) Prins, L. J.; Huskens, J.; De, J. F.; Timmerman, P.; Reinhoudt, D. N. *Nature* **1999**, *398*, 498 (f) Ajami, D.; Hou, J.-L.; Dale, T. J.; Barrett, E.; Rebek, J., Jr. *Proc Natl Acad Sci U S A* **2009**, *106*, 10430 (g) Ajami, D.; Hou, J.-L.; Dale, T. J.; Barrett, E.; Rebek, J., Jr. *Proc. Natl. Acad. Sci. U. S. A.* **2009**, *106*, 10430 (h) Crego-Calama, M.; Reinhoudt, D. N.; ten, C. M. G. J. *Top. Curr. Chem.* **2005**, *249*, 285.

(33) (a) Schnarr, N. A.; Kennan, A. J. *J. Am. Chem. Soc.* **2003**, *125*, 667 (b) Bilgicer, B.; Xing, X.; Kumar, K. *J. Am. Chem. Soc.* **2001**, *123*, 11815.

(34) (a) Rowan, S. J. H., D. G.; Brady, P. A.; Sanders, J. K. M. *J. Am. Chem. Soc.* **1997**, 2578 (b) Rowan, S. J. R., D. J.; Sanders *J. Org. Chem.* **1999**, 5804 (c) Rowan, S. J. C., S. J.; Cousins, G. R. L.; Sanders, J. K. M.; Stoddart, J. F. *Angew.*

Chem., Int. Ed. **2002**, 2943 (d) Corbett, P. T. L., J.; Vial, L.; West, K. R.; Wietor, J.-L.; Sanders, J. K. M.; Otto, S. *Chem. Rev.* **2006**, 3652.

(35) Saur, I.; Scopelliti, R.; Severin, K. *Chem.--Eur. J.* **2006**, *12*, 1058.

(36) (a) Collin, J.-P.; Dietrich-Buchecker, C.; Gavina, P.; Jimenez-Molero, M. C.; Sauvage, J.-P. *Acc. Chem. Res.* **2001**, *34*, 477 (b) Jimenez, M. C.; Dietrich-Buchecker, C.; Sauvage, J.-P.; De, C. A. *Angew. Chem., Int. Ed.* **2000**, *39*, 1295 (c) Amabilino, D. B.; Dietrich-Buchecker, C. O.; Sauvage, J.-P. *J. Am. Chem. Soc.* **1996**, *118*, 3285 (d) Frey, J.; Tock, C.; Collin, J.-P.; Heitz, V.; Sauvage, J.-P.; Rissanen, K. *J. Am. Chem. Soc.* **2008**, *130*, 11013 (e) Nierengarten, J. F.; Dietrich-Buchecker, C. O.; Sauvage, J. P. *J. Am. Chem. Soc.* **1994**, *116*, 375 (f) Sauvage, J. P.; Weiss, J. *J. Am. Chem. Soc.* **1985**, *107*, 6108(g) Solladie, N.; Chambron, J.-C.; Sauvage, J.-P. *J. Am. Chem. Soc.* **1999**, *121*, 3684.

(37) (a) Baxter, P. N.; Hanan, G. S.; Lehn, J.-M. *Chem. Commun.* **1996**, 2019 (b) Smith, V. C. M.; Lehn, J.-M. *Chem. Commun.* **1996**, 2733 (c) Lehn, J.-M. *Chem.--Eur. J.* **2000**, *6*, 2097 (d) Hasenknopf, B.; Lehn, J.-M.; Baum, G.; Fenske, D. *Proc. Natl. Acad. Sci. U. S. A.* **1996**, *93*, 1397 (e) Sleiman, H.; Baxter, P.; Lehn, J.-M.; Rissanen, K. *J. Chem. Soc., Chem. Commun.* **1995**, 715.

(38) Dietrich-Buchecker, C. O.; Sauvage, J. P.; Kintzinger, J. P. *Tetrahedron Lett.* **1983**, *24*, 5095.

(39) (a) Schmittel, M.; Ganz, A. *Chem. Commun.* **1997**, 999 (b) Schmittel, M.; Ammon, H.; Kalsani, V.; Wiegrefe, A.; Michel, C. *Chem. Commun.* **2002**, 2566 (c) Schmittel, M.; Ganz, A.; Fenske, D. *Org. Lett.* **2002**, *4*, 2289 (d) Kalsani, V.; Ammon, H.; Jaeckel, F.; Rabe, J. P.; Schmittel, M. *Chem.--Eur. J.* **2004**, *10*, 5481 (e) Kalsani, V.; Bodenstedt, H.; Fenske, D.; Schmittel, M. *Eur. J. Inorg. Chem.* **2005**, 1841 (f) Schmittel, M.; Kalsani, V.; Kishore, R. S. K.; Coelfen, H.; Bats, J. W. *J. Am. Chem. Soc.* **2005**, *127*, 11544 (g) Kishore, R. S. K.; Kalsani, V.; Schmittel, M. *Chem. Commun.* **2006**, 3690 (h) Kishore, R. S. K.; Paululat, T.; Schmittel, M. *Chem.--Eur. J.* **2006**, *12*, 8136 (i) Schmittel, M.; Kalsani, V.; Mal, P.; Bats, J. W. *Inorg. Chem.* **2006**, *45*, 6370 (j) Schmittel, M.; He, B.; Kalsani, V.; Bats, J. W. *Org. Biomol. Chem.* **2007**, *5*, 2395 (k) Schmittel, M.; Kalsani, V.; Michel, C.; Mal, P.; Ammon, H.; Jaeckel, F.; Rabe, J. P. *Chem.--Eur. J.* **2007**, *13*, 6223 (l) Schmittel, M.; Kishore, R. S. K.; Bats, J. W. *Org. Biomol. Chem.* **2007**, *5*, 78(m) Schmittel, M.; He, B. *Chem. Commun.* **2008**, 4723 (n) Schmittel, M.; He, B.; Mal, P. *Org. Lett.* **2008**, *10*, 2513 (o) Fan, J.; Bats, J. W.; Schmittel, M. *Inorg. Chem.* **2009**, *48*, 6338 (p) Schmittel, M.; He, B.; Fan, J.; Bats, J. W.; Engeser, M.; Schlosser, M.; Deiseroth, H.-J. *Inorg. Chem.* **2009**, *48*, 8192 (q) Schmittel, M.; Mahata, K. *Inorg. Chem.* **2009**, *48*, 822.

(40) Yoshizawa, M.; Nagao, M.; Kumazawa, K.; Fujita, M. *J. Organomet. Chem.* **2005**, *690*, 5383.

(41) Yamanaka, M.; Yamada, Y.; Sei, Y.; Yamaguchi, K.; Kobayashi, K. *J. Am. Chem. Soc.* **2006**, *128*, 1531.

(42) Kumazawa, K.; Biradha, K.; Kusukawa, T.; Okano, T.; Fujita, M. *Angew. Chem., Int. Ed.* **2003**, *42*, 3909.

(43) Lee, J.; Ghosh, K.; Stang, P. J. *J. Am. Chem. Soc.* **2009**, *131*, 12028.

(44) Wang, M.; Vajpayee, V.; Shanmugaraju, S.; Zheng, Y. R.; Zhao, Z.; Kim, H.; Mukherjee, P. S.; Chi, K. W.; Stang, P. J. *Inorg Chem* **2011**, *50*, 1506.

(45) (a) Fiedler, D.; Leung, D. H.; Bergman, R. G.; Raymond, K. N. *Acc. Chem. Res.* **2005**, *38*, 349 (b) Pluth, M. D.; Bergman, R. G.; Raymond, K. N. *Acc. Chem. Res.* **2009**, *42*, 1650 (c) Pluth, M. D.; Raymond, K. N. *Chem. Soc. Rev.* **2007**, *36*, 161 (d) Pluth, M. D.; Bergman, G.; Raymond, K. N. *Chemtracts* **2004**, *17*, 515 (e) Yoshizawa, M.; Klosterman, J. K.; Fujita, M. *Angew. Chem., Int. Ed.* **2009**, *48*, 3418 (f) Klosterman, J. K.; Yamauchi, Y.; Fujita, M. *Chem. Soc. Rev.* **2009**, *38*, 1714 (g) Kawano, M.; Fujita, M. *Coord. Chem. Rev.* **2007**, *251*, 2592 (h) Maurizot, V.; Yoshizawa, M.; Kawano, M.; Fujita, M. *Dalton Trans.* **2006**, 2750(i) Yoshizawa, M.; Fujita, M. *Pure Appl. Chem.* **2005**, *77*, 1107 (j) Wiester, M. J.; Ulmann, P. A.; Mirkin, C. A. *Angew. Chem., Int. Ed.* **2011**, *50*, 114.

(46) Northrop, B. H.; Yang, H.-B.; Stang, P. J. *Chem. Commun.* **2008**, 5896.

(47) Frechet, J. M. J. *Science* **1994**, *263*, 1710.

(48) (a) Yang, H.-B.; Hawkridge, A. M.; Huang, S. D.; Das, N.; Bunge, S. D.; Muddiman, D. C.; Stang, P. J. *J. Am. Chem. Soc.* **2007**, *129*, 2120 (b) Yang, H.-B.; Das, N.; Huang, F.; Hawkridge, A. M.; Muddiman, D. C.; Stang, P. J. *J. Am. Chem. Soc.* **2006**, *128*, 10014.

(49) Ghosh, K.; Yang, H.-B.; Northrop, B. H.; Lyndon, M. M.; Zheng, Y.-R.; Muddiman, D. C.; Stang, P. J. *J. Am. Chem. Soc.* **2008**, *130*, 5320.

(50) (a) Yang, H.-B.; Ghosh, K.; Zhao, Y.; Northrop, B. H.; Lyndon, M. M.; Muddiman, D. C.; White, H. S.; Stang, P. J. *J. Am. Chem. Soc.* **2008**, *130*, 839 (b) Yang, H.-B.; Ghosh, K.; Northrop, B. H.; Zheng, Y.-R.; Lyndon, M. M.; Muddiman, D. C.; Stang, P. J. *J. Am. Chem. Soc.* **2007**, *129*, 14187.

(51) (a) Murase, T.; Sato, S.; Fujita, M. *Angew. Chem., Int. Ed.* **2007**, *46*, 1083 (b) Murase, T.; Sato, S.; Fujita, M. *Angew. Chem., Int. Ed.* **2007**, *46*, 5133 (c) Kamiya, N.; Tominaga, M.; Sato, S.; Fujita, M. *J. Am. Chem. Soc.* **2007**, *129*, 3816 (d) Sato, S.; Iida, J.; Suzuki, K.; Kawano, M.; Ozeki, T.; Fujita, M. *Science* **2006**, *313*, 1273 (e) Suzuki, K.; Takao, K.; Sato, S.; Fujita, M. *J. Am. Chem. Soc.* **2010**, *132*, 2544 (f) Suzuki, K.; Sato, S.; Fujita, M. *Nat. Chem.* **2010**, *2*, 25 (g) Ikemi, M.; Kikuchi, T.; Matsumura, S.; Shiba, K.; Sato, S.; Fujita, M. *Chem. Sci.*

2010, *1*, 68 (h) Dolain, C.; Hatakeyama, Y.; Sawada, T.; Tashiro, S.; Fujita, M. *J. Am. Chem. Soc.* **2010**, *132*, 5564.

CHAPTER 2

DYNAMIC COMPONENT EXCHANGE WITHIN COORDINATION-DRIVEN SELF-ASSEMBLED SUPRAMOLECULAR SYSTEMS

2.1 Introduction

During the last two decades, coordination-driven self-assembly has become a well-established methodology in supramolecular chemistry for constructing ensembles of varying structural motifs, as evidenced by the development of diverse metallo-supramolecular helicates, polygons, and polyhedra.[1] As most investigations focus largely on the structural features of these supramolecules, reports about the dynamic characteristics of such structures are limited.[2] That said, the dynamic nature of self-assembly is widely recognized as a significant feature of supramolecular assemblies.[3] Detailed mechanistic studies are not only important for understanding of self-assembly processes of both two-component and multicomponent supramolecular systems, but are also crucial to the use of supramolecular assemblies in applications such as the construction of constitutional dynamic libraries,[4] the self-assembly of supramolecular polymers,[5] and the ability to control supramolecular transformations.[6]

One of the most fundamental features of the dynamic nature of coordination-driven and indeed all supramolecular self-assembly is dynamic component exchange—the mutual exchange of molecular components between the supramolecular

assemblies under thermodynamic control.[3b,c] Although such constitutional dynamic features have been routinely used in explaining experimental results and developing theoretical understanding of supramolecular self-assembly,[7] very few examples have been reported that directly and quantitatively characterize such exchanges in self-assembled supramolecules.[8] Very recently, Rebek and coworkers demonstrated an innovative way to characterize such dynamic features of supramolecular capsules using a fluorescent resonance energy transfer (FRET) technique, but these studies have so far been limited to hydrogen bond-driven self-assemblies.[8] For coordination-driven self-assembly, such reports are rare,[2f] likely because of the lack of a suitable characterization method.

Isotopic labeling is an appropriate tool to characterize dynamic exchanges in metallo-supramolecular assemblies. Indeed, isotopic labeling has been widely used in biological studies, such as proteomics, and used in the quantitative study of proteins based on mass spectral characterization.[9] Herein, we demonstrate an isotopic labeling-based method capable of direct and quantitative characterization of the constitutional dynamic feature of coordination-driven self-assembly, using electrospray ionization mass spectrometry (ESI-MS). This method allows for a thorough study of the poorly understood dynamic nature of Pt-N coordination-driven self-assembly.[1b,e,10] With this technique, the dynamic ligand exchange process, as well as the subsequent equilibration under thermodynamic control, can be directly monitored in both two- and multicomponent supramolecular systems.

2.2 Results and Discussion

We have employed the isotopically labeled (^{1}H/^{2}D) pyridyl ligands **2.1** and **2.2** (Figure 2.1) in self-assembly with organoplatinum acceptors **2.3** and **2.4** to form supramolecular polygons **2.5**[11] and **2.6**[12] based on the directional bonding approach. ESI-MS was used to observe and characterize the dynamic ligand exchange between these self-assemblies. Combining **2.1** or **2.2** with organoplatinum acceptors **2.3** or **2.4** results in the self-assembly of isotopically pure supramolecular polygons **2.5a/b** or **2.6a/b**. As shown in Scheme 2.1, mixing homoisotopic rectangles (**2.5a** or **2.5b**) and/or homoisotopic triangles (**2.6a** or **2.6b**) leads to heteroisotopic polygons **2.5c** or **2.6c** and **2.6d** due to ligand exchange. These species can be easily distinguished by mass spectral analysis. More importantly, the relative distribution of the isotopically varying supramolecular entities in the mixture can be quantitatively calculated based on the intensities of their corresponding spectral signals.

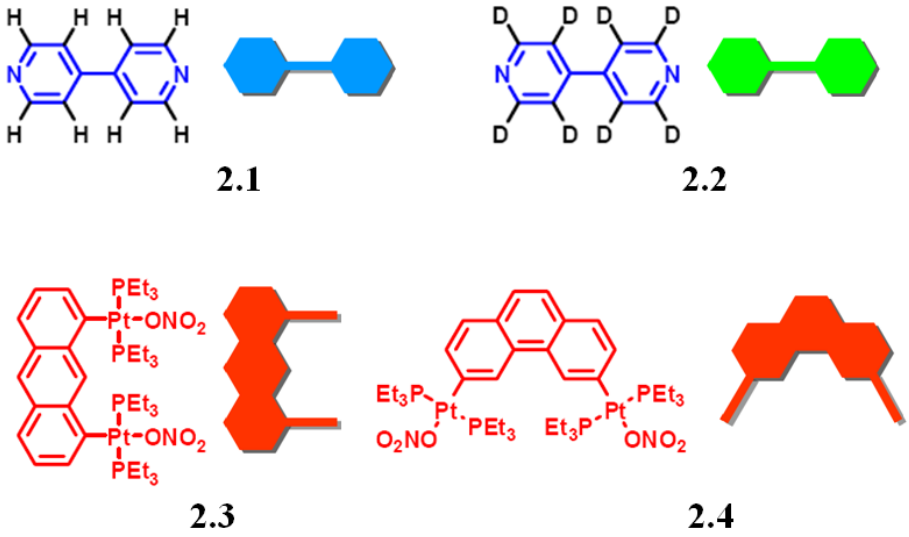

Figure 2.1. Schematic and molecular structures of linear dipyridyl donors **2.1** and **2.2** as well as 0 ° and 60 ° organoplatinum acceptors **2.3** and **2.4**.

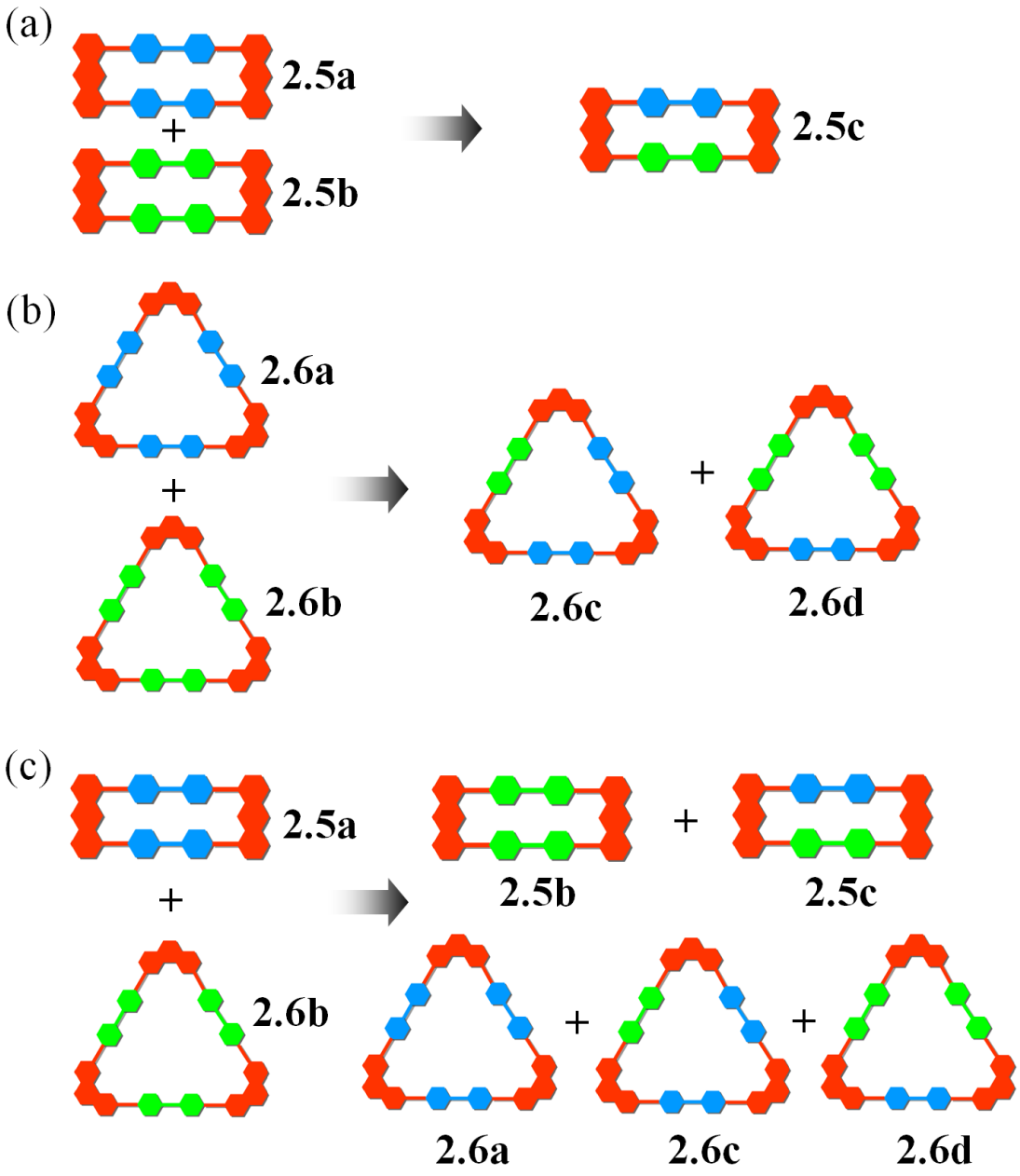

Scheme 2.1. Schematic representation of the dynamic ligand exchange between the same (a and b) and different types (c) of supramolecular polygons (rectangles: **2.5a** and **2.5b**; triangles: **2.6a** and **2.6b**) with isotope label (^{1}H / ^{2}D).

In order to explore the dynamic ligand exchange between two-component supramolecular systems, individually prepared **2.5a/b** or **2.6a/b** were mixed in a 1:1 ratio and heated to 64 ± 1 ℃ in an aqueous acetone solution (*v/v* 1:1) (Scheme 2.1a and b). ESI-MS was used to monitor ligand exchange over a period of days (Figure 2.2). Initially, in each mixture, only those signals corresponding to homoisotopic polygons ([**2.5a** – $3ONO_2]^{3+}$**:** m/z = 817.3; [**2.5b** – $3ONO_2]^{3+}$**:** m/z = 822.7; [**2.6a** – $4ONO_2]^{4+}$**:** m/z = 927.3; [**2.6b** – $4ONO_2]^{4+}$**:** m/z = 933.3) were observed and in similar intensities (Figure 2.3d and 2.4e). Upon heating at 64 ± 1 ℃, signals corresponding to polygons **2.5c**, **2.6c**, and **2.6d** could be resolved at m/z = 820.0 ([**2.5c** – $3ONO_2]^{3+}$), m/z = 929.3 ([**2.6c** – $4ONO_2]^{4+}$), and m/z = 931.3 ([**2.6d** – $4ONO_2]^{4+}$) (Figure 2.2), clearly indicating dynamic ligand exchange between the supramolecules. After 10–20 days, the dynamic ligand exchange processes reached equilibrium as indicated by the unchanging ESI-MS signals. The resulting equilibrium mixtures represented, in each case (Figure 2.3e and 2.4f), statistical product distributions: rectangles: **2.5a**: **2.5c**: **2.5b** = 1.04: 2.00: 1.16 (theoretical value: 1: 2: 1); triangles: **2.6a**: **2.6c**: **2.6d**: **2.6b** = 1.00: 3.00: 2.89: 0.987 (theoretical value: 1: 3: 3: 1).

It was reported that mixing molecular clip **2.3** and 60 ° organoplatinum acceptor **2.4** with bipyridyl ligand **2.1** in a 1:1:2 ratio resulted in a self-sorted supramolecular system with simultaneous formation of both supramolecular rectangle **2.5a** and triangle **2.5a**.[10a] It would be valuable to monitor whether these self-sorted supramolecules could exchange their components. Thus, similar mass spectral studies were also carried out on this three-component, self-sorted supramolecular system containing supramolecular polygons **2.5a** and **2.5b** (Scheme 2.1c). Dynamic ligand exchange between these different

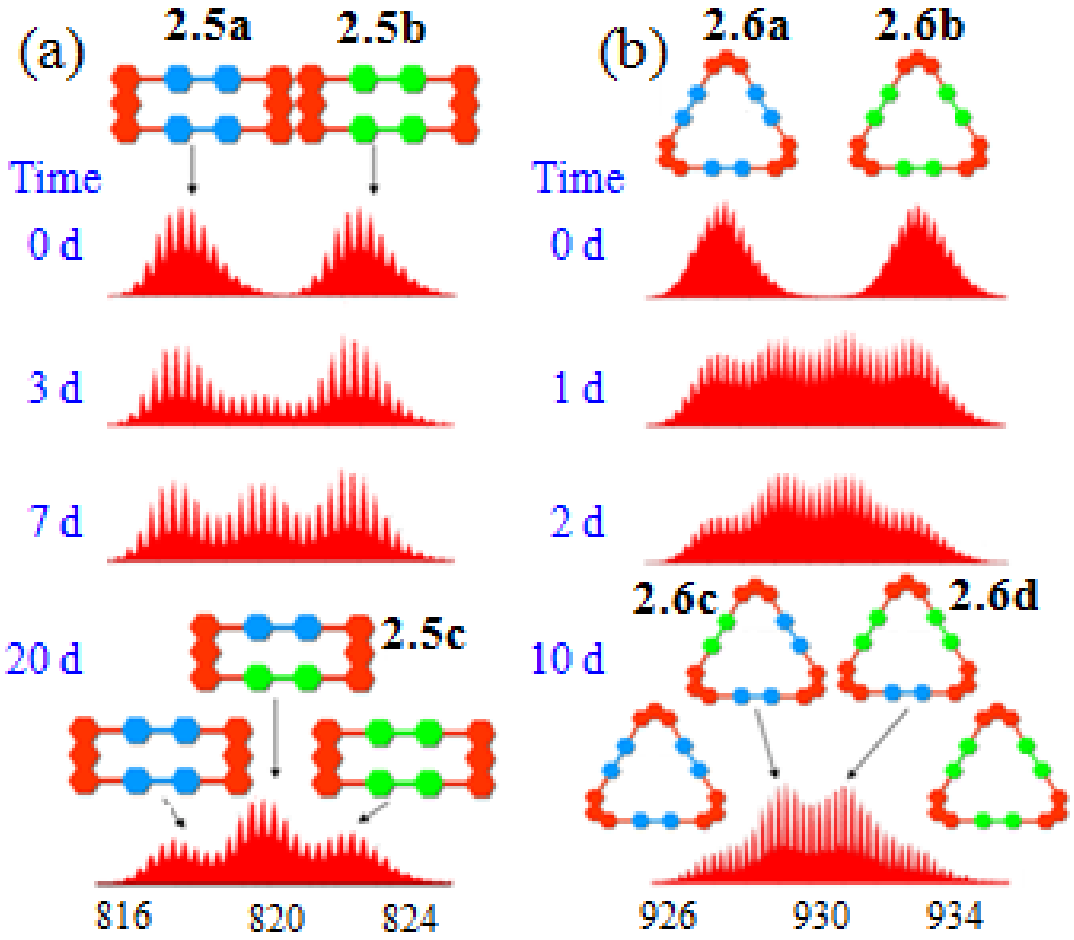

Figure 2.2. ESI-MS spectra of dynamic ligand exchange between (a) supramolecular rectangles (**2.5a** and **2.5b**) and (b) supramolecular triangles (**2.6a** and **2.6b**) recorded at different time intervals (d: day).

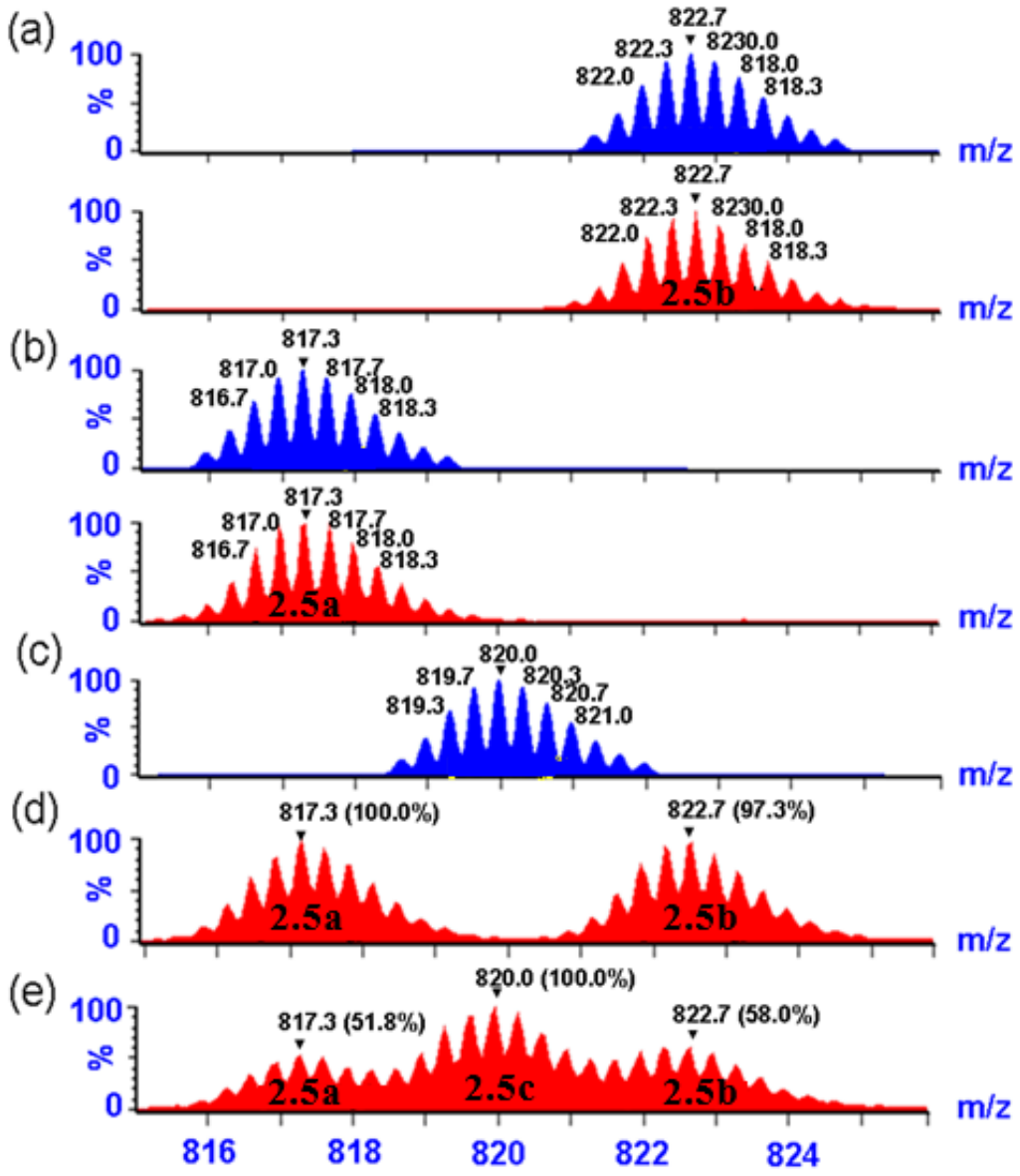

Figure 2.3. Calculated (blue) and experimental (red) ESI-MS spectra (Acetone-d_6/D_2O 1:1) (a) individually prepared **2.5b**, (b) individually prepared **2.5a**, (c) **2.5c** (calculated) (d) initial mixture of **2.5a** and **2.5b**, and (e) equilibrated mixture of **2.5a**, **2.5b**, and **2.5c**.

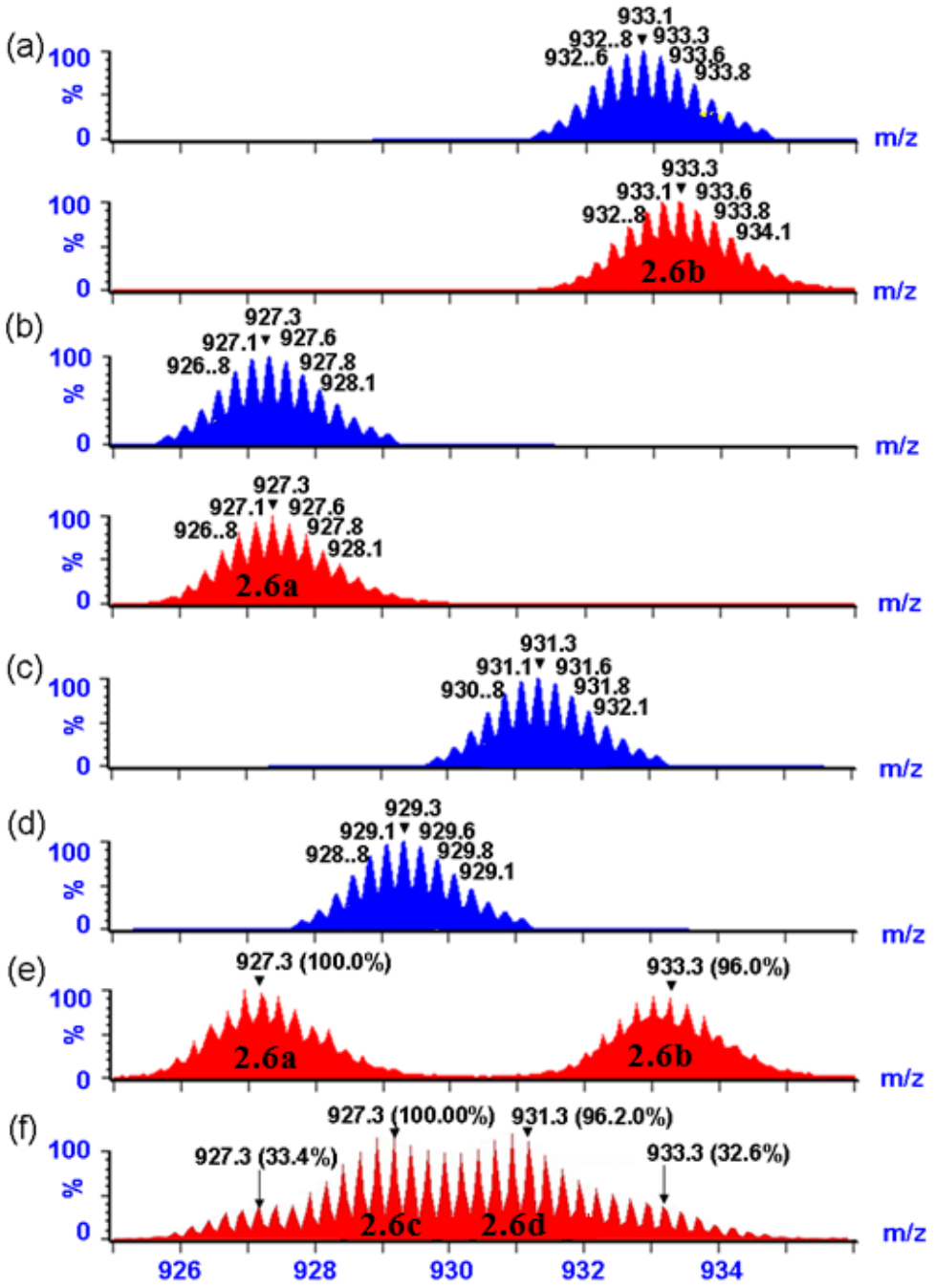

Figure 2.4. Calculated (blue) and experimental (red) ESI-MS spectra (Acetone-d_6/D_2O 1:1) (a) individually prepared **2.6b**, (b) individually prepared **2.6a**, (c) **2.6c** (calculated), (d) **2.6d** (calculated), (e) initial mixture of **2.6a** and **2.6b**, and (f) equilibrated mixture of **2.6a**, **2.6b**, **2.6c**, and **2.6d**.

polygons was also observed, as indicated by the increase of mass spectral signals corresponding to **2.5b**, **2.5c**, **2.6a**, **2.6c**, and **2.6d** (Figure 2.5) in addition to the peaks for **2.5a** and **2.6b**, upon heating the mixture at 64 ± 1 ℃ in an aqueous acetone solution (*v/v* 1:1) for 20 d.

In addition to the mass spectral characterizations, NMR spectral studies were also employed to monitor these exchange processes. For ligand exchange between structures of the same motif (**2.5a**/**b** or **2.6a**/**b**), no significant change could be found in either the $^{31}P\{^{1}H\}$ or ^{1}H NMR spectra during the exchange, as expected. Dynamic ligand exchange between **2.5a** and **2.6b** caused an increase in the signals at 8.31 ppm and 8.52 ppm, as regular pyridyl ligand **2.1** gradually replaced the deuterated component **2.2** in the triangle **2.6b**. The combined results from ESI mass spectrometry and NMR spectroscopy not only unambiguously supported the dynamic ligand exchange of these metallosupramolecular polygons, but also directly demonstrated the subsequent equilibration under thermodynamic control. For the exchange reaction of rectangles (**2.5a** + **2.5b** ⇆ 2 **2.5c**), constitutional dynamic exchange allowed for the redistribution of the isotopically different **2.5a**, **2.5b**, and **2.5c** from the initial input ratio of 1: 1: 0 towards the equilibrium value of 1: 1: 2, which agrees well with the thermodynamic equilibrium constant of $K = 4$ based on statistical factors.[14] Due to the similar intrinsic stabilities of **2.5a**, **2.5b**, and **2.5c**, such a dynamic redistribution process is mainly entropically-driven.

Furthermore, quantitative mass spectral results acquired over time allowed for the kinetics of supramolecular dynamic ligand exchange to be determined. Analysis of the kinetic data (Table 2.1) shows a first-order kinetic process with a rate of $k = 0.0024\ h^{-1}$ for the dynamic ligand exchange between **2.5a** and **2.5b**, as shown in Figure 2.6 (R^2 =

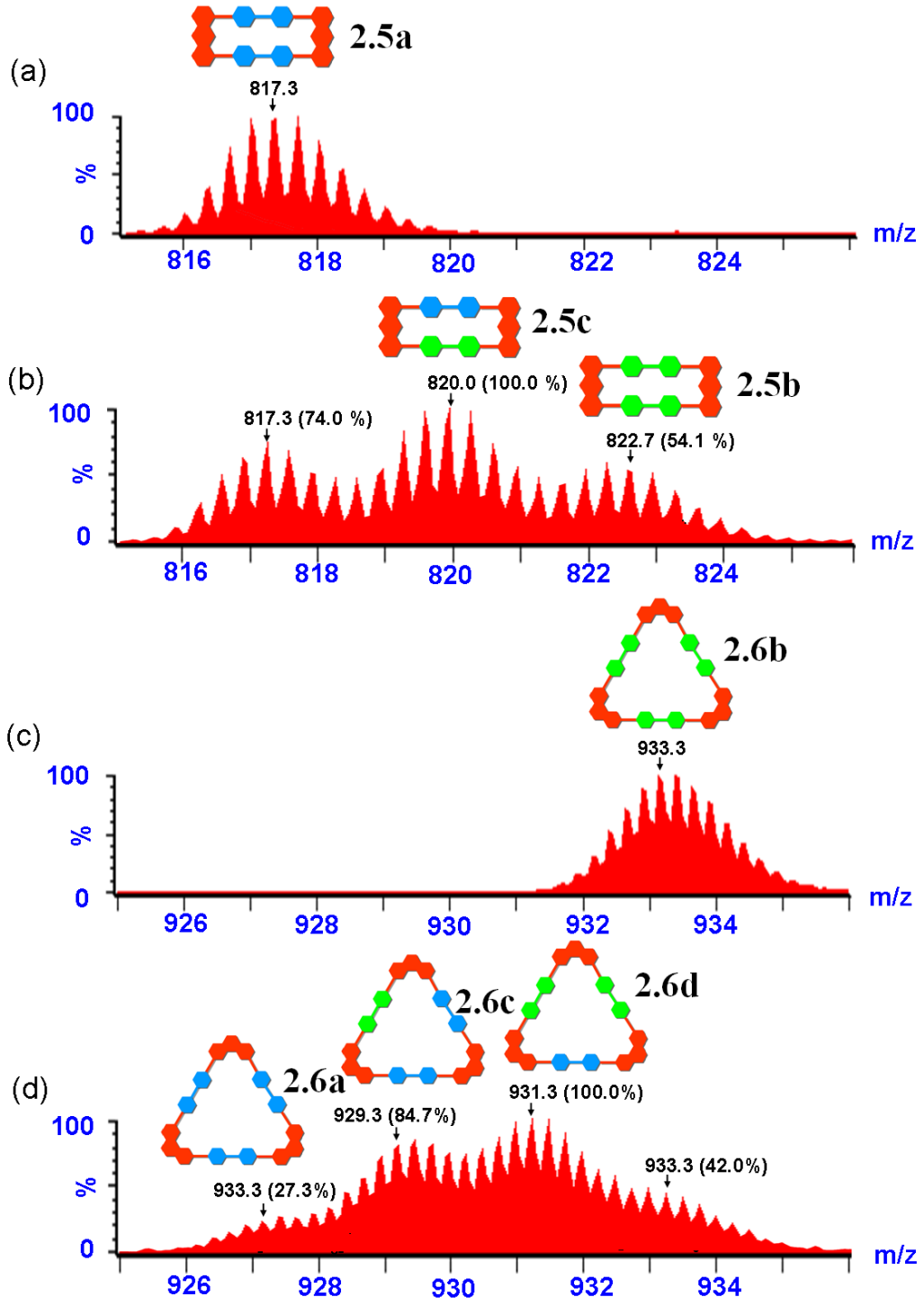

Figure 2.5. ESI-MS spectra (Acetone-d_6/D_2O 1:1) (a) and (c) initial mixture of **2.5a** and **2.6b** an (b) and (d) equilibrated mixture of **2.5a**, **2.5b**, **2.5c**, **2.6a**, **2.6b**, **2.6c**, and **2.6d**.

Table 2.1. Kinetic data extracted from ESI-MS spectra of ligand exchange between **2.5a** and **2.5b**.

t (h)	$[\mathbf{2.5c}]_t$ / $[\mathbf{2.5a}]_t$ *	$[\mathbf{2.5a}]_0$ / $[\mathbf{2.5a}]_t$	Ln($[\mathbf{2.5a}]_0$ / $[\mathbf{2.5a}]_t$)
0	0. 000	1.00	0. 000
20	0. 133	1.07	0. 064
43	0. 210	1.11	0. 100
66	0. 373	1.19	0. 171
89	0. 470	1.24	0. 211
161	0. 978	1.49	0. 398
206	1. 24	1.62	0. 482

* $[\mathbf{2.5c}]_t$ / $[\mathbf{2.5a}]_t$ is determined by the ratio of the intensity of peaks for **2.5c** (820.0) and **2.5a** (817.3) in the ESI-MS spectra recorded at specific time (**t**).

∵ Rectangle (**2.5a)** + Rectangle (**2.5b)** ⇆ 2 Rectangle (**2.5c)**
∴ $[\mathbf{2.5a}]_0 = [\mathbf{2.5a}]_t + [\mathbf{2.5c}]_t$ /2
∴ $[\mathbf{2.5a}]_0$ / $[\mathbf{2.5a}]_t = 1 + ([\mathbf{2.5c}]_t$ / $[\mathbf{2.5a}]_t)$ /2

The apparent rate constant *k* for the dynamic exchange between rectangles **2.5a** and **2.5b** was determined by fitting the data to the first-order kinetic equation:

$$\text{Ln}([\mathbf{2.5a}]_0 / [\mathbf{2.5a}]_t) = k\mathbf{t}$$

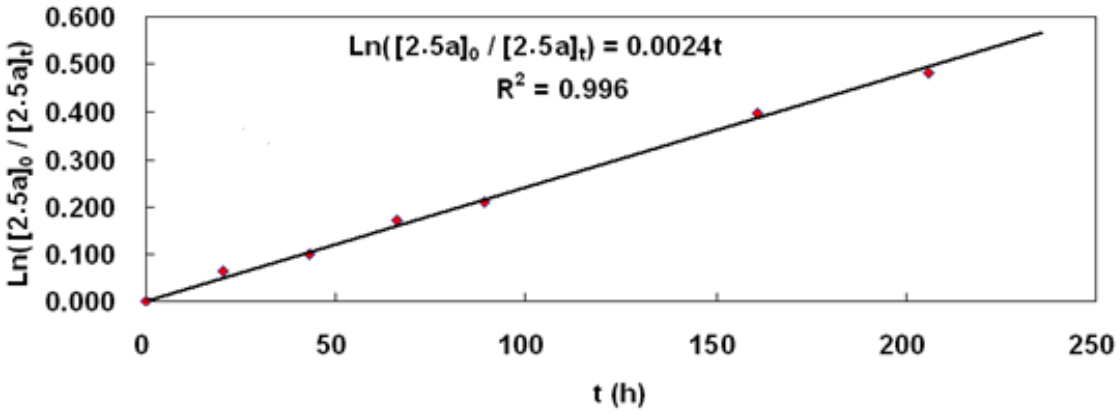

Figure 2.6. The first-order kinetic treatment of the data obtained at varied time intervals (0–240 h) for ligand exchange between **2.5a** and **2.5b**.

0.996). Presumably, the first-order exchange kinetics correspond to the ring-opening of rectangular supramolecules upon nucleophilic attack on the Pt-N coordination bond by a nitrate anion as the rate determining step. Nitrate anions and the cationic rectangle are likely to form an ion pair in the acetone solution,[13] and the ring-opening step could be consequently considered as an intramolecular process of the ion pair, whereby the first-order kinetics can be established.

We have also explored the influence of temperature, solvent, and counter anion on the ligand exchange process between **2.5a** and **2.5b**. As may be expected, decreasing the temperature significantly slows the exchange process. At 25–30 ℃ the exchange is no longer observed (Figure 2.7a), even after 20 d. Interestingly, as seen in Figure 2.7b, decreasing the percentage of water in the solution can significantly accelerate the rate of the exchange process. Upon heating at 64 ± 1 ℃ in an aqueous acetone solution (*v/v* 15:1), the exchange process reaches equilibrium within 1 d. Additionally, changing the counter anion from nitrate (NO_3^-) to hexafluorophosphate (PF_6^-) anions results in no exchange, as observed by ESI-MS spectra (Figure 2.7c).The influence of solvent and counter anion further substantiates the role of the nitrate anions in the rate-determining step of the ligand exchange process: nitrate anions are more nucleophilic when fewer water molecules are present, and when the counter anion is exchanged from NO_3^- to PF_6^-, the dynamic exchange does not proceed as PF_6^- is a less nucleophilic anion.

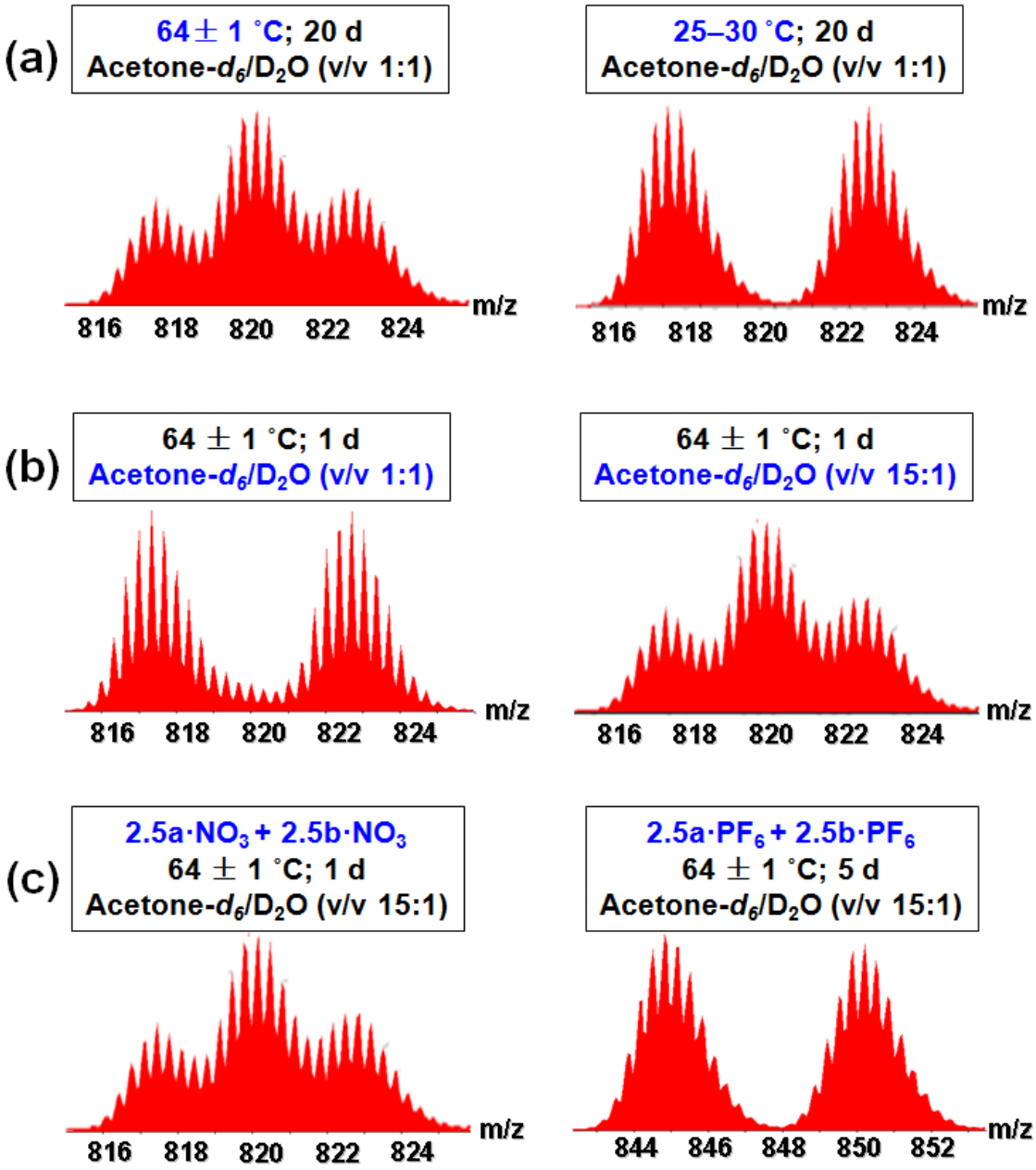

Figure 2.7. ESI-MS spectra of ligand exchange between **2.5a** and **2.5b** influenced by differences in (a) temperature, (b) solvent, and (c) counter anion.

2.3 Conclusion

In conclusion, we have directly demonstrated the constitutional dynamic exchange of Pt-N coordination-driven self-assembled supramolecular polygons (triangles and rectangles) using stable isotope labeling ($^{1}H/^{2}D$) of the pyridyl donors and ESI mass spectrometry together with NMR spectroscopy. Both the thermodynamic and kinetic aspects of such exchange processes have been established based on quantitative mass spectral results. Further investigation showed that, as expected, the exchange is highly dependent on experimental conditions such as temperature, solvent, and counter anions. The isotope labeling-based mass spectral technique described here represents a new way to directly and quantitative study supramolecular dynamics.

2.4 References

(1) (a) Stang, P. J.; Olenyuk, B. *Acc. Chem. Res.* **1997**, *30*, 502. (b) Leininger, S.; Olenyuk, B.; Stang, P. J. *Chem. Rev.* **2000**, *100*, 853. (c) Holliday, B. J.; Mirkin, C. A. *Angew. Chem. Int. Ed.* **2001**, *40*, 2022. (d) Fujita, M.; Umemoto, K.; Yoshizawa, M.; Fujita, N.; Kusukawa, T.; Biradha, K. *Chem. Commun.* **2001**, 509. (e) Seidel, S. R.; Stang, P. J. *Acc. Chem. Res.* **2002**, *35*, 972. (f) (b) Ruben, M.; Rojo, J.; Romero-Salguero, F. J.; Uppadine, L. H.; Lehn, J.-M. *Angew. Chem. Int. Ed.* **2004**, *43*, 3644. (g) Fiedler, D.; Leung, D. H.; Bergman, R. G.; Raymond, K. N. *Acc. Chem. Res.* **2005**, *38*, 351. (h) Fujita, M.; Tominaga, M.; Hori, A.; Therrien, B. *Acc. Chem. Res.* **2005**, *38*, 369. (i) Lukin, O.; Voegtle, F. *Angew. Chem. Int. Ed.* **2005**, *44*, 1456. (j) Severin, K. *Chem. Commun.* **2006**, 3859. (k) Nitschke, J. R. *Acc. Chem. Res.* **2007**, *40*, 103. (l) Pitt, M. A.; Johnson, D. W. *Chem. Soc. Rev.* **2007**, *36*, 1441. (m) Northrop, B. H.; Yang, H.-B.; Stang, P. J. *Chem. Commun.* **2008**, 5896. (n) Schmittel, M.; Mahata, K. *Angew. Chem. Int. Ed.* **2008**, *47*, 5284.

(2) (a) Hori, A.; Akasaka, A.; Biradha, K.; Sakamoto, S.; Yamaguchi, K.; Fujita, M. *Angew. Chem. Int. Ed.* **2002**, *41*, 3269. (b) Yamamoto, T.; Arif, A. M.; Stang, P. J. *J. Am. Chem. Soc.* **2003**, *125*, 12309. (c) Davis, A. V.; Raymond, K. N. *J. Am. Chem. Soc.* **2005**, *127*, 7912. (d) Davis, A. V.; Fiedler, D.; Seeber, G.; Zahl, A.; Van Eldik, R.; Raymond, K. N. *J. Am. Chem. Soc.* **2006**, *128*, 1324. (e) Pluth, M. D.; Raymond, K. N. *Chem. Soc. Rev.* **2006**, *36*, 161. (f) Claessens, C. G.; Vicente-Arana, M. J.; Torres, T. *Chem. Commun.* **2008**, 6378. (g) Levin, M. D.; Stang, P. J. *J. Am. Chem. Soc.* **2000**, *122*, 7428.

(3) (a) Lehn, J.-M. *Proc. Natl. Acad. Sci. U.S.A.* **2002**, *99*, 4763. (b) Davis, A. V.; Yeh, R. M.; Raymond, K. N. *Proc. Natl. Acad. Sci. U.S.A.* **2002**, *99*, 4793. (c) Lehn, J.-M. *Chem. Soc. Rev.* **2007**, *36*, 151.

(4) (a) Wheaton, C. A.; Jennings, M. C.; Puddephatt, R. J. *J. Am. Chem. Soc.* **2006**, *128*, 15370. (b) Chow, C.-F.; Fujii, S.; Lehn, J.-M. *Angew. Chem. Int. Ed.* **2007**, *46*, 5007. (c) Friese, V. A.; Kurth, D. G. *Coord. Chem. Rev.* **2008**, *252*, 199.

(5) (a) Barboiu, M.; Vaughan, G.; Graff, R.; Lehn, J.-M. *J. Am. Chem. Soc.* **2003**, *125*, 10257. (b) Giuseppone, N.; Schmitt, J.-L.; Lehn, J.-M. *J. Am. Chem. Soc.* **2006**, *128*, 16748.

(6) (a) Heo, J.; Jeon, Y.-M.; Mirkin, C. A. *J. Am. Chem. Soc.* **2007**, *129*, 7712. (b) Hiraoka, S.; Sakata, Y.; Shionoya, M. *J. Am. Chem. Soc.* **2008**, *130*, 10058. (c) Zhao, L; Northrop, B. H.; Stang, P. J. *J. Am. Chem. Soc.* **2008**, *130*, 11886.

(7) (a) Ercolani, G.; Mandolini, L.; Mencarelli, P.; Roelens, S. *J. Am. Chem. Soc.* **1993**, *115*, 3901. (b) Ercolani, G. *J. Phys. Chem. B* **1998**, *102*, 5699. (c) Ercolani, G. *J. Phys. Chem. B* **2003**, *107*, 5052. (d) Ercolani, G. *J. Am. Chem. Soc.* **2003**, *125*, 16097.

(8) (a) Barrett, E. S.; Dale, T. J.; Rebek, J., Jr. *J. Am. Chem. Soc.* **2007**, *129*, 3818. (b) Barrett, E. S.; Dale, T. J.; Rebek, J., Jr. *J. Am. Chem. Soc.* **2007**, *129*, 8818. (c) Barrett, E. S.; Dale, T. J.; Rebek, J., Jr. *J. Am. Chem. Soc.* **2008**, *130*, 2344.

(9) (a) Ong, S.-E.; Foster, L. J.; Mann, M. *Methods* **2003**, *29*, 124, and references therein. (b) Ong, S.-E.; Mann, M. *Nat. Chem. Biol.* **2005**, 1, 252, and references therein.

(10) (a) Addicott, C.; Das, N.; Stang, P. J. *Inorg. Chem.* **2004**, *43*, 5335. (b) Yang, H.-B.; Ghosh, K.; Northrop, B. H.; Stang, P. J. *Org. Lett.* **2007**, *9*, 1561. (c) Zheng Y.-R.; Yang, H.-B.; Northrop, B. H.; Ghosh, K.; Stang, P. J. *Inorg. Chem.* **2008**, *47*, 4706. (d) Northrop, B. H.; Yang, H.-B.; Stang, P. J. *Inorg. Chem.* **2008**, *47*, 11257.

(11) Kuehl, C. J.; Huang, S. D.; Stang, P. J. *J. Am. Chem. Soc.* **2001**, *123*, 9634.

(12) Kryschenko, Y. K.; Seidel, S. R.; Arif, A. M.; Stang, P. J. *J. Am. Chem. Soc.* **2003**, *125*, 5193.

(13) (a) Ercolani, G.; Piguet, C.; Borkovec, M.; Hamacek, J. *J. Phys. Chem. B* **2007**, *111*, 12195. (b) Vacek, J.; Caskey, D. C.; Horinek, D.; Shoemaker, R. K.; Stang, P. J.; Michl, J. *J. Am. Chem. Soc.* **2008**, *130*, 7629

CHAPTER 3

SELF-SORTING IN MULTICOMPONENT SUPRAMOLECULAR SYSTEMS

3.1 Introduction

Self-sorting, the mutual recognition of complementary components within a mixture, is a critical phenomenon in many biological systems. When specific information is encoded within the structural aspects of molecular subunits, multiple supramolecular structures can be obtained from complex, multicomponent mixtures via self-sorting processes.[1] Through detailed investigations of the self-sorting process, valuable insight into analogous biological self-sorting processes may be obtained. Toward this aim, pioneering synthetic self-sorting systems based upon metal-ligand coordination bonds,[2] hydrogen bonds,[3] solvophobic effects,[4] and dynamic covalent chemistry[5] have been developed.

In the area of synthetic self-sorting systems driven by metal-ligand coordination bonding interactions, a great number of valuable studies have been presented in the past decades. For example, Raymond et al. observed self-sorting of three supramolecular triple helicates containing two metal centers based solely on the lengths of rigid spacers separating two catecholate ligands.[2b] Stack and coworkers reported that self-sorting can also be directed by chirality of ligands for simultaneous production of two supramolecular double helicates.[2g] Recently, Stang and coworkers have reported the self-

sorting of multiform 2D supramolecular polygons (rectangle, triangle, and square) via the treatment of a 4,4'-dipyridyl donor with three different organoplatinum acceptors of varying bonding angles.[7] For these self-sorting systems, it was found that size, angle, and chirality, the major factors directing the self-sorting, can all be considered as geometric features of the molecular components. Thus, the question is whether these geometry directing self-sorting systems are exceptional cases, or if the geometric features encoded in the molecular building blocks can be used as a major factor to direct self-sorting in multicomponent supramolecular systems, in general.

Coordination-driven self-assembly based on the directional bonding approach[8] has proven to be a successful strategy for constructing metal-organic supramolecules of high complexity. In the last two decades, an extensive collection of 2D polygons and 3D polyhedra have been developed using this technique. In the directional bonding approach, the geometry, e.g., shape and size, of the molecular building blocks are the most important structural factors dictating the self-assembled supramolecular structure. Thus, supramolecular systems of polygons and polyhedra based on the directional bonding approach are a fertile ground for studying geometric-directed self-sorting behavior. Very few examples, however, have been reported that involve the self-sorting of building blocks during the assembly of supramolecular polygons or polyhedrons.

Herein, we have carried out a study of three self-sorting systems **SS_1**–**SS_3** with 2D and 3D Pt(II)-based supramolecular polygons and cages, which is mainly directed by the size of the different organic ligands. Despite the possibility of forming a myriad of oligomeric structures, discrete supramolecular rectangles and triangles, as well as prisms, are strongly preferred in the mixtures, representative of size-selective self-sorting.

As a further step into ordered multicomponent supramolecular systems of higher complexity, investigations of self-sorting with additional components and higher structural diversity, still directed by geometric features, have also been performed. We carried out a detailed study of nine increasingly complicated self-sorting systems **SS_4–SS_{12}**, each of which shows self-sorting into three to four 2D and/or 3D supramolecular components. These self-sorting systems include six different structural motifs (rectangular,[9] triangular,[10] rhomboid,[11] distorted,[12] nondistorted triangular prism,[13] and triangular bipyramidal[14]) developed by the directional bonding approach. In these nine self-sorting systems **SS_4–SS_{12}**, geometric differences encoded within the rigid and directional molecular components, i.e., size, angle, and number of binding sites, are the major driving forces directing the self-sorting process.

In addition, to obtain insight into the dynamic nature of the self-sorting processes, we carried out a mass spectral study to monitor the self-sorting process and to explore the key variables of temperature and solvent that are capable of affecting these systems.

3.2 Results and Discussion

3.2.1 Size selective self-sorting of supramolecular rectangles

When molecular clip **3.01** is mixed with two different sized linear bipyridyl linkers **3.02** (0.72 nm) and **3.03** (1.65 nm) in a 2:1:1 ratio and heated at 60–65 ˚C for 45 h in an aqueous acetone solution (*v/v* 1:1), a three-component self-sorting system **SS_1** with two molecular rectangles **3.04** and **3.05**[9] of different sizes is formed (Scheme 3.1). The self-sorting process was followed by ^{31}P and ^{1}H multinuclear NMR spectroscopy as shown in Figures 3.1 and 3.2, respectively. After 1 h, the mixture changes from a suspension to a clear solution. The ^{31}P $\{^{1}H\}$ NMR spectrum of this reaction mixture

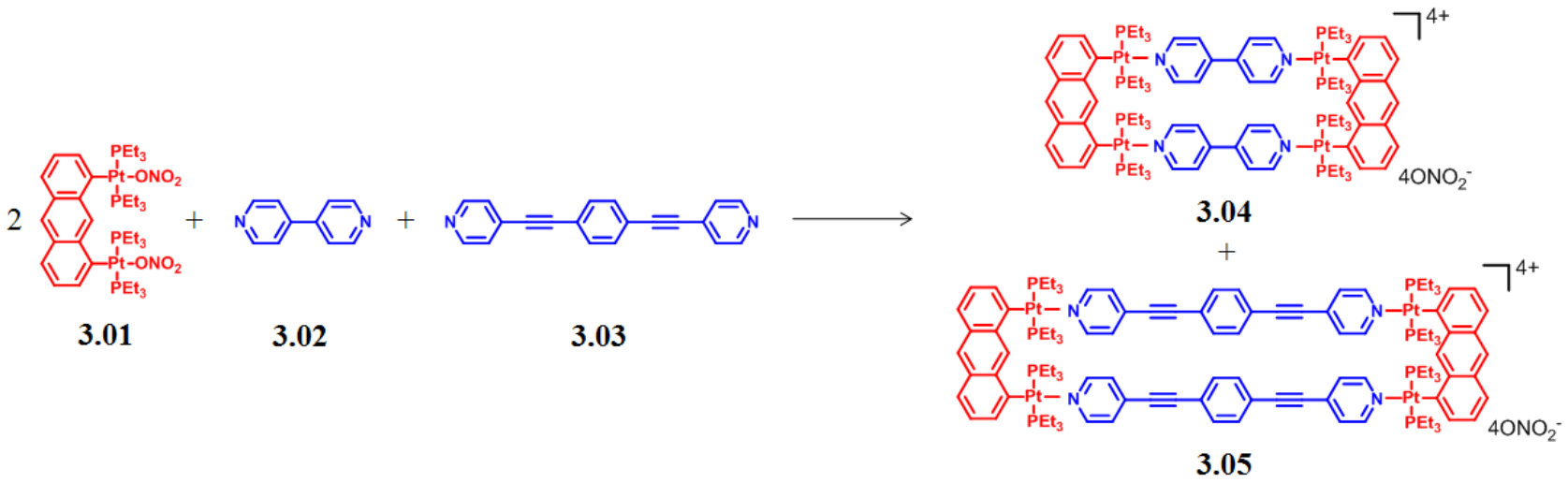

Scheme 3.1. Three-component self-sorting system **SS$_1$** with two supramolecular rectangles **3.04** and **3.05**[10] of different sizes

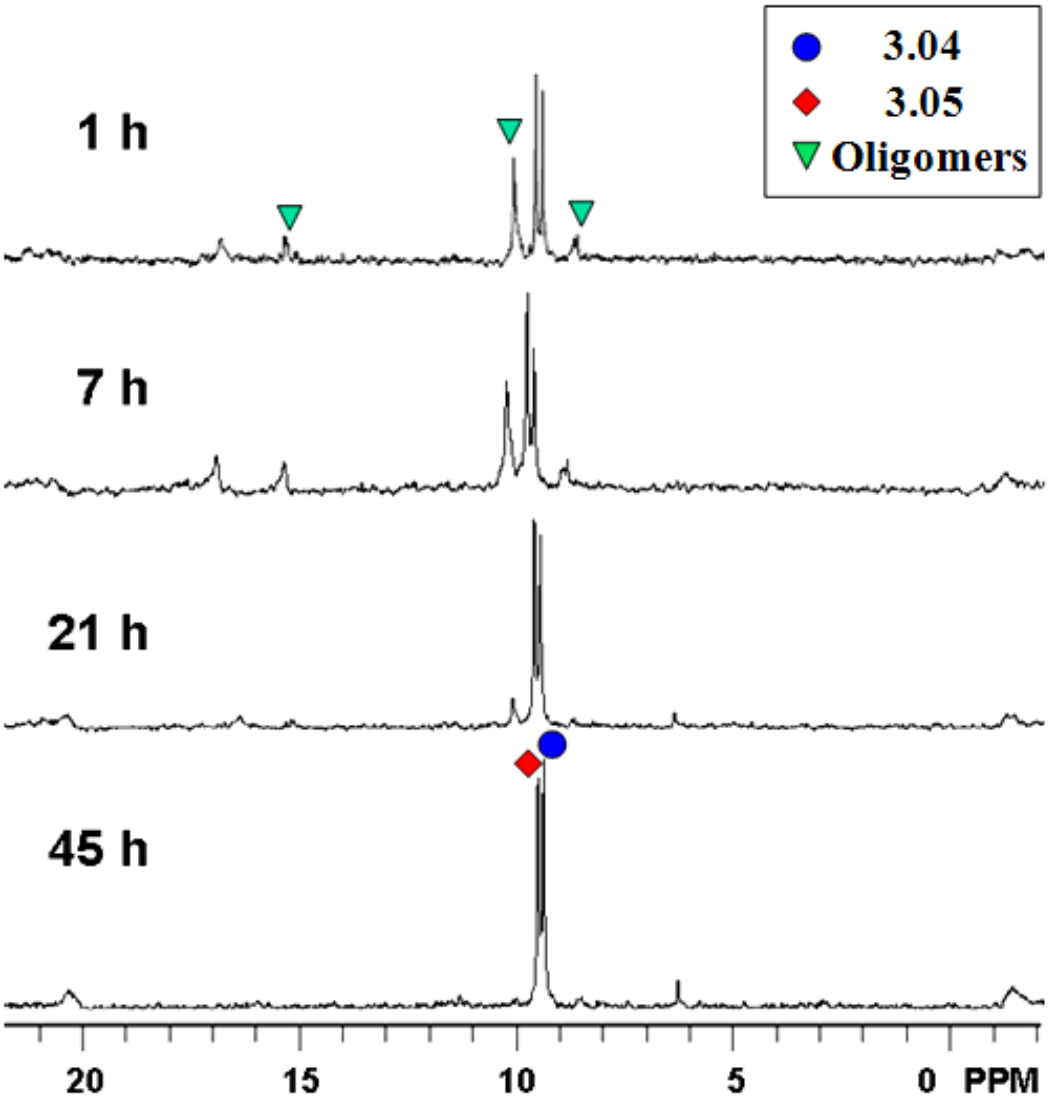

Figure 3.1. $^{31}P\{^{1}H\}$ NMR spectra (Acetone-d_6/D_2O 1:1) recorded at 1 h, 7 h, 21 h, and 45 h time intervals during the formation of rectangles **3.04** and **3.05**

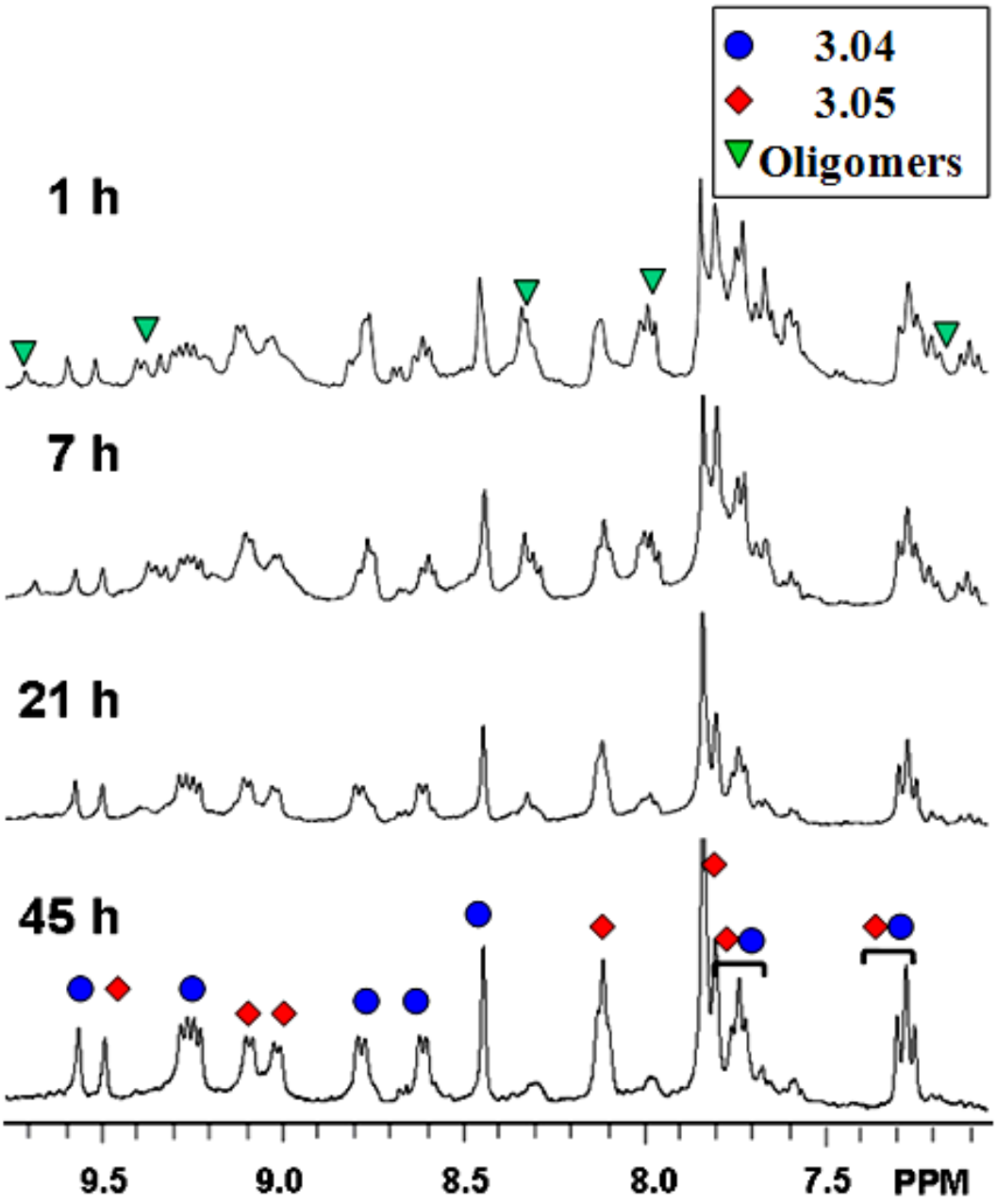

Figure 3.2. Partial ^{1}H NMR spectra (Acetone-d_6/D_2O 1:1) recorded for **SS_1** at 1 h, 7 h, 21 h, and 45 h time intervals during the formation of supramolecular rectangles **3.04** and **3.05**

shows intense peaks at 8.95 ppm and 9.10 ppm with concomitant ^{195}Pt satellites for **3.04** and **3.05**, flanked by unassignable signals that are representative of oligomeric byproducts. Likewise, peaks attributable to rectangles **3.04** and **3.05** (e.g., δ = 9.52 ppm, H_9 in **3.04**; δ = 9.45 ppm, H_9 in **3.05**) can be found in the ^{1}H NMR spectrum after 1 h of heating, though broad peaks and unassignable signals belonging to oligomeric byproducts are also observed. After 21 h, the broad byproduct peaks at 7.89 ppm, 8.22 ppm, 9.30 ppm, and 9.64 ppm decrease significantly while the intense peaks for **3.04** and **3.05** remain in the ^{1}H NMR spectrum, indicating that most oligomeric byproducts have dynamically self-sorted to the desired products. After 45 h, two sets of sharp signals (consistent with those previously reported[10] for **3.04** and **3.05**) remain in the NMR spectrum, indicating the presence of two highly symmetric Pt(II)-based supramolecular species in solution.

The formation of the desired supramolecular rectangles is further confirmed by ESI mass spectrometry, as shown in Figure 3.3. The ESI mass peaks corresponding to the consecutive loss of nitrate anions from the small rectangle **3.04**: m/z = 1256.2 $[M - 2NO_3]^{2+}$ and m/z = 816.8 $[M - 3NO_3]^{3+}$ are observed, as are those corresponding to the formation of the large rectangle, **3.05**, at m/z = 1379.8 $[M – 2NO_3]^{2+}$and m/z = 899.5 $[M - 3NO_3]^{3+}$. All of these peaks were isotopically resolved and agree with their theoretical distributions.

The combined evidence from ^{1}H and ^{31}P NMR spectroscopy as well as ESI mass spectrometry clearly indicate the formation of two discrete molecular rectangles **3.04** and **3.05**, from a complex mixture via a dynamic self-sorting process. In order to further study such size selective self-sorting processes in the self-assembly of 2D Pt(II)- based

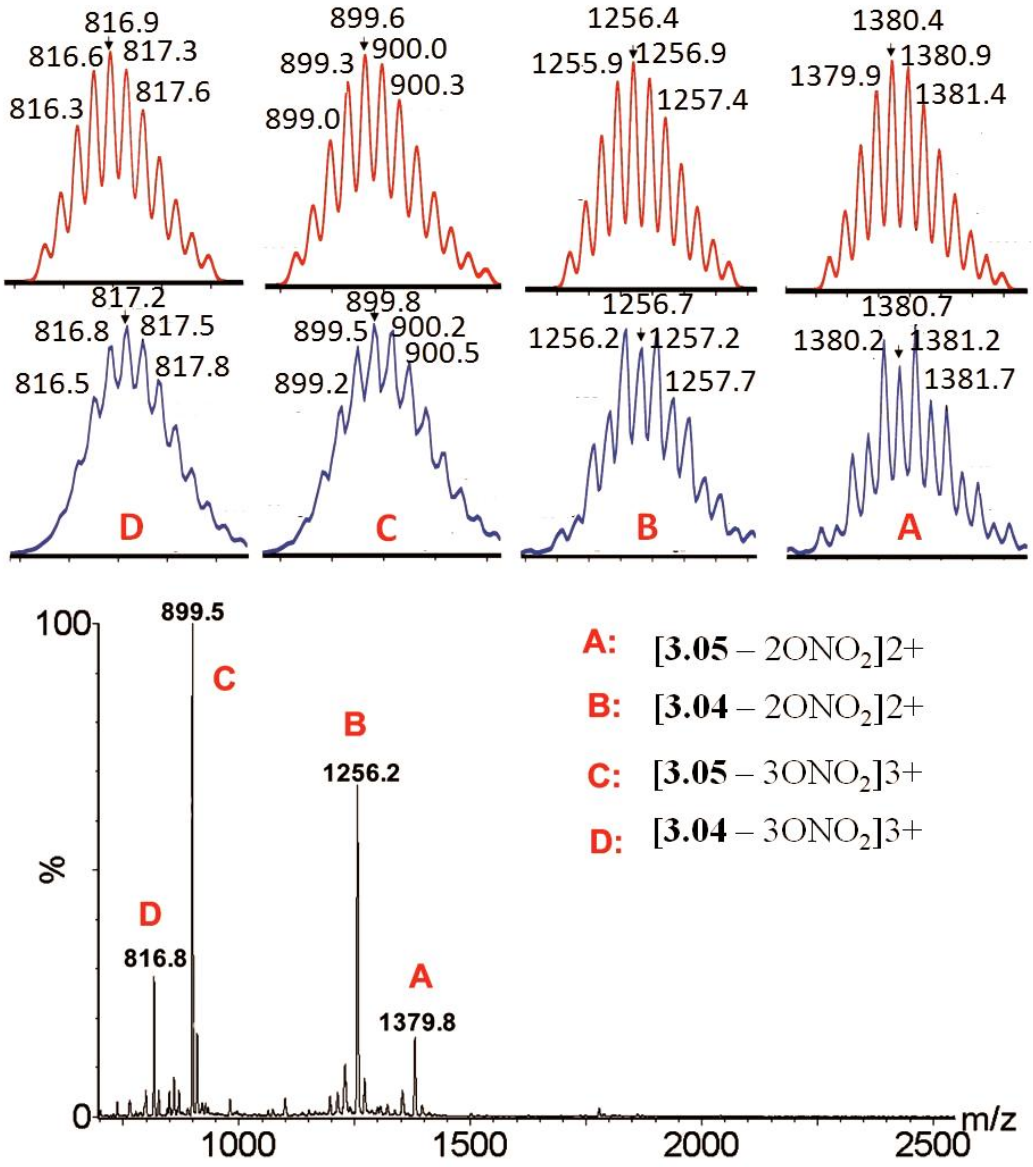

Figure 3.3. Full ESI mass spectrum (Acetone-d_6/D_2O 1:1) of **SS_1** containing supramolecular rectangles **3.04** and **3.05** (Experimental patterns: blue; Calculated distributions: red)

supramolecular systems, another supramolecular system was investigated by mixing 60 ° organoplatinum acceptor **3.06** with linear linkers **3.02** and **3.03**, resulting in the self-sorting of supramolecular triangles (**3.07**: small triangle[12] and **3.08**: large triangle)[10] as shown in Scheme 3.2.

3.2.2 Size selective self-sorting of supramolecular triangles

Heating an aqueous acetone solution (*v/v* 1:1) containing 60 ° di-Pt(II) acceptor **3.06** and two dipyridyl linkers **3.02** and **3.03** in a 2:1:1 ratio for 65 h results in the formation of a three-component self-sorting system $\mathbf{SS_2}$ with two discrete molecular triangles **3.07** and **3.08** as the main products (Scheme 3.2). The $^{31}P\{^{1}H\}$ NMR spectrum of the reaction mixture shows sharp peaks at 15.19 ppm (**3.07**) and 15.27 ppm (**3.08**). Two sets of signals corresponding to **3.07** and **3.08** are clearly presented in the ^{1}H NMR spectrum as well. Signals indicative of minor impurities can, however, be observed in the NMR spectrum even after prolonged heating. ESI mass spectrometry provides further evidence for the formation of the two discrete different sized triangles. The ESI mass spectrum exhibits peaks at m/z = 1916.1 and m/z = 927.1, corresponding to $[M - 2NO_3]^{2+}$ and $[M - 4NO_3]^{4+}$ for **3.07** as well as peaks at *m/z* = 2102.2 and *m/z* = 1019.8, corresponding to $[M - 2NO_3]^{2+}$ and $[M - 4NO_3]^{4+}$ for **3.08**. All peaks were isotopically resolved and are in agreement with their theoretical distributions.

The collective experimental and analytical data clearly indicate that the formation of different 2D polygons of the same shape but different size can be achieved from a complex mixture via the self-sorting process. Extending beyond the 2D polygons, the self-sorting of 3D supramolecular structures is expected to be more challenging.

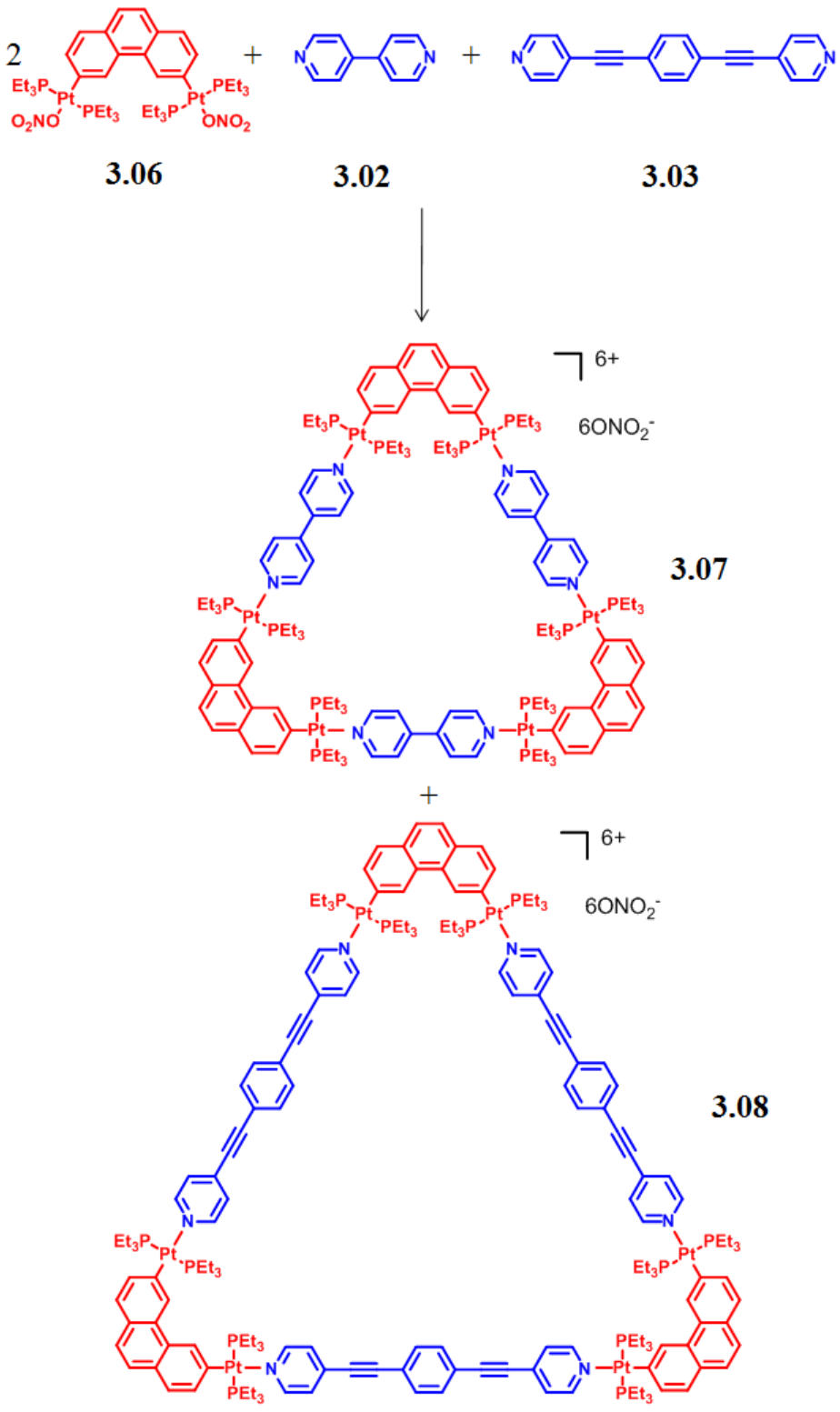

Scheme 3.2. Three-component self-sorting system **SS_2** with two discrete supramolecular triangles **3.07** and **3.08**

3.2.3 Size selective self-sorting of supramolecular prisms

The investigation of size selective self-sorting in the self-assembly of 3D polygons was carried out by mixing molecular clip **3.01** with two tritopic donors **3.09** and **3.10** in a 3:1:1 ratio, as shown in Scheme 3.3. Analysis of the mixture using multinuclear NMR ^{31}P and ^{1}H spectroscopy (Figures 3.4) and ESI mass spectrometry (Figures 3.5) show that distorted triangular prisms **3.11** (small distorted triangular prism) and **3.12** (large distorted triangular prism) [12] were formed in the three-component self-sorting system $\mathbf{SS_3}$.

The mixture changes from a suspension to a clear solution after 1 h and displays a highly disordered ^{31}P {^{1}H} and ^{1}H NMR spectra. After 3 h, initial formation of **3.11** and **3.12** is clearly indicated by the ^{31}P {^{1}H} NMR spectrum (Figures 3.4a), wherein two peaks at 11.12 ppm and 10.16 ppm with concomitant ^{195}Pt satellites for **3.11** and **3.12** appear. There exist, however, multiple unassignable peaks, such as those at 15.31 ppm, 9.85 ppm and 8.87 ppm, that are representative of oligomeric byproduct in solution. At the 3 h time interval, signals for **3.11** and **3.12** cannot be identified in the ^{1}H NMR spectrum (Figures 3.4b) because of the breadth of peaks corresponding to the oligomeric byproducts. After 12 h, peaks attributable to discrete **3.11** and **3.12** can be identified in both the ^{31}P {^{1}H}pr NMR spectrum and the ^{1}H NMR spectrum, as the intensities of peaks corresponding to oligomeric byproducts are significantly decreased. After 24 h, in the ^{31}P {^{1}H} and ^{1}H NMR spectra (Figures 3.4), clearly identifiable peaks reveal the formation of two different sized discrete supramolecular 3D cages **3.11** and **3.12** as the major self-sorted species in the solution.

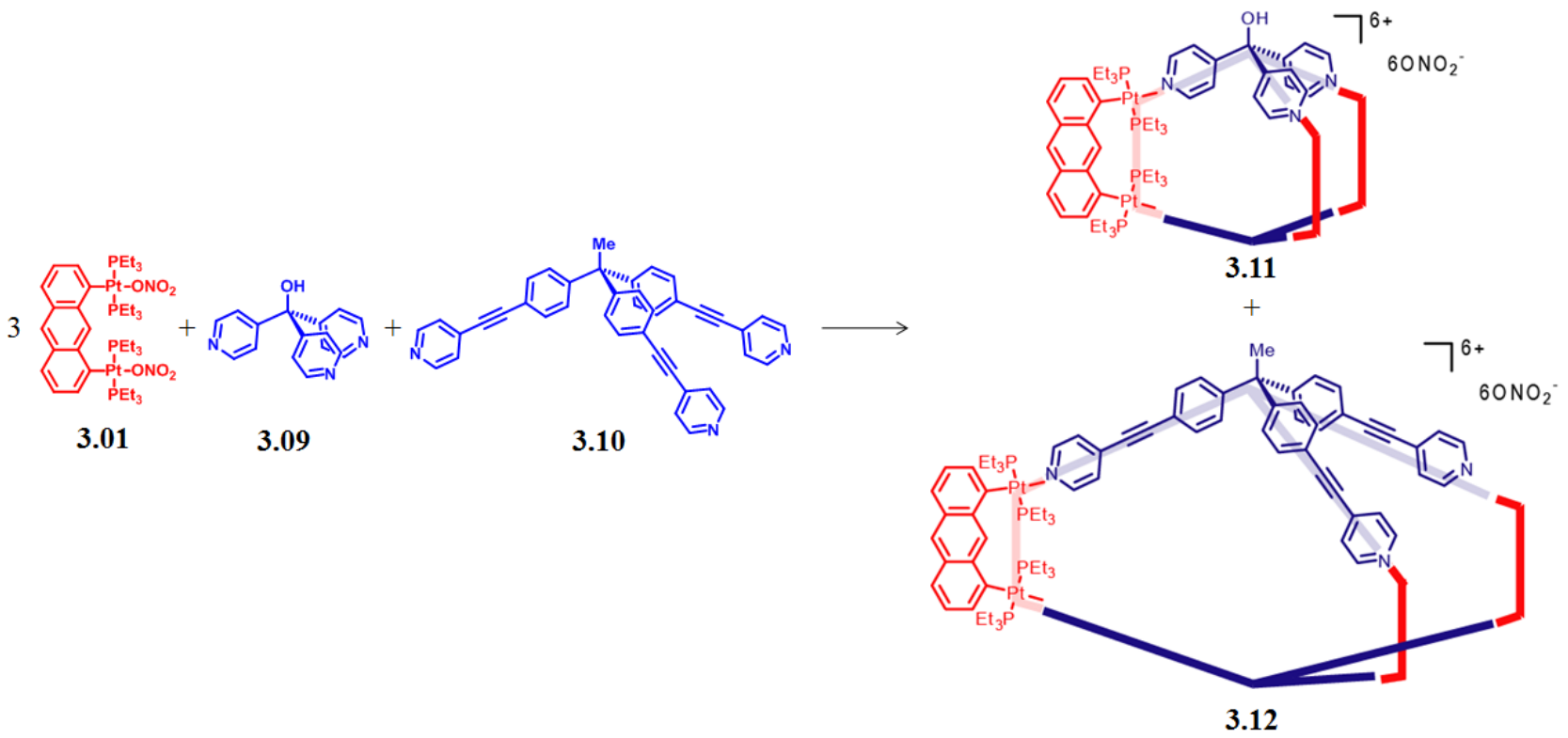

Scheme 3.3. Three-component self-sorting system **SS$_3$** with two discrete supramolecular bipyramids **3.11** and **3.12**

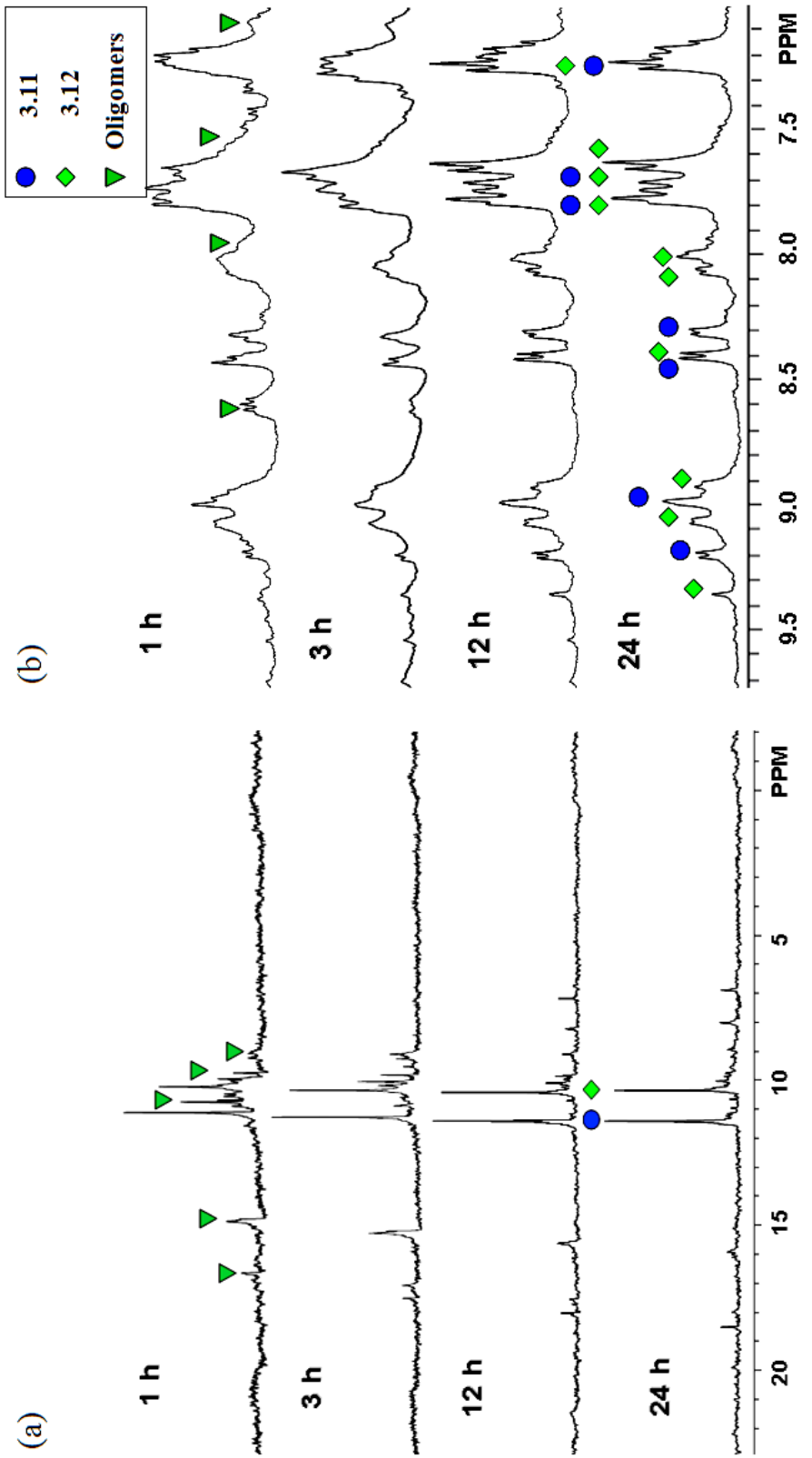

Figure 3.4. NMR spectra: (a) $^{31}P\{^{1}H\}$ NMR spectra and (b) partial ^{1}H NMR spectra (Acetone-d_6/D_2O 1:1) recorded for $\mathbf{SS_3}$ at 1 h, 3 h, 12 h, and 24 h time intervals during the formation of supramolecular rectangles **3.11** and **3.12**

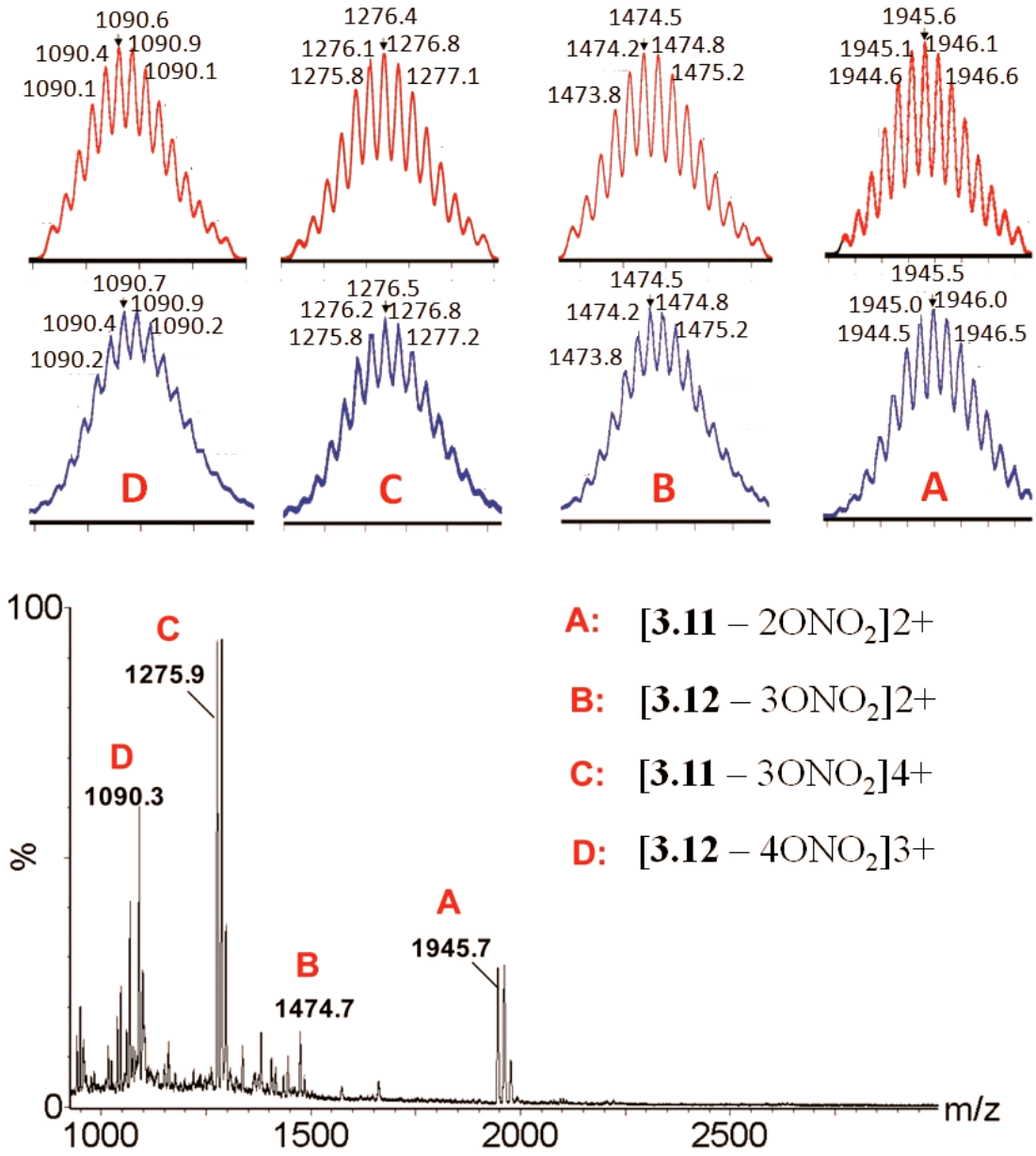

Figure 3.5. Full ESI mass spectrum (Acetone-d_6/D_2O 1:1) of **SS_3** containing supramolecular rectangles **3.11** and **3.12** (Experimental patterns: blue; Calculated distributions: red)

ESI mass spectrometry (Figure 3.5) confirms the self-sorting of different sized supramolecular 3D cages **3.11** and **3.12** in the mixture. The ESI mass peaks corresponding to the consecutive loss of nitrate anions from the small cage **3.11** at m/z = 1946.0 $[M - 2NO_3]^{2+}$ and m/z = 1276.5 $[M - 3NO_3]^{3+}$ are observed, as are those corresponding to the formation of the large cage **3.12** at m/z = 1474.5 $[M - 3NO_3]^{2+}$and m/z = 1090.4 $[M - 4NO_3]^{3+}$. All peaks were isotopically resolved and agree with their theoretical distribution.

3.2.4 Four-component self-sorting with "molecular clip"

As a further step into multicomponent supramolecular systems of higher complexity, an investigation of self-sorting of more components and higher structural diversity was deemed valuable. Self-sorting studies involving molecular clip **3.01** with pyridyl donors **3.02**, **3.03**, **3.09**, and **3.10** led to multicomponent supramolecular systems of relatively higher complexity, as shown in Scheme 3.4.

The four-component self-sorting system **SS_4** was carried out by mixing molecular clip **3.01** with two different sized linear bipyridyl linkers **3.02** and **3.03** and a tripyridyl donor **3.09** in a 7:2:2:2 ratio, as shown in Scheme 3.4. After 1 h heating at 65–70 ℃, **SS_4** changed from a suspension to a clear solution. The $^{31}P\{^1H\}$ NMR spectrum (Figure 3.6a) of the reaction mixture showed a highly complex pattern of signals that was representative of disordered oligomeric intermediates (**3.01**, **3.02**, **3.03**, and **3.09**). Likewise, broad peaks belonging to oligomeric intermediates were found in the ^1H NMR spectrum (Figure 3.6b).

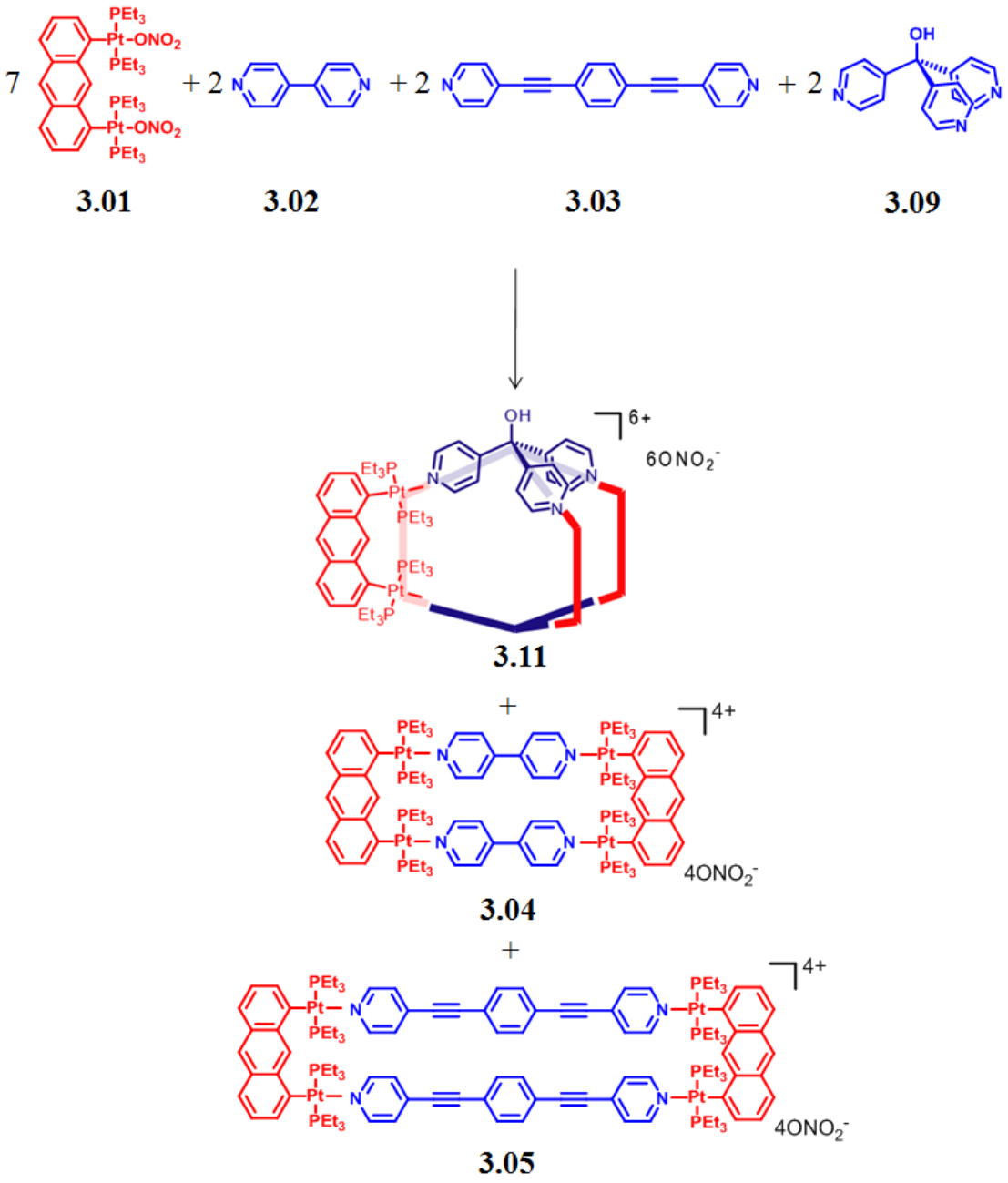

Scheme 3.4. Four-component self-sorting system **SS$_4$** with supramolecular rectangles **3.04** and **3.05** and prism **3.11**

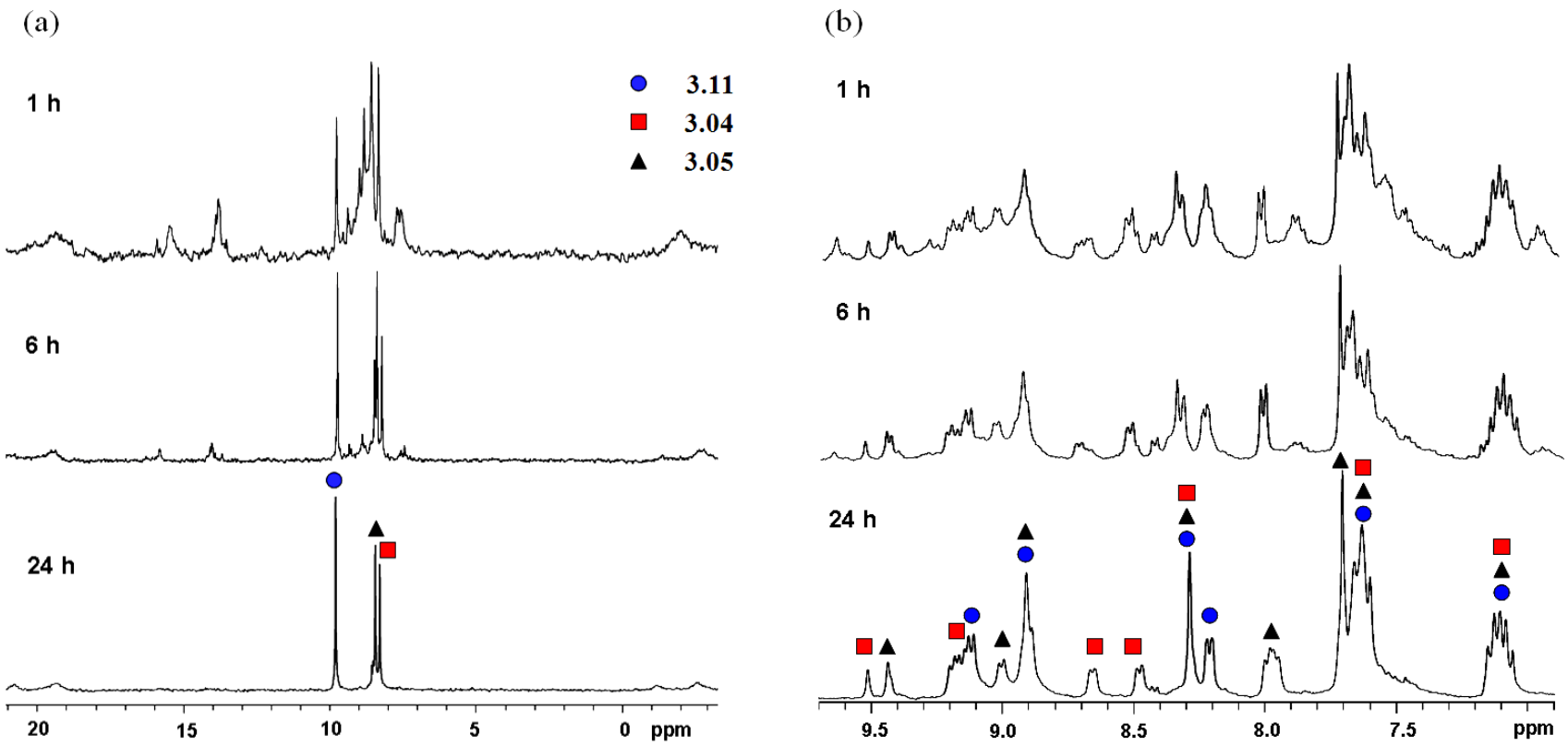

Figure 3.6. NMR spectra: (a) $^{31}P\{^{1}H\}$ NMR spectra and (b) partial ^{1}H NMR spectra (Acetone-d_6/D_2O 1:1) recorded for **SS_4** at 1 h, 3 h, 12 h, and 24 h time intervals during the formation of supramolecular rectangles **3.11** and **3.12**

However, after 24 h only, three sets of sharp signals (consistent with those previously reported for **3.04**, **3.05**,[9] and **3.11**[12]) were observed in the NMR spectra, as shown in Figure 3.6, indicating that the random intermediates initially formed were dynamically and selectively converted to specific supramolecular assemblies (**3.04**, **3.05**, and **3.11**) in the equilibrated mixture. In contrast, the hetero-assembled products involving different ligands were not found. The selective formations of such supramolecuar rectangles **3.04** and **3.05** and distorted triangular prism **3.11** were further confirmed by ESI mass spectrometry. The ESI mass peaks corresponding to the consecutive loss of nitrate anions from the prism **3.11**: m/z = 1944.8 $[M - 2NO_3]^{2+}$ and m/z = 1275.9 $[M - 3NO_3]^{3+}$ were observed, as were those corresponding to the formation of the different sized rectangles, **3.04**: m/z = 1256.7 $[M - 2NO_3]^{2+}$ and m/z = 816.9 $[M - 3NO_3]^{3+}$, and **3.05**: m/z = 1380.3 $[M - 2NO_3]^{2+}$ and m/z = 899.2 $[M - 3NO_3]^{3+}$, each of which is in agreement with those reported previously. Thus, the collective analytical data from NMR and ESI-MS clearly indicate a self-sorting system involving 2D and 3D supramolecular structures **3.04**, **3.05**, and **3.11** has been obtained from a complex mixture of molecular acceptor **3.01** and donors **3.02**, **3.03**, and **3.09**.

Three different self-sorting systems $\mathbf{SS_5}$–$\mathbf{SS_7}$, each involving three out of the five species **3.04**, **3.05**, **3.11**, **3.12**, and **3.14**, were obtained by mixing multiple molecular subunits in an aqueous acetone solution (Scheme 3.5). Initially, oligomeric intermediates were formed from the random combination of various molecular components in all mixtures, as indicated by the ^{31}P and the ^{1}H NMR spectra. These disordered intermediates slowly converted into discrete supramolecular structures, as evidenced by the sharpening of their NMR spectra over a 24–48 h period of heating at 65–70 ℃.

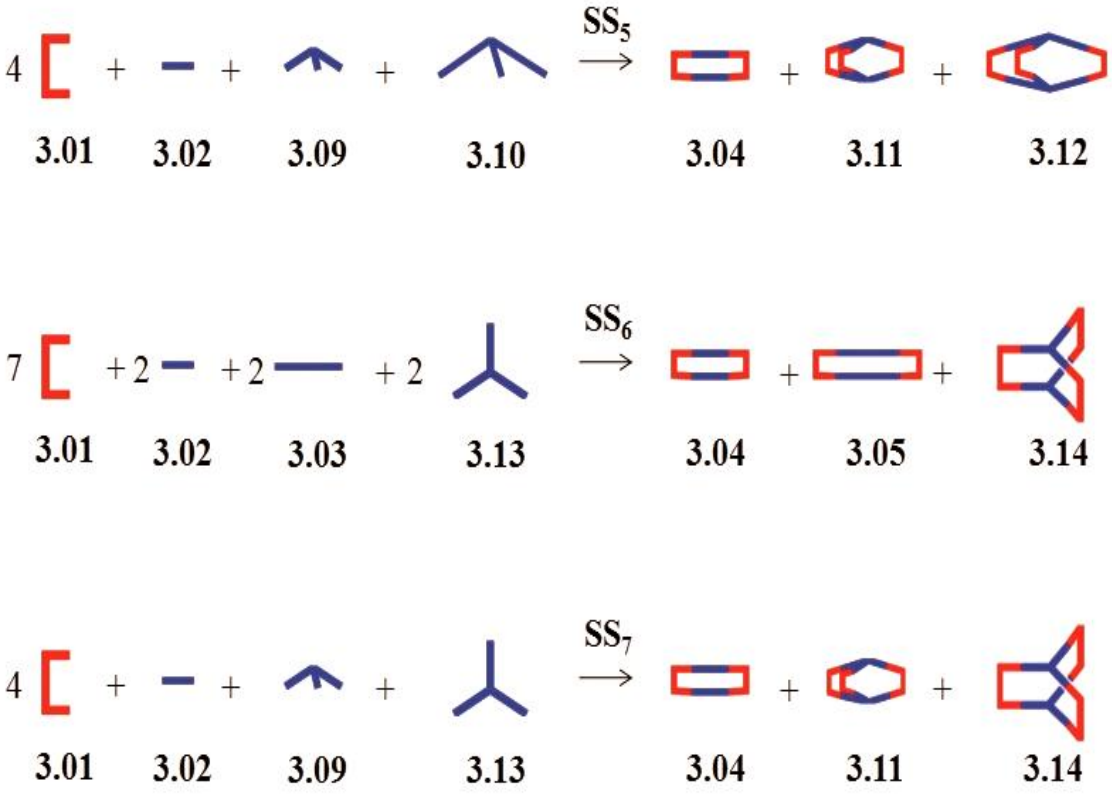

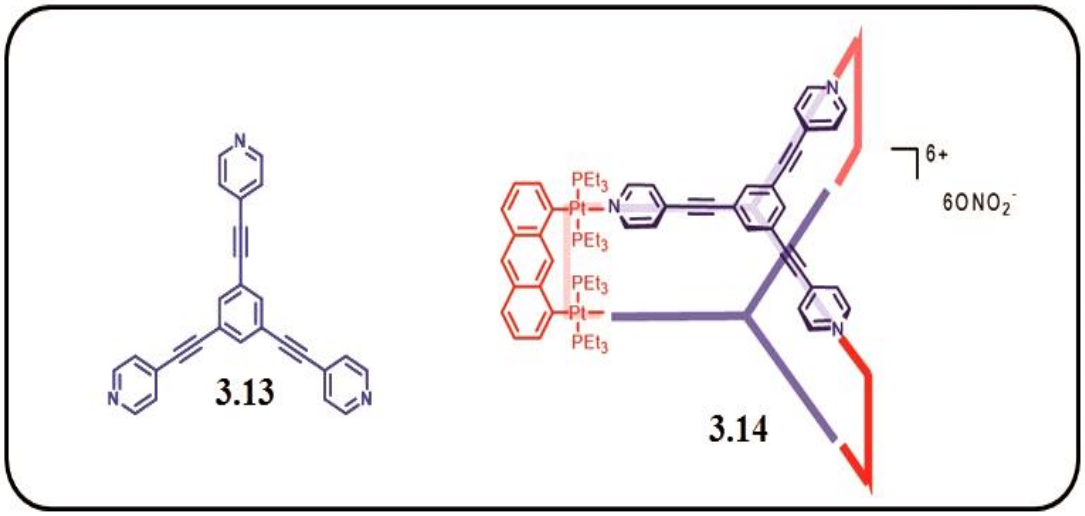

Scheme 3.5. Four-component self-sorting systems **SS$_5$**, **SS$_6$**, and **SS$_7$** with supramolecular rectangles **3.04** and **3.05** and prism **3.11**, **3.12**, and **3.14**

Equilibrated mixtures **SS_5–SS_7** contain only discrete two-component assemblies **3.04**, **3.05**, **3.11**, **3.12**, and **3.14** as supported by sharp and identifiable spectroscopic signals (**SS_5**: 8.32 ppm for **3.04**; 8.83 ppm for **3.12**; 9.81 ppm for **3.11**, **SS_6**: 8.32 ppm for **3.04**; 8.48 ppm for **3.05**; 8.65 ppm for **3.14**, and **SS_7**: 8.32 ppm for **3.04**; 8.65 ppm for **3.14**; 9.81 ppm for **3.11**) in the $^{31}P\{^{1}H\}$ NMR spectra (Figures 3.7a–c). In both **SS_6** and **SS_7**, a small peak at 9.01 ppm appears and is believed to indicate a small amount of disordered byproduct. Similarly, the ^{1}H NMR spectra (Figures 3.7d–f) show intense identifiable signals corresponding to the different self-sorted supramolecular species, each of which is consistent with those reported previously, despite a partial overlapping of some signals.

The selective formation of discrete supramolecular rectangles and 3D cages in these complex mixtures of **SS_5–SS_7** is further characterized by ESI mass spectrometry, as shown in Figure 3.8. Identifiable signals for the consecutive loss of nitrate anions from **3.04**, **3.05**, **3.11**, **3.12**, and **3.14** can be found in the ESI mass spectra of **SS_5–SS_7**: e.g., intense peaks for **3.04**: m/z = 1256.7 $[M - 2NO_3]^{2+}$ and m/z = 816.9 $[M - 3NO_3]^{3+}$, **3.05**: m/z = 1380.3 $[M - 2NO_3]^{2+}$ and m/z = 899.2 $[M - 3NO_3]^{3+}$, **3.11**: m/z = 1944.8 $[M - 2NO_3]^{2+}$ and m/z = 1275.9 $[M - 3NO_3]^{3+}$, **3.12**: m/z = 1474.5 $[M - 3NO_3]^{3+}$ and m/z = 1090.4 $[M - 4NO_3]^{4+}$, and **3.14**: m/z = 1354.1$[M - 3NO_3]^{3+}$ and m/z = 1000.4 $[M - 4NO_3]^{4+}$. Each of these peaks is consistent with those previously reported.[9,12] The combined data from ^{31}P and ^{1}H multinuclear NMR spectroscopy as well as ESI mass spectrometry clearly indicate that high-fidelity self-sorting has been achieved in systems **SS_5–SS_7**.

The major factors directing self-sorting are the multiple different geometric features of these pyridyl ligands (**3.02**, **3.03**, **3.09**, and **3.10**). The size difference between

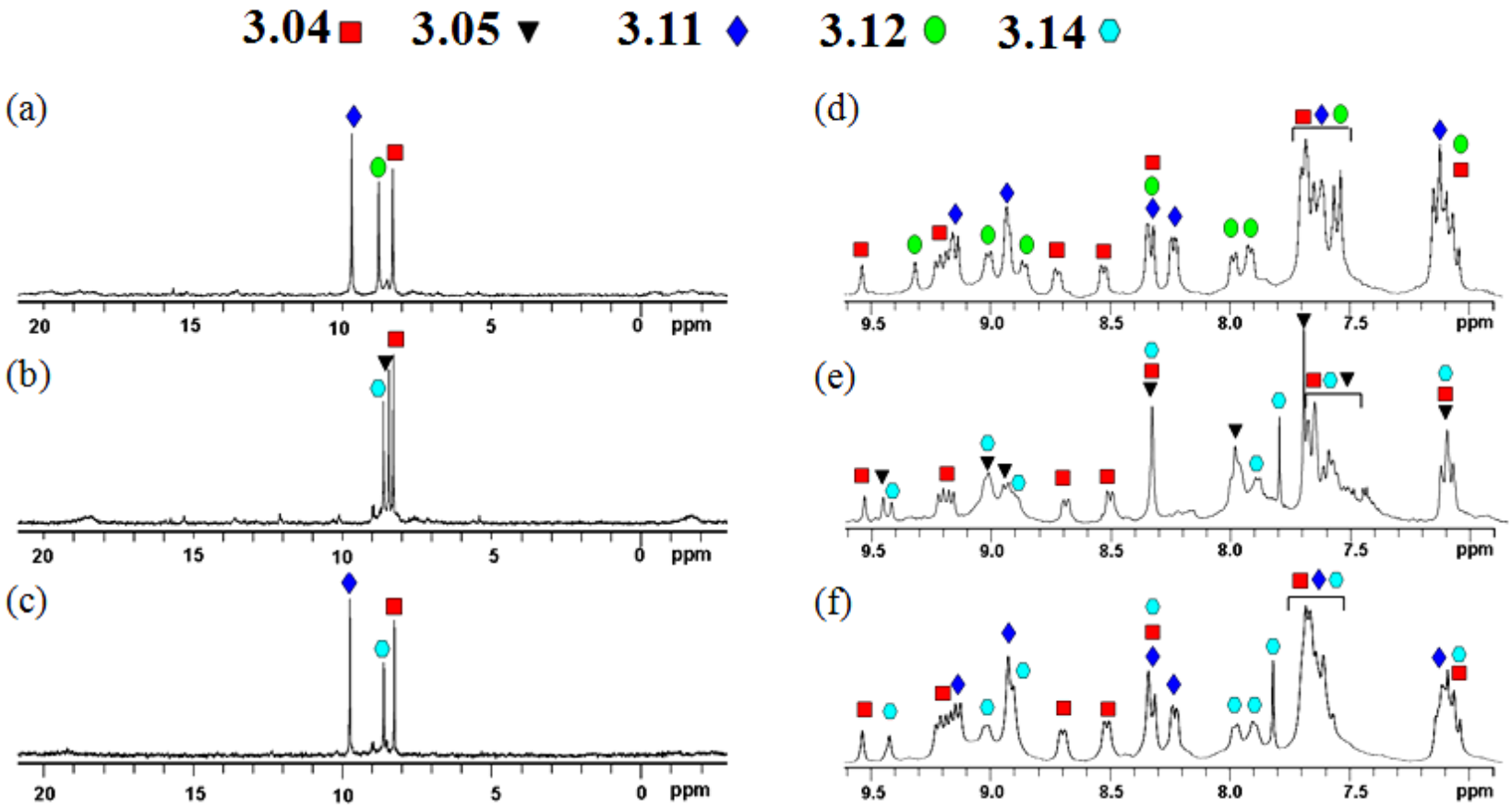

Figure 3.7. NMR spectra: (a,b,c) $^{31}P\{^{1}H\}$ NMR spectra and (d,e,f) partial ^{1}H NMR spectra (Acetone-d_6/D_2O 1:1) recorded for **SS_5**, **SS_6,** and **SS_7** with formation of supramolecular rectangles **3.04** and **3.05** and prism **3.11**, **3.12**, and **3.14**

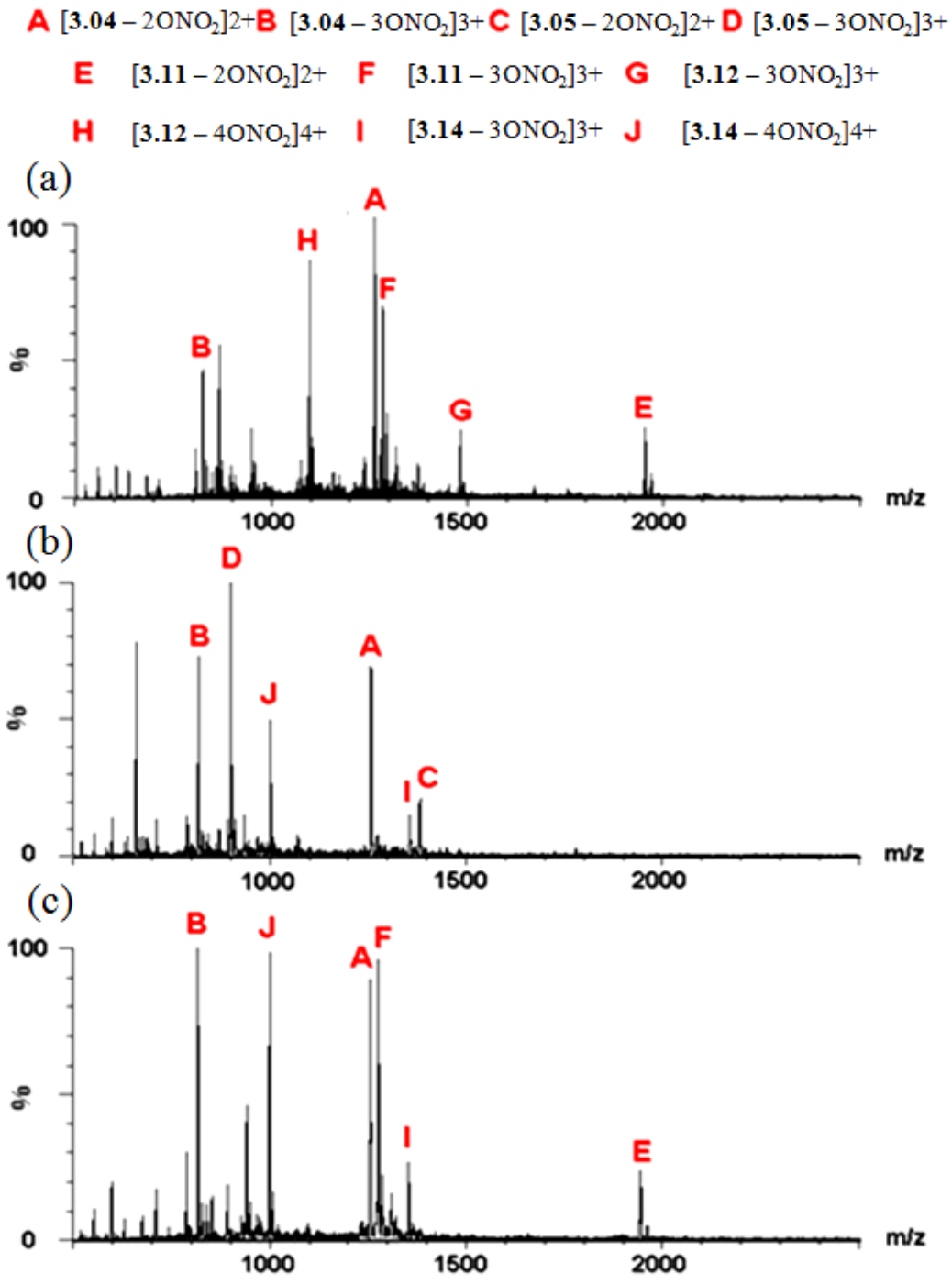

Figure 3.8. ESI-MS for self-sorting systems (a) $\mathbf{SS_5}$, (b) $\mathbf{SS_6}$, and (c) $\mathbf{SS_7}$ with supramolecular rectangles **3.04** and **3.05** and prism **3.11**, **3.12**, and **3.14**

3.02 and **3.03** as well as **3.09** and **3.10**, along with the varied number of binding sites between **3.02**/**3.03** and **3.09**, allow for the self-recognition of ligands of the same geometry to proceed via two-component assembly into discrete supramolecular assemblies **3.04**, **3.05**, **3.11**, and **3.12**. The successful achievement of these four-component self-sorting systems **SS_4–SS_7**, indicates the generality of self-sorting behavior for the self-assembly of these structural motifs (rectangles and distorted and nondistorted triangular prisms), which is the first step toward the construction of highly diverse multicomponent supramolecular systems via self-sorting.

3.2.5 Four-component self-sorting with 60 ° acceptor

To further demonstrate the generality of geometric, selective self-sorting in coordination-driven self-assembly, detailed investigations into supramolecular species assembled by additional molecular components were necessary. Thus, a 60 ° organoplatinum acceptor **3.06**, which is a widely utilized molecular subunit capable of assembling 2D supramolecular structures such as rhomboids and triangles as well as 3D triangular bipyramids, has been investigated.

Three different self-sorting systems **SS_8–SS_{10}**, each involving three out of the five different assemblies **3.07**, **3.08**, **3.17**, **3.18**, and **3.19**, were carried out, as shown in Scheme 3.6. The 60 ° organoplatinum acceptor **3.06** was mixed with complementary ditopic and tritopic pyridyl donors **3.02**, **3.03**, **3.10**, **3.15**, and **3.16** in an aqueous acetone solution (*v/v* 1:1) and heated at 65–70 ℃. The ^{31}P and ^{1}H multinuclear NMR spectra of these mixtures were used to follow the self-sorting processes, and the sharpening, over time, of both the $^{31}P\{^{1}H\}$ and ^{1}H NMR spectra was observed for each mixture during continual heating (24–48 h). These results indicate that oligomeric intermediates formed

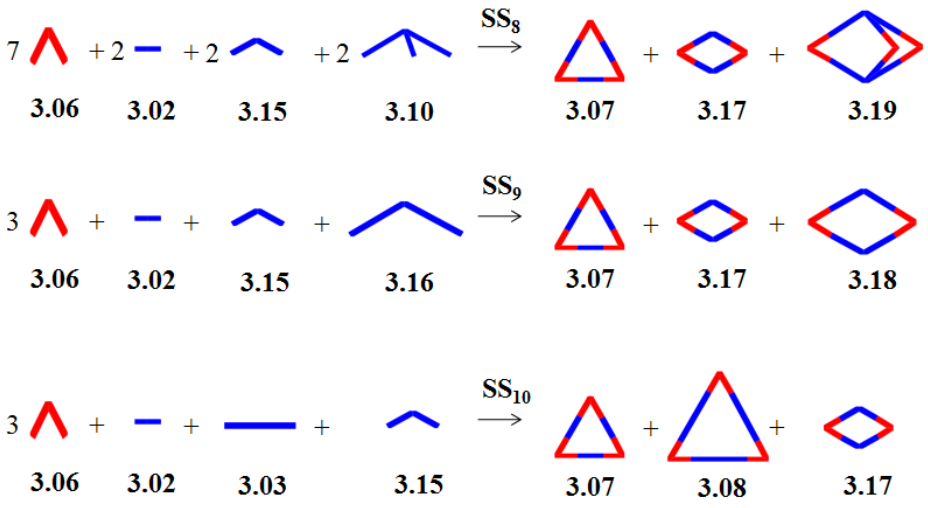

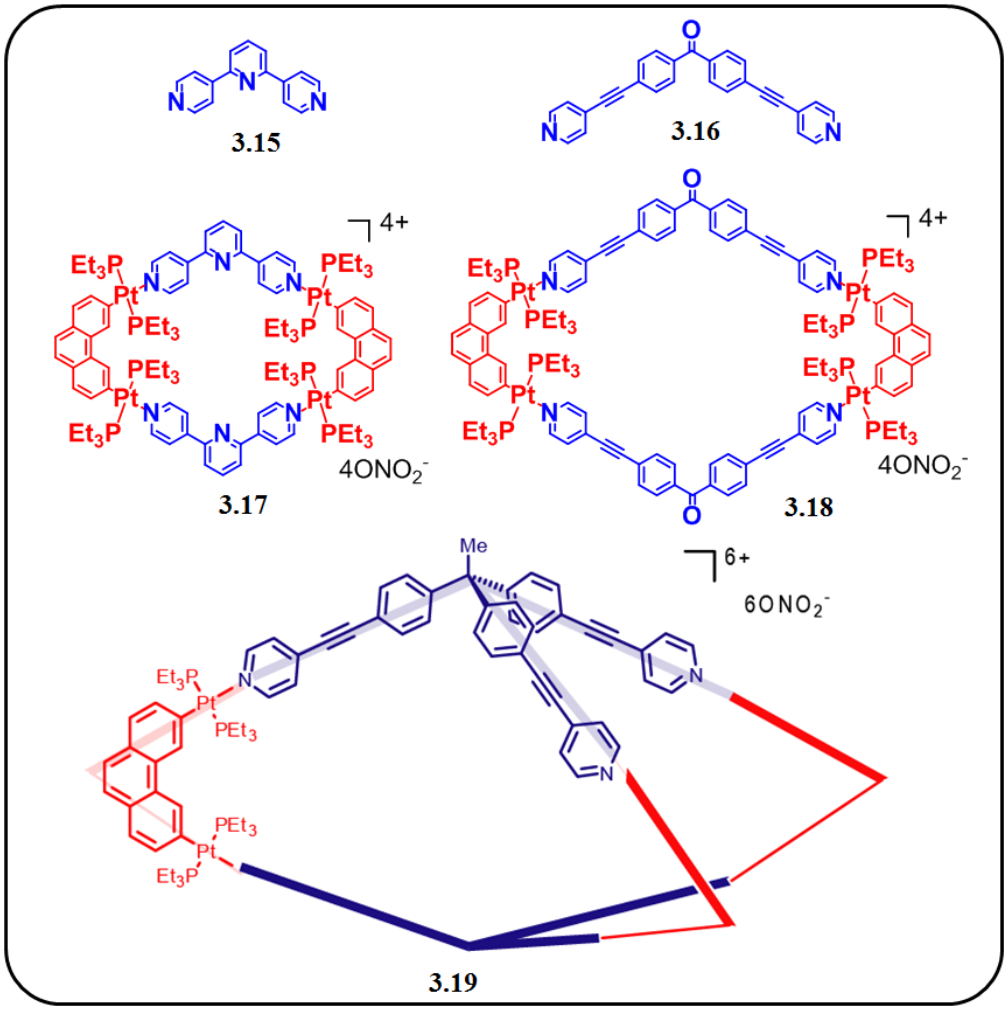

Scheme 3.6. Four-component self-sorting systems **SS$_8$**, **SS$_9$**, and **SS$_{10}$** with supramolecular triagnles **3.07** and **3.08**, rhomboids **3.17**, and **3.18**, and prism **3.19**

from the random combination of various building blocks were initially present, but were later dynamically converted to discrete supramolecular products. Species **3.07**, **3.08**, **3.17**, **3.18**, and **3.19** were formed as the predominant products in the fully equilibrated mixtures. Figure 3.9 presents the $^{31}P\{^{1}H\}$ and ^{1}H NMR spectra of self-sorting systems **SS$_8$**–**SS$_{10}$** after full equilibration. As expected, the $^{31}P\{^{1}H\}$ NMR spectra for each of **SS$_8$**–**SS$_{10}$** (Figures 3.9a–c) show peaks that are consistent with those of the individually prepared assemblies (**SS$_8$**: 14.31 ppm for **3.07**; 14.40 ppm for **3.19**; 14.43 ppm for **3.17**, **SS$_9$**: 14.31 ppm for **3.07**; 14.38 ppm for **3.18**; 14.43 ppm for **3.17**, and **SS$_{10}$**: 14.31 ppm for **3.07**; 14.43 ppm for **3.17**), though overlap of signals from **3.08** and **3.17** of **SS$_{10}$** at 14.41 ppm can be seen. Correspondingly, three sets of signals for discrete, self-assembled supramolecules in each self-sorting system can be clearly identified in each ^{1}H NMR spectrum (Figure 3.9d–f), though some small broad peaks associated with minor amounts of disordered structures can also be found in the ^{1}H NMR spectra (**SS$_8$**: 7.12 ppm, 7.82 ppm, and 8.12 ppm; **SS$_9$**: 7.48 ppm; **SS$_{10}$**: 7.48 ppm, 8.12 ppm, and 8.54 ppm).

The formation of discrete supramolecular species **3.07**, **3.08**, **3.17**, **3.18**, and **3.19** in complex mixtures **SS$_8$**–**SS$_{10}$** is further supported by ESI mass spectrometry, as shown in Figure 3.10. Signals for the consecutive loss of nitrate anions from **3.07**, **3.08**, **3.17**, **3.18**, and **3.19** (**3.07**: m/z = 1916.6 $[M - 2NO_3]^{2+}$ and m/z = 927.06 $[M - 4NO_3]^{4+}$, **3.08**: m/z = 1381.5 $[M - 3NO_3]^{3+}$ and m/z = 1020.6 $[M - 4NO_3]^{4+}$, **3.17**: m/z = 1333.4 $[M - 2NO_3]^{2+}$ and m/z = 868.3 $[M - 3NO_3]^{3+}$, **3.18**: m/z = 1484.5 $[M - 2NO_3]^{2+}$ and m/z = 969.0 $[M - 3NO_3]^{3+}$, and **3.19**: m/z = 1474.5$[M - 3NO_3]^{3+}$ and m/z = 1090.4 $[M - 4NO_3]^{4+}$) are observed in the ESI mass spectra and are consistent with previously reported results. The results of both multinuclear NMR spectroscopy and ESI mass spectrometry indicate

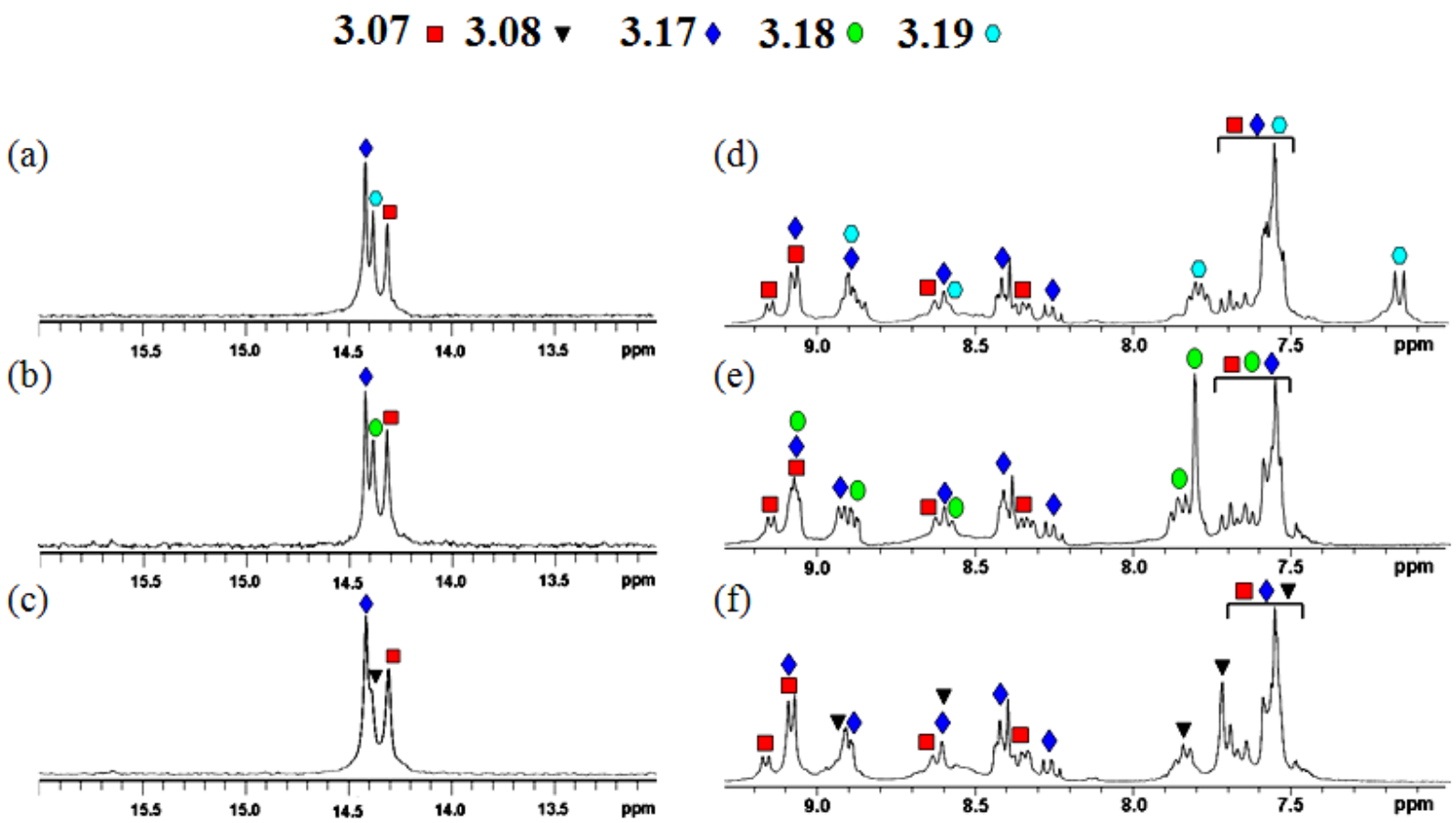

Figure 3.9. NMR spectra: (a,b,c) $^{31}P\{^{1}H\}$ NMR spectra and (d,e,f) partial ^{1}H NMR spectra (Acetone-d_6/D_2O 1:1) recorded for **SS_8**, **SS_9,** and **SS_{10}** with formation of supramolecular triagnles **3.07** and **3.08**, rhomboids **3.17**, and **3.18**, and prism **3.19** with formation of supramolecular rectangles **3.04** and **3.05** and prism **3.11**, **3.12**, and **3.14**

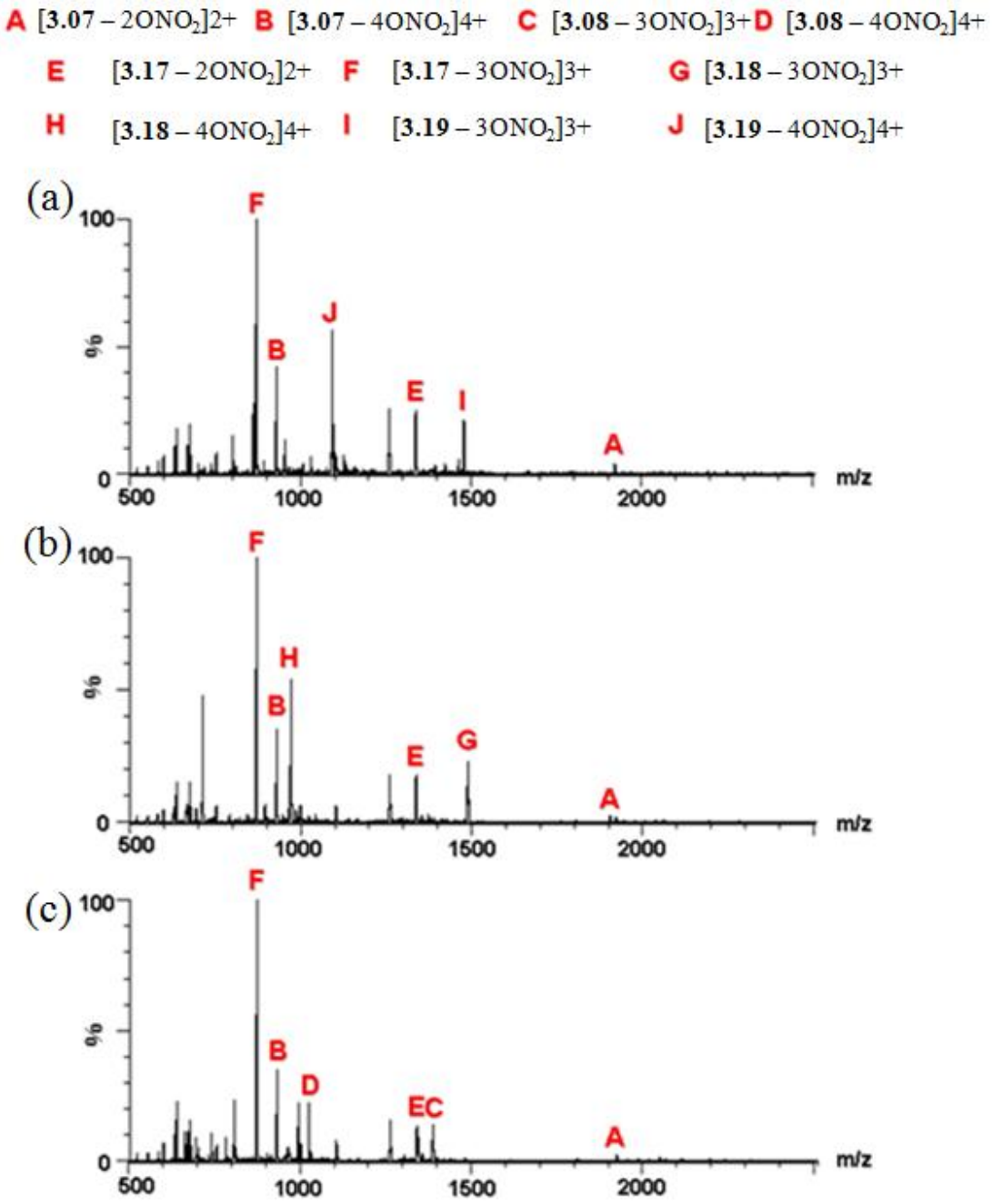

Figure 3.10. ESI-MS for self-sorting systems (a) **SS$_8$**, (b) **SS$_9$**, and (c) **SS$_{10}$** with supramolecular triangles **3.07** and **3.08**, rhomboids **3.17**, and **3.18**, and prism **3.19**

the successful achievement of self-sorting within systems **SS_8**–**SS_{10}**, with a high degree of structural diversity (triangles, rhomboids, and triangular bipyramids).

3.2.6 Four-compoent self-sorting with "molecular clip" and 60 ° acceptor

Additional investigations exploring geometry-directed self-sorting involving the combination of two organic donors and two organoplatinum acceptors have also been performed. Self-sorting system **SS_{11}**, for example, involves mixing molecular clip **3.01** and 60 ° organoplatinum acceptor **3.06** with different sized linear dipyridyl donors **3.02** and **3.03** in a 1:1:1:1 ratio in aqueous acetone solution (*v/v* 1:1). The equilibrated self-sorting system produces only two-component assemblies **3.04**, **3.05**, **3.07**, and **3.08** as a result of high-fidelity self-sorting (Scheme 3.7a).

The self-sorting process was followed by ^{31}P and ^{1}H multinuclear NMR spectroscopy. Disordered oligomeric intermediates were initially formed as indicated by signals at 7.54 ppm, 8.94 ppm, 9.11 ppm 14.03 ppm, and 15.80 ppm in the $^{31}P\{^{1}H\}$ NMR spectra, as well as unidentifiable broad peaks in the ^{1}H NMR spectra recorded at 6 and 24 h time intervals. A significantly long heating time (72 h) at 65–70 ℃ was necessary to accomplish self-sorting. The $^{31}P\{^{1}H\}$ and the ^{1}H NMR spectra of the resulting **SS_{11}** mixture is shown in Figure 3.11. Four peaks corresponding to the different sized supramolecular rectangles and triangles at 8.32 ppm (**3.04**[9]), 8.48 ppm (**3.05**[9]), 14.32 ppm (**3.07**[10]), and 14.40 ppm (**3.08**) are seen in the $^{31}P\{^{1}H\}$ NMR spectrum (Figure 3.11a). Likewise, four sets of signals for these different sized rectangles and triangles can be clearly identified within the ^{1}H NMR spectrum, as shown in Figure 3.11b, the chemical shifts of which are consistent with those previously reported.[9,10] Certain minor

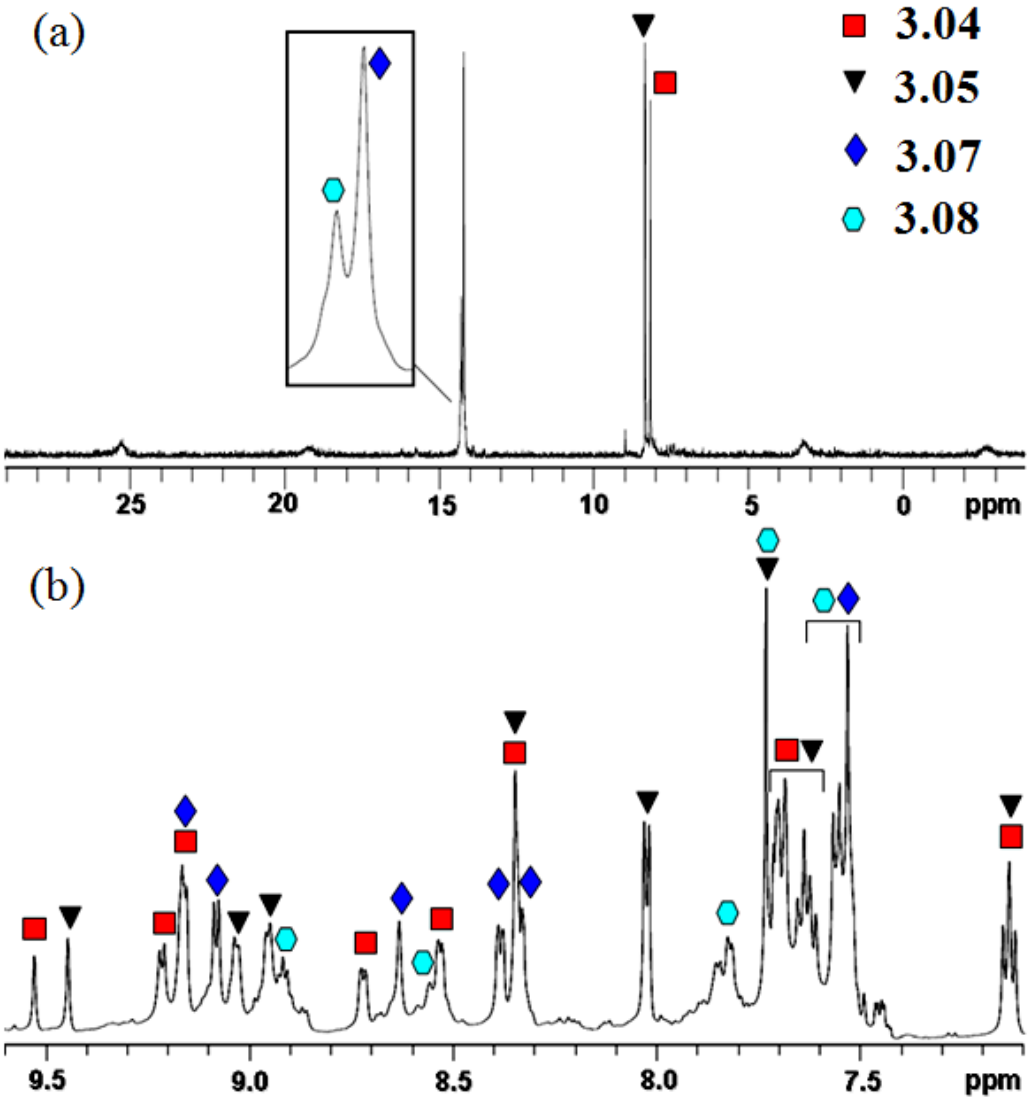

Figure 3.11. $^{31}P\{^{1}H\}$ (a) and Partial ^{1}H (b) NMR spectra (Acetone-d_6/D_2O 1:1) recorded for self-sorting system $\mathbf{SS_{11}}$ (supramolecular rectangles **3.04** and **3.05**, triangles **3.07** and **3.08**).

signals that are representative of a small amount of disordered byproducts can still be found as minor peaks in the ^{1}H NMR spectrum, such as those at 7.45 ppm and 8.90 ppm. These peaks persist even with longer heating. ESI mass spectrometry was also used to characterize this self-sorting system. Intense ESI mass peaks corresponding to the consecutive loss of nitrate anions from four self-sorted supramolecular structures can be observed.

The use of two organoplatinum acceptors and two organic donors in such complex self-sorting systems can be extended to three-dimensions by mixing molecular clip **3.01** and 60 °acceptor **3.06** with ditopic and tritopic pyridyl donors **3.02** and **3.10** in a 3:3:3:2 ratio, resulting in self-sorting system $\mathbf{SS_{12}}$ (Scheme 3.7b). This self-sorting system is capable of selectively forming 2D supramolecular polygons (rectangle **3.04** and triangle **3.07**) as well as 3D cages (distorted triangular prism **3.12** and triangular bipyramid **3.19**) with the exclusion of mixed products from the multicomponent ensembles of different organoplatinum acceptors and pyridyl donors, as shown in Scheme 3.7b. ^{31}P and ^{1}H multinuclear NMR spectroscopy was applied to study the self-sorting

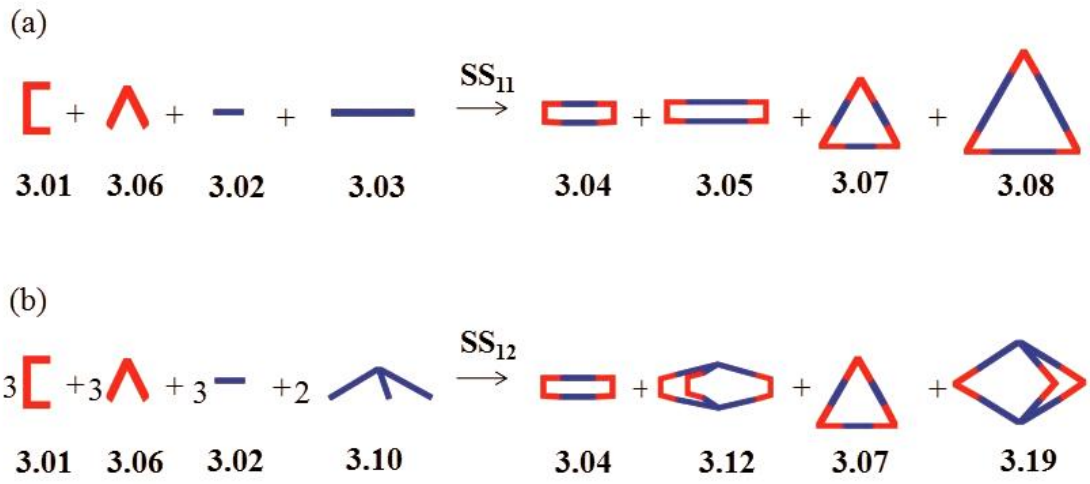

Scheme 3.7. Four-component self-sorting systems $\mathbf{SS_{11}}$ (a) and $\mathbf{SS_{12}}$ (b) with supramolecular rectangles **3.04** and **3.05**, triangles **3.07** and **3.08**, and prism **3.11** and **3.19**

process. It was observed that the mixture remained highly disordered after 6 h of heating, as indicated by unassignable signals at 8.83 ppm, 13.98 ppm, and 15.97 ppm in the $^{31}P\{^{1}H\}$ NMR spectra. Over time and with continual heating, these oligomeric peaks decreased as the peaks of **3.04**, **3.07**, **3.12**, and **3.19** sharpened, indicating that the mixture slowly approached equilibrium. After 96 h of heating at 65–70 ℃, four different 2D and 3D supramolecular structures (**3.04**, **3.07**, **3.12**, and **3.19**) were self-sorted in $\mathbf{SS_{12}}$ as supported by ^{31}P and ^{1}H multinuclear NMR spectroscopy as well as ESI mass spectrometry. Within the $^{31}P\{^{1}H\}$ NMR spectrum, peaks at 8.33 ppm (**3.04**[9]), 8.83 ppm (**3.12**[12]), 14.32 ppm (**3.07**[10]), and 14.39 ppm (**3.19**[11]) clearly indicated the formation of the four discrete supramolecular species as the predominant products of the reaction. Similarly, the ^{1}H NMR spectrum displayed identifiable signals belonging to **3.04**, **3.07**, **3.12**, and **3.19**, along with small broad peaks attributable to disordered structures (7.88 ppm and 9.05 ppm) that could still be found. Data from ESI-MS studies also supported the formation of the four discrete supramolecular entities.

3.2.7 Mass spectral investigation on the self-sorting process

When these different molecular components coexist in one mixture, two classes of assemblies are possible: two-component assembly (e.g., in the $\mathbf{SS_4}$ system, molecular clip **3.01** combines with identical donors (**3.02**, **3.03**, and **3.09**) producing discrete structures (**3.04**, **3.05**, and **3.11**)) and multicomponent ensembles, resulting from mixed products composed of nonidentical ligands (e.g., in $\mathbf{SS_4}$, a three-component species which formed by the aggregation of acceptor **3.01** together with nonidentical donors **3.02** and **3.03**). The multicomponent assembly mainly contributes to the formation of disordered oligomeric species in the initial stages of self-sorting.

A mass spectral study was carried out to investigate the self-sorting process in **SS_4**. After 1 h of heating at 65–70 ℃, the ESI mass spectrum (Figure 3.12a) shows intense signals corresponding to fragments of intermediates formed by multicomponent assembly, e.g., *m/z* = 858.2 for [2(**3.01**) + (**3.02**) + (**3.03**) – $3NO_3$]$^{3+}$, *m/z* = 1310.0 for [2(**3.01**) + (**3.02**) + (**3.08**) – $2NO_3$]$^{2+}$, and *m/z* = 1372.4 for [2(**3.01**) + (**3.03**) + (**3.08**) – $2NO_3$]$^{2+}$, etc. The mass spectral results confirm the initially random combination of these building blocks, resulting in the formation of oligomeric species, in agreement with the observation of the NMR spectra. After 24 h, the mixture was self-sorted. In the ESI mass spectrum shown in Figure 3.12b, the peaks previously observed for multicomponent esembles have disminished, and instead, those corresponding to the two-component species (prism **3.11**, rectangles **3.04** and **3.05**) dominate the spectrum, e.g., *m/z* = 1256.6 for [2(**3.01**) + 2(**3.02**) – $2NO_3$]$^{2+}$ for rectangle **3.04**, *m/z* = 899.5 for [2(**3.01**) + 2(**3.03**) – $3NO_3$]$^{3+}$ for rectangle **3.04**, *m/z* = 1275.9 for [3(**3.01**) + 2(**3.08**) – $3NO_3$]$^{3+}$ for prism **3.11**.

This mass spectral study clearly supports that multicomponent ensembles can be formed through the initial random combination of molecular subunits, but by self-sorting, the mixture can gradually converge to the two-component supramolecular structures. The fundamental driving force in the self-sorting system is the thermodynamic stability of self-assembled products dictated by the geometric information of the molecular building blocks. For example, in **SS_4**, the multicomponent self-assembly of molecular clip **3.01** with different ligands bearing varying geometric features would result in highly strained structures, e.g., a trapezoid formed from [2(**3.01**) + (**3.02**) + (**3.03**)], or larger disordered aggregates, because of the geometric mismatch between different ligands. As compared with **3.04**, **3.05**, and **3.11** formed from building blocks of the same geometry, such

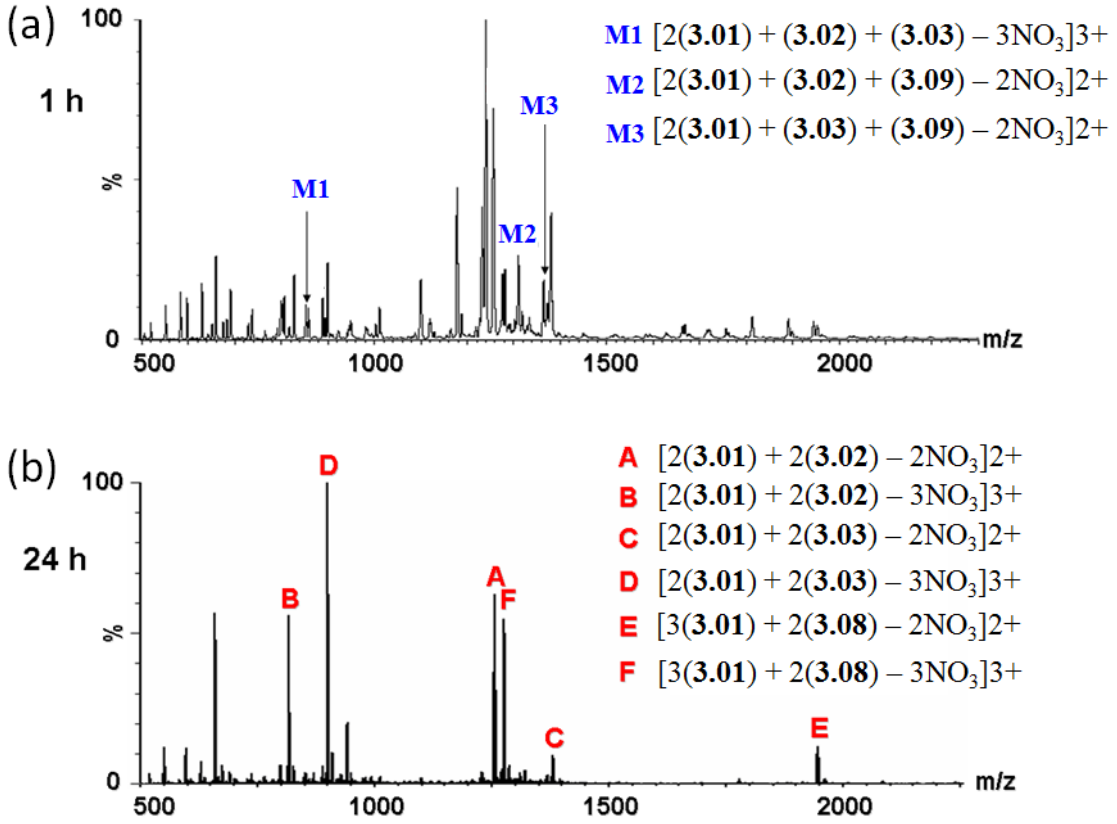

Figure 3.12. Full ESI mass spectrum (Acetone-d_6/D_2O 1:1) recorded for **SS_4** at 1 h (a) and 24 h (b) time intervals during the formation of supramolecular rectangles **3.04** and **3.05** and prism **3.11**

multicomponent structures are enthalpically and entropically unfavored. Thus, thermodynamically-selective dynamic self-assembly allows for **3.04**, **3.05**, and **3.11** to be generated, embodying geometry-directed self-sorting.

3.2.8 Variables that affect the fidelity of self-sorting processes

In addition to geometric differences, experimental factors such as temperature and solvent may influence the efficiency of self-sorting during coordination-driven self-assembly. The dynamics of self-sorting are largely dependent on temperature and solvent, and therefore, the effects of varying these two parameters have been investigated in the cases of $\mathbf{SS_4}$ and $\mathbf{SS_9}$.

To investigate the effect of temperature changes on self-sorting processes, the molecular subunits of $\mathbf{SS_4}$ were mixed in an aqueous acetone solution (*v/v* 1:1) and heated at 65–70 ℃ for 1 h. As a result, disordered oligomeric species were formed via the initial random combination of acceptors and donors as implied by the $^{31}P\{^1H\}$ (Figure 3.13a) and ^1H NMR spectra. This mixture was then separated into three samples that were kept at 25–30 ℃, 45–50 ℃, and 65–70 ℃, respectively, until each reached thermodynamic equilibrium. ^{31}P and ^1H multinuclear NMR spectroscopy was used to monitor the self-sorting process within each mixture. Results from the $^{31}P\{^1H\}$ NMR spectra of these three mixtures, shown in Figure 3.13b-d**,** as well as the ^1H NMR spectra, indicate that a decrease of temperature causes a significant decrease in the rate of the self-sorting process: Decreasing the reaction temperature from 65–70 ℃ to 45–50 ℃ resulted in a significant increase in the time required for self-sorting (from 24 h to 120 h), while at low temperatures of 25–30 ℃, the self-sorting process occured extremely slowly and could

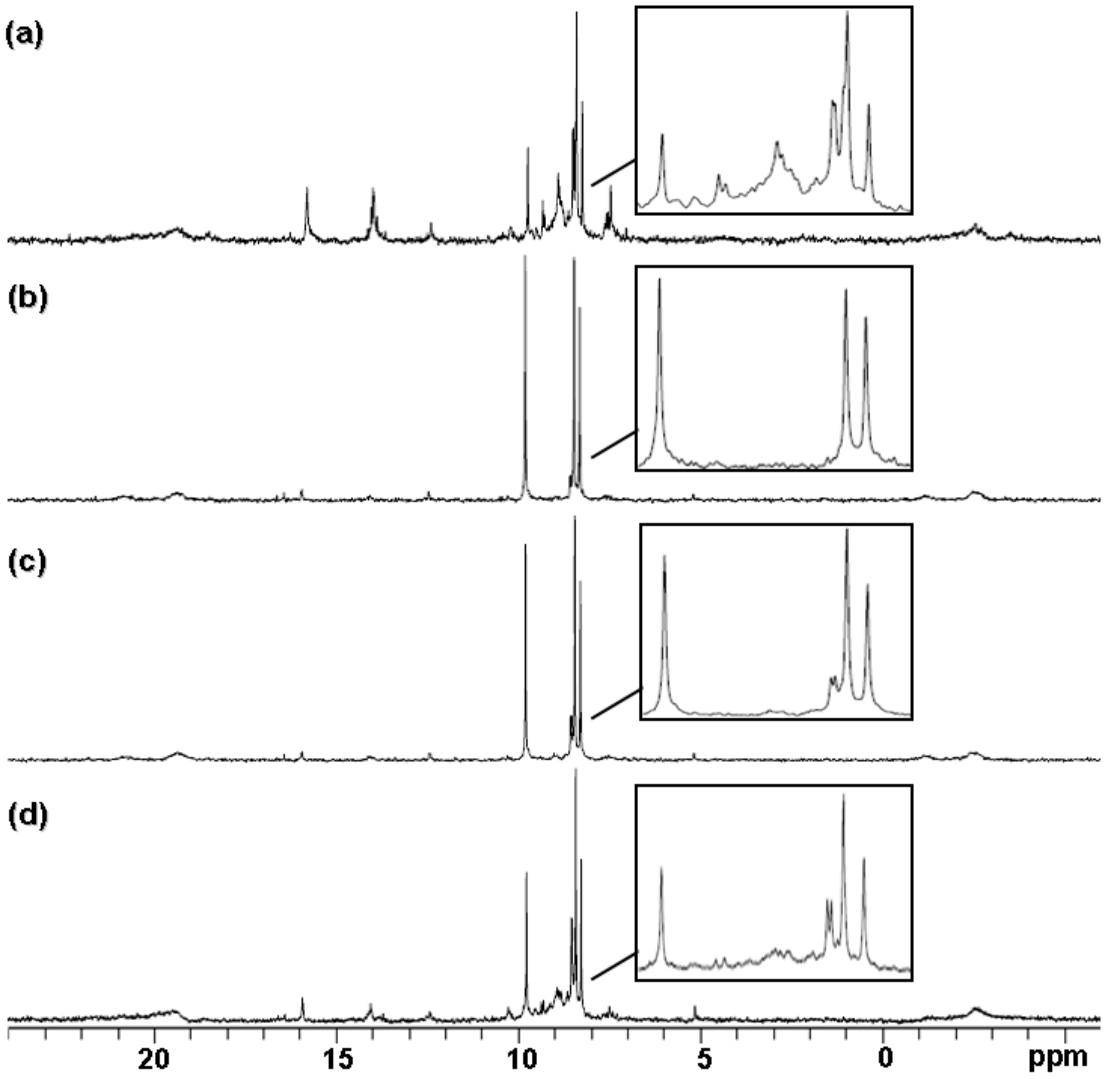

Figure 3.13. $^{31}P\{^{1}H\}$ NMR spectra (Acetone-d_6/D_2O 1:1) recorded for mixtures of **SS_4** (**3.04**, **3.05**, and **3.11**) heated at (a) 65–70 ℃ for 1 h, (b) 65–70 ℃ for 24 h, (c) 45-50 ℃ for 120 h, and (d) 25-30 ℃ for 20 d.

not reach an equilibrium even after 20 d. Similar temperature effects were found within the self-sorting system **SS$_9$** as indicated by the multinuclear NMR spectral results.

Self-assembly is sensitive to changes of solvent due to the different thermodynamic stabilities of the species formed by the self-assembly of molecular subunits in different media. To test how solvent affects self-sorting, a study of both **SS$_4$** and **SS$_9$** was carried out in two different solvent systems: CD_2Cl_2 and Acetone-d_6/D_2O (20:1). The self-sorted mixtures were obtained by initial heating of an aqueous acetone solution (*v/v* 1:1) for 24 h, then concentrating to dryness and redissolving in either CD_2Cl_2 or Acetone-d_6/D_2O (20:1), and finally heating each (CD_2Cl_2: 45–50 ℃; Acetone-d_6/D_2O (20:1): 60–65 ℃) until achieving equilibrium. As characterized by ^{31}P and ^{1}H multinuclear NMR spectroscopy, the nature of the solvent has little effect in **SS$_9$**, but significantly affects the self-sorting system **SS$_4$**.

Mixtures of **SS$_9$** in either CD_2Cl_2 or Acetone-d_6/D_2O (20:1) were capable of self-sorting after 36 h of heating as evidenced by the identifiable signals corresponding to the discrete supramolecular species in the $^{31}P\{^{1}H\}$ and ^{1}H NMR spectra. However, in the case of **SS$_4$**, supramolecular species **3.04**, **3.05**, and **3.11** in the mixtures of both CD_2Cl_2 and Acetone-d_6/D_2O (20:1) were significantly disordered after 36 h heating, as evidenced by the replacement of three intense peaks with multiple unassignable signals within the $^{31}P\{^{1}H\}$ NMR spectra (Figure 3.14b-c) and the appearance of broad signals in the ^{1}H NMR spectra. Thus, destruction of the ordered supramolecular species occurred as a result of the change of solvent for **SS$_4$**. Moreover, it was found that the solvent effects on **SS$_4$** were reversible. Upon concentrating the disordered CD_2Cl_2 or Acetone-d_6/D_2O (20:1) mixture of **SS$_4$** to dryness and redissolving in Acetone-d_6/D_2O (1:1), the self-sorted

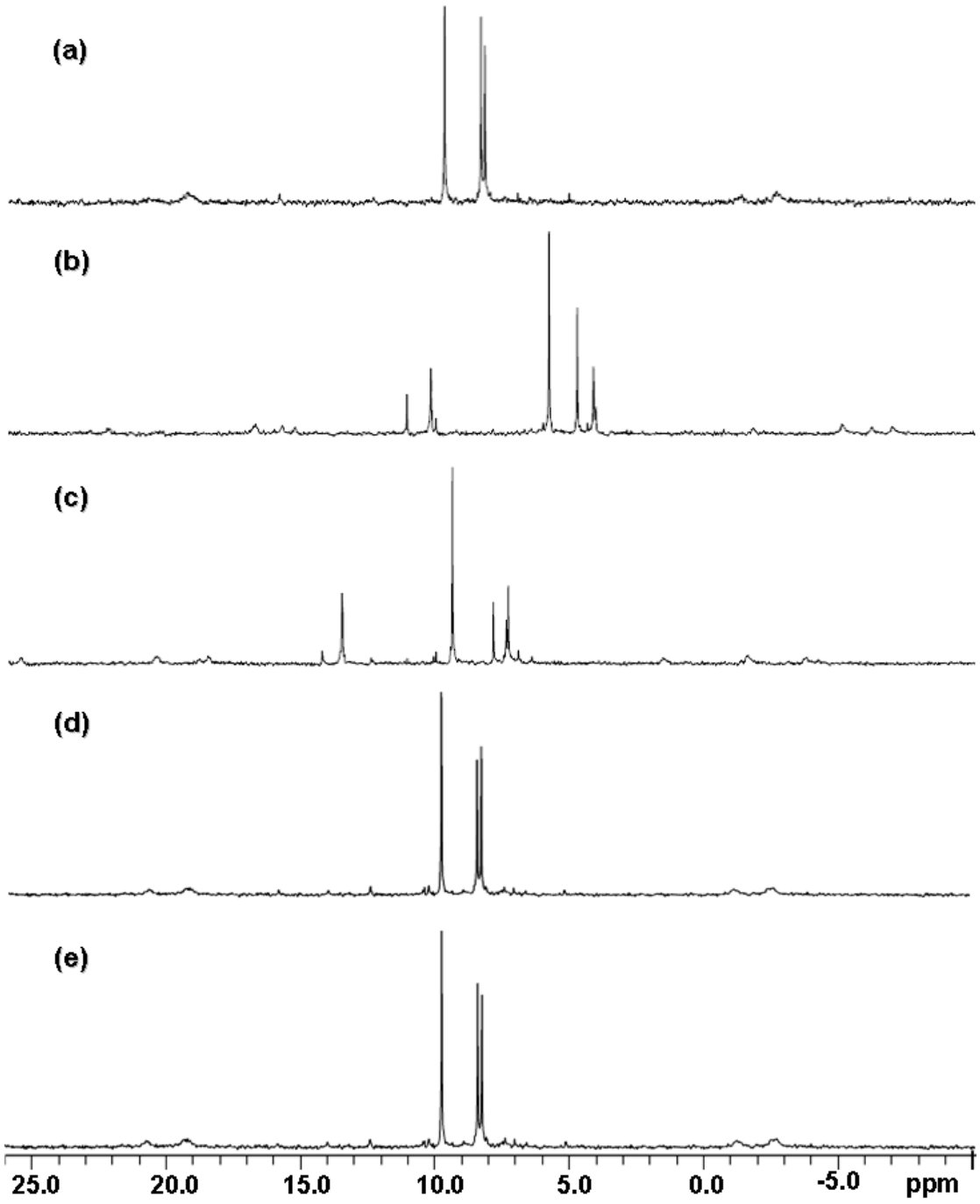

Figure 3.14. $^{31}P\{^{1}H\}$ NMR spectra of **SS$_4$** in varied solvents: (a) Acetone-d_6/D_2O (1:1), (b) CD_2Cl_2, (c) Acetone-d_6/D_2O (20:1), (d) Acetone-d_6/D_2O (1:1) after removal of CD_2Cl_2, and (e) Acetone-d_6/D_2O (1:1) after removal of Acetone-d_6/D_2O (20:1).

mixture was again achieved as evidenced by the $^{31}P\{^{1}H\}$ (Figure 3.14d–e) and ^{1}H NMR spectra. Hence, the combined data indicate that the choice of solvent is critical to the efficiency of self-sorting in the coordination-driven self-assembly of organoplatinum supramolecules.

3.3 Conclusion

In conclusion, both the three- and four-component self-sorting of twelve different complex mixtures has been clearly demonstrated, each of which is capable of selectively producing discrete supramolecular structures of a variety of 2D and 3D topologies. In all self-sorting systems, the formation of discrete self-sorted products is supported by multinuclear NMR spectroscopy and ESI mass spectrometry. The observed self-sorting can be directed by either size alone or together with the angles and number of binding sites of organic ligands. Such self-sorting is achieved via a thermodynamic self-correction process, by which multicomponent species can be gradually "corrected" to two-component products. In addition, the experimental variables of temperature and solvent have been investigated and shown to be capable of affecting such self-sorting systems. As expected, temperature changes have a dramatic effect on the rate of the self-sorting process. Different solvents present a significant, yet reversible, change in the fidelity of self-sorting.

The successful self-sorting in twelve systems, including ten different 2D and 3D supramolecular structures (**3.04**, **3.05**, **3.11**, **3.12**, **3.14**, **3.07**, **3.08**, **3.17**, **3.18**, and **3.19**) and six different structural motifs (rectangle, triangle, rhomboid, normal and distorted triangular prism, and triangular bipyramid), reveals the high generality of geometrically-directed self-sorting behavior in the coordination-driven self-assembly of supramolecular

polygons and cages, and also represents a promising approach towards the build-up of structurally diverse multicomponent supramolecular systems. The implications of this research go beyond the comprehensive study of self-sorting in coordination driven self-assembly; Many recent reports have been focused on the synthesis and self-assembly of functionalized supramolecules.[15] Provided that high-fidelity self-sorting can be extended to these new functionalized systems, this current research can be extended to the development of multifunctionalized, multicomponent supramolecular systems. The spontaneous self-assembly and self-sorting of multiple, discrete, functionalized supramolecules could lead to integrated systems wherein many functional molecules are able to collaborate to achieve functions in a manner akin to natural biological systems. Thus, we envision that detailed studies of the self-sorting of multicomponent supramolecular systems can pave the way towards the construction of complex, functional systems and have implications in the related processes that govern the assembly of more complex biological structures throughout nature.

3.4 References

(1) (a) Lehn, J.-M. *Science* **2002**, *295*, 2400. (b) Lehn, J.-M. *Rep. Prog. Phys.* **2004**, *67*, 249. (c) Hollingsworth, M. D. *Science* **2002**, *295*, 2410. (d) Wu, A.; Isaacs, L. *J. Am. Chem. Soc.* **2003**, *125*, 4831.

(2) (a) Krämer, R.; Lehn, J.-M.; Marquis-Rigault, A. *Proc. Natl. Acad. Sci. U.S.A.* **1993**, *90*, 5394. (b) Caulder, D. L.; Raymond, K. N. *Angew. Chem., Int. Ed. Engl.* **1997**, *36*, 1440. (c) Masood, M. A.; Enemark, E. J.; Stack, T. D. P. *Angew. Chem., Int. Ed.* **1998**, *37*, 928. (d) Enemark, E. J.; Stack, T. D. P. *Angew. Chem., Int. Ed.* **1998**, *37*, 932. (e) Stiller, R.; Lehn, J.-M. *Eur. J. Inorg. Chem.* **1998**, 977. (f) Taylor, P. N.; Anderson, H. L. *J. Am. Chem. Soc.* **1999**, *121*, 11538. (g) Albrecht, M.; Schneider, M.; Röttele, H. *Angew. Chem., Int. Ed* **1999**, *38*, 557. (h) Kondo, T.; Oyama, K.-I.; Yoshida, K. *Angew. Chem., Int. Ed.* **2001**, *40*, 894. (i) Pinalli, R.; Cristini, V.; Sottili, V.; Geremia, S.; Campagnolo, M.; Caneschi, A.; Dalcanale E. *J. Am. Chem. Soc.* **2004**, *126*, 6516. (j) Kamada, T.; Aratani, N.; Ikeda, T.; Shibata, N.; Higuchi, Y.; Wakamiya A.; Yamaguchi, S.; Kim, K. S.; Yoon, Z. S.; Kim, D.; Osuka A. *J. Am. Chem. Soc.* **2006**, *128*, 7670. (k) Saur, I.; Scopelliti, R.;

Severin, K. *Chem. Eur. J.* **2006**, *12*, 1058. (l) Langner, A.; Tait, S. L.; Lin, N.; Rajadurai, C.; Ruben, M.; Kern, K. *Proc. Natl. Acad. Sci. U.S.A.* **2007**, *104*, 17927.

(3) (a) Jolliffe, K. A.; Timmerman, P.; Reinhoudt, D. N. *Angew. Chem., Int. Ed.* **1999**, *38*, 933. (b) Cai, M.; Shi, X.; Sidorov, V.; Fabris, D.; Lam, Y.-F.; Davis, J. T. *Tetrahedron* **2002**, *58*, 661. (c) Corbin, P. S.; Lawless, L. J.; Li, Z.; Ma, Y.; Witmer, M. J.; Zimmerman, S. C. *Proc. Natl. Acad. Sci. U.S.A.* **2002**, *99*, 5099. (d) Ma, Y.; Kolotuchin, S. V.; Zimmerman, S. C. *J. Am. Chem. Soc.* **2002**, *124*, 13757. (e) Wu, A.; Chakraborty, A.; Fettinger, J. C.; Flowers, R. A., II.; Isaacs, L. *Angew. Chem., Int. Ed.* **2002**, *41*, 4028. (f) Mukhopadhyay, P.; Zavalij, P. Y.; Isaacs, L. *J. Am. Chem. Soc.* **2006**, *128*, 12098.

(4) (a) Bilgiçer, B.; Xing, X.; Kumar, K. *J. Am. Chem. Soc.* **2001**, *123*, 11815. (b) Schnarr, N. A.; Kennan, A. J. *J. Am. Chem. Soc.* **2003**, *125*, 667.

(5) (a) Rowan, S. J.; Hamilton, D. G.; Brady, P. A.; Sanders, J. K. M. *J. Am. Chem. Soc.* **1997**, *119*, 2578. (b) Rowan, S. J.; Reynolds, D. J.; Sanders, J. K. M. *J. Org. Chem.* **1999**, *64*, 5804. (c) Rowan, S. J.; Cantrill, S. J.; Cousins, G. R. L.; Sanders, J. K. M.; Stoddart, J. F. *Angew. Chem., Int. Ed.* **2002**, *41*, 2943. (d) Corbett, P. T.; Leclaire, J.; Vial, L.; West, K. R.; Wietor, J.-L.; Sanders, J. K. M.; Otto, S. *Chem. Rev.* **2006**, *106*, 3652.

(6) Ziegler, M.; Miranda, J. J.; Andersen, U. N.; Raymond, K. N. *Angew. Chem., Int. Ed.* **2001**, *40*, 733.

(7) (a) Addicott, C.; Das, N.; Stang, P. J. *Inorg. Chem.* **2004**, *43*, 5335. (b) Yang, H.-B.; Ghosh, K.; Northrop, B. H.; Stang, P. J. *Org. Lett.* **2007**, *9*, 1561.

(8) (a) Stang, P. J.; Olenyuk, B. *Acc. Chem. Res.* **1997**, *30*, 502. (b) Leininger, S.; Olenyuk, B.; Stang, P. J. *Chem. Rev.* **2000**, *100*, 853. (c) Seidel, S. R.; Stang, P. J. *Acc. Chem. Res.* **2002**, *35*, 972. (d) Schwab, P. F. H.; Levin, M. D.; Michl, J. *Chem. Rev.* **1999**, *99*, 1863. (e) Holliday, B. J.; Mirkin, C. A. *Angew. Chem. Int. Ed.* **2001**, *40*, 2022. (f) Cotton, F. A.; Lin, C.; Murillo, C. A. *Acc. Chem. Res.* **2001**, *34*, 759. (g) Fujita, M.; Tominaga, M.; Hori, A.; Therrien, B. *Acc. Chem. Res.* **2005**, *38*, 369. (h) Fiedler, D.; Leung, D. H.; Bergman, R. G.; Raymond, K. N. *Acc. Chem. Res.* **2005**, *38*, 349.

(9) Kuehl, C. J.; Huang, S. D.; Stang, P. J. *J. Am. Chem. Soc.* **2001**, *123*, 9634.

(10) Kryschenko, Y. K.; Seidel, S. R.; Arif, A. M.; Stang, P. J. *J. Am. Chem. Soc.* **2003**, *125*, 5193.

(11) Yang, H.-B.; Ghosh, K.; Arif, A. M.; Stang, P. J. *J. Org. Chem.* **2006**, *71*, 9464.

(12) Kuehl, C. J.; Kryschenko, Y. K.; Radhakrishnan, U.; Seidel, S. R.; Huang, S. D.; Stang, P. J. *Proc. Natl. Acad. Sci. U.S.A.* **2002**, *99*, 4932.

(13) Addicott, C.; Oesterling, I.; Yamamoto, T.; Muellen, K.; Stang, P. J. *J. Org. Chem.* **2005**, *70*, 797.

(14) Kuehl, C. J.; Yamamoto, T.; Seidel, S. R.; Stang, P. J. *Org. Lett.* **2002**, *4*, 913.

(15) (a) Yang, H.-B.; Das, N.; Huang, F.; Hawkridge, A. M.; Muddiman, D. C.; Stang, P. J. *J. Am. Chem. Soc.* **2006**, *128*, 10014. (b) Yang, H.-B.; Hawkridge, A. M.; Huang, S. D.; Das, N.; Bunge, S. D.; Muddiman, D. C.; Stang, P. J. *J. Am. Chem. Soc.* **2007**, *129*, 2120. (c) Yang, H.-B.; Ghosh, K.; Northrop, B. H.; Zheng, Y.-R.; Lyndon, M. M.; Muddiman, D.C.; Stang, P. J. *J. Am. Chem. Soc.* **2007**, *129*, 14187. (d) Yang, H.-B.; Ghosh, K.; Zhao, Y.; Northrop, B. H.; Lyndon, M. M.; Muddiman, D. C.; White, H. S.; Stang, P. J. *J. Am. Chem. Soc.* **2008**, *130*, 839. (e) Ghosh, K; Yang, H.-B.; Northrop, B. H.; Lyndon, M. M.; Zheng, Y.-R.; Muddiman, D. C.; Stang, P. J. *J. Am. Chem. Soc.* **2008**, *130*, 5320. (f) Brian, H. N.; Yang, H.-B.; Stang, P. J. *Chem. Commun.* **2008**, 5896.

CHAPTER 4

SELECTIVE SELF-ASSEMBLY OF MULTICOMPONENT SUPRAMOLECULAR STRUCTURES AND SUPRAMOLECULAR TRANSFORMATION

4.1 Introduction

Over the last two decades, the design of coordination-driven self-assembly has been largely constrained to two-component assembly, in which only one metallic and one organic component is used.[1-5] The two-component assembly endows coordination-driven self-assembly with easy control and design, but significantly limits the versatility of molecular components involved, and, therefore, the diversity of supramolecules assembled.[6] With the aim of broadening the diversity of coordination-driven self-assembly, it is essential to explore controlled self-assembly within a multicomponent system.

Multicomponent selective self-assembly represents a unique self-assembly process by which multiple components can selectively recognize and combine with each other to generate one singular supramolecular structure within a mixture.[7] In the area of coordination-driven self-assembly, several methods have been developed to achieve multicomponent selective self-assembly. Sauvage[11] and Lehn,[12] in a pioneering study, used topological information to guide the selective self-assembly of multicomponent pseudorotaxanes. Recently, it was found that steric hindrance could be exploited to

control multicomponent selective self-assembly, as shown by the impressive examples from Schmittel,[13] Fujita,[14] and Kobayashi.[15] However, incorporation of either topological or steric information into molecular components requires significant synthetic effort. Fujita demonstrated a facile selective self-assembly of a 3D trigonal prism by mixing Palladium (II) acceptors with di- and trioptic pyridyl ligands, but a template was essential for this self-assembly.[16]

In our recent reports,[17] we demonstrated that square planar Pt(II) was able to selectively coordinate with one carboxylate and one pyridyl ligand to form an asymmetrical self-assembly. This selective self-assembly has also been observed in similar Pd(II) coordination complexes.[18] In these studies, both carboxylate and pyridyl compartments are integrated in one molecular building block. By separating the carboxylate and pyridyl components onto two different molecular subunits, selective self-assembly may result in an efficient way to form multicomponent ensembles with Pt(II) acceptors. In this chapter, we present a design of multicomponent selective self-assembly using the coordination-driven self-assembly of a 90^{o} Pt(II) acceptor with various carboxylate ligands and pyridyl donors. A judicious choice of molecular building blocks permits selective self-assembly in the formation of a variety of three-component 2D supramolecular rectangles and 3D prisms in a simple, efficient manner.

In addition to being a useful method for building multicomponent supramolecular architectures, selective self-assembly can also be used to achieve supramolecular transformations. Supamolecular transformations represent a novel supramolecular phenomenon whereby a supramolecular species can alter its structure (and composition) upon suitable external stimulus. Such supramolecular transformations have been reported

that rely upon triggering by light, solvent variation, or chemical signals.[19] For example, Mirkin et al. reported a novel synthetic strategy for the spontaneous and reversible transformation between a homochiral helical polymer and a metal-organic triangle simply through the addition of an appropriate solvent.[19b] Recently, we have also demonstrated a supramolecular transformation from a large hexagon to two smaller triangles by alternation of the structural configuration of the molecular subunits.[19c] In this chapter, we investigate supramolecular transformations based on multicomponent selective self-assembly. Upon addition of suitable molecular components or supramolecules, selective self-assembly results in either a global change or partial modification of the staring two-component structures.

4.2 Results and Discussion

4.2.1 Selective self-assembly of a multicomponent supramolecular rectangle

Cis-$Pt(PEt_3)_2(OTf)_2$ **4.01** was mixed with dicarboxylate ligand **4.02** and linear dipyridyl donor **4.03** in a 2:1:1 ratio, followed by the addition of D_2O and Acetone-d_6. After 3h of heating at 75 ℃, all solvent was removed from the clear solution, and Acetone-d_6 was added into the mixture. An equilibrium was reached after an additional 5 h of heating at 75 ℃, forming the supramolecular rectangle **4.04**, as shown in Scheme 4.1. ^{31}P and ^{1}H multinuclear NMR spectroscopy and ESI mass spectrometry were used to characterize **4.04**.

In the $^{31}P\{^{1}H\}$ NMR spectrum (Figure 4.1b), two coupled doublets at 6.60 ppm and 1.06 ppm ($^{2}J_{P\text{-}P}$ = 22.0 Hz) of approximately equal intensity with concomitant ^{195}Pt satellites were found, indicating that the Pt(II) centers of **4.04** bear a three-component

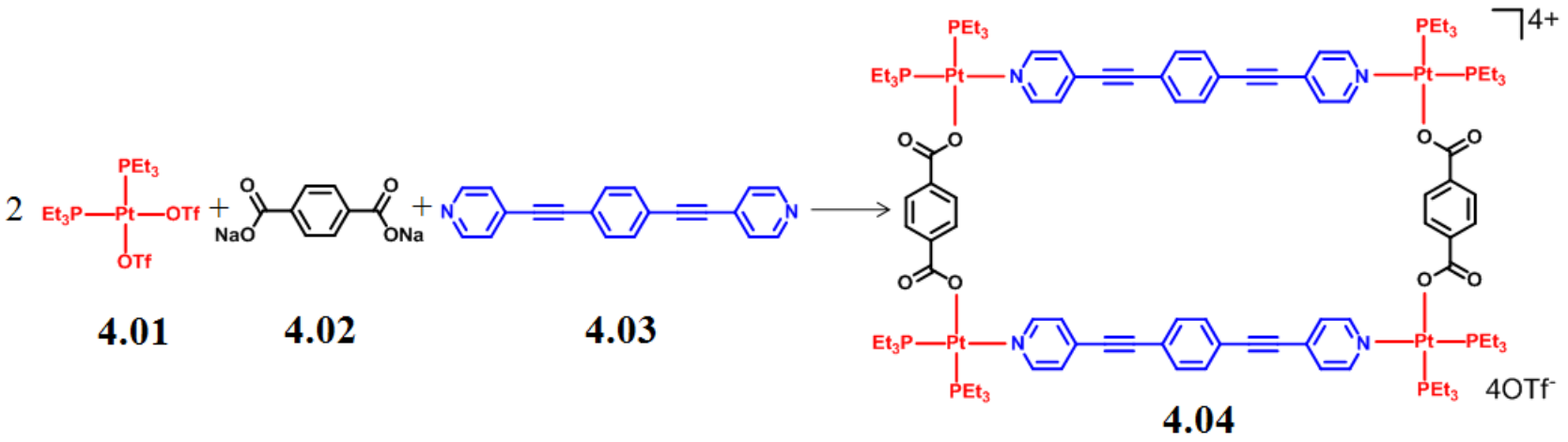

Scheme 4.1. Selective self-assembly of a multicomponent rectangle **4.04** by the combination of *cis*-$Pt(PEt_3)_2(OTf)_2$ **4.01**, dicarboxylate ligand **4.02**, and linear dipyridyl donor **4.03**.

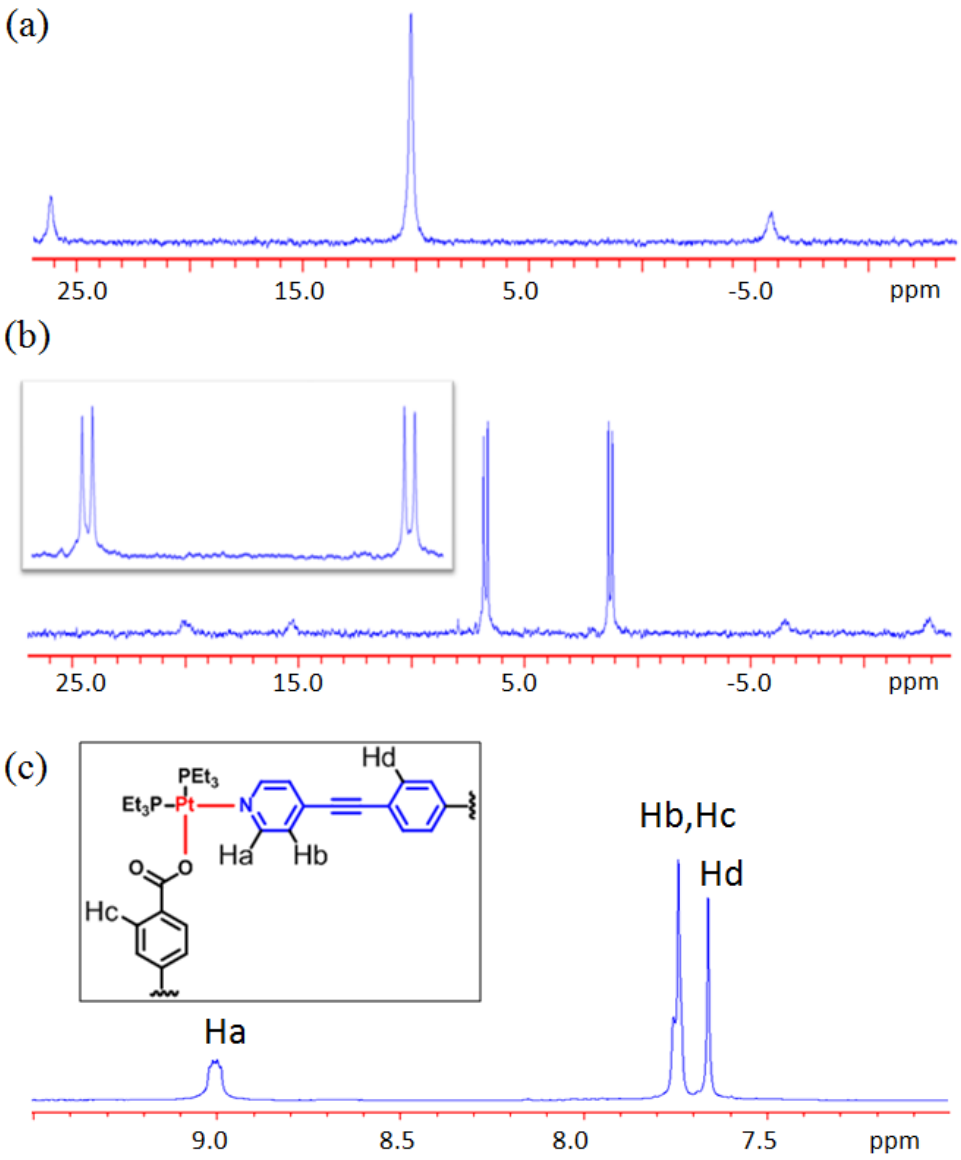

Figure 4.1. $^{31}P\{^{1}H\}$ NMR spectra of *cis*-$Pt(PEt_3)_2(OTf)_2$ **4.01** (a) the multicomponent supramolecular rectangle **4.04** (b), and partial ^{1}H NMR spectrum (c) of **4.04**.

coordination motif with pyridyl and carboxylate moieties.[20] The doublet at 1.06 ppm is shifted approximately 12 ppm upfield relative to **4.01** (Figure 4.1a) upon coordination, and corresponds to the phosphorous nuclei trans to the pyridine ring, while the doublet at 6.60 ppm is due to the phosphorous nuclei opposite to the carboxylate group.[20a–c] The two signals are coupled indicating that chemically inequivalent phosphorous nuclei are bound to the same Pt(II) centers. This is expected for the three-component coordination motif of rectangle **4.04**. In the ^{1}H NMR spectrum (Figure 4.1c), signals corresponding to the coordinated pyridine and carboxylate ligands were identified at 9.00 ppm ($H_{\alpha\text{-Py}}$), 7.74 ppm ($H_{\beta\text{-Py}}$), and 7.66 ppm (H_{phenyl}). The sharp and identifiable signals in both the $^{31}P\{^{1}H\}$ and ^{1}H NMR spectra support the self-assembly of the highly symmetric rectangle **4.04** as the predominant product in the mixture, and rule out the formation of two-component assemblies or oligomers. ESI mass spectrometry further confirms the formation of a [4+2+2] multicomponent supramolecular rectangle, **4.04**. In Figure 4.2, peaks attributable to **4.04** with the loss of two and three triflate anions can be observed at *m/z* = 1455.69 ($[M - 2OTf]^{2+}$) and *m/z* = 920.88 ($[M - 3OTf]^{3+}$). All these peaks are isotopically resolved and in good agreement with their theoretical distributions.

4.2.2 Selective self-assembly of multicomponent supramolecular prisms

To date, the selective self-assembly of 3D supramolecules has always required a template,[16] and rarely occurs based solely on the intrinsic information of the complementary subunits.[13] Herein, we present a selective self-assembly of 3D supramolecular prisms by mixing a 90^{o} Pt(II) acceptor, carboxylate ligands, and different multipyridyl ligands, as shown in Scheme 4.2.

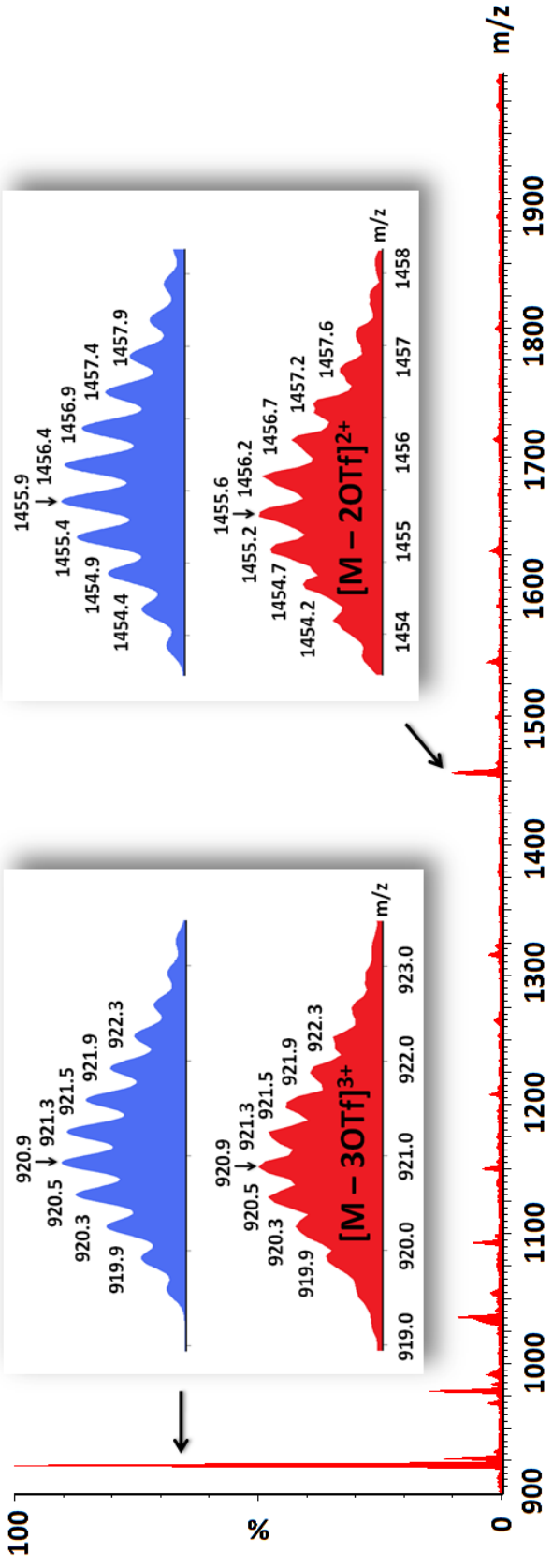

Figure 4.2. Full ESI mass spectrum of the solution of the multicomponent supramolecular rectangle **4.04**.

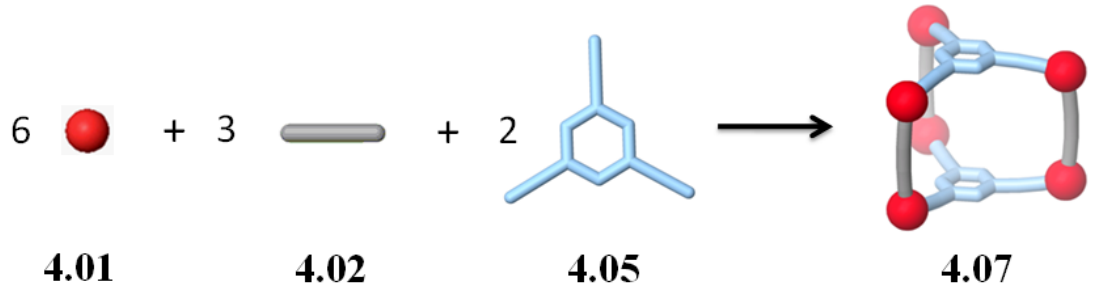

4.01 **4.02** **4.05** **4.07**

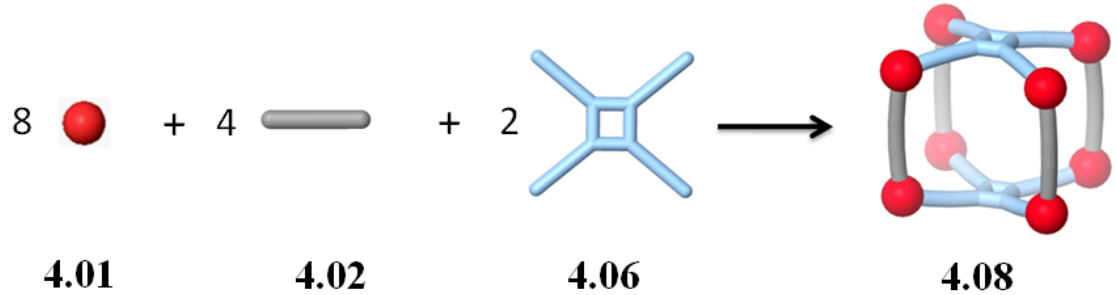

4.01 **4.02** **4.06** **4.08**

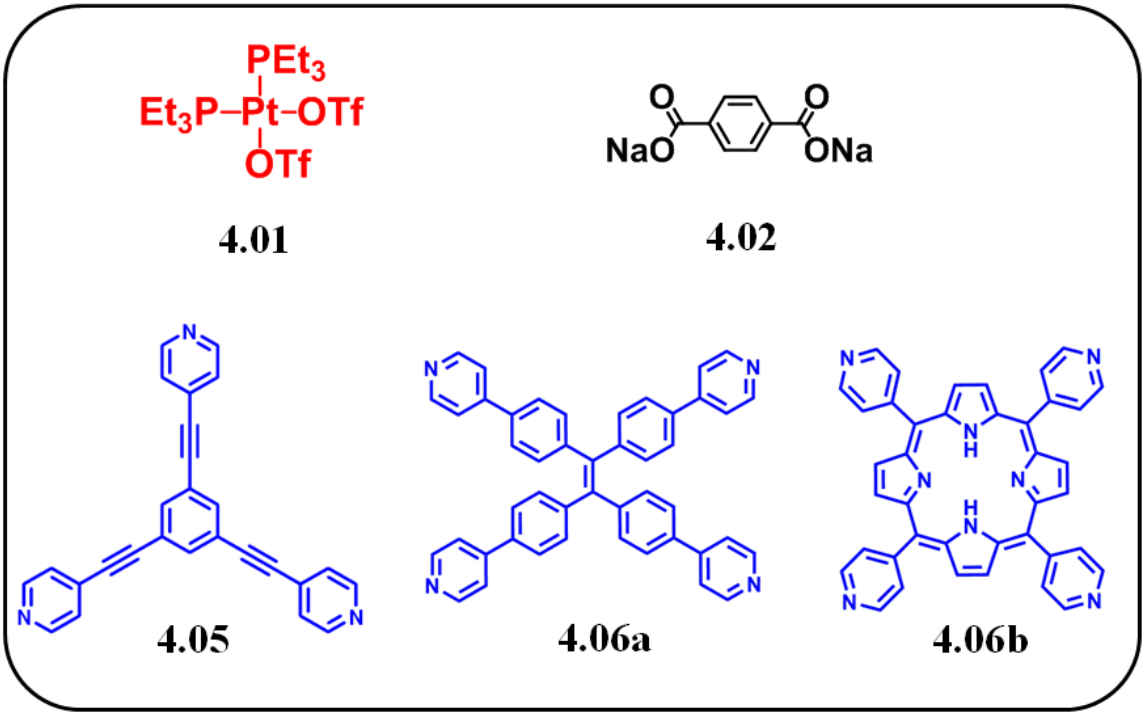
PEt3
Et3P–Pt–OTf
OTf
O
O
NaO
ONa
N
N
N

Mixing *cis*-$Pt(PEt_3)_2(OTf)_2$ **4.01** and carboxylate ligand **4.02** with tri-/tetrapyridyl donors **4.05**/**4.06** in a specific ratio (for **4.07**: **1**:**2**:**5** = 6:3:2; for **4.08**: **1**:**2**:**6** = 8:4:2), after equilibration, supramolecular prisms **4.07** and **4.08** were formed as the predominant species. The $^{31}P\{^1H\}$ NMR spectra (Figure 4.3) of **4.07** and **4.08** are dominated by two coupled doublets (**7**: 6.56 ppm and 1.01 ppm, $^2J_{P\text{-}P}$ = 22.0 Hz; **4.08a**: 5.88 ppm and 1.08 ppm, $^2J_{P\text{-}P}$ = 21.4 Hz; **4.08b**: 5.07 ppm and -0.34 ppm, $^2J_{P\text{-}P}$ = 21.4 Hz) of similar intensity with concomitant ^{195}Pt satellites. These data, as expected, confirm the three-component coordination environment of supramolecular prisms **4.07**/**4.08** and rule out the formation of two-component complexes or oligomers. Likewise, in the ^1H NMR spectra, signals attributable to the coordinated pyridyl and carboxylate moieties are observed for **4.07**: 9.02 ppm ($H_{\alpha\text{-}Py}$), 7.75 ppm ($H_{\beta\text{-}Py}$), 7.77 ppm (H_{phenyl}); for **4.08a**: 8.87 ppm ($H_{\alpha\text{-}Py}$), 7.89 ppm ($H_{\beta\text{-}Py}$), 7.60 ppm (H_{phenyl}); for **4.08b**: 9.27 ppm ($H_{\alpha\text{-}Py}$), 8.34 ppm ($H_{\beta\text{-}Py}$), 8.09 ppm (H_{phenyl}). The sharp signals in both the $^{31}P\{^1H\}$ and ^1H NMR spectra support the formation of highly symmetric supramolecules **4.07** and **4.08**.

ESI mass spectral results further support the self-assembly of supramolecular prisms **4.07** and **4.08**. As shown in Figure 4.4, intense ESI mass peaks corresponding to consecutive loss of triflate anions from trigonal prism **4.07**: *m/z* = 2218.76 $[M - 2OTf]^{2+}$ and *m/z* = 1429.59 $[M - 3OTf]^{3+}$ were observed, as were those corresponding to the tetragonal prisms: **4.08a** at *m/z* = 2037.75 $[M - 3PF_6]^{3+}$ and *m/z* = 1164.50 $[M - 5PF_6]^{6+}$ and **4.08b** at *m/z* = 2022.71 $[M - 3PF_6]^{3+}$ and *m/z* = 1155.62 $[M - 5PF_6]^{5+}$. All of these peaks are isotopically resolved and agree well with their theoretical distributions.

While suitable X-ray-quality crystals were not obtained, a computational study together with PGSE NMR measurements was carried out to gain insight into the

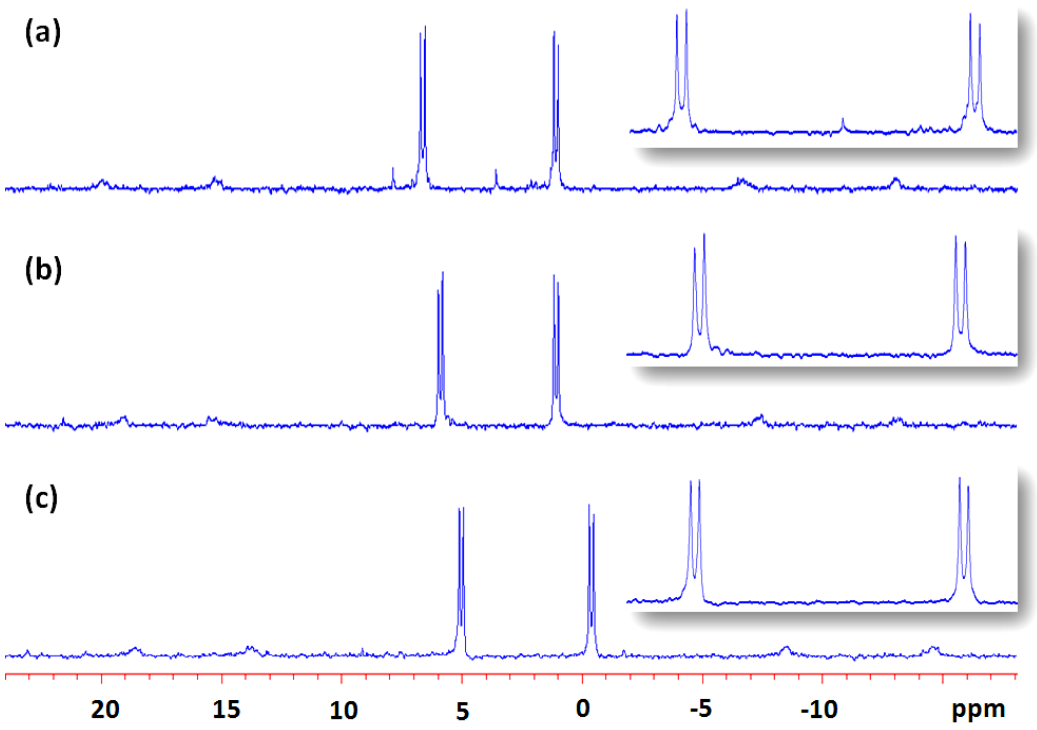

Figure 4.3 $^{31}P\{^{1}H\}$ NMR spectra of the trigonal prism **4.07** (a) and tetragonal prisms **4.08a** (b) and **4.08b** (c).

structural characteristics of these assemblies.[21] A molecular dynamics simulation using Maestro and Macromodel with a MMFF or MM2* force field, at 300K, in the gas phase was applied to equilibrate each supramolecule, and the output of the simulation was then minimized to full convergence. As shown in Figure 4.5, models of assemblies **4.07** and **4.08** adopt trigonal and tetragonal prismatic structures, respectively, with radii of 1.2 nm (**4.07**), 1.3 nm (**4.08a**), and 1.2 nm (**4.08b**). PGSE NMR experiments were carried out to measure the hydrodynamic radius for these assemblies, and the results agree with the values from the model structures: 1.21 ± 0.01 nm (**4.07**), 1.16 ± 0.03 nm (**4.08a**), and 1.09 ± 0.01 nm (**4.08b**).

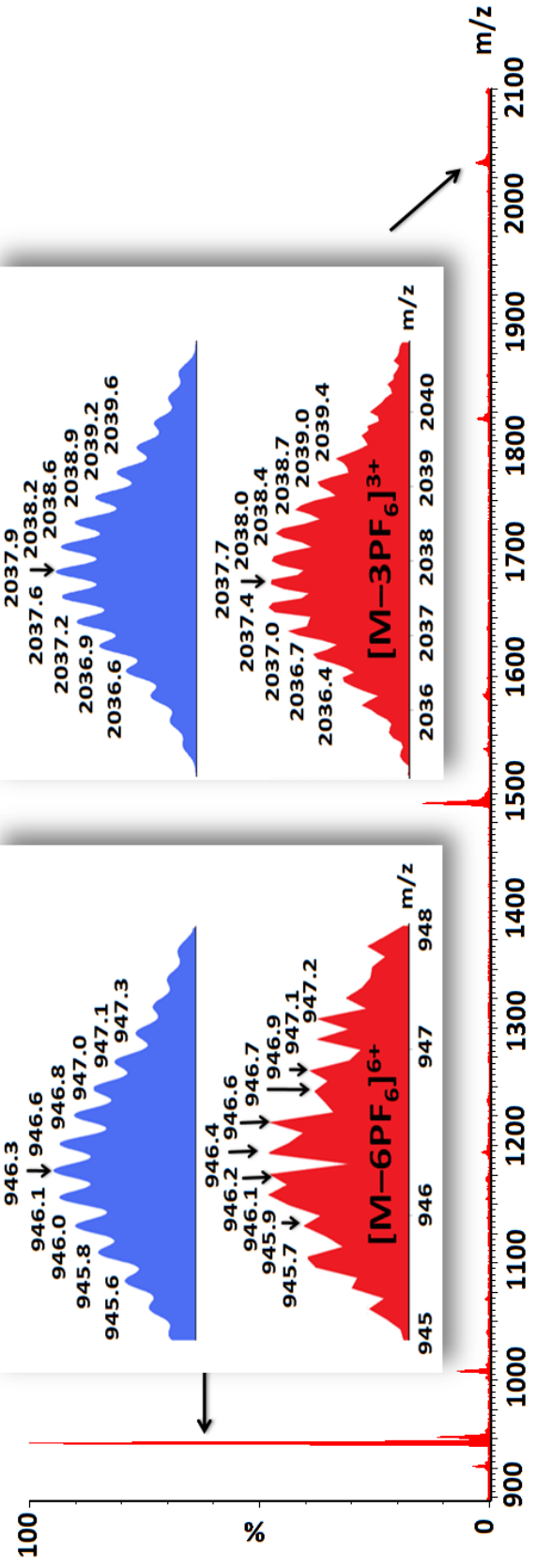

Figure 4.4. Full ESI mass spectrum of the solution of the multicomponent supramolecular tetragonal prism **4.08a**.

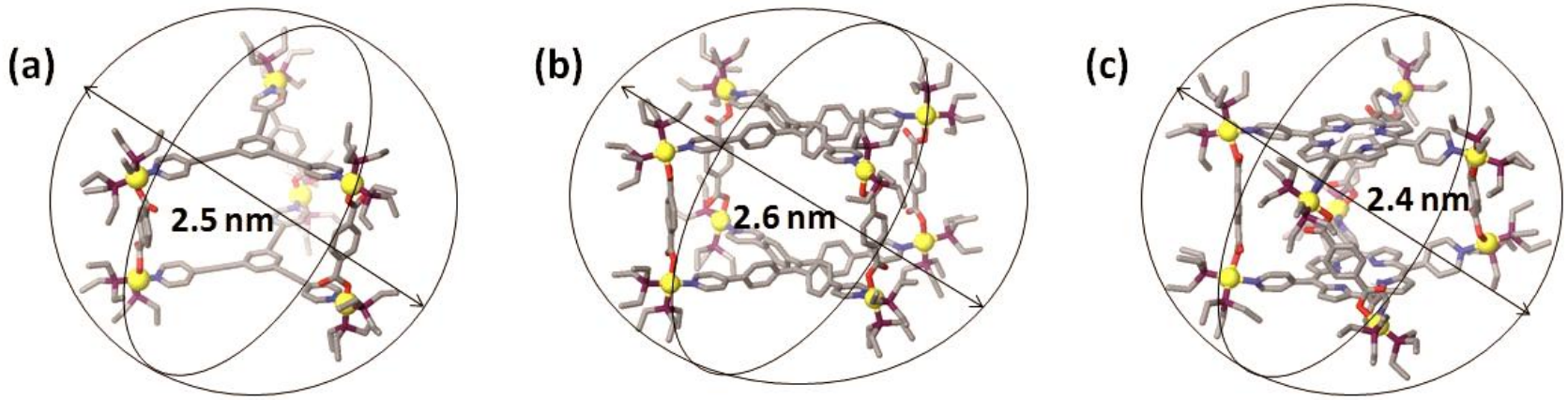

Figure 4.5. Computational simulations of trigonal prism **4.07** (a) and tetragonal prisms **4.08a** (b) and **4.08b** (c).

4.2.3 Selective self-assembly of multicomponent hexagonal prisms of variable size

The formation of hexagonal prisms of variable size can be achieved by the design shown in Scheme 4.3. The linear carboxylate donors **4.02**, **4.09**, and **4.10** are used as pillars, whereas hexa-(4-(4-pyridyl)phenyl) benzene **4.11**, containing six pyridyl groups, and cis-$Pt(PEt_3)_2(OTf)_2$ **4.01** are selected as faces and corners, respectively. Hexapyridyl donor **1** and carboxylate ligands **4.02**, **4.09**, or **4.10** were mixed with acceptor *cis*-$Pt(PEt_3)_2(OTf)_2$ **4.01** in a 1:3:6 ratio and heated at 50–56 ℃ for 6 h in aqueous acetone. Upon ion exchange with KPF_6, hexagonal prisms **4.12**–**4.14** were obtained. The $^{31}P\{^1H\}$NMR spectra of prisms **4.12**–**4.14** showed two coupled doublets peaks (**4.12**: 6.19 and 1.06 ppm, $^2J_{p\text{-}p}$ = 21.30 Hz; **4.13**: 6.56 and 1.10 ppm, $^2J_{p\text{-}p}$ = 21.30 Hz; **4.14**: 6.99 and 2.13 ppm, $^2J_{p\text{-}p}$ = 21.30 Hz) of approximately equal intensities with concomitant ^{195}Pt satellites. These signals were shifted upfield for **4.12**: 6.31 and 11.44 ppm; **4.13**: 5.77 and 11.22 ppm; **4.14**: 5.34 and 10.19 ppm, as compared to the 90 °Pt(II) acceptor **4.01** (δ = 12.50 ppm). This result agrees with the coordination motif of Pt(II) in **4.12**–**4.14**.[18] In the ^{1}H NMR spectra of **4.12**–**4.14**, the α- and β- pyridyl hydrogen signals both experience downfield shifts (**4.12**: 0.25 and 0.46 ppm; **4.13**: 0.45 and 0.68 ppm; **4.14**: 0.44 and 0.65 ppm) as compared with their chemical shifts in the precursor building block **4.11**. These shifts are associated with the loss of electron density upon coordination to the platinum metal centers. The sharp NMR spectral signals together with the solubility of the assemblies indicate that a self-assembly of high symmetry was formed as the major product in each reaction, and the formation of homoligated species and oligomers can be ruled out.

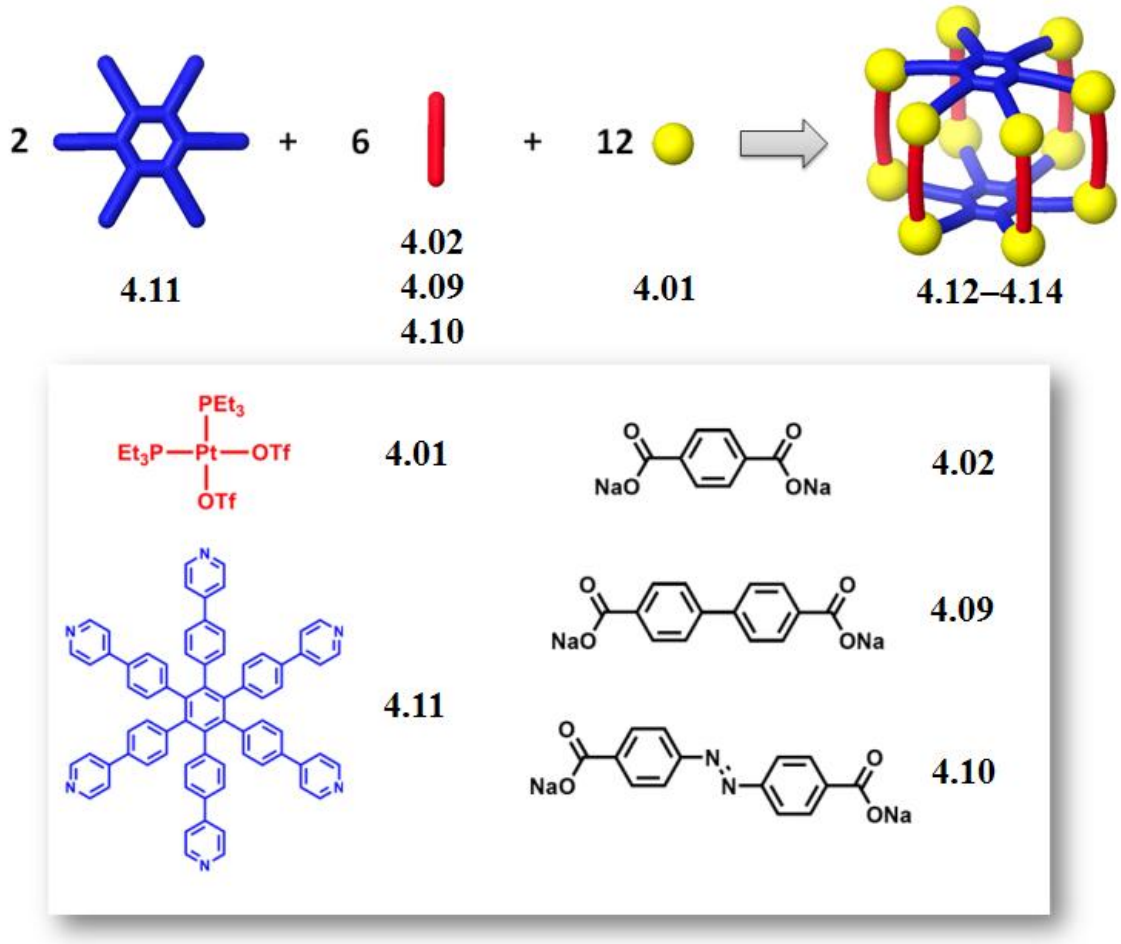

Scheme 4.3. Selective self-assembly of supramolecular hexagonal prisms of variable size by mixing 90° Pt(II) acceptor **4.01**, hexapyridyl ligand **4.11**, and different ditopic carboxylate donors **4.02**, **4.09**, and **4.10**

Further evidence for the formation of assemblies **4.12**–**4.14** was obtained by ESI-MS. The ESI-MS of **4.12** exhibited peaks for [**4.12**-4PF_6]$^{4+}$ and [**4.12**-5PF_6]$^{5+}$ at *m/z* = 2328.3 and 1834.1, respectively. Likewise, peaks attributable to **4.13** were found at *m/z* = 1924.7 [**4.13**-5PF_6]$^{5+}$, as were those corresponding to **4.14**: *m/z* = 1958.4 [**4.14**-5PF_6]$^{5+}$ and *m/z* = 1607.9 [**4.14**-6PF_6]$^{6+}$. All ESI-MS signals are in good agreement with their theoretical distributions.

4.2.4 Supramolecular transformations

We investigated supramolecular transformations in multicomponent selective self-assembly as shown in Scheme 4.4, wherein 90^{o} Pt(II) acceptor **4.01** and pyridyl ligands **4.03**, **4.04**, and **4.05b** self-assemble into well-defined two-component supramolecular structures **4.15**, **4.16**, and **4.17**. Addition of neutral triangle **4.18**, assembled by the mixing of 90^{o} Pt(II) acceptor **4.01** and the carboxylate ligand **4.02**, is able to convert the two-component species into multicomponent supramolecules of different topologies (**4.04**, **4.07**, and **4.08b**).

The two-component ensembles **4.15**, **4.16**, and **4.17**, as well as the neutral triangle **4.18**, were obtained by mixing 90^{o} Pt(II) acceptor **4.01** with pyridyl ligands **4.03**, **4.04**, and **4.05b** and carboxylate donor **2** in a 1:1 (**4.15**), 3:2 (**4.16**), 2:1 (**4.17**), and 1:1 (**4.18**) ratio. Each structure was characterized by ^{31}P and ^{1}H multinuclear NMR spectroscopy, ESI mass spectrometry, and PGSE NMR measurements. In the ^{31}P{^{1}H} NMR spectra (Figure 4.6a–d), only one intense singlet (**4.15**: 0.36 ppm; **4.16**: 0.29 ppm; **4.17**: 0.90 ppm; **4.18**: 3.52 ppm) with concomitant ^{195}Pt satellites can be found. Likewise, the ^{1}H NMR spectra show sharp signals assigned to coordinated pyridyl moieties (e.g., δ = 9.28 ppm, $H_{\alpha\text{-Py}}$ in **4.15**; δ = 9.32 ppm, $H_{\alpha\text{-Py}}$ in **4.16**; δ = 9.75 ppm, $H_{\alpha\text{-Py}}$ in **4.17**) and the carboxylate moieties (δ = 7.74 ppm in **4.18**). These NMR spectral results are in accord with the highly symmetric structures of **4.15**, **4.16**, **4.17**, and **4.18**. ESI mass spectrometry further confirms the structural assignments given to these assemblies. Signals for the [4 + 4] and [6 + 4] self-assembly of **4.15** and **4.16** can be found at m/z = 1869.91 [**4.15** – 2OTf]$^{2+}$, m/z = 1197.08 [**4.15** – 3OTf]$^{3+}$, m/z = 1818.36 [**4.16** – 3OTf]$^{3+}$, and m/z = 1326.65 [**4.16** – 4OTf]$^{4+}$. The [6 + 3] self-assembly of trigonal prism **4.17** was

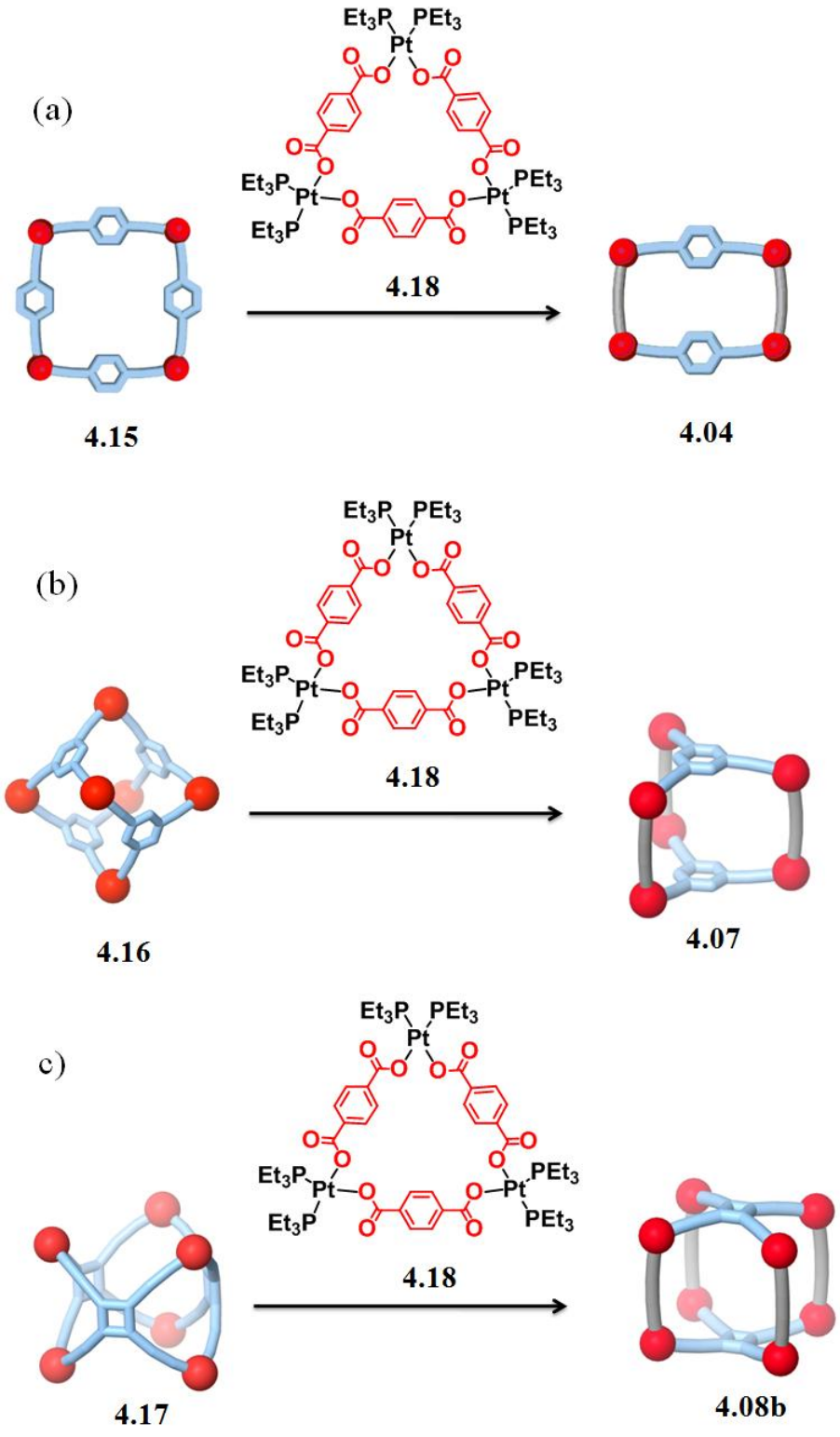

Scheme 4.4. Supramolecular transformations of square **4.15**, truncated tetrahedron **4.16**, and trigonal prism **4.17** into rectangle **4.04**, trigonal prism **4.07**, and tetragonal prism **4.08b** upon addition of neutral triangle **4.18** assembled by *cis*-$Pt(PEt_3)_2(OTf)_2$ **4.01** and carboxylate ligand **4.02**.

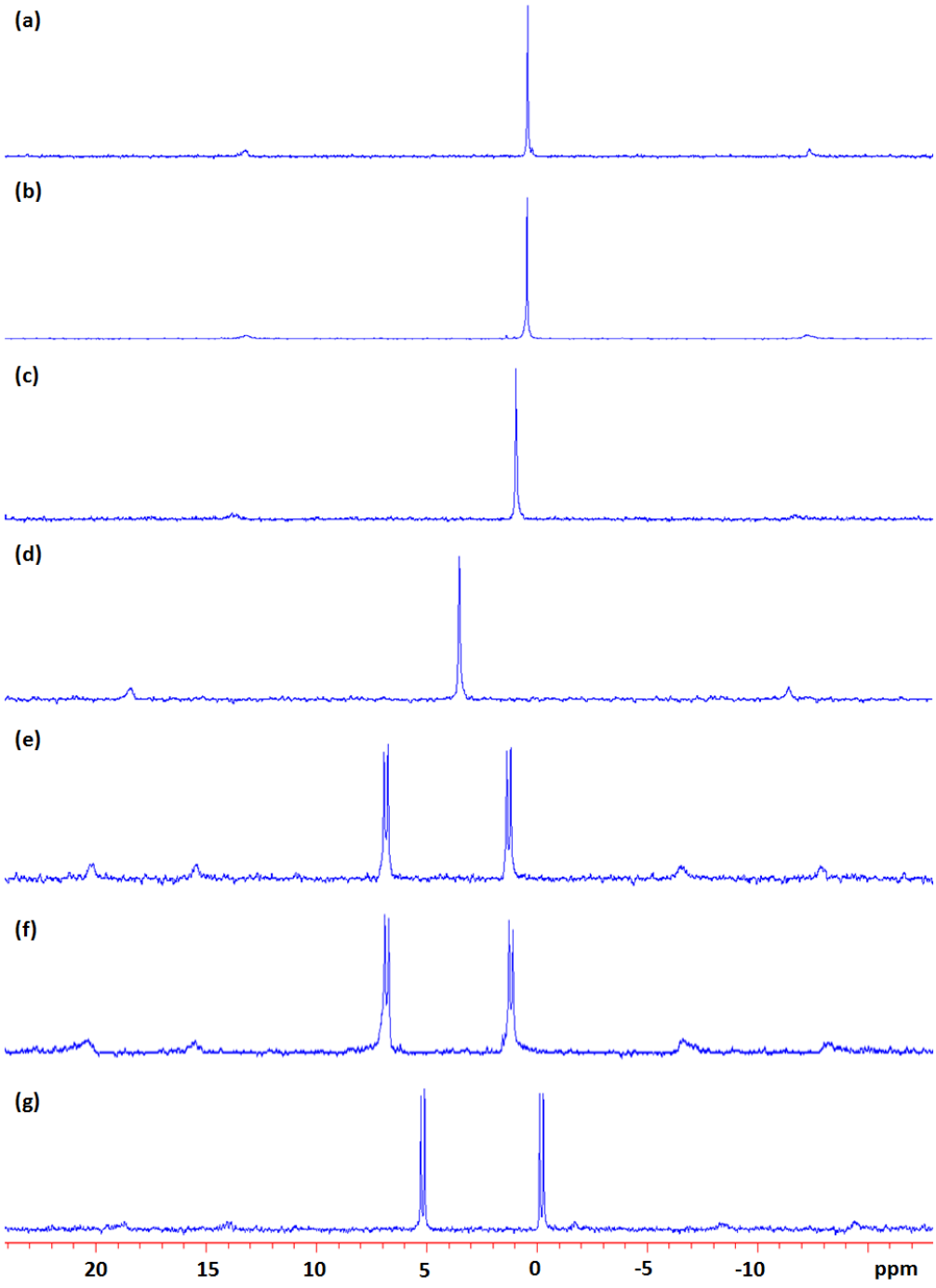

Figure 4.6. $^{31}P\{^{1}H\}$ NMR spectra of two-component self-assemblies **4.15** (a), **4.16** (b), and **4.17** (c), and neutral triangle **4.18** (d), as well as multicomponent rectangle **4.04** (e), trigonal prism **4.07** (f), and tetragonal prism **4.08b** (g) obtained via supramolecular transformations.

also supported by observation of isotopically resolved signals at m/z = 2966.57 [**4.17** – 2OTf]$^{2+}$, m/z = 1408.99 [**4.17** – 4OTf]$^{4+}$, and m/z = 1097.48 [**4.17** – 5OTf]$^{5+}$. Those for larger assemblies, such as [4 + 4], [5 + 5], and [6 + 6], could not be found, ruling out the possibility of forming larger prisms.[23] For the neutral triangle **4.18**, the molecular ion peak for the [3 + 3] self-assembly was found at m/z = 1787.12 [**4.18** + H]$^{+}$ and m/z = 1809.11 [**4.18** + Na]$^{+}$, along with the signal for [**4.18** + 2Na]$^{2+}$ at m/z = 916.16. There are no molecular ion peaks for the [2 + 2] or [4 + 4] ensembles observed in the mass spectrum, thus excluding the possible formation of a [2 + 2] rectangle and [4 + 4] square. Furthermore, a PGSE NMR study was also carried out to estimate the size of trigonal prism **4.17**, and the experimental radius of 1.70 ± 0.04 nm is in good agreement with the computational value of 1.6 nm from the MMFF modeling.[21]

The transformation of the two-component self-assemblies into the three-component assemblies was carried out by the addition of a solution of the previously formed two-component product to the neutral triangle **4.18**. After 5 h of heating at 75 ℃, a clear solution was obtained and characterized by ^{31}P and ^{1}H multinuclear NMR spectroscopy. In the ^{31}P{^{1}H} NMR spectra (Figure 4.6e–g), two intense coupled doublet peaks (Figure 4.6e: 6.63 ppm and 1.08 ppm, $^{2}J_{P\text{-}P}$ = 22.0 Hz for **4.04**; Figure 4.6f: 6.63 ppm and 1.03 ppm, $^{2}J_{P\text{-}P}$ = 21.4 Hz for **4.07**; Figure 4.6g: 5.03 ppm and -0.35 ppm, $^{2}J_{P\text{-}P}$ = 21.4 Hz for **4.08b**) with concomitant ^{195}Pt satellites were found, which were in good agreement with those observed in Figure 4.1 and 4.3 for the authentic three-component cages. Likewise, in the ^{1}H NMR spectra, the thus transformed two-component to three-component structures match the signals of the authentic ensembles. Peaks corresponding

to the starting two-component structures were absent in both $^{31}P\{^{1}H\}$ and ^{1}H NMR spectra. These NMR data clearly indicate that the two-component assemblies have been entirely transformed into the three-component structures.

To further investigate the supramolecular transformation process, we carried out a study of the gradual transformation of square **4.15** to rectangle **4.04**: equivalencies of 10%, 25%, 50%, and 100% of neutral triangle **4.18** were added to an acetone solution of square **9** and the mixtures were heated at 75 ℃ for 5 h. The resulting clear solutions were characterized by ^{31}P and ^{1}H multinuclear NMR spectroscopy. As indicated by the $^{31}P\{^{1}H\}$ NMR spectra (Figure 4.7), increasing the amount of **4.18** resulted in a decrease of the signal (δ = 0.36 ppm) for square **4.15** and the simultaneous formation of signals around 6.63 ppm and 0.99 ppm attributable to three-component complexes. A similar result can be observed in ^{1}H NMR spectra, by comparing the signals for $H_{\alpha\text{-Py}}$ of **4.15** (δ = 9.28 ppm) and **4.04** (δ = 9.00 ppm). These ^{31}P and ^{1}H NMR spectral results demonstrate the gradual transformation of three-component complexes from the two-component species upon addition of the neutral triangle. During the transformation process, an intermediate was also observed in addition to rectangle **4.04**, as indicated by the multiplets around 6.63 ppm and 0.99 ppm in Figure 4.7b–d. Isotopically resolved signals in the ESI mass spectrum (Figure 4.8) at m/z = 722.6 $[M - 3OTf]^{3+}$ and 1158.2 $[M - 2OTf]^{2+}$ suggest this intermediate is formed by [3 + 2 + 1] assembly of Pt(II) acceptor **4.01**, pyridyl donor **4.03**, and carboxylate ligand **4.02**, and these signals cannot be found in the spectrum of pure rectangle **4.04**, square **4.15**, or neutral triangle **4.18**. The intermediate is formed due to the improper ratio of square and neutral triangle for generating [4 + 2 + 2] rectangle **4.04**. Once 100% of neutral triangle **4.18** was added, square **4.15** can be fully altered to **4.04**.

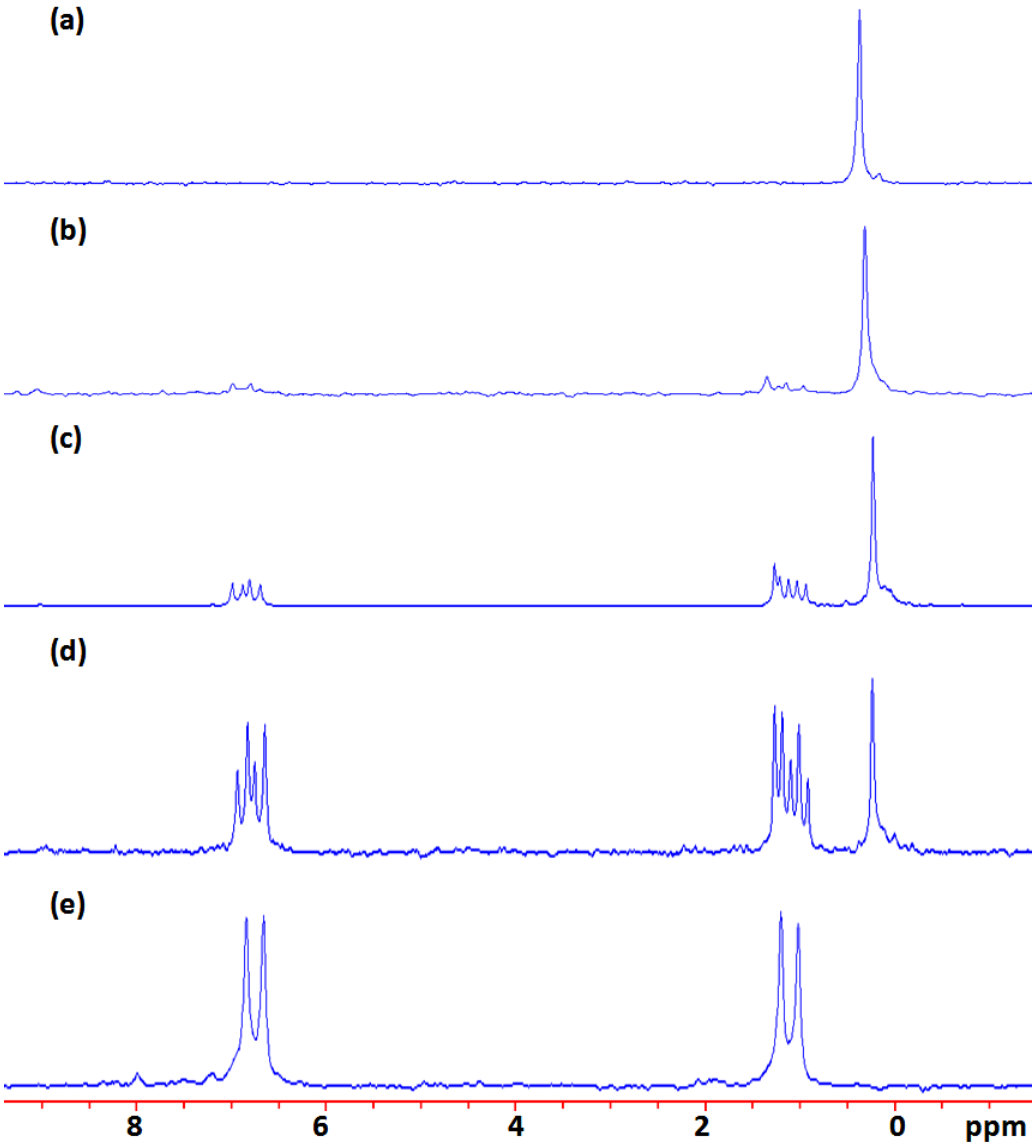

Figure 4.7. $^{31}P\{^{1}H\}$ NMR spectra for mixtures of square **4.15** upon addition of 0% (a), 10% (b), 25% (c), 50% (d), and 100% (e) of neutral triangle **4.18**.

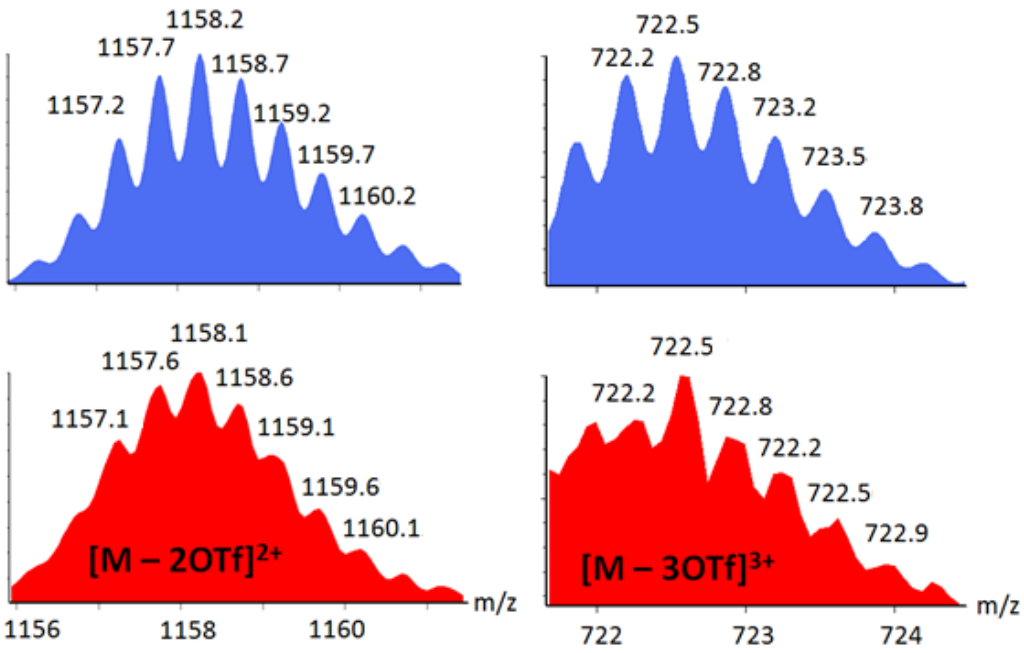

Figure 4.8. Calculated (blue, top) and Experimental (red, bottom) ESI mass spectrum of the intermediate formed during the gradual transformation

4.2.5 Supramolecular modifications

Partial structural modification of supramolecules can be achieved via addition of molecular subunits resulting in supramolecular transformations. As shown in Scheme 4.5, the two-component starting material **4.19** can be transformed into a three-component structure **4.20** by addition of carboxylate ligand **4.02** or together with cis-$Pt(PEt_3)_2(OTf)_2$ **4.01**. The resulting three-component species possesses a square pyramid-like shape which resembles half of the octahedral starting structure.

The starting two-component ensemble **4.19** was obtained by mixing 90^o Pt(II) acceptor **4.01** with tritopic pyridyl ligands **4.21** in a 3:2 ratio in an acetone solution. The structure was characterized by ^{31}P and ^{1}H multinuclear NMR spectroscopy and ESI mass spectrometry. In the $^{31}P\{^{1}H\}$ NMR spectrum (Figure 4.9a), only one intense singlet at 0.33 ppm with concomitant ^{195}Pt satellites can be found. Likewise, the ^{1}H NMR spectra

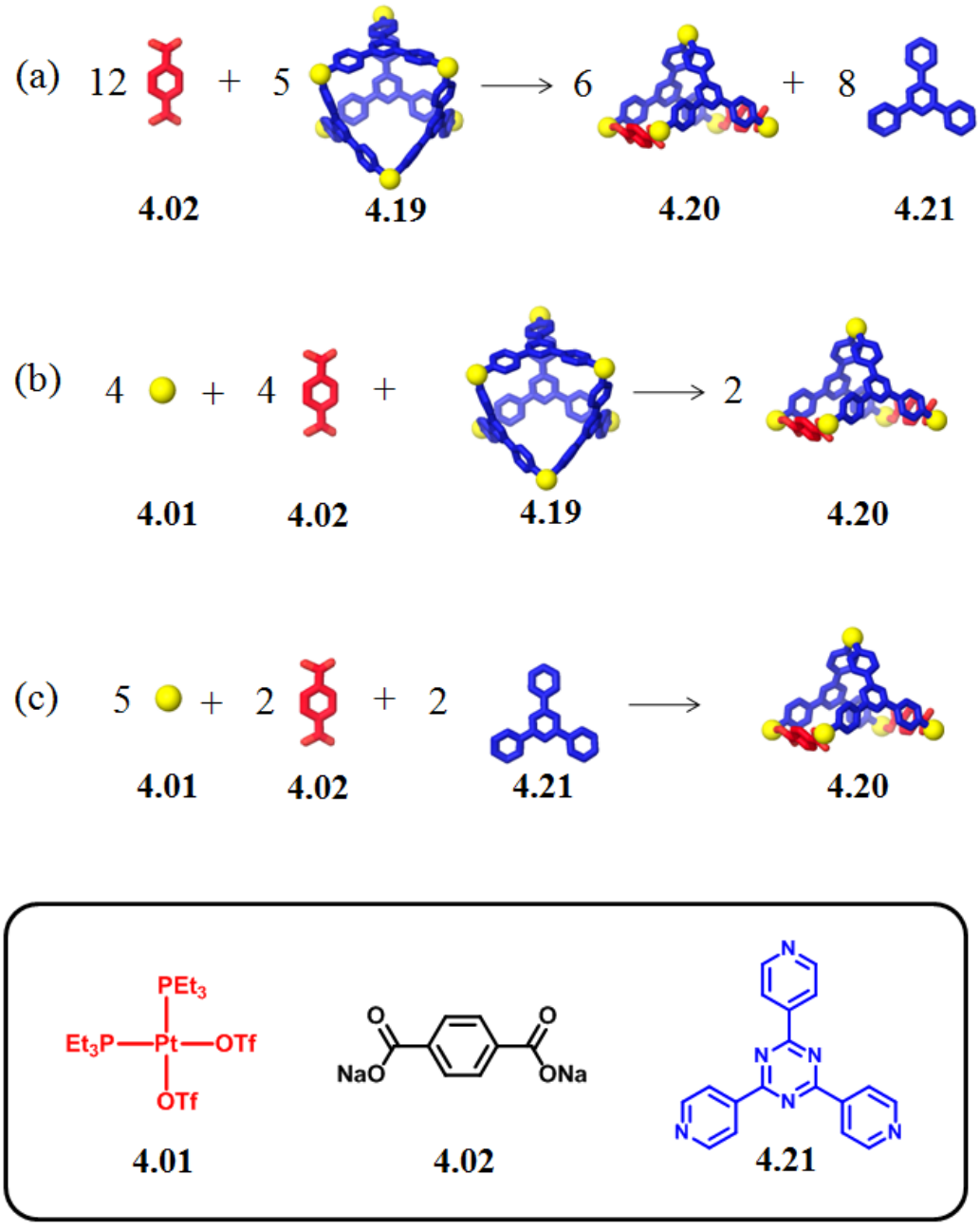

Scheme 4.5. Supramolecular modifications (a,b) of two-component starting material **4.19** to three-component structure **4.20**, and (c) self-assembly of **4.20** via combination of *cis*-$Pt(PEt_3)_2(OTf)_2$ **4.01**, carboxylate ligand **4.02**, and tritopic pyridyl donor **4.21**

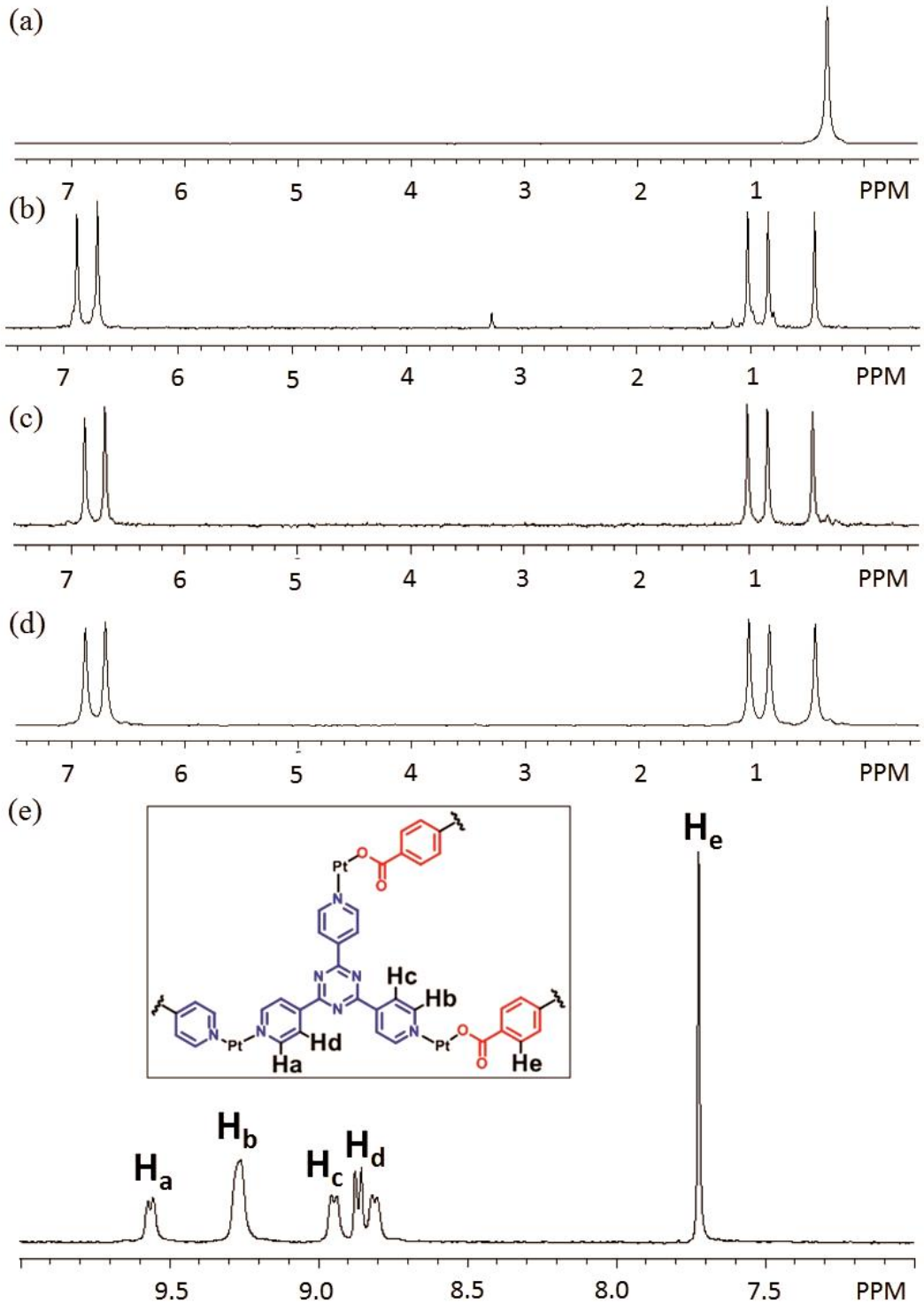

Figure 4.9. $^{31}P\{^{1}H\}$ NMR spectra of **4.20** (b,c) modified from **4.19** (a) and assembled (d) by *cis*-$Pt(PEt_3)_2(OTf)_2$ **4.01**, ditopic carboxylate ligand **4.02**, and tritopic pyridyl donor **4.21**, and its ^{1}H NMR spectrum (e).

show sharp signals assigned to coordinated pyridyl moieties (δ = 9.64 ppm, $H_{\alpha\text{-Py}}$; δ = 8.94 ppm, $H_{\beta\text{-Py}}$). ESI mass spectrometry further confirms the [6 + 4] self-assembly of **4.19**. Signals can be found at m/z = 1725.9 [**4.19** – 3OTf]$^{3+}$, m/z = 1257.1 [**4.19** – 4OTf]$^{4+}$, and m/z = 975.9 [**4.19** – 5OTf]$^{5+}$, and the 3+ and 4+ signals are isotopically resolved. Both NMR and ESI-MS strongly support the formation of **4.19** as the sole species in solution.

To achieve the transformation (Scheme 4.5a), an aqueous solution of carboxylate ligand **4.02** was added to the acetone solution of structure **4.19**, and the mixture was stirred at 70 ℃ for 1 h. Following removal of all solvent, acetone-d_6 was added to dissolve the mixture, which was allowed to re-equilibrate after 3 h of heating at 75 ℃. The solid product **4.20** was isolated by ion exchange with KPF_6. ^{31}P and ^{1}H multinuclear NMR spectroscopy and ESI-MS were used to characterize the mixture. In the $^{31}P\{^{1}H\}$ NMR spectra (Figure 4.9b), two coupled doublets at 6.75 ppm and 0.90 ppm and a singlet at 0.42 ppm with concomitant ^{195}Pt satellites were found, which were in good agreement with the hybrid coordination motifs (cis-$Pt(Py)_2$ and cis-Pt(COO)(Py)) of Pt(II) centers in transformed ensemble **4.20**. In the ^{1}H NMR spectra (Figure 4.9e), well-defined proton signals indicated two types of pyridyl protons in the structures at a ratio of 2:1 (δ = 9.55 ppm for $H_{\alpha\text{-Py}}$ in cis-$Pt(Py)_2$ and δ = 9.25 ppm for $H_{\alpha\text{-Py}}$ in Pt(COO)(Py)), matching the structural features of **4.20**. Isotopically resolved signals observed in the ESI mass spectrum of the isolated species (Figure 4.10) at m/z = 1844.0 [M – $2PF_6$]$^{2+}$, m/z = 1181.1 [M – $3PF_6$]$^{3+}$ and m/z = 849.9 [M – $4PF_6$]$^{4+}$ further support a [5 + 2 + 2] self-assembly of **4.20** as the major product in the mixture. Moreover, as shown in Figure 4.11, the X-ray analysis of a single crystal of the isolated product unambiguously shows the

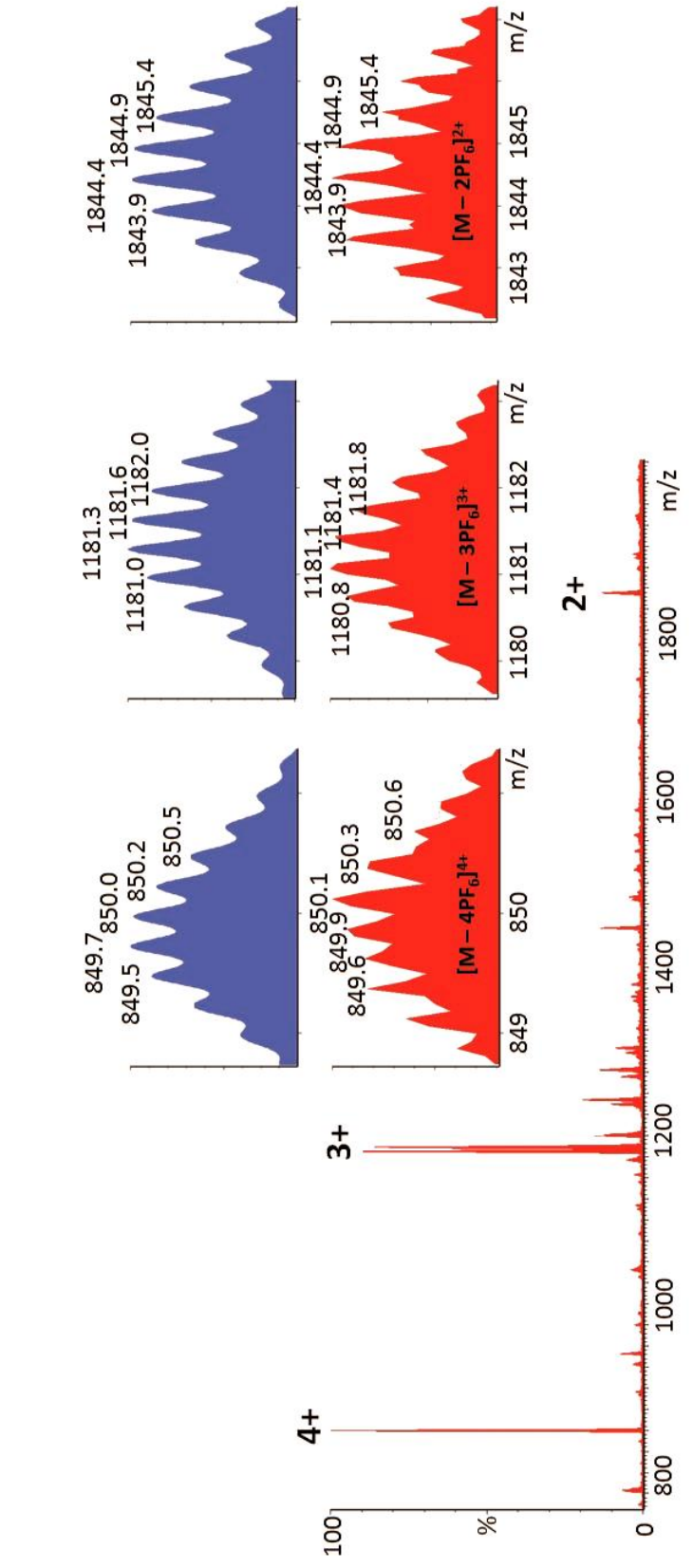

Figure 4.10. Full ESI mass spectrum of the solution of the modified three-component structure **4.20**

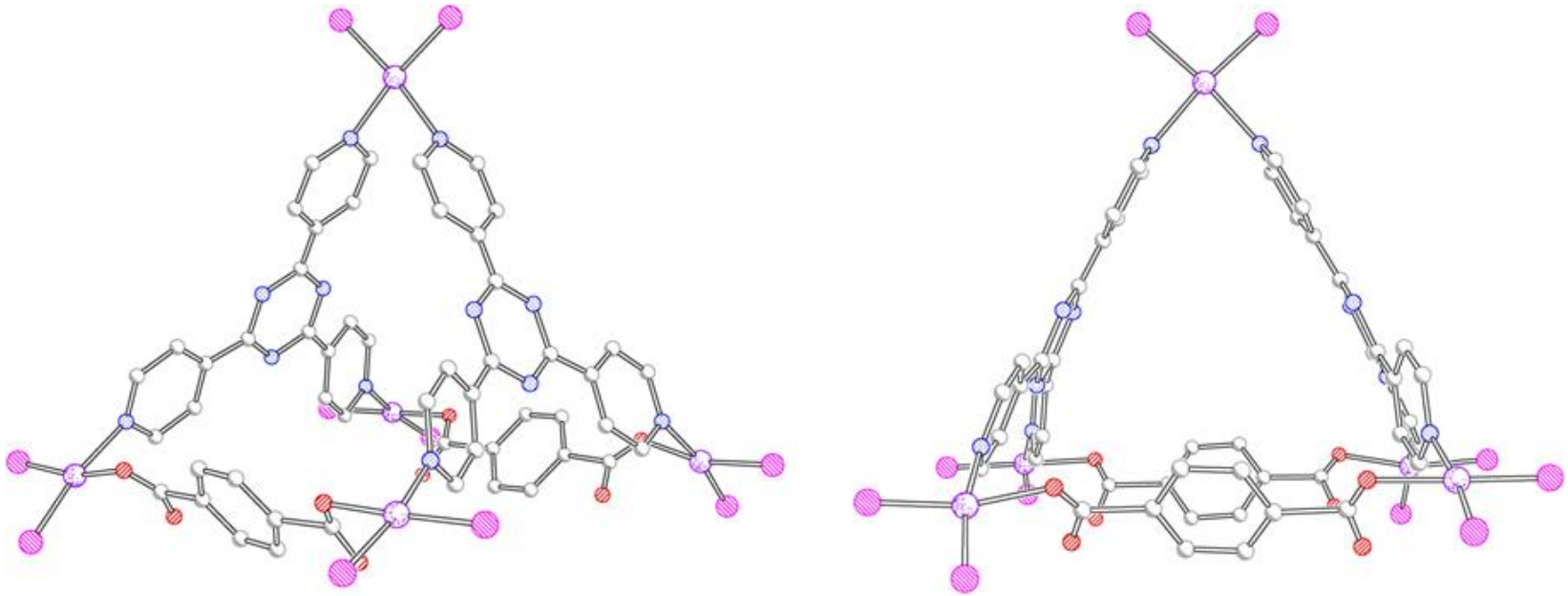

Figure 4.11. Different views of the X-ray crystal structure of **4.20** (anions and ethyl groups on phosphines are omitted for clarity)

structure of three-component **4.20**. Combined analysis from NMR, MS, and X-ray characterization indicated that three-component self-assembly **4.20** was the predominant species, resulting from the supramolecular transformation of the starting material **4.19**. In this case, a byproduct in the form of a free tripyridyl ligand was also produced, which precipitated out. To fully utilize all molecular components in a supramolecular modification, pathway 2 (Scheme 4.5b) was attempted, in which cis-$Pt(PEt_3)_2(OTf)_2$ **4.01** was also added. Following an analogous experimental procedure, three-component structure **4.20** can be obtained as evidenced by the identical NMR spectra (Figure 4.9c). In this case, there is no free tripyridyl donor produced and more transformed product **4.20** was obtained. The three-component supramolecule **4.20** can also be individually prepared via combination of Pt(II) acceptor **4.01**, carboxylate ligand **4.02**, and pyridyl donor **4.21** in a 5:2:2 ratio, as shown in Scheme 4.5c. The NMR spectra (Figure 4.9d) are identical to those obtained from the supramolecular modification.

Another interesting supramolecular modification was also achieved, as shown in Scheme 4.6. In this case, the modified three-component species **4.22** is structurally similar to the basic structure **4.19**, but in **4.22**, one of the tripyridyl donors is replaced by a tricarboxylate ligand, **4.23**. The modification was performed following an analogous experimental procedure in which one equiv. of tricarboxylate ligand **4.23** was added (Scheme 4.6a). In the $^{31}P\{^1H\}$ NMR spectrum (Figure 4.12b) of the mixture, two coupled doublet peaks at 6.63 ppm and 0.80 ppm, along with a singlet at 0.47 ppm with concomitant ^{195}Pt satellites were found, indicative of the hybrid coordination motifs of the Pt(II) centers in three-component ensemble **4.22**. In the ^1H NMR spectrum, signals identified for two types of pyridyl protons, corresponding to the different coordination

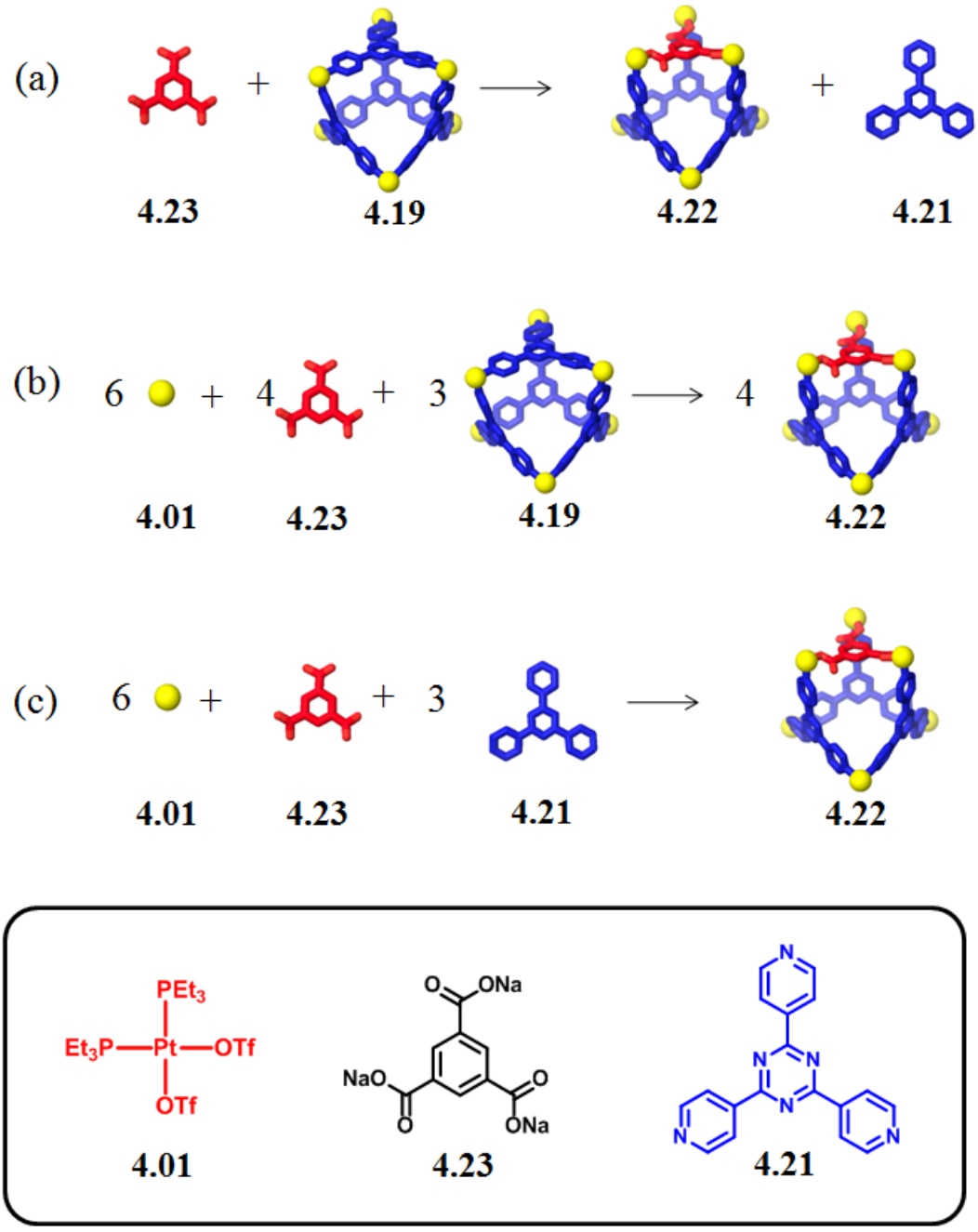

Scheme 4.6. Supramolecular modifications (a,b) of two-component starting material **4.19** to three-component structure **4.22**, and (c) self-assembly of **4.22** via combination of *cis*-$Pt(PEt_3)_2(OTf)_2$ **4.01**, tricarboxylate ligand **4.23**, and tritopic pyridyl donor **4.21**

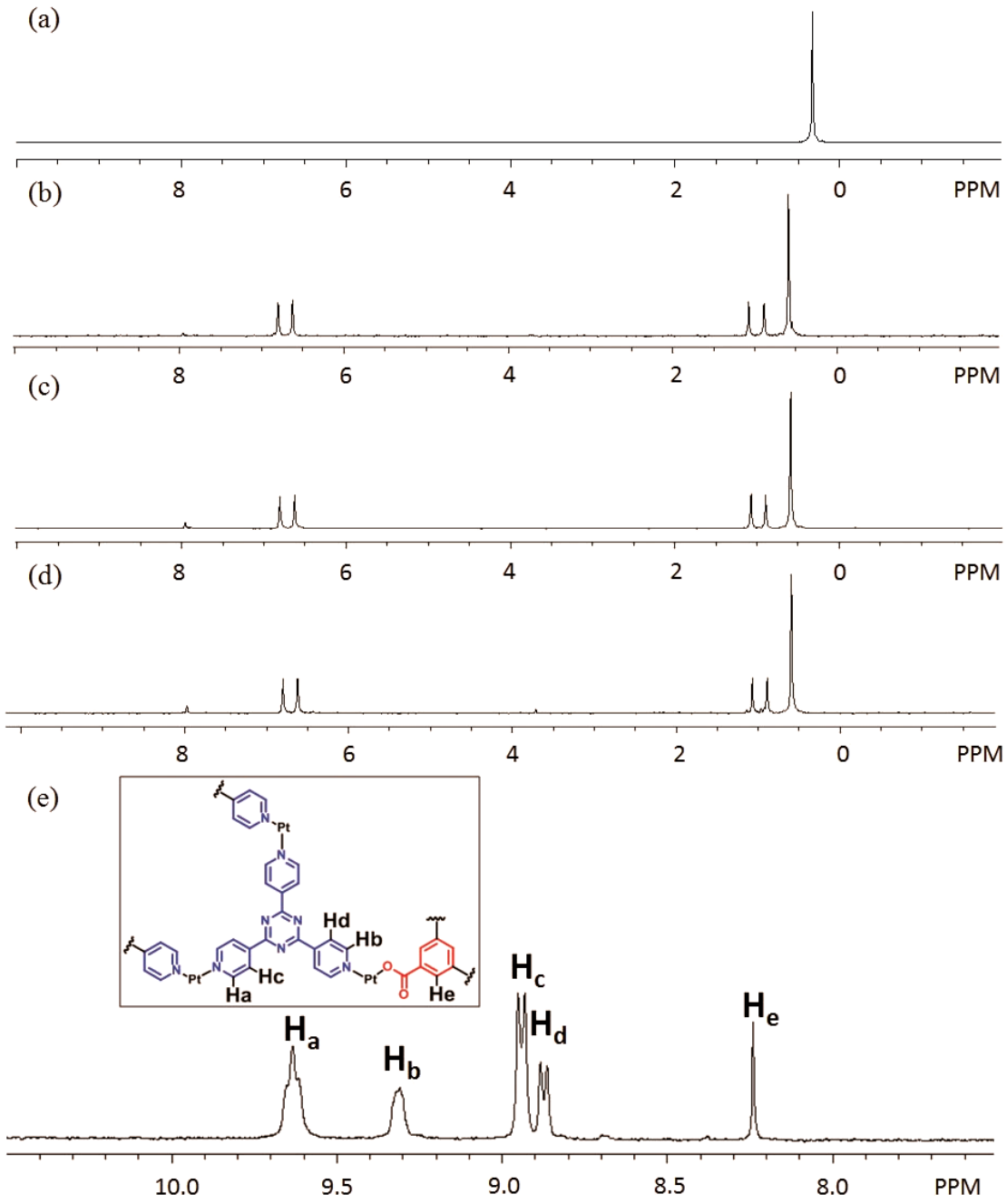

Figure 4.12. $^{31}P\{^{1}H\}$ NMR spectra of **4.22** (b,c) modified from **4.19** (a) and assembled (d) by *cis*-$Pt(PEt_3)_2(OTf)_2$ **4.01**, tricarboxylate ligand **4.23**, and tritopic pyridyl donor **4.21**, and its ^{1}H NMR spectrum (e).

motifs of Pt(II), are in a ratio of 1:3, consistent with the structural features of **4.22**. In the ESI mass spectrum (Figure 4.13), the isotopically resolved signals at m/z = 2386.8 [M – 2OTf]$^{2+}$, m/z = 1541.6 [M – 3OTf]$^{3+}$, and m/z = 1118.8 [M – 4OTf]$^{4+}$ further indicate that the [6+3+1] self-assembly of **4.22** is the predominate product in the reaction. As shown in pathway 2 in Scheme 4.6b, addition of cis-Pt(PEt_3)$_2$(OTf)$_2$ **4.01** is also able to fully use all molecular components to achieve a supramolecular modification, as indicated by the identical NMR in Figure 4.12c. In addition, the three-component supramolecule **4.22** was also independently prepared via the combination of Pt(II) acceptor **4.01**, tripyridyl donor **4.21**, and carboxylate ligand **4.23** in a 6:3:1 ratio (Scheme 4.6c). The NMR spectra (Figure 4.12d) are identical to those obtained from the supramolecular modification.

Such modifications can also be achieved gradually. We carried out a study of the gradual transformation of the two-component starting material **4.19** to the three-component structure **4.22**: 0%, 30%, 60%, and 100% of tricarboxylate ligand **4.23** was added to the two-component structure **4.19**, respectively, and the transformed product was obtained following the same experimental procedure. The resulting mixtures were characterized by ^{31}P and ^{1}H multinuclear NMR spectroscopy. As indicated by the ^{31}P{^{1}H} NMR spectra (Figure 4.14), the gradual transformation of **4.19** to **4.22** results in a decrease of the signal (δ = 0.33 ppm) for the starting material **4.19** and the simultaneous development of signals around 6.63 ppm, 0.80 ppm, and 0.47 ppm, attributable to the three-component complex **4.22**, without generating any other signals. A similar result can be observed in the ^{1}H NMR spectra by comparing the signals for $H_{\alpha\text{-Py}}$ of the two-component assembly (δ = 9.64 ppm) and the three-component complexes (δ = 9.31 ppm).

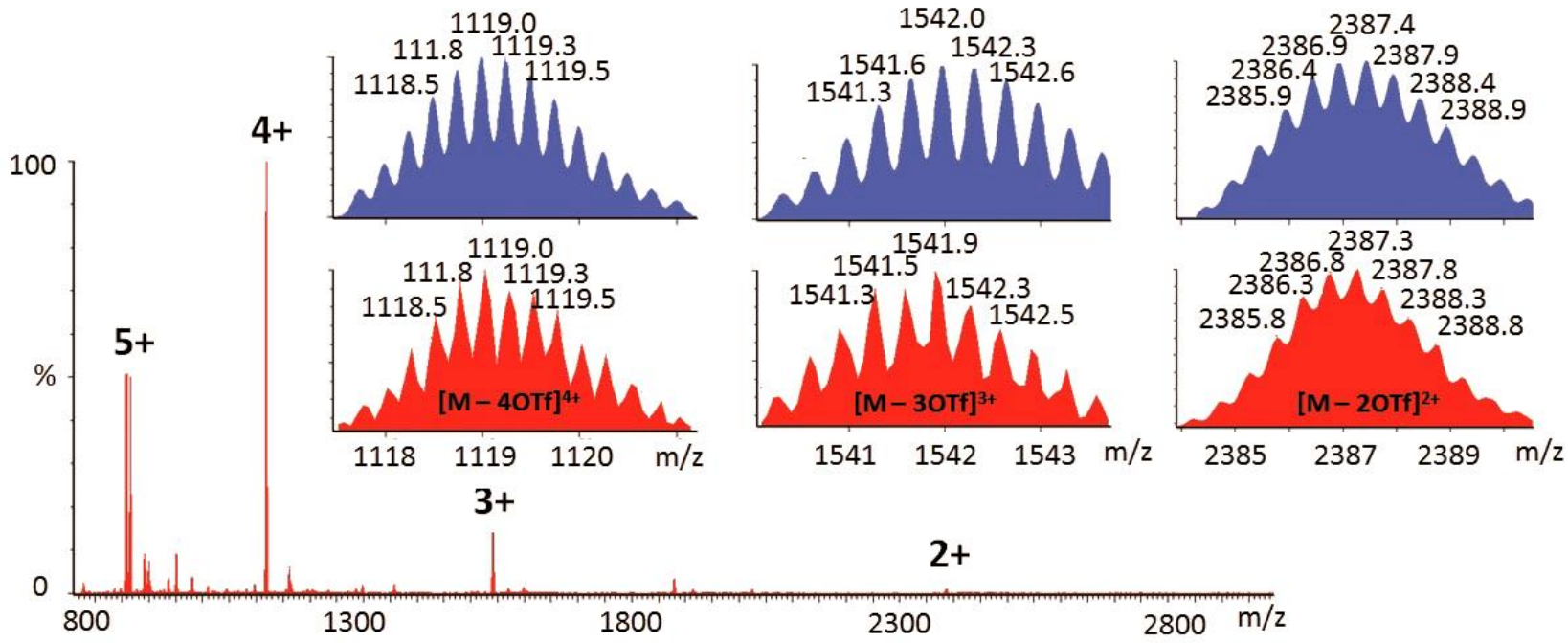

Figure 4.13. Full ESI mass spectrum of the solution of the modified three-component structure **4.22**

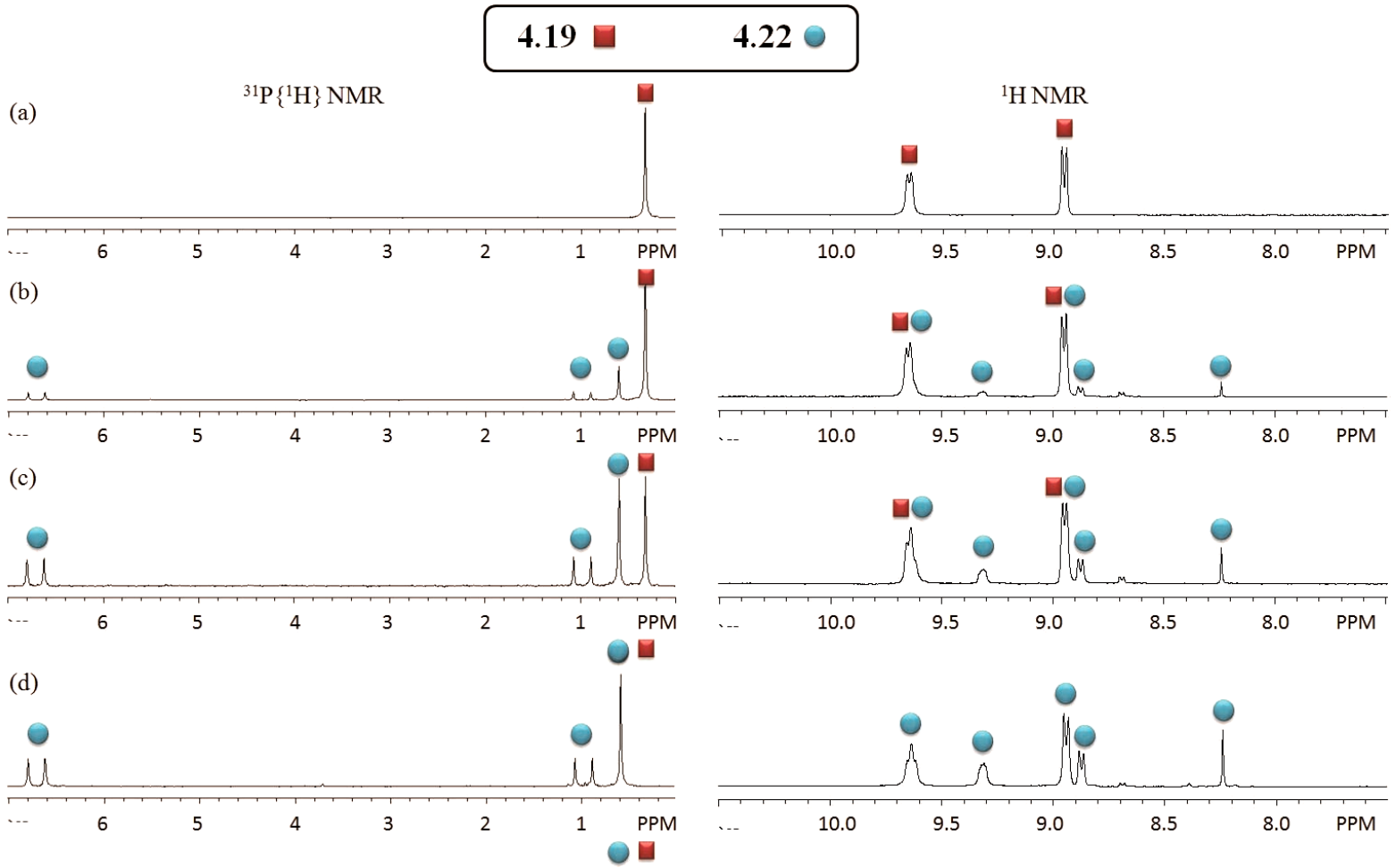

Figure 4.14. $^{31}P\{^{1}H\}$ NMR and partial ^{1}H NMR spectra of the gradual transformation of **4.19** to **4.22** upon addition of 0 eqiv.(a), 0.3 equiv. (b), 0.6 equiv. (c), and 1.0 equiv. (d) of **4.23**

In addition, the ratios of **4.19** and **4.22** in the mixture, calculated from the integrations of proton signals, agree well with the expected values: experimental results are 3.2:1 and 1.9:3 upon addition of 30% and 60%, respectively, and the theoretical values are 3:1 and 2:3. These ^{31}P and ^{1}H NMR spectral results indicate that supramolecular modification is the major process in the mixture and may be achieved gradually.

4.3 Conclusion

We describe here a facile and very efficient approach for selective construction of well-defined multicomponent 2D and 3D supramolecular structures of various motifs. Upon the combination of 90 ° Pt(II) acceptor with appropriate carboxylate ligands and pyridyl donors in a proper ratio, coordination-driven self-assembly allows for the selective formation of a multicomponent supramolecular rectangle and prisms. These multicomponent complexes can also be obtained by a novel supramolecule-to-supramolecule transformation from the two-component assemblies. Characterization via multinuclear (^{31}P and ^{1}H) NMR spectroscopy clearly reveals the three-component coordination nature of these assembled supramolecules as well as their high structural symmetry. ESI mass spectrometry and PGSE NMR measurements, together with computational simulations, further identified the composition and size of these multicomponent assemblies.

In addition, supramolecular transformation from the two-component assemblies to three-component structures was also achieved using selective self-assembly. Two-component coordination supramolecules were used as starting materials to which extra molecular components or supramolecules were added. These starting structures can be postassembled into three-component supramolecular architectures of higher complexity.

Characterization via NMR spectroscopy, ESI-MS, and X-ray crystallography strongly supports such transformations. These supramolecular transformations provide a new strategy to construct supramolecular architectures by invoking alterations of pre-assembled supramolecules, in contrast to the bottom-up approach of using a wide range of building blocks. Moreover, supramolecular modifications derived from supramolecular transformations suggest an innovative way to modify self-assembled supramolecular species.

4.4 References

(1) (a) Stang, P. J.; Olenyuk, B. *Acc. Chem. Res.* **1997**, *30*, 502. (b) Leininger, S.; Olenyuk, B.; Stang, P. J. *Chem. Rev.* **2000**, *100*, 853. (c) Holliday, B. J.; Mirkin, C. A. *Angew. Chem., Int. Ed.* **2001**, *40*, 2022. (d) Fujita, M.; Umemoto, K.; Yoshizawa, M.; Fujita, N.; Kusukawa, T.; Biradha, K. *Chem. Commun.* **2001**, 509. (e) Seidel, S. R.; Stang, P. J. *Acc. Chem. Res.* **2002**, *35*, 972. (f) (b) Ruben, M.; Rojo, J.; Romero-Salguero, F. J.; Uppadine, L. H.; Lehn, J.-M. *Angew. Chem., Int. Ed.* **2004**, *43*, 3644. (g) Fiedler, D.; Leung, D. H.; Bergman, R. G.; Raymond, K. N. *Acc. Chem. Res.* **2005**, *38*, 351. (h) Fujita, M.; Tominaga, M.; Hori, A.; Therrien, B. *Acc. Chem. Res.* **2005**, *38*, 369. (i) Lukin, O.; Voegtle, F. *Angew. Chem., Int. Ed.* **2005**, *44*, 1456. (j) Severin, K. *Chem. Commun.* **2006**, 3859. (k) Nitschke, J. R. *Acc. Chem. Res.* **2007**, *40*, 103. (l) Pitt, M. A.; Johnson, D. W. *Chem. Soc. Rev.* **2007**, *36*, 1441. (m) Oliver, C. G.; Ulman, P. A.; Wiester, M. J.; Mirkin, C. A. *Acc. Chem. Res.* **2008**, *41*, 1618. (n) Parkash, M. J.; Lah, M. S. *Chem. Commun.* **2009**, 3326.

(2) (a) Yang, H.-B.; Das, N.; Huang, F.; Hawkridge, A. M.; Muddiman, D. C.; Stang, P. J. *J. Am. Chem. Soc.* **2006**, *128*, 10014. (b) Yang, H.-B.; Hawkridge, A. M.; Huang, S. D.; Das, N.; Bunge, S. D.; Muddiman, D. C.; Stang, P. J. *J. Am. Chem. Soc.* **2007**, *129*, 2120. (c) Baytekin, H. T.; Sahre, M.; Rang, A.; Engeser, M.; Schulz, A.; Schalley, C. A. *Small* **2008**, *4*, 1823. (d) Yang, H.-B.; Northrop, B. H.; Zheng, Y.-R.; Ghosh, K.; Lyndon, M. M.; Muddiman, D. C.; Stang, P. J. *J. Org. Chem.* **2009**, *74*, 3524. (e) Yang, H.-B.; Northrop, B. H.; Zheng, Y.-R.; Ghosh, K.; Stang, P. J. *J. Org. Chem.* **2009**, *74*, 7067. (f) Zheng, Y.-R.; Ghosh, K.; Yang, H.-B.; Stang, P. J. *Inorg. Chem.* **2010**, *49*, 4747.

(3) (a) Pluth, M. D.; Bergman, R. G.; Raymond, K. N. *J. Am. Chem. Soc.* **2008**, *130*, 6362. (b) Klosterman, J. K.; Yamauchi, Y.; Fujita, M. *Chem. Soc. Rev.* **2009**, *38*, 1714. (c) Yamauchia, Y.; Yoshizawa, M.; Akita, M.; Fujita, M. *Prod. Nat. Acd. Sci. USA* **2009**, *106*, 10435. (d) Hatakeyama, Y.; Sawada, T.; Kawano, M.; Fujita, M. *Angew. Chem., Int. Ed.* **2009**, *48*, 8695. (e) Pluth, M. D.; Fiedler, D.; Mugridge,

J. S.; Bergman, R. G.; Raymond, K. N. *Prod. Nat. Acd. Sci. USA* **2009**, *106*, 10438. (f) Mal, P.; Breiner, B.; Rissanen, K.; Nitschke, J. R. *Science* **2009**, *324*, 1697. (g) Sawada, T.; Fujita, M. *J. Am. Chem. Soc.* **2010**, *132*, 7194.

(4) (a) Yoshizawa, M.; Tamura, M.; Fujita, M. *Science* **2006**, *312*, 251. (b) Pluth, Michael D.; Bergman, Robert G.; Raymond, Kenneth N. *Science* **2007**, *316*, 85. (c) Pluth, M. D.; Bergman, R. G.; Raymond, K. N. *Acc. Chem. Res.* **2009**, *42*, 1650. (d) Yoshizawa, M; Klosterman, J. K.; Fujita, M. *Angew. Chem., Int. Ed.* **2009**, *48*, 3418.

(5) (a) Yamashita, K.-I.; Kawano, M.; Fujita, M. *Chem. Commun.* **2007**, *40*, 4102. (b) Lee, S. J. Lin, W. *Acc. Chem. Res.* **2008**, *41*, 521. (c) Steed, J. W. *Chem. Soc. Rev.* **2009**, *38*, 506. (d) Liu, Y.; Wu, X.; He, C.; Jiao, Y.; Duan, C. *Chem. Commun.* **2009**, *48*, 7554.

(6) De, S; Mahata, K. Schmittel, M. *Chem. Soc. Rev.* **2010**, *39*, 1555.

(7) (a) Lehn, J.-M. *Science* **2002**, *295*, 2400. (b) Lehn, J.-M. *Rep. Prog. Phys.* **2004**, *67*, 249. (c) Lehn, J.-M. *Chem. Soc. Rev.* **2008**, 36, 151.

(8) (a) Abad-Zapatero, C.; Abdel-Meguid, S. S.; Johnson, J. E.; Leslie, A. G. W.; Rayment, I.; Rossmann, M. G.; Suck, D.; Tsukihara, T. *Nature* **1980**, *286*, 33. (b) Rossmann, M. G.; Arnold, E.; Erickson, J. W.; Frankenberger, E. A.; Griffith, J. P.; Hecht, H. J.; Johnson, J. E.; Kamer, G.; Luo, M.; Mosser, A. G.; Mosser, A. G.; Rueckert, R. R.; Sherry, B.; Vriend, G. *Nature* **1985**, *317*, 145.

(9) Groll, M.; Dizel, L.; Lowe, J.; Stock, D.; Bochter, M.; Bartunik, H. D. Huber, R. *Nature* **1997**, *386*, 463.

(10) (a) Zheng, Y.-R.; Yang, H.-B.; Northrop, B. H.; Ghosh, K.; Stang, P. J. *Inorg. Chem.* **2008**, *47*, 4706. (b) Northrop, B. H.; Yang, H.-B.; Stang, P. J. *Inorg. Chem.* **2008**, *47*, 11257. (c) Northrop, B. H.; Zheng, Y.-R.; Chi, K.-W.; Stang, P. J. *Acc. Chem. Res.* **2009**, *42*, 1554. (d) Zheng, Y.-R.; Yang, H.-B.; Ghosh, K.; Zhao, L.; Stang, P. J. *Chem. Eur. J.* **2009**, *15*, 7203.

(11) (a) Sauvage, J.-P.; Weiss, J. *J. Am. Chem. Soc.* **1985**, *107*, 6108. (b) Nierengarten, J. F.; Dietrich-Buchecker, C. O.; Sauvage, J.-P. *J. Am. Chem. Soc.* **1994**, *116*, 375. (c) Amabilino, D. A.; Dietrich-Buchecker, C. O.; Sauvage, J.-P. *J. Am. Chem. Soc*. **1996**, *118*, 3285. (d) Solladié, N.; Chambron, J.-C.; Sauvage, J.-P. *J. Am. Chem. Soc*. **1999**, *121*, 3684.

(12) Sleiman, H.; Baxter, P.; Lehn, J.-M.; Rissanen, K. *J. Chem. Soc., Chem. Commu*n. **1995**, 715.

(13) (a) Schmittel, M.; Ganz, A.; *Chem. Commun.* **1997**, 999. (b) Schmittel, M.; Ganz, A.; Fenske, D. *Org. Lett.* **2002**, *4*, 2289. (c) Schmittel, M.; Ammon, H.; Kalsani,

V.; Wiegrefe, A.; Michel, C. *Chem. Commun.* **2002**, 2566. (d) Schmittel, M..; Kalsani, V.; Fenske, D.; Wiegrefe, A. *Chem. Commun.* **2004**, *5*, 490. (e) Schmittel M.; Kalsani V.; Bats J. W. *Inorg. Chem.* **2005**, *44*, 4115. (f) Schmittel, M.; Mahata, K. *Angew. Chem., Int. Ed.* **2008**, *47*, 5284. (g) Schmittel, M.; Mahata, K. *Inorg. Chem.* **2009**, *48*, 822. (h) Fan, J.; Bats, J. W.; Schmittel, M. *Inorg. Chem.* **2009**, *48*, 6338. (i) Mahata, K.; Schmittel, M. *J. Am. Chem. Soc.* **2009**, *131*, 16544.

(14) (a) Yoshizawa, M.; Nagao, M.; Kumazawa, K.; Fujita, M. *J. Organomet. Chem.* **2005**, *690*, 5383. (b) Yamauchi, Y.; Fujita, M. *Chem. Commun*. **2010**, *46*, 5897.

(15) Yamanaka, M.; Yamada, Y.; Sei, Y.; Yamaguchi, K.; Kobayashi, K. *J. Am. Chem. Soc.* **2006**, *128*, 1531.

(16) (a) Kumazawa, K.; Biradha, K.; Kusukawa, T.; Okano, T.; Fujita, M. *Angew. Chem., Int. Ed.* **2003**, *42*, 3909. (b) Yoshizawa, M.; Nakagawa, J.; Kurnazawa, K.; Nagao, M.; Kawano, M.; Ozeki, T.; Fujita, M. *Angew. Chem., Int. Ed.* **2005**, *44*, 1810.

(17) Chi. K.-W.; Addicott, C.; Arif, A. M.; Stang, P. J. *J.* Am. *Chem. Soc*. **2004**, *126*, 16569.

(18) (a) Ghosh, S.; Turner, D. R.; Batten, S. R.; Mukherjee, P. S. *Dalton Trans.* **2007**, 1869. (b) Isaacs, L.; Witt, D. *Angew. Chem., Int. Ed.* **2002**, *41*, 1905.

(19) (a) Sun, S.-S.; Anspach, J. A.; Lees, A. J. *Inorg. Chem.* **2002**, *41*, 1862. (b) Sun, S.-S.; Stern, C. L.; Nguyen, S. T.; Hupp, J. T. *J. Am. Chem. Soc.* **2004**, *126*, 6314. (c) Heo, J.; Jeon, Y.-M.; Mirkin, C. A. *J. Am. Chem. Soc.* **2007**, *129*, 7712. (d) Zhao, L.; Northrop, B. H.; Stang, P. J. *J. Am. Chem. Soc.* **2008**, *130*, 11886. (e) Campbell, V. E.; Hatten, X.; Delsuc, N.; Kauffmann, B.; Huc, I.; Nitschke, J. R. *Nature Chem.* **2010**, *2*, 684.

(20) (a) Chi, K.-W.; Addicott, C.; Arif, A. M.; Stang, P. J. *J. Am. Chem. Soc.* **2004**, *126*, 16569. (b) Chi, K.-W.; Addicott, C.; Kryschenko, Y. K.; Stang, P. J. *J. Org. Chem.* **2004**, *69*, 964. (c) Chi, K.-W.; Addicott, C.; Moon, M.-E.; Lee, H. J.; Yoon, S. C.; Stang, P. J. *J. Org. Chem.* **2006**, *71*, 6662. (d) Ghosh, S.; Turner, D. R.; Batten, S. R.; Mukherjee, P. S. *Dalton Trans.* **2007**, 1869.

(21) (a) Yang, H.-B.; Ghosh, K.; Northrop, B. H.; Zheng, Y.-R.; Lyndon, M. M.; Muddiman, D. C.; Stang, P. J. *J. Am. Chem. Soc*. **2007**, *129*, 14187; (b) Northrop, B. H.; Gloeckner, A.; Stang, P. J. *J. Org. Chem.* **2008**, *73*, 1787; (c) Zhao, L.; Northrop, B. H.; Zheng, Y.-R.; Yang, H.-B.; Lee, H. J.; Lee, Y. M.; Park, J. Y.; Chi, K.-W.; Stang, P. J. *J. Org. Chem.* **2008**, *73*, 6580.

CHAPTER 5

COORDINATION-DRIVEN SELF-ASSEMBLY OF CAGES CAPABLE OF ENCAPSULATING 1,3,5-TRIPHENYL BENZENE

5.1 Introduction

Coordination-driven self-assembly is a successful methodology for preparing three-dimensional (3D) supramolecular structures.[1] During the past two decades, a variety of novel 3D coordinative structures of high complexity, high symmetry, and well-defined sizes and shapes, such as tetrahedra, cubes, double squares, cuboctahedra, adamantanoids, dodecahedra, and a sphere, have been developed.[2] Among these 3D supramolecules, tetrahedral structures represent one of the most widely studied systems because of their unique structural features and fascinating host-guest properties, as evidenced by the impressive results of Raymond[6] and Fujita.[7] However, the design of tetrahedral structures is still limited.[6-8]

The two-component self-assembly of a hexapyridyl ligand and a 90 ° acceptor forms a tetrahedral structure, wherein the hexadentate ligands act as faces and the platinum acceptors are the connectors at the corners, as shown in Scheme 5.1. We carried out the self-assembly of hexapyridyl donor **5.2**[9] with 90 ° platinum acceptor **5.1**, resulting in a truncated tetrahedron **5.3** in quantitative yield. The structures were characterized by

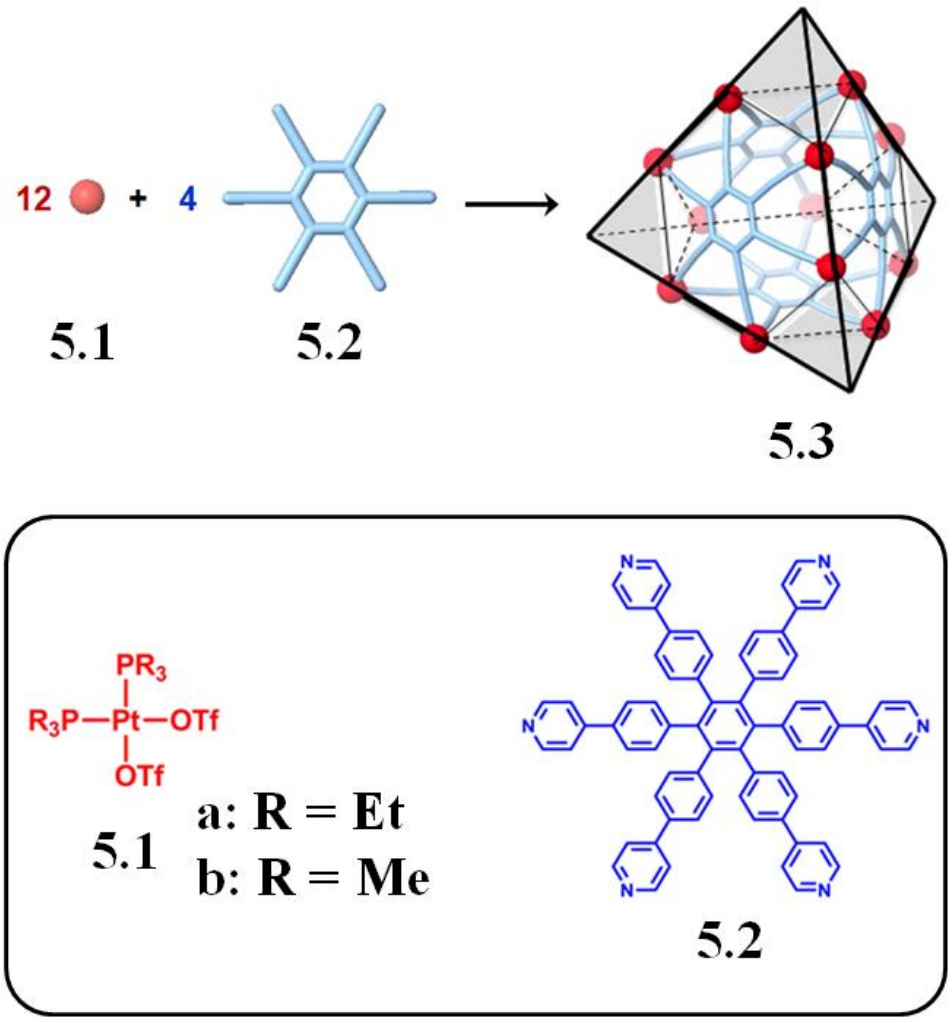

Scheme 5.1. Graphical representation of the [12+4] self-assembly of 90^{o} Pt(II) acceptors **5.1** and hexapyridyl ligand **5.2** into a truncated tetrahedron **5.3**.

multinuclear (^{31}P and ^{1}H) NMR spectroscopy, electrospray ionization mass spectrometry (ESI-MS), pulsed field gradient spin-echo (PGSE) NMR, as well as X-ray crystallography. Furthermore, it was found that truncated tetrahedron **5.3b** is able to encapsulate 1,3,5-triphenylbenzene **5.4** in an aqueous acetone solution. This host-guest complex was characterized by NMR spectroscopy and ESI-MS as well as computational simulations.

5.2 Results and Discussion

By mixing 90 ° platinum acceptor **5.1** and hexapyridyl donor **5.2**[9] in a 3:1 ratio in an acetone-d_6/CD_3NO_2 (*v/v* 7:3) solution for **5.3a** and an aqueous acetone solution (*v/v* 1:1) for **5.3b**, self-assembly of truncated tetrahedra **5.3** were obtained after 16 h of heating at 80 ℃. Assemblies **5.3** can be quantitatively isolated via ion exchange with KPF_6.

In the $^{31}P\{^1H\}$ NMR spectra (Figure 5.1) of **5.3**, only singlets at 0.92 ppm (**5.3a**) and -28.2 ppm (**5.3b**) with concomitant ^{195}Pt satellites can be found for the coordinated platinum centers. Likewise, the ^1H NMR spectra also exhibit sharp signals for the pyridyl protons of **5.3** ($\delta_{Py\alpha\text{-}H}$: 8.91 ppm and $\delta_{Py\beta\text{-}H}$: 7.44 ppm for **5.3a**; $\delta_{Py\alpha\text{-}H}$: 8.68 ppm and $\delta_{Py\beta\text{-}H}$: 7.48 ppm for **5.3b**), with approximately 0.1 ppm ($H_{Py\text{-}\beta}$) and 0.2–4 ppm ($H_{Py\text{-}\alpha}$) downfield shifts due to the loss of electron density upon coordination to the platinum centers. Signals corresponding to the phenyl protons on the donors are split into two sets of doublets, presumably caused by the difference between the exterior and interior of the cage structure. In the ESI mass spectra of **5.3**, peaks corresponding to [**5.03a** – $5PF_6$]$^{5+}$ and [**5.3a** – $6PF_6$]$^{6+}$ can be found at m/z = 2383.1 and m/z = 1961.9, as are those for **5.3b** at m/z = 2197.0 [**5.3b** – 5OTf]$^{5+}$ and m/z = 1806.2 [**5.3b** – 6OTf]$^{6+}$. These signals are isotopically resolved and in good agreement with their theoretical distributions.

The structure of **5.3** was unambiguously determined by X-ray diffraction analysis using synchrotron radiation. X-ray quality crystals of **5.3a** were obtained by slow diffusion of pentane into acetone solution of **5.3a**. As shown in Figure 5.2, the structure has a truncated tetrahedral shape with a diameter of 3.6 nm, and bears a 1.0 nm cavity in its core. The shortest Pt-Pt distance is 1.1 nm. The PF_6^- anions are found surrounding the

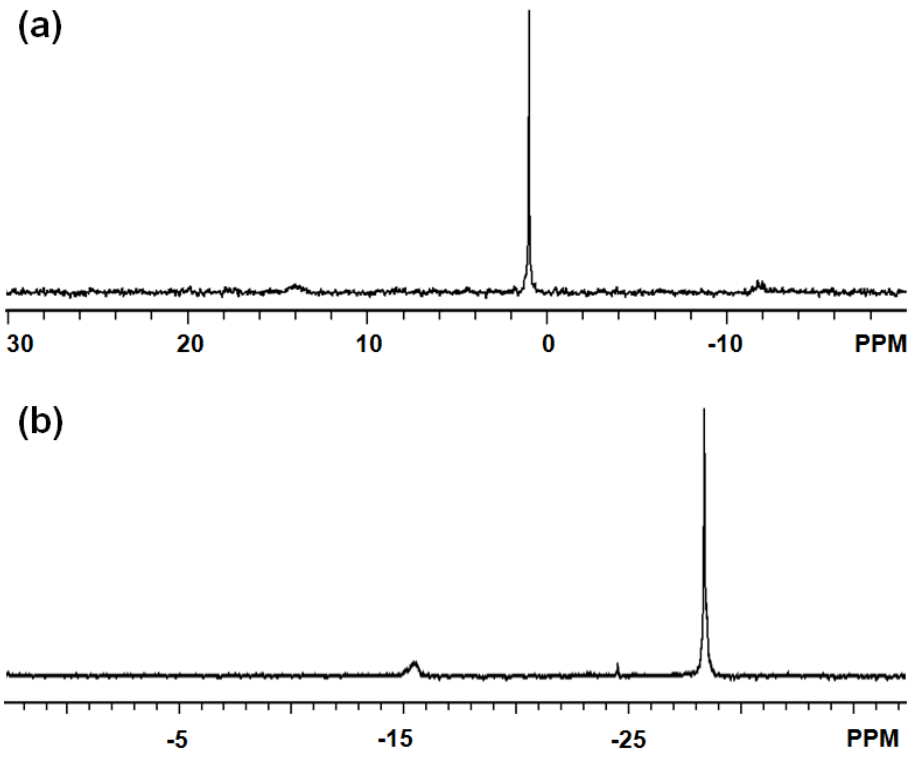

Figure 5.1. $^{31}P\{^{1}H\}$ NMR spectra of truncated tetrahedra **5.3a** in acetone-d_6/CD_3NO_2 (a) and **5.3b** in acetone-d_6/D_2O (b).

structure but not in the cavity, and the shortest Pt-F distance was measured to be 0.48 nm. The Pt atoms in the structure are coordinated by two PEt_3 and two nitrogen atoms from the pyridine moieties, resulting in a distorted square planar geometry. The mean values from the square planar Pt(II) are N-Pt-N 80.6 °, P-Pt-P 98.2 °, N-Pt-P 90.6 °, Pt-P 2.28 Å, and Pt-N 2.09 Å.

PGSE NMR measurements were also used to characterize the structures in solution. Using the translational self-diffusion coefficient measured by PGSE NMR in conjunction with the Stokes-Einstein equation, the "effective size" of the overall assembly in acetone-d_6 was obtained: 3.35 ± 0.15 nm for **5.3a** and 3.23 ± 0.21 nm for **5.3b**, which are in good agreement with that of the crystal structure.

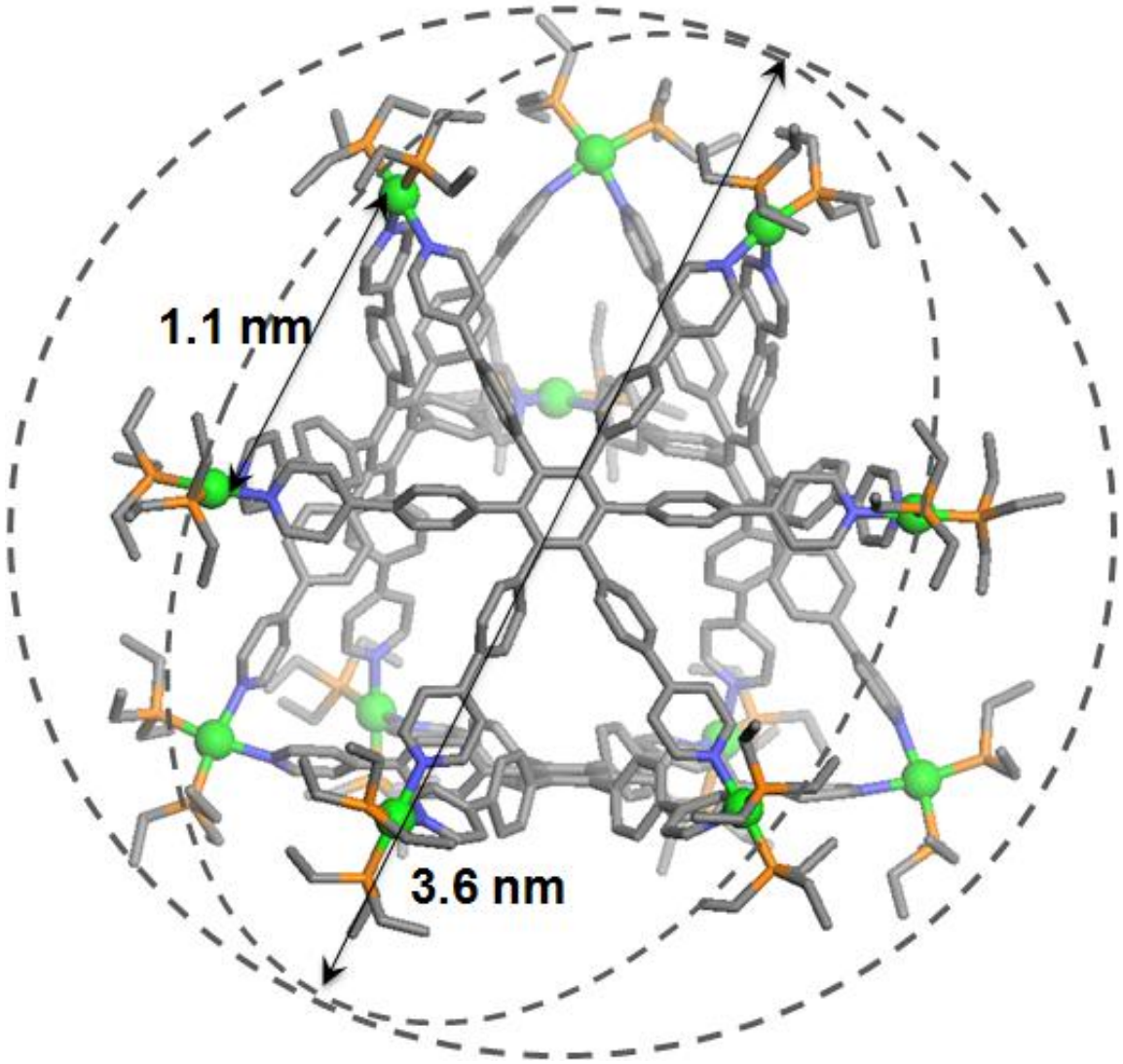

Figure 5.2. Crystal structure of truncated tetrahedron **3a** (Pt: green; C: grey; N: blue; P: Orange; protons, solvent, and PF_6^- omitted for clarity).

The host-guest properties of **5.3** were also studied. Accounting for the symmetry and size of the host, 1,3,5-triphenylbenzene **5.4** was chosen for these investigations. The experiment was carried out by mixing **5.1b** and **5.2** in a 3:1 ratio with excess triphenylbenzene **5.4** in an aqueous acetone solution (*v/v* 1:1). After 16 h of heating at 70 ℃, the encapsulated complex **5.3b 5.4**$_3$ was formed.

The singlet at -28.2 ppm with concomitant ^{195}Pt satellites in the ^{31}P{^{1}H} NMR spectrum and the identifiable peaks (δ = 8.76 ppm $H_{Py\text{-}\alpha\text{-}\mathbf{5.3b}}$; δ = 7.36 ppm $H_{Py\text{-}\beta\text{-}\mathbf{5.3b}}$; δ = 6.94 ppm $H_{Phenyl\text{-}\mathbf{5.3b}}$) in the ^{1}H NMR spectra (Figure 5.3c) show the formation of a truncated tetrahedron. By comparing the ^{1}H NMR spectra of **5.4** (acetone-d_6), **5.3b** (acetone-d_6/D_2O = 1:1), and **5.3b 5.4**$_3$ (acetone-d_6/D_2O = 1:1) in Figure 5.3b, signals are found at 7.25 ppm (Δδ = -0.6 ppm, $H_{Phenyl\text{-}\mathbf{5.4}}$), 7.06 ppm (Δδ = 0.24 ppm, $H_{Phenyl\text{-}\mathbf{5.3b}}$), and 6.35 ppm (Δδ = -1.0–1.8 ppm, $H_{Phenyl\text{-}\mathbf{5.4}}$), indicating that the triphenylbenzene **5.4** is encapsulated in the truncated tetrahedron **5.3b**. Integration of the peaks at 8.76 ppm ($H_{Py\text{-}\alpha\text{-}\mathbf{5.3b}}$) and 6.35 ppm ($H_{Phenyl\text{-}\mathbf{5.4}}$) suggest that three guest molecules are encapsulated in each cage. In the ESI mass spectra (Figure 5.3d), isotopically resolved signals at m/z = 2380.8 [**3b 4**$_3$ – 5OTf]$^{5+}$ and m/z = 1959.3 [**5.3b 5.4**$_3$ – 6OTf]$^{6+}$ confirm the complex **5.3b 5.4**$_3$. Elemental analysis of the isolated complex is also consistent with the composition of **5.3b 5.4**$_3$.

While X-ray quality crystals for **5.3b 5.4**$_3$ were not obtained, a computational simulation was used to gain insight into the structural features of the encapsulated complex.[10] A molecular dynamics simulation using a molecular mechanics force field (MMFF), 300K, in the gas phase was used to equilibrate the supramolecule, and the output of the simulation was then minimized to full convergence. As shown in Figure 5.4,

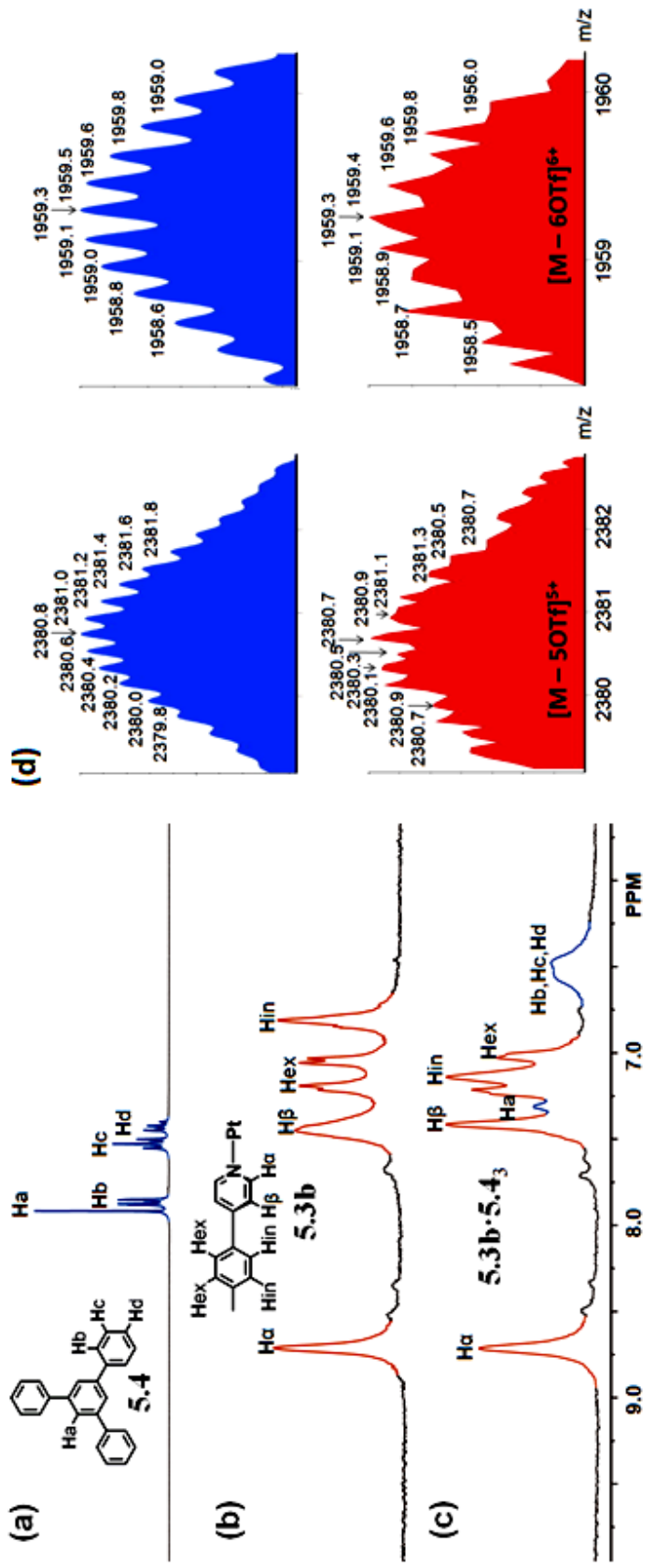

Figure 5.3. Partial ^{1}H NMR spectra of "free" **5.4** in acetone-d_6 (a), **5.3b** in acetone-d_6/D_2O (b), and the encapsulated complex **5.3b** **5.4**$_3$ in acetone-d_6/D_2O (c) and its ESI mass spectra (d).

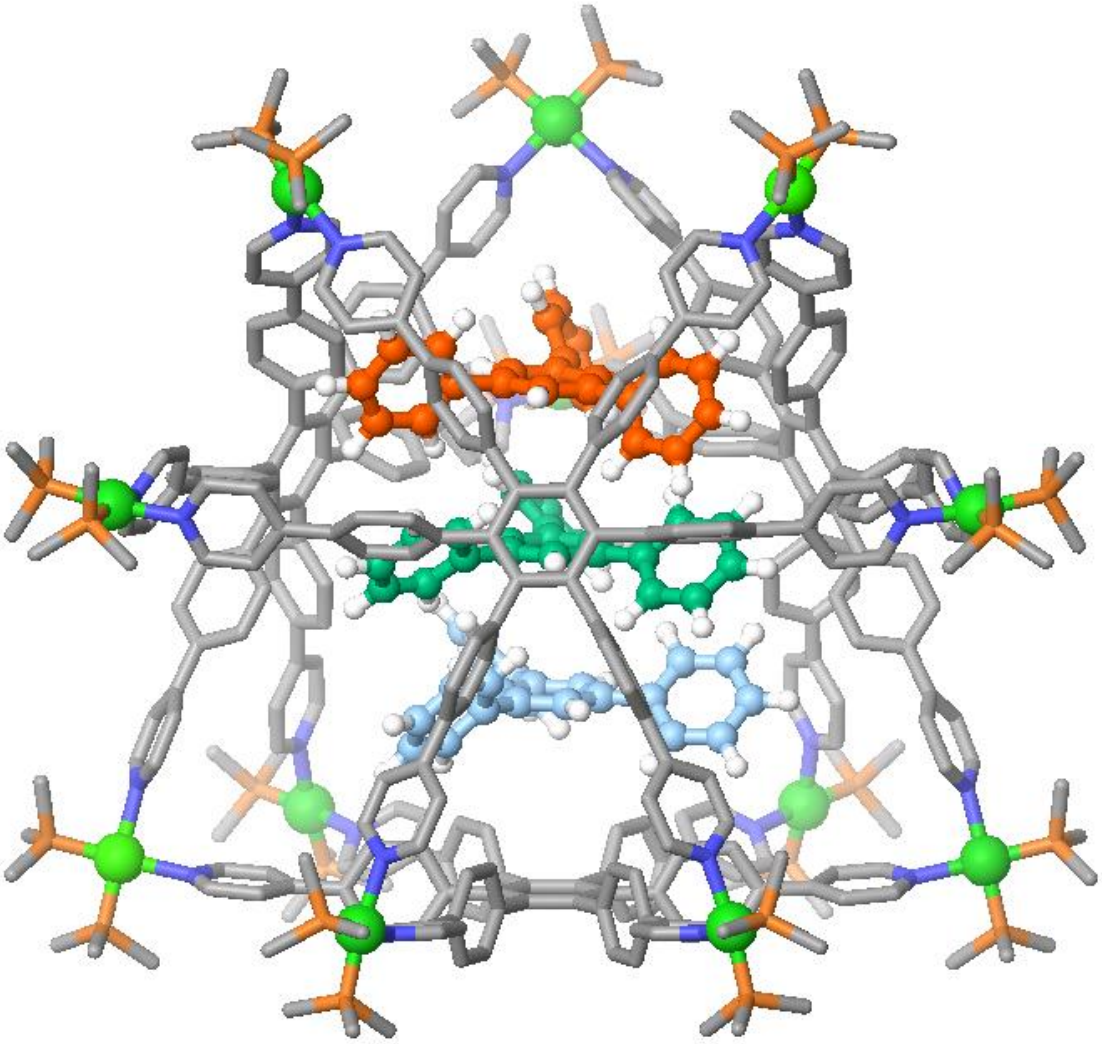

Figure 5.4. Computational model (MMFF) of the encapsulated complex **5.3b•5.4$_3$** (For clarity, the three guest molecules are labeled as blue, green, and orange).

in the model of **5.3b 5.4**$_3$, three triphenylbenzene molecules **5.4** are stacked within the cavity of **5.3b**. The distance between these guests is about 0.43 nm, and that between the guest and the interior of the cage is 0.36–0.43 nm.

5.3 Conclusion

In conclusion, we report the facile synthesis of a new type of 3D truncated tetrahedra via coordination-driven self-assembly, wherein the highly symmetrical hexapyridyl ligands act as faces and 90 ° platinum acceptors are connectors at the edges. These truncated tetrahedra show a unique 3D nanoscale pore, and preliminary studies indicate the nano-cavity is able to encapsulate 1,3,5-triphenylbenzene.

5.4 References

(1) (a) Leininger, S.; Olenyuk, B.; Stang, P. J. *Chem. Rev.* **2000**, *100*, 853. (b) Seidel, S. R.; Stang, P. J. *Acc. Chem. Res.* **2002**, *35*, 972. (c) Holliday, B. J.; Mirkin, C. A. *Angew. Chem., Int. Ed.* **2001**, *40*, 2022. (d) Fujita, M.; Umemoto, K.; Yoshizawa, M.; Fujita, N.; Kusukawa, T.; Biradha, K. *Chem. Commun.* **2001**, 509. (e) Fiedler, D.; Leung, D. H.; Bergman, R. G.; Raymond, K. N. *Acc. Chem. Res.* **2005**, *38*, 351. (f) Fujita, M.; Tominaga, M.; Hori, A.; Therrien, B. *Acc. Chem. Res.* **2005**, *38*, 369. (g) Ruben, M.; Rojo, J.; Romero-Salguero, F. J.; Uppadine, L. H.; Lehn, J.-M. *Angew. Chem., Int. Ed.* **2004**, *43*, 3644. (h) Severin, K. *Chem. Commun.* **2006**, 3859. (i) Nitschke, J. R. *Acc. Chem. Res.* **2007**, *40*, 103. (j) Oliveri, C. G.; Ulmann, P. A.; Wiester, M. J.; Mirkin, C. A. *Acc. Chem. Res.* **2008**, *41*, 1618. (k) Ward, M. D. *Chem. Commun.* **2009**, *30*, 4487. (l) Jin, P.; Dalgarno, S. J.; Atwood, J. L. *Coord. Chem. Rev*. **2010**, *254*, 1760.

(2) (a) Fujita, M.; Oguro, D.; Miyazawa, M.; Oka, H.; Yamaguchi, K.; Ogura, K. *Nature* **1995**, *378*, 469. (b) Parac, T. N.; Caulder, D. L.; Raymond, K. N. *J. Am. Chem. Soc.* **1998**, *120*, 8003. (c) Johannessen, S. C.; Brisbois, R. G.; Fischer, J. P.; Grieco, P. A.; Counterman, A. E.; Clemmer, D. E. *J. Am. Chem. Soc.* **2001**, *123*, 3818. (d) Roche, S.; Haslam, C.; Adams, H.; Heath, S. L.; Thomas, J. A. *Chem. Commun.* **1998**, 1681. (e) Fujita, M.; Yu, S.-Y.; Kusukawa, T.; Funaki, H.; Ogura, K.; Yamaguchi, K. *Angew, Chem. Int. Ed. Engl.* **1998**, *37*, 2082. (f) Olenyuk, B.; Whiteford, J. A.; Fechtenkotter, A.; Stang, P. J. *Nature*, **1999**, *398*, 796. (g) Schweiger, M.; Seidel, S. R.; Schmitz, M.; Stang, P. J. *Org. Lett.* **2000**, *2*, 1255. (h) Olenyuk, B.; Levin, M. D.; Whiteford, J. A.; Shield, J. E.; Stang, P. J. *J. Am. Chem. Soc.* **1999**, *121*, 10434. (i) Suzuki, K.; Kawano, M.; Sato, S.; Fujita, M. *J. Am. Chem. Soc.* **2007**, *129*, 10652. (j) Ghosh, K. Hu, J.; White, H. S.; Stang, P. J.

J. Am. Chem. Soc. **2009**, *131*, 6695. (k) Suzuki, K.; Tominaga, M.; Kawano, M.; Fujita, M. *Chem. Commun.* **2009**, *13*, 1638. (l) Zheng, Y.-R. Ghosh, K.; Yang, H.-B.; Stang, P. J. *Inorg. Chem.* **2010**, *114*, 9007. (m) Sun, Q.-F.; Iwasa, J.; Ogawa, D.; Ishido, Y.; Sato, S.; Ozeki, T.; Sei, Y.; Yamaguchi, K.; Fujita, M. *Science* **2010**, *328*, 1144.

(3) (a) Rosi, N. L.; Eckert, J.; Eddaoudi, M.; Vodak, D. T.; Kim, J.; O'Keeffe, M.; Yaghi, O. M. *Science* **2003**, *300*, 1127. (b) Trembleau, Laurent; Rebek, Julius, Jr. *Science* **2003**, *301*, 1219. (c) Yoshizawa, M.; Tamura, M.; Fujita, M. *Science* **2006**, *312*, 251. (d) Pluth, Michael D.; Bergman, Robert G.; Raymond, Kenneth N. *Science* **2007**, *316*, 85.

(4) Northrop, B. H.; Yang, H.-B. Stang, P. J. *Chem. Commun.* **2008**, 5896.

(5) (a) Sato, S.; Iida, J.; Suzuki, K.; Kawano, M.; Ozeki, T.; Fujita, M. *Science* **2006**, *313*, 1273. (b) Kamiya, N.; Tominaga, M.; Sato, S.; Fujita, M. *J. Am. Chem. Soc.* **2007**, *129*, 3816. (c) Murase, T.; Sato, S.; Fujita, M. *Angew. Chem., Int. Ed.* **2007**, *46*, 5133. (d) Zheng, Y.-R; Ghosh, K.; Yang, H.-B.; Stang, P. J. *Inorg. Chem.* **2010**, 49, 4747.

(6) (a) Pluth, M. D.; Bergman, R. G.; Raymond, K. N. *Acc. Chem. Res.* **2009**, *42*, 1650. (b) Pluth, M. D.; Fiedler, D.; Mugridge, J. S.; Bergman, R. G.; Raymond, K. N. *Proc. Natl. Acad. Sci. USA* **2009**, *106*, 10438. (c) Brown, C. J.; Bergman, R. G.; Raymond, K. N. *J. Am. Chem. Soc.* **2009**, *131*, 17530. (d) Hastings, C. J.; Pluth, M. D.; Bergman, R. G.; Raymond, K. N. *J. Am. Chem. Soc.* **2010**, *132*, 6938.

(7) (a) Yoshizawa, M; Klosterman, J. K.; Fujita, M. *Angew. Chem., Int. Ed.* **2009**, *48*, 3418. (b) Murase, T.; Horiuchi, S.; Fujita, M. *J. Am. Chem. Soc.* **2010**, *132*, 2866. (c) Dolain, C.; Hatakeyama, Y.; Sawada, T.; Tashiro, S.; Fujita, M. *J. Am. Chem. Soc.* **2010**, *132*, 5644. (d) Horiuchi, S.; Nishioka, Y.; Murase, T.; Fujita, M. *Chem. Commun.* **2010**, *46*, 3460. (e) Murase, T.; Otsuka, K.; Fujita, M. *J. Am. Chem. Soc.* **2010**, *132*, 7864.

(8) (a) Leininger, S.; Fan, J.; Schmitz, M.; Stang, P. J. *Proc. Natl. Acad. Sci. USA* **2000**, *97*, 1380. (b) Schweiger, M.; Yamamoto, T.; Stang, P. J.; Blaeser, D.; Boese, R. *J. Org. Chem.* **2005**, *70*, 4861.

(9) (a) Rathore, R.; Burns, C. L.; Guzei, I. A. *J. Org. Chem.* **2004**, *69*, 1524. (b) Hoffmann, M.; Kärnbratt, J.; Chuan, M. H.; Herz, L. M.; Albinsson, B.; Anderson, H. L. *Angew. Chem., Int. Ed.* **2008**, *47*, 4993.

(10) Caskey, D. C.; Yamamoto, T.; Addicott, C.; Shoemaker, R. K.; Vacek, J.; Hawkridge, A. M.; Muddiman, D. C.; Kottas, G. S.; Michl, J.; Stang, P. J. *J. Am. Chem. Soc.* **2008**, *130*, 7620, and references therein.

CHAPTER 6

GUEST ENCAPSULATION DIRECTED BY SUPRAMOLECULAR TRANSFORMATION

6.1 Introduction

The ability to exhibit host-guest chemistry is considered one of the most interesting features of self-assembled supramolecules.[1] By virtue of the great progress in coordination-driven self-assembly,[2] the host-guest chemistry of coordination supramolecules has rapidly developed in the past decade. Various interesting and valuable coordination supramolecular containers have been designed and constructed.[3] For example, Raymond's tetrahedra[3d] and Fujita's truncated tetrahedra[3b] are elegant examples, which use metal-organic supramolecules, exploiting their precious host-guest properties. Research on the host-guest chemistry of self-assembled metal-organic cages not only enhances the capability of encapsulating an extensive collection of guest molecules, but also leads to a variety of useful applications,[4] e.g., catalysts for organic reactions, containers for stabilizing active species, molecular flasks, etc. Nitschke et al. recently reported that air-sensitive white phosphorous can be stabilized within a Fe(II) tetrahedral cage.[4f] In a recent study, Fujita and coworkers demonstrated that a coordination supramolecule is able to alter biological properties as a result of its host-guest properties.[4g]

It is commonly known that the host-guest properties of coordination supramolecules are directly related to their structural features as the noncovalent interactions holding host and guest molecules together are critical. Supramolecular transformations (see Chapter 4) have emerged as a powerful method to tailor the structural features of self-assembled supramolecules.[5] Thus, supramolecular transformation is a promising new technique to control the host-chemistry properties of coordination-driven self-assembled supramolecular structure, though reports applying this technique are not known. In this chapter, we present the design of guest encapsulation within a multicomponent coordination supramolecular system, which is achieved by a supramolecular transformation of a two-component species to a three-component structure, as shown in Scheme 6.1. The starting two-component supramolecule **6.1** is not able to encapsulate coronene. However, after the addition of suitable molecular subunits, it is transformed into a three-component prism, which encapsulates coronene with a high affinity. The transformation and host-guest chemistry have been examined by NMR spectroscopy and ESI mass spectrometry.

6.2 Results and Discussion

The two-component starting ensemble **6.1** was obtained by mixing the cis-$Pt(PMe_3)_2(OTf)_2$ **6.2** with tritopic pyridyl ligand **6.3** in a 3:2 ratio in an aqueous acetone solution (*v/v* = 1:3). The structure was characterized by ^{31}P and ^{1}H multinuclear NMR spectroscopy and ESI mass spectrometry. In the $^{31}P\{^{1}H\}$ NMR spectra (Figure 6.1a), only one singlet at -28.4 ppm with concomitant ^{195}Pt satellites can be found. Likewise, the ^{1}H NMR spectra show sharp signals assigned to **6.1** (δ = 9.34 ppm, $H_{\alpha\text{-Py}}$; δ = 8.88 ppm, $H_{\beta\text{-Py}}$). In ESI-MS, isotopically resolved signals corresponding to the [6 + 4] self-

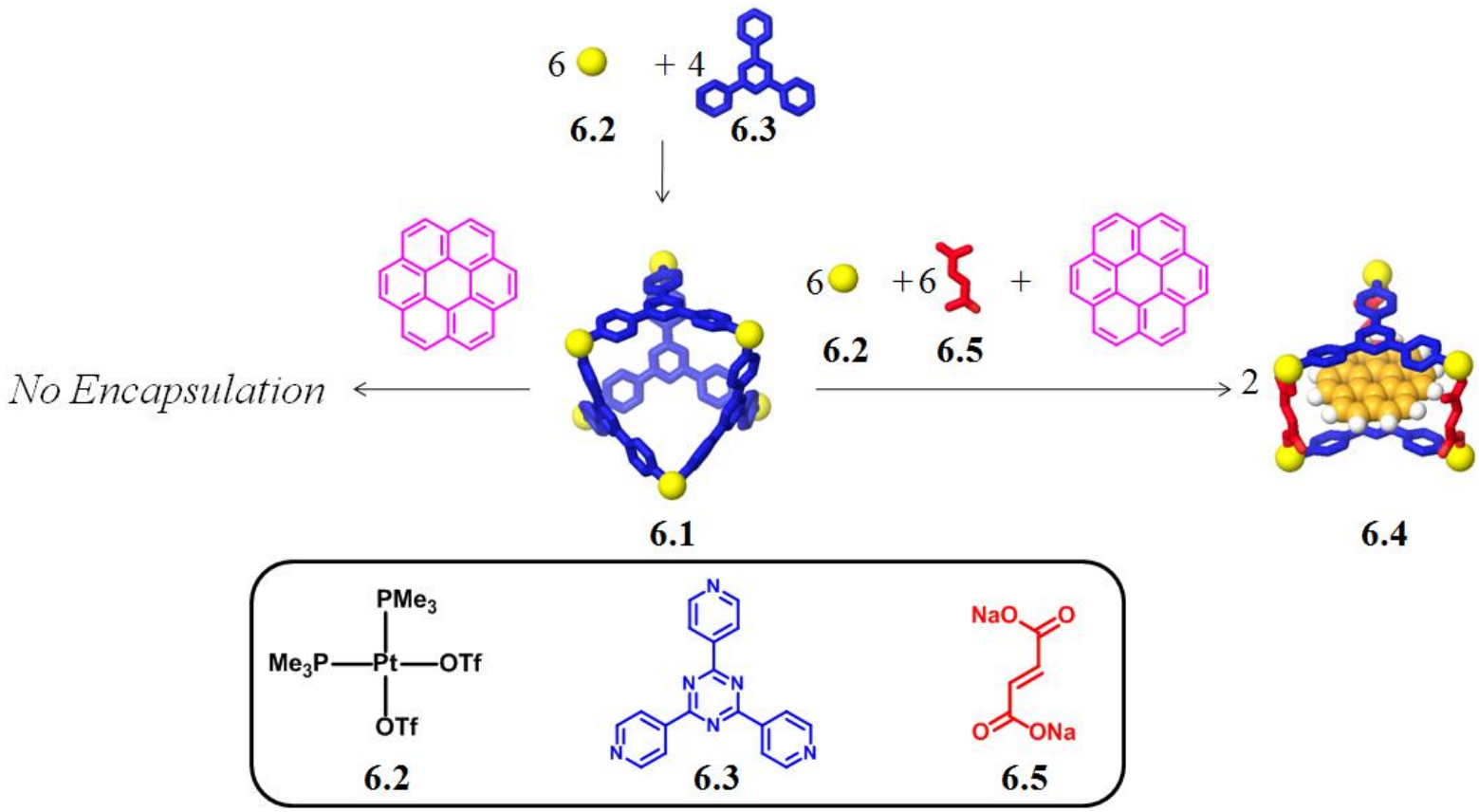

Scheme 6.1. Schematic representation of the supramolecular transformation of **6.1** to **6.4** resulting in encapsulation of coronene.

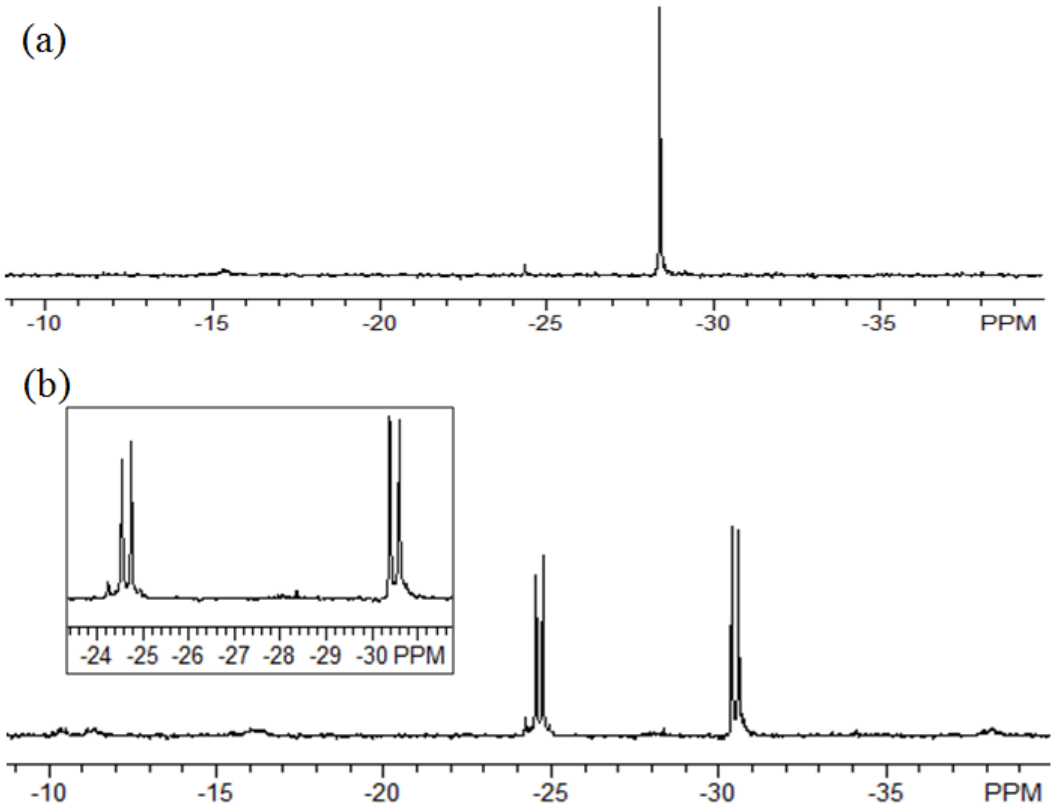

Figure 6.1. $^{31}P\{^{1}H\}$ NMR spectra of **6.1** and the transformed **6.4**.

assembly of **6.1** were observed at m/z = 1130.9 [**6.1** – 4OTf]$^{4+}$, m/z = 1557.4 [**6.1** – 3OTf]$^{3+}$. The host-guest chemistry between **6.1** and coronene was examined in two different ways: addition of coronene before and after self-assembly occured. However, in either case, the two-component supramolecular cage is not able to encapsulate, as evidenced by the unchanged signals for coronene and **6.1** in the ^{1}H NMR spectra (Figure 6.2c), as well as no indicative signals in the ESI-MS.

The supramolecular transformation of two-component species **6.1** into the three-component structure **6.4** was achieved by the addition of cis-Pt$(PMe_3)_2(OTf)_2$ **6.2** and carboxylate ligand **6.5** in presence of excess coronene. After 5 h of heating at 75 ℃, the colorless suspension turned orange. ^{31}P and ^{1}H multinuclear NMR spectroscopy was used

to characterize the mixture. In the $^{31}P\{^{1}H\}$ NMR spectra (Figure 6.1b), two coupled doublets at −24.8 ppm and −30.6 ppm with concomitant ^{195}Pt satellites were observed and the singlet at -28.4 ppm for the stating material **6.1** was absent. This observation indicates the success of transforming **6.1** into **6.4** in the mixture. In the ^{1}H NMR spectra (Figure 6.2d), sharp and well-defined signals at 8.84 ppm ($H_{Py\text{-}\alpha}$), 7.40 ppm ($H_{Py\text{-}\beta}$), and 7.08 ppm (H_{phenyl}) support the formation of a highly symmetrical three-component structure, **6.4**. The shifted proton signal at 8.15 ppm ($\Delta\delta$ = −0.83 ppm) for coronene clearly indicates that encapsulation has occurred within the aromatic cavity of prism **6.4**. Integration of the resonances indicates one coronene is present in each cage.

ESI mass spectral studies strongly support the formation of a host-guest complex. In the ESI mass spectrum (Figure 6.3), major peaks at m/z = 911.9 and 1265.5 are observed, corresponding to $[M - 4OTf]^{4+}$ and $[M - 3OTf]^{3+}$ of the complex **6.4**. Both isotopically resolved patterns match with their theoretical distributions. Elemental analysis of the isolated complex is also consistent with the composition of **6.4**.

While X-ray quality crystals for **6.4** were not obtained, a computational simulation was used to gain insight into the structural features of the encapsulated complex **6.4**.[6] A molecular dynamics simulation using a molecular mechanics force field (MM2*), 300K, in the gas phase was used to equilibrate each supramolecule, and the output of the simulation was then minimized to full convergence. As shown in Figure 6.4, in the model of **6.4**, one coronene molecule is stacked between two tripyridyl panels of the host and the average distance between them is about 0.35 nm. This is an ideal distance for π-π interactions, and as such, π-π interactions are likely a major driving force for the encapsulation.

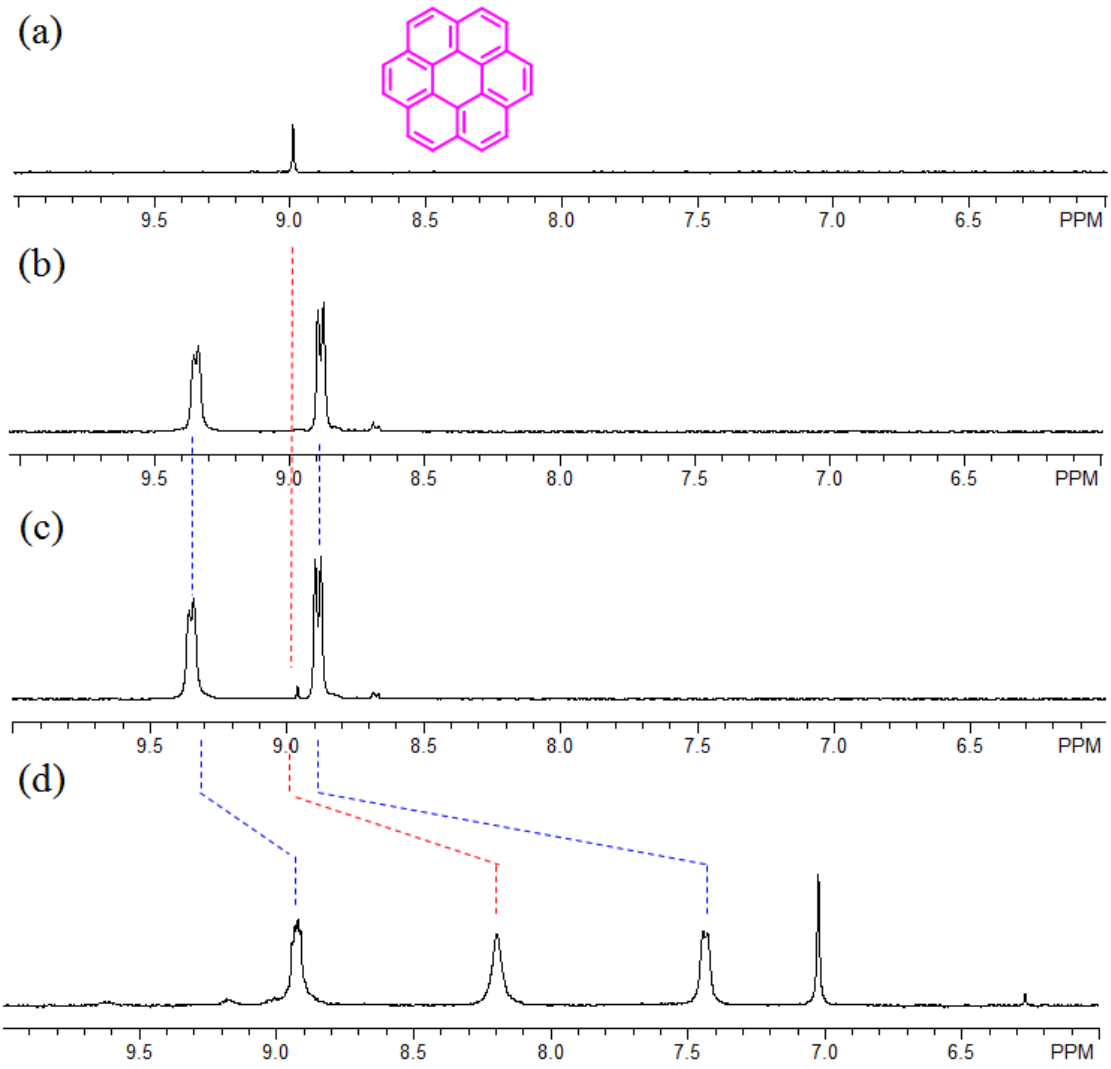

Figure 6.2. Partial ^{1}H NMR spectra of coronene (a), **6.1** (b), mixture of **6.1** and coronene (c), and transformation from **6.1** to **6.4** with encapsulation of coronene (d) by addition of *cis*-$Pt(PMe_3)_2(OTf)_2$ **6.2** and carboxylate ligand **6.5**.

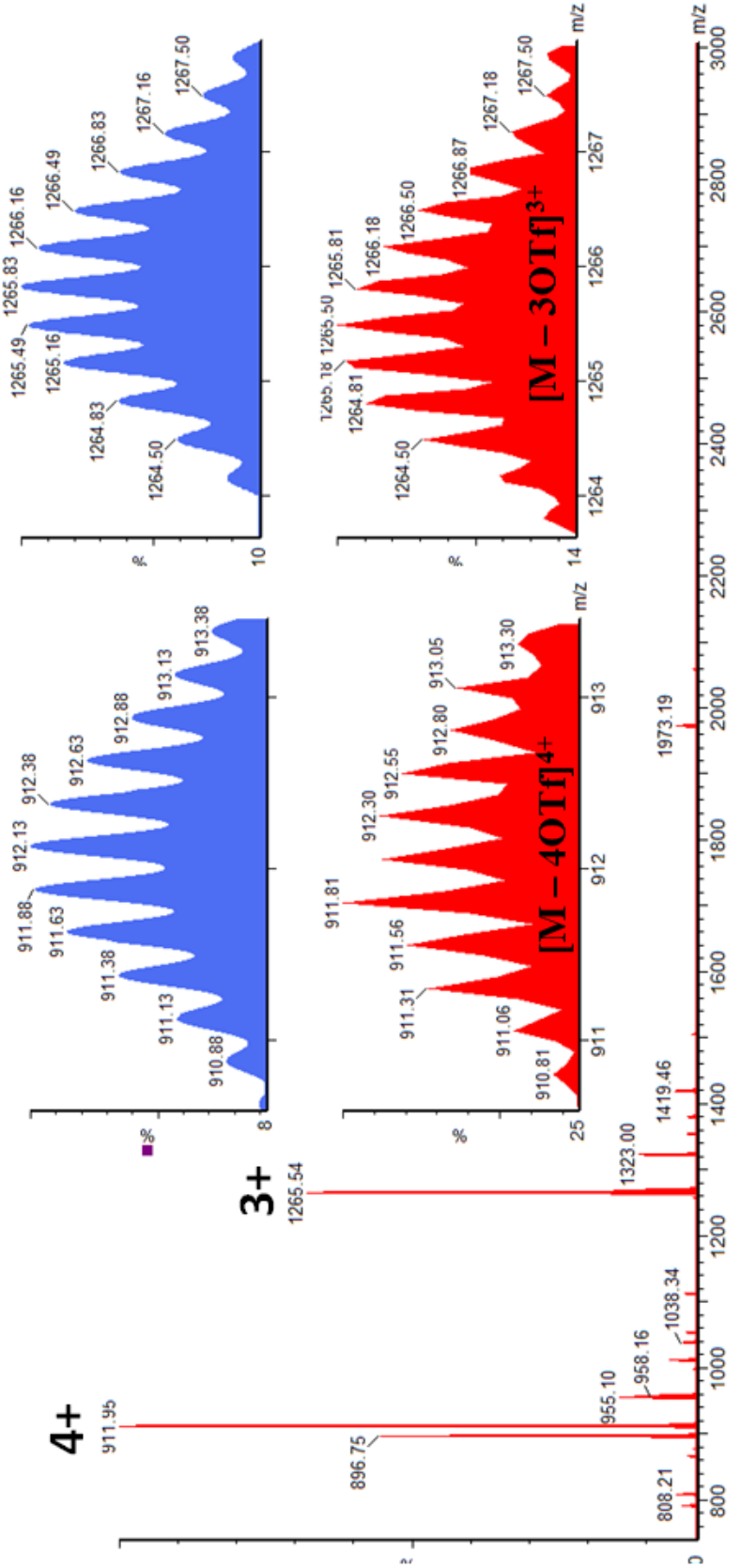

Figure 6.3. Full ESI mass spectrum of the solution of the transformed three-component supramolecular prism **6.4** encapsulating coronene.

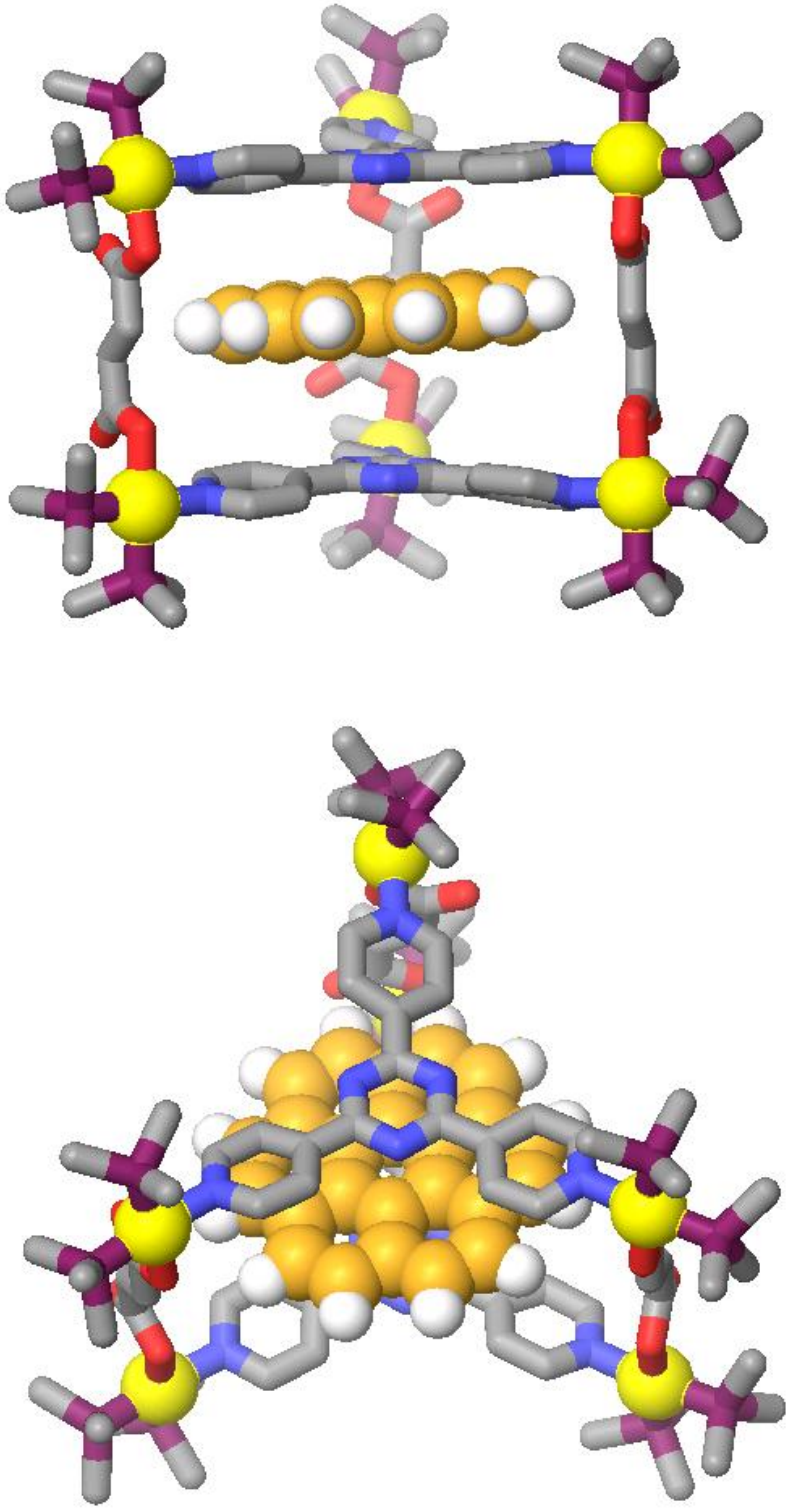

Figure 6.4. Different views of the MM2* computational simulation of three-component trigonal prism **6.4** with encapsulated coronene.

6.3 Conclusion

In conclusion, we have studied the use of supramolecular transformation to alter the host-guest properties of a coordination supramolecular system resulting in the encapsulation of coronene. The transformation and subsequent host-guest chemistry are strongly supported by NMR spectroscopy and ESI mass spectrometry. In this study, the supramolecular transformation allowed for the conversion of a two-component species, which is unable to capture coronene to a three-component prism which encapsulates coronene with a high affinity. This study represents our initial attempt to develop valuable applications based on the selective self-assembly of multicomponent supramolecular systems and supramolecular transformations in combination with host-guest chemistry. By virtue of the generality of multicomponent selective self-assembly and the power of supramolecular transformation, these results provide a basis for future design strategies seeking to alter the host-guest properties of coordination-based supramolecular systems as well as the development of tunable host-guest supramolecular systems.

6.4 References

(1) (a) Rebek, J., Jr. *Chem. Soc. Rev.* **1996**, *25*, 255. (b) Hof, F.; Rebek, J., Jr. *Prod. Nat. Acd. Sci. USA* **2002**, *99*, 4775. (c) Palmer, L. C.; Rebek, J., Jr. *Org. Biom. Chem.* **2004**, *2*, 3051. (d) Albrecht, M.; Janser, I.; Froehlich, R. *Chem. Commun.* **2005**, *2*, 157. (e) Rebek, J., Jr. *Angew. Chem., Int. Ed.* **2005**, *44*, 2068. (f) Crego-Calama, M.; Reinhoudt, D. N.; ten Cate, M. G. J. *Top. Curr. Chem.* **2005**, *249*, 285. (g) Scarso, A.; Rebek, J., Jr. *Top. Curr. Chem.* **2006**, *265*, 1. (h) Ludden, M. J. W.; Reinhoudt, D. N.; Huskens, J. *Chem. Soc. Rev.* **2006**, *35*, 1122. (i) Oshovsky, G. V.; Reinhoudt, D. N.; Verboom, W. *Angew. Chem., Int. Ed.* **2007**, *46*, 2366. (j) Rebek, J., Jr. *Chem. Commun.* **2007**, *27*, 2777.

(2) (a) Leininger, S.; Olenyuk, B.; Stang, P. J. *Chem. Rev.* **2000**, *100*, 853. (b) Seidel, S. R.; Stang, P. J. *Acc. Chem. Res.* **2002**, *35*, 972. (c) Holliday, B. J.; Mirkin, C. A. *Angew. Chem., Int. Ed.* **2001**, *40*, 2022. (d) Fujita, M.; Umemoto, K.; Yoshizawa, M.; Fujita, N.; Kusukawa, T.; Biradha, K. *Chem. Commun.* **2001**, 509. (e) Fiedler,

D.; Leung, D. H.; Bergman, R. G.; Raymond, K. N. *Acc. Chem. Res.* **2005**, *38*, 351. (f) Ruben, M.; Rojo, J.; Romero-Salguero, F. J.; Uppadine, L. H.; Lehn, J.-M. *Angew. Chem., Int. Ed.* **2004**, *43*, 3644. (g) Severin, K. *Chem. Commun.* **2006**, 3859. (h) Nitschke, J. R. *Acc. Chem. Res.* **2007**, *40*, 103. (i) Oliveri, C. G.; Ulmann, P. A.; Wiester, M. J.; Mirkin, C. A. *Acc. Chem. Res.* **2008**, *41*, 1618. (j) Ward, M. D. *Chem. Commun.* **2009**, *30*, 4487. (k) Jin, P.; Dalgarno, S. J.; Atwood, J. L. *Coord. Chem. Rev*. **2010**, *254*, 1760.

(3) (a) Beer, P. D.; Gale, P. A. *Angew. Chem., Int. Ed.* **2001**, *40*, 486. (b) Fujita, M.; Tominaga, M.; Hori, A.; Therrien, B. *Acc. Chem. Res.* **2005**, *38*, 369. (c) Maurizot, V.; Yoshizawa, M.; Kawano, M.; Fujita, M. *Dalton Trans.* **2006**, *23*, 2750. (d) Pluth, M. D.; Raymond, K. N. *Chem. Soc. Rev.* **2007**, *36*, 161.

(4) (a) Pluth, M. D.; Bergman, R. G.; Raymond, K. N. *J. Am. Chem. Soc.* **2008**, *130*, 6362. (b) Klosterman, J. K.; Yamauchi, Y.; Fujita, M. *Chem. Soc. Rev.* **2009**, *38*, 1714. (c) Yamauchia, Y.; Yoshizawa, M.; Akita, M.; Fujita, M. *Prod. Nat. Acd. Sci. USA* **2009**, *106*, 10435. (d) Hatakeyama, Y.; Sawada, T.; Kawano, M.; Fujita, M. *Angew. Chem., Int. Ed.* **2009**, *48*, 8695. (e) Pluth, M. D.; Fiedler, D.; Mugridge, J. S.; Bergman, R. G.; Raymond, K. N. *Prod. Nat. Acd. Sci. USA* **2009**, *106*, 10438. (f) Mal, P.; Breiner, B.; Rissanen, K.; Nitschke, J. R. *Science* **2009**, *324*, 1697. (g) Sawada, T.; Fujita, M. *J. Am. Chem. Soc.* **2010**, *132*, 7194. (h) Fiedler, D.; Leung, D. H.; Bergman, R. G.; Raymond, K. N. *Acc. Chem. Res.* **2005**, *38*, 349. (i) Pluth, M. D.; Bergman, R. G.; Raymond, K. N. *Acc. Chem. Res.* **2009**, *42*, 1650. (j) Yoshizawa, M.; Klosterman, J. K.; Fujita, M. *Angew. Chem., Int. Ed.* **2009**, *48*, 3418.

(5) (a) Sun, S.-S.; Anspach, J. A.; Lees, A. J. *Inorg. Chem.* **2002**, *41*, 1862. (b) Sun, S.-S.; Stern, C. L.; Nguyen, S. T.; Hupp, J. T. *J. Am. Chem. Soc.* **2004**, *126*, 6314. (c) Heo, J.; Jeon, Y.-M.; Mirkin, C. A. *J. Am. Chem. Soc.* **2007**, *129*, 7712. (d) Zhao, L.; Northrop, B. H.; Stang, P. J. *J. Am. Chem. Soc.* **2008**, *130*, 11886. (e) Campbell, V. E.; Hatten, X.; Delsuc, N.; Kauffmann, B.; Huc, I.; Nitschke, J. R. *Nature Chem.* **2010**, *2*, 684.

(6) (a) Yang, H.-B.; Ghosh, K.; Northrop, B. H.; Zheng, Y.-R.; Lyndon, M. M.; Muddiman, D. C.; Stang, P. J. *J. Am. Chem. Soc.* **2007**, *129*, 14187; (b) Northrop, B. H.; Gloeckner, A.; Stang, P. J. *J. Org. Chem.* **2008**, *73*, 1787; (c) Zhao, L.; Northrop, B. H.; Zheng, Y.-R.; Yang, H.-B.; Lee, H. J.; Lee, Y. M.; Park, J. Y.; Chi, K.-W.; Stang, P. J. *J. Org. Chem.* **2008**, *73*, 6580.

CHAPTER 7

COORDINATION-DRIVEN SELF-ASSEMBLY OF 3D SUPRAMOLECULAR DENDRIMERS

7.1 Introduction

Dendrimers of high complexity have emerged as one of the most important structures of interest in chemistry, biology, and medical research.[1,2] By merging dedrimer chemistry with the concepts of self-assembly, complicated dendritic structures can be synthesized in a simple manner. For example, one-dimensional (1D) helical supramolecular dendrimers that vividly mimic natural pore-forming proteins can be efficiently self-assembled by employing a library of amphiphilic dendritic peptides.[2a-c] Recently, a variety of two-dimensional (2D) structures, such as rhomboidal, square, and hexagonal supramolecular dendrimers have been prepared via coordination-driven self-assembly.[3,4] Most reported systems are limited to helical and 2D structures. As compared with 1D and 2D structures, three-dimensional (3D) assemblies exhibit a finite cavity of well-defined shape and size, and can be valuable in applications such as guest encapsulation, gas storage, catalysis, and drug delivery.[5] However, 3D supramolecular dendrimers are still rare,[2d] mainly because of the design constraints of rigid well-defined 3D structures.

Coordination-driven self-assembly has proven to be a successful methodology for constructing 3D supramolecules as indicated by the variety of elaborate supramolecular

cages, prisms, and polydedra of well-defined shapes and sizes formed by this method.[6] Self-assembled 3D supramolecules have proven to be useful in capturing guest molecules, supramolecular catalysis, and in accessing unusual reactions by virtue of their 3D nano-cavities.[7] Covalent modifications of molecular subunits can endow assemblies with a wide variety of fascinating structural and functional properties.[8] Because of their robust structures, unique confined spaces, and designable frameworks, coordination-driven self-assembled 3D metallosupramolecules are promising candidates for constructing 3D supramolecular dendrimers.

We have recently prepared 2D hexagonal and 3D cuboctahedral multifunctional scaffolds with a precise number, position, and orientation of functional groups by chemical tailoring of molecular subunits.[10] Encouraged by the power and versatility of this methodology, we extended it to the construction of 3D supramolecular dendrimers, and hereby present the self-assembly of 120° diplatinum acceptors **7.1** with tritopic donors **7.2a**–**d**, substituted with Fréchet-type dendrons from [G-0] to [G-3].[10] As shown in Scheme 7.1, coordination-driven self-assembly allows for quantitative generation of a series of supramolecular dendrimers **7.3a**–**d** possessing a rigid 3D adamantanoid core. These structures have been identified by multinuclear (^{31}P and ^{1}H) NMR spectroscopy and electrospray ionization (ESI) mass spectrometry, as well as pulsed field gradient spin-echo (PGSE) NMR measurement together with computational simulations.

7.2 Results and Discussion

[G-0]–[G-3] tripyridyl donors **7.2a–d** were prepared by substituting tripyridin-4-yl methanol with Fréchet-type dendrons. A CD_2Cl_2 solution of tripyridyl

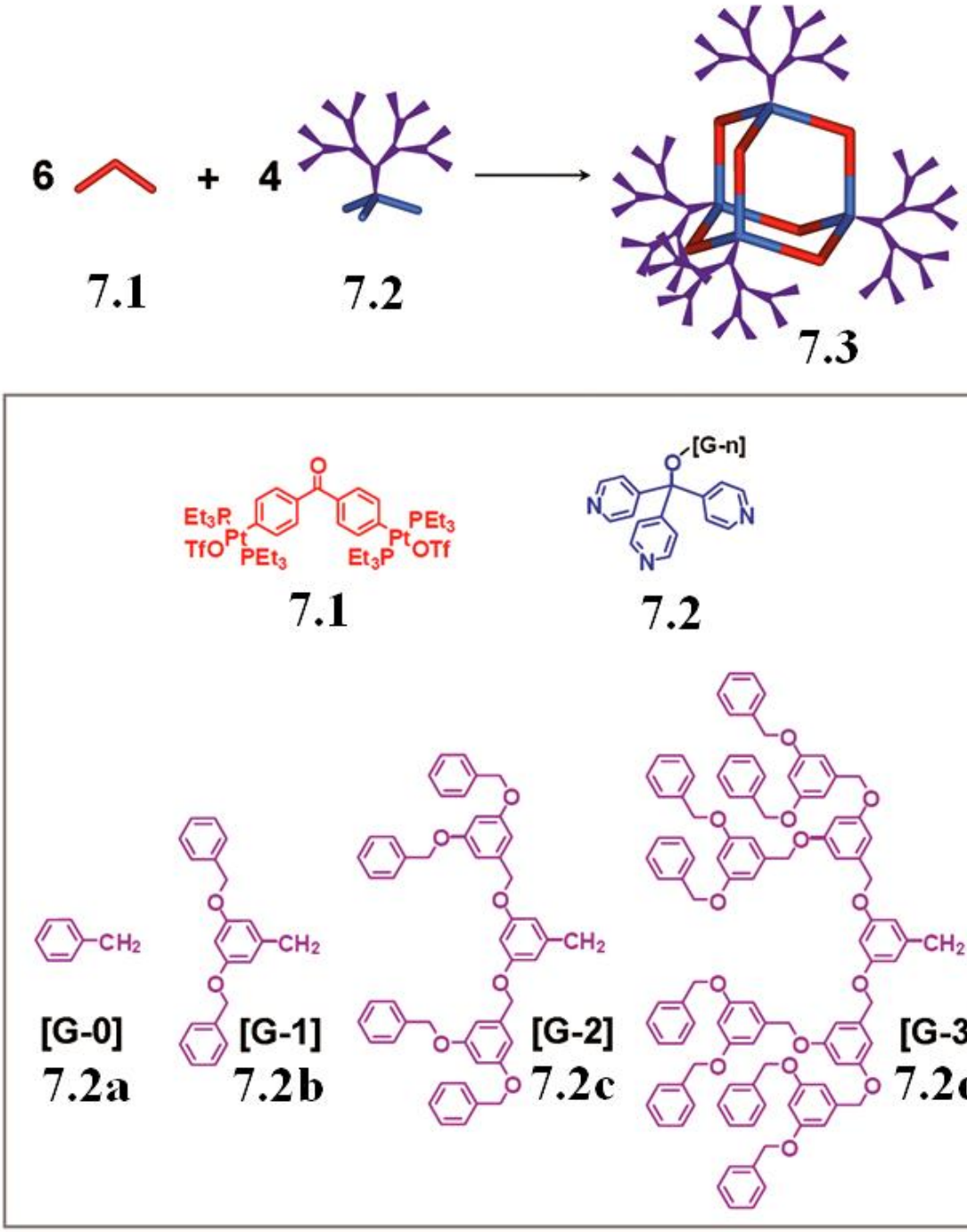

Scheme 7.1. Representation of the [6+4] self-assembly of adamantanoid supramolecular dendrimers

donor **7.2** was slowly added to an acetone-d_6 solution of 120 ° organoplatinum acceptor **1** in a 2:3 ratio. After stirring for 15 min at RT, the [6 + 4] self-assembly of adamantanoid [G-0]–[G-3] dendrimers **7.3a–d** were quantitatively obtained. In the $^{31}P\{^{1}H\}$ NMR spectra (Figure 7.1a and b) of these mixtures, only a sharp singlet (**7.3a**: 14.06 ppm; **7.3b**: 14.06 ppm; **7.3c**: 14.05 ppm; **7.3d**: 14.01 ppm) with concomitant ^{195}Pt satellites can be found. Due to the formation of the Pt-N coordination bond, the signals are shifted upfield from that of the organoplatinum acceptor **7.1** by approximately 9.0 ppm. Likewise, the ^{1}H NMR spectra exhibit sharp signals for the pyridyl protons with small shifts downfield ($\triangle\delta_{Py\alpha\text{-}H}$: 0.30 ppm; $\triangle\delta_{Py\beta\text{-}H}$: 0.75 ppm) due to the loss of electron density that occurs upon coordination. The well-defined sharp NMR signals in both the ^{31}P and ^{1}H NMR agree with the high symmetry of **7.3** and rule out the formation of oligomers.

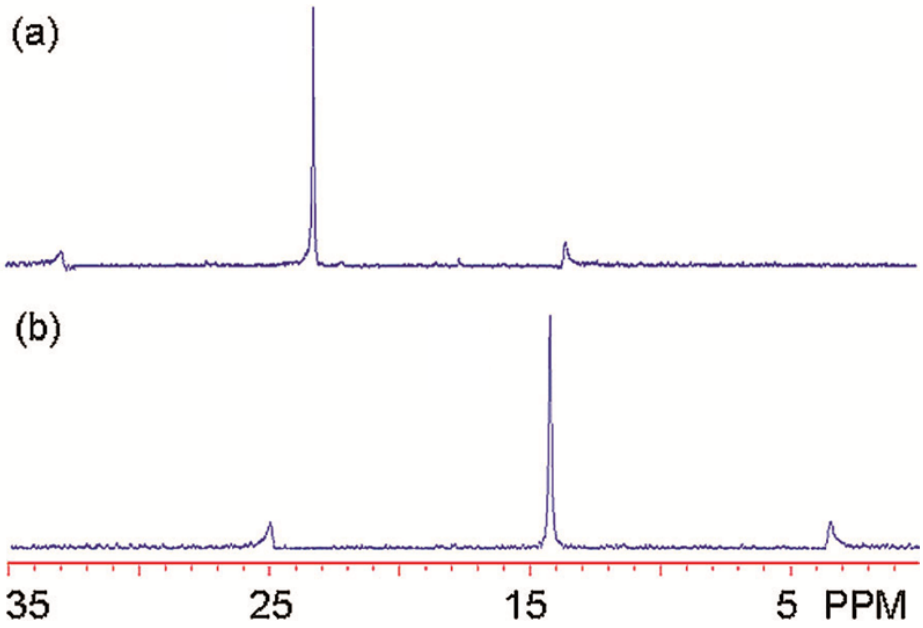

Figure 7.1. $^{31}P\{^{1}H\}$ NMR (300 MHz, Acetone-d_6/CD_2Cl_2: 1/1) Spectra of (a) 120 ° Organoplatinum Acceptor **7.1** and (b) [G-3] Supramolecular Dendrimer **7.3d**.

ESI mass spectrometry further confirmed the [6 + 4] self-assembly of supramolecular dendrimers. In the ESI mass spectrum of the [G-0] adamantanoid dendrimer **7.3a**, peaks corresponding to $[M - 4OTf]^{4+}$ and $[M - 5OTf]^{5+}$ can be found at *m/z* = 1742.4 and *m/z* = 1427.3. The ESI mass peak for loss of triflate anions from [G-1] adamantanoid dendrimer **7.3b** at *m/z* = 1912.2 $[M - 5OTf]^{5+}$ is observed. Simlar peaks are observed for the [G-2] adamantanoid dendrimer **7.3c** at *m/z* = 2251.6 $[M - 5OTf]^{5+}$ (Figure 7.2). All ESI mass peaks are isotopically resolved and agree with their theoretical distributions. However, for the [G-3] adamantanoid dendrimer **7.3d**, an isotopically resolved ESI mass signal was not obtained because of its high molecular weight

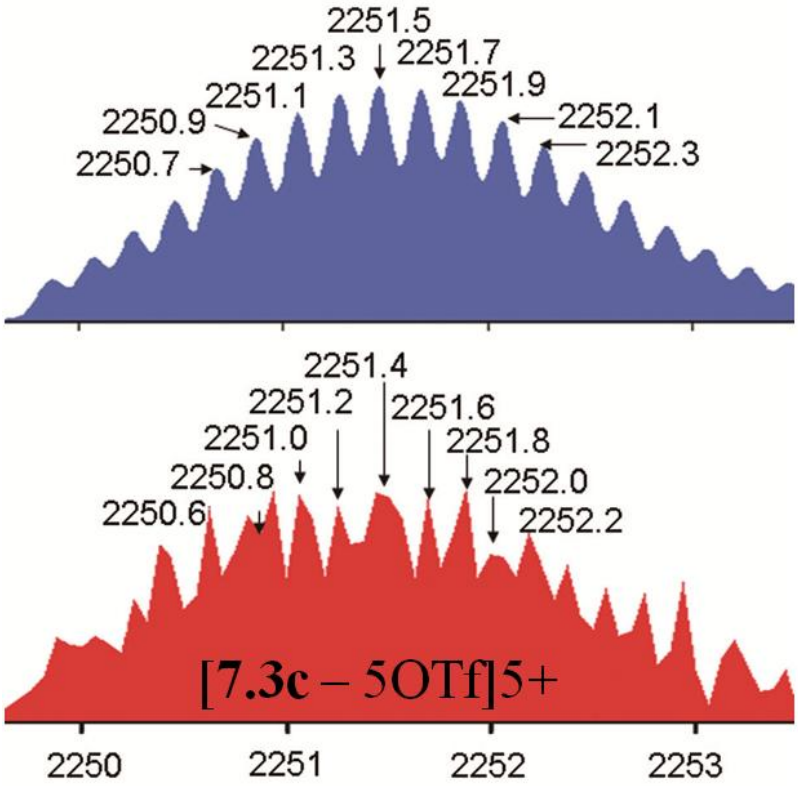

Figure 7.2. Calculated (blue, top) and Experimental (red, bottom) ESI Mass Spectra of [G-2] Supramolecular Dendrimer **7.3c**.

As suitable X-ray quality crystals could not be obtained, a computational study was carried out to gain insight into the structural characteristics of these assemblies. A 1.0 ns molecular dynamics simulation (MMFF force field, 300K, gas phase) was used to equilibrate each supramolecule, and the output of the simulation was then minimized to full convergence. As shown in Figure 7.3, each assembly has a 3.0 nm adamantanoid core with T_d symmetry, and the size of the overall structure is increased from 3.0 nm (for [G-0] **7.3a**) to 4.6 nm (for [G-3] **7.3d**). In **7.3d**, the adamantanoid core is partially covered by a dendritic shell.

PGSE NMR measurements were used to characterize these structures by determination of their translational self-diffusion coefficients. By applying the Stokes-Einstein equation, the "effective size" of the overall assembly in solution was obtained.[11] The ^{1}H PGSE for all assemblies were determined in acetone-d_6 (see Supporting Information) : **7.3a**: 3.0 ± 0.1 nm; **7.3b**: 4.0 ± 0.12 nm; **7.3c**: 4.5 ± 0.1 nm; **7.3d**: 4.5 ± 0.15 nm. As shown in Figure 7.3, these diameters are in good agreement with the computational values (**7.3a**: 3.0 nm; **7.3b**: 3.8 nm; **7.3c**: 4.3 nm; **7.3d**: 4.6 nm) from molecular force field modeling. Since the dendrons on the exterior spread around the adamantanoid core instead of extending out, the size increase from **7.3c** to **7.3d** is minor, as apparent by their similar sizes from the PGSE NMR measurements.

7.3 Conclusion

In conclusion, we have developed a convergent synthesis of 3D metallosupramolecular dendrimers via coordination-driven self-assembly, wherein the exterior dendrons are introduced by pre-assembly modification of molecular subunits. These supramolecular dendrimers possess a unique 3D adamantanoid core, which is part-

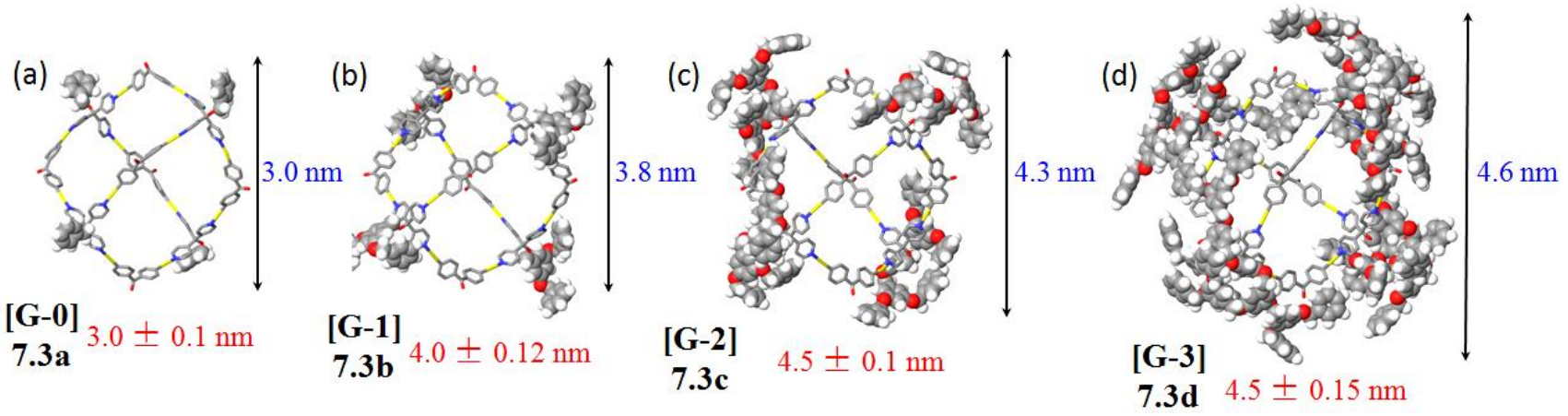

Figure 7.3. Computational simulations (MMFF force field) of 3-D dendrimers **7.3a–d** (protons and triethyl phosphrous moieties of adamantanoid core omitted for clarity) and their calculated (blue) sizes as well as experimental (red) values from PGSE NMR measurements.

ially covered by the dendritic exterior. Exploration of the interior environment would be interesting and valuable. Furthermore, functionalization of dendrons and/or the supramolecular core should allow access to 3D hollow supramolecular functional systems with potential applications in guest encapsulation, nanoreactors, and drug delivery.

7.4 References

(1) (a) Hawker, C. J.; Fréchet, J. M. J. *J. Am. Chem. Soc.* **1990**, *112*, 7638. (b) Fréchet, J. M. J.; Tomalia, D. A. *Dendrimers and Other Dendritic Polymers*; VCH-Wiley: New York, **2000**. (c) Grayson, S. M.; Fréchet, J. M. J. *Chem. Rev.* **2001**, *101*, 3819. (d) Hecht, S.; Fréchet, J. M. J. *Angew. Chem., Int. Ed.* **2001**, *40*, 74-91. (e) Hecht, S.; Vladimirov, N.; Fréchet, J. M. J. *J. Am. Chem. Soc.* **2001**, *123*, 18. (f) Fréchet, J. M. J. *Proc. Natl. Acad. Sci. U.S.A.* **2002**, *99*, 4782. (g) Landskron, K.; Ozin, G. A. *Science* **2004**, *306*, 1529. (h) Lee, C. C.; MacKay, J. A.; Fréchet, J. M. J.; Szoka, F. C. *Nature Biotech.* **2005**, 23, 1517. (i) Medina, S. H.; E.l-Sayed, M. E. H. *Chem. Rev.* **2009**, *109*, 3141.

(2) (a) Percec, V.; Dulcey, A. E.; Balagurusamy, V. S. K.; Miura, Y.; Smidrkal, J.; Peterca, M.; Nummelin, S.; Edlund, U.; Hudson, S. D.; Heiney, P. A.; Duan, H.; Magonov, S. N.; Vinogradov, S. A. *Nature* **2004**, *430*, 764-768. (b) Percec, V.; Dulcey, A. E.; Peterca, M.; Ilies, M.; Sienkowska, M. J.; Heiney, P. A. *J. Am. Chem. Soc.* **2005**, *127*, 17902. (c) Percec, V.; Dulcey, A. E.; Peterca, M.; Adelman, P.; Samant, R.; Balagurusamy, V. S. K.; Heiney, P. A. *J. Am. Chem. Soc.* **2007**, *129*, 5992. (d) Percec, V.; Peterca, M.; Dulcey, A. E.; Imam, M. R.; Hudson, S. D.; Nummelin, S.; Adelman, P.; Heiney, P. A. *J. Am. Chem. Soc.* **2008**, *130*, 13079. (e) Rudick, J. G.; Percec, V. *Acc. Chem. Res.* **2008**, *41*, 1641. (f) Rosen, B. M.; Wilson, C. J.; Wilson, D. A.; Peterca, M.; Imam, M. R.; Percec, V. *Chem. Rev.* **2009,** *109*, 6275.

(3) (a) Yang, H.-B.; Das, N.; Huang, F.; Hawkridge, A. M.; Muddiman, D. C.; Stang, P. J. *J. Am. Chem. Soc.* **2006**, *128*, 10014. (b) Yang, H.-B.; Hawkridge, A. M.; Huang, S. D.; Das, N.; Bunge, S. D.; Muddiman, D. C.; Stang, P. J. *J. Am. Chem. Soc.* **2007**, *129*, 2120. (c) Yang, H.-B.; Northrop, B. H.; Zheng, Y.-R.; Ghosh, K.; Lyndon, M. M.; Muddiman, D. C.; Stang, P. J. *J. Org. Chem.* **2009**, *74*, 3524. (d) Yang, H.-B.; Northrop, B. H.; Zheng, Y.-R.; Ghosh, K.; Stang, P. J. *J. Org. Chem.* **2009**, *74*, 7067.

(4) Baytekin, H. T.; Sahre, M.; Rang, A.; Engeser, M.; Schulz, A.; Schalley, C. A. *Small* **2008**, *4*, 1823.

(5) (a) Rosi, N. L.; Eckert, J.; Eddaoudi, M.; Vodak, D. T.; Kim, J.; O'Keeffe, M.; Yaghi, O. M. *Science* **2003**, *300*, 1127. (b) Trembleau, Laurent; Rebek, Julius, Jr. *Science* **2003**, *301*, 1219. (c) Yoshizawa, M.; Tamura, M.; Fujita, M. *Science*

2006, *312*, 251. (d) Pluth, Michael D.; Bergman, Robert G.; Raymond, Kenneth N. *Science* **2007**, *316*, 85.

(6) (a) Stang, P. J.; Olenyuk, B. *Acc. Chem. Res.* **1997**, *30*, 502. (b) Leininger, S.; Olenyuk, B.; Stang, P. J. *Chem. Rev.* **2000**, *100*, 853. (c) Seidel, S. R.; Stang, P. J. *Acc. Chem. Res.* **2002**, *35*, 972. (d) Fiedler, D.; Leung, D. H.; Bergman, R. G.; Raymond, K. N. *Acc. Chem. Res.* **2005**, *38*, 351. (e) Fujita, M.; Tominaga, M.; Hori, A.; Therrien, B. *Acc. Chem. Res.* **2005**, *38*, 369.

(7) (a) Pluth, M. D.; Bergman, R. G.; Raymond, K. N. *Acc. Chem. Res.* **2009**, *42*, 1650. (b) Yoshizawa, M; Klosterman, J. K.; Fujita, M. *Angew. Chem., Int. Ed.* **2009**, *48*, 3418.

(8) Northrop, B. H.; Yang, H.-B. Stang, P. J. *Chem. Commun.* **2008**, 5896.

(9) (a) Sato, S.; Iida, J.; Suzuki, K.; Kawano, M.; Ozeki, T.; Fujita, M. *Science* **2006**, *313*, 1273. (b) Kamiya, N.; Tominaga, M.; Sato, S.; Fujita, M. *J. Am. Chem. Soc.* **2007**, *129*, 3816. (c) Murase, T.; Sato, S.; Fujita, M. *Angew. Chem., Int. Ed.* **2007**, *46*, 5133. (d) Suzuki, K.; Kawano, M.; Sato, S.; Fujita, M. *J. Am. Chem. Soc.* **2007**, *129*, 10652. (e) Suzuki, K.; Sato, S.; Fujita, M. *Nature Chem.* **2010**, *2*, 25.

(10) (a) Yang, H.-B.; Ghosh, K.; Northrop, B. H.; Zheng, Y.-R.; Lyndon, M. M.; Muddiman, D. C.; Stang, P. J. *J. Am. Chem. Soc.* **2007**, *129*, 14187. (b) Yang, H.-B.; Ghosh, K.; Zhao, Y.; Northrop, B. H.; Lyndon, M. M.; Muddiman, D. C.; White, H. S.; Stang, P. J. *J. Am. Chem. Soc.* **2008**, *130*, 839. (c) Ghosh, K.; Hu, J.; White, H. S.; Stang, P. J. *J. Am. Chem. Soc.* **2009**, *131*, 6695.

(11) Caskey, D. C.; Yamamoto, T.; Addicott, C.; Shoemaker, R. K.; Vacek, J.; Hawkridge, A. M.; Muddiman, D. C.; Kottas, G. S.; Michl, J.; Stang, P. J. *J. Am. Chem. Soc.* **2008**, *130*, 7620, and references therein.

CHAPTER 8

CONCLUSION AND PROSPECTIVE

8.1 Conclusion

My graduate research over the past four years (2007–2011) has focused on the chemistry of coordination-driven self-assembled supramolecular systems with the purpose of obtaining control over coordination supramolecular systems of high complexity and subsequent applications. To achieve these goals, I have been working on three aspects of coordination supramolecular chemistry: 1. Understanding the fundamental dynamic properties of coordination supramolecular systems; 2. Developing approaches to control multicomponent supramolecular systems resulting in self-sorting and selective self-assembly; 3. Searching for potential applications of coordination supramolecular systems based on host-guest chemistry and functionalization. These three aspects of my research have been divided into six chapters of this thesis, as shown below.

8.1.1 Dynamic properties of coordination supramolecular systems

In Chapter 2, I have demonstrated a detailed study concerning dynamic exchange of Pt-N coordination-driven self-assembled supramolecular systems using stable isotope labeling ($^{1}H/^{2}D$) and ESI mass spectrometry together with NMR spectroscopy. Both the thermodynamic and kinetic aspects of such exchange processes have been established based on quantitative mass spectral results. Further investigation showed that, as expected, the exchange is highly dependent on experimental conditions such as

temperature, solvent, and counter anions. These results are not only crucial for understanding and controlling the self-assembly of supramolecular systems, but also important for the use of supramolecular assemblies in further applications.

8.1.2 Self-assembly in multicomponent supramolecular systems: self-sorting and selective self-assembly

In Chapter 3, an approach based on the manipulation of the geometric features of molecular components has been developed to control self-sorting within multicomponent supramolecular systems. Twelve different self-sorting systems have been demonstrated, each of which involves three or four different molecular components. Such self-sorting behavior allows for the selective and simultaneous formation of multiple, discrete supramolecules. The observed self-sorting can be directed by either the size alone, or together with the angle and number of binding sites of organic ligands. The success of self-sorting not only provides an efficient approach for controlling multicomponent supramolecular systems but also represents a significant pathway for supramolecular chemistry to go beyond the paradigm of studying only one supramolecule.

In Chapter 4, I report a facile and efficient approach for the selective self-assembly of well-defined multicomponent 2D and 3D supramolecular structures of various motifs. Upon the combination of 90 ° Pt(II) acceptor with appropriate carboxylate ligands and pyridyl donors in a proper ratio, selective coordination at the Pt(II) centers allows for the selective formation of a multicomponent supramolecular rectangle and prisms. More interestingly, supramolecular transformations and modifications from the two-component assemblies to three-component structures were also achieved based on this selective self-assembly theme. Selective self-assembly allows supramolecular

chemistry to construct architectures of higher complexity as compared to traditional two-component self-assembly, and the supramolecular transformations and modifications provide a new strategy to construct supramolecular architectures by applying pre-assembled supramolecules, in contrast to the bottom-up approach by using a wide range of building blocks.

8.1.3 Potential applications of coordination supramolecular systems

In Chapter 5, I report the facile synthesis of a new type of 3D truncated tetrahedra via coordination-driven self-assembly wherein the highly symmetrical hexapyridyl ligand acts as the faces and 90 ° organoplatinum acceptors are connectors at the edges. These truncated tetrahedra show a unique 3D nanoscale pore, and preliminary studies indicate the nano-cavity is able to encapsulate 1,3,5-triphenylbenzene. This study represents an initial attempt to develop valuable applications based on the host-guest chemistry of coordination supramolecular systems.

In Chapter 6, I demonstrate a study of using supramolecular transformation to alter the host-guest properties of a coordination supramolecular system, resulting in the encapsulation of coronene. In this study, supramolecular transformation allows for the conversion of a two-component species, which is not able to capture coronene, to a three-component prism that encapsulates coronene with high affinity. By virtue of the generality of multicomponent selective self-assembly and the power of supramolecular transformation, this approach may lead to future designs of tunable host-guest supramolecular systems.

In Chapter 7, I have developed a convergent synthesis of nanoscale metallosupramolecular dendrimers via coordination-driven self-assembly wherein the

exterior dendrons were introduced by functionalization of the molecular components. These supramolecular dendrimers show a unique 3D adamantanoid core, which is partially covered by the dendritic exterior. Exploration of this interior environment would be interesting and valuable. These nanoscale supramolecular dendrimers are a suitable scaffold for the development of new applications, such as guest encapsulation, nanoreactors, and drug delivery.

8.2 Prospective

This work helped not only to further the understanding of coordination-driven self-assembly, but also to enhance our capability of controlling supramolecular systems of high complexity, thus allowing for the development of interesting applications. More importantly, these investigations provide important implications for designing prospective supramolecular systems which can be useful in a variety of applications, e.g., biomimics, drug delivery, and reaction catalysts. Several preliminary designs have been proposed.

Supramolecular transformations and modifications can be developed to reversibly change supramolecular structures, going beyond the irreversible transformations we currently employ. For example, by using acid-base stimulus, we may be able to transform three-component supramolecules back to Pt(II)-Pyridine coordination compounds via protonation of the carboxylate donors. Together with host-guest chemistry, such reversible transformations of supramolecular systems may result in reversibly tunable host-guest supramolecular systems, which not only encapsulate but also allow for the release of the encapsulated species. Such tunable host-guest systems are important for further applications in drug delivery.

Functionalization is an important way for supramolecular systems to achieve applications. Supramolecular modifications can be used to achieve postassembly functionalization by using functionalized molecular components. For example, the carboxylate components used to modify Pt(II)-Pyridine supramolecular structures can be synthesized to bear specific functional groups, e.g., long hydrophobic chains or photochemical or electrochemical-responsive moieties, and as a result of supramolecular modifications, the modified three-component supramolecular structure can be functionalized. Supramolecular modifications are able to change both structural and functional features of supramolecular systems, which is a valuable biomimic of post-translational pathways used in biological systems.

By integration with host-guest chemistry, the self-sorting of coordination supramolecular systems can be very interesting. If a collection of self-sorted supramolecules are hosts towards different guest molecules, self-sorted systems may represent a library of supramolecular hosts allowing for the encapsulation of diverse guest molecules. Such libraries can be a fertile ground for developing interesting chemistry. For example, an acid and a base may no longer react in a mixture while they are captured by their hosts. Similarly, organic reactants can proceed via multiple reaction pathways within varying catalytic supramolecular hosts, all in one solution.

CHAPTER 9

EXPERIMENTAL

9.1 General Methods

Solvents used in the reactions were purchased from Fisher, Optima grade, and purified in the following manner: Toluene was distilled from sodium metal; ether and THF were distilled from potassium/benzophenone complex; methylene chloride was distilled from calcium hydride. The filtration device was assembled by tightly placing a filter inside a 9-inch pipette. Deuterated solvents were purchased from Cambridge Isotope Laboratories. NMR spectra were recorded on a Varian Unity 300 spectrometer. The ^{1}H NMR chemical shifts are reported relative to residual solvent signals (CD_2Cl_2: δ = 5.32 ppm; $CDCl_3$: δ = 7.26 ppm; Acetone-d_6: δ = 2.05 ppm; D_2O: δ = 4.80 ppm), and ^{31}P NMR resonances are referenced to an external unlocked sample of 85% H_3PO_4 (δ 0.0). ^{13}C NMR specrtra were recoded at 75 MHz, and all chemical shifts are reported relative to residual solvent signals ($CDCl_3$: δ = 77.8 ppm; Acetone-d_6: δ = 29.8 ppm). Mass spectra were recorded on a Micromass Quattro II triple-quadrupole mass spectrometer using electrospray ionization with a MassLynx operating system, and sample concerntration was around 0.05–1 mM.

9.2 General Procedure for the Dynamic Ligand Exchange Experiment

Individually prepared rectangles (**2.5a** and **2.5b**) and triangles (**2.6a** and **2.6b**) were mixed in 1:1 ([**2.5a**]$_0$= 2.14 mM and [**2.5b**]$_0$ =2.14 mM), 1:1 ([**2.6a**]$_0$ =1.43 mM and

[**2.6b**]$_0$ =1.43 mM), and 3:2 ([**2.5a**]$_0$= 2.14 mM and [**2.6b**]$_0$ =1.43 mM) ratios in an aqueous acetone solution (Acetone-d_6/D_2O 1:1) to carry out the study of ligand exchange between the same (**2.5a** + **2.5b** as well as **2.6a** + **2.6b**) and different (**2.5a** + **2.6b**) types of polygons. Upon heating at 64 ± 1 ℃, the mixtures were periodically transferred for ESI-MS and NMR analysis.

9.3 General Procedure for Self-sorting

Appropriate organoplatinum acceptors and pyridyl donors were placed in a 2-dram vial, followed by the addition of the mixed solvent Acetone-d_6/D_2O (*v/v* 1:1), which was then sealed with Teflon tape and immersed in an oil bath at 65–70 ℃. The clear solution was periodically transferred to an NMR tube for analysis. After three or four sets of signals corresponding to discrete supramolecular structures were clearly presented in the NMR spectra with no further changes, the reaction mixture was characterized by ESI-MS.

9.4 General Procedure for Selective Self-assembly

Cis-$Pt(PEt_3)_2(OTf)_2$ **4.01** along with various carboxylate and pyridyl donors were placed in a 2-dram vial, followed by addition of D_2O (0.2 mL) and Acetone-d_6 (0.8 mL). After 3 h of heating at 75 ℃, all solvent was removed by N_2 flow, and then dried under vacuum. Acetone-d_6 (0.7 mL) was then added into each mixture. A clear solution was obtained after an additional 5 h of heating at 75 ℃. The resulted multicomponent supramolecules were isolated via precipitation by addition of Et_2O or KPF_6.

9.5 General Procedure for Supramolecular Transformation

Two-component self-assembly **4.15**, **4.16**, and **4.17** was obtained in Acetone-d_6 or CD_3NO_2/CD_2Cl_2 mixed solvent, and neutral triangle **12** was formed in Acetone-d_6. Two-

component self-assembly was then slowly added into the solution of neutral triangle in a 3:4 (**4.15**:**4.18**), 1:2 (**4.16**:**4.18**), and 1:2 (**4.17**:**4.18**) ratio, respectively. After 5 h of heating at 75 ^{o}C, clear solutions were obtained and concentrated by N_2 flow. Multinuclear (^{31}P and ^{1}H) NMR spectroscopy was used to characterize the solutions.

9.6 General Procedure for Supramolecular Modification

Two-component self-assembly **4.19** was obtained in Acetone-d_6. The acetone solution of **4.19** was then slowly added into the aqueous solution of carboxylate ligand **4.02**/**4.23** or suspension of **4.02**/**4.23** and **4.01** in a 5:12 (**4.19**:**4.02**), 1:4:4 (**4.19**:**4.02:4.01**), 1:1 (**4.19**:**4.23**), and 3:4:6 (**4.19**:**4.23:4.01**), ratio, respectively. After 1 h of heating at 70 ℃, all solvent was removed by N_2 flow, and then dried under vacuum. Acetone-d_6 (0.7 mL) was then added into each mixture. A suspension or solution was obtained after an additional 5 h of heating at 75 ℃. The suspension or solution was filtered and the modified three-component supramolecules were isolated via precipitation by addition of KPF_6.

9.7 Experimental Details for the Pulsed Field Gradient Spin Echo (PGSE) NMR Measurement

Pulsed gradient spin-echo (PGSE) NMR diffusion measurements were done by pulse-sequence method developed by Stejskal and Tanner:

$$\mathrm{In}(I/I_0) = \gamma_x^2\delta^2G^2(\Delta - \delta/3)D$$

γ_x : Gyromagnetic ratio of the x-nucleus

δ: Length of the gradient pulse

G: Gradient strength

Δ: Delay between the midpoints of gradients

D: Diffusion coeffient

Temp: 298K

Instrument: Inova 500 MHz

Stokes-Einstein Equation: The molecular size is obtained from the diffusion coefficient via the Stokes-Einstein equation shown below:

$$D = k_B T/6\pi\eta r$$

k_B: Bolzmann constant

T: Absolute temperature

r: Hydrodynamic radius of the species under investigation

D: Diffusion coeffient

Gradient Calibration: The gradient strengths need to be carefully calibrated to obtain accurate D values to fit equation (1). Gradient strengths were calibrated using the width (in Hz) of a sample of known length along the NMR-tube (Z) axis; back-calculation of the coil constant from a diffusion experiment on D_2O using $D = 1.9 \times 10^{-5}$ cm^2/s for D_2O at 298K[2] was used to calculate the gradient strengths of both the probes.

Issue of Viscosity: The effect of variable viscosity in different batches of same solvents was examined using the D values observed for the residual protons of the solvent resonance.

Pulse Sequence: Stejskal-Tanner pulse sequence

9.8 Details for the Computational Simulations Using Maestro and Macromodel

The license for Maestro and Macromodel was bought from Schrödinger™.

All computational models were initially built using Maestro, and then minimized by Macromodel. Molecular dynamics simulations using a MMFF or MM2* force field, 300K, in the gas phase was used to equilibrate each supramolecule, and the output of the simulation was then minimized to full convergence.

Parameters Used for Dynamics Simulations:

Force Field: MMFF and MM2*

Solvent: None

Electrostatic Treatment: Constant Dielectric

Dielectric Constant: 1.0

Charge from: Force Field

Cutoff: Normal

Minimization Method: PRCG

Maximum Iterations: 50000

Convergence Threshold: 0.0500

Dynamics: Stochastic Dynamics

SHAKE: Nothing

Simulation Temperature (K): 300.0

Time Step (fs): 1.500

Equilibration Time (ps): 1000.0

Simulation Time (ps): 10000.0

9.9 X-Ray Crystallographic Data of Truncated Tetrahedron

The diffraction data from single crystals of **5.3a** mounted on a loop were collected at 90 K on an ADSC Quantum 210 CCD diffractometer with a synchrotron radiation (λ = 0.90000 Å) at Macromolecular Crystallography Beamline 6B1, Pohang Accelerator Laboratory (PAL), Pohang, Korea. The raw data were processed and scaled using the program HKL2000. The structure was solved by direct methods, and the refinements were carried out with full-matrix least-squares on F^2 with appropriate software implemented in SHELXTL program package. X-ray data for **5.3a**: $C_{108}H_{138}F_{36}N_6P_{12}Pt_3$, M = 3161.15, tetragonal, P-42_1c (No. 114), a = 32.987(5) Å, c = 31.918(6) Å, V =34730(10) Å^3, Z = 8, T = 90 K, μ(synchrotron) = 4.137 mm^{-1}, d_{calc} = 1.209 g cm^{-3}, 154346 reflections measured, 23131 unique (R_{int} = 0.0674), R_1 = 0.0841, wR_2 = 0.2244 for 19314 reflections ($I > 2\sigma(I)$), R_1 = 0.0981, wR_2 = 0.2396 (all data), GoF = 1.060, Flack = 0.015(6), 1487 parameters and 3157 restraints. All the nonhydrogen atoms were refined anisotropically. Hydrogen atoms were added to their geometrically ideal positions.

9.10 General Procedure for the Preparation of Dendron-substituted Donors **7.2a–d**

Tripyridin-4-yl methanol (60 mg, 0.23 mmol) and NaH (30 mg, 1.2 mmol) were placed in a 25 mL Schlenk flask followed by addition of 3 mL anhydrous DMF and 3 ml THF. The mixture was stirred for 30 min. The appropriate [Gn]-Br[1] (for [G0]-Br: 39 mg, 0.23 mmol; for [G1]-Br: 89 mg, 0.23 mmol; for [G2]-Br: 185 mg, 0.229 mmol; for [G3]-Br: 378 mg, 0.228 mmol) was then added under nitrogen. The reaction was continued at 60 ^{o}C for another 1.5 h and then quenched by 10 mL of water, extracted with CH_2Cl_2 (3 × 20 mL), and dried ($MgSO_4$). The solvent was removed by evaporation on a rotary

evaporator. The residue was purified by column chromatography on silica gel to give compounds **7.2a–d**.

9.11 General Procedure for the Preparation of [G-0]–[G-3] 3D Aadamantanoid Supramolecular Dendrimers **7.3a–d**

To a 0.5 mL acetone-d_6 solution of 120° organoplatinum acceptor **7.1** (3.80 mg, 2.83 μmol) was added a 0.5 mL CD_2Cl_2 solution of the appropriate [G0]–[G3] dendric donor **7.2a**–**d** (for **7.2a**: 0.67 mg, 1.9 μmol; for **7.2b**: 1.08 mg, 1.91 μmol; for **7.2c**: 1.89 mg, 1.91 μmol; for **7.2d**: 3.50 mg, 1.90 μmol;), drop by drop, with continuous stirring (10 min). The reaction mixture was stirred overnight at room temperature. The solution was evaporated to dryness, and the product was collected.

9.12 Materials

Platinum acceptors **2.3/3.01**,[2] **2.4/3.06**,[3] **4.01/5.01a**,[4] **5.01b/6.2**,[4] and **7.1**,[5] pyridyl donors (**3.03/4.03**,[2] **3.09**,[6] **3.10**,[6] **3.13/4.05**,[7] **4.11/5.2**[8]), and self-assemblies (rectangles[1]: **2.5a**, **3.04**, and **3.05**; triangles[3]: **2.6a** and **3.07**; prisms[6–9]: **3.11**, **3.12**, **3.14**, and **3.19**) were prepared according to literature procedures. 4,4'-dipyridyl-d_8 **2.2** was purchased from C/D/N Isotope Inc. All other reagents were purchased from Sigma-Aldrich, Alfa-Aesar, Strem, and TCI-American, without further purification unless specified otherwise.

9.13 Synthesis of Compounds

9.13.1 Self-sorting of SS_1

Molecular "Clip" **3.01** (4.44 mg, 0.00382 mmol), 4,4'-dipyridyl **3.02** (0.30 mg, 0.0019 mmol), and 1,4-bis(4-pyridylethynyl)benzene **3.03** (0.53 mg, 0.0019 mmol) were placed in a 2-dram vial, following by adding 0.8 mL of a mixture of solvent (Acetone-d_6

/D_2O 1:1), which was then sealed with Teflon tape and immersed in an oil bath at 60-65 ℃ for 45 h. The yellow orange solution was periodically transferred to an NMR tube for analysis. After two sets of signals corresponding to **3.05** and **3.06** were clearly presented in the NMR spectra with no further changes, the reaction mixture were characterized by ESI/MS. ^{1}H NMR (Acetone-d_6 /D_2O: 1/1, 300 MHz) For **3.05**: δ 9.53 (s, 2H, H_9), 9.21 (d, ^3J = 5.8 Hz, 4H, $H_{\alpha\text{-Py}}$), 9.18 (d, ^3J = 5.4 Hz, 2H, $H_{\alpha'\text{-Py}}$), 8.71 (d, ^3J = 5.4 Hz, 4H, $H_{\beta\text{-Py}}$), 8.53 (d, ^3J = 5.4 Hz, 4H, $H_{\beta'\text{-Py}}$), 8.37 (s, 2H, H_{10}), 7.71 (d, ^3J = 10.5 Hz, 4H, $H_{4,5}$), 7.62 (m, 4H, $H_{2,7}$), 7.14 (t, ^3J = 7.2 Hz, 4H, $H_{3,6}$), 1.45 (m, 48H, PCH_2CH$_3$), 0.84 (m, 72H, PCH$_2$CH_3). For **3.06**: δ 9.45 (s, 2H, H_9), 9.03 (d, 4H, ^3J = 5.1 Hz, $H_{\alpha\text{-Py}}$), 8.95 (d, 4H, ^3J = 5.4 Hz, $H_{\alpha'\text{-Py}}$), 8.36 (s, 2H, H_{10}), 8.03 (m, 8H, $H_{\beta\text{-Py}}$), 7.74 (s, 8H, $H_{\text{phenylene}}$), 7.71 (d, 4H, ^3J = 10.5 Hz, $H_{4,5}$), 7.64 (m, 4H, $H_{2,7}$), 7.14 (t, ^3J = 7.2 Hz, 4H, $H_{3,6}$), 1.45 (m, 48H, PCH_2CH$_3$), 0.84 (m, 72H, PCH$_2$CH_3). ^{31}P {^{1}H} NMR (Acetone-d_6 /D_2O: 1/1, 121.4 MHz) For **3.05**: δ 8.95 (^{195}Pt satellites, $^1J_{\text{Pt-P}}$ = 2671 Hz). For **3.06**: δ 9.10 (^{195}Pt satellites, $^1J_{\text{Pt-P}}$ = 2671 Hz).

9.13.2 Self-sorting of SS_2

60 ° organoplatinum acceptor **3.06** (4.44 mg, 0.00382 mmol), 4,4'-dipyridyl **3.02** (0.30 mg, 0.0019 mmol), and 1,4-Bis(4-pyridylethynyl)benzene **3.03** (0.53 mg, 0.0019 mmol) were placed in a 2-dram vial, following by adding 1.4 mL of a mixture of solvent (Acetone-d_6 /D_2O 1:1), which was then sealed with Teflon tape and immersed in an oil bath at 60-65 ℃ for 65 h. After two sets of signals corresponding to **3.07** and **3.08** were clearly presented in the NMR with no further changes spectra, the reaction mixture were characterized by ESI/MS. ^{1}H NMR (Acetone-d_6 /D_2O: 1/1, 300 MHz) For **3.07**: δ 9.11 (d, ^3J = 5.7 Hz, 6H, $H_{\alpha\text{-Py}}$), 9.06 (d, ^3J = 5.7 Hz, 6H, $H_{\alpha'\text{-Py}}$), 8.62 (s, 6H, $H_{4,5}$), 8.32 (d, ^3J =

6.3 Hz, 6H, $H_{\beta\text{-Py}}$), 8.29 (d, ^3J = 6.0 Hz, 6H, $H_{\beta'\text{-Py}}$), 7.65 (d, ^3J = 8.4 Hz, 6H, $H_{2,7}$), 7.54 (m, 12H, $H_{1,8,9,10}$), 1.30 (m, 72H, PCH_2CH_3), 1.07 (m, 108H, PCH_2CH_3). For **3.08**: δ 8.87 (m, 12H, $H_{\alpha\text{-Py}}$), 8.54 (s, 6H, $H_{4,5}$), 7.80 (d, 12H, ^3J = 6.6 Hz, $H_{\beta\text{-Py}}$), 7.71 (s, 12H, $H_{phenylene}$), 7.65 (d, ^3J = 8.4 Hz, 6H, $H_{2,7}$), 7.54 (m, 12H, $H_{1,8,9,10}$), 1.30 (m, 72H, PCH_2CH_3), 1.07 (m, 108H, PCH_2CH_3). ^{31}P {^1H} NMR (Acetone-d_6 /D_2O: 1/1, 121.4 MHz) For **3.07**: δ 15.19 (^{195}Pt satellites, $^1J_{Pt\text{-}P}$ = 2639 Hz). For **3.08**: δ 15.27 (^{195}Pt satellites, $^1J_{Pt\text{-}P}$ = 2654 Hz).

9.13.3 Self-sorting of SS_3

Molecular "Clip" **3.01** (7.92 mg, 0.00681 mmol), tritopic tectons **3.09** (0.59 mg, 0.0022 mmol), and **3.10** (1.29 mg, 0.00230 mmol) were placed in a 2-dram vial, followed by adding 0.8 mL of a mixture of solvent (Acetone-d_6 /D_2O 1:1), which was then sealed with Teflon tape and immersed in an oil bath at 65-70 ℃ for 24 h. The yellow orange solution was periodically transferred to an NMR tube for analysis. After two sets of signals corresponding to **3.11** and **3.12** were clearly presented in the NMR spectra with no further changes, the reaction mixture were characterized by ESI/MS. ^1H NMR (Acetone-d_6 /D_2O: 1/1 300 MHz) For **3.11**: δ 9.14 (d, 6H, ^3J = 6.3 Hz, $H_{\alpha\text{-Py}}$), 8.98 (m, 9H, $H_{\alpha'\text{-Py},9}$), 8.36 (s, 3H, H_{10}), 8.25 (d, 6H, ^3J = 4.2 Hz, $H_{\beta\text{-Py}}$), 7.72 (m, 12H, $H_{\beta'\text{-Py}}$, $H_{4,5}$), 7.68 (d, 6H, ^3J = 9.9 Hz, $H_{2,7}$), 7.14 (m, 6H, $H_{3,6}$), 1.40 (m, 72H, PCH_2CH_3), 0.82 (m, 108H, PCH_2CH_3). For **3.12**: δ 9.32 (s, 3H, H_9), 9.01 (d, 6H, ^3J = 5.1 Hz, $H_{\alpha\text{-Py}}$), 8.91 (d, 6H, ^3J = 4.8 Hz, $H_{\alpha'\text{-Py}}$), 8.36 (s, 3H, H_{10}), 8.00 (d, 6H, ^3J = 6.0 Hz, $H_{\beta\text{-Py}}$), 7.95 (d, 6H, ^3J = 6.0 Hz, $H_{\beta\text{-Py}}$), 7.73 (m, 12H, $H_{4,5,2,7}$), 7.57 (d, 12H, ^3J = 8.4 Hz, $H_{3,5\text{-phenylene}}$), 7.17 (d, 12H, ^3J = 8.1 Hz, $H_{2,6\text{-phenylene}}$), 7.14 (m, 6H, $H_{3,6}$), 1.40 (m, 72H, PCH_2CH_3), 0.82 (m,

108H, PCH_2CH_3). $^{31}P\{^1H\}$ NMR (Acetone-d_6/D_2O: 1/1 121.4 MHz) **3.11**: δ 11.12 (^{195}Pt satellites, $^1J_{Pt\text{-}P}$ = 2639 Hz). For **3.12**: δ 10.16 (^{195}Pt satellites, $^1J_{Pt\text{-}P}$ = 2654 Hz).

9.13.4 Self-sorting of SS_4

Molecular "Clip" **3.01** (10.56 mg, 0.00908 mmol), 4,4'-dipyridyl **3.02** (0.40 mg, 0.0026 mmol), 1,4-bis(4-pyridylethynyl)benzene **3.03** (0.71 mg, 0.0025 mmol), and tritopic tecton **3.09** (0.70 mg, 0.0026 mmol) were added to 1.1 mL of mixed solvent. After 24 h heating, **3.04**, **3.05**, and **3.11** were formed predominantly. ^1H NMR (Acetone-d_6/D_2O: 1/1, 300 MHz) For **3.04**: δ 9.53 (s, 2H, H_9), 9.21 (d, ^3J = 5.8 Hz, 4H, $H_{\alpha\text{-}Py}$), 9.18 (d, ^3J = 5.4 Hz, 2H, $H_{\alpha'\text{-}Py}$), 8.71 (d, ^3J = 5.4 Hz, 4H, $H_{\beta\text{-}Py}$), 8.53 (d, ^3J = 5.4 Hz, 4H, $H_{\beta'\text{-}Py}$), 8.37 (s, 2H, H_{10}), 7.71 (d, ^3J = 10.5 Hz, 4H, $H_{4,5}$), 7.62 (m, 4H, $H_{2,7}$), 7.14 (t, ^3J = 7.2 Hz, 4H, $H_{3,6}$), 1.45 (m, 48H, PCH_2CH_3), 0.84 (m, 72H, PCH_2CH_3) ppm. For **3.05**: δ 9.45 (s, 2H, H_9), 9.03 (d, 4H, ^3J = 5.1 Hz, $H_{\alpha\text{-}Py}$), 8.95 (d, 4H, ^3J = 5.4 Hz, $H_{\alpha'\text{-}Py}$), 8.36 (s, 2H, H_{10}), 8.03 (m, 8H, $H_{\beta\text{-}Py}$), 7.74 (s, 8H, $H_{phenylene}$), 7.71 (d, 4H, ^3J = 10.5 Hz, $H_{4,5}$), 7.64 (m, 4H, $H_{2,7}$), 7.14 (t, ^3J = 7.2 Hz, 4H, $H_{3,6}$), 1.45 (m, 48H, PCH_2CH_3), 0.84 (m, 72H, PCH_2CH_3) ppm. For **3.11**: δ 9.14 (d, 6H, ^3J = 6.3 Hz, $H_{\alpha\text{-}Py}$), 8.98 (m, 9H, $H_{\alpha'\text{-}Py,9}$), 8.36 (s, 3H, H_{10}), 8.25 (d, 6H, ^3J = 4.2 Hz, $H_{\beta\text{-}Py}$), 7.72 (m, 12H, $H_{\beta'\text{-}Py}$, $H_{4,5}$), 7.68 (d, 6H, ^3J = 9.9 Hz, $H_{2,7}$), 7.14 (m, 6H, $H_{3,6}$), 1.40 (m, 72H, PCH_2CH_3), 0.82 (m, 108H, PCH_2CH_3) ppm. $^{31}P\{^1H\}$ NMR (Acetone-d_6/D_2O: 1/1, 121.4 MHz) For **3.04**: δ 8.32 (^{195}Pt satellites, $^1J_{Pt\text{-}P}$ = 2640 Hz) ppm. For **3.05**: δ 8.48 (^{195}Pt satellites, $^1J_{Pt\text{-}P}$ = 2640 Hz) ppm. For **3.11**: δ 9.81 (^{195}Pt satellites, $^1J_{Pt\text{-}P}$ = 2651 Hz) ppm.

9.13.5 Self-sorting of SS_5

Molecular "Clip" **3.01** (11.98 mg, 0.0103 mmol), 4,4'-dipyridyl **3.02** (0.43 mg, 0.0028 mmol), tritopic tectons **3.09** (0.68 mg, 0.0026 mmol) and **3.10** (1.35 mg, 0.0024 mmol) were added to 1.1 mL of mixed solvent. After 24 h heating, **3.04**, **3.11**, and **3.12** were formed predominantly. ^{1}H NMR (Acetone-d_6 /D_2O: 1/1, 300 MHz) For **3.04**: δ 9.53 (s, 2H, H_9), 9.21 (d, ^{3}J = 5.8 Hz, 4H, $H_{\alpha\text{-Py}}$), 9.18 (d, ^{3}J = 5.4 Hz, 2H, $H_{\alpha'\text{-Py}}$), 8.71 (d, ^{3}J = 5.4 Hz, 4H, $H_{\beta\text{-Py}}$), 8.53 (d, ^{3}J = 5.4 Hz, 4H, $H_{\beta'\text{-Py}}$), 8.37 (s, 2H, H_{10}), 7.71 (d, ^{3}J = 10.5 Hz, 4H, $H_{4,5}$), 7.62 (m, 4H, $H_{2,7}$), 7.14 (t, ^{3}J = 7.2 Hz, 4H, $H_{3,6}$), 1.45 (m, 48H, PCH_2CH_3), 0.84 (m, 72H, PCH_2CH_3) ppm. For **3.11**: δ 9.14 (d, 6H, ^{3}J = 6.3 Hz, $H_{\alpha\text{-Py}}$), 8.98 (m, 9H, $H_{\alpha'\text{-Py},9}$), 8.36 (s, 3H, H_{10}), 8.25 (d, 6H, ^{3}J = 4.2 Hz, $H_{\beta\text{-Py}}$), 7.72 (m, 12H, $H_{\beta'\text{-Py}}$, $H_{4,5}$), 7.68 (d, 6H, ^{3}J = 9.9 Hz, $H_{2,7}$), 7.14 (m, 6H, $H_{3,6}$), 1.40 (m, 72H, PCH_2CH_3), 0.82 (m, 108H, PCH_2CH_3) ppm. For **3.12**: δ 9.32 (s, 3H, H_9), 9.01 (d, 6H, ^{3}J = 5.1 Hz, $H_{\alpha\text{-Py}}$), 8.91 (d, 6H, ^{3}J = 4.8 Hz, $H_{\alpha'\text{-Py}}$), 8.36 (s, 3H, H_{10}), 8.00 (d, 6H, ^{3}J = 6.0 Hz, $H_{\beta\text{-Py}}$), 7.95 (d, 6H, ^{3}J = 6.0 Hz, $H_{\beta\text{-Py}}$), 7.73 (m, 12H, $H_{4,5,2,7}$), 7.57 (d, 12H, ^{3}J = 8.4 Hz, $H_{3,5\text{-phenylene}}$), 7.17 (d, 12H, ^{3}J = 8.1 Hz, $H_{2,6\text{-phenylene}}$), 7.14 (m, 6H, $H_{3,6}$), 1.40 (m, 72H, PCH_2CH_3), 0.82 (m, 108H, PCH_2CH_3) ppm. $^{31}P\{^{1}H\}$ NMR (Acetone-d_6 /D_2O: 1/1, 121.4 MHz) For **3.04**: δ 8.32 (^{195}Pt satellites, $^{1}J_{Pt\text{-}P}$ = 2636 Hz) ppm. For **3.11**: δ 9.81 (^{195}Pt satellites, $^{1}J_{Pt\text{-}P}$ = 2649 Hz) ppm. For **3.12**: δ 8.83 (^{195}Pt satellites, $^{1}J_{Pt\text{-}P}$ = 2655 Hz) ppm.

9.13.6 Self-sorting of SS_6

Molecular "Clip" **3.01** (16.09 mg, 0.01383 mmol), 4,4'-dipyridyl **3.02** (0.60 mg, 0.0038 mmol), 1,4-bis(4-pyridylethynyl)benzene **3.03** (1.16 mg, 0.00414 mmol), and tritopic tecton **3.13** (1.49 mg, 0.00391 mmol) were added to 2.0 mL of mixed solvent. After 48 h heating, **3.04**, **3.05**, and **3.14** were formed predominantly. ^{1}H NMR (Acetone-

d_6/D_2O: 1/1, 300 MHz) For **3.04**: δ 9.53 (s, 2H, H_9), 9.21 (d, ^3J = 5.8 Hz, 4H, $H_{\alpha\text{-Py}}$), 9.18 (d, ^3J = 5.4 Hz, 2H, $H_{\alpha'\text{-Py}}$), 8.71 (d, ^3J = 5.4 Hz, 4H, $H_{\beta\text{-Py}}$), 8.53 (d, ^3J = 5.4 Hz, 4H, $H_{\beta'\text{-Py}}$), 8.37 (s, 2H, H_{10}), 7.71 (d, ^3J = 10.5 Hz, 4H, $H_{4,5}$), 7.62 (m, 4H, $H_{2,7}$), 7.14 (t, ^3J = 7.2 Hz, 4H, $H_{3,6}$), 1.45 (m, 48H, PCH_2CH_3), 0.84 (m, 72H, PCH_2CH_3) ppm. For **3.05**: δ 9.45 (s, 2H, H_9), 9.02 (m, 4H, $H_{\alpha\text{-Py}}$), 8.94 (d, 4H, ^3J = 5.4 Hz, $H_{\alpha'\text{-Py}}$), 8.36 (s, 2H, H_{10}), 8.03 (m, 8H, $H_{\beta\text{-Py}}$), 7.74 (s, 8H, $H_{\text{phenylene}}$), 7.71 (d, 4H, ^3J = 10.5 Hz, $H_{4,5}$), 7.64 (m, 4H, $H_{2,7}$), 7.14 (t, ^3J = 7.2 Hz, 4H, $H_{3,6}$), 1.45 (m, 48H, PCH_2CH_3), 0.84 (m, 72H, PCH_2CH_3) ppm. For **3.14**: δ 9.41 (s, 3H, H_9), 9.02 (m, 6H, $H_{\alpha\text{-Py}}$), 8.90 (d, 6H, ^3J = 5.4 Hz, $H_{\alpha'\text{-Py}}$), 8.36 (s, 3H, H_{10}), 7.92 (m, 12H, $H_{\beta\text{-Py}}$), 7.69 (d, 6H, ^3J = 9.9 Hz, $H_{2,7}$), 7.85 (s, 6H, H_{Benzene}), 7.62 (d, 6H, ^3J = 9.9 Hz, $H_{2,7}$), 7.15 (m, 6H, $H_{3,6}$), 1.40 (m, 72H, PCH_2CH_3), 0.82 (m, 108H, PCH_2CH_3) ppm. $^{31}P\{^1H\}$ NMR (Acetone-d_6 /D_2O: 1/1, 121.4 MHz) For **3.04**: δ 8.33 (^{195}Pt satellites, $^1J_{\text{Pt-P}}$ = 2648 Hz) ppm. For **3.05**: δ 8.48 (^{195}Pt satellites, $^1J_{\text{Pt-P}}$ = 2648 Hz) ppm. For **3.14**: δ 8.65 (^{195}Pt satellites, $^1J_{\text{Pt-P}}$ = 2648 Hz) ppm.

9.13.7 Self-sorting of SS_7

Molecular “Clip” **3.01** (13.43 mg, 0.01155 mmol), 4,4’-dipyridyl **3.02** (0.49 mg, 0.0031 mmol), tritopic tectons **3.09** (0.73 mg, 0.0028 mmol) and **3.13** (1.08 mg, 0.00283 mmol) were added to 2.0 mL of mixed solvent. After 48 h heating, **3.04**, **3.11**, and **3.14** were formed predominantly. ^1H NMR (Acetone-d_6 /D_2O: 1/1, 300 MHz) For **3.04**: δ 9.53 (s, 2H, H_9), 9.21 (d, ^3J = 5.8 Hz, 4H, $H_{\alpha\text{-Py}}$), 9.18 (d, ^3J = 5.4 Hz, 2H, $H_{\alpha'\text{-Py}}$), 8.71 (d, ^3J = 5.4 Hz, 4H, $H_{\beta\text{-Py}}$), 8.53 (d, ^3J = 5.4 Hz, 4H, $H_{\beta'\text{-Py}}$), 8.37 (s, 2H, H_{10}), 7.71 (d, ^3J = 10.5 Hz, 4H, $H_{4,5}$), 7.62 (m, 4H, $H_{2,7}$), 7.14 (t, ^3J = 7.2 Hz, 4H, $H_{3,6}$), 1.45 (m, 48H, PCH_2CH_3), 0.84 (m, 72H, PCH_2CH_3) ppm. For **3.11**: δ 9.14 (d, 6H, ^3J = 6.3 Hz, $H_{\alpha\text{-Py}}$), 8.98 (m, 9H, $H_{\alpha'\text{-Py},9}$), 8.36 (s, 3H, H_{10}), 8.25 (d, 6H, ^3J = 4.2 Hz, $H_{\beta\text{-Py}}$), 7.72 (m, 12H, $H_{\beta'\text{-Py}}$, $H_{4,5}$),

7.68 (d, 6H, ^{3}J = 9.9 Hz, $H_{2,7}$), 7.14 (m, 6H, $H_{3,6}$), 1.40 (m, 72H, PCH_2CH$_3$), 0.82 (m, 108H, PCH$_2$CH_3) ppm. For **3.14**: δ 9.41 (s, 3H, H_9), 9.02 (m, 6H, $H_{\alpha\text{-Py}}$), 8.90 (d, 6H, ^{3}J = 5.4 Hz, $H_{\alpha'\text{-Py}}$), 8.36 (s, 3H, H_{10}), 7.92 (m, 12H, $H_{\beta\text{-Py}}$), 7.69 (d, 6H, ^{3}J = 9.9 Hz, $H_{2,7}$), 7.85 (s, 6H, H_{Benzene}), 7.62 (d, 6H, ^{3}J = 9.9 Hz, $H_{2,7}$), 7.15 (m, 6H, $H_{3,6}$), 1.40 (m, 72H, PCH_2CH$_3$), 0.82 (m, 108H, PCH$_2$CH_3) ppm. ^{31}P{^{1}H} NMR (Acetone-d_6/D$_2$O: 1/1, 121.4 MHz) For **3.04**: δ 8.33 (^{195}Pt satellites, $^{1}J_{\text{Pt-P}}$ = 2651 Hz) ppm. For **3.11**: δ 9.81 (^{195}Pt satellites, $^{1}J_{\text{Pt-P}}$ = 2654 Hz) ppm. For **3.14**: δ 8.65 (^{195}Pt satellites, $^{1}J_{\text{Pt-P}}$ = 2651 Hz) ppm.

9.13.8 Synthesis of 120 °dipydyl donor 3.15

A 50 mL Schlenk flask was charged with 2,6-dibromopyridine (200 mg, 0.844 mmol), pyridin-4-ylboronic acid (230 mg, 1.87 mmol), and Pd(PPh$_3$)$_4$ (60 mg, 0.052 mmol), degassed, and back-filled three times with N_2(g). Dry toluene (6 mL) and ethanol (6 mL) as well as Na_2CO_3 (200 mg, 1.89 mmol) in 6 ml distilled water were then gradually introduced into the mixture via syringe. The reaction was allowed to stir at 90 ℃ for 24 h under N_2. The reaction mixture was partitioned between water (75 mL) and CH_2Cl_2 (60 mL). The organic layer was separated and extracted further with CH_2Cl_2 (3 × 30 mL). The combined organic layers were dried ($MgSO_4$), filtered, and evaporated. The resulting residues were purified by column chromatography on silica gel with chromatography eluent: ethyl acetate/methanol (3:20). Yield 136 mg (off white solid), 69.1 %. Mp 147-149 ℃; ^{1}H NMR ($CDCl_3$, 300MHz) δ 8.78 (d, 4H, *J*=6.0 Hz, H_α-Py), 8.03 (d, 4H, *J*=6.0 Hz, H_β-Py), 7.96 (m, 1H, H_4-Py), 7.87 (m, 2H, $H_{3,5}$-Py) ppm. ^{13}C NMR ($CDCl_3$, 300MHz) δ 154.85, 150.69, 146.19, 138.52, 121,31, 120.94 ppm. HRMS (ESI-TOF): *m/z* 234.1026 ([M+H]$^+$; calcd for $C_{15}H_{12}N_3$: 234.1031)

9.13.9 Synthesis of 120 ° dipydyl donor 3.16

A 50 mL Schlenk flask was charged with bis(4-bromophenyl)methanone (203 mg, 0.597 mmol), 4-ethynylpyridine hydrochloride (250 mg, 1.79 mmol), $Pd(PPh_3)_4$ (67 mg, 0.058 mmol), and CuI (10 mg, 0.053 mmol), degassed, and back-filled three times with N_2(g). Dry THF (15 mL) and triethylamine (5 mL) were then introduced into the reaction via syringe. The reaction was allowed to stir at 60 ℃ for 48 h under N_2. The reaction mixture was partitioned between water (30 mL) and CH_2Cl_2 (40 mL). The organic layer was separated and extracted further with CH_2Cl_2 (3 × 30 mL). The combined organic layers were dried ($MgSO_4$), filtered, and evaporated. The resulting residues were purified by column chromatography on silica gel with chromatography eluent: dichloromethane/acetone (3:1). Yield 123 mg (off white solid), 53.6 %. Mp 245 ℃ decomposition; ^{1}H NMR ($CDCl_3$, 300MHz) δ 8.64 (d, 4H, *J*=6.0 Hz, H_α-Py), 7.81 (d, 4H, *J*=8.4 Hz, H_α-Phenylene), 7.67 (d, 4H, *J*=8.4 Hz, H_β-Phenylene), 7.41 (d, 4H, *J*=6.0 Hz, H_β-Py) ppm. ^{13}C NMR ($CDCl_3$, 300MHz) δ 195.07, 149.83, 137.51, 132.11, 131.33, 130.28, 126.69, 125.99, 93.24, 89.68 ppm. HRMS (ESI-TOF): *m/z* 385.1341 ([M+H]+; calcd for C27H17N2O: 385.1341).

9.13.10 Self-assembly of rhomboid 3.17

60 ° organoplatinum acceptor **3.06** (7.98 mg, 0.00686 mmol) and 2,6-dipyridyl pyridine **3.15** (1.61 mg, 0.00690 mmol) were added to 1.0 mL of Acetone-d_6/D_2O mixed solvent (*v/v* 1:1). After 6 h of heating at 65–70 ℃, **3.17** was formed quantitatively in the solution and isolated by removal of all solvent. Yield: 9.39 mg, 98 %. ^{1}H NMR (Acetone-d_6 /D_2O: 1/1, 300 MHz) for **3.17**: δ 9.06 (m, 4H, $H_{\alpha\text{-Py}}$), 8.87 (m, 4H, $H_{\alpha'\text{-Py}}$), 8.62 (s, 4H, $H_{4,5}$), 8.41 (m, 12H, $H_{\beta\text{-Py}}$, 3,5-Py), 8.25 (m, 2H, $H_{4\text{-Py}}$), 7.71 (d, 4H, $H_{2,7}$), 7.54 (m, 8H,

$H_{1,8,9,10}$), 1.33 (m, 48H, PC*H*2CH3), 1.05 (m, 72H, PCH2C*H*3) ppm. 31P{1H} NMR (Acetone-d_6 /D_2O: 1/1, 121.4 MHz) for **3.17**: δ 14.42 (^{195}Pt satellites, $^1J_{Pt\text{-}P}$ = 2687 Hz) ppm. MS (ESI) for **3.17** (C106H158N10O12P8Pt4): *m/z*: 1333.8 $[M - 2NO_3]^{2+}$, 868.5 $[M - 3NO_3]^{3+}$.

9.13.11 Self-assembly of rhomboid 3.18

60 °organoplatinum acceptor **3.06** (4.75 mg, 0.00408 mmol) and bis(4-(pyridin-4-ylethynyl)phenyl) methanone **3.16** (1.57 mg, 0.00408 mmol) were added to 0.8 mL of Acetone-d_6/D_2O mixed solvent *(v/v* 1:1). After 6 h of heating at 65–70 ℃, **3.18** was formed quantitatively in the solution and isolated by removal of all solvent. Yield: 6.13 mg, 97 % ^{1}H NMR (Acetone-d_6 /D_2O: 1/1, 300 MHz) for **3.18**: δ 8.92 (d, 8H, ^3J = 6.0 Hz, $H_{\alpha\text{-Py}}$), 8.58 (s, 4H, $H_{4,5}$),7.84 (m, 8H, $H_{\beta\text{-Py}}$), 7.81 (s, 8H, $H_{Phenylene}$), 7.63 (d, 4H, $H_{2,7}$), 7.54 (m, 8H, $H_{1,8,9,10}$), 1.33 (m, 48H, PC*H*2CH3), 1.05 (m, 72H, PCH2C*H*3) ppm. 31P{1H} NMR (Acetone-d_6 /D_2O: 1/1, 121.4 MHz) for **3.18**: δ 14.39 (^{195}Pt satellites, $^1J_{Pt\text{-}P}$ = 2690 Hz) ppm. MS (ESI) for **3.18** (C130H168N8O14P8Pt4): *m/z*: 1484.4 $[M - 2NO_3]^{2+}$, 969.2 $[M - 3NO_3]^{3+}$.

9.13.12 Self-sorting of SS_8

60 °organoplatinum acceptor **3.06** (13.01 mg, 0.01119 mmol), 4,4'-dipyridyl **3.02** (0.51 mg, 0.0033 mmol), 2,6-dipyridyl pyridine **3.15** (0.76 mg, 0.0033 mmol), and tritopic tecton **3.10** (1.75 mg, 0.00312 mmol) were added to 1.2 mL of mixed solvent. After 24 h heating, **3.07**, **3.17**, and **3.19** were formed predominantly. ^{1}H NMR (Acetone-d_6 /D_2O: 1/1, 300 MHz) For **3.07**: δ 9.16 (d, ^3J = 5.7 Hz, 6H, $H_{\alpha\text{-Py}}$), 9.09 (d, ^3J = 5.7 Hz, 6H, $H_{\alpha'\text{-Py}}$), 8.65 (s, 6H, $H_{4,5}$), 8.35 (m, 12H, $H_{\beta\text{-Py}}$), 7.54 (m, 18H, $H_{1,2,7,8,9,10}$), 1.33 (m, 72H, PCH_2CH$_3$), 1.05 (m, 108H, PCH$_2$CH_3) ppm. For **3.17**: δ 9.09 (d, 4H, ^3J = 5.7 Hz,

$H_{\alpha\text{-Py}}$), 8.87 (m, 4H, $H_{\alpha'\text{-Py}}$), 8.62 (s, 4H, $H_{4,5}$), 8.41 (m, 12H, $H_{\beta\text{-Py, 3,5-Py}}$), 8.25 (m, 2H, $H_{4\text{-Py}}$), 7.54 (m, 12H, $H_{1,2,7,8,9,10}$), 1.33 (m, 48H, PCH_2CH_3), 1.05 (m, 72H, PCH_2CH_3) ppm. For **3.19**: δ 8.91 (m, 12H, $H_{\alpha\text{-Py}}$), 8.61 (s, 6H, $H_{4,5}$), 7.78 (m, 12H, $H_{\beta\text{-Py}}$), 7.54 (m, 30H, $H_{1,2,7,8,9,10,\ \alpha\text{-Phenylene}}$), 7.15 (d, 12H, ^3J = 8.7 Hz, $H_{1,2,7,8,9,10,\ \beta\text{-Phenylene}}$), 1.33 (m, 72H, PCH_2CH_3), 1.05 (m, 108H, PCH_2CH_3) ppm. $^{31}P\{^1H\}$ NMR (Acetone-d_6 /D_2O: 1/1, 121.4 MHz) For **3.07**: δ 14.31 (^{195}Pt satellites, $^1J_{Pt\text{-}P}$ = 2695 Hz) ppm. For **3.17**: δ 14.42 (^{195}Pt satellites, $^1J_{Pt\text{-}P}$ = 2695 Hz) ppm. For **3.19**: δ 14.38 (^{195}Pt satellites, $^1J_{Pt\text{-}P}$ = 2695 Hz) ppm.

9.13.13 Self-sorting of SS_9

60 ° organoplatinum acceptor **3.06** (9.96 mg, 0.00856 mmol), 4,4'-dipyridyl **3.02** (0.45 mg, 0.0029 mmol), 2,6-dipyridyl pyridine **3.15** (0.67 mg, 0.0029 mmol), and bis(4-(pyridin-4-ylethynyl)phenyl) methanone **3.16** (1.08 mg, 0.00281 mmol) were added to 1.4 mL of mixed solvent. After 24 h heating, **3.07**, **3.17**, and **3.18** were formed predominantly. ^1H NMR (Acetone-d_6 /D_2O: 1/1, 300 MHz) **3.07**: δ 9.16 (d, ^3J = 5.7 Hz, 6H, $H_{\alpha\text{-Py}}$), 9.06 (m, 6H, $H_{\alpha'\text{-Py}}$), 8.65 (s, 6H, $H_{4,5}$), 8.35 (m, 12H, $H_{\beta\text{-Py}}$), 7.54 (m, 18H, $H_{1,2,7,8,9,10}$), 1.33 (m, 72H, PCH_2CH_3), 1.05 (m, 108H, PCH_2CH_3) ppm. For **3.17**: δ 9.06 (m, 4H, $H_{\alpha\text{-Py}}$), 8.87 (m, 4H, $H_{\alpha'\text{-Py}}$), 8.62 (s, 4H, $H_{4,5}$), 8.41 (m, 12H, $H_{\beta\text{-Py, 3,5-Py}}$), 8.25 (m, 2H, $H_{4\text{-Py}}$), 7.54 (m, 12H, $H_{1,2,7,8,9,10}$), 1.33 (m, 48H, PCH_2CH_3), 1.05 (m, 72H, PCH_2CH_3) ppm. For **3.18**: δ 8.92 (d, 8H, ^3J = 6.0 Hz, $H_{\alpha\text{-Py}}$), 8.58 (s, 4H, $H_{4,5}$),7.84 (m, 8H, $H_{\beta\text{-Py}}$), 7.81 (s, 8H, $H_{Phenylene}$), 7.54 (m, 16H, $H_{1,2,7,8,9,10}$), 1.33 (m, 48H, PCH_2CH_3), 1.05 (m, 72H, PCH_2CH_3) ppm. $^{31}P\{^1H\}$ NMR (Acetone-d_6 /D_2O: 1/1, 121.4 MHz) For **3.07**: δ 14.32 (^{195}Pt satellites, $^1J_{Pt\text{-}P}$ = 2690 Hz) ppm. For **3.17**: δ 14.43 (^{195}Pt satellites, $^1J_{Pt\text{-}P}$ = 2690 Hz) ppm. For **3.18**: δ 14.39 (^{195}Pt satellites, $^1J_{Pt\text{-}P}$ = 2690 Hz) ppm.

9.13.14 Self-sorting of SS_{10}

60 ° organoplatinum acceptor **3.06** (9.21 mg, 0.00792 mmol), 4,4'-dipyridyl **3.02** (0.42 mg, 0.0027 mmol), 1,4-bis(4-pyridylethynyl)benzene **3.03** (0.71 mg, 0.0025 mmol), and 2,6-dipyridyl pyridine **3.15** (0.63 mg, 0.0027 mmol) were added to 1.2 mL of mixed solvent. After 48 h heating, **3.07**, **3.08**, and **3.17** were formed predominantly. ^{1}H NMR (Acetone-d_6 /D_2O: 1/1, 300 MHz) For **3.07**: δ 9.16 (d, ^{3}J = 5.7 Hz, 6H, $H_{\alpha\text{-Py}}$), 9.06 (m, 6H, $H_{\alpha'\text{-Py}}$), 8.65 (s, 6H, $H_{4,5}$), 8.35 (m, 12H, $H_{\beta\text{-Py}}$), 7.54 (m, 18H, $H_{1,2,7,8,9,10}$), 1.33 (m, 72H, PCH_2CH$_3$), 1.05 (m, 108H, PCH$_2$CH_3) ppm. For **3.08**: δ 8.90 (m, 12H, $H_{\alpha\text{-Py}}$), 8.62 (s, 6H, $H_{4,5}$), 7.84 (d, 12H, ^{3}J = 6.6 Hz, $H_{\beta\text{-Py}}$), 7.73 (s, 12H, $H_{\text{phenylene}}$), 7.54 (m, 18H, $H_{1,2,7,8,9,10}$), 1.30 (m, 72H, PCH_2CH$_3$), 1.07 (m, 108H, PCH$_2$CH_3) ppm. For **3.17**: δ 9.06 (m, 4H, $H_{\alpha\text{-Py}}$), 8.87 (m, 4H, $H_{\alpha'\text{-Py}}$), 8.62 (s, 4H, $H_{4,5}$), 8.41 (m, 12H, $H_{\beta\text{-Py, 3,5-Py}}$), 8.25 (m, 2H, $H_{4\text{-Py}}$), 7.54 (m, 12H, $H_{1,2,7,8,9,10}$), 1.33 (m, 48H, PCH_2CH$_3$), 1.05 (m, 72H, PCH$_2$CH_3) ppm. ^{31}P{^{1}H} NMR (Acetone-d_6 /D_2O: 1/1, 121.4 MHz) For **3.07**: δ 14.32 (^{195}Pt satellites, $^{1}J_{\text{Pt-P}}$ = 2687 Hz) ppm. For **3.08**: δ 14.42 (^{195}Pt satellites, $^{1}J_{\text{Pt-P}}$ = 2687 Hz) ppm. For **3.17**: δ 14.42 (^{195}Pt satellites, $^{1}J_{\text{Pt-P}}$ = 2687 Hz) ppm.

9.13.15 Self-sorting of SS_{11}

Molecular "Clip" **3.01** (11.61 mg, 0.00998 mmol), 60 ° organoplatinum acceptor **3.06** (11.67 mg, 0.0100 mmol), 4,4'-dipyridyl **3.02** (1.56 mg, 0.00998 mmol), and 1,4-bis(4-pyridylethynyl)benzene **3.03** (2.81 mg, 0.0100 mmol) were added to 1.7 mL of mixed solvent. After 72 h heating, **3.04**, **3.05**, **3.07**, and **3.08** were formed predominantly. ^{1}H NMR (Acetone-d_6 /D_2O: 1/1, 500 MHz) For **3.04**: δ 9.53 (s, 2H, H_9), 9.21 (d, ^{3}J = 5.8 Hz, 4H, $H_{\alpha\text{-Py}}$), 9.18 (d, ^{3}J = 5.4 Hz, 2H, $H_{\alpha'\text{-Py}}$), 8.71 (d, ^{3}J = 5.4 Hz, 4H, $H_{\beta\text{-Py}}$), 8.53 (d, ^{3}J = 5.4 Hz, 4H, $H_{\beta'\text{-Py}}$), 8.37 (s, 2H, H_{10}), 7.71 (d, ^{3}J = 10.5 Hz, 4H, $H_{4,5}$), 7.62 (m, 4H,

$H_{2,7}$), 7.14 (t, ^3J = 7.2 Hz, 4H, $H_{3,6}$), 1.45 (m, 48H, PCH_2CH$_3$), 0.84 (m, 72H, PCH$_2$CH_3) ppm. For **3.05**: δ 9.45 (s, 2H, H_9), 9.02 (m, 4H, $H_{\alpha\text{-Py}}$), 8.94 (d, 4H, ^3J = 5.4 Hz, $H_{\alpha'\text{-Py}}$), 8.36 (s, 2H, H_{10}), 8.03 (m, 8H, $H_{\beta\text{-Py}}$), 7.74 (s, 8H, $H_{\text{phenylene}}$), 7.71 (d, 4H, ^3J = 10.5 Hz, $H_{4,5}$), 7.64 (m, 4H, $H_{2,7}$), 7.14 (t, ^3J = 7.2 Hz, 4H, $H_{3,6}$), 1.45 (m, 48H, PCH_2CH$_3$), 0.84 (m, 72H, PCH$_2$CH_3) ppm. For **3.07**: δ 9.16 (d, ^3J = 5.7 Hz, 6H, $H_{\alpha\text{-Py}}$), 9.06 (m, 6H, $H_{\alpha'\text{-Py}}$), 8.65 (s, 6H, $H_{4,5}$), 8.35 (m, 12H, $H_{\beta\text{-Py}}$), 7.54 (m, 18H, $H_{1,2,7,8,9,10}$), 1.33 (m, 72H, PCH_2CH$_3$), 1.05 (m, 108H, PCH$_2$CH_3) ppm. For **3.08**: δ 8.90 (m, 12H, $H_{\alpha\text{-Py}}$), 8.62 (s, 6H, $H_{4,5}$), 7.84 (d, 12H, ^3J = 6.6 Hz, $H_{\beta\text{-Py}}$), 7.73 (s, 12H, $H_{\text{phenylene}}$), 7.54 (m, 18H, $H_{1,2,7,8,9,10}$), 1.30 (m, 72H, PCH_2CH$_3$), 1.07 (m, 108H, PCH$_2$CH_3) ppm. ^{31}P{^{1}H} NMR (Acetone-d_6 /D$_2$O: 1/1, 121.4 MHz) For **3.04**: δ 8.33 (^{195}Pt satellites, $^1J_{\text{Pt-P}}$ = 2639 Hz) ppm. For **3.05**: δ 8.48 (^{195}Pt satellites, $^1J_{\text{Pt-P}}$ = 2639 Hz) ppm. For **3.07**: δ 14.32 (^{195}Pt satellites, $^1J_{\text{Pt-P}}$ = 2673 Hz) ppm. For **3.08**: δ 14.40 (^{195}Pt satellites, $^1J_{\text{Pt-P}}$ = 2673 Hz) ppm.

9.13.16 Self-sorting of SS_{12}

Molecular "Clip" **3.01** (7.52 mg, 0.00647 mmol), 60 ° organoplatinum acceptor **3.06** (7.50 mg, 0.00645 mmol), 4,4'-dipyridyl **3.02** (1.00 mg, 0.00640 mmol), and tritopic tectons **3.10** (2.43 mg, 0.00433 mmol) were added to 1.2 mL of mixed solvent. After 96 h heating, **3.04**, **3.12**, **3.07**, and **3.19** were formed predominantly. ^{1}H NMR (Acetone-d_6 /D$_2$O: 1/1, 500 MHz) For **3.04**: δ 9.53 (s, 2H, H_9), 9.21 (d, ^3J = 5.8 Hz, 4H, $H_{\alpha\text{-Py}}$), 9.18 (d, ^3J = 5.4 Hz, 2H, $H_{\alpha'\text{-Py}}$), 8.71 (d, ^3J = 5.4 Hz, 4H, $H_{\beta\text{-Py}}$), 8.53 (d, ^3J = 5.4 Hz, 4H, $H_{\beta'\text{-Py}}$), 8.37 (s, 2H, H_{10}), 7.71 (d, ^3J = 10.5 Hz, 4H, $H_{4,5}$), 7.62 (m, 4H, $H_{2,7}$), 7.14 (t, ^3J = 7.2 Hz, 4H, $H_{3,6}$), 1.45 (m, 48H, PCH_2CH$_3$), 0.84 (m, 72H, PCH$_2$CH_3) ppm. For **3.12**: δ 9.32 (s, 3H, H_9), 9.01 (d, 6H, ^3J = 5.1 Hz, $H_{\alpha\text{-Py}}$), 8.91 (d, 6H, ^3J = 4.8 Hz, $H_{\alpha'\text{-Py}}$), 8.36 (s, 3H, H_{10}), 8.00 (d, 6H, ^3J = 6.0 Hz, $H_{\beta\text{-Py}}$), 7.95 (d, 6H, ^3J = 6.0 Hz, $H_{\beta\text{-Py}}$), 7.73 (m, 12H,

$H_{4,5,2,7}$), 7.57 (d, 12H, ^3J = 8.4 Hz, $H_{3,5\text{-phenylene}}$), 7.17 (d, 12H, ^3J = 8.1 Hz, $H_{2,6\text{-phenylene}}$), 7.14 (m, 6H, $H_{3,6}$), 1.40 (m, 72H, PCH_2CH_3), 0.82 (m, 108H, PCH_2CH_3) ppm. For **3.07**: δ 9.16 (d, ^3J = 5.7 Hz, 6H, $H_{\alpha\text{-Py}}$), 9.06 (m, 6H, $H_{\alpha'\text{-Py}}$), 8.65 (s, 6H, $H_{4,5}$), 8.35 (m, 12H, $H_{\beta\text{-Py}}$), 7.54 (m, 18H, $H_{1,2,7,8,9,10}$), 1.33 (m, 72H, PCH_2CH_3), 1.05 (m, 108H, PCH_2CH_3) ppm. For **3.19**: δ 8.91 (m, 12H, $H_{\alpha\text{-Py}}$), 8.61 (s, 6H, $H_{4,5}$), 7.78 (m, 12H, $H_{\beta\text{-Py}}$), 7.54 (m, 30H, $H_{1,2,7,8,9,10,\ \alpha\text{-Phenylene}}$), 7.15 (d, 12H, ^3J = 8.7 Hz, $H_{1,2,7,8,9,10,\ \beta\text{-Phenylene}}$), 1.33 (m, 72H, PCH_2CH_3), 1.05 (m, 108H, PCH_2CH_3) ppm. $^{31}P\{^1H\}$ NMR (Acetone-d_6/D_2O: 1/1, 121.4 MHz) **3.04**: δ 8.33 (^{195}Pt satellites, $^1J_{Pt\text{-}P}$ = 2638 Hz) ppm. For **3.12**: δ 8.83 (^{195}Pt satellites, $^1J_{Pt\text{-}P}$ = 2637 Hz) ppm. For **3.07**: δ 14.32 (^{195}Pt satellites, $^1J_{Pt\text{-}P}$ = 2667 Hz) ppm. For **3.19**: δ 14.39 (^{195}Pt satellites, $^1J_{Pt\text{-}P}$ = 2667 Hz) ppm.

9.13.17 Selective self-assembly of 4.04

Reaction scale: *Cis*-$Pt(PEt_3)_2(OTf)_2$ **4.01** (5.37 mg, 7.36 μmol), carboxylate ligand **4.02** (0.77 mg, 3.7 μmol), and ditopic pyridyl ligand **4.03** (1.03 mg, 3.68 μmol). Yield: 5.32 mg, 90%. MS (ESI) calcd for $[M - 2OTf]^{2+}$ *m/z* 1455.85, found 1455.69; calcd for $[M - 3OTf]^{3+}$ *m/z* 920.92, found 920.88. ^1H NMR (Acetone-d_6, 300MHz) δ 9.00 (s, 8H, $H_{\alpha\text{-Py}}$), 7.74 (m, 16H, $H_{\beta\text{-Py}}$ and $H_{phenyl\text{-}Py}$), 7,66 (s, 8H, H_{phneyl}), 1.92 (m, 48H, PCH_2CH_3), 1.21 (m, 72H, PCH_2CH_3). $^{31}P\{^1H\}$ NMR (Acetone-d_6, 121.4 MHz) δ 6.60 (d, $^2J_{P\text{-}P}$ = 22.0 Hz, ^{195}Pt satellites, $^1J_{Pt\text{-}P}$ = 3242 Hz), 1.06 (d, $^2J_{P\text{-}P}$ = 22.0 Hz, ^{195}Pt satellites, $^1J_{Pt\text{-}P}$ = 3427 Hz). Anal. Calcd for $C_{108}H_{152}F_{12}N_4O_{20}P_8Pt_4S_4$: C, 40.40; H, 4.77; N, 1.74. Found: C, 40.04; H, 4.70; N, 1.71.

9.13.18 Selective self-assembly of 4.07

Reaction scale: *Cis*-Pt(PEt_3)$_2$(OTf)$_2$ **4.01** (4.88 mg, 6.69 μmol), carboxylate ligand **4.02** (0.71 mg, 3.4 μmol), and tritopic pyridyl ligand **4.05** (0.84 mg, 2.2 μmol). Yield: 4.81mg, 91%. MS (ESI) calcd for $[M - 2OTf]^{2+}$ *m/z* 2218.98, found 2218.76; calcd for $[M - 3OTf]^{3+}$ *m/z* 1429.67, found 1429.59. ^{1}H NMR (Acetone-d_6, 300MHz) δ 9.02 (s, 12H, $H_{\alpha\text{-Py}}$), 7,88 (s, 12H, $H_{\text{phneyl-Py}}$), 7.75 (m, 24H, $H_{\beta\text{-Py}}$ and H_{phenyl}), 1.89 (m, 72H, PCH_2CH_3), 1.20 (m, 108H, PCH_2CH_3). ^{31}P{^{1}H} NMR (Acetone-d_6, 121.4 MHz) δ 6.56 (d, $^2J_{\text{P-P}}$ = 22.0 Hz, ^{195}Pt satellites, $^1J_{\text{Pt-P}}$ = 3227 Hz), 1.01 (d, $^2J_{\text{P-P}}$ = 22.0 Hz, ^{195}Pt satellites, $^1J_{\text{Pt-P}}$ = 3404 Hz). Anal. Calcd for $C_{156}H_{222}F_{18}N_6O_{30}P_{12}Pt_6S_6$: C, 39.55; H, 4.72; N, 1.77. Found: C, 39.92; H, 4.54; N, 1.79.

9.13.19 Selective self-assembly of 4.08a

Reaction scale: *Cis*-Pt(PEt_3)$_2$(OTf)$_2$ **4.01** (5.22 mg, 7.16 μmol), carboxylate ligand **4.02** (0.75 mg, 3.6 μmol), and tetratopic pyridyl ligand **4.06a** (1.14 mg, 1.78 μmol). Yield: 5.65 mg, 96%. MS (ESI) calcd for $[M - 3PF_6]^{3+}$ *m/z* 2037.86, found 2037.75; calcd for $[M - 5PF_6]^{5+}$ *m/z* 1164.51, found 1164.50. ^{1}H NMR (Acetone-d_6, 300MHz) δ 8.87 (s, 16H, $H_{\alpha\text{-Py}}$), 7,89 (d, *J* = 6 Hz, 16H, $H_{\alpha\text{-phneyl-Py}}$), 7.60 (m, 32H, $H_{\beta\text{-Py}}$ and H_{phenyl}), 7,20 (d, *J* = 6 Hz, 16H, $H_{\beta\text{-phneyl-Py}}$), 1.89 (m, 96H, PCH_2CH_3), 1.17 (m, 144H, PCH_2CH_3). ^{31}P{^{1}H} NMR (Acetone-d_6, 121.4 MHz) δ 5.88 (d, $^2J_{\text{P-P}}$ = 21.4 Hz, ^{195}Pt satellites, $^1J_{\text{Pt-P}}$ = 3270 Hz), 1.08 (d, $^2J_{\text{P-P}}$ = 21.4 Hz, ^{195}Pt satellites, $^1J_{\text{Pt-P}}$ = 3448 Hz). Anal. Calcd for $C_{220}H_{320}F_{48}N_8O_{16}P_{24}Pt_8$: C, 40.35; H, 4.93; N, 1.71. Found: C, 40.71; H, 5.08; N, 1.74.

9.13.20 Selective self-assembly of 4.08b

Reaction scale: *Cis*-Pt(PEt_3)$_2$(OTf)$_2$ **4.01** (4.52 mg, 6.10 μmol), carboxylate ligand **4.02** (0.63 mg, 3.0 μmol), and tetratopic pyridyl ligand **4.06b** (0.94 mg, 1.5 μmol). Yield:

4.81 mg, 95%. MS (ESI) calcd for $[M - 3PF_6]^{3+}$ *m/z* 2022.83, found 2022.71; calcd for $[M - 5PF_6]^{5+}$ *m/z* 1155.71, found 1155.62. ^{1}H NMR (CD_3NO_2, 300MHz) δ 9.27 (m, 24H, $H_{\alpha\text{-Py}}$ and $H_{Pyrrole}$), 8.34 (d, *J* = 5.7 Hz, 16H, $H_{\beta\text{-Py}}$), 8.08 (s, 16H, H_{phneyl}), 7.12 (s, 8H, $H_{Pyrrole}$), 2.24 (m, 96H, PCH_2CH_3), 1.39 (m, 144H, PCH_2CH_3). -3.28 (s, 4H, $H_{N\text{-}H}$). ^{31}P{^{1}H} NMR (CD_3NO_2, 121.4 MHz) δ 5.07 (d, $^2J_{P\text{-}P}$ = 21.4 Hz, ^{195}Pt satellites, $^1J_{Pt\text{-}P}$ = 3270 Hz), -0.34 (d, $^2J_{P\text{-}P}$ = 21.4 Hz, ^{195}Pt satellites, $^1J_{Pt\text{-}P}$ = 3462 Hz). Anal. Calcd for $C_{208}H_{308}F_{48}N_{16}O_{16}P_{24}Pt_8$: C, 38.41; H, 4.77; N, 3.45. Found: C, 38.07; H, 4.92; N, 3.41.

9.13.21 Selective self-assembly of 4.12

Reaction scale: *Cis*-$Pt(PEt_3)_2(OTf)_2$ **4.01** (6.51 mg, 8.93 μmol), carboxylate ligand **4.02** (0.94 mg, 4.5 μmol), and hexatopic pyridyl ligand **4.11** (1.48 mg, 1.48 μmol). Yield: 7.10 mg, 96%. MS (ESI) calcd for $[M - 4PF_6]^{4+}$ *m/z* 2328.3, found 2328.3; calcd for $[M - 5PF_6]^{5+}$ *m/z* 1834.1, found 1834.0. ^{1}H NMR (Acetone-d_6, 300 MHz): *δ* 8.76 (s, 24H, H_α-Py for donor **4.11**), 7.80 (d, *J* = 6.0 Hz, 24H, H_{phenyl} for donor **4.02**), 7.57 (s, 24H, H_β-Py for donor **4.11**), 7.50 (d, *J* = 9.0 Hz, 24H, H_{phenyl} for donor **4.11**), 7.20 (d, *J* = 6.0 Hz, 24H, H_{phenyl} for donor **1**), 1.92-1.77 (m, 144H, PCH_2CH_3), 1.35-1.14(m, 216H, PCH_2CH_3); ^{31}P {^{1}H} NMR (Acetone-d_6, 121.4 MHz): *δ* 6.19 (d, $^2J_{P\text{-}P}$ = 21.85 Hz, ^{195}Pt satellites, $^1J_{Pt\text{-}P}$ = 3228 Hz), 1.06 (d, $^2J_{P\text{-}P}$ = 21.85 Hz, ^{195}Pt satellites, $^1J_{Pt\text{-}P}$ = 3403 Hz); Anal. Calcd for $C_{336}H_{480}F_{72}N_{12}O_{24}P_{36}Pt_{12}$: C, 40.78; H, 4.89; N, 1.70. Found: C, 40.49; H, 5.02; N, 1.80.

9.13.22 Selective self-assembly of 4.13

Reaction scale: *Cis*-$Pt(PEt_3)_2(OTf)_2$ **4.01** (5.85 mg, 8.02 μmol), carboxylate ligand **4.09** (1.15 mg, 4.0 μmol), and hexatopic pyridyl ligand **4.11** (1.33 mg, 1.33 μmol). Yield: 6.53 mg, 94%. MS (ESI) calcd for $[M - 5PF_6]^{5+}$ *m/z* 1924.7, found 1924.7. ^{1}H NMR (Acetone-d_6, 300 MHz): *δ* 8.96 (s, 24H, H_α-Py for donor **4.11**), 8.03 (d, *J* = 9.0 Hz, 24H,

H_{phenyl} for donor **4.09**), 7.71 (s, 48H, H_{β}-Py for donor **4.11** and H_{phenyl} for donor **4.09**), 7.49 (d, *J* = 6.0 Hz, 12H, H_{phenyl} for donor **1**), 7.30 (d, *J* = 9.0 Hz, 12H, H_{phenyl} for donor **4.11**), 7.10 (d, *J* = 6.0 Hz, 12H, H_{phenyl} for donor **1**), 6.88 (d, *J* = 9.0 Hz, 12H, H_{phenyl} for donor **4.11**), 1.92-1.81 (m, 144H, PCH_2CH_3), 1.39-1.18 (m, 216H, PCH_2CH_3); ^{31}P {^{1}H} NMR (Acetone-d_6, 121.4 MHz): δ 6.73 (d, $^{2}J_{P\text{-}P}$ = 21.85 Hz, ^{195}Pt satellites, $^{1}J_{Pt\text{-}P}$ = 3201 Hz), 1.10 (d, $^{2}J_{P\text{-}P}$ = 21.85 Hz, ^{195}Pt satellites, $^{1}J_{Pt\text{-}P}$ = 3437 Hz); Anal. Calcd for $C_{372}H_{504}F_{72}N_{12}O_{24}P_{36}Pt_{12}$: C, 43.16; H, 4.91; N, 1.62. Found: C, 42.95; H, 5.04; N, 1.67.

9.13.23 Selective self-assembly of 4.14

Reaction scale: *Cis*-$Pt(PEt_3)_2(OTf)_2$ **4.01** (6.15 mg, 8.43 μmol), carboxylate ligand **4.10** (1.32 mg, 4.21 μmol), and hexatopic pyridyl ligand **4.11** (1.40 mg, 1.41 μmol). Yield: 6.75 mg, 91%. MS (ESI) calcd for $[M - 5PF_6]^{5+}$ *m/z* 1958.4, found 1958.4; calcd for $[M - 6PF_6]^{6+}$ *m/z* 1607.9, found 1607.8. ^{1}H NMR (Acetone-d_6, 300 MHz): δ 8.95 (s, 24H, H_{α}-Py for donor **4.11**), 7.99-7.81 (m, 72H, H_{β}-Py for donor **1** and H_{phenyl} for donor **4.10**), 7.63 (d, J = 9.0 Hz, 12H, H_{phenyl} for donor **4.11**), 7.36-7.28(m, 24H, H_{phenyl} for donor **4.11**), 7.01 (d, *J* = 9.0 Hz, 12H, H_{phenyl} for donor **4.11**), 1.89-1.76 (m, 144H, PCH_2CH_3), 1.33-1.21 (m, 216H, PCH_2CH_3); ^{31}P {^{1}H} NMR (Acetone-d_6, 121.4 MHz): δ 7.16 (d, $^{2}J_{P\text{-}P}$ = 21.85 Hz, ^{195}Pt satellites, $^{1}J_{Pt\text{-}P}$ = 3170 Hz), 2.13 (d, $^{2}J_{P\text{-}P}$ = 21.85 Hz, ^{195}Pt satellites, $^{1}J_{Pt\text{-}P}$ = 3388 Hz); Anal. Calcd for $C_{372}H_{504}F_{72}N_{24}O_{24}P_{36}Pt_{12}$: C, 42.47; H, 4.83; N, 3.20. Found: C, 42.14; H, 4.81; N, 3.13.

9.13.24 Self-assembly of 4.15

Cis-$Pt(PEt_3)_2(OTf)_2$ **4.01** (5.07 mg, 6.95 μmol) and ditopic pyridyl ligand **4.03** (1.95 mg, 6.96 μmol) were placed in a 2-dram vial, followed by addition of 0.7 mL Acetone-d_6, which was then sealed with Teflon tape and immersed in an oil bath at 70 ℃

for 2 h. Solid product was obtained by removing the solvent under vacuum. Yield: 6.80 mg, 97%. MS (ESI) calcd for $[M - 2OTf]^{2+}$ *m/z* 1869.84, found 1869.91; calcd for $[M - 3OTf]^{3+}$ *m/z* 1197.25, found 1197.08. ^{1}H NMR (Acetone-d_6, 300MHz) δ 9.28 (d, *J* = 4.8 Hz, 16H, $H_{\alpha\text{-Py}}$), 7.79 (d, *J* = 6.0 Hz, 16H, $H_{\beta\text{-Py}}$), 7.69 (s, 16H, $H_{\text{phneyl-Py}}$), 2.08 (m, 48H, PCH_2CH_3), 1.29 (m, 72H, PCH_2CH_3). $^{31}P\{^{1}H\}$ NMR (Acetone-d_6, 121.4 MHz) δ 0.36 (s, ^{195}Pt satellites, $^{1}J_{\text{Pt-P}}$ = 3099 Hz). Anal. Calcd for $C_{136}H_{168}F_{24}N_8O_{24}P_8Pt_4S_8$: C, 40.44; H, 4.19; N, 2.77. Found: C, 40.65; H, 4.21; N, 2.64.

9.13.25 Self-assembly of 4.16

Cis-$Pt(PEt_3)_2(OTf)_2$ **4.01** (4.51 mg, 6.18 μmol) and tritopic pyridyl ligand **4.05** (1.55 mg, 4.06 μmol) were placed in a 2-dram vial, followed by addition of 0.7 mL Acetone-d_6, which was then sealed with Teflon tape and immersed in an oil bath at 70 ℃ for 2 h. Solid product was obtained by removing the solvent under vacuum. Yield: 5.94 mg, 98%. MS (ESI) calcd for $[M - 3OTf]^{3+}$ *m/z* 1818.32, found 1818.36; calcd for $[M - 4OTf]^{4+}$ *m/z* 1326.75, found 1326.65. ^{1}H NMR (Acetone-d_6, 300MHz) δ 9.32 (d, *J* = 4.8 Hz, 24H, $H_{\alpha\text{-Py}}$), 8.04 (s, 12H, $H_{\text{phneyl-Py}}$), 7.83 (d, *J* = 6.3 Hz, 24H, $H_{\beta\text{-Py}}$), 2.09 (m, 72H, PCH_2CH_3), 1.29 (m, 108H, PCH_2CH_3). $^{31}P\{^{1}H\}$ NMR (Acetone-d_6, 121.4 MHz) δ 0.29 (s, ^{195}Pt satellites, $^{1}J_{\text{Pt-P}}$ = 3083 Hz). Anal. Calcd for $C_{192}H_{240}F_{36}N_{12}O_{36}P_{12}Pt_6S_{12}$: C, 39.07; H, 4.10; N, 2.85. Found: C, 39.25; H, 4.18; N, 2.81.

9.13.26 Self-assembly of 4.17

To a 1.2 mL CD_2Cl_2 suspension of tetratopic pyridyl ligand **4.06b** (2.46 mg, 3.97 μmol) was added a 0.4 mL CD_3NO_2 solution of *Cis*-$Pt(PEt_3)_2(OTf)_2$ **4.01** (5.89 mg, 8.07 μmol), drop by drop, with continuous stirring (5 min). The reaction mixture was stirred at room temperature for 1 h, and then heated up to 70 ℃ for overnight. The solution was

evaporated to dryness, and the product was collected. Yield: 8.18mg, 98%. MS (ESI) calcd for $[M - 2OTf]^{2+}$ *m/z* 2966.54, found 2966.57; calcd for $[M - 4OTf]^{4+}$ *m/z* 1409.04, found 1408.99; calcd for $[M - 5OTf]^{5+}$ *m/z* 1097.44, found 1097.48. ^{1}H NMR (CD_2Cl_2/CD_3NO_2: 3/1, 300MHz) δ 9.75 (dd, J_1 = 4.8 Hz and J_2 = 36 Hz, 24H, $H_{\alpha\text{-Py}}$), 8.98 (m, 36H, $H_{\beta\text{-Py}}$ and $H_{Pyrrole}$), 8.51 (s, 12H, $H_{Pyrrole}$), 2.32 (m, 72H, PCH_2CH_3), 1.60 (m, 108H, PCH_2CH_3). $^{31}P\{^{1}H\}$ NMR (CD_2Cl_2/CD_3NO_2: 3/1, 121.4 MHz) δ 0.90 (s, ^{195}Pt satellites, $^{1}J_{Pt\text{-}P}$ = 3070 Hz). Anal. Calcd for $C_{204}H_{258}F_{36}N_{24}O_{36}P_{12}Pt_6S_{12}$: C, 39.31; H, 4.17; N, 5.39. Found: C, 39.83; H, 4.35; N, 5.16.

9.13.27 Self-assembly of 4.18

Cis-$Pt(PEt_3)_2(OTf)_2$ **4.01** (2.12 mg, 2.91 μmol) and carboxylate ligand **4.02** (0.61 mg, 2.9 μmol) were placed in a 2-dram vial, followed by addition of 0.08 mL H_2O and 0.8 Acetone, which was then sealed with Teflon tape and immersed in an oil bath at 70 ℃ for 2 h. The solvent was then removed by N_2 flow, and the solid mixture was dried under vacuum. 0.6 mL Acetone-d_6 was added to the dried mixture and after 4 h of heating at 70 ℃, the neutral triangle was formed. Yield: 1.56 mg, 90 %. MS (ESI) calcd for $[M + H]^{+}$ *m/z* 1787.38, found 1787.12; calcd for $[M + Na]^{+}$ *m/z* 1809.47, found 1809.11; calcd for $[M + 2Na]^{2+}$ *m/z* 916.23, found 916.16. ^{1}H NMR (Acetone-d_6, 300MHz) δ 7.74 (s, 12H, H_{Phenyl}), 2.00 (m, 36H, PCH_2CH_3), 1.23 (m, 54H, PCH_2CH_3). $^{31}P\{^{1}H\}$ NMR (Acetone-d_6, 121.4 MHz) δ 3.52 (s, ^{195}Pt satellites, $^{1}J_{Pt\text{-}P}$ = 3619 Hz).

9.13.28 Self-assembly of 4.19

Cis-$Pt(PEt_3)_2(OTf)_2$ **4.01** (6.08 mg, 8.34 μmol) and tripyridyl ligand **4.21** (1.67 mg, 5.35 μmol) were placed in a 2-dram vial, followed by addition of 0.8 Acetone-d_8, which was then sealed with Teflon tape and immersed in an oil bath at 70 ℃ for 3 h. The

truncated tetrahedron **4.19** was formed and isolated by removal of all solvent. Yield: 10.21 mg, 98%. MS (ESI) calcd for $[M - 3OTf]^{3+}$ *m/z* = 1726.0, found 1725.9; calcd for $[M - 4OTf]^{4+}$ *m/z* = 976.0, found 975.9. ^{1}H NMR (Acetone-d_6, 300MHz) δ 9.64 (d, J_1 = 5.1 Hz, 24H, $H_{\alpha\text{-Py}}$), 8.94 (d, J_1 = 6.3 Hz, 24H, $H_{\beta\text{-Py}}$), 1.96 (m, 72H, PCH_2CH_3), 1.23 (m, 108H, PCH_2CH_3). ^{31}P{^{1}H} NMR (Acetone-d_6, 121.4 MHz) δ 0.33 (s, ^{195}Pt satellites, $^{1}J_{Pt\text{-}P}$ = 3085 Hz).

9.13.29 Self-assembly of 4.20

4.20 can be obtained via three different ways:

(1) supramolecular modification with addition of carboxylate ligand: To 1.0 ml acetone solution of **4.19** (8.15 mg, 1.45 μmol), 0.2 ml aqueous solution of carboxylate donor **4.02** (0.73 mg, 3.5 μmol) was added in a 2-dram vial, which was then sealed with Teflon tape and immersed in an oil bath at 70 ℃ for 1 h. The solvent was then removed by N_2 flow, and the solid mixture was dried under vacuum. 0.7 mL Acetone-d_6 was added to the dried mixture and after 5 h of heating at 75 ℃, the square pyramid **4.20** was formed and isolated by addition of aqueous solution of KPF_6. Yield: 6.33 mg, 91%;

(2) supramolecular modification with addition of carxylate ligand and Pt(II) acceptor: 1.0 ml acetone solution of **4.19** (7.22 mg, 1.28 μmol) was added to a 0.1 ml water suspension of c*is*-$Pt(PEt_3)_2(OTf)_2$ **4.01** (3.74 mg, 5.13 μmol), carboxylate donor **4.02** (1.08 mg, 5.14 μmol) in a 2-dram vial, which was then sealed with Teflon tape and immersed in an oil bath at 70 ℃ for 1 h. The solvent was then removed by N_2 flow, and the solid mixture was dried under vacuum. 0.7 mL Acetone-d_6 was added to the dried mixture and after 5 h of heating at 75 ℃, the square pyramid **4.20** was formed and isolated by addition of aqueous solution of KPF_6. Yield: 9.56 mg, 93%;

(3) self-assembly of molecular components: *Cis*-$Pt(PEt_3)_2(OTf)_2$ **4.01** (10.17 mg, 13.95 μmol), carboxylate donor **4.02** (1.17 mg, 5.57 μmol), and tripyridyl ligand **4.21** (1.74 mg, 5.57 μmol) were placed in a 2-dram vial, followed by addition of 0.08 mL H_2O and 0.8 Acetone, which was then sealed with Teflon tape and immersed in an oil bath at 70 ℃ for 1 h. The solvent was then removed by N_2 flow, and the solid mixture was dried under vacuum. 0.7 mL Acetone-d_6 was added to the dried mixture and after 5 h of heating at 75 ℃, the square pyramid **4.20** was formed and isolated by addition of aqueous solution of KPF_6. Yield: 10.62 mg, 95%. MS (ESI) calcd for $[M - 3PF_6]^{3+}$ *m/z* = 1181.0, found 1181.1; calcd for $[M - 2PF_6]^{2+}$ *m/z* = 1844.4, found 1844.4. ^{1}H NMR (Acetone-d_6, 300MHz) δ 9.56 (d, J_1 = 5.1 Hz, 4H, $H_{\alpha\text{-}Py(PyPtPy)}$), 9.26 (m, 8H, $H_{\alpha\text{-}Py(COOPtPy)}$), 8.94 (d, J_1 = 5.1 Hz, 4H, $H_{\beta\text{-}Py(COOPtPy)}$), 8.86 (d, J_1 = 6.3 Hz, 4H, $H_{\beta'\text{-}Py(PyPtPy)}$), 8.04 (d, J_1 = 5.1 Hz, 4H, $H_{\beta\text{-}Py(COOPtPy)}$), 7.72 (s, 8H, H_{Phenyl}), 1.83 (m, 60H, PCH_2CH_3), 1.09 (m, 90H, PCH_2CH_3). $^{31}P\{^1H\}$ NMR (Acetone-d_6, 121.4 MHz) δ 6.70 (d, $^2J_{P\text{-}P}$ = 22.0 Hz, ^{195}Pt satellites, $^1J_{Pt\text{-}P}$ = 3264 Hz), 0.84 (d, $^2J_{P\text{-}P}$ = 22.0 Hz, ^{195}Pt satellites, $^1J_{Pt\text{-}P}$ = 3429 Hz), 0.31 (s, ^{195}Pt satellites, $^1J_{Pt\text{-}P}$ = 3102 Hz).

9.13.30 Self-assembly of 4.22

4.22 can be obtained via three different ways:

(1) supramolecular modification with addition of carboxylate ligand: To 1.0 ml acetone solution of **4.19** (8.93 mg, 1.58 μmol), 0.2 ml aqueous solution of carboxylate donor **4.23** (0.43 mg, 1.58 μmol) was added in a 2-dram vial, which was then sealed with Teflon tape and immersed in an oil bath at 70 ℃ for 1 h. The solvent was then removed by N_2 flow, and the solid mixture was dried under vacuum. 0.7 mL Acetone-d_6 was added

to the dried mixture and after 5 h of heating at 75 ℃, the truncated tetrahedron **4.22** was formed and isolated by addition of aqueous solution of Et_2O. Yield: 7.41 mg, 92%;

(2) supramolecular modification with addition of carxylate ligand and Pt(II) acceptor: 1.0 ml acetone solution of **4.19** (6.71 mg, 1.19 μmol) was added to a 0.1 ml water suspension of c*is*-$Pt(PEt_3)_2(OTf)_2$ **4.01** (1.84 mg, 2.52 μmol), carboxylate donor **4.23** (0.45 mg, 1.65 μmol) in a 2-dram vial, which was then sealed with Teflon tape and immersed in an oil bath at 70 ℃ for 1 h. The solvent was then removed by N_2 flow, and the solid mixture was dried under vacuum. 0.7 mL Acetone-d_6 was added to the dried mixture and after 5 h of heating at 75 ℃, the truncated tetrahedron **4.22** was formed and isolated by addition of aqueous solution of Et_2O. Yield: 7.26 mg, 90%;

(3) self-assembly of molecular components: *Cis*-$Pt(PEt_3)_2(OTf)_2$ **4.01** (8.15 mg, 11.17 μmol), carboxylate donor **4.23** (0.53 mg, 1.94 μmol), and tripyridyl ligand **4.21** (1.71 mg, 5.48 μmol) were placed in a 2-dram vial, followed by addition of 0.08 mL H_2O and 0.8 Acetone, which was then sealed with Teflon tape and immersed in an oil bath at 70 ℃ for 1 h. The solvent was then removed by N_2 flow, and the solid mixture was dried under vacuum. 0.7 mL Acetone-d_6 was added to the dried mixture and after 5 h of heating at 75 ℃, the truncated tetrahedron **4.22** was formed and isolated by addition of aqueous solution of Et_2O. Yield: 8.60 mg, 91%. MS (ESI) calcd for $[M - 2OTf]^{2+}$ *m/z* = 2387.4, found 2387.3; $[M - 3OTf]^{3+}$ *m/z* = 1542.0, found 1541.9; calcd for $[M - 4OTf]^{4+}$ *m/z* = 1119.0, found 1119.0. ^1H NMR (Acetone-d_6, 300MHz) δ 9.64 (m, 12H, $H_{\alpha\text{-}Py(PyPtPy)}$), 9.31 (m, 6H, $H_{\alpha\text{-}Py(COOPtPy)}$), 8.93 (d, J_1 = 6.3 Hz, 4H, $H_{\beta\text{-}Py(PyPtPy)}$), 8.86 (d, J_1 = 6.0 Hz, 4H, $H_{\beta'\text{-}Py(PyPtPy)}$), 8.24 (s, 3H, H_{Phenyl}), 8.04 (d, J_1 = 5.1 Hz, 4H, $H_{\beta\text{-}Py(PyPtPy)}$), 1.94 (m, 72H, PCH_2CH_3), 1.24 (m, 108H, PCH_2CH_3). $^{31}P\{^1H\}$ NMR (Acetone-d_6, 121.4 MHz) δ 6.62

(d, $^{2}J_{P\text{-}P}$ = 22.0 Hz, ^{195}Pt satellites, $^{1}J_{Pt\text{-}P}$ = 3242 Hz), 0.90 (d, $^{2}J_{P\text{-}P}$ = 22.0 Hz, ^{195}Pt satellites, $^{1}J_{Pt\text{-}P}$ = 3473 Hz), 0.59 (s, ^{195}Pt satellites, $^{1}J_{Pt\text{-}P}$ = 3112 Hz).

9.13.31 Self-assembly of 5.3a

90 °acceptor **5.1a** (5.87 mg, 8.05 mmol) and hexapyridyl donor **5.2** (2.65 mg, 2.66 mmol) were placed in a 2-dram vial followed by addition of 1.0 mL CD_3NO_2/Acetone-d_6 (*v/v* 7/3) solvent. The mixture was stirred at 80 ℃ for 16 h, and the truncated tetrahedron **5.3a** was formed. The solvent was then removed by evaporation under N_2 flow and vacuum. 0.8 ml Acetone was added to the mixture to dissolve the self-assembly. The OTf–counterions were exchanged for PF_6^- using an aqueous solution of KPF_6 to precipitate the product, which was collected and washed with excess water and then dried in vacuum. Yield: 7.90 mg, 93 %. ^{1}H NMR (CD_3NO_2/Acetone-d_6: 3/7, 300 MHz): δ 8.91 (m, 48H, $H_{\alpha\text{-Py}}$), 7.58 (d, J_1 = 5.1 Hz, 24H, $H_{\beta\text{-Py}}$), 7.44 (d, J_1 = 5.1 Hz, 24H, $H_{\beta\text{-Py}}$), 7.14 (dd, J_1 = 7.8 Hz, J_2 = 33.9 Hz, 48H, Ph$H_{exterior}$), 6.94 (dd, J_1 = 6.0 Hz, J_2 = 6.3 Hz, 48H, Ph$H_{interior}$), 2.10 (m, 144H, PC*H*2CH3), 1.29 (m, 216H, PCH2C*H*3). ^{31}P{^{1}H} NMR (CD_3NO_2/Acetone-d_6: 3/7, 121.4 MHz): δ 0.92 (s, $^{1}J_{Pt\text{-}P}$ = 3121 Hz). Anal. Calcd for $C_{432}H_{552}F_{144}N_{24}P_{48}Pt_{12}$: C, 41.03; H, 4.40; N, 2.66. Found: C, 40.80; H, 4.50; N, 2.65.

9.13.32 Self-assembly of 5.3b

90 ° acceptor **5.1b** (3.57 mg, 5.53 mmol) and hexapyridyl donor **5.2** (1.83 mg, 1.84 mmol) were placed in a 2-dram vial followed by addition of 1.0 mL D_2O/Acetone-d_6 (*v/v* 1/1) solvent. The mixture was stirred at 80 ℃ for 16 h, and the truncated tetrahedron **5.3b** was formed. The OTf–counterions were exchanged for PF_6^- using an aqueous solution of KPF_6 to precipitate the product, which was collected and washed with excess water and then dried in vacuum. Yield: 4.86 mg, 91 %. ^{1}H NMR (D_2O/Acetone-d_6: 1/1,

300 MHz): δ 8.68 (m, 48H, $H_{\alpha\text{-Py}}$), 7.48 (m, 48H, $H_{\beta\text{-Py}}$), 7.03 (dd, J_1 = 7.8 Hz, J_2 = 37.2 Hz, 48H, PhH_{exterior}), 6.78 (m, 48H, PhH_{interior}), 1.81 (d, J = 10.8 Hz, 216H, PC*H*3). $^{31}P\{^1H\}$ NMR (D_2O/Acetone-d_6: 1/1, 121.4 MHz): δ -28.2 ppm (s, $^1J_{\text{Pt-P}}$ = 3110 Hz). Anal. Calcd for $C_{360}H_{408}F_{144}N_{24}P_{48}Pt_{12}$: C, 37.16; H, 3.53; N, 2.89. Found: C, 37.53; H, 3.80; N, 2.82.

9.13.33 Self-assembly of 5.3b 5.4$_3$

90 ° acceptor **5.1b** (4.36 mg, 5.53 mmol), hexapyridyl donor **5.2** (1.83 mg, 1.84 mmol), and 1,3,5-triphenylbenzene **5.4** (3.31 mg, 10.8 mmol) were placed in a 2-dram vial followed by addition of 1.0 mL D_2O/Acetone-d_6 (*v/v* 1/1) solvent. The mixture was stirred at 80 ℃ for 16 h, and the encapsulated complex **5.3b 5.4$_3$** was formed. Excess **5.4** was filtered. The OTf–counterions were exchanged for PF_6^- using an aqueous solution of KPF_6 to precipitate the product, which was collected and washed with excess water and then dried in vacuum. Yield: 5.49 mg, 95 %. ^1H NMR (D_2O/Acetone-d_6: 1/1, 300 MHz): δ 8.76 (s, 48H, $H_{\alpha\text{-Py}}$), 7.36 (s, 48H, $H_{\beta\text{-Py}}$), 6.94 (m, 105H, Ph$H_{\mathbf{3b}\text{ and }\mathbf{4}}$), 6.35 (m, 45H, Ph$H_{\mathbf{4}}$), 1.63 (d, J = 4.2 Hz, 216H, PC*H*3). $^{31}P\{^1H\}$ NMR (D_2O/Acetone-d_6: 1/1, 121.4 MHz): δ -28.2 (s, $^1J_{\text{Pt-P}}$ = 3111 Hz). Anal. Calcd for $C_{432}H_{462}F_{144}N_{24}P_{48}Pt_{12}$: C, 41.33; H, 3.71; N, 2.68. Found: C, 40.95; H, 3.63; N, 2.83.

9.13.34 Self-assembly of 6.1

Cis-$Pt(PMe_3)_2(OTf)_2$ **6.2** (6.30 mg, 9.77 μmol) and tripyridyl ligand **6.3** (2.03 mg, 6.50 μmol) were placed in a 2-dram vial, followed by addition of 0.08 ml D_2O and 0.8 ml Acetone-d_6, which was then sealed with Teflon tape and immersed in an oil bath at 70 ℃ for 3 h. The truncated tetrahedron **6.1** was formed and isolated by removal of all solvent. Yield: 8.16 mg, 98%. MS (ESI) calcd for $[M - 3OTf]^{3+}$ *m/z* = 1557.4, found 1557.3;

calcd for $[M - 4OTf]^{4+}$ *m/z* = 1130.8, found 1130.9. ^{1}H NMR (Acetone-d_6:D_2O 10:1, 300MHz) δ 9.34 (d, J_1 = 4.8 Hz, 24H, $H_{\alpha\text{-Py}}$), 8.88 (d, J_1 = 6.3 Hz, 24H, $H_{\beta\text{-Py}}$), 1.69 (d, J_1 = 11.4 Hz, 108H, PC*H*$_3$). ^{31}P{^{1}H} NMR Acetone-d_6:D_2O 10:1, 121.4 MHz) δ -28.4 (s, ^{195}Pt satellites, $^{1}J_{\text{Pt-P}}$ = 3133 Hz).

9.13.35 Self-assembly of 6.4

0.8 ml aqueous acetone solution (*v/v* 1:10) of two-component self-assembly **6.1** (5.28 mg, 1.03 μmol) was added to a water suspension (0.1 ml) of *cis*-$Pt(PMe_3)_2(OTf)_2$ **6.2** (3.98 mg, 6.17 μmol) and carboxylate ligand **6.5** (0.99 mg, 6.18 μmol) in a 2-dram vial, followed by addition of coronene (3.00 mg, 10.0 μmol), which was then sealed with Teflon tape and immersed in an oil bath at 70 ℃ for 3 h. The resulted orange suspension was filtered and the three-component prism **6.4** was isolated by removal of all solvent. Yield: 9.85 mg, 93%. MS (ESI) calcd for $[M - 3OTf]^{3+}$ *m/z* = 1265.5, found 1265.5; calcd for $[M - 4OTf]^{4+}$ *m/z* = 911.9, found 911.8. ^{1}H NMR (Acetone-d_6:D_2O 10:1, 300MHz) δ 8.84 (m, 12H, $H_{\alpha\text{-Py}}$), 8.15 (s, 12H, H_{Coronene}), 7.40 (d, J_1 = 5.7 Hz, 12H, $H_{\beta\text{-Py}}$), 7.08 (s, 6H, H_{olefin}), 1.82 (d, J_1 = 11.7 Hz, 54H, PC*H*$_3$), 1.37 (d, J_1 = 11.7 Hz, 54H, PC*H*$_3$). ^{31}P{^{1}H} NMR Acetone-d_6:D_2O 10:1, 121.4 MHz) δ -24.75 (d, J_1 = 24.4 Hz, ^{195}Pt satellites, $^{1}J_{\text{Pt-P}}$ = 3255 Hz), -30.59 (d, J_1 = 24.4 Hz, ^{195}Pt satellites, $^{1}J_{\text{Pt-P}}$ = 3474 Hz).

9.13.36 Synthesis of [G-0] dendron-substituted tripyridyl donors 7.2a

Yield: 64 mg (white solid), 80%. Mp: 179–181 ^{o}C. ^{1}H NMR ($CDCl_3$, 300 MHz): δ 8.64 (d, *J* = 4.8 Hz, 6H, $H_{\alpha\text{-Py}}$), 7.35 (m, 11H, $H_{\beta\text{-Py}}$ and Ph*H*), 4.16 (s, 2H, PhC*H*2O). ^{13}C NMR ($CDCl_3$, 75 MHz): δ 150.5, 150.1, 137.3, 128.9, 128.2, 127.3, 123.2, 85.1, 66.9. HR-MS (ESI-TOF): calculated for $[M + 1]^{+}$ 354.1608, found 354.1606.

9.13.37 Synthesis of [G-1] dendron-substituted tripyridyl donors 7.2b

Yield: 97 mg (white solid), 75%. Mp: 168–170 ^{o}C. ^{1}H NMR ($CDCl_3$, 300 MHz): δ 8.62 (d, *J* = 4.8 Hz, 6H, $H_{\alpha\text{-Py}}$), 7.31 (m, 16H, $H_{\beta\text{-Py}}$ and Ph*H*), 6.58 (s, 1H, Ph*H*), 6.55 (s, 2H, Ph*H*), 5.04 (s, 4H, PhC*H*2O), 4.07 (s, 2H, PhC*H*2O). ^{13}C NMR ($CDCl_3$, 75 MHz): δ 160.3, 150.5, 150.0, 139.6, 136.9, 128.9, 128.3, 127.7, 123.1, 106.2, 101.5, 85.1, 70.4, 66.8. HR-MS (ESI-TOF): calculated for $[M + 1]^+$ 566.2449, found 566.2444.

9.13.38 Synthesis of [G-2] dendron-substituted tripyridyl donors 7.2c

Yield: 150 mg (white solid), 66.2%. Mp: 74–76 ^{o}C. ^{1}H NMR ($CDCl_3$, 300 MHz): δ 8.65 (s, 6H, $H_{\alpha\text{-Py}}$), 7.31 (m, 26H, $H_{\beta\text{-Py}}$ and Ph*H*), 6.67 (s, 4H, Ph*H*), 6.53 (m, 5H, Ph*H*), 5.02 (s, 8H, PhC*H*2O), 4.97 (s, 4H, PhC*H*2O), 4.07 (s, 2H, PhC*H*2O). ^{13}C NMR ($CDCl_3$, 75 MHz): δ 160.4, 160.3, 150.5, 150.0, 139.6, 139.4, 136.9, 128.8, 128.3, 127.8, 123.1, 106.6, 106.3, 101.6, 101.4, 85.1, 70.3, 70.2, 66.7. HR-MS (ESI-TOF): calculated for $[M + 1]^+$ 990.4122, found 990.4118.

9.13.39 Synthesis of [G-3] dendron-substituted tripyridyl donors 7.2d

Yield: 254 mg (white solid), 60.6%. Mp: 62–64 ^{o}C. ^{1}H NMR (Acetone-d_6, 300 MHz): δ 8.56 (d, *J* = 5.1 Hz, 6H, $H_{\alpha\text{-Py}}$), 7.28 (m, 46H, $H_{\beta\text{-Py}}$ and Ph*H*), 6.71 (s, 12H, Ph*H*), 6.59 (m, 9H, Ph*H*), 5.05 (s, 24H, PhC*H*2O), 4.99 (s, 4H, PhC*H*2O), 4.13 (s, 2H, PhC*H*2O). ^{13}C NMR (Acetone-d_6, 75 MHz): δ 161.2, 161.0, 151.1, 150.9, 141.0, 140.9, 138.3, 129.4, 128.7, 128.6, 123.9, 107.2, 106.9, 102.3, 102.0, 85.7, 70.6, 70.4, 67.2. HR-MS (ESI-TOF): calculated for $[M + 1]^+$ 1838.7462, found 1838.7473.

9.13.40 Self-assembly of [G-0] adamantanoid dendrimer 7.3a

Yield: 4.29 mg, 96%. ^{1}H NMR (Acetone-d_6/CD_2Cl_2: 1/1, 300 MHz): δ 8.96 (s, 24H, $H_{\alpha\text{-Py}}$), 8.11 (s, 24H, $H_{\beta\text{-Py}}$), 7.38 (m, 68H, Ph$H_{\text{acceptor and donor}}$), 4.40 (s, 8H, PhC*H*2O), 1.40 (m, 144H, PC*H*2CH3), 1.10 (m, 216H, PCH2C*H*3). ^{31}P{^{1}H} NMR (Acetone-d_6/CD_2Cl_2: 1/1, 121.4 MHz): δ 14.06 (s, $^{1}J_{\text{Pt-P}}$ = 2652.3 Hz). Anal. Calcd for $C_{326}H_{484}F_{36}O_{46}N_{12}P_{24}Pt_{12}S_{12}$: C, 41.39; H, 5.16; N, 1.78. Found: C, 41.06; H, 5.17; N, 2.00.

9.13.41 Self-assembly of [G-1] adamantanoid dendrimer 7.3b

Yield: 4.73 mg, 97%. ^{1}H NMR (Acetone-d_6/CD_2Cl_2: 1/1, 300 MHz): δ 8.94 (s, 24H, $H_{\alpha\text{-Py}}$), 8.10 (s, 24H, $H_{\beta\text{-Py}}$), 7.35 (m, 88H, Ph$H_{\text{acceptor and donor}}$), 6.81 (s, 8H, Ph*H*), 6.64 (s, 4H, Ph*H*), 5.10 (s, 16H, PhC*H*2O), 4.35 (s, 8H, PhC*H*2O), 1.40 (m, 144H, PC*H*2CH3), 1.09 (m, 216H, PCH2C*H*3). ^{31}P{^{1}H} NMR (Acetone-d_6/CD_2Cl_2: 1/1, 121.4 MHz): δ 14.06 (s, $^{1}J_{\text{Pt-P}}$ = 2654.9 Hz). Anal. Calcd for $C_{382}H_{532}F_{36}O_{54}N_{12}P_{24}Pt_{12}S_{12}$: C, 44.50; H, 5.20; N, 1.63. Found: C, 44.65; H, 5.40; N, 1.78.

9.13.42 Self-assembly of [G-2] adamantanoid dendrimer 7.3c

Yield: 5.46 mg, 96%. ^{1}H NMR (Acetone-d_6/CD_2Cl_2: 1/1, 300 MHz): δ 8.94 (s, 24H, $H_{\alpha\text{-Py}}$), 8.11 (s, 24H, $H_{\beta\text{-Py}}$), 7.32 (m, 128H, Ph$H_{\text{acceptor and donor}}$), 6.81 (s, 8H, Ph*H*), 6.74 (m, 20H, Ph*H*), 6.59 (s, 8H, Ph*H*), 5.06 (s, 48H, PhC*H*2O), 4.35 (s, 8H, PhC*H*2O), 1.38 (m, 144H, PC*H*2CH3), 1.07 (m, 216H, PCH2C*H*3). ^{31}P{^{1}H} NMR (Acetone-d_6/CD_2Cl_2: 1/1, 121.4 MHz): δ 14.05 (s, $^{1}J_{\text{Pt-P}}$ = 2655.4 Hz). Anal. Calcd for $C_{494}H_{628}F_{36}O_{70}N_{12}P_{24}Pt_{12}S_{12}$: C, 49.41; H, 5.27; N, 1.40. Found: C, 49.50; H, 5.41; N, 1.55.

9.13.43 Self-assembly of [G-3] adamantanoid dendrimer 7.3d

Yield: 6.93 mg, 95%. ^{1}H NMR (Acetone-d_6/CD_2Cl_2: 1/1, 300 MHz): δ 8.92 (s, 24H, $H_{\alpha\text{-Py}}$), 8.10 (s, 24H, $H_{\beta\text{-Py}}$), 7.30 (m, 208H, Ph$H_{\text{acceptor and donor}}$), 6.82 (s, 8H, Ph*H*), 6.68 (m, 52H, Ph*H*), 6.55 (s, 24H, Ph*H*), 5.00 (s, 112H, PhC*H*2O), 4.34 (s, 8H, PhC*H*2O), 1.38 (m, 144H, PC*H*2CH3), 1.07 (m, 216H, PCH2C*H*3). ^{31}P{^{1}H} NMR (Acetone-d_6/CD_2Cl_2: 1/1, 121.4 MHz): δ 14.01 (s, $^{1}J_{\text{Pt-P}}$ = 2653.6 Hz). Anal. Calcd for $C_{718}H_{820}F_{36}O_{102}N_{12}P_{24}Pt_{12}S_{12}$: C, 55.99; H, 5.37; N, 1.09. Found: C, 55.64; H, 5.42; N, 1.27.

9.14 Crystal Data of Truncated Tetrahedron **5.3a**

The diffraction data from single crystals of **5.3a** mounted on a loop were collected at 90 K on an ADSC Quantum 210 CCD diffractometer with a synchrotron radiation (λ = 0.90000 Å) at Macromolecular Crystallography Beamline 6B1, Pohang Accelerator Laboratory (PAL), Pohang, Korea. Crystal data and structure refinement for **5.3a** is shown in Table 9.1.

Table 9.1. Crystal data and structure refinement for **5.3a**

Identification code	**5.3a**	
Empirical formula	C108 H138 F36 N6 P12 Pt3	
Formula weight	3161.15	
Temperature	90(2) K	
Wavelength	0.90000 Å	
Crystal system	Tetragonal	
Space group	$P\text{-}42_1/c$	
Unit cell dimensions	a = 32.987(5) Å	α = 90 °
	b = 32.987(5) Å	β = 90 °
	c = 31.918(6) Å	γ = 90 °
Volume	34730(10) $Å^3$	
Z	8	
Density (calculated)	1.209 g/cm^3	
Absorption coefficient	4.137 mm^{-1}	
F(000)	12528	
Crystal size	0.42 × 0.42 × 0.38 mm^3	
Theta range for data collection	1.56 to 30.37 °	
Index ranges	$-36 \le h \le 36$, $-36 \le k \le 37$, $-32 \le l \le 32$	
Reflections collected	154346	
Independent reflections	23131 [R_{int} = 0.0674]	
Completeness to theta = 25.00 °	99.0 %	
Absorption correction	Semi-empirical from equivalents	
Max. and min. transmission	0.3024 and 0.2754	
Refinement method	Full-matrix least-squares on F^2	
Data / restraints / parameters	23131 / 1356 / 1487	
Goodness-of-fit on F^2	1.050	
Final R indices [I>2sigma(I)]	R_1 = 0.0841, wR_2 = 0.2244	
R indices (all data)	R_1 = 0.0981, wR_2 = 0.2396	
Absolute structure parameter	0.015(6)	
Extinction coefficient	0.00123(6)	
Largest diff. peak and hole	2.491 and -1.069 e.$Å^{-3}$	

9.15 References

(1) Kuehl, C. J.; Huang, S. D.; Stang, P. J. *J. Am. Chem. Soc.* **2001**, *123*, 9634.

(2) Kryschenko, Y. K.; Seidel, S. R.; Arif, A. M.; Stang, P. J. *J. Am. Chem. Soc.* **2003**, *125*, 5193.

(3) Stang, P. J.; Cao, D. H.; Saito, S.; Arif, A. M. *J. Am. Chem. Soc.* **1995**, *117*, 6273.

(4) Leininger, S.; Schmitz, M.; Stang, P. J. *Org. Lett.* **1999**, *1*, 1921.

(5) Kuehl, C. J.; Kryschenko, Y. K.; Radhakrishnan, U.; Seidel, S. R.; Huang, S. D.; Stang, P. J. *Proc. Natl. Acad. Sci. U.S.A.* **2002**, *99*, 4932.

(6) Kuehl, C. J.; Yamamoto, T.; Seidel, S. R.; Stang, P. J. *Org. Lett.* **2002**, *4*, 913.

(7) (a) Rathore, R.; Burns, C. L.; Guzei, I. A. *J. Org. Chem.* **2004**, *69*, 1524. (b) Hoffmann, M.; Kärnbratt, J.; Chuan, M. H.; Herz, L. M.; Albinsson, B.; Anderson, H. L. *Angew. Chem., Int. Ed.* **2008**, *47*, 4993.

(8) Yang, H.-B.; Ghosh, K.; Arif, A. M.; Stang, P. J. *J. Org. Chem.* **2006**, *71*, 9464.

(9) (a) Hawker, C. J.; Fréchet, J. M. J. *J. Am. Chem. Soc.* **1990**, *112*, 7638. (b) Yang, H.-B.; Hawkridge, A. M.; Huang, S. D.; Das, N.; Bunge, S. D.; Muddiman, D. C.; Stang, P. J. *J. Am. Chem. Soc.* **2006**, *129*, 2120.

APPENDIX

REFERENCE NMR AND MASS SPECTRA

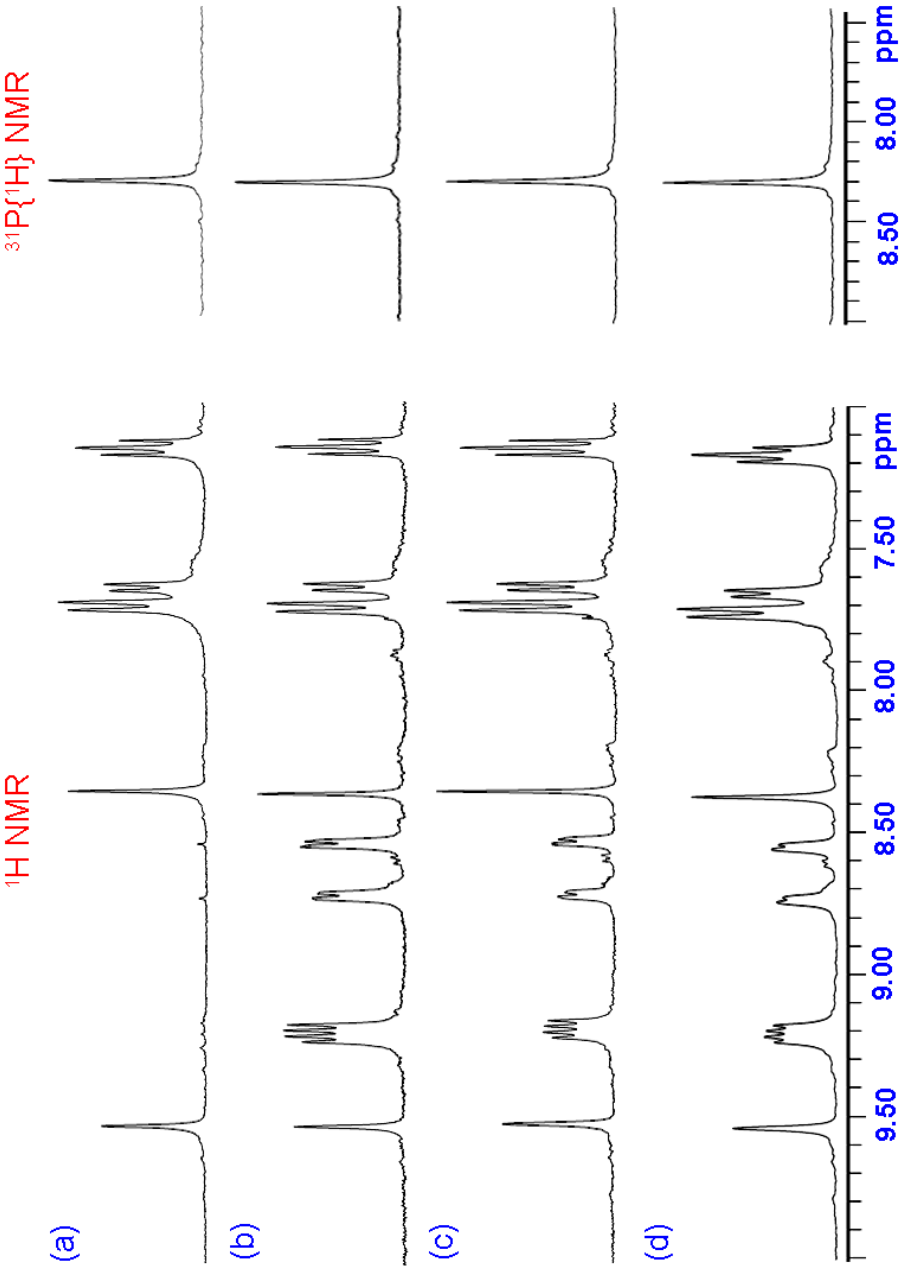

Figure A.1. ^{1}H and $^{31}P\{^{1}H\}$ NMR spectra of (a) individually prepared **2.5b**, (b) individually prepared **2.5a**, (c) initial mixture of **2.5a** and **2.5b**, and (d) equilibrated mixture of **2.5a**, **2.5b**, and **2.5c**.

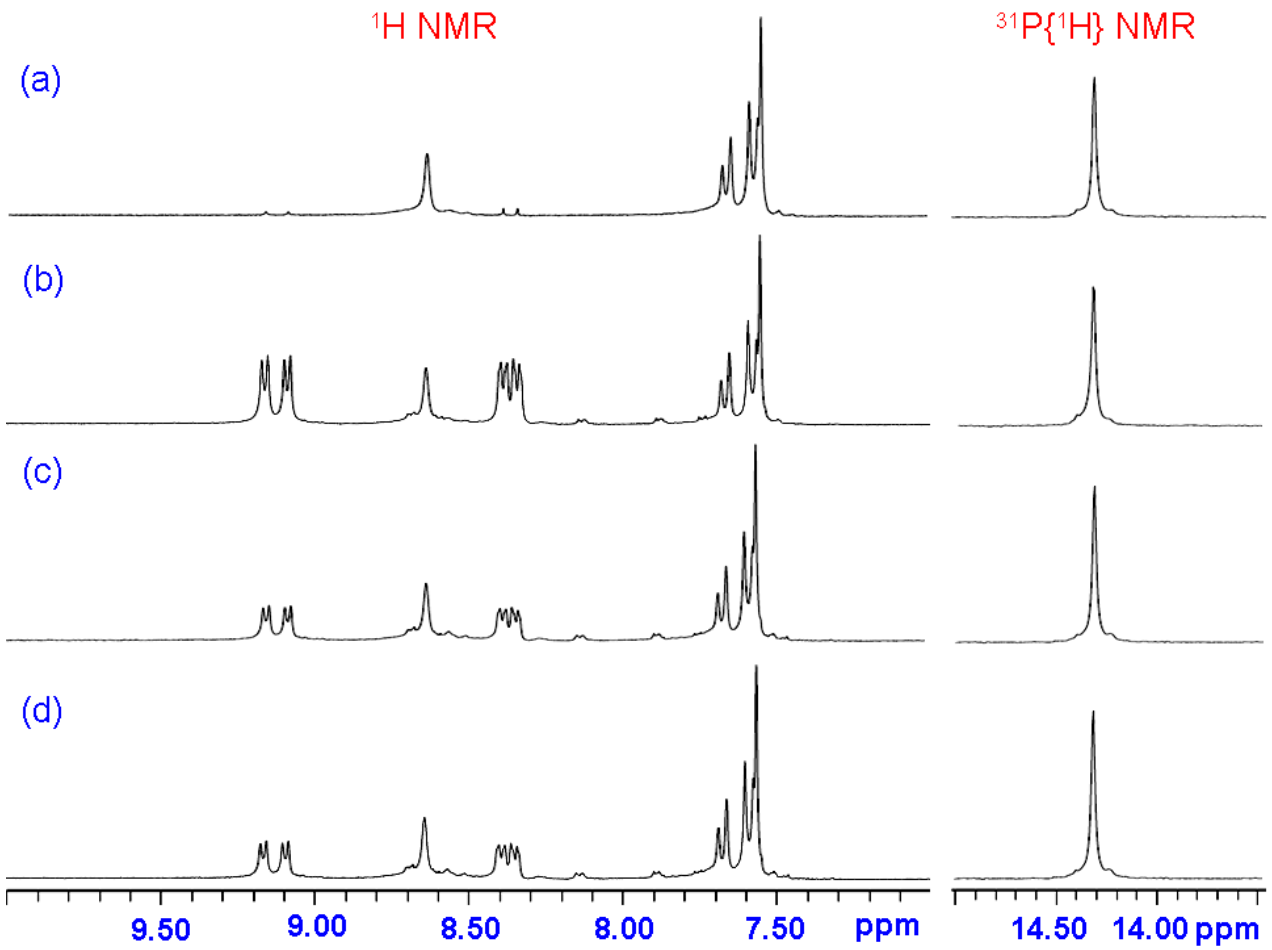

Figure A.2. ^{1}H and ^{31}P{^{1}H} NMR spectra of (a) individually prepared **2.6b**, (b) individually prepared **2.6a**, (c) initial mixture of **2.6a** and **2.6b**, and (d) equilibrated mixture of **2.6a**, **2.6b**, **2.6c**, and **2.6d**..

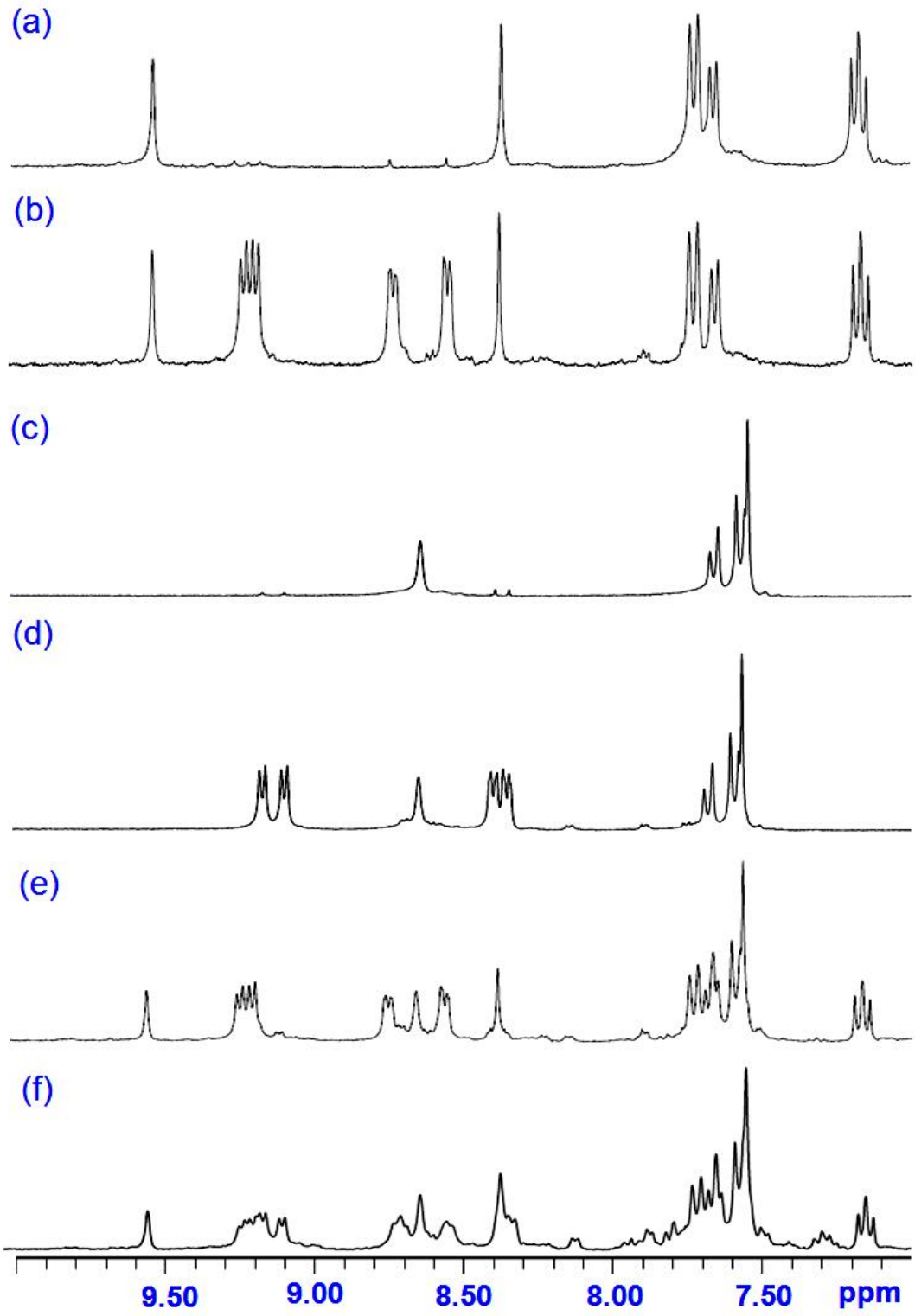

Figure A.3. ^{1}H NMR spectra of (a) individually prepared **2.5b**, (b) individually prepared **2.5a**, (c) individually prepared **2.6b**, (d) individually prepared **2.6a**, (e) initial mixture of **2.5a** and **2.6b**, and (f) equilibrated mixture of **2.5a**, **2.5b**, **2.5c**, **2.6a**, **2.6b**, **2.6c**, and **2.6d**.

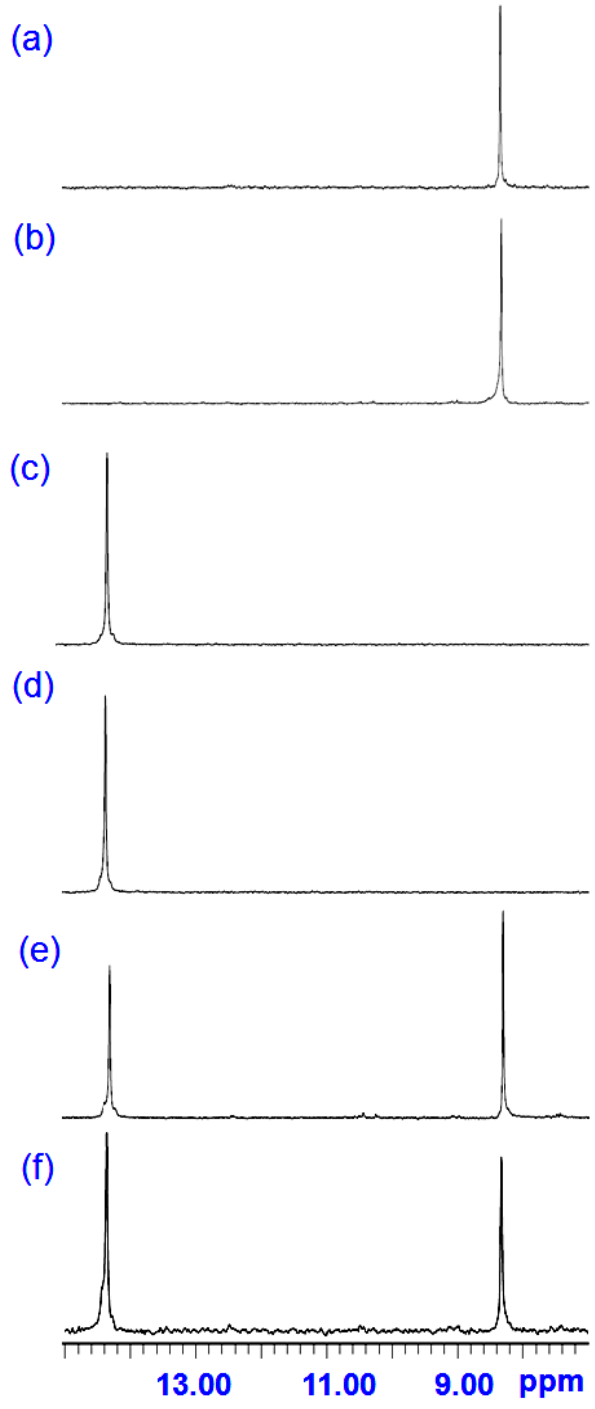

Figure A.4. $^{31}P\{^{1}H\}$ NMR spectra of (a) individually prepared **2.5b**, (b) individually prepared **2.5a**, (c) individually prepared **2.6b**, (d) individually prepared **2.6a**, (e) initial mixture of **2.5a** and **2.6b**, and (f) equilibrated mixture of **2.5a**, **2.5b**, **2.5c**, **2.6a**, **2.6b**, **2.6c**, and **2.6d**.

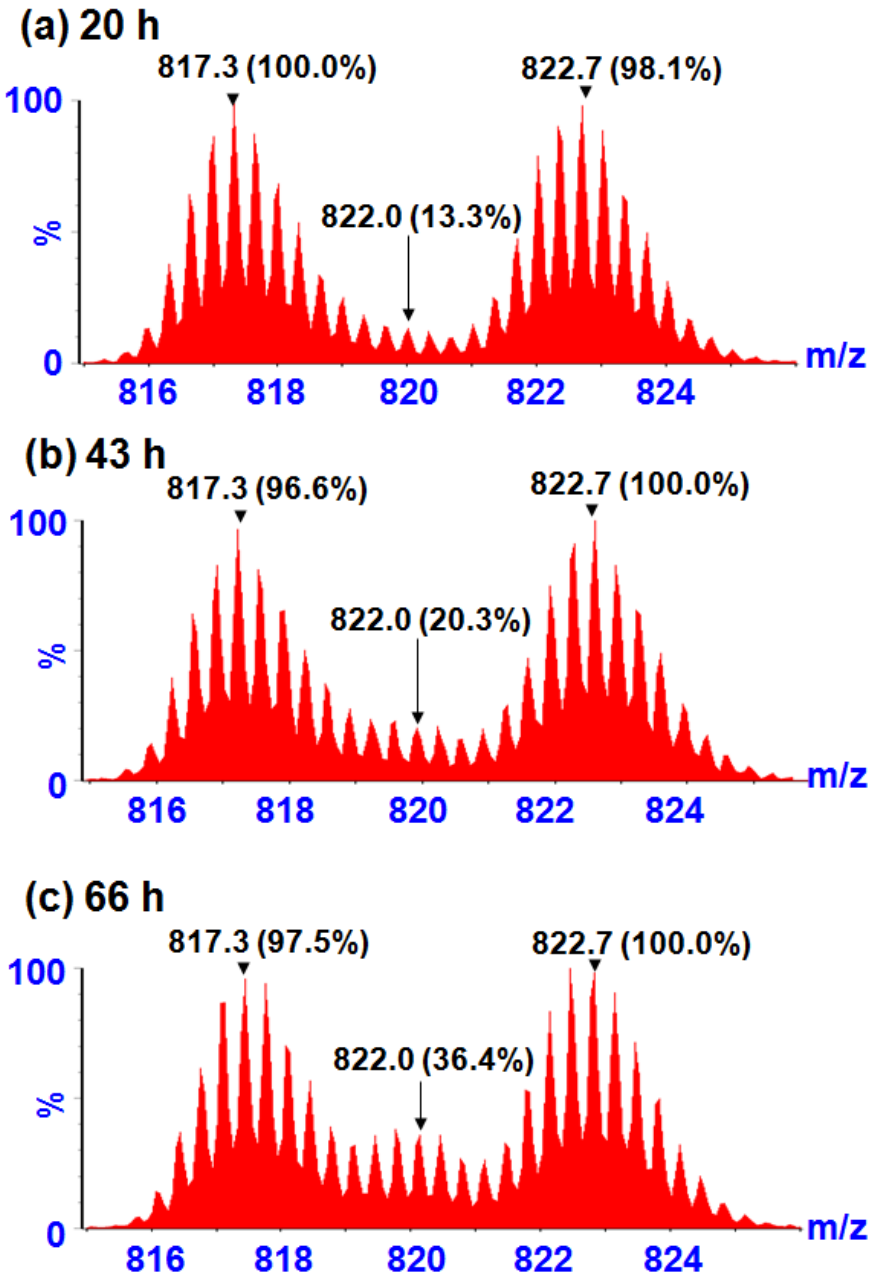

Figure A.5. ESI-MS spectra (Acetone-d_6/D_2O 1:1) for dynamic ligand exchange between **2.5a** and **2.5b** recorded at different time intervals: (a) 20 h, (b) 43 h, (c) 66 h,

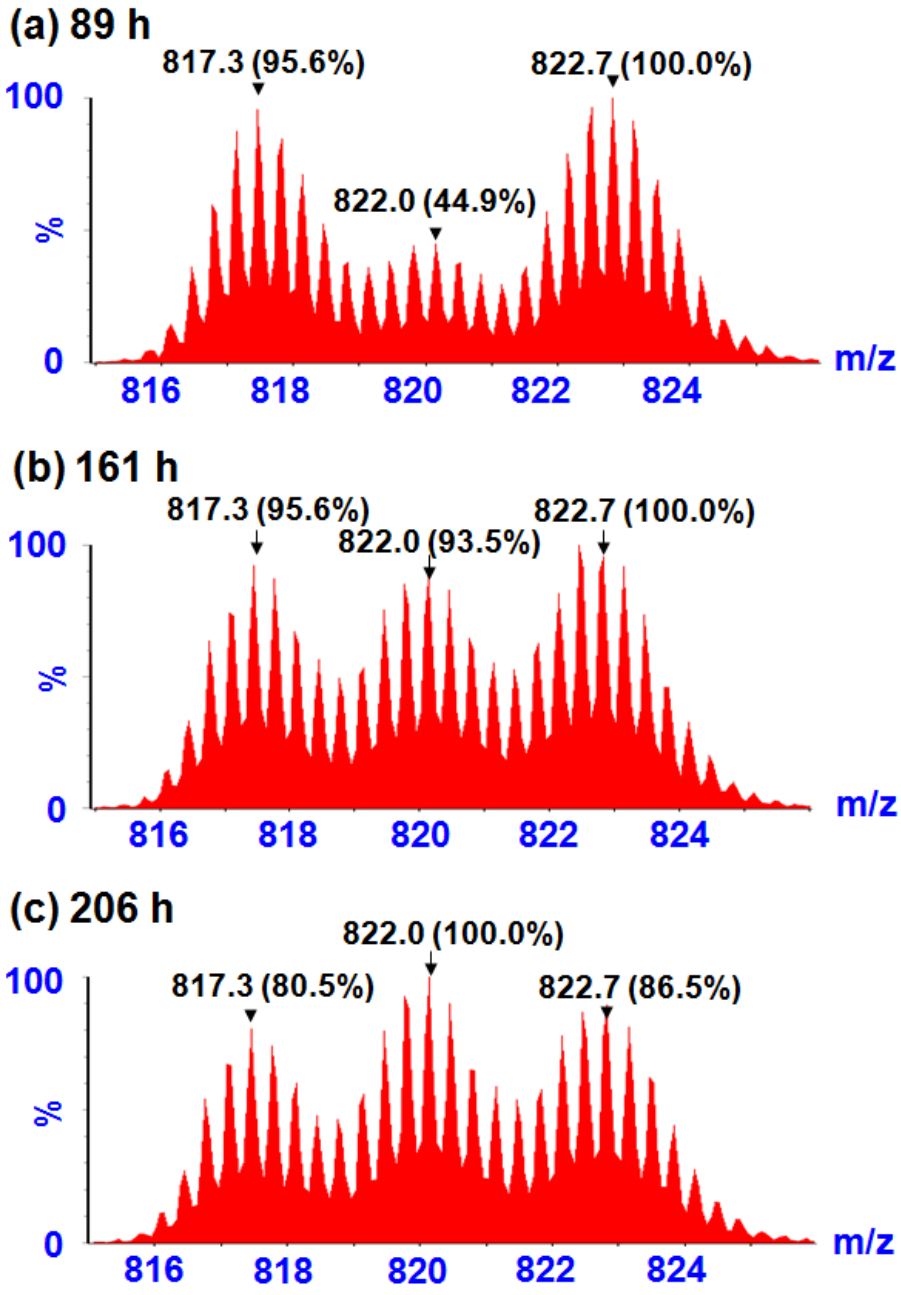

Figure A.6. ESI-MS spectra (Acetone-d_6/D_2O 1:1) for dynamic ligand exchange between **2.5a** and **2.5b** recorded at different time intervals: (a) 89 h, (b) 161 h, (c) 206 h,

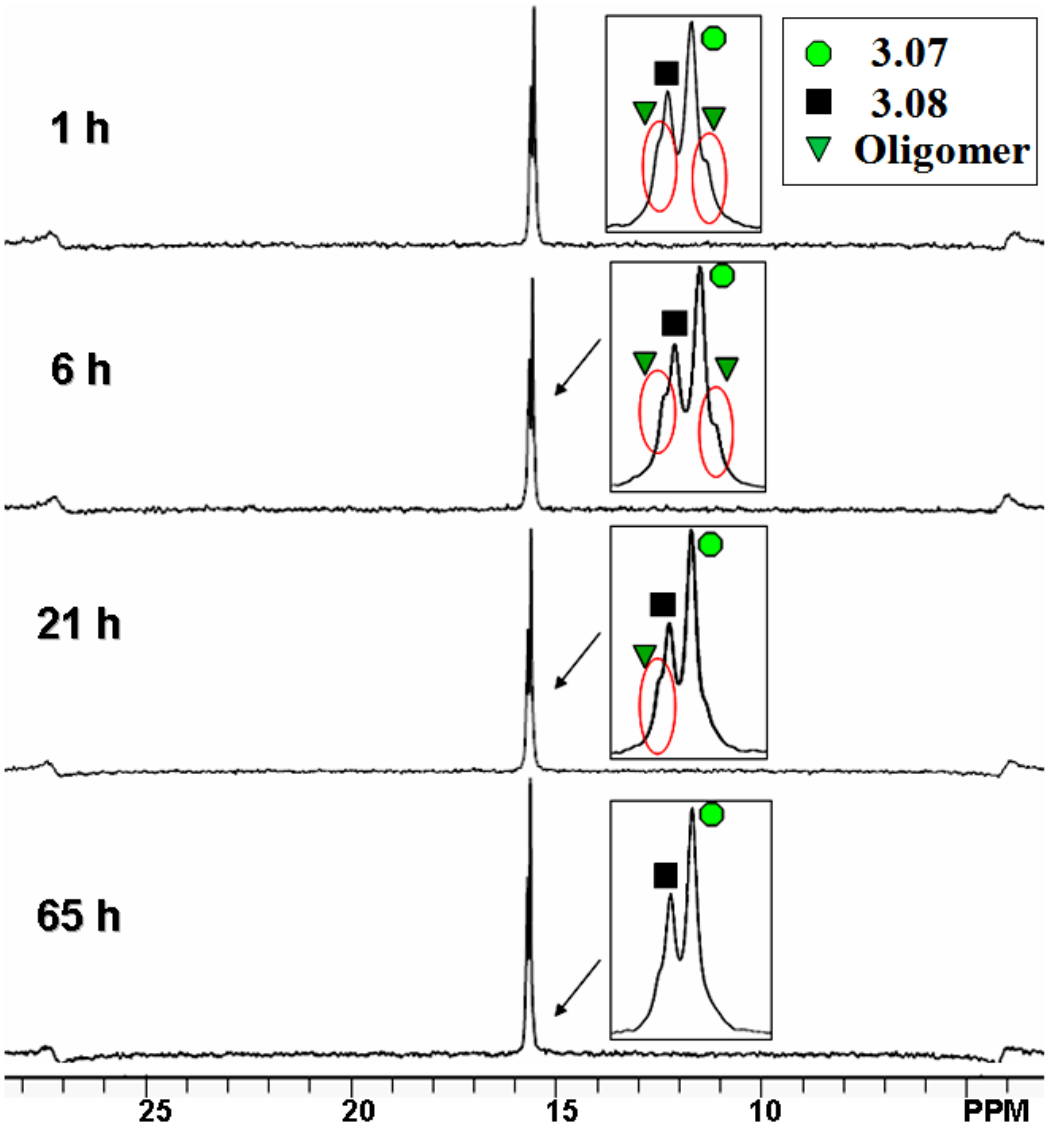

Figure A.7. $^{31}P\{^{1}H\}$ NMR spectra (Acetone-d_6/D_2O 1/1) of product mixture containing supramolecular triangles **3.07** and **3.08**.

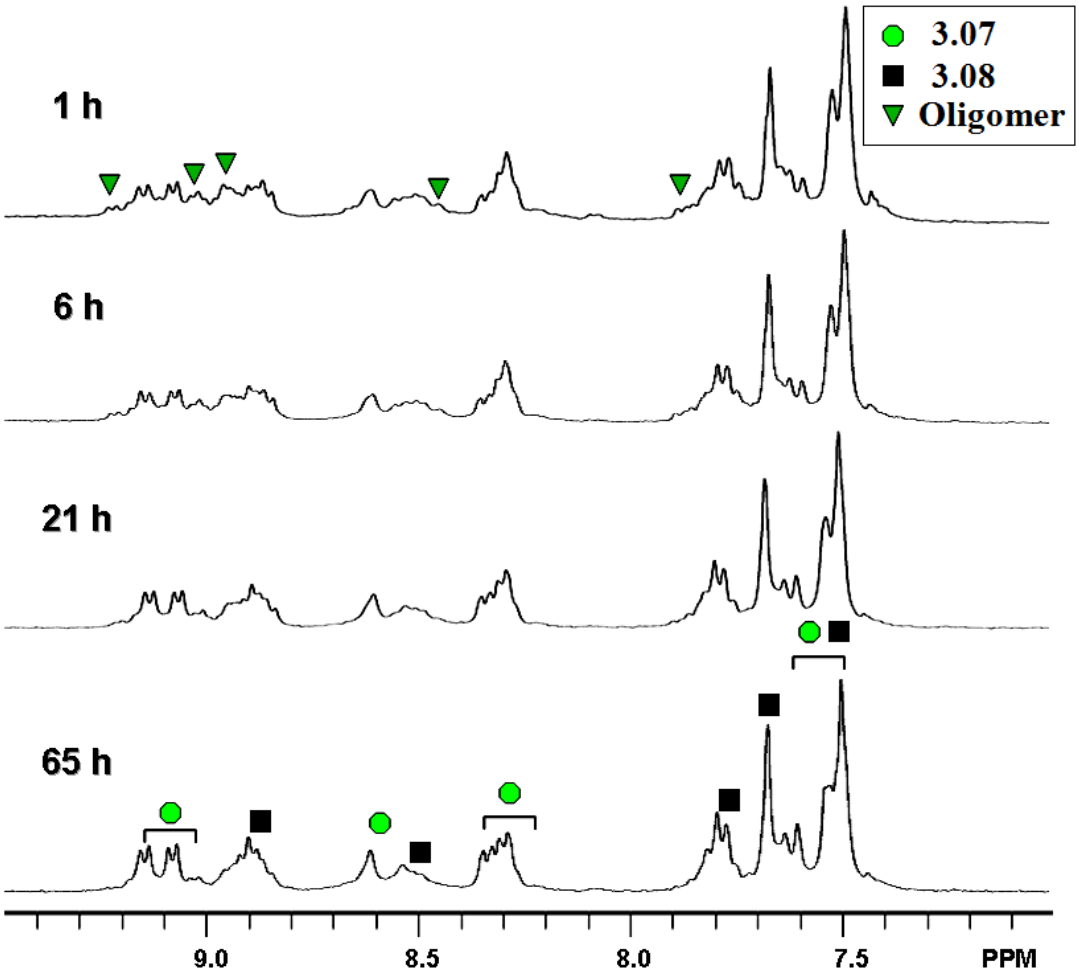

Figure A.8. ^{1}H NMR spectra (Acetone-d_6/D_2O 1/1) of product mixture containing supramolecular triangles **3.07** and **3.08**.

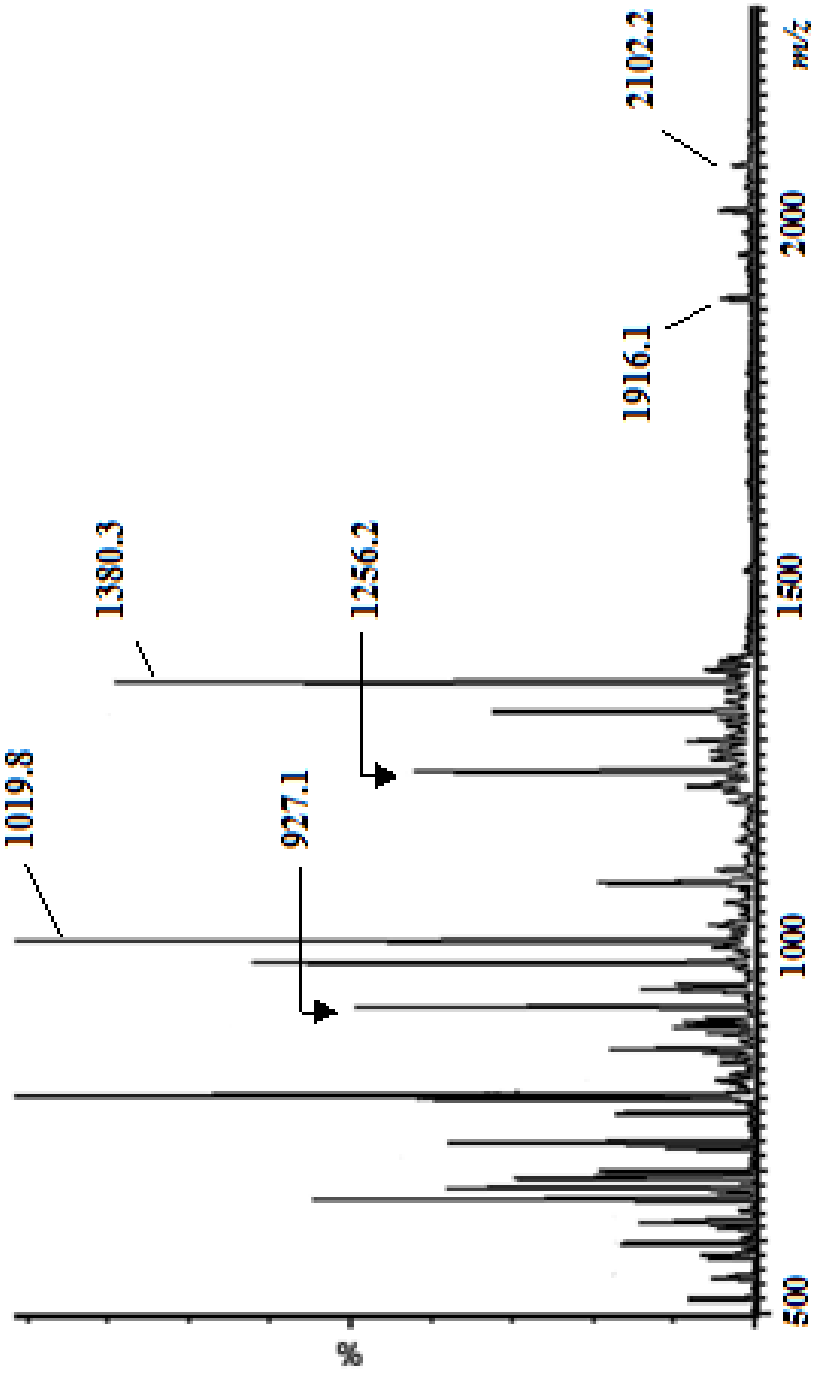

Figure A.9. Full ESI mass spectrum (Acetone-d_6/D_2O 1/1) of product mixture containing supramolecular triangles **3.07** (m/z: 1916.1, 1256.2, and 927.1) and **3.08** (m/z: 2102.2, 1380.3, and 1019.8).

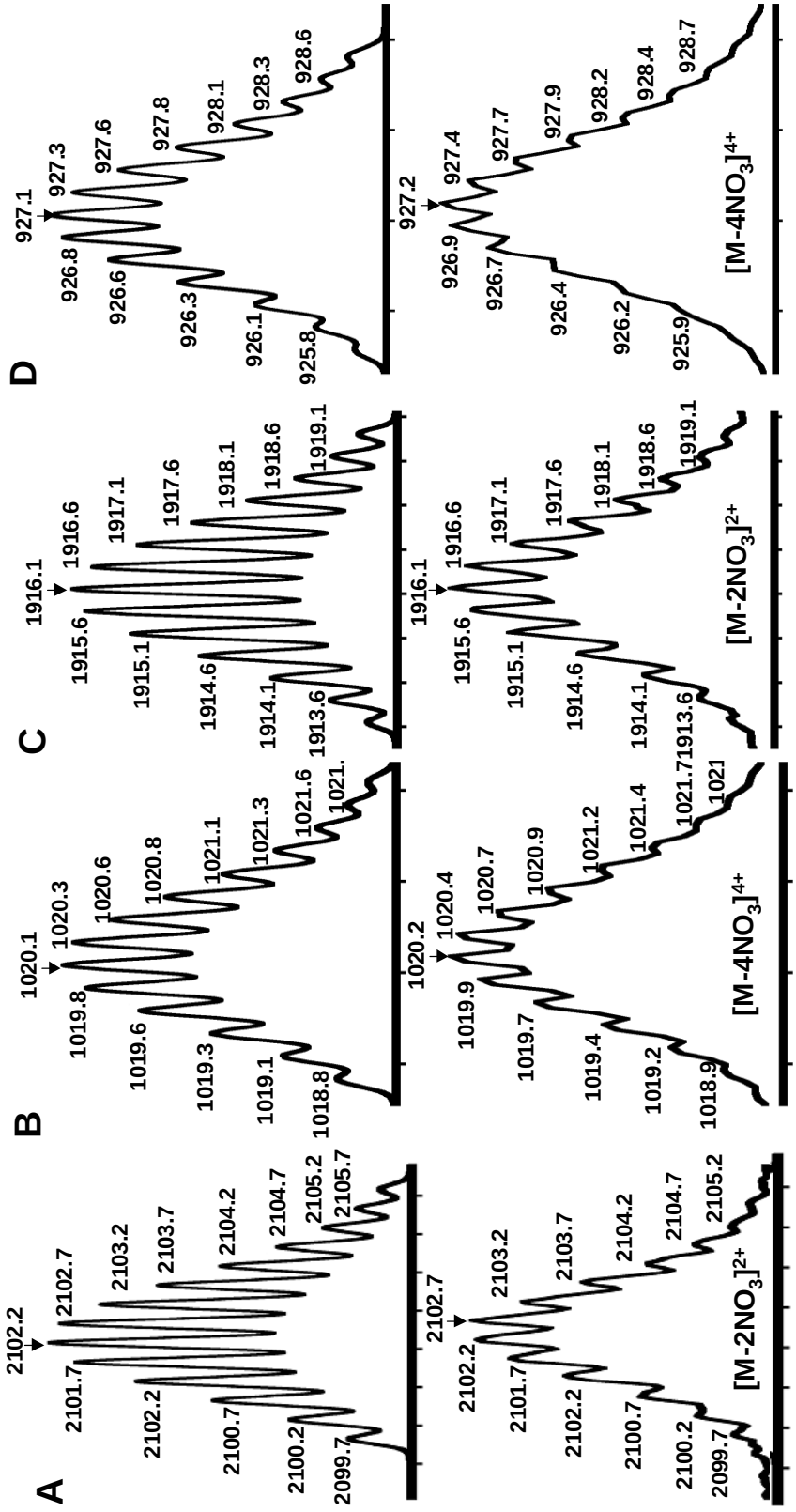

Figure A.9. Calculated (top) and experimental (bottom) ESI mass spectra (Acetone-d_6/D_2O 1/1) of product mixture containing supramolecular triangles **3.08** (A and B) and **3.07** (C and D).

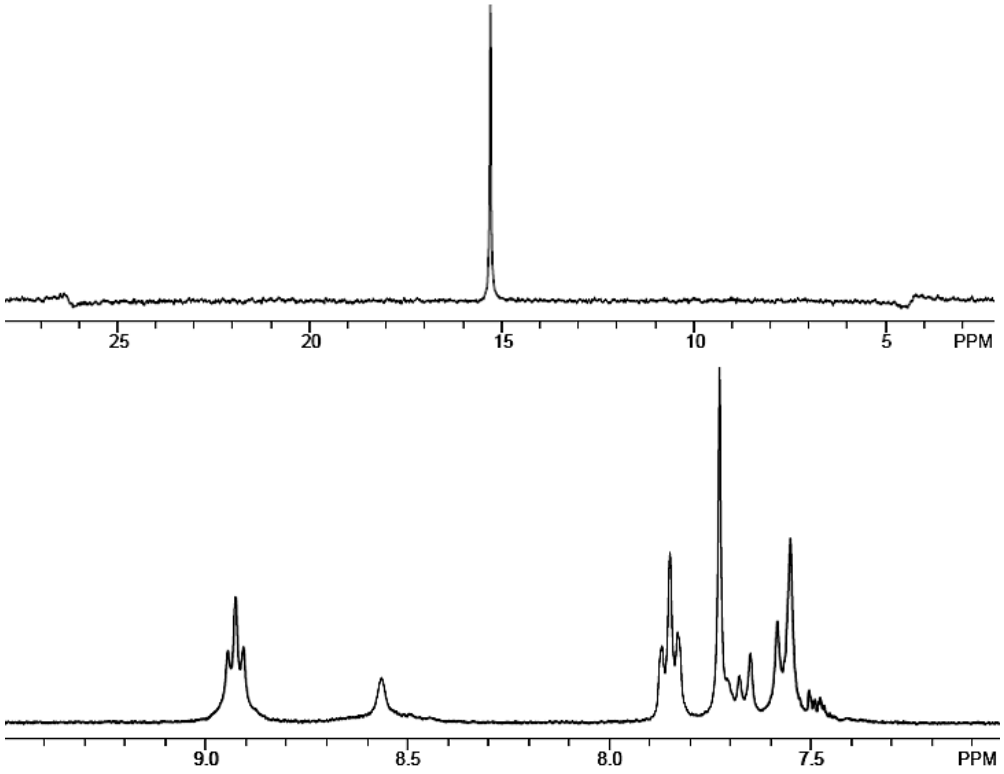

Figure A.11. $^{31}P\{^{1}H\}$ (top) and partial ^{1}H NMR (bottom) spectra (Acetone-d_6/D_2O 1/1) of the supramolecular triangle **3.08**.

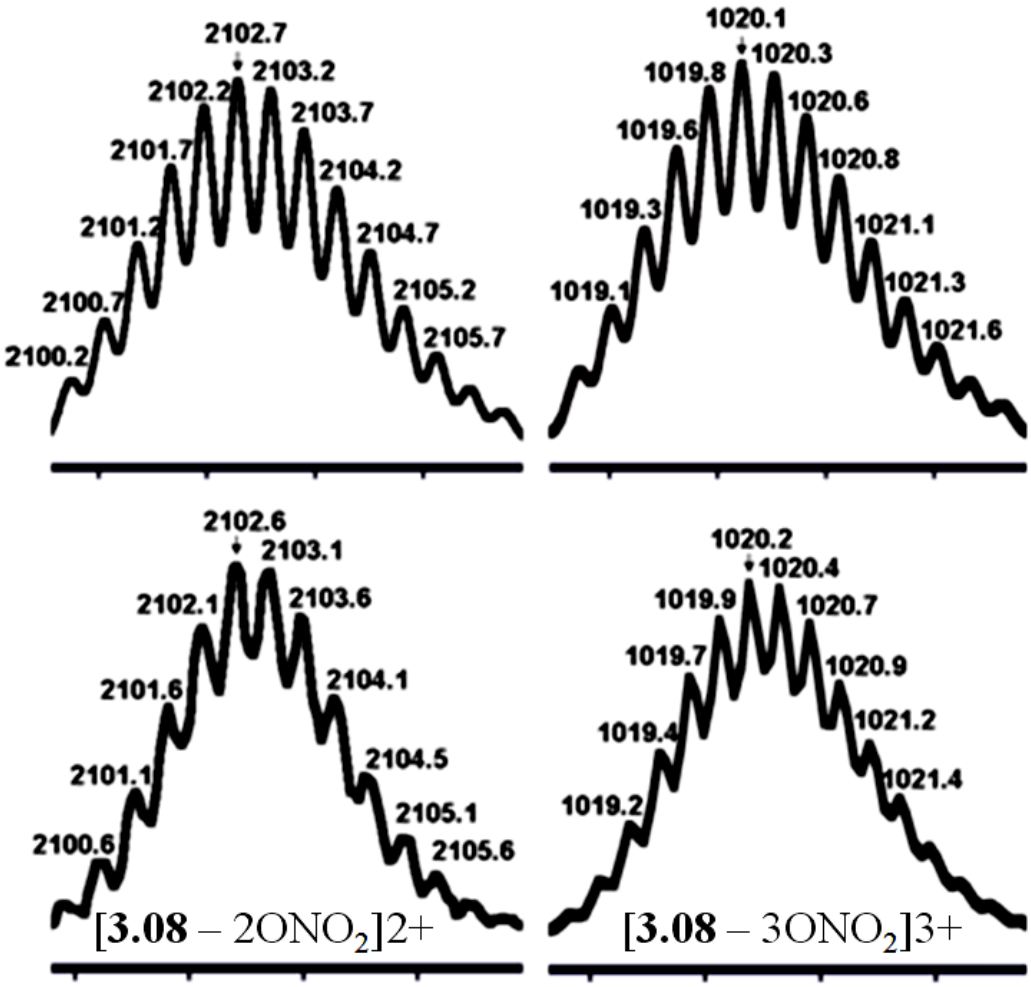

Figure A.12. Calculated (top) and experimental (bottom) ESI mass spectra (Acetone-d_6/D_2O 1/1) of the supramolecular triangle **3.08**.

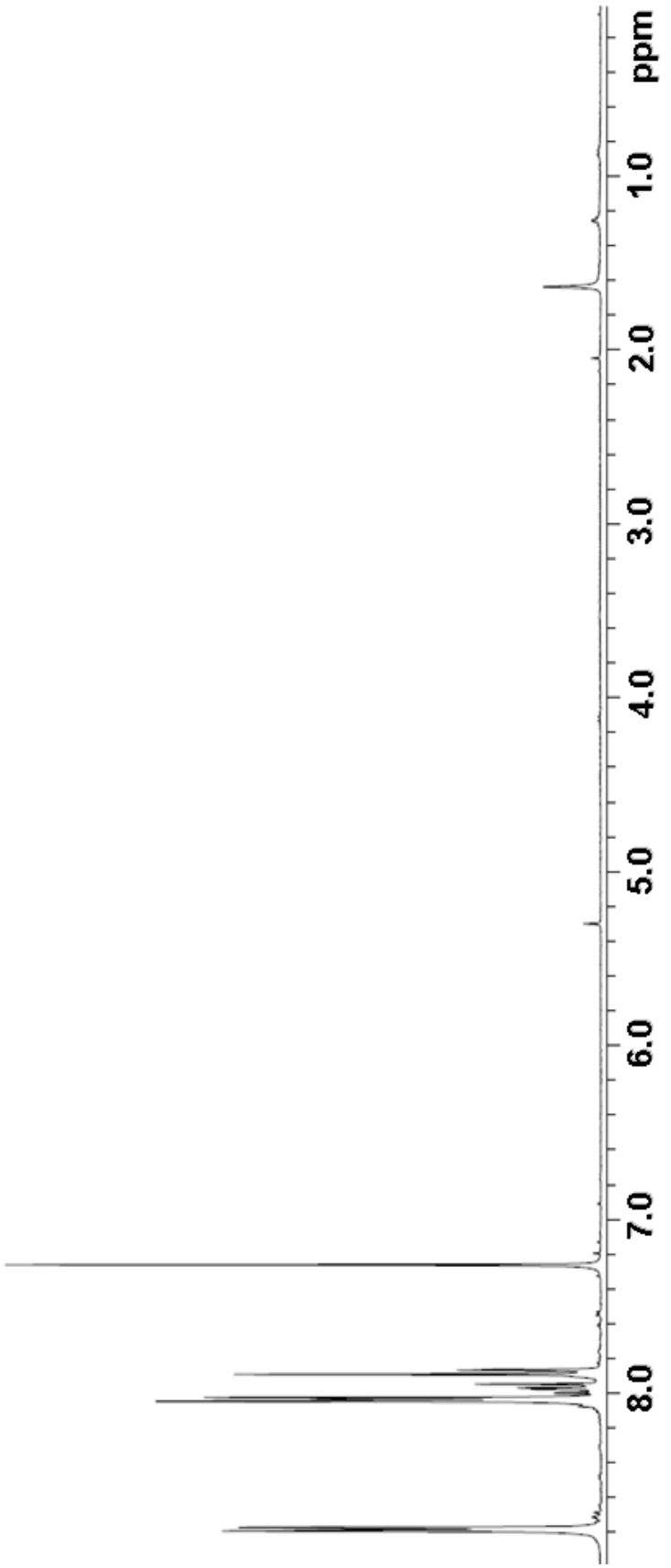

Figure A.13. ^{1}H NMR spectrum of **3.08** in $CDCl_3$.

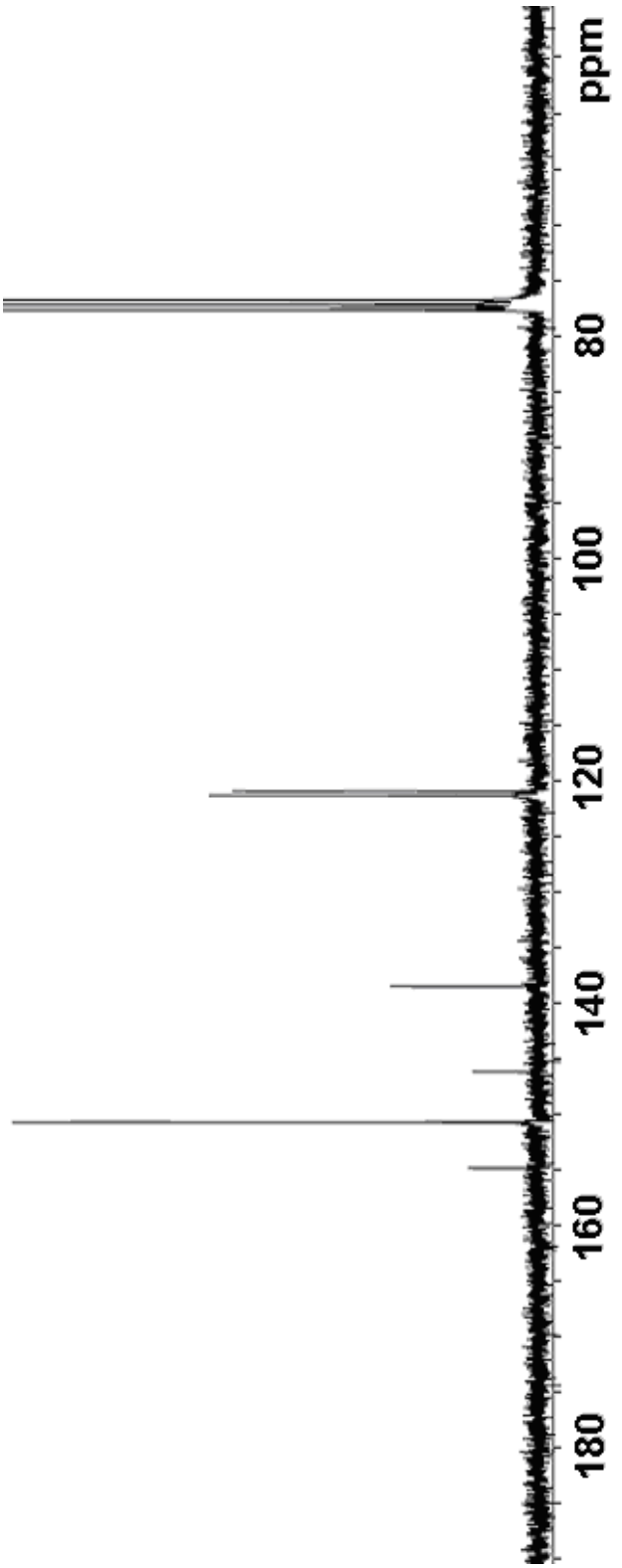

Figure A.14. ^{13}C NMR spectrum of **3.08** in $CDCl_3$..

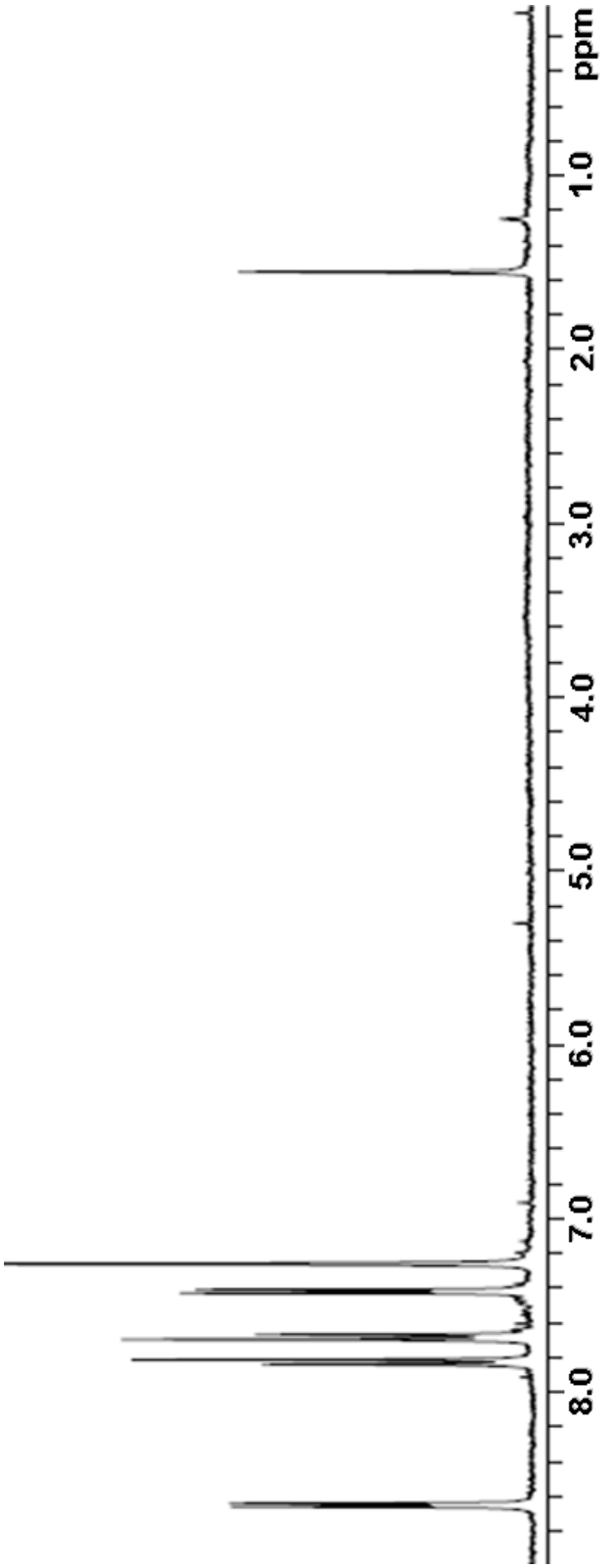

Figure A.15. ^{1}H NMR spectrum of **3.09** in $CDCl_3$.

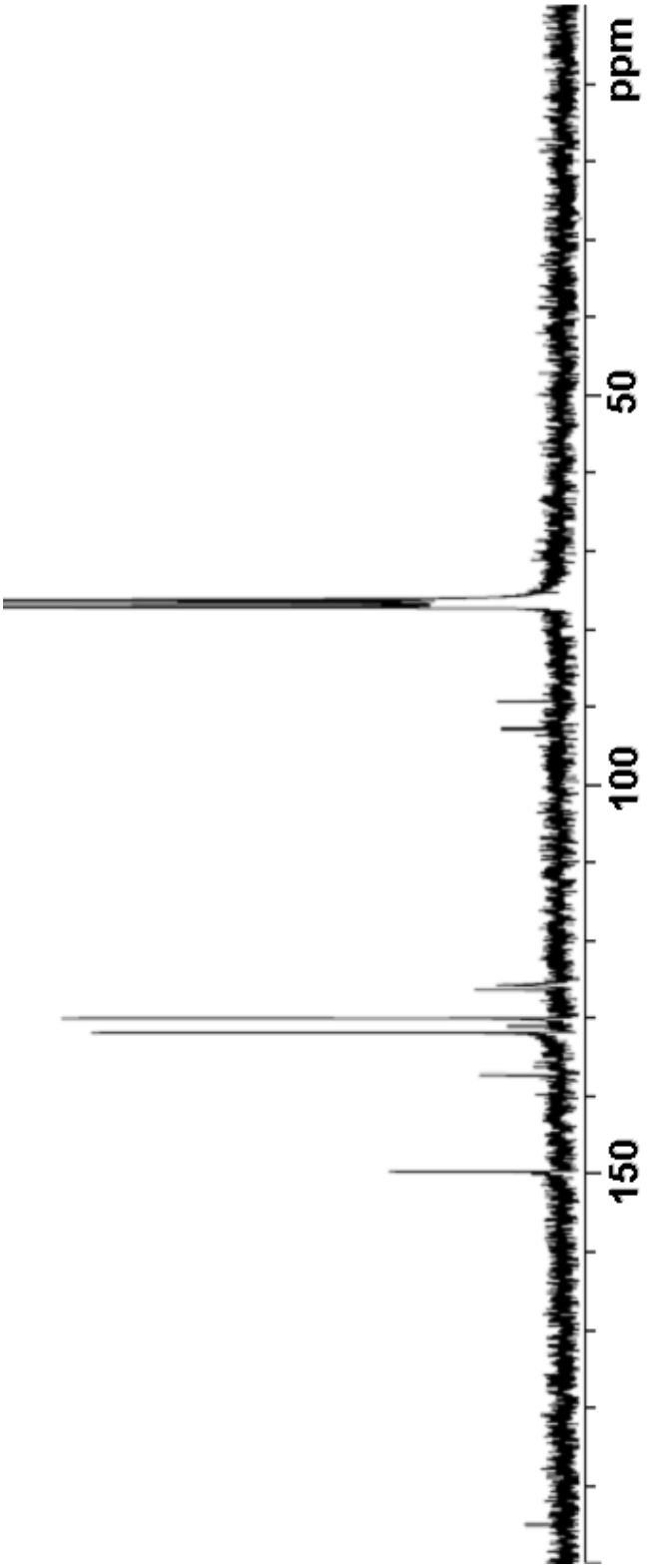

Figure A.16. ^{13}C NMR spectrum of **3.09** in $CDCl_3$..

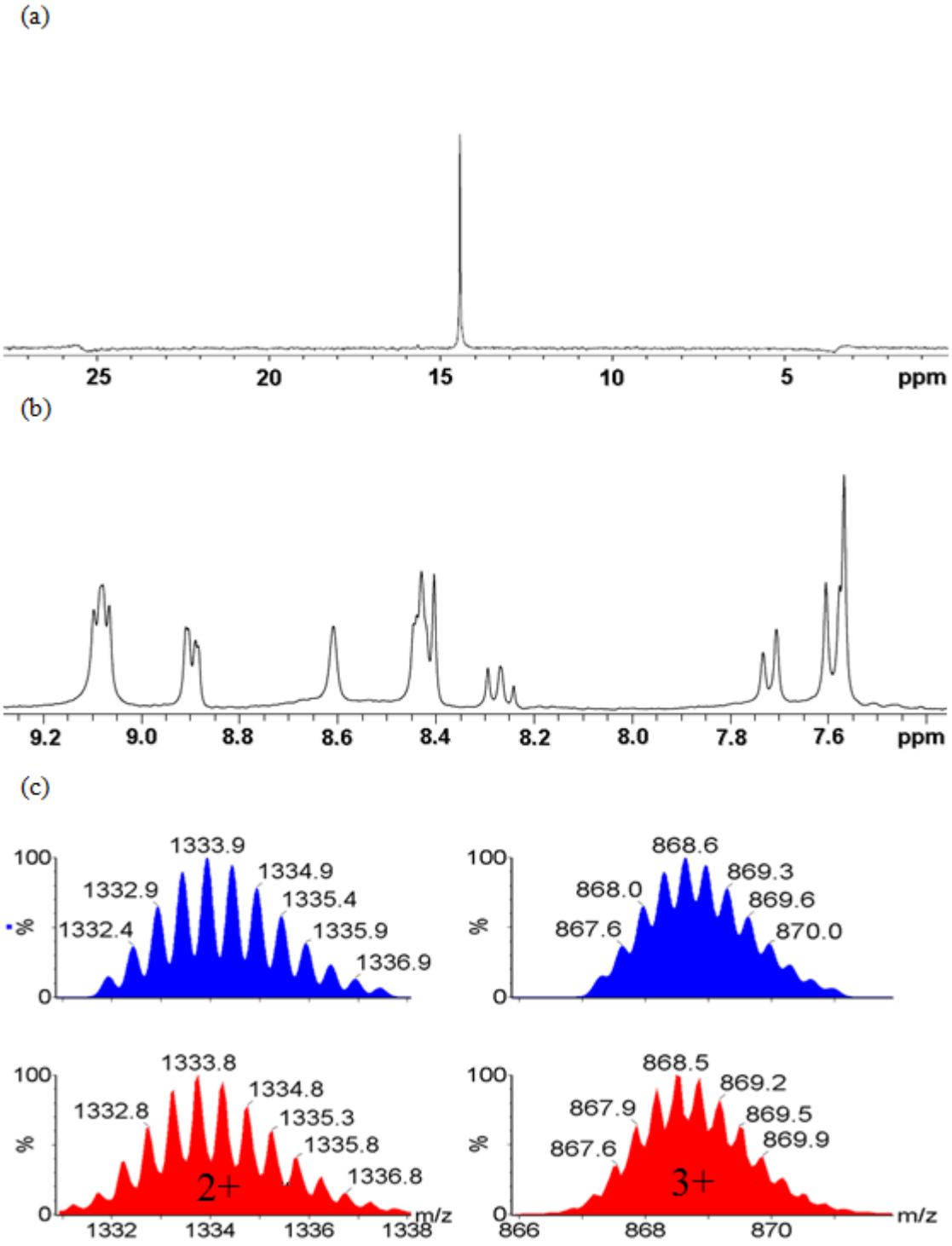

Figure A.17. (a) $^{31}P\{^{1}H\}$ and (b) Partial ^{1}H NMR spectra and (c) Calculated (top, blue) and experimental (bottom, red) ESI-MS of self-assembly **3.17** in Acetone-d_6/D_2O (v/v 1:1).

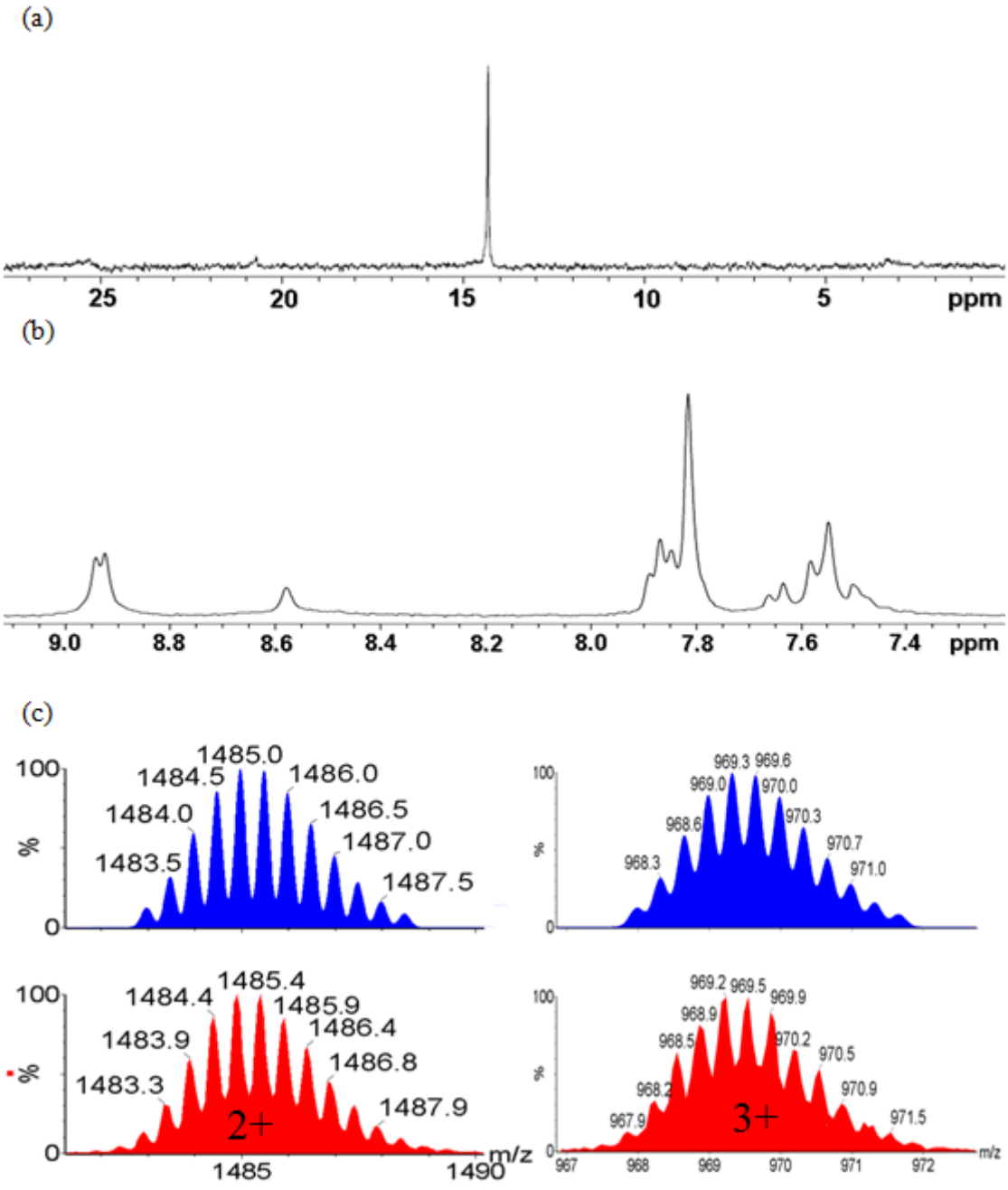

Figure A.18. (a) $^{31}P\{^{1}H\}$ and (b) Partial ^{1}H NMR spectra and (c) Calculated (top, blue) and experimental (bottom, red) ESI-MS of self-assembly **3.18** in Acetone-d_6/D_2O (v/v 1:1).

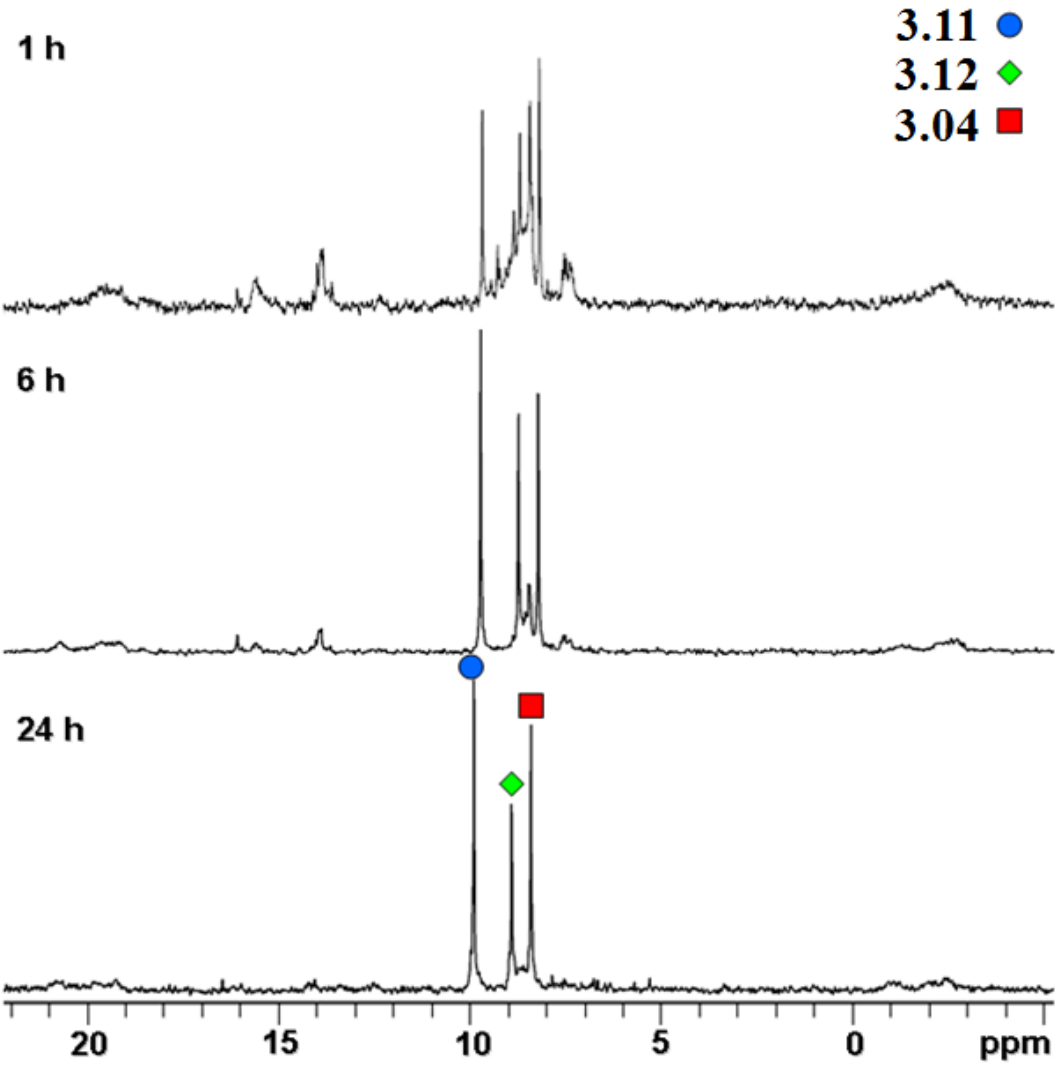

Figure A.19. $^{31}P\{^{1}H\}$ NMR trace spectra of self-sorting system **SS$_5$** in Acetone-d_6/D_2O (v/v 1:1) heating at 65—70 ℃.

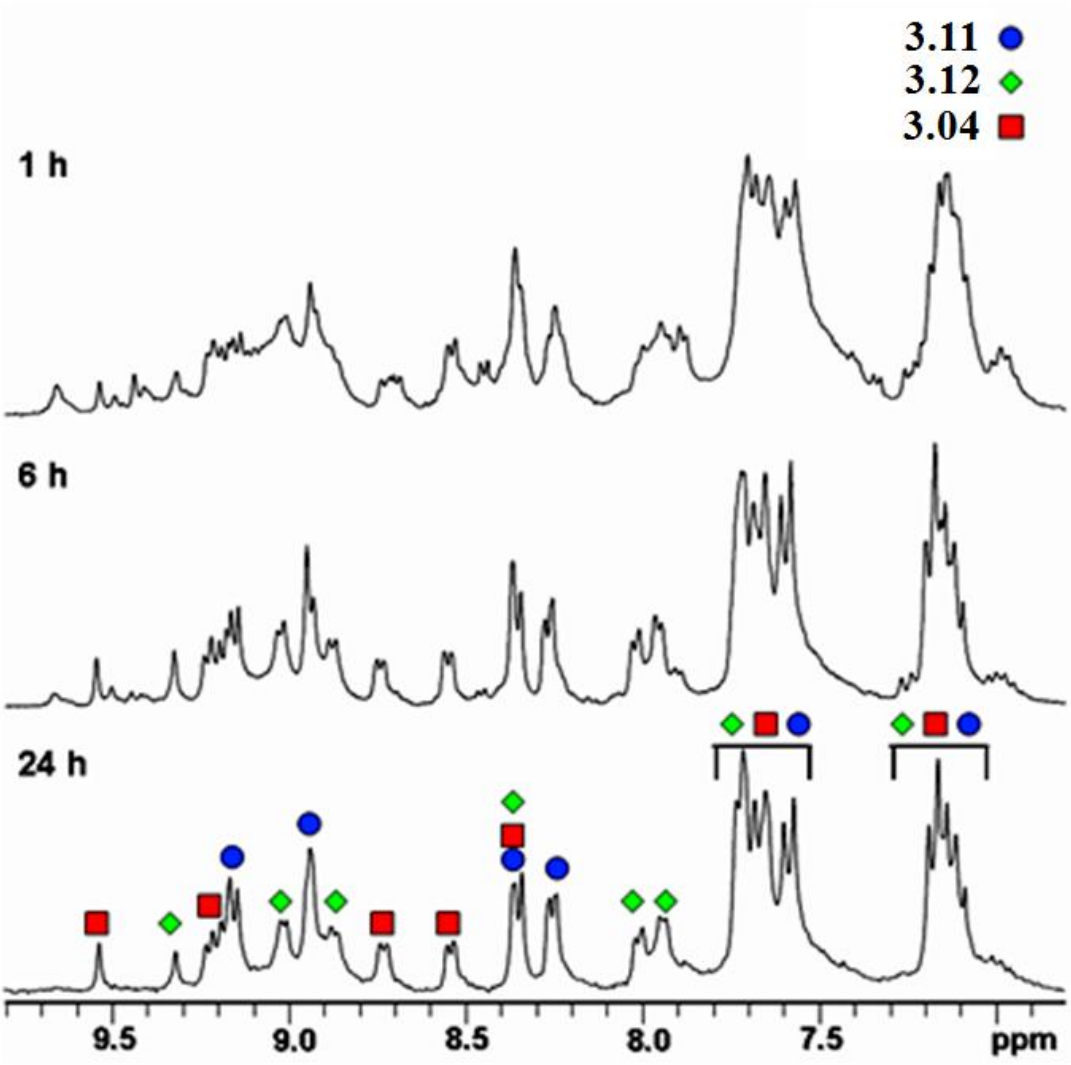

Figure A.20. ^{1}H NMR trace spectra of self-sorting system **SS$_5$** in Acetone-d_6/D_2O (v/v 1:1) heating at 65—70 ℃.

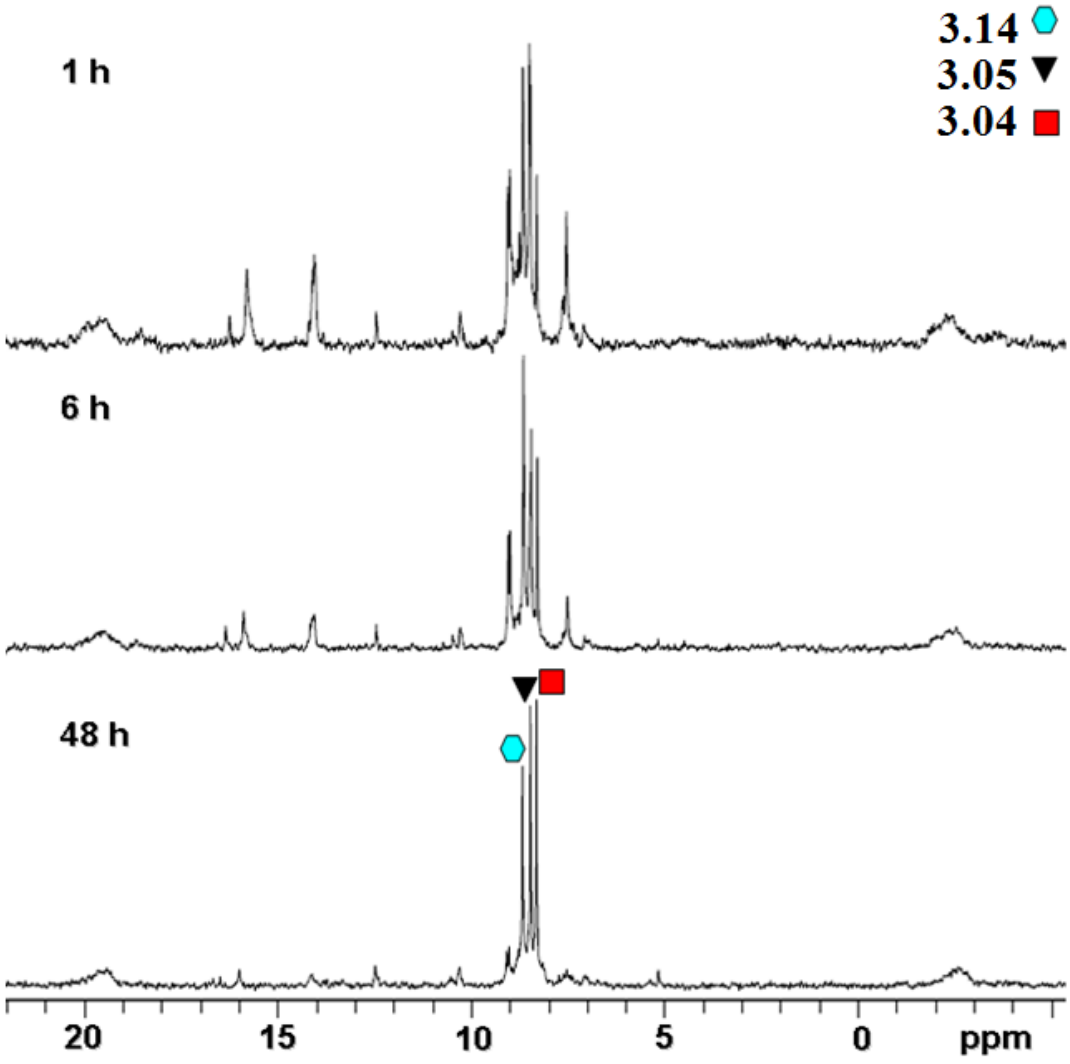

Figure A.21. $^{31}P\{^{1}H\}$ NMR trace spectra of self-sorting system **SS$_6$** in Acetone-d_6/D_2O (v/v 1:1) heating at 65—70 ℃.

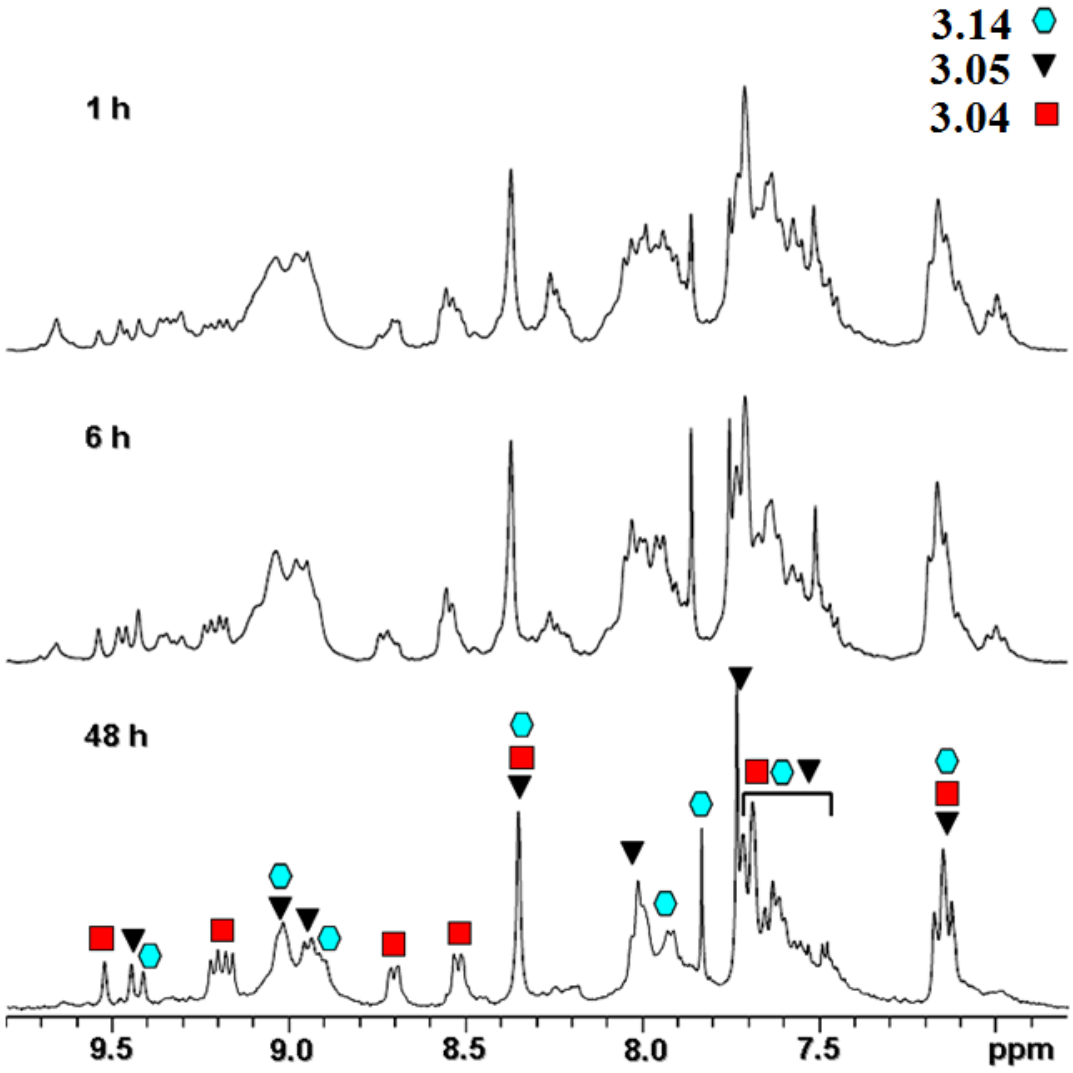

Figure A.22. ^{1}H NMR trace spectra of self-sorting system **SS$_6$** in Acetone-d_6/D_2O (v/v 1:1) heating at 65—70 ℃.

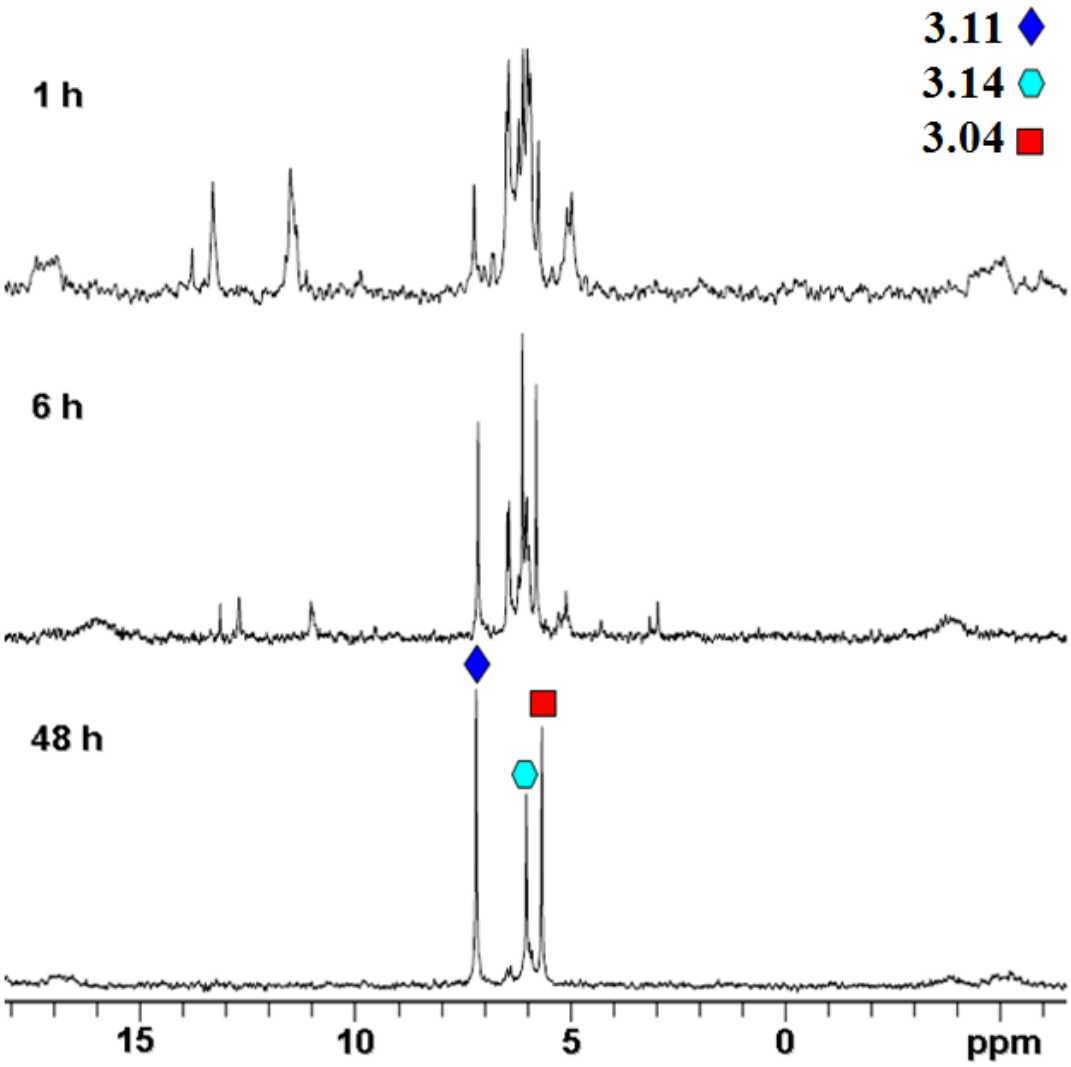

Figure A.23. $^{31}P\{^{1}H\}$ NMR trace spectra of self-sorting system **SS$_7$** in Acetone-d_6/D_2O (v/v 1:1) heating at 65—70 ℃.

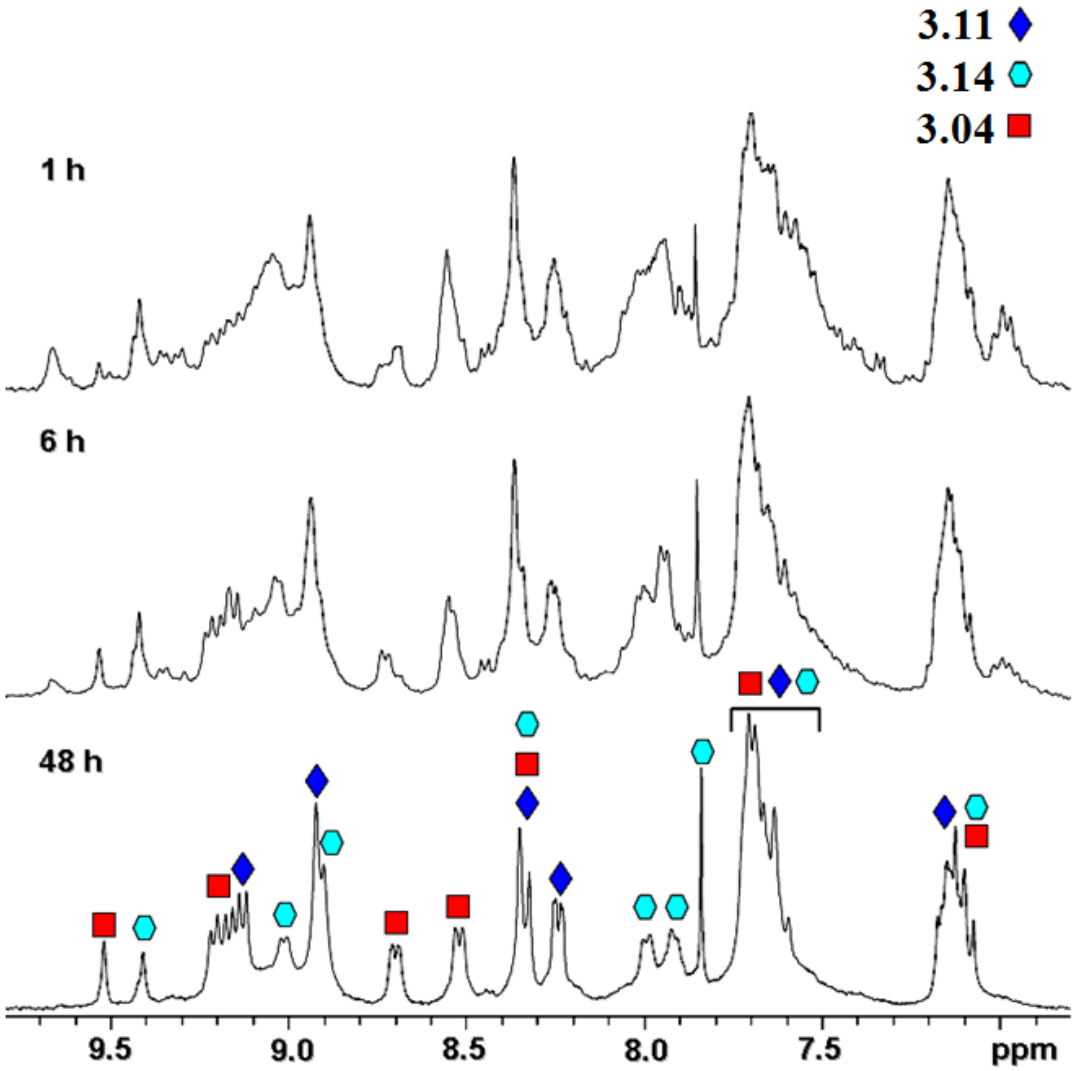

Figure A.24. ^{1}H NMR trace spectra of self-sorting system **SS$_7$** in Acetone-d_6/D_2O (v/v 1:1) heating at 65—70 ℃.

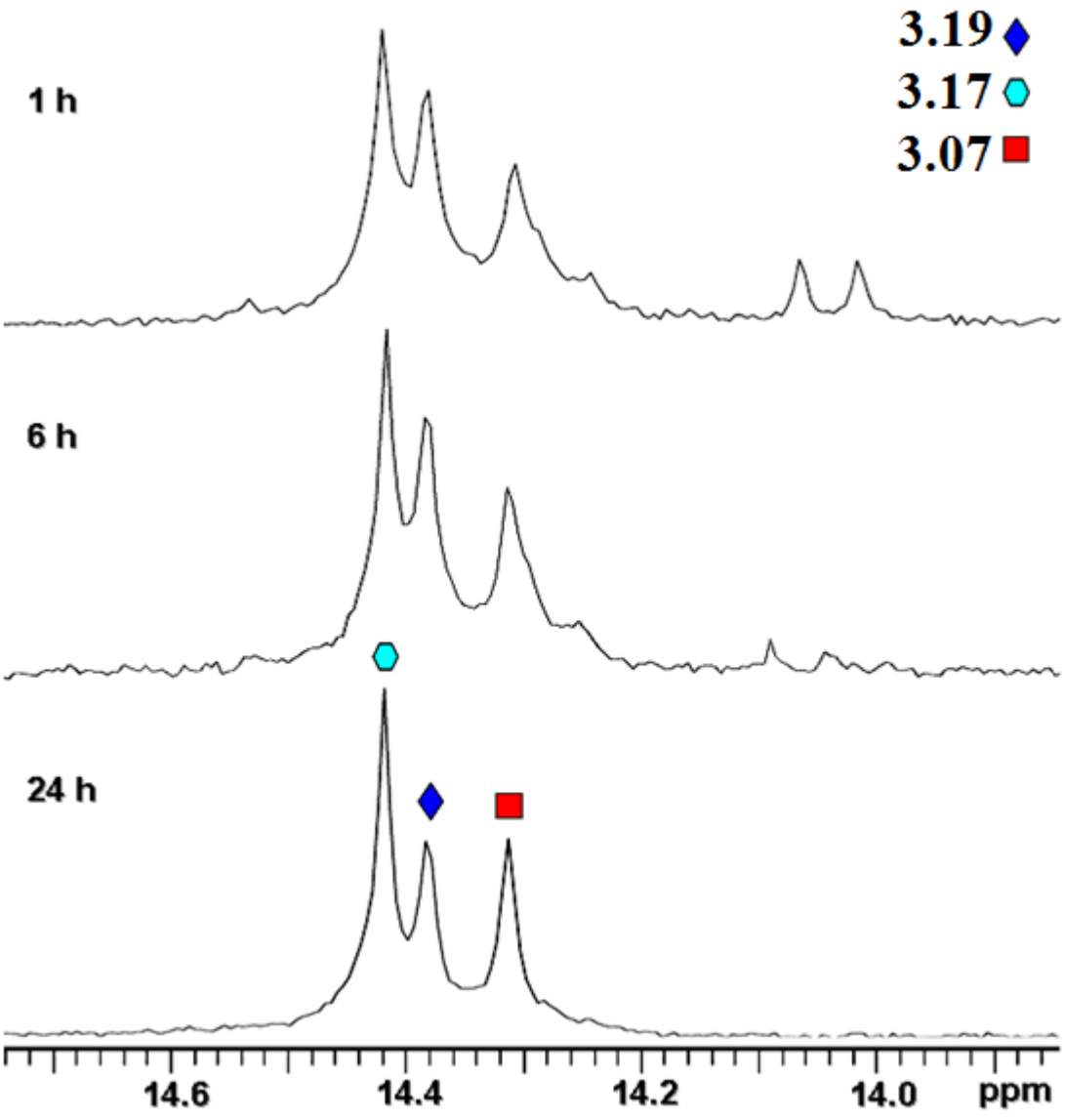

Figure A.25. $^{31}P\{^{1}H\}$ NMR trace spectra of self-sorting system **SS_8** in Acetone-d_6/D_2O (v/v 1:1) heating at 65—70 ℃.

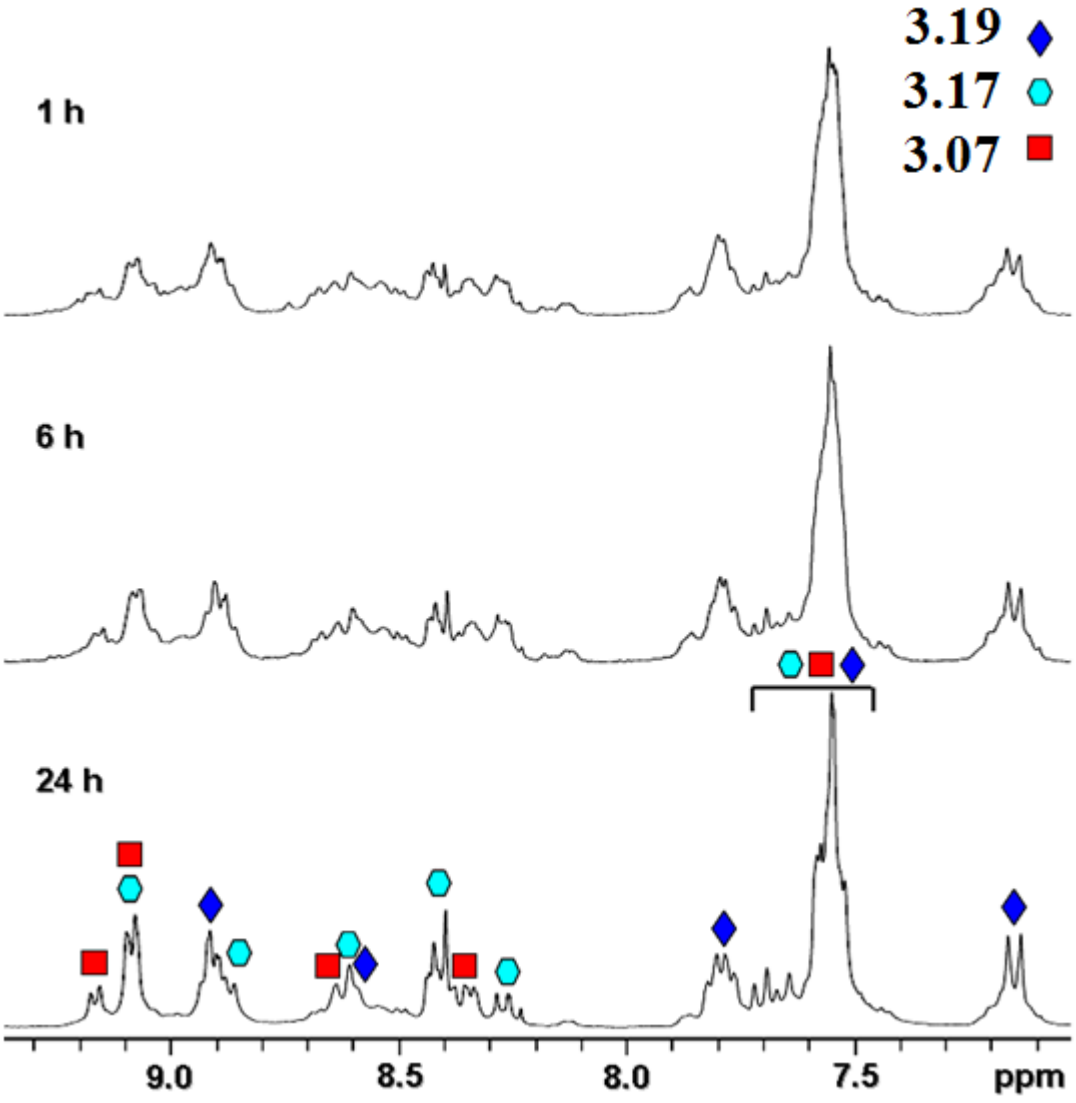

Figure A.26. ^{1}H NMR trace spectra of self-sorting system **SS$_8$** in Acetone-d_6/D_2O (v/v 1:1) heating at 65—70 ℃.

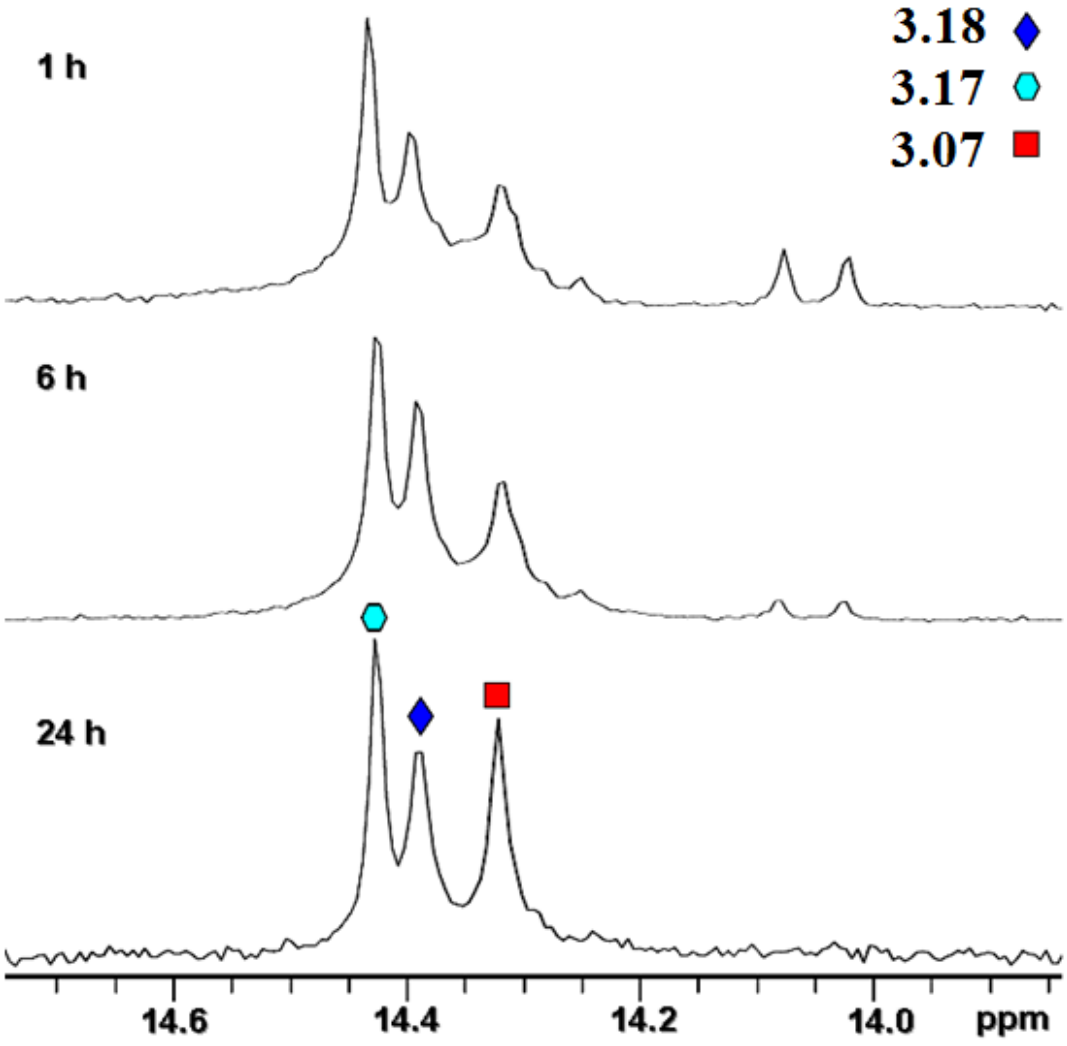

Figure A.27. $^{31}P\{^{1}H\}$ NMR trace spectra of self-sorting system **SS$_9$** in Acetone-d_6/D_2O (v/v 1:1) heating at 65—70 ℃.

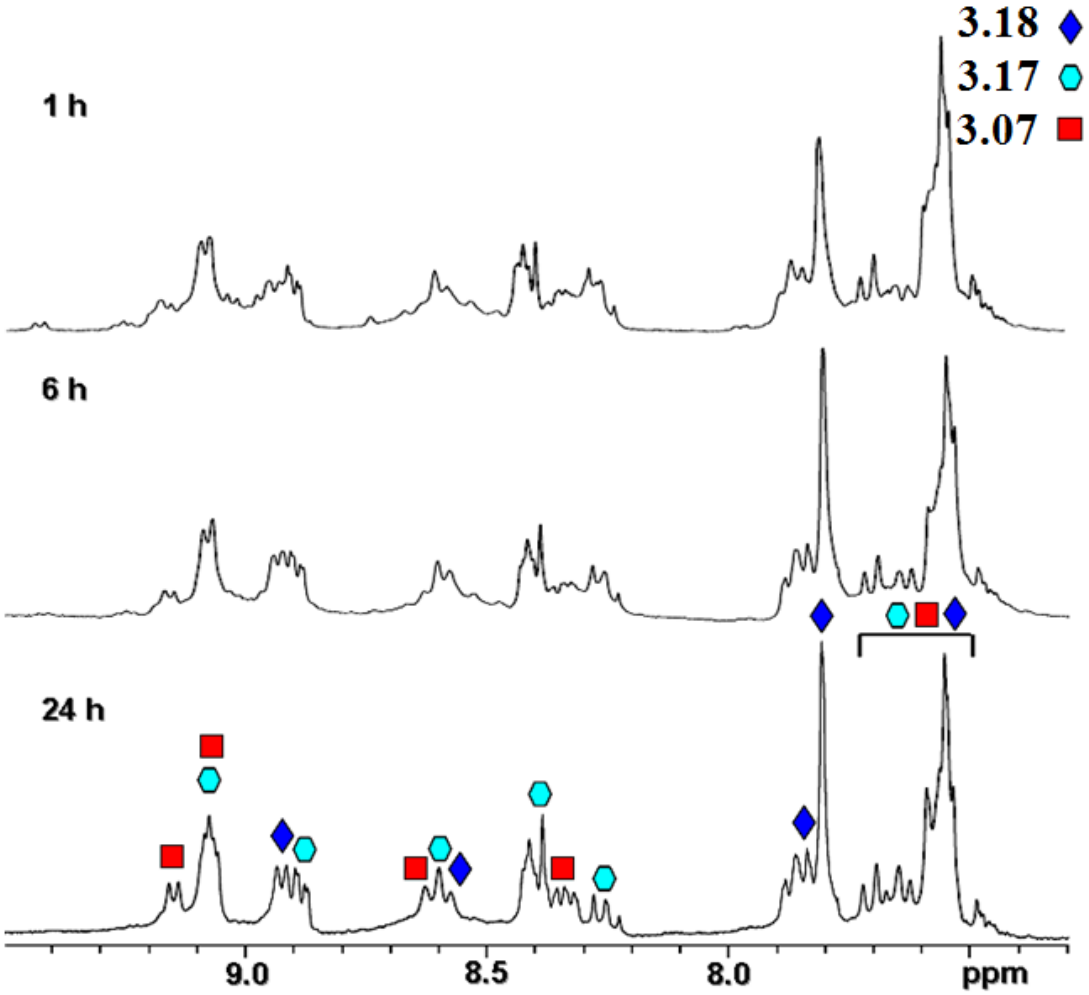

Figure A.28. ^{1}H NMR trace spectra of self-sorting system **SS$_9$** in Acetone-d_6/D_2O (v/v 1:1) heating at 65—70 ℃.

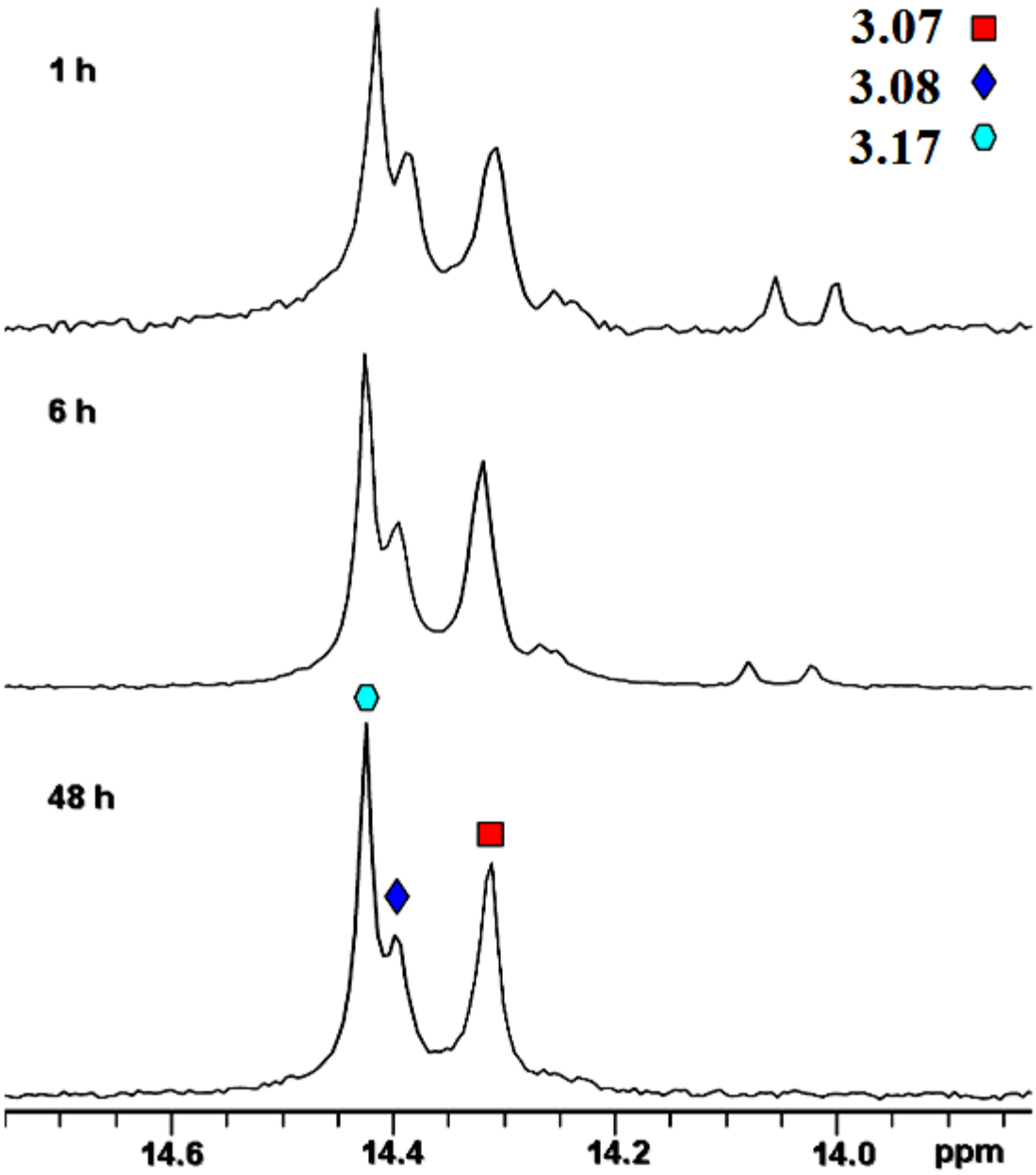

Figure A.29. $^{31}P\{^{1}H\}$ NMR trace spectra of self-sorting system **SS$_{10}$** in Acetone-d_6/D_2O (v/v 1:1) heating at 65—70 ℃.

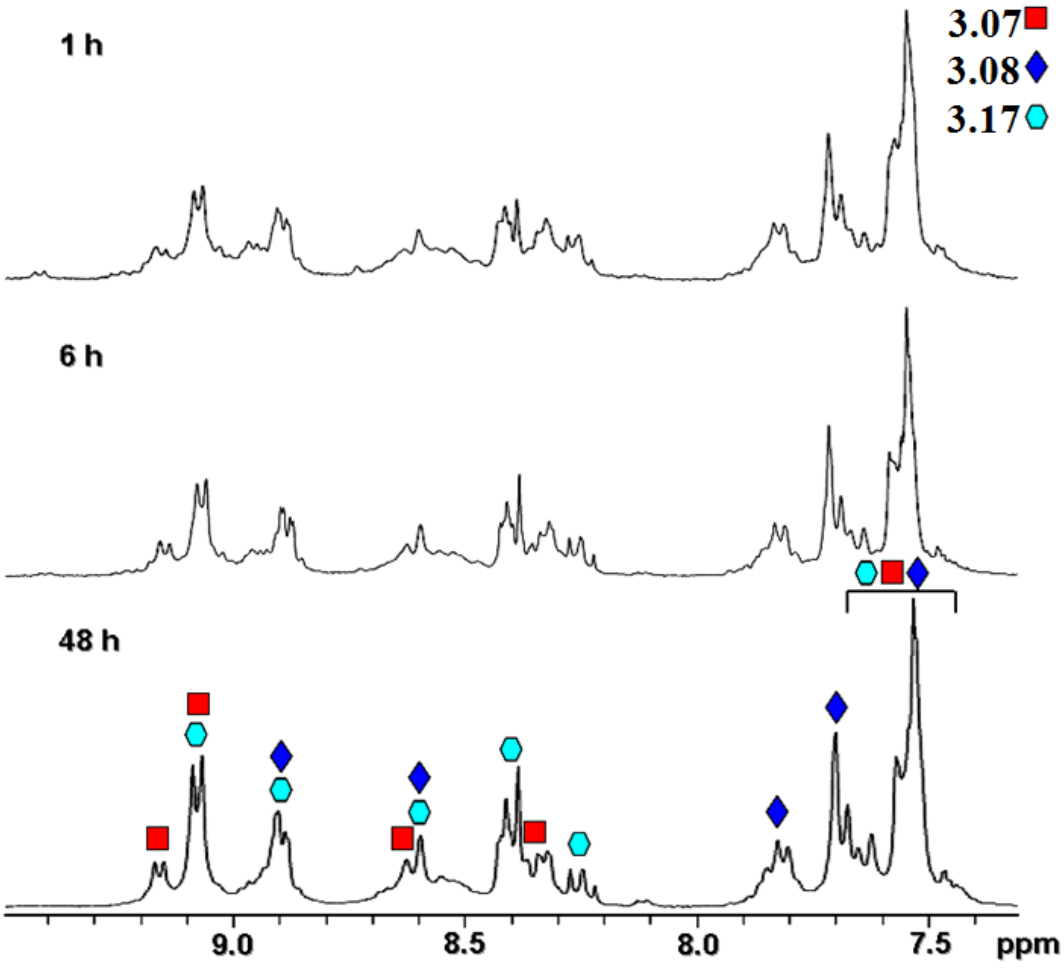

Figure A.30. ^{1}H NMR trace spectra of self-sorting system **SS$_{10}$** in Acetone-d_6/D_2O (v/v 1:1) heating at 65—70 ℃.

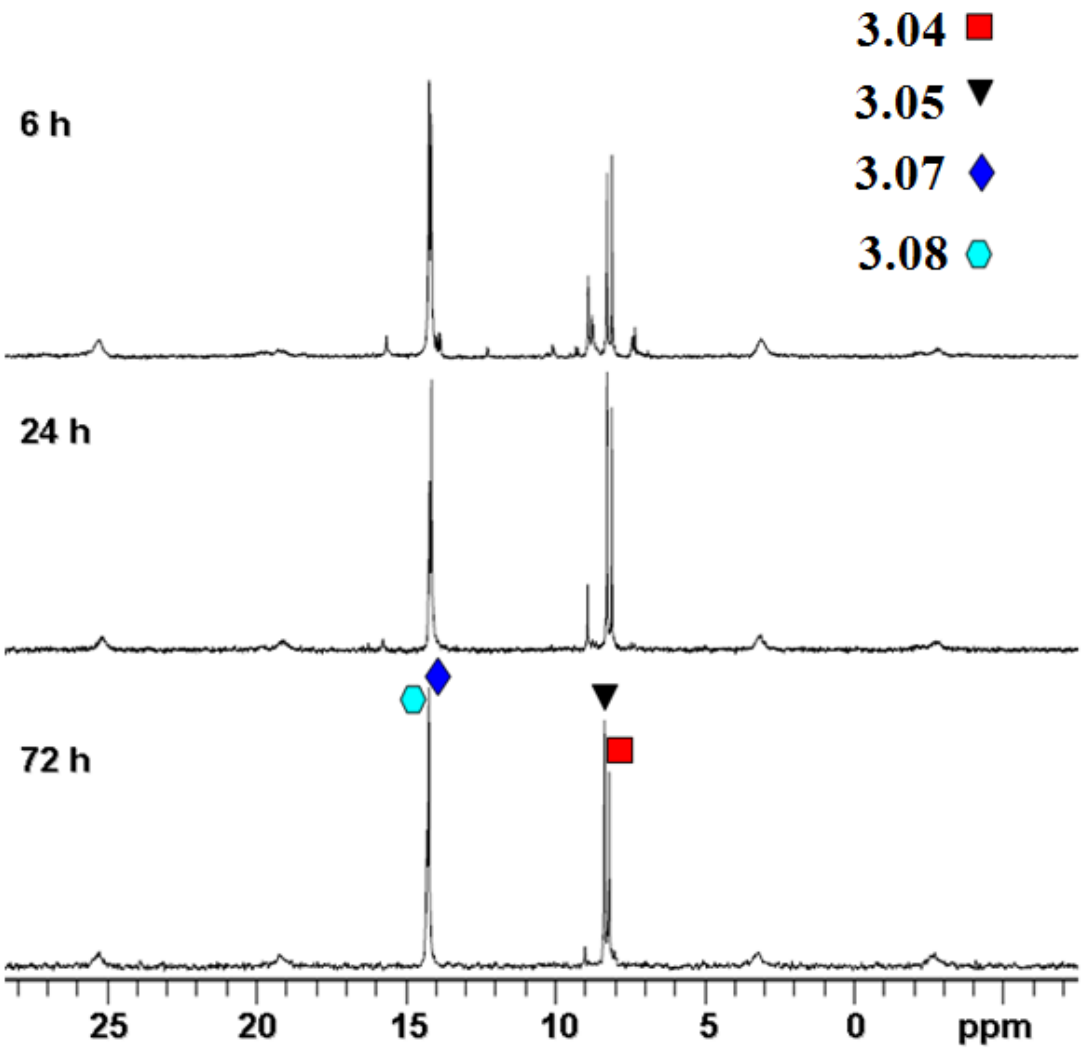

Figure A.31. $^{31}P\{^{1}H\}$ NMR trace spectra of self-sorting system **SS$_{11}$** in Acetone-d_6/D_2O (v/v 1:1) heating at 65—70 ℃.

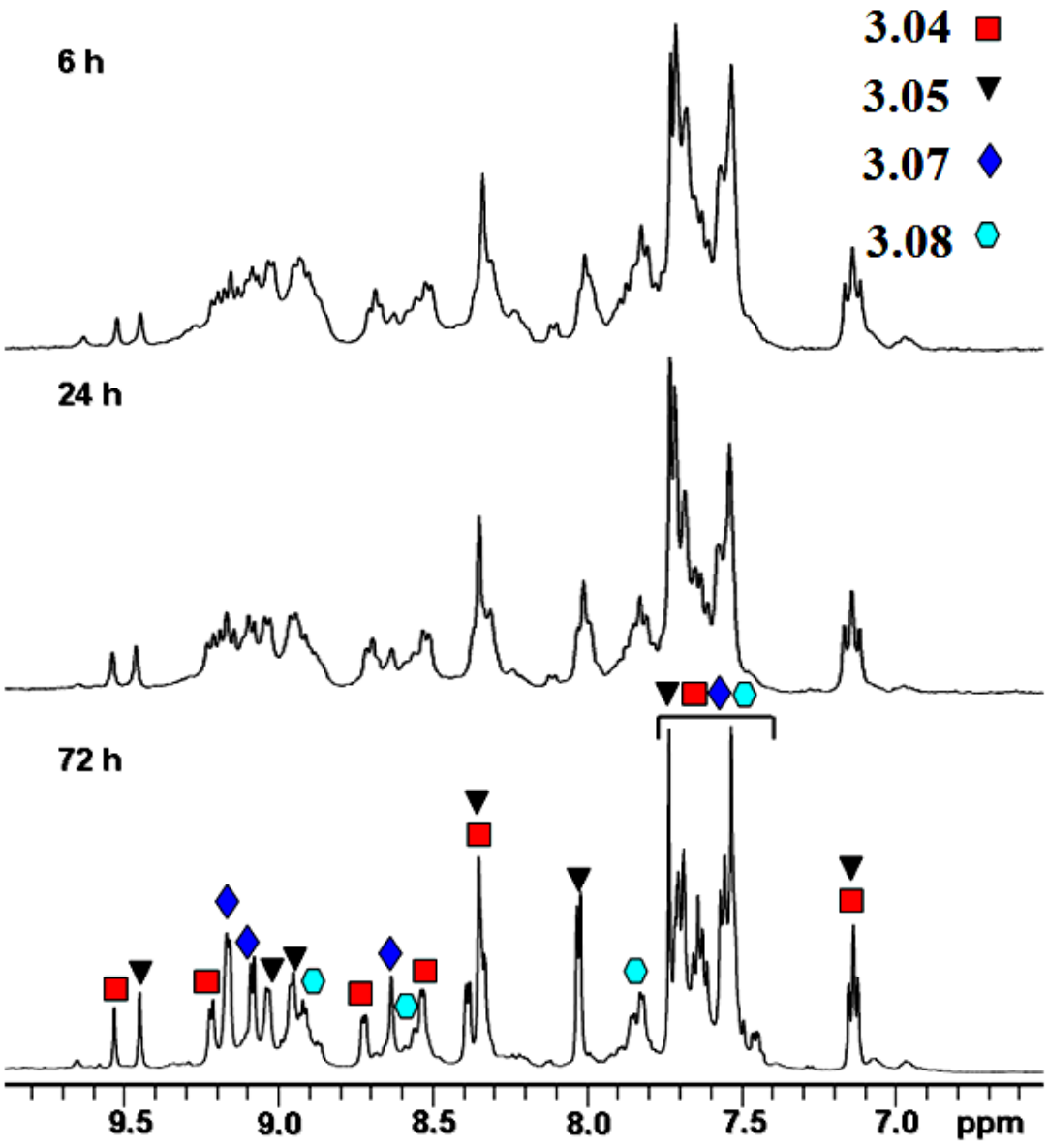

Figure A.32. ^{1}H NMR trace spectra of self-sorting system **SS$_{11}$** in Acetone-d_6/D_2O (v/v 1:1) heating at 65—70 ℃.

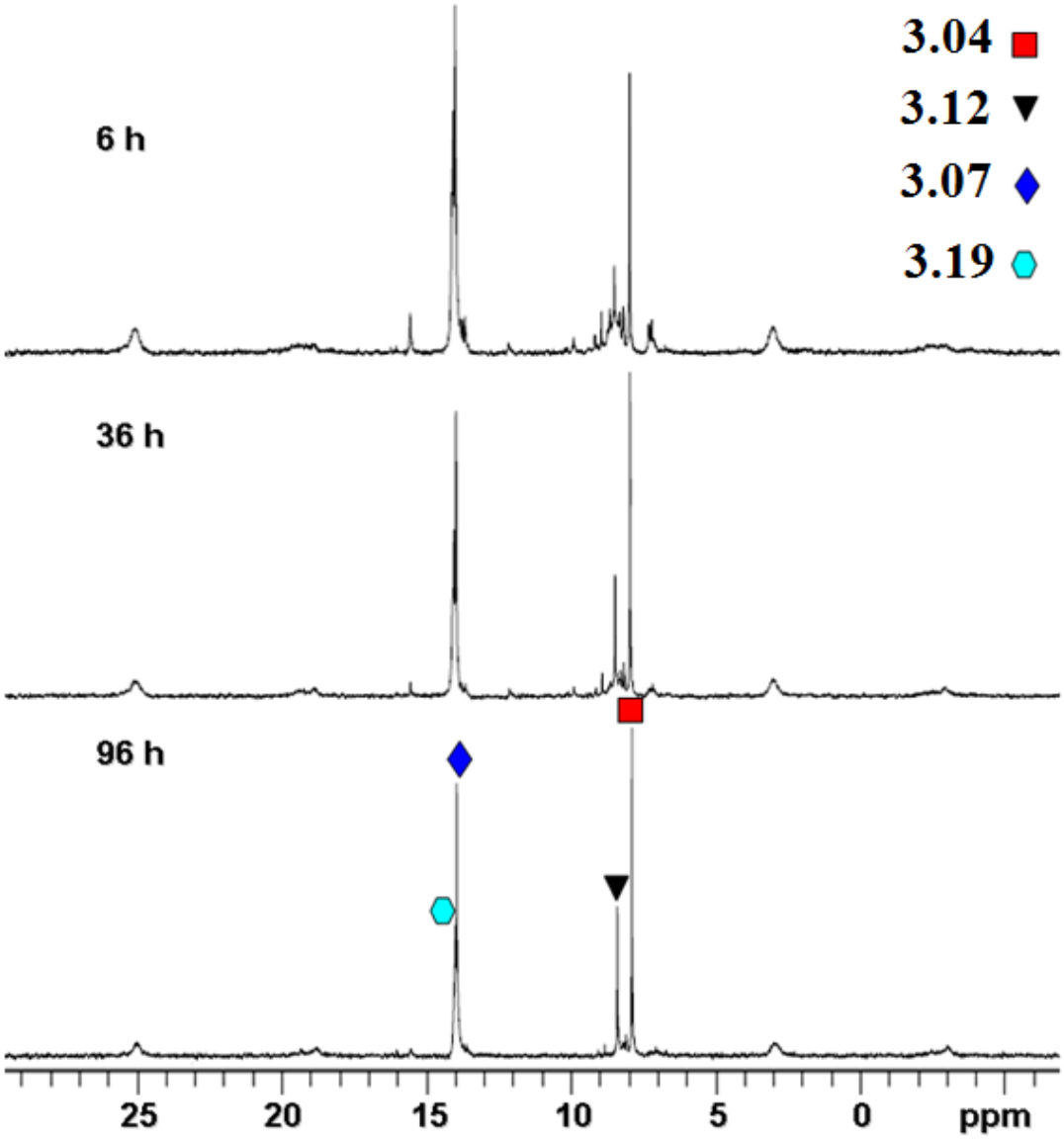

Figure A.33. $^{31}P\{^{1}H\}$ NMR trace spectra of self-sorting system **SS$_{12}$** in Acetone-d_6/D_2O (v/v 1:1) heating at 65—70 ℃.

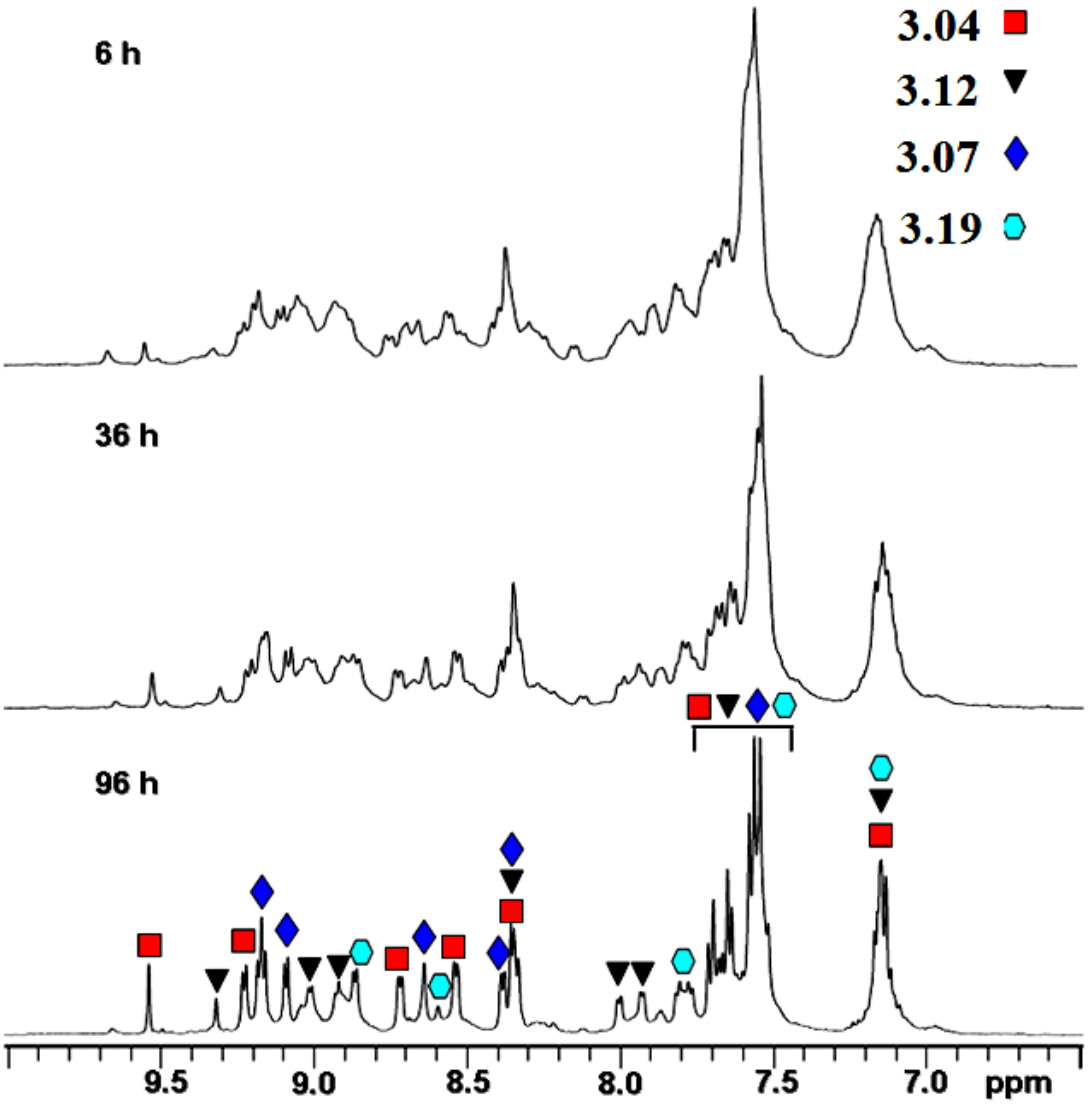

Figure A.34. ^{1}H NMR trace spectra of self-sorting system **SS$_{12}$** in Acetone-d_6/D_2O (v/v 1:1) heating at 65—70 ℃.

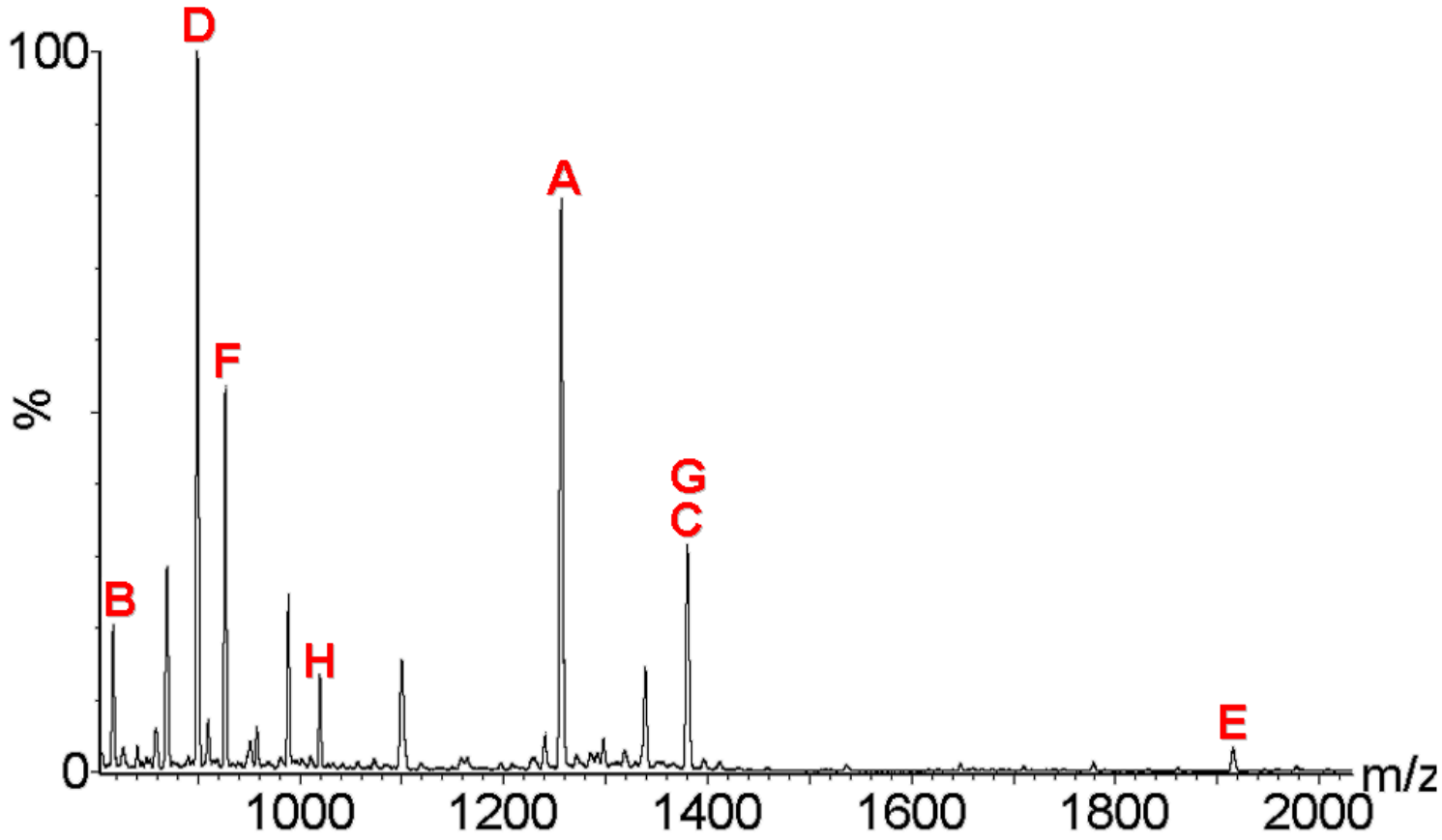

Figure A.35. Full ESI mass spectrum (Acetone-d_6/D_2O 1:1) of self-sorting systems **SS_{11}**: **3.04** (A,B), **3.05**(C,D), **3.07**(E,F), and **3.08**(G,H).

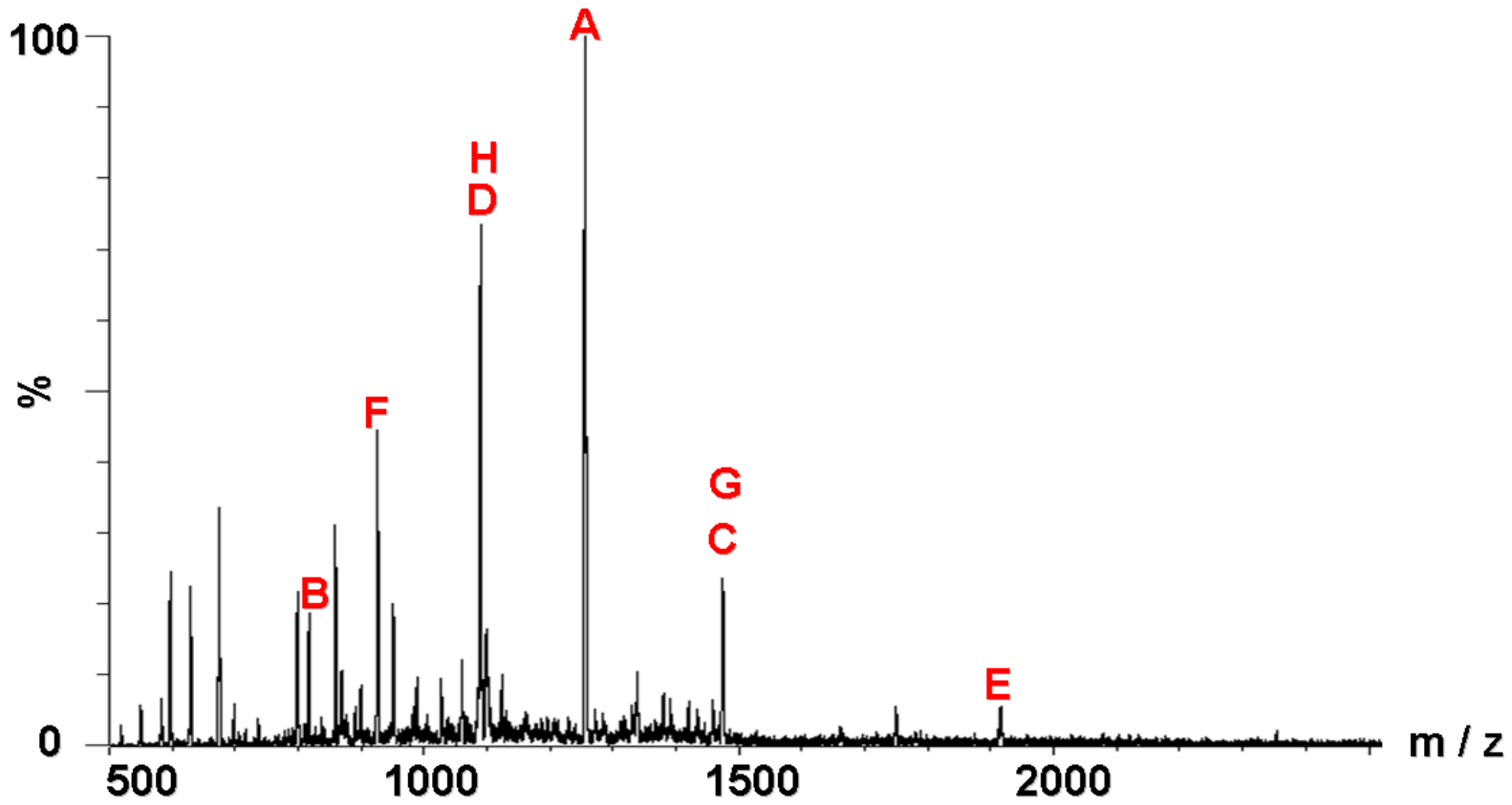

Figure A.36. Full ESI mass spectrum (Acetone-d_6/D_2O 1:1) of self-sorting systems $\mathbf{SS_{12}}$: **3.04** (A,B), **3.12**(C,D), **3.07**(E,F), and **3.19**(G,H).

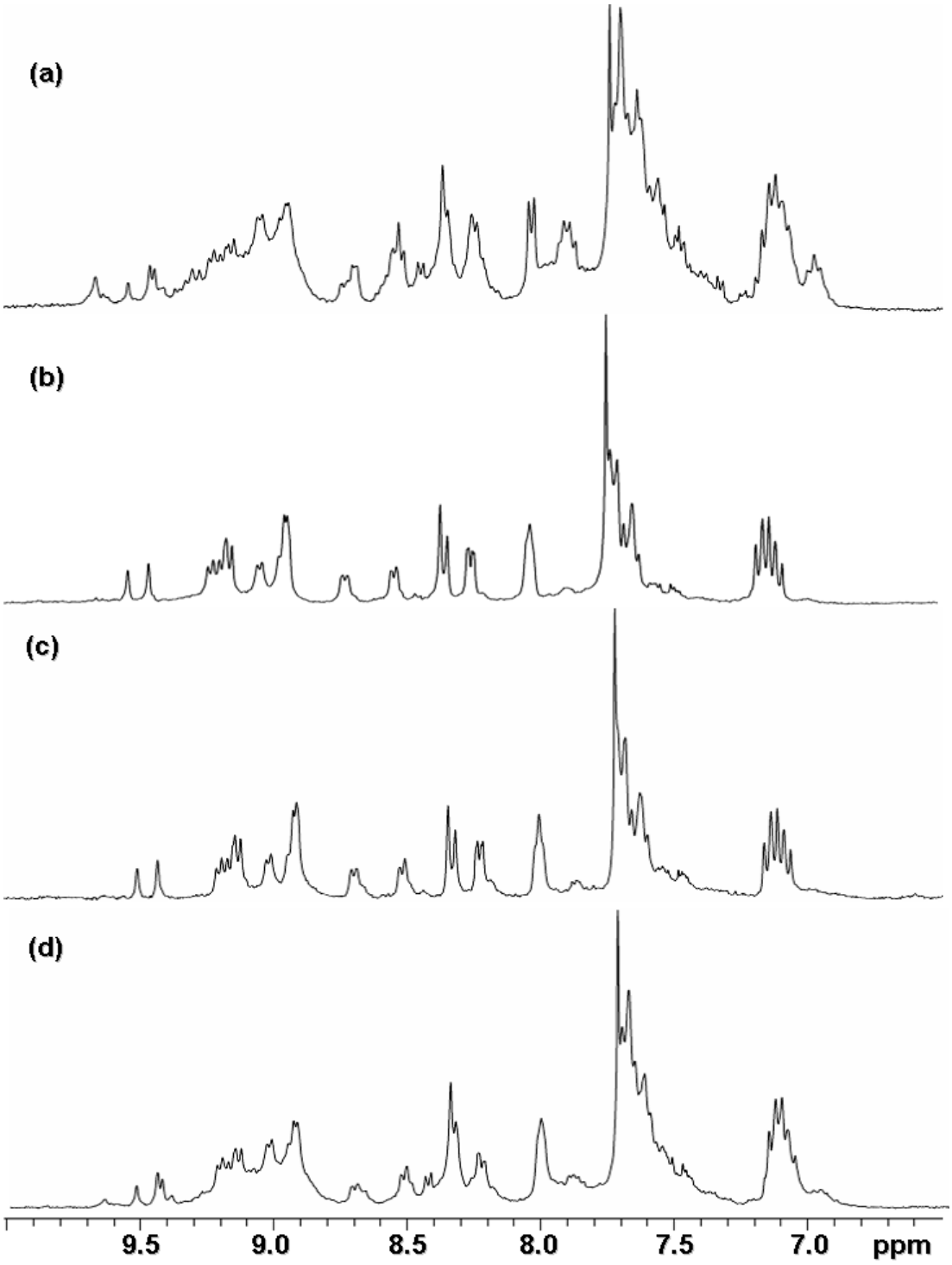

Figure A.37. ^{1}H NMR spectra (Acetone-d_6/D_2O 1:1) recorded for mixtures of **SS_4** (**3.04**, **3.05**, and **3.11**) heated at varied temperature achieved at different time (a) 65—70 ℃ at 1 h; (b) 65—70 ℃ at 24 h; (c) 45—50 ℃ at 120 h; (d) 25—30 ℃ at 20 d.

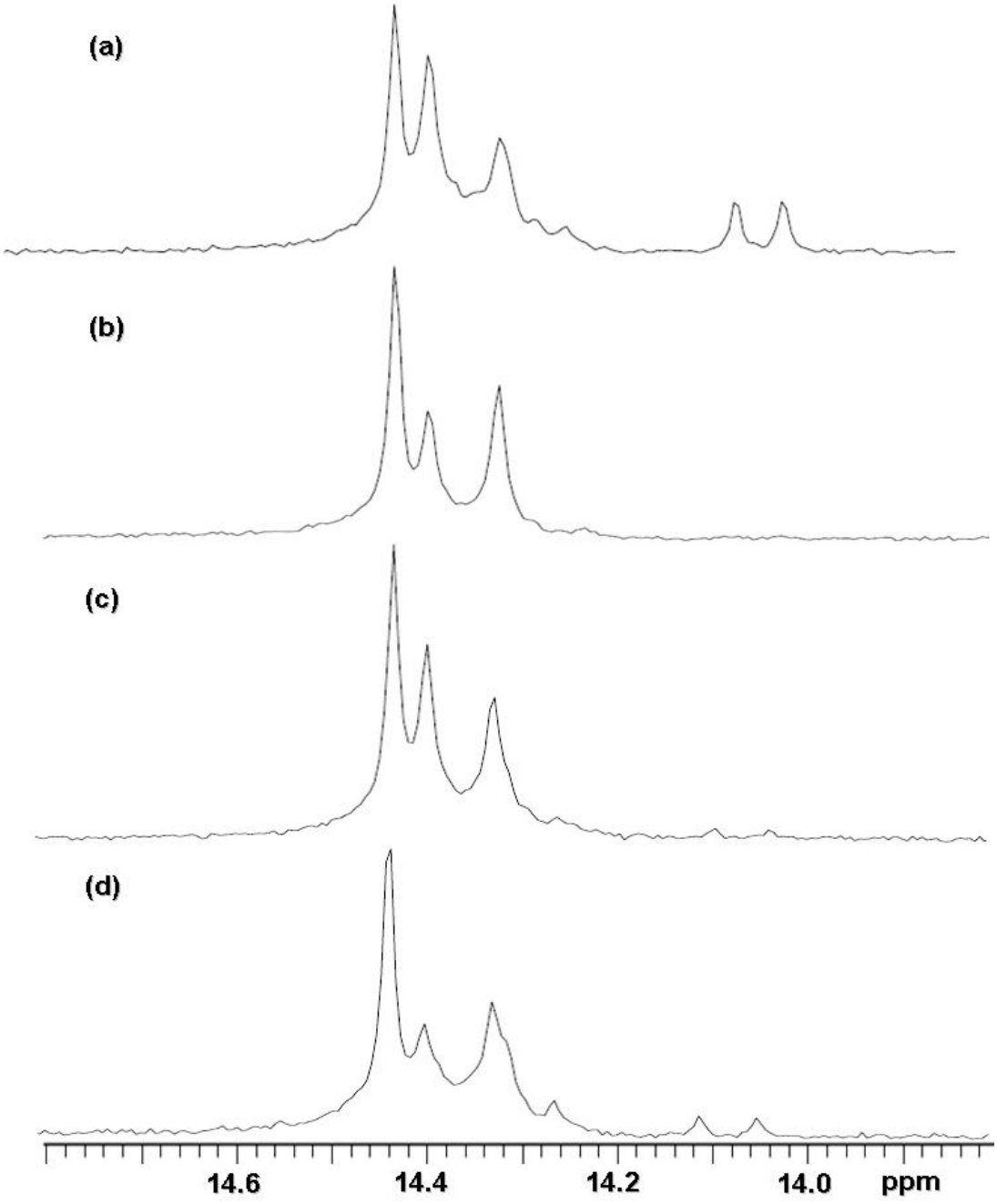

Figure A.38. $^{31}P\{^{1}H\}$ NMR spectra (Acetone-d_6/D_2O 1:1) recorded for mixtures of **SS_9** (**3.07**, **3.17**, and **3.18**) heated at varied temperature achieved at different time (a) 65—70 ℃ at 1 h; (b) 65—70 ℃ at 24 h; (c) 45—50 ℃ at 48 h; (d) 25—30 ℃ at 20 d.

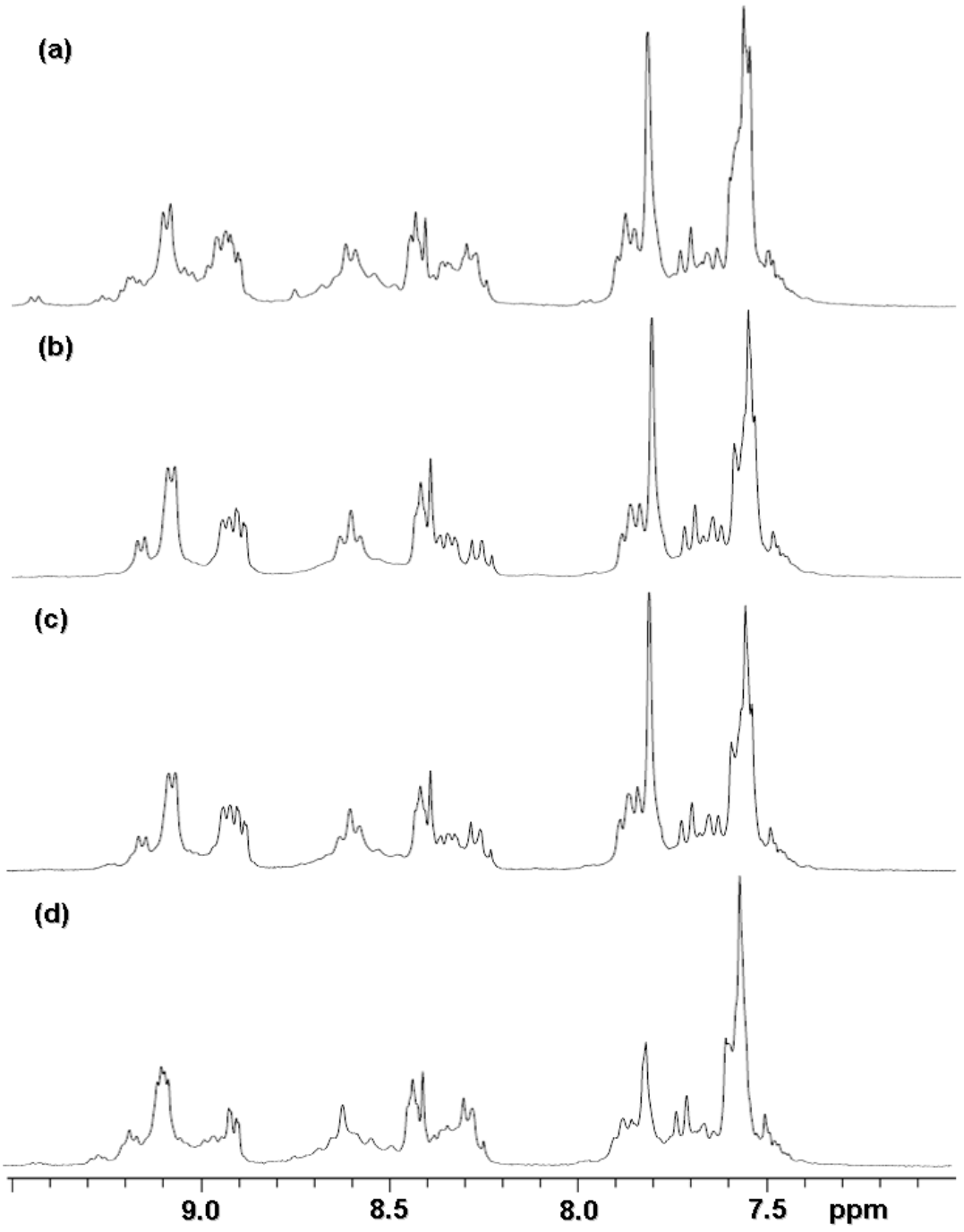

Figure A.39. ^{1}H NMR spectra (Acetone-d_6/D_2O 1:1) recorded for mixtures of **SS_9** (**3.07**, **3.17**, and **3.18**) heated at varied temperature achieved at different time (a) 65—70 ℃ at 1 h; (b) 65—70 ℃ at 24 h; (c) 45—50 ℃ at 48 h; (d) 25—30 ℃ at 20 d.

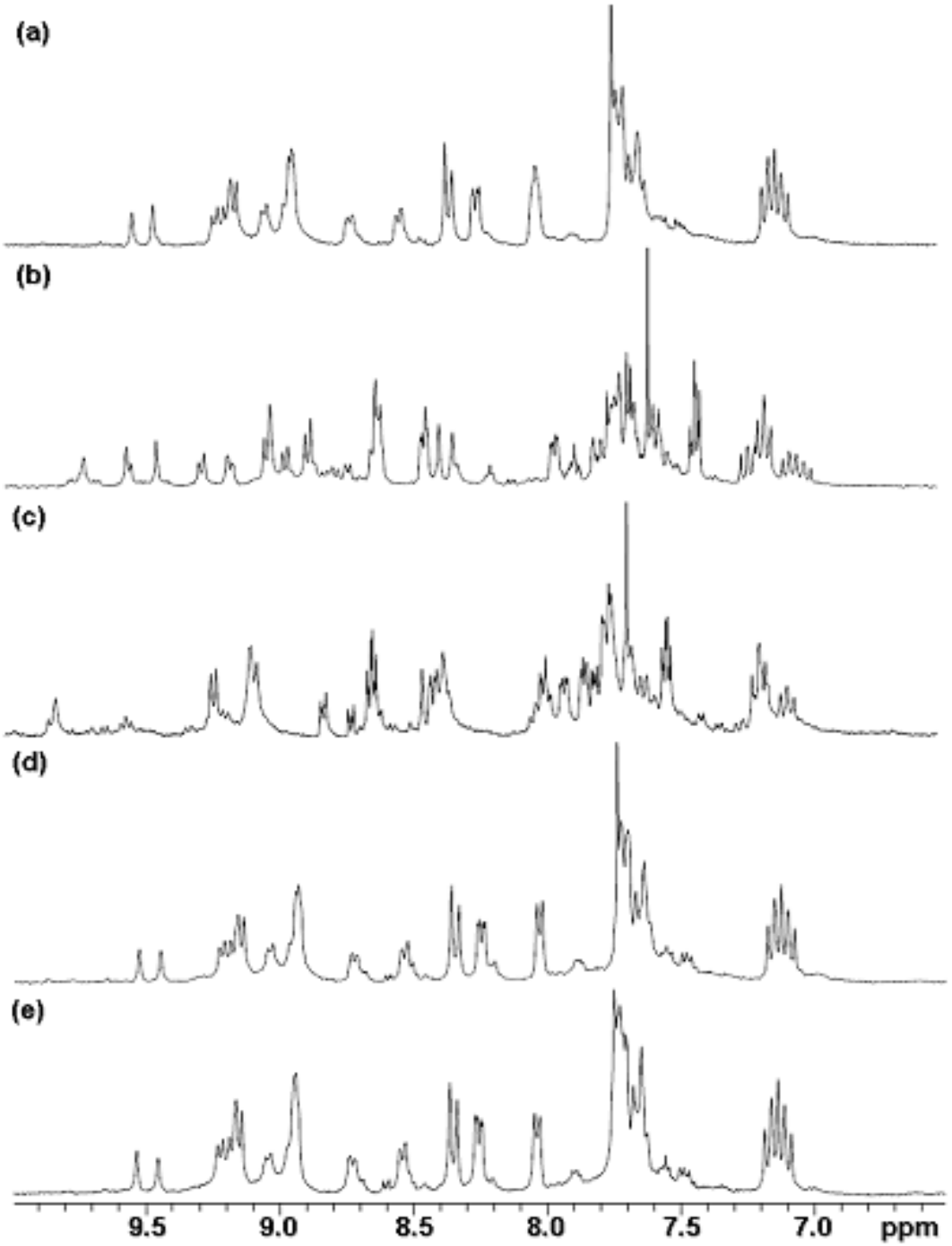

Figure A.40. Partial ^{1}H NMR spectra of **SS$_4$** in varied solvents: (a) Acetone-d_6/D_2O (1:1); (b) CD_2Cl_2; (c) Acetone-d_6/D_2O (20:1); (d) Acetone-d_6/D_2O (1:1) after removal of CD_2Cl_2; (e) Acetone-d_6/D_2O (1:1) after removal of Acetone-d_6/D_2O (20:1).

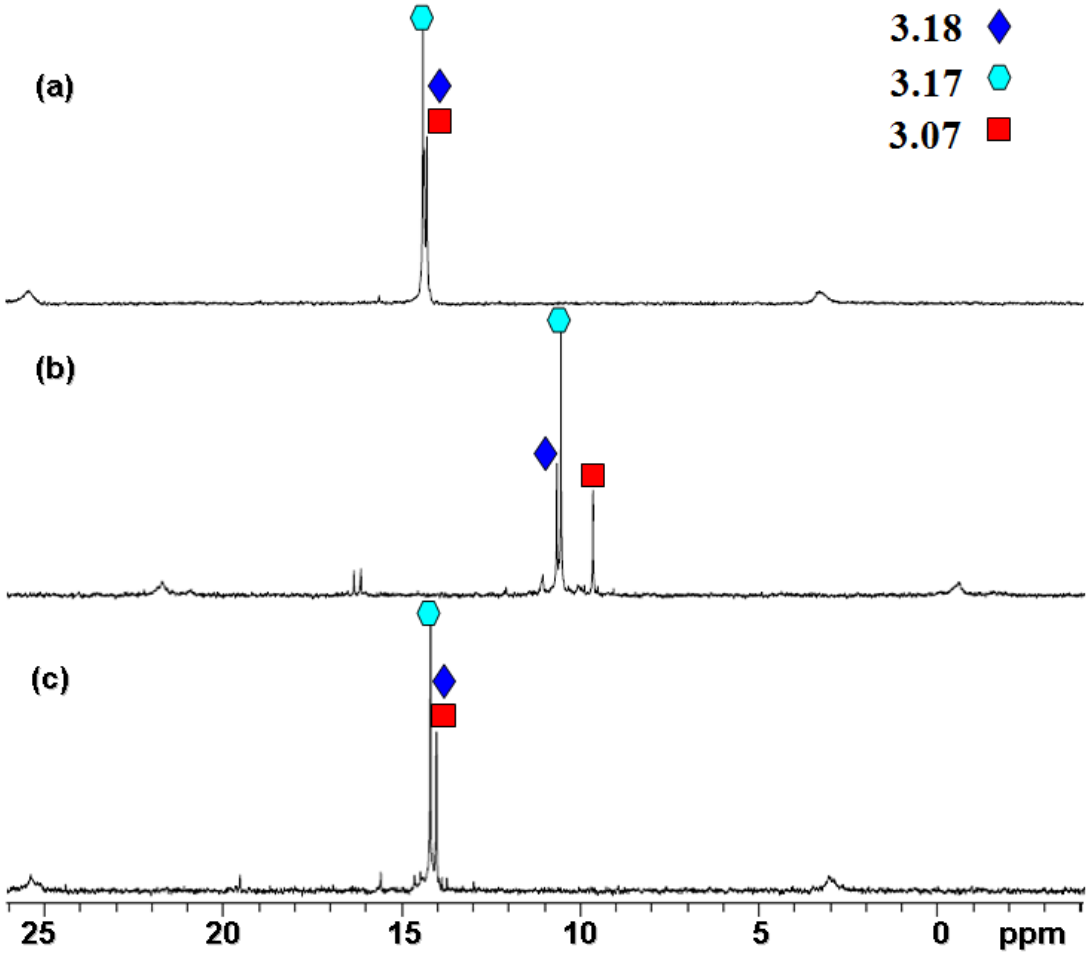

Figure A.41. $^{31}P\{^{1}H\}$ NMR spectra of **SS$_9$** in varied solvents: (a) Acetone-d_6/D_2O (1:1); (b) CD_2Cl_2; (c) Acetone-d_6/D_2O (20:1).

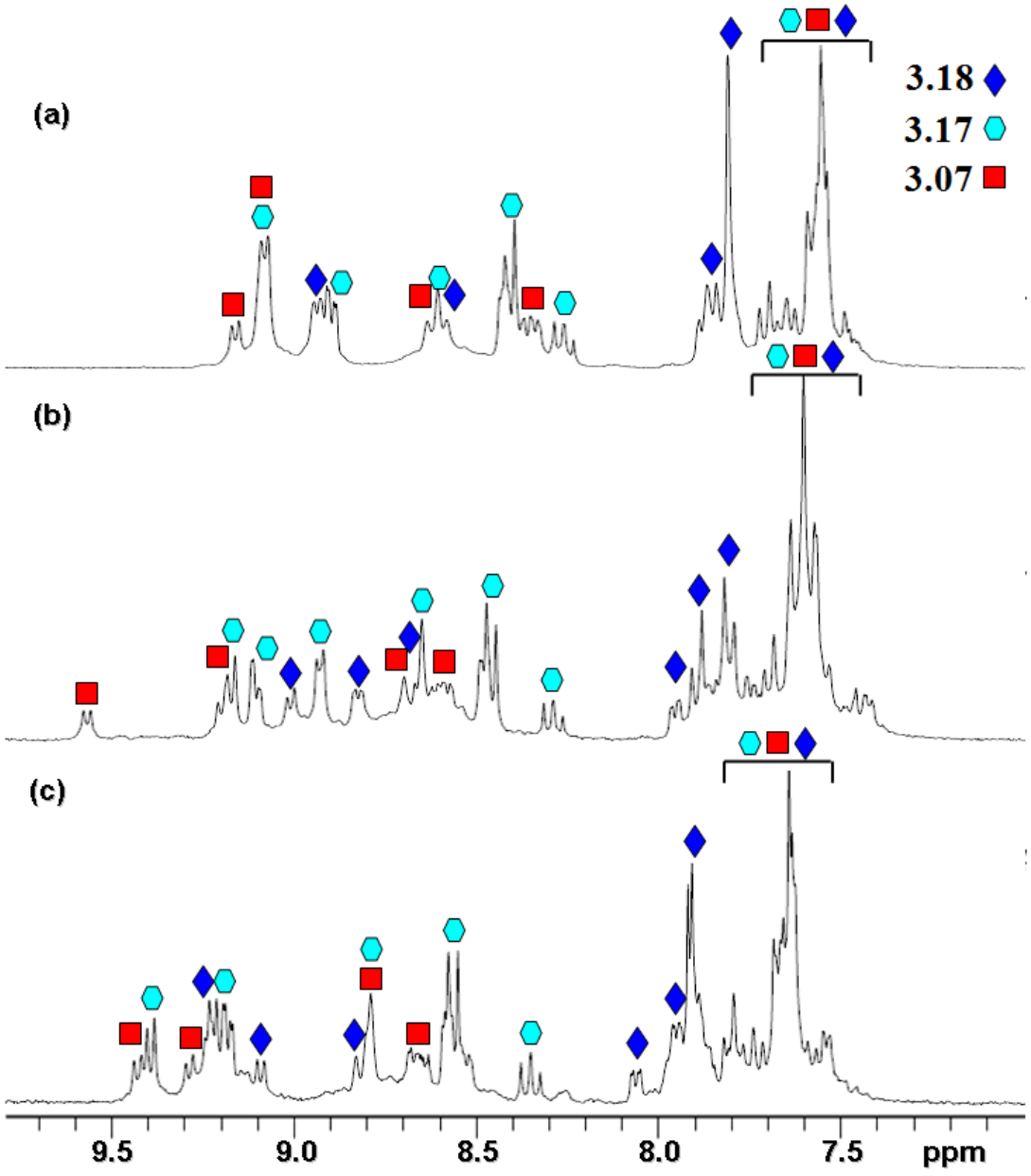

Figure A.42. ^{1}H NMR spectra of **SS$_9$** in varied solvents: (a) Acetone-d_6/D_2O (1:1); (b) CD_2Cl_2; (c) Acetone-d_6/D_2O (20:1).

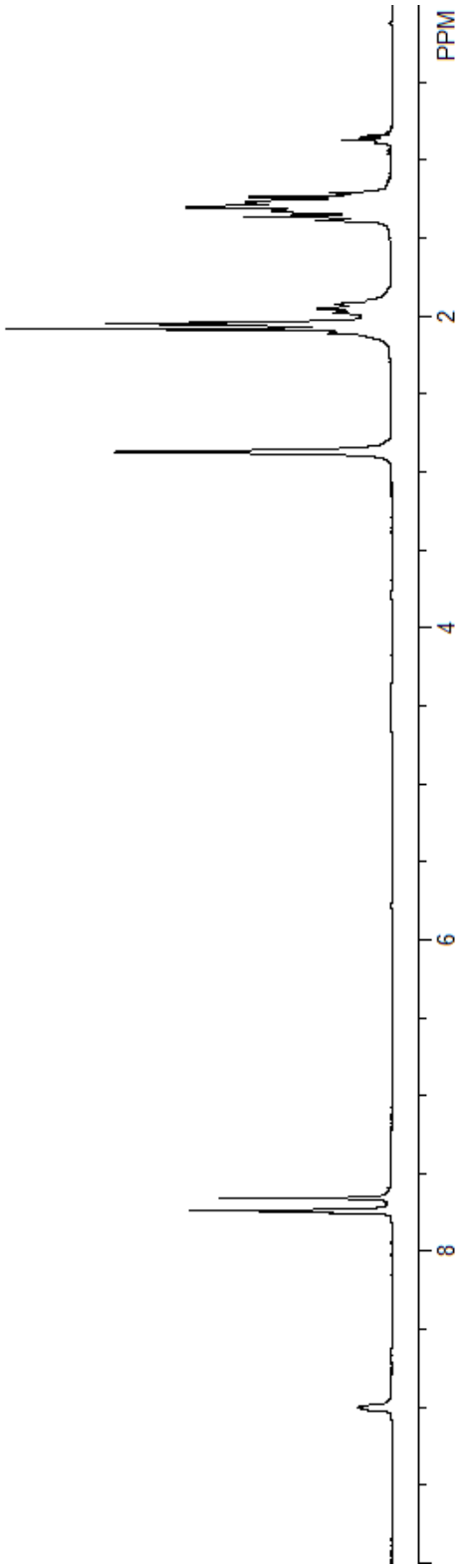

Figure A.43. ^{1}H NMR (Acetone-d_6, 300MHz) spectrum of multicomponent supramolecular rectangle **4.04**.

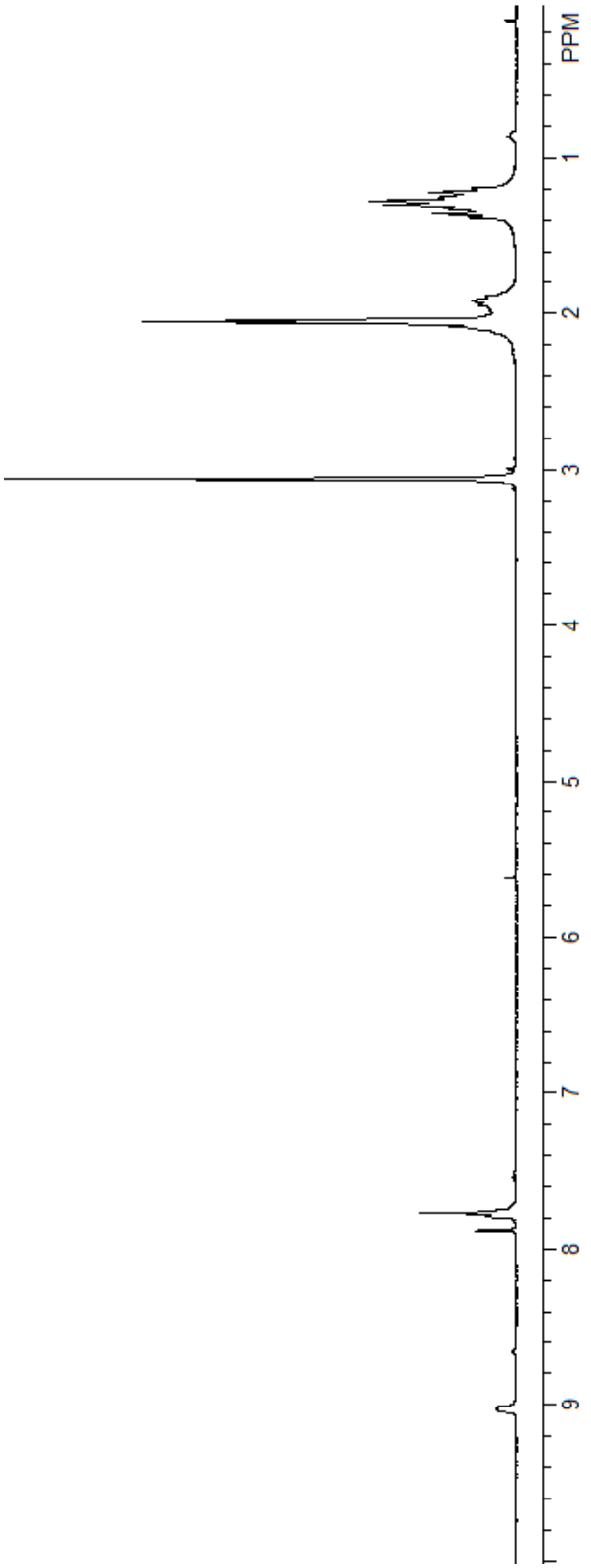

Figure A.44. ^{1}H NMR (Acetone-d_6, 300MHz) spectrum of multicomponent supramolecular rectangle **4.07**.

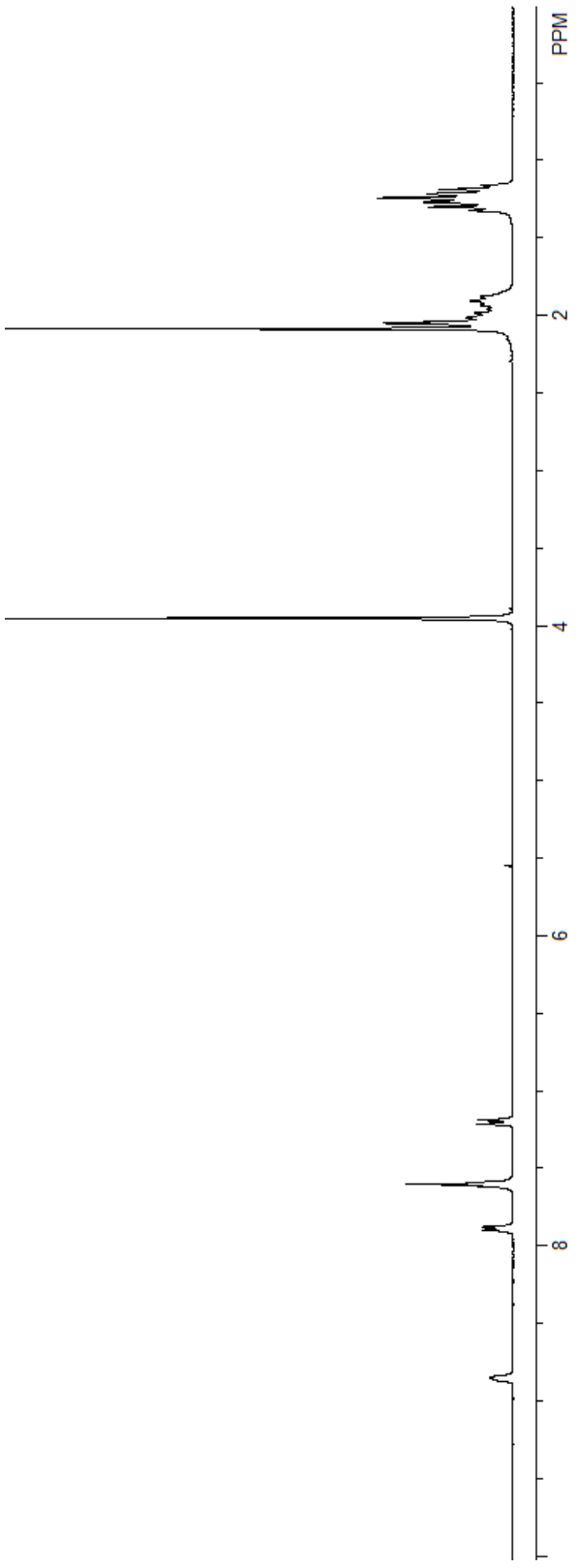

Figure A.45. ^{1}H NMR (Acetone-d_6/D_2O 10:1, 300MHz) spectrum of multicomponent supramolecular rectangle **4.08a**.

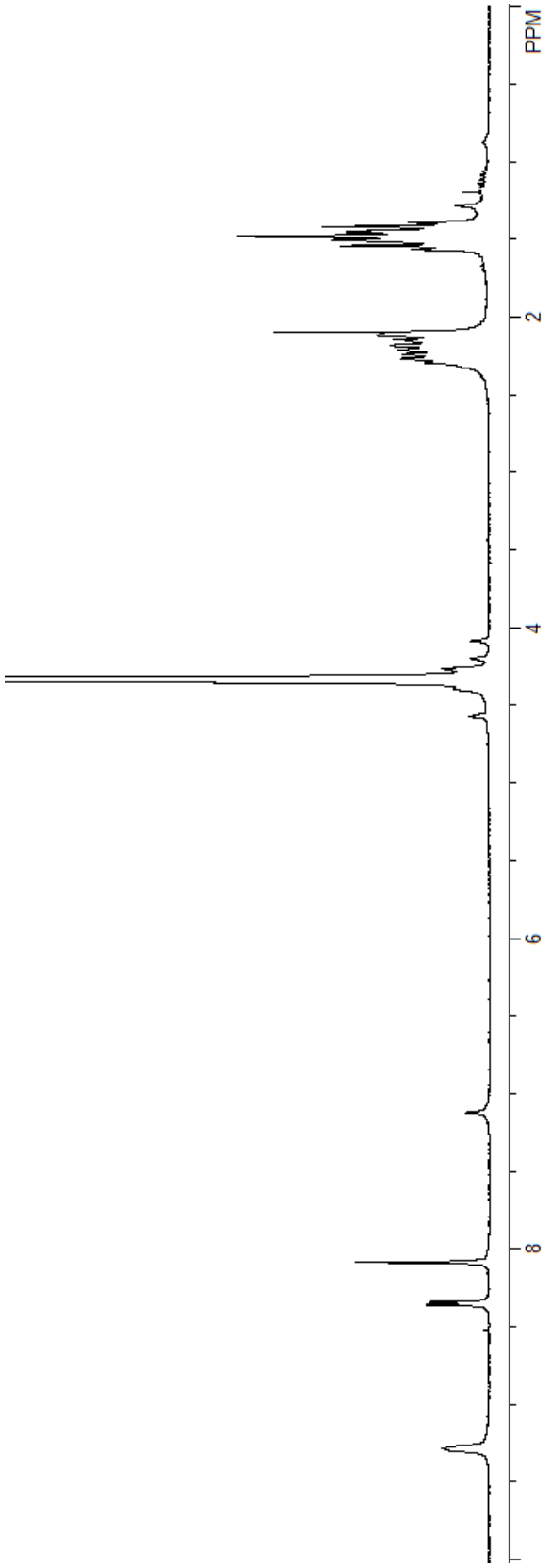

Figure A.46. ^{1}H NMR (CD_3NO_2, 300MHz) spectrum of multicomponent supramolecular rectangle **4.08b**.

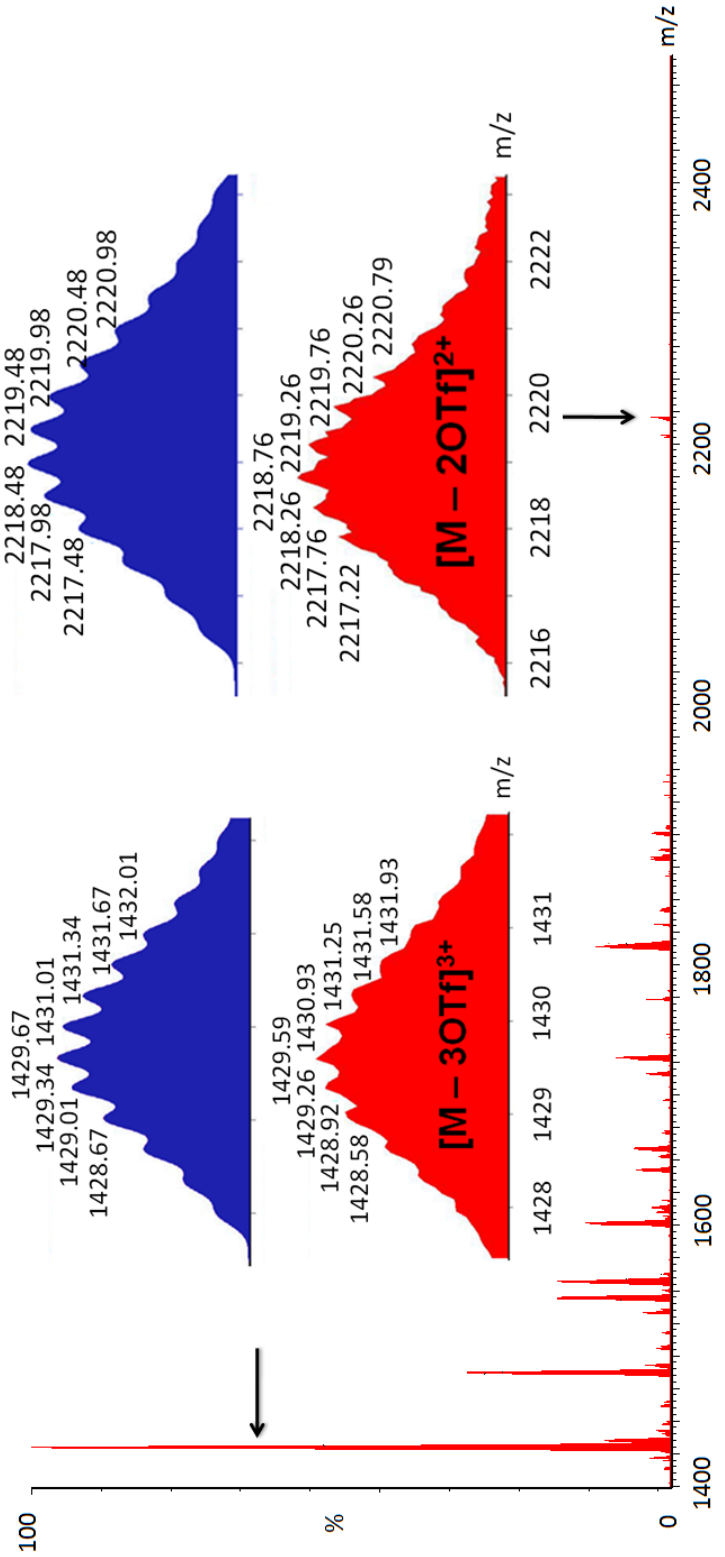

Figure A.47. ESI mass spectrum of multicomponent supramolecular trigonal prism **4.07**.

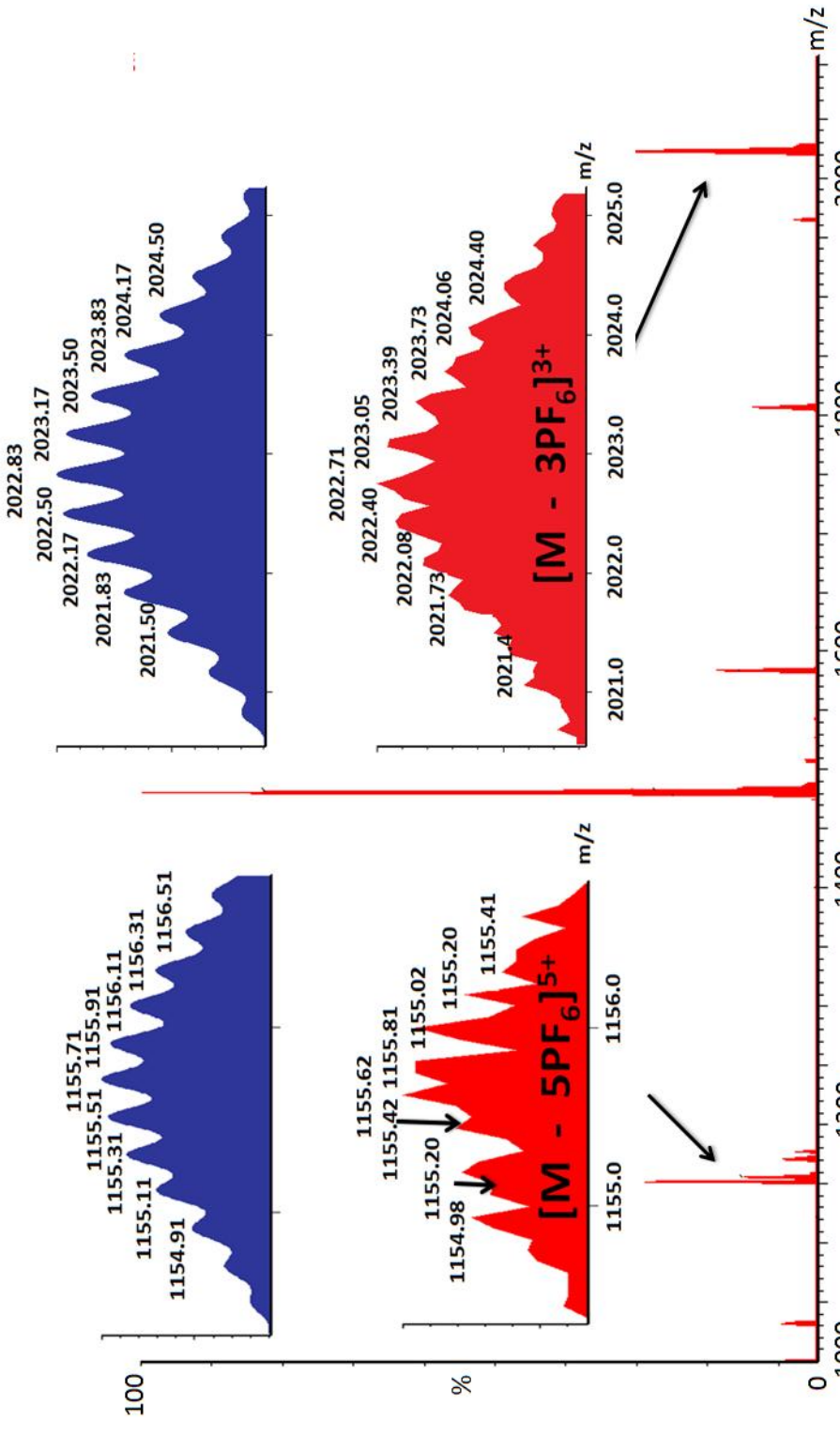

Figure A.48. ESI mass spectrum of multicomponent supramolecular tetragonal prism **4.08b**.

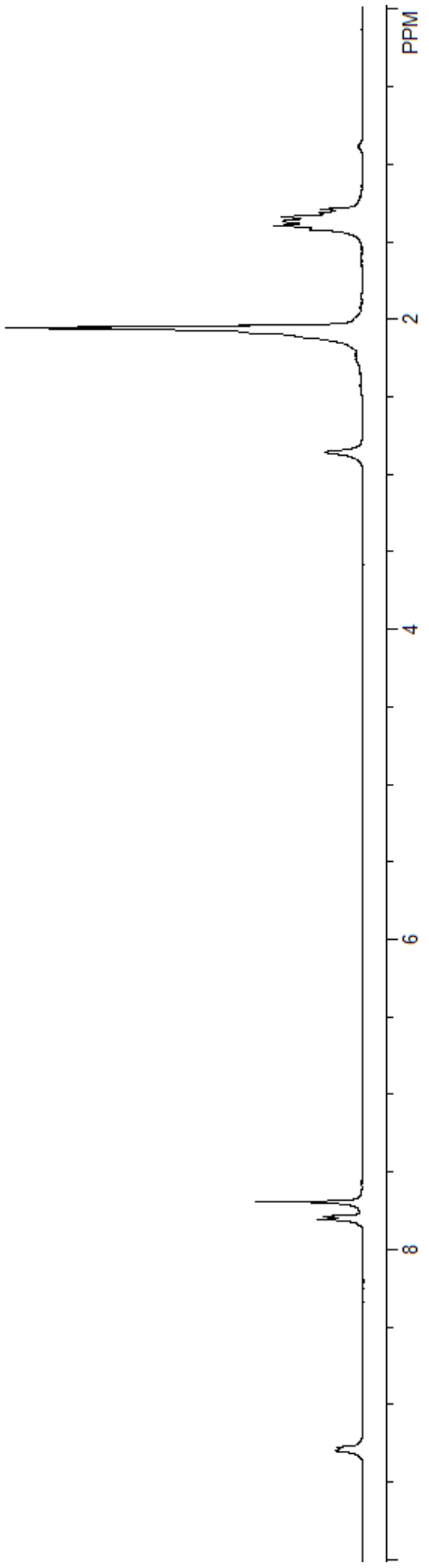

Figure A.49. ^{1}H NMR (Acetone-d_6, 300MHz) spectrum of two-component supramolecular square **4.15**.

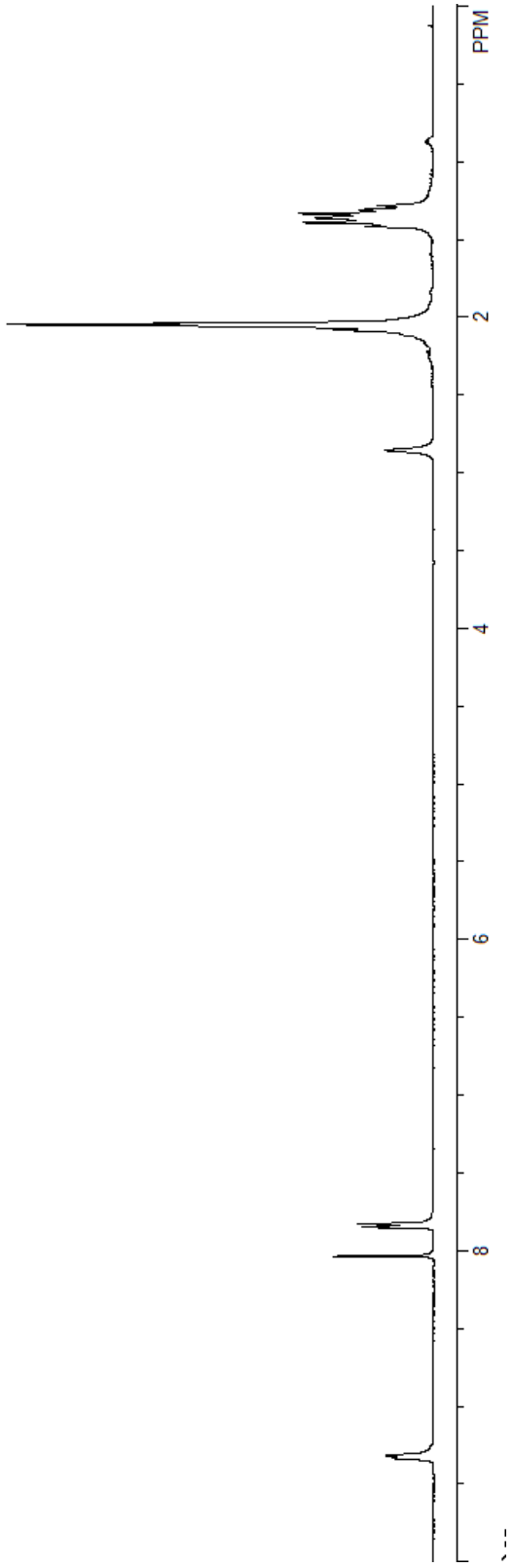

Figure A.50. ^{1}H NMR (Acetone-d_6, 300MHz) spectrum of two-component truncated tetrahedron **4.16**.

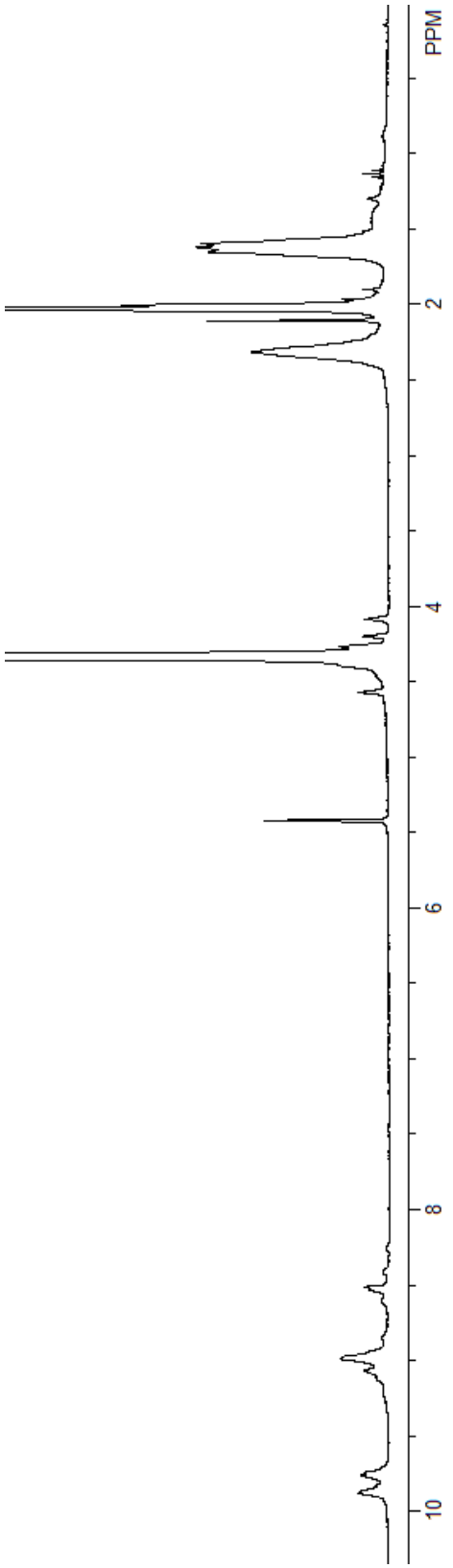

Figure A.51. ^{1}H NMR (CD_3NO_2/CD_2Cl_2 5:1 300MHz) spectrum of two-component trigonal prism **4.17**.

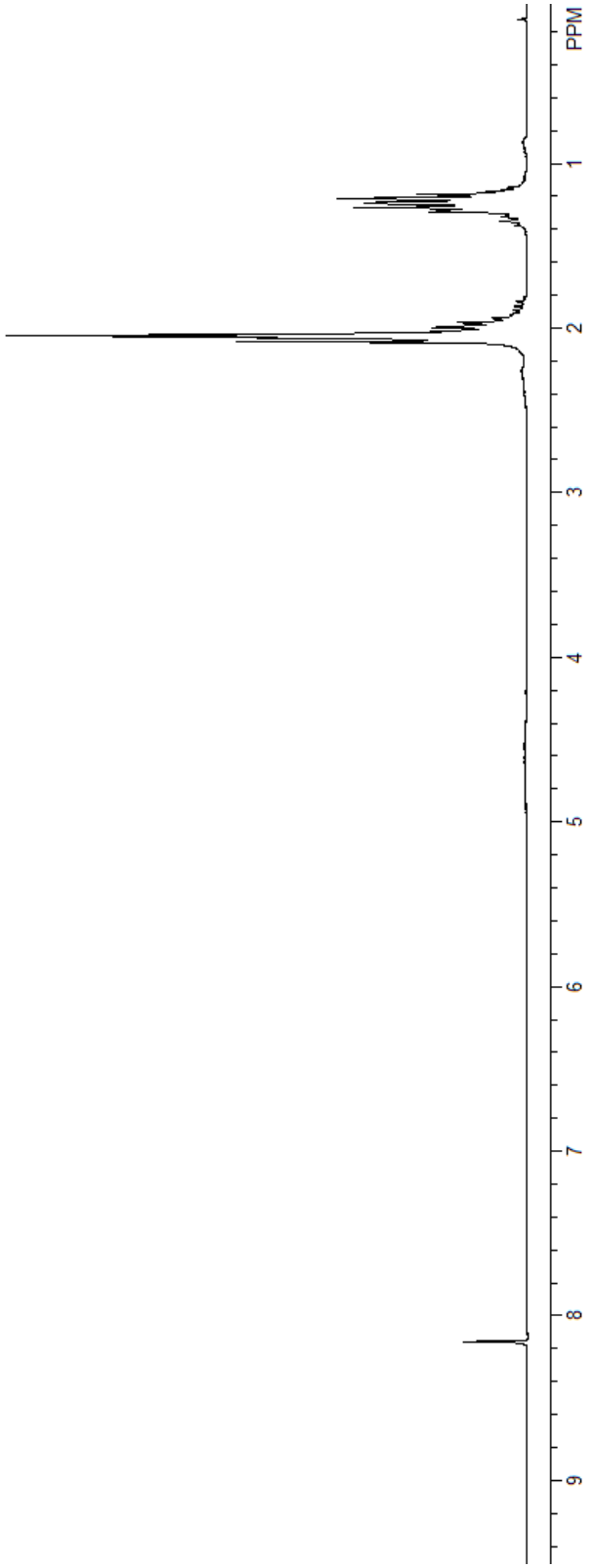

Figure A.52. ^{1}H NMR (Acetone-d_6, 300MHz) spectrum of two-component neutral triangle **4.18**.

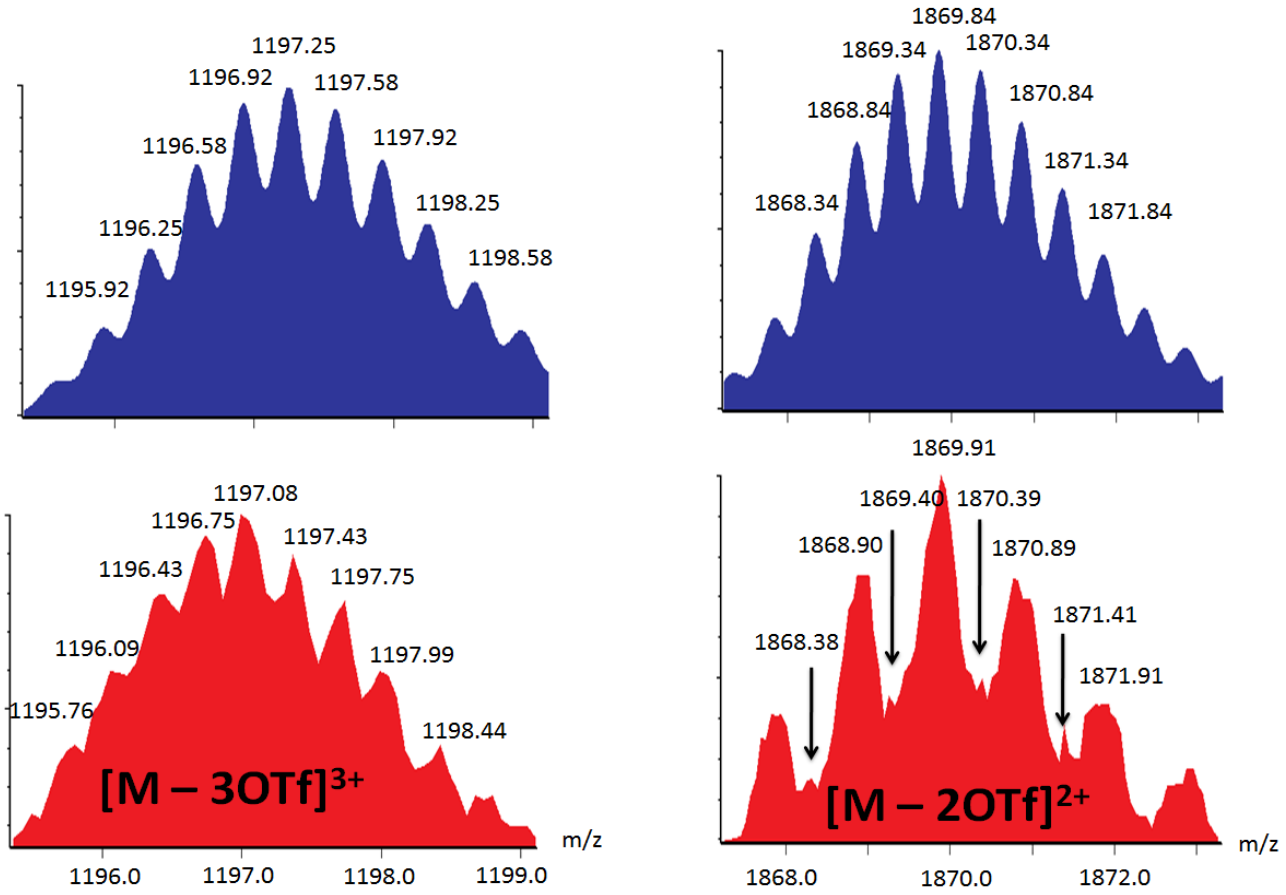

Figure A.53. Calculated (top) and experimental (bottom) ESI mass spectrum of two-component square **4.15**

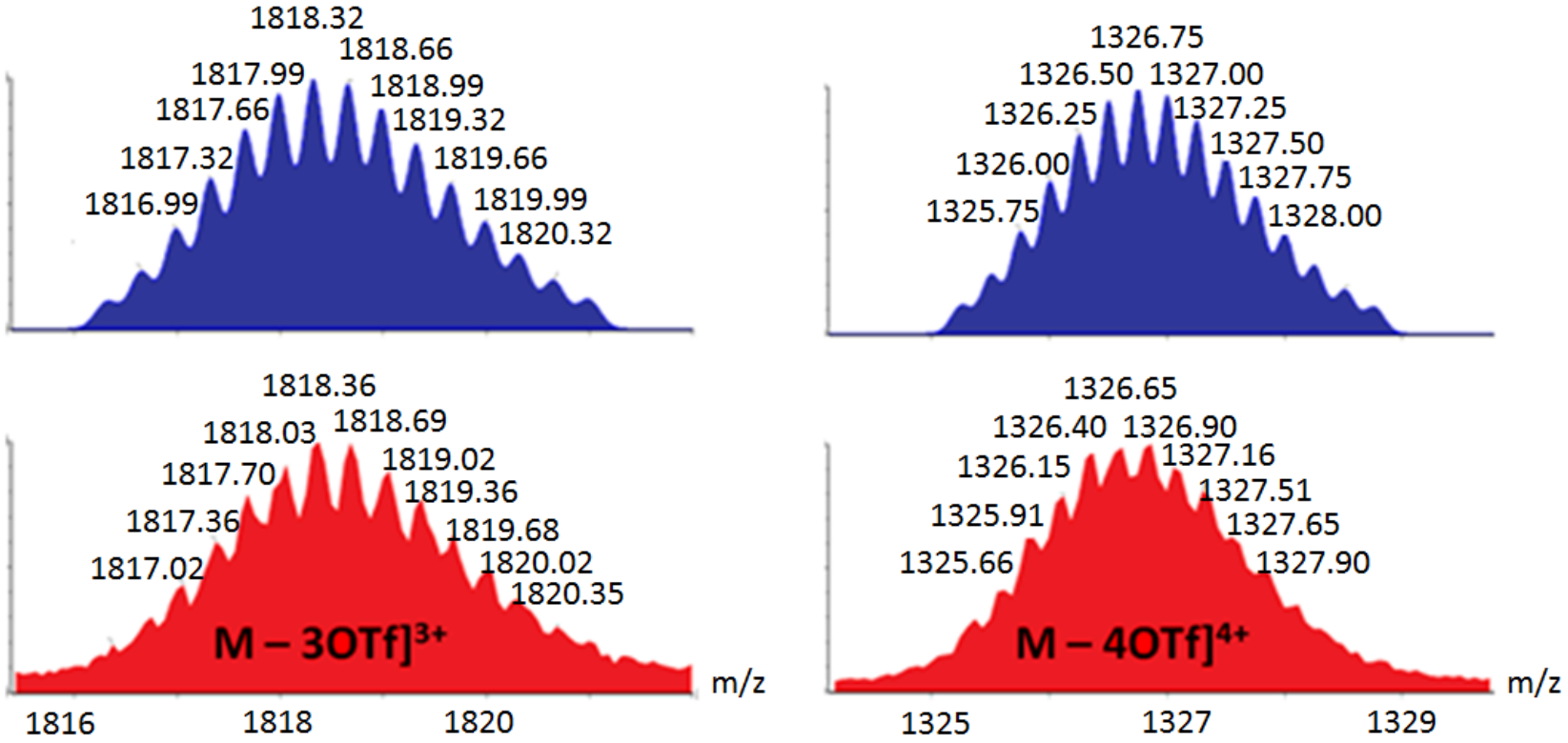

Figure A.54. Calculated (top) and experimental (bottom) ESI mass spectrum of two-component truncated tetrahedron **4.16**

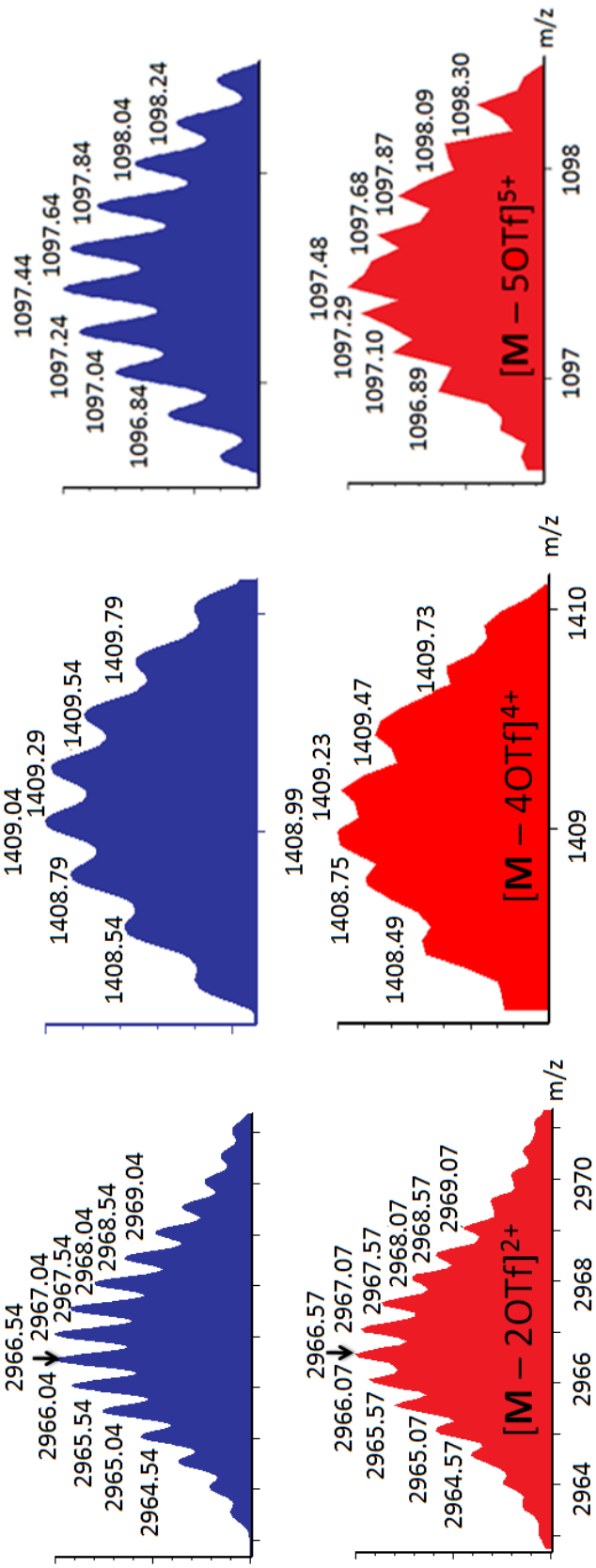

Figure A.55. Calculated (top) and experimental (bottom) ESI mass spectrum of two-component trigonal prism **4.17**

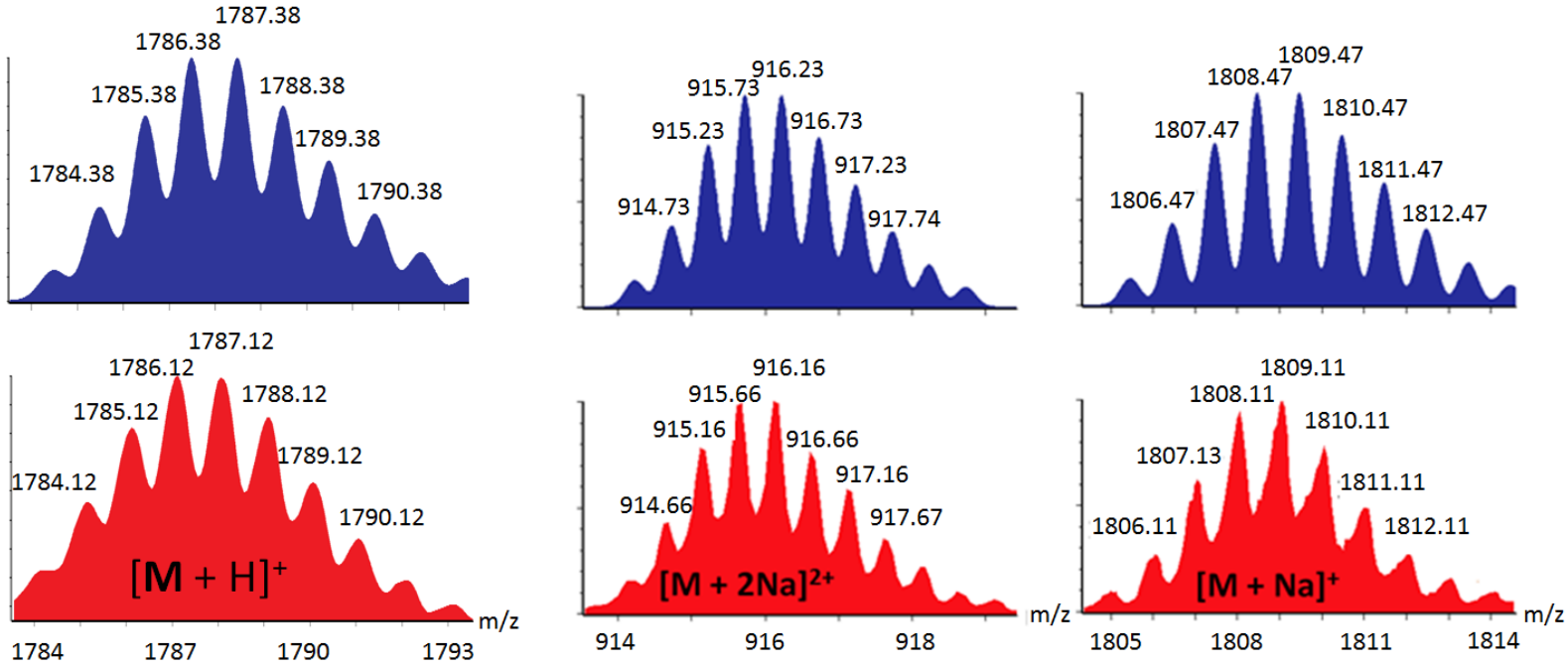

Figure A.56. Calculated (top) and experimental (bottom) ESI mass spectrum of two-component neutral triangle **4.18**

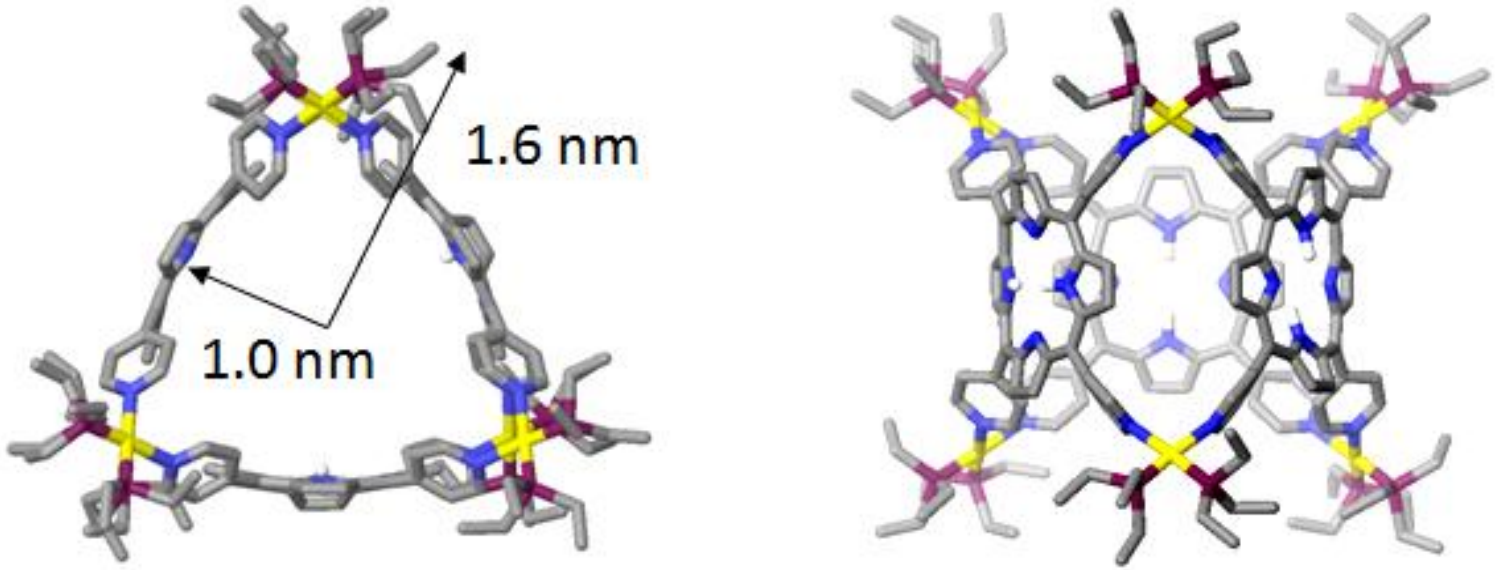

Figure A.57. Different views of the computational model (MMFF) of homoleptic self-assembly **4.17** and its estimated size.

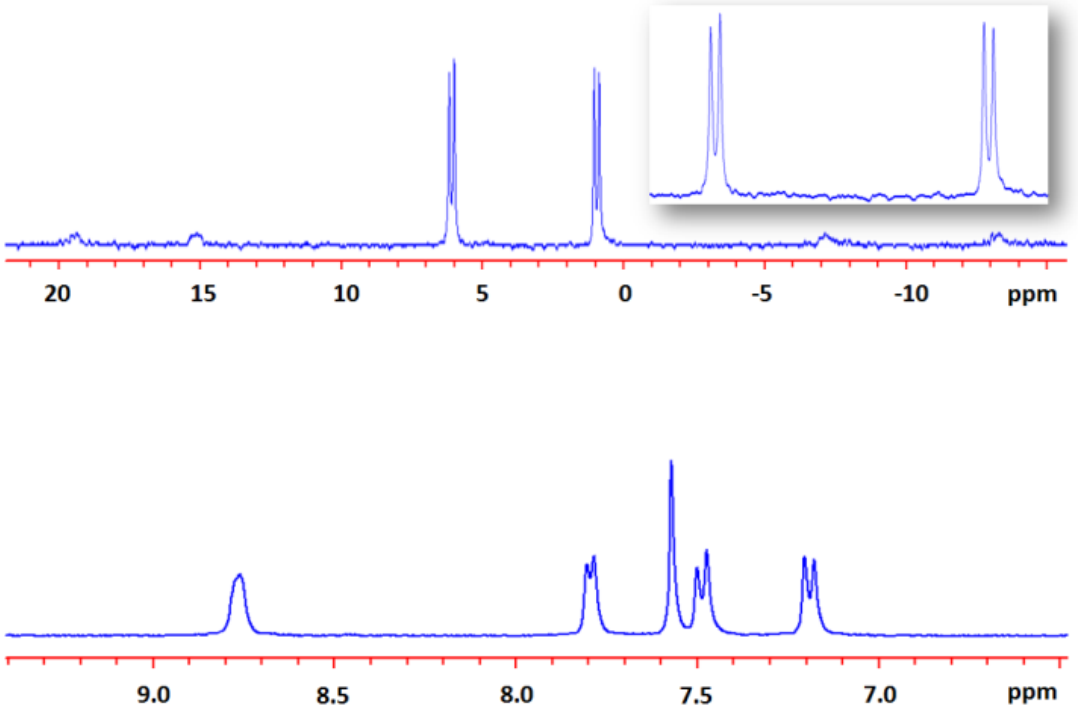

Figure A.58. $^{31}P\{^{1}H\}$ (top) and partial ^{1}H NMR (bottom) spectra (Acetone-d_6) of the supramolecular hexagonal prism **3.12**.

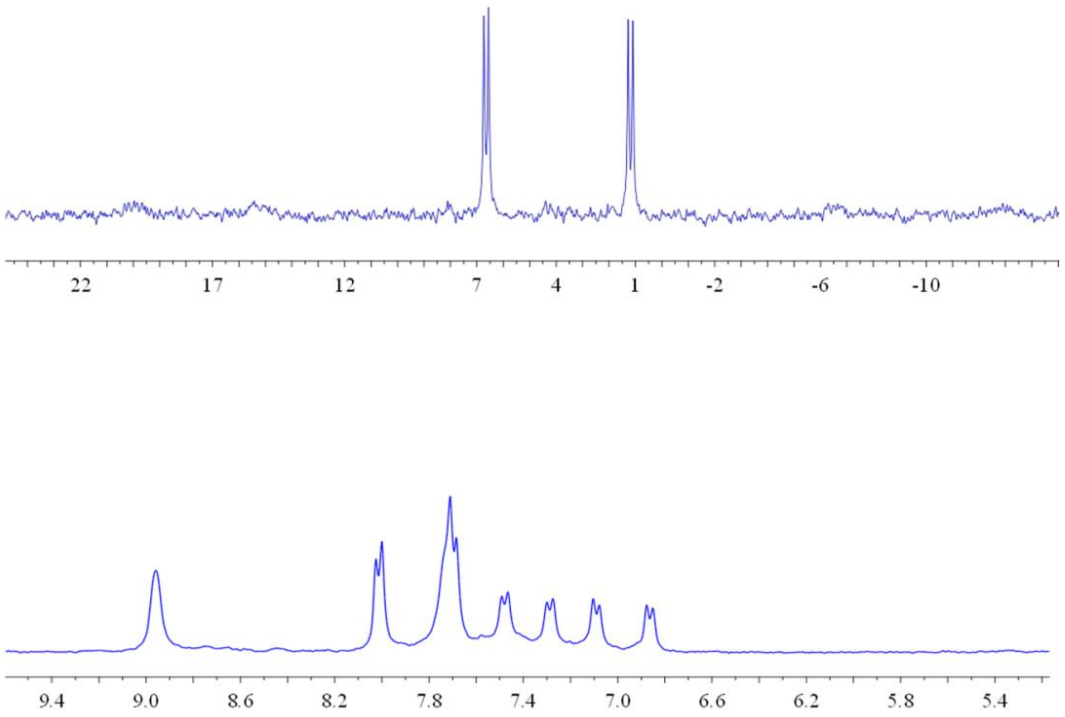

Figure A.59. $^{31}P\{^{1}H\}$ (top) and partial ^{1}H NMR (bottom) spectra (Acetone-d_6) of the supramolecular hexagonal prism **3.13**.

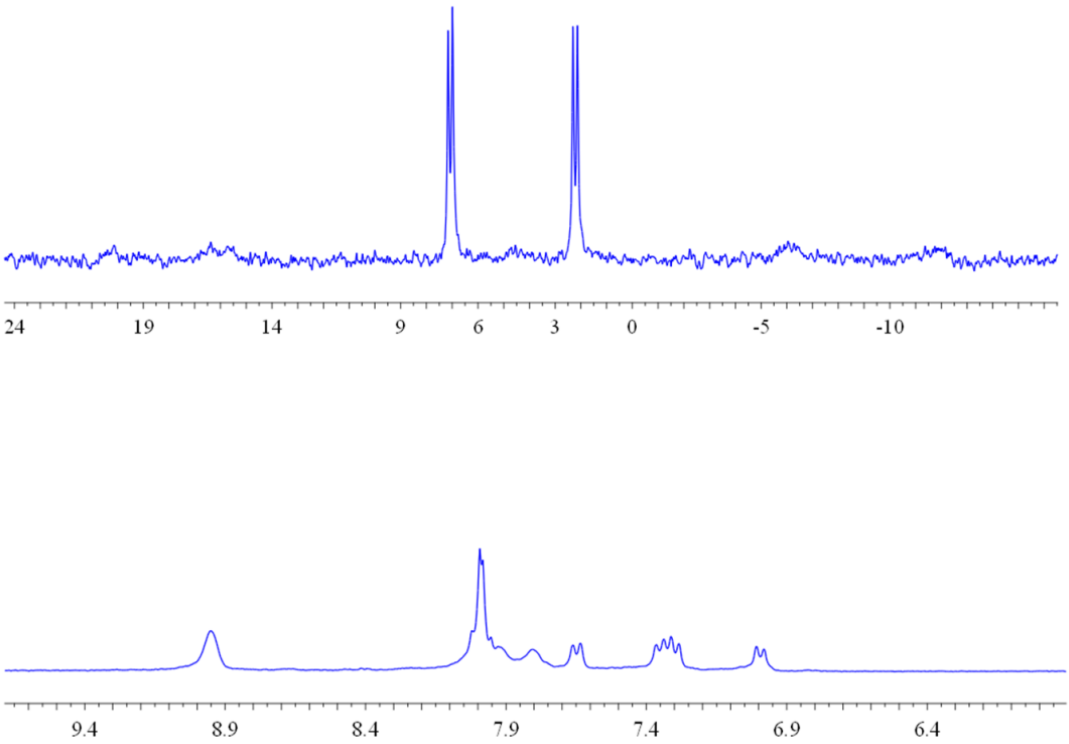

Figure A.60. $^{31}P\{^{1}H\}$ (top) and partial ^{1}H NMR (bottom) spectra (Acetone-d_6) of the supramolecular hexagonal prism **3.14**.

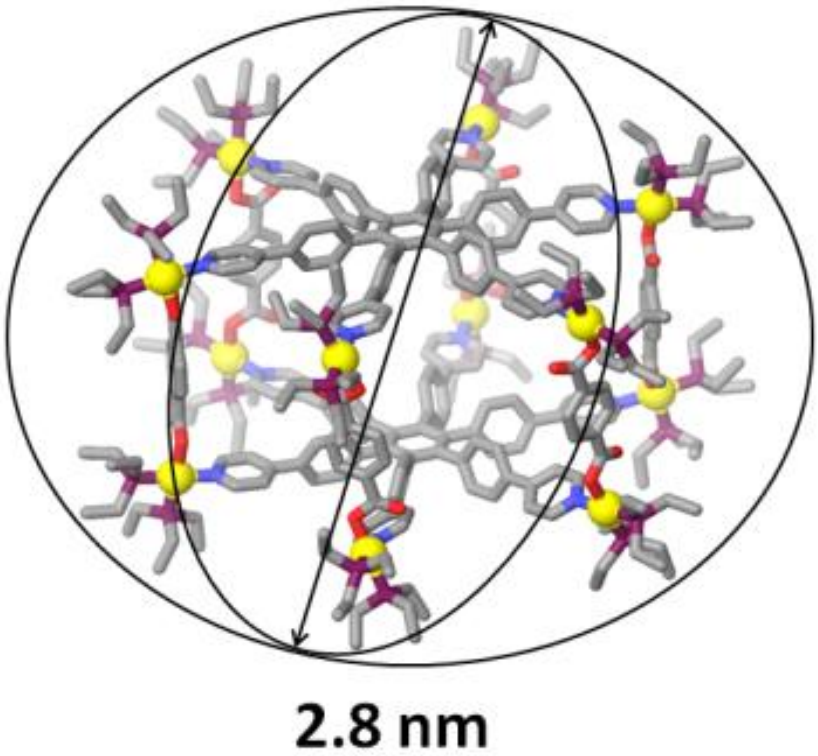

Figure A.61. Computational model (MMFF) of supramolecular hexagonal prism **4.12**

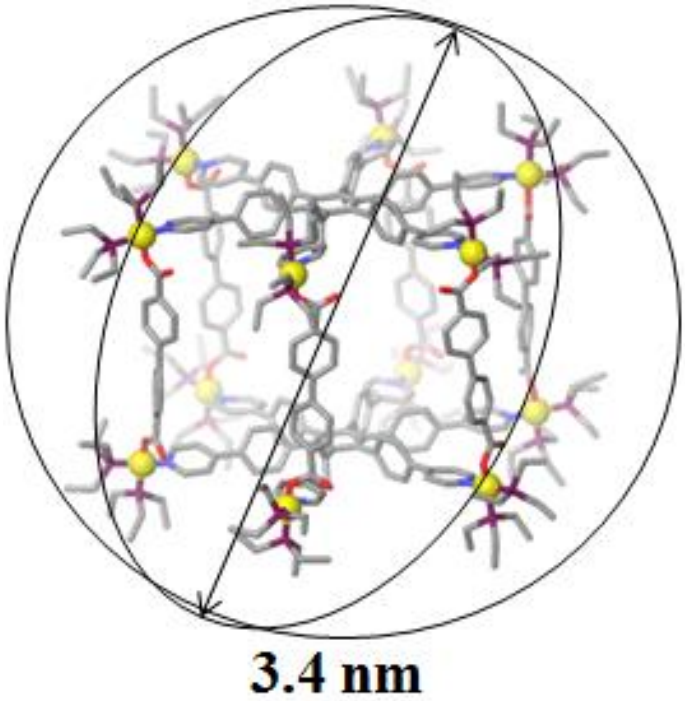

Figure A.62. Computational model (MMFF) of supramolecular hexagonal prism **4.13**

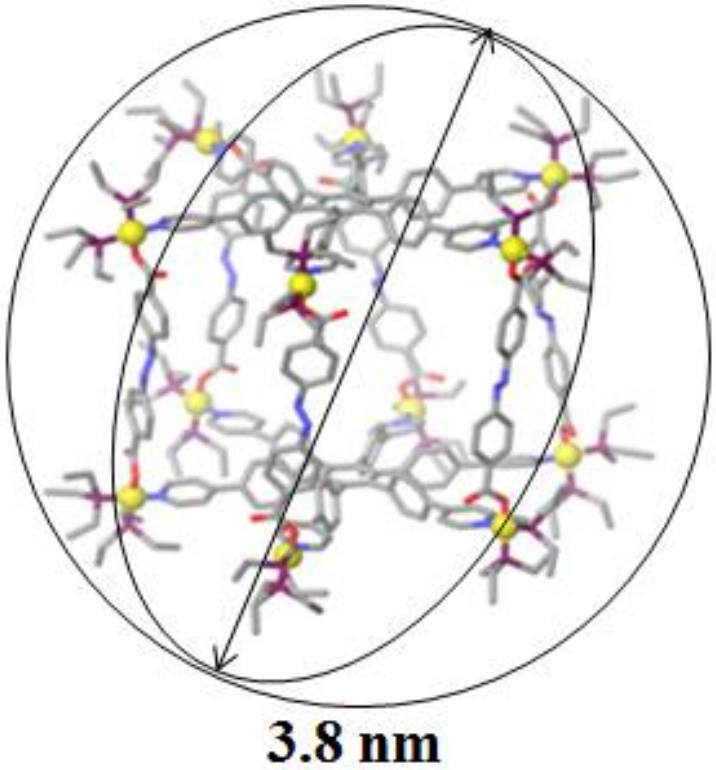

Figure A.63. Computational model (MMFF) of supramolecular hexagonal prism **4.14**

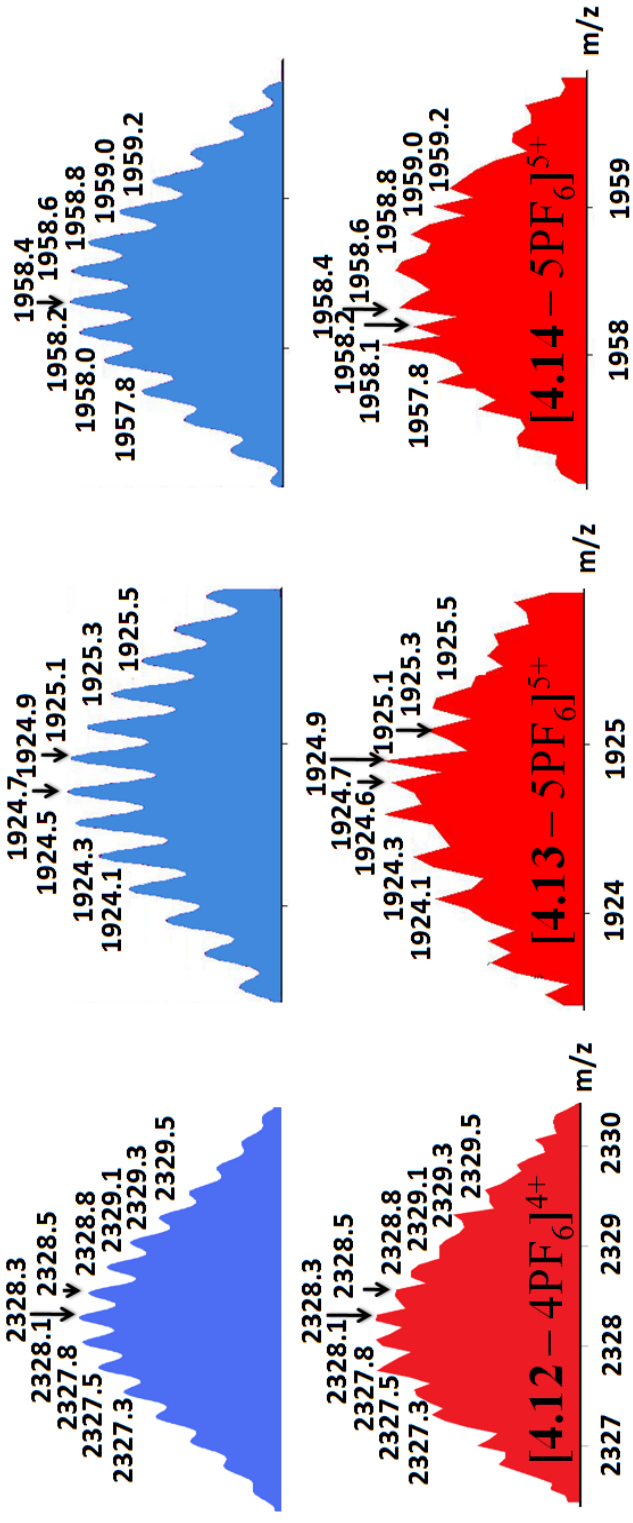

Figure A.64. Calculated (top) and experimental (bottom) ESI mass spectrum of three-component hexagonal prism **4.12–4.14**

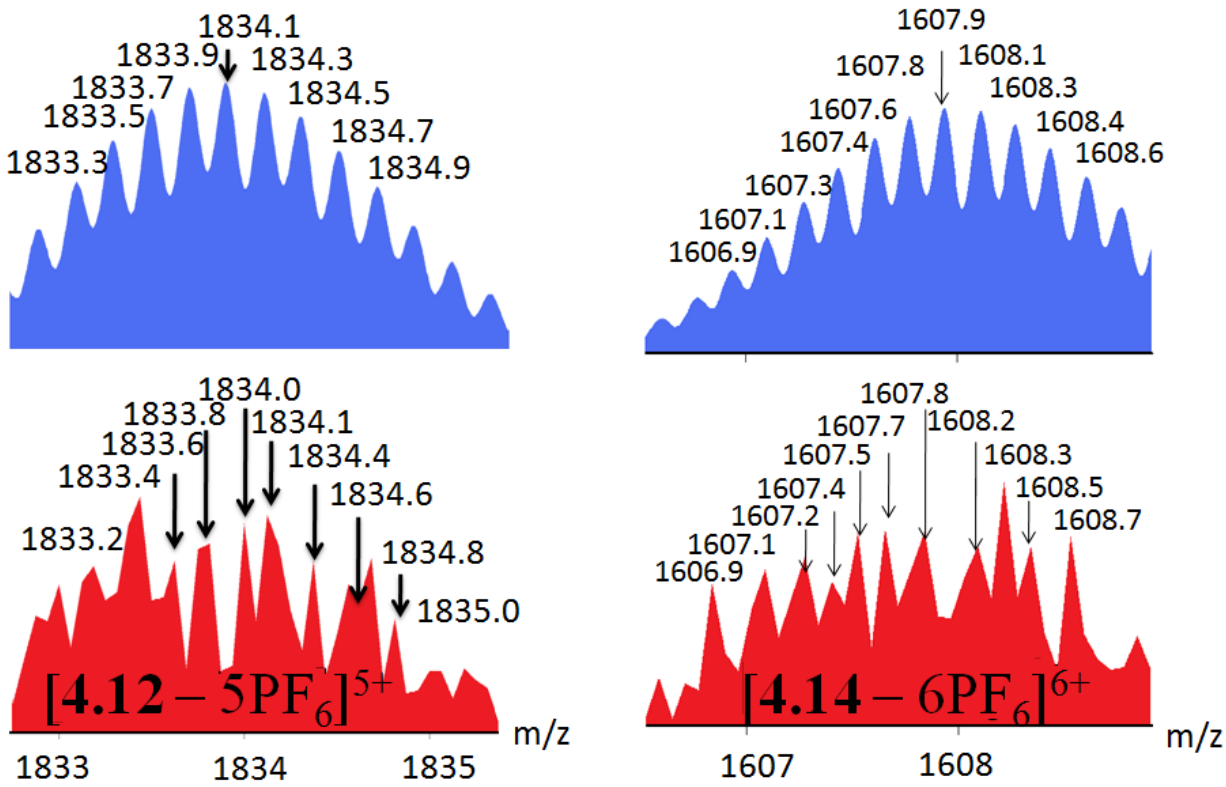

Figure A.65. Calculated (top) and experimental (bottom) ESI mass spectrum of three-component hexagonal prism **4.12** and **4.14**

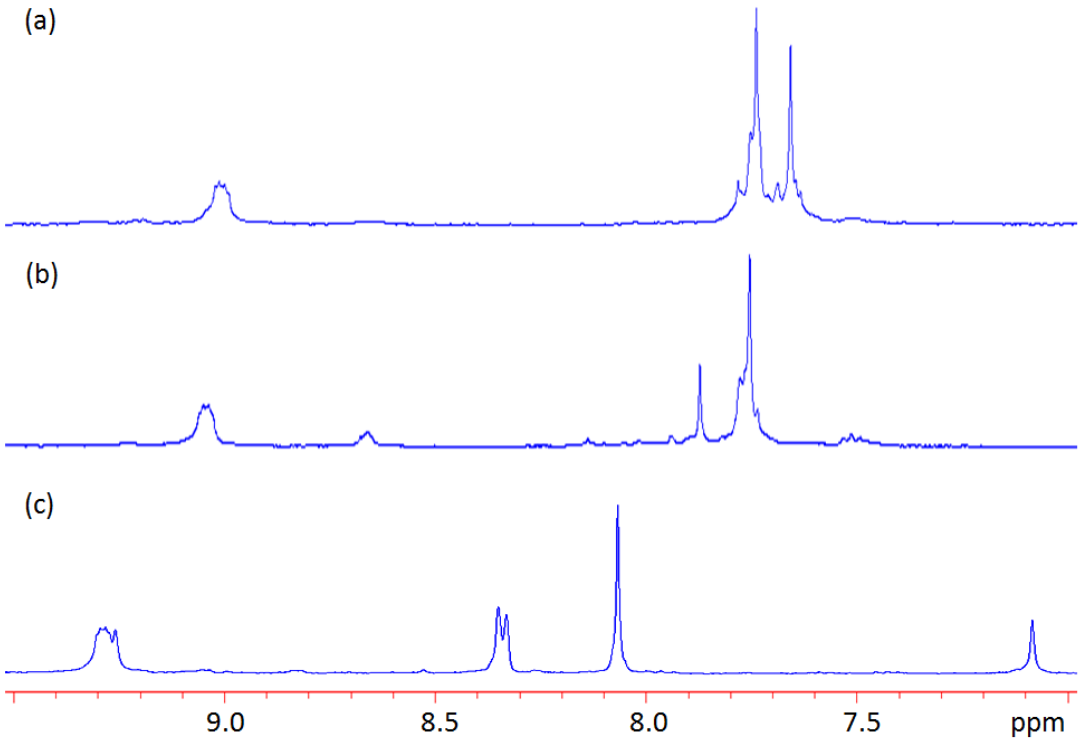

Figure A.66. Partial ^{1}H NMR spectra of multicomponent supramolecular rectangle **4.04** (a), trigonal prism **4.07** (b), and tetragonal prism **4.08b** (c) obtained via supramolecular transformations.

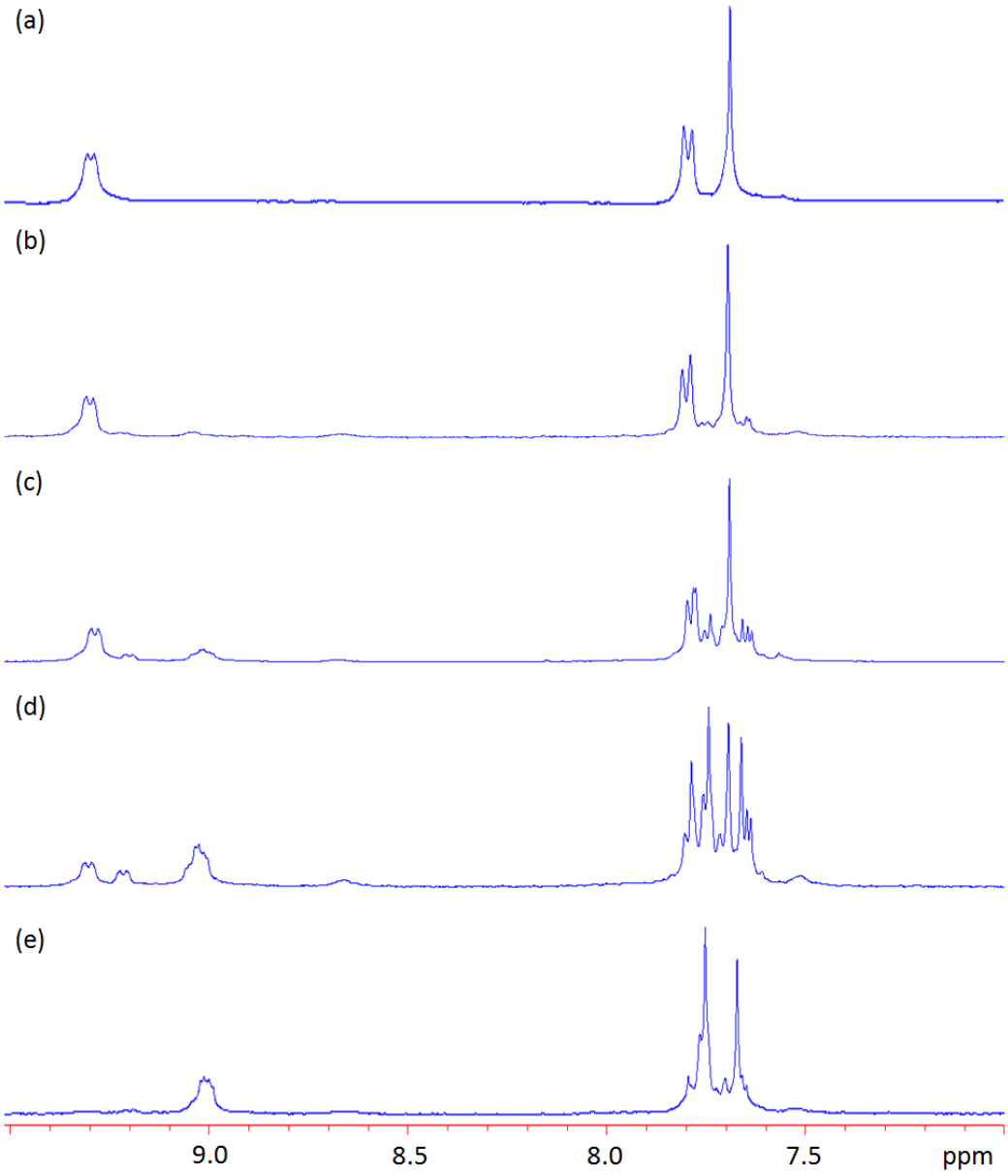

Figure A.67. Partial ^{1}H NMR spectra for mixtures of square **4.15** upon addition of 0% (a), 10% (b), 25% (c), 50% (d), and 100% (e) of neutral triangle **4.18**.

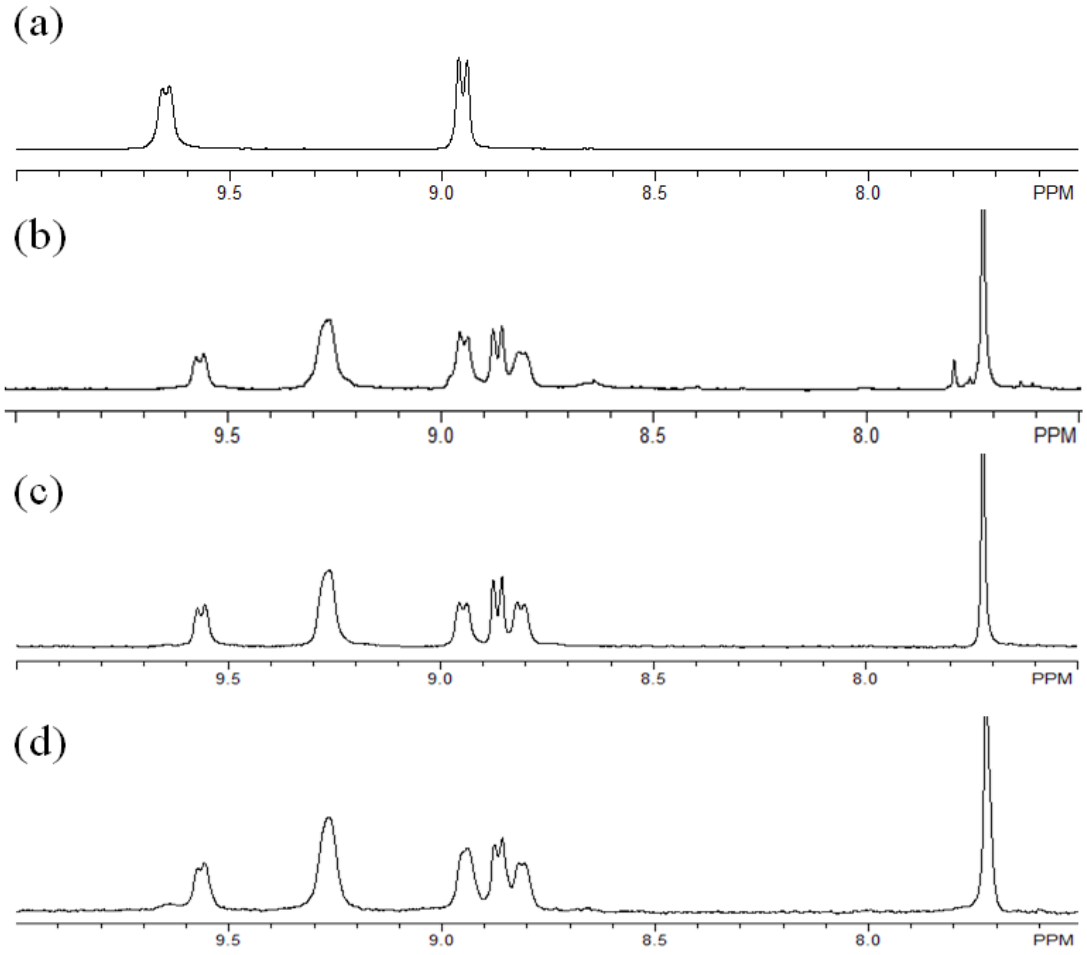

Figure A.68. Partial ^{1}H NMR spectra of **4.20** (b,c) modified from **4.19** (a) and assembled (d) by *cis*-$Pt(PEt_3)_2(OTf)_2$ **4.01**, ditopic carboxylate ligand **4.02**, and tritopic pyridyl donor **4.21**.

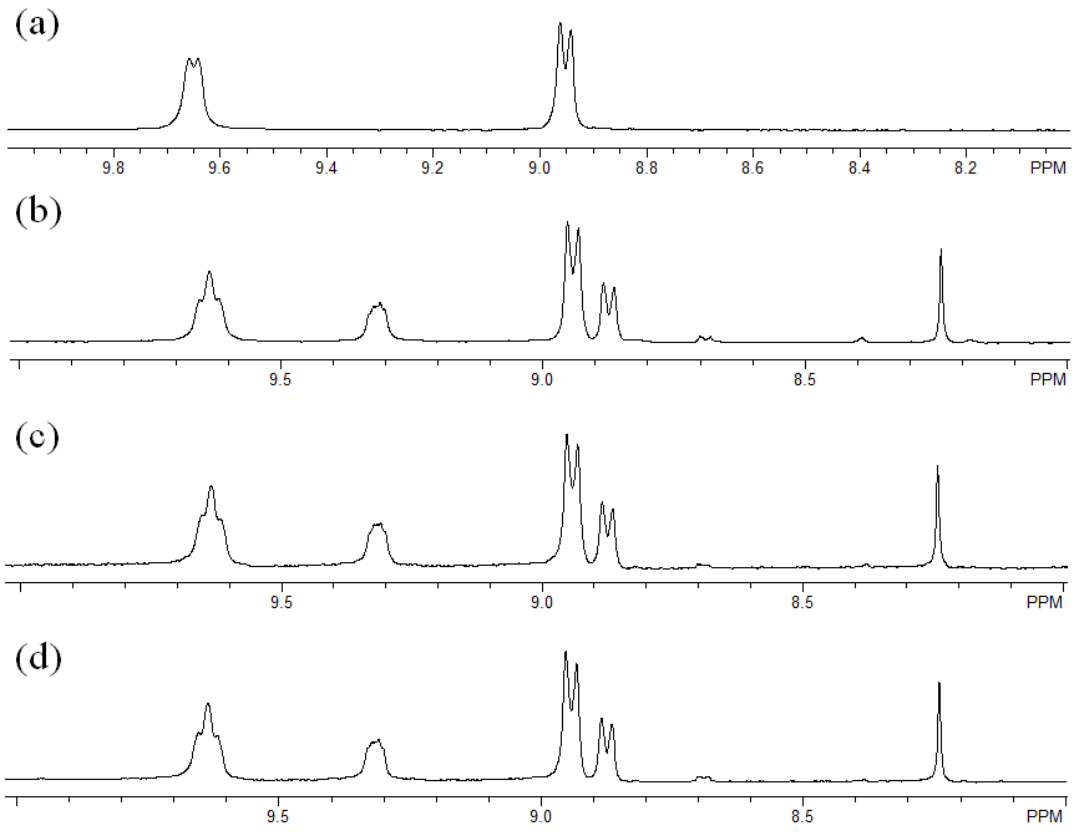

Figure A.69. Partial ^{1}H NMR spectra of **4.22** (b,c) modified from **4.19** (a) and assembled (d) by *cis*-$Pt(PEt_3)_2(OTf)_2$ **4.01**, tritopic carboxylate ligand **4.23**, and tritopic pyridyl donor **4.21**.

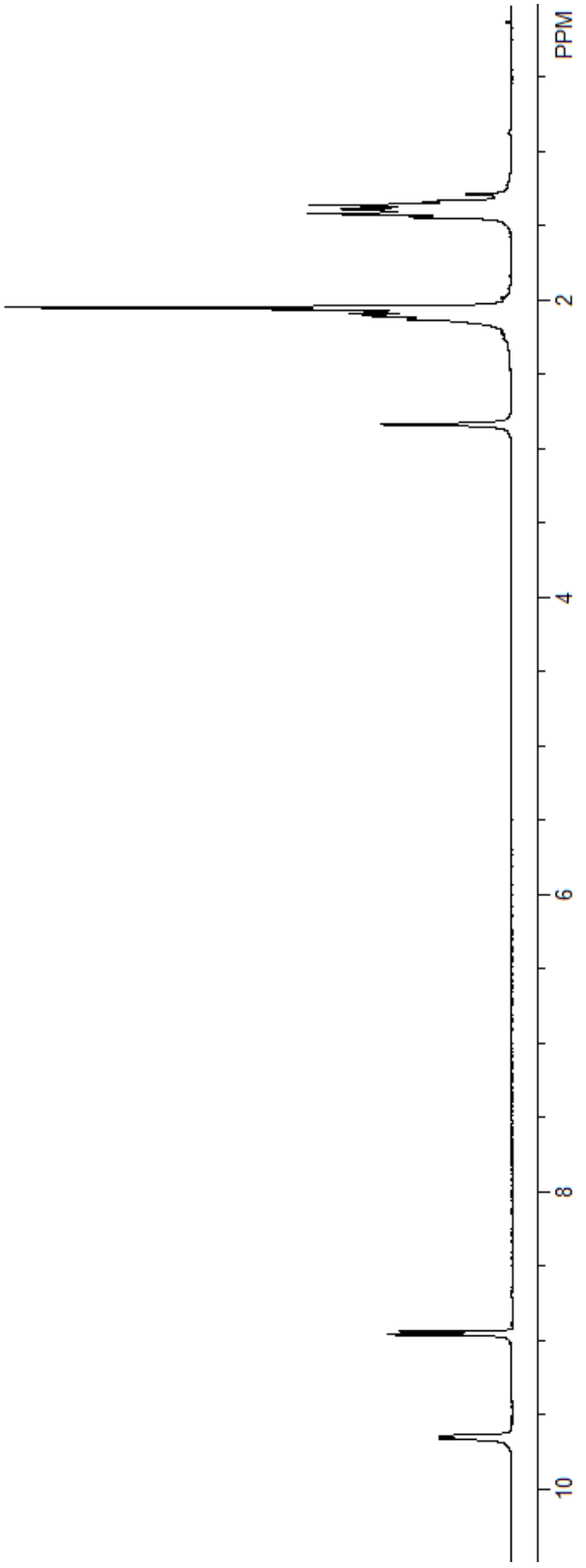

Figure A.70. ^{1}H NMR spectrum (Acetone-d_6, 300 MHz) of **4.19**

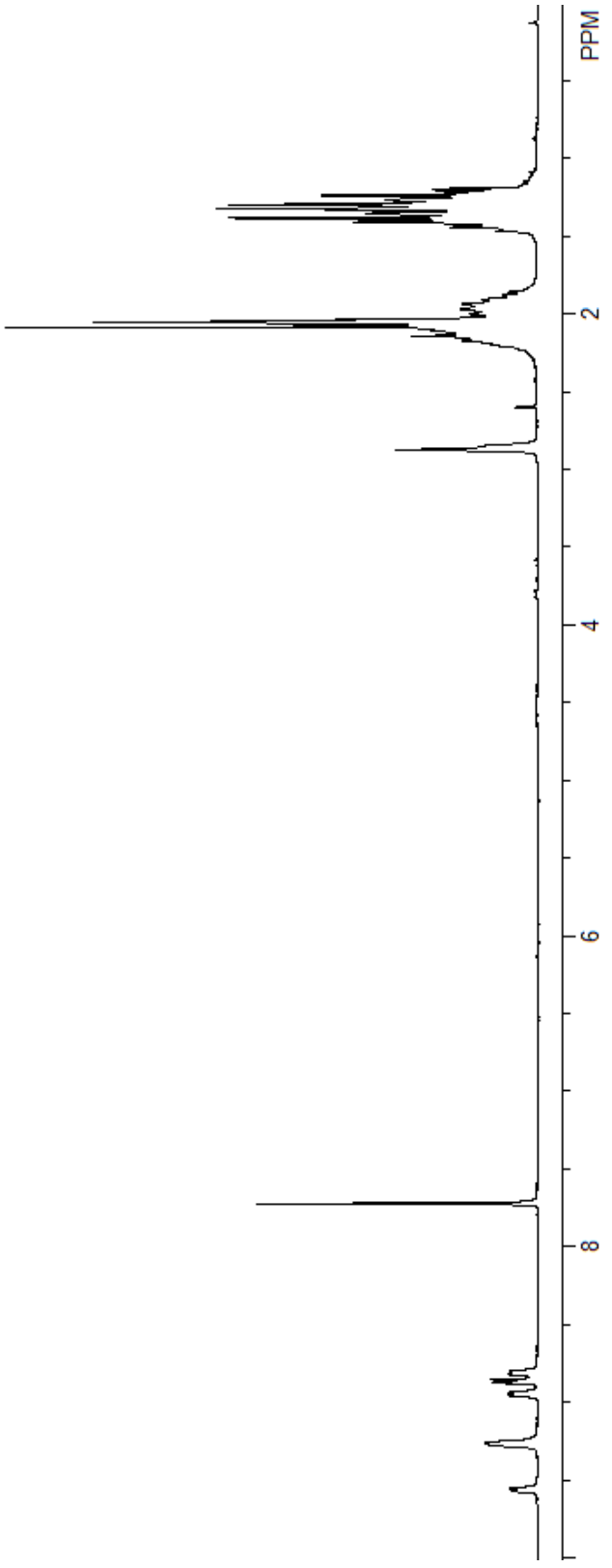

Figure A.71. ^{1}H NMR spectrum (Acetone-d_6, 300 MHz) of **4.20**

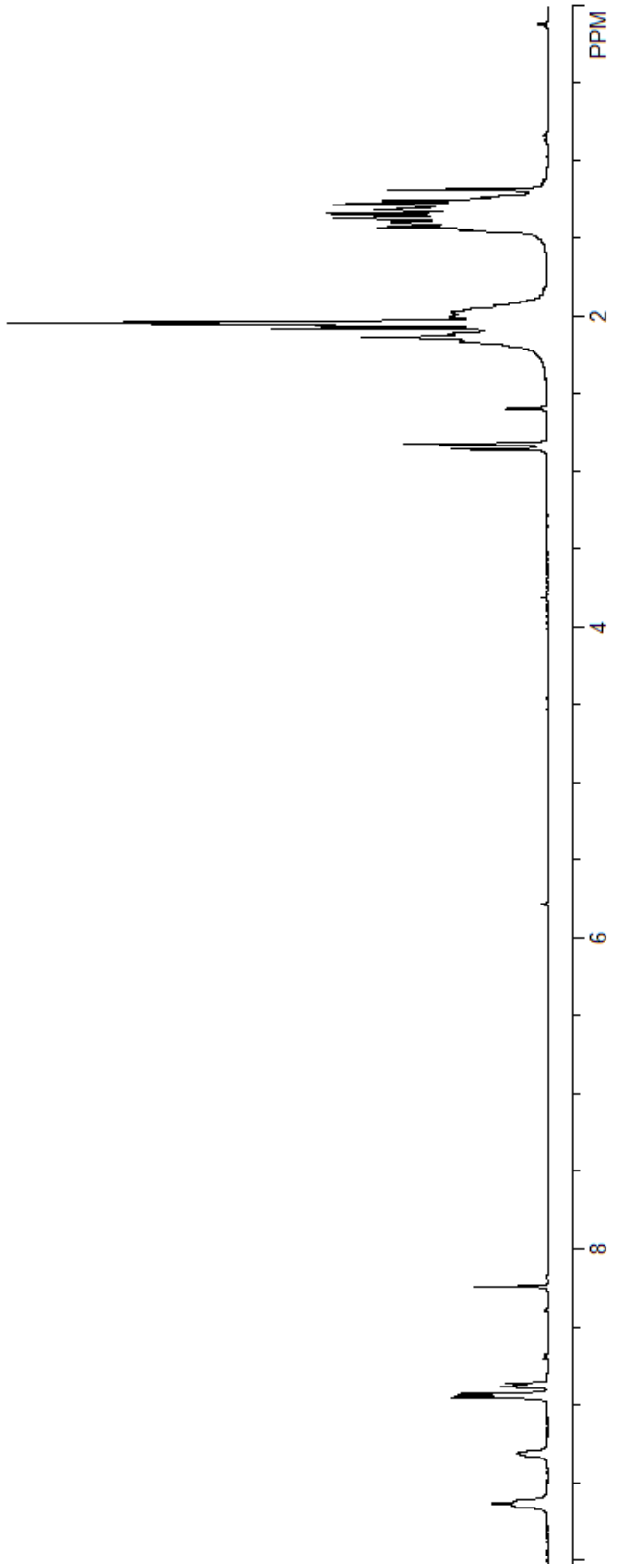

Figure A.72. ^{1}H NMR spectrum (Acetone-d6, 300 MHz) of **4.22**

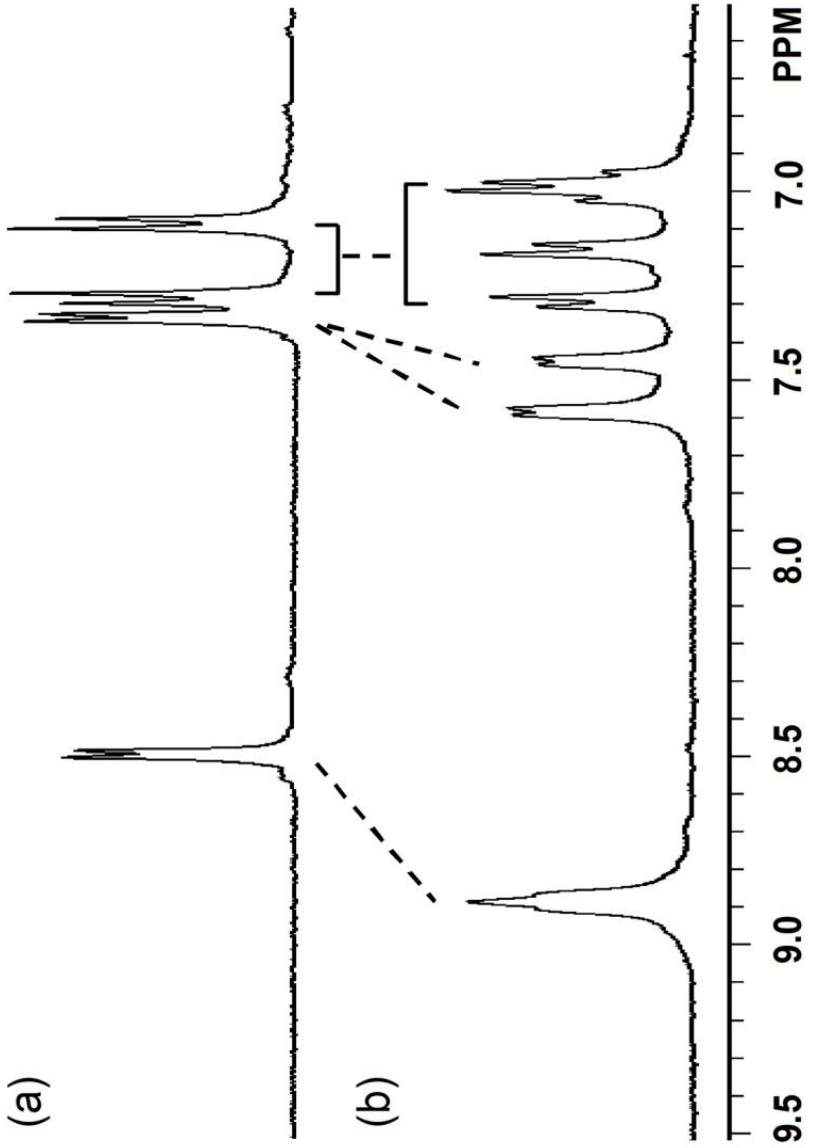

Figure A.73. Partial ^{1}H NMR (300MHz) spectra of hexapyridyl ligand **5.2** (a) and truncated tetrahedron **5.3a** (b)

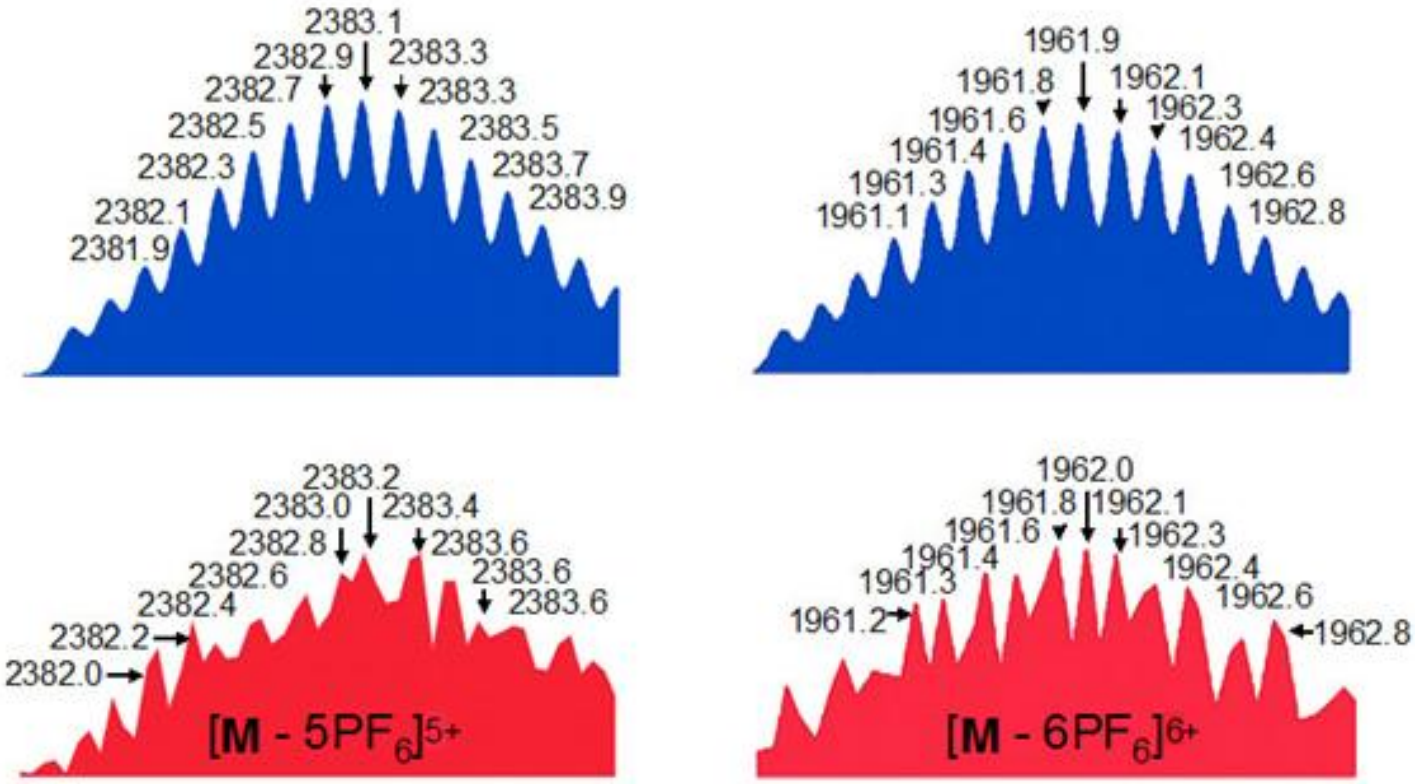

Figure A.74. Calculated (top) and Experimental (bottom) ESI mass spectra of **5.3a**

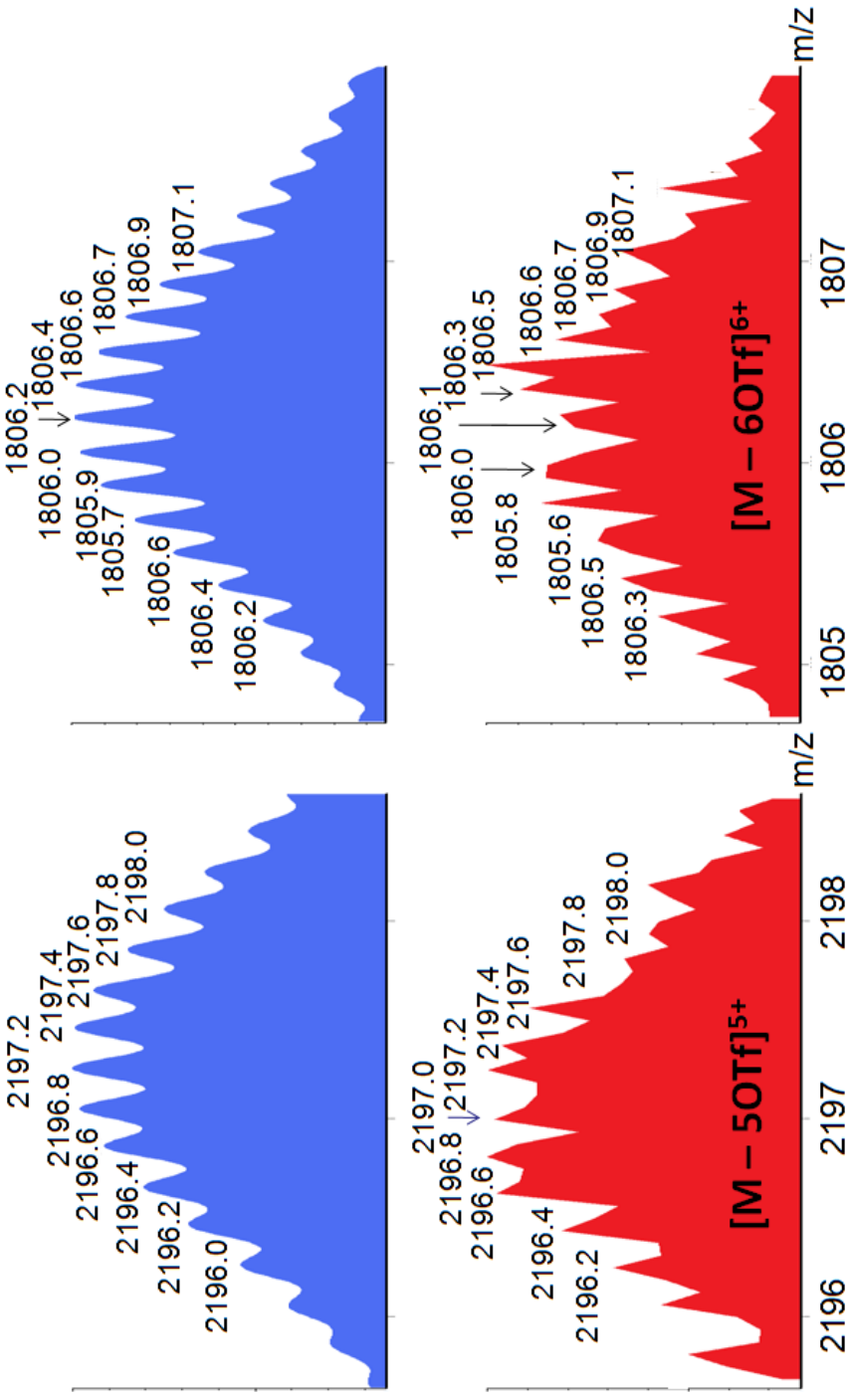

Figure A.75. Calculated (top) and Experimental (bottom) ESI mass spectra of **5.3b**

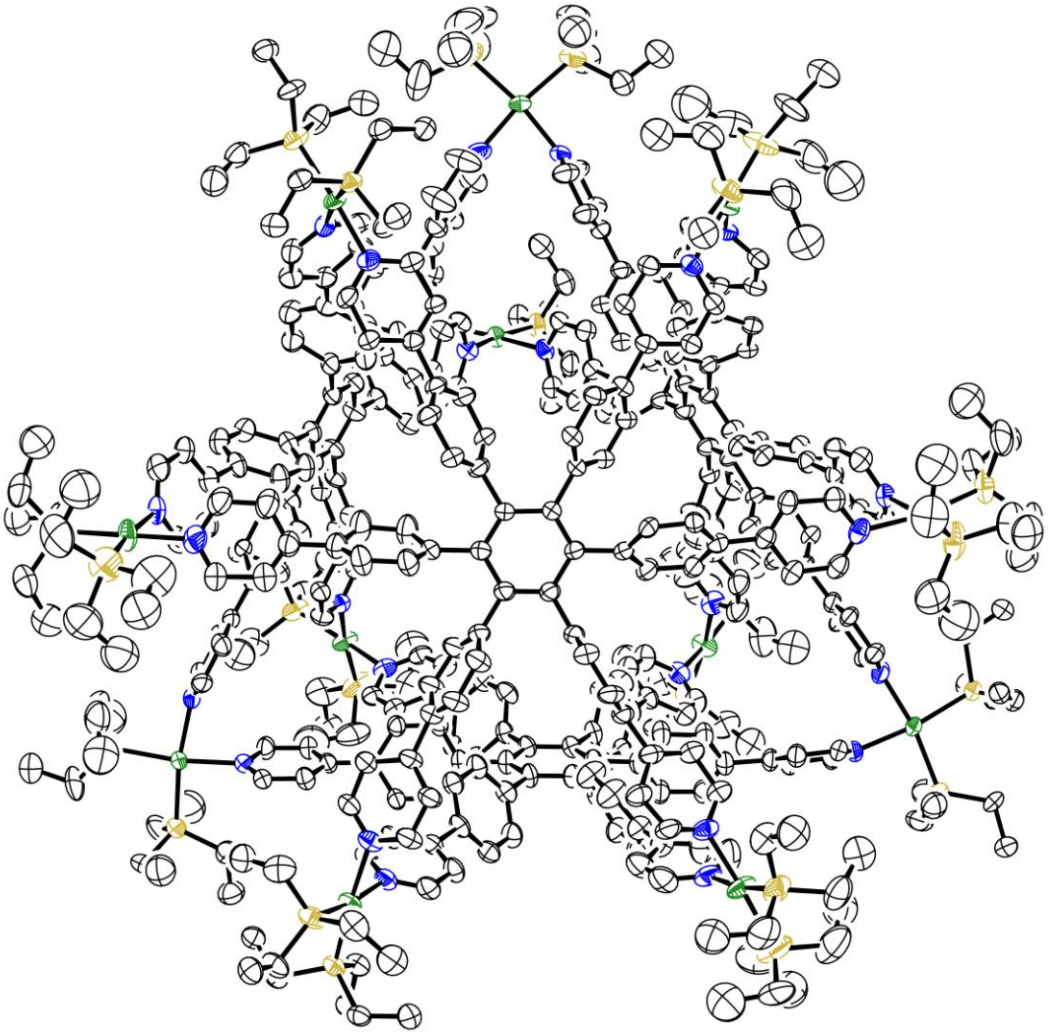

Figure A.76. X-ray crystal structure of **5.3a** with 30 % probability (Pt: green; P: yellow; N: blue; C: white).

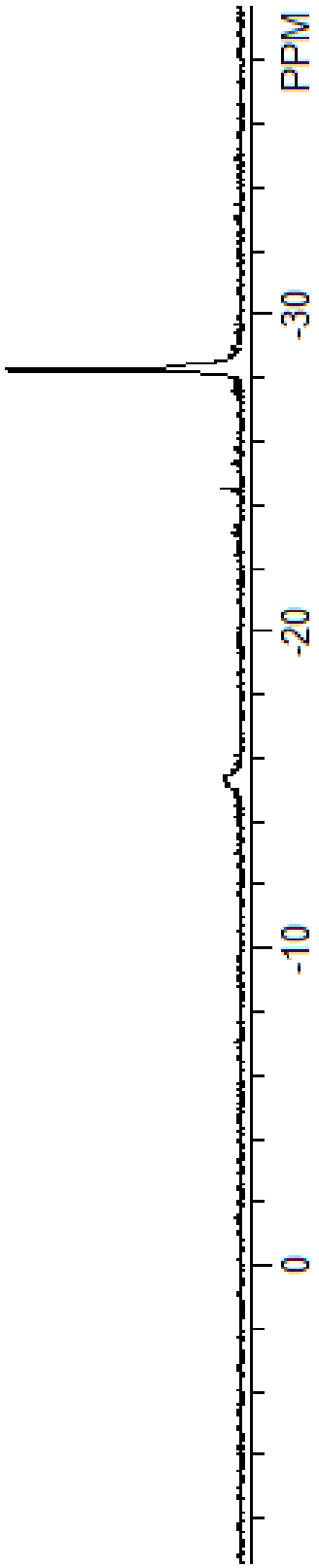

Figure A.77. $^{31}P\{^{1}H\}$ NMR (300MHz) spectra of the encapsulated complex **5.3b•5.4**$_3$.

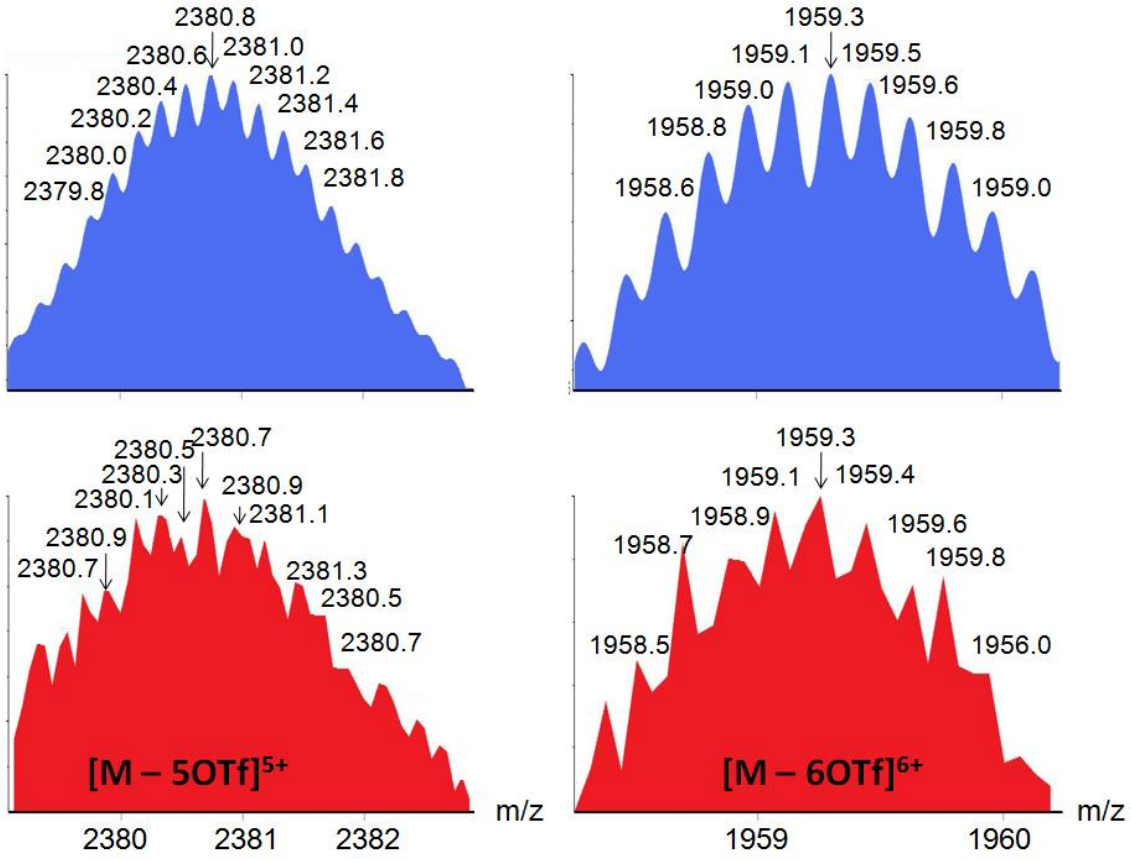

Figure A.78. Calculated (top) and Experimental (bottom) ESI mass spectra of the encapsulated complex **5.3b•5.4**$_3$.

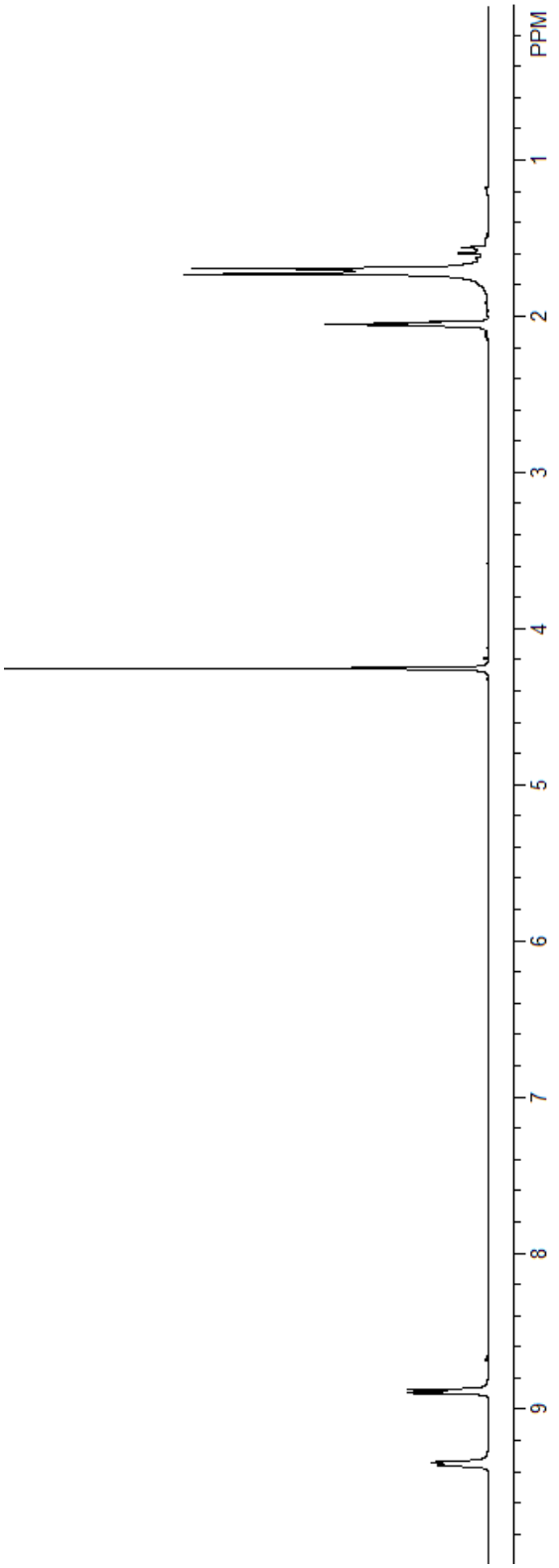

Figure A.80. ^{1}H NMR (Acetone-d_6/D_2O 10:1, 300MHz) spectra of the two-component self-assembly of **6.1**

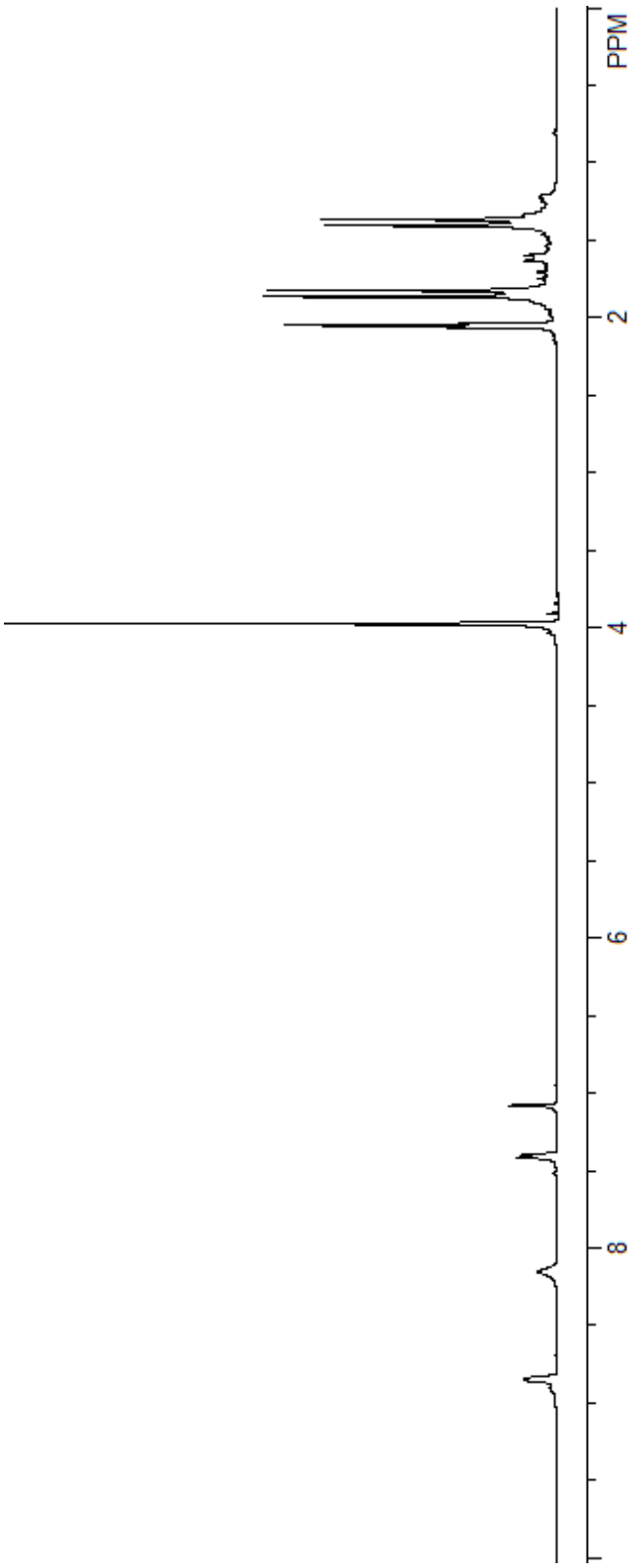

Figure A.81. ^{1}H NMR (Acetone-d_6/D_2O 10:1, 300MHz) spectra of the encapsulated complex **6.4**

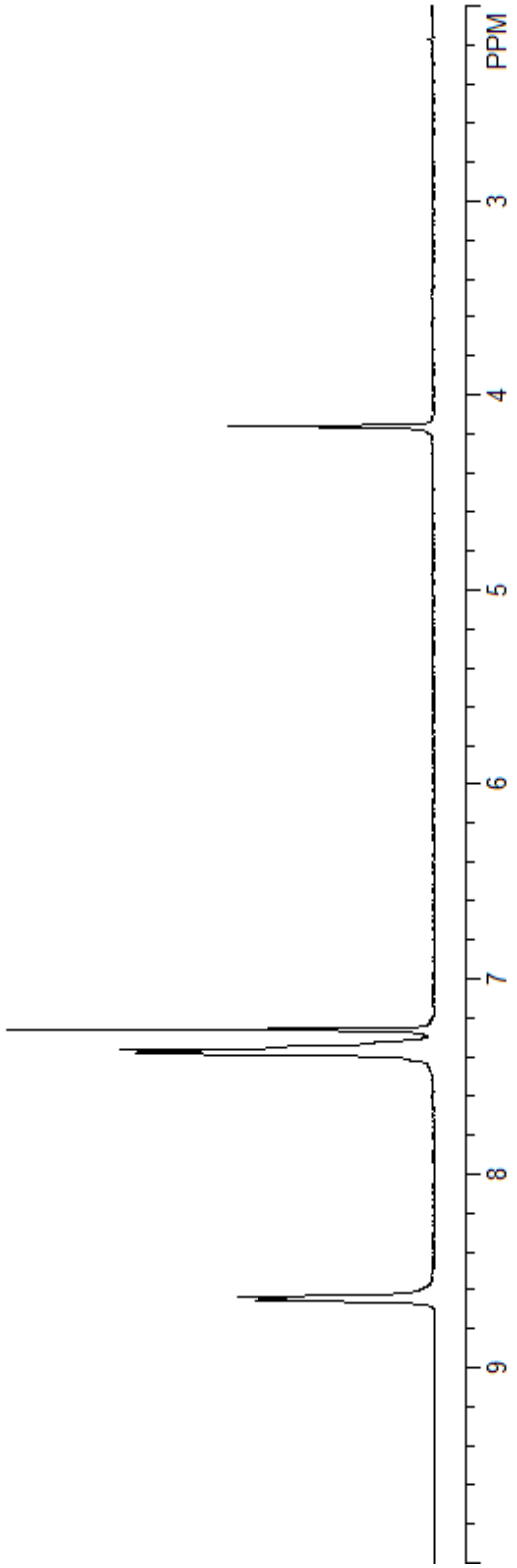

Figure A.82. ^{1}H NMR ($CDCl_3$, 300MHz) spectra of **6.2a**

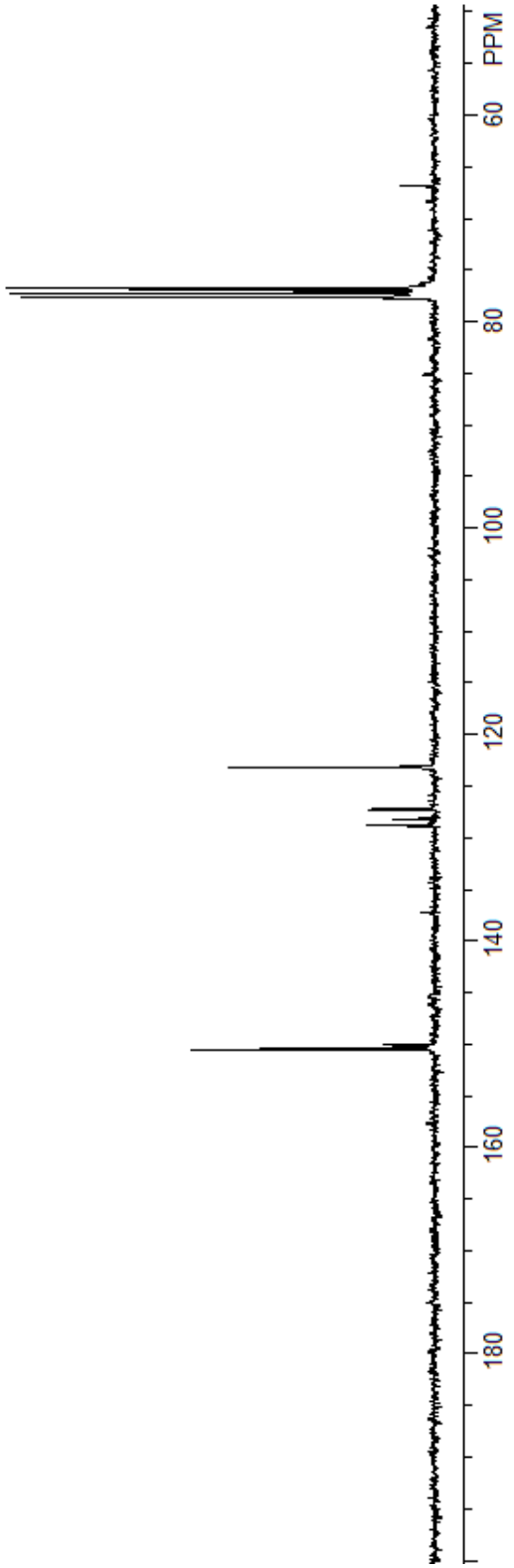

Figure A.83. ^{13}C NMR ($CDCl_3$, 300MHz) spectra of **6.2a**

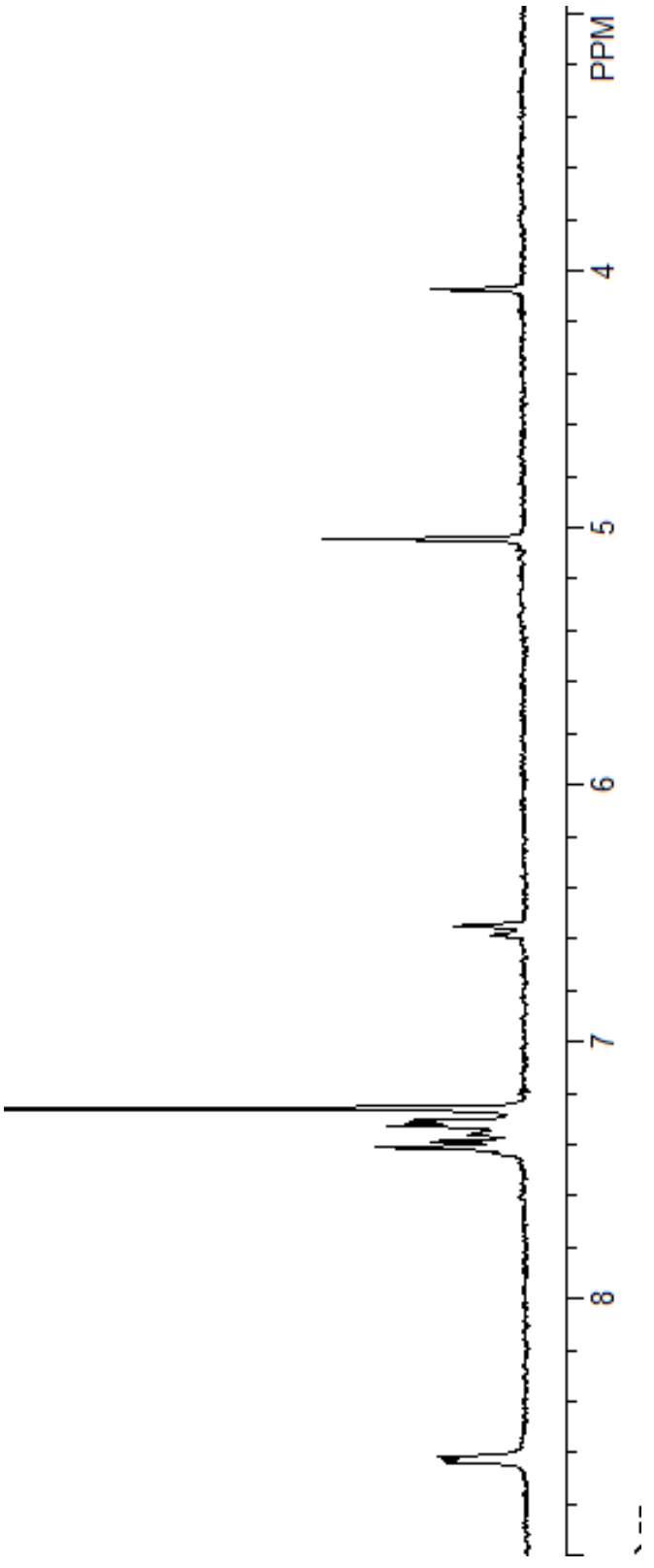

Figure A.84. ^{1}H NMR ($CDCl_3$, 300MHz) spectra of **6.2b**

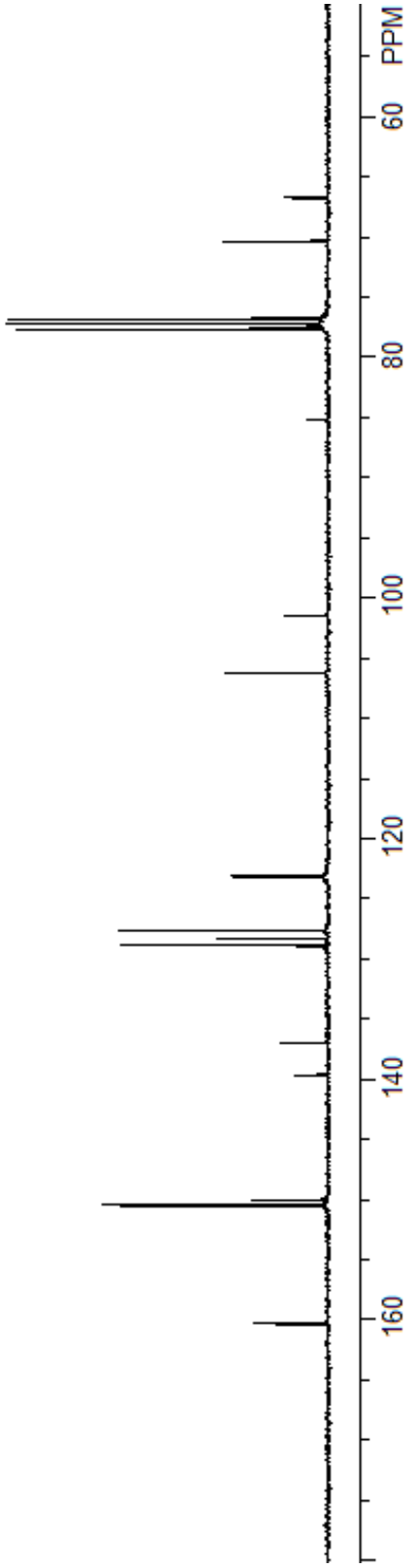

Figure A.85. ^{13}C NMR ($CDCl_3$, 300MHz) spectra of **6.2b**

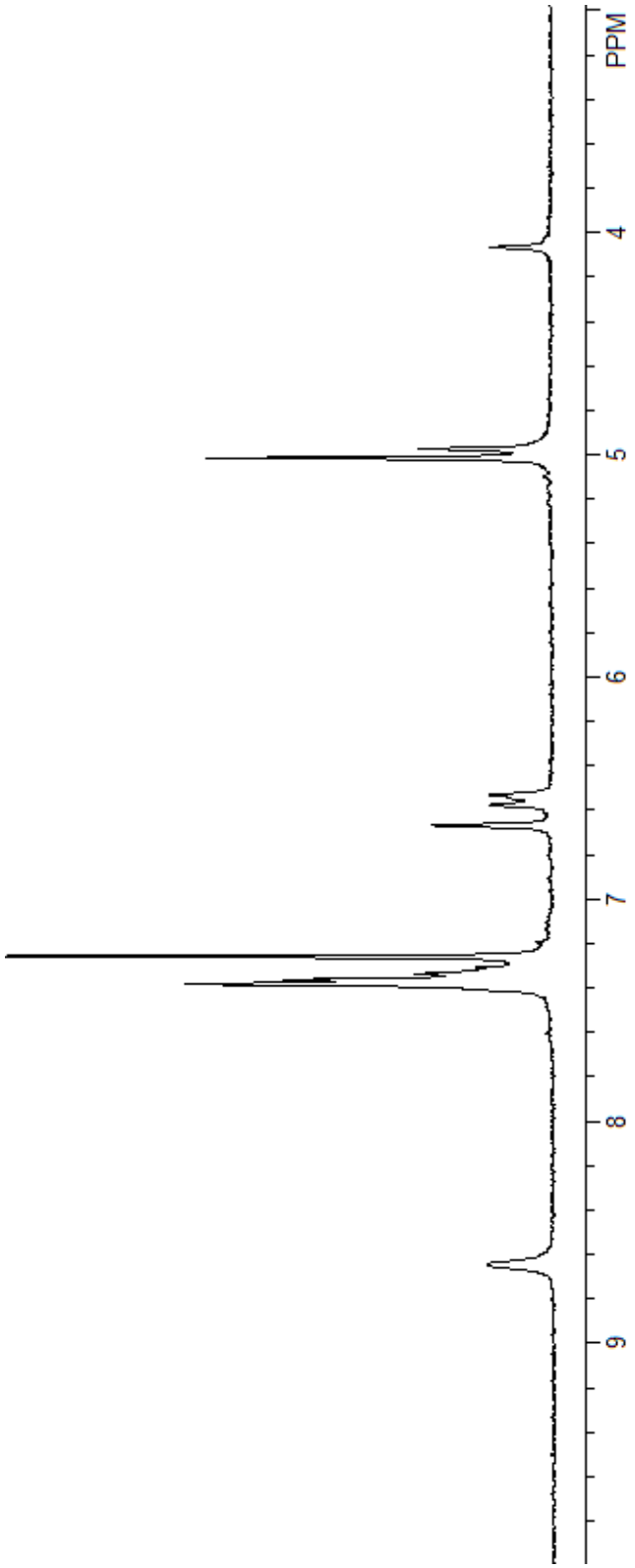

Figure A.86. ^{1}H NMR ($CDCl_3$, 300MHz) spectra of **6.2c**

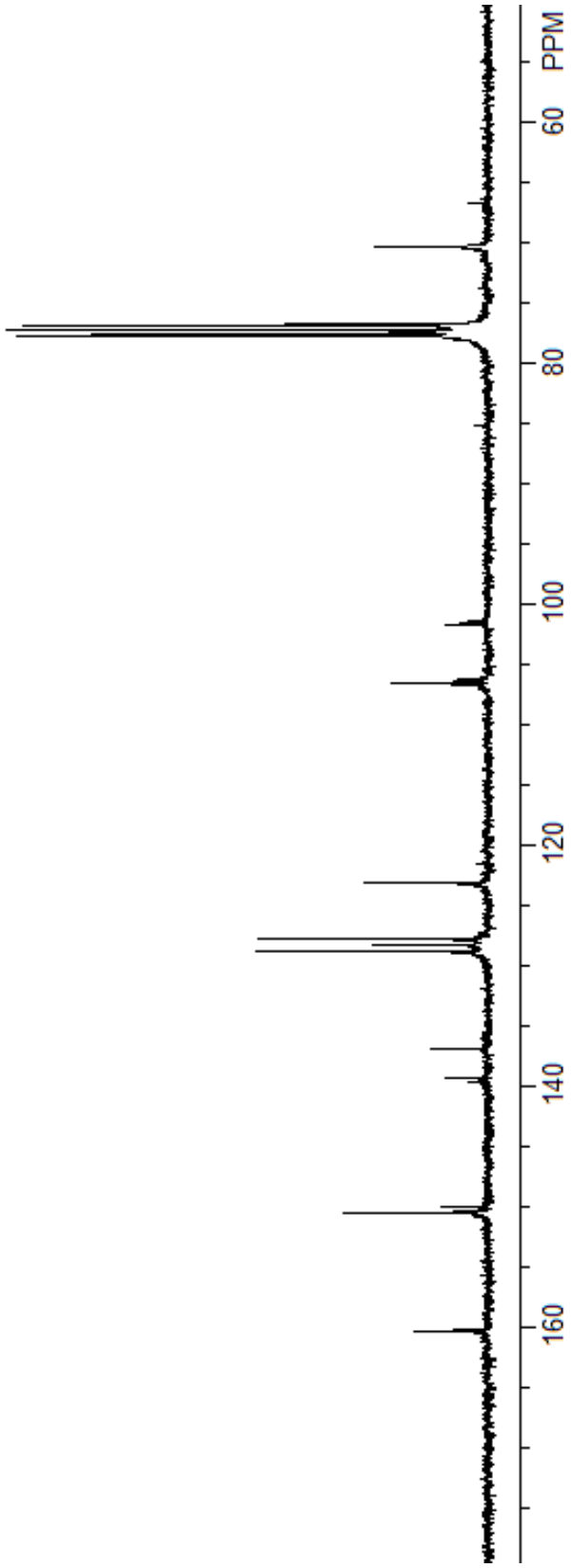

Figure A.87. ^{13}C NMR ($CDCl_3$, 300MHz) spectra of **6.2c**

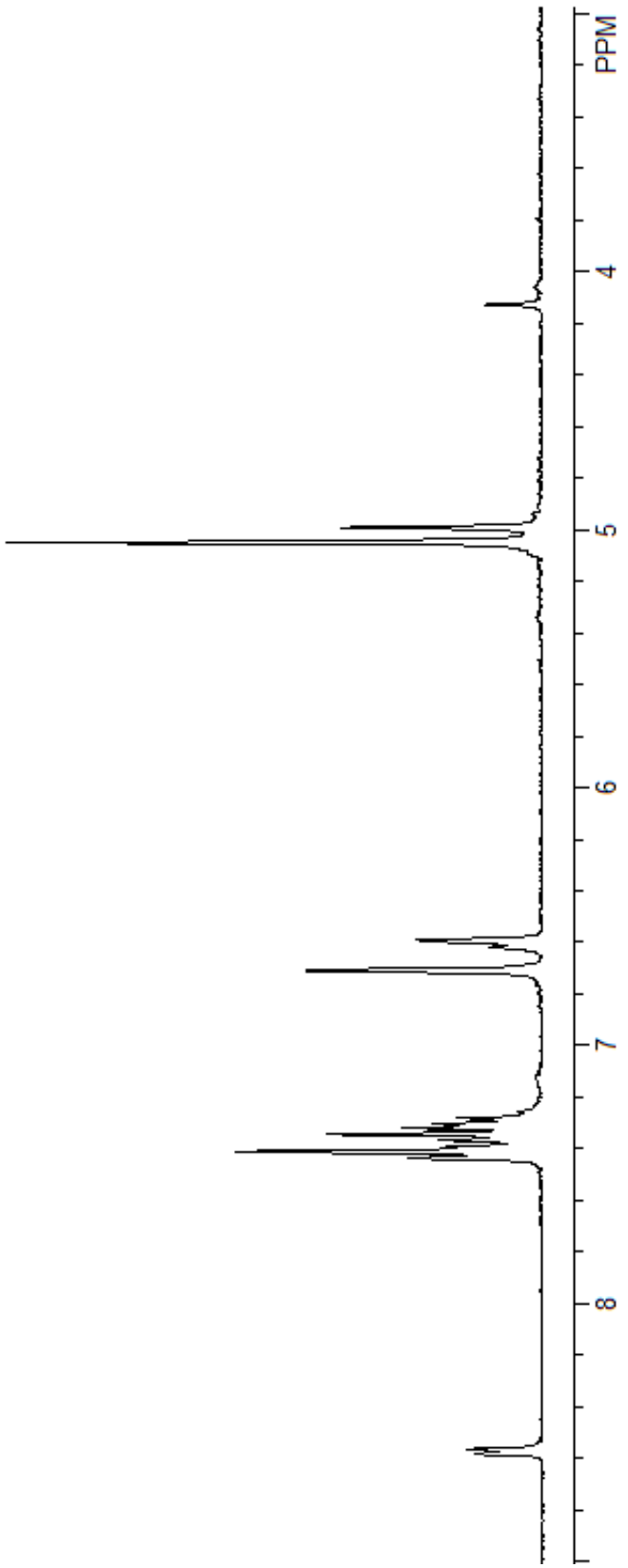

Figure A.88. ^{1}H NMR (Acetone-d_6, 300MHz) spectra of **6.2d**

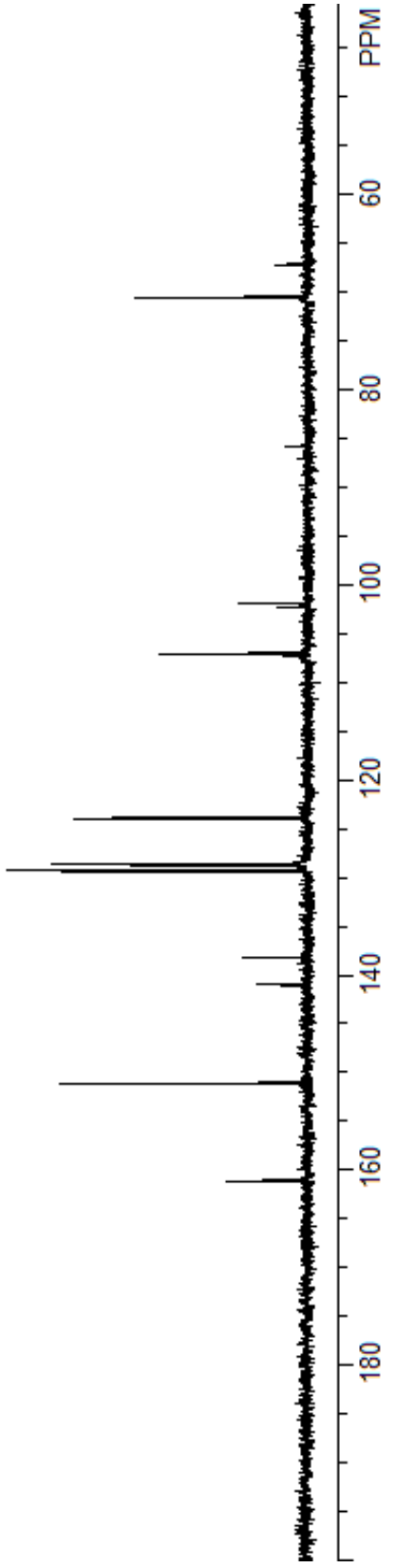

Figure A.89. ^{13}C NMR (Acetone-d_6, 300MHz) spectra of **6.2d**

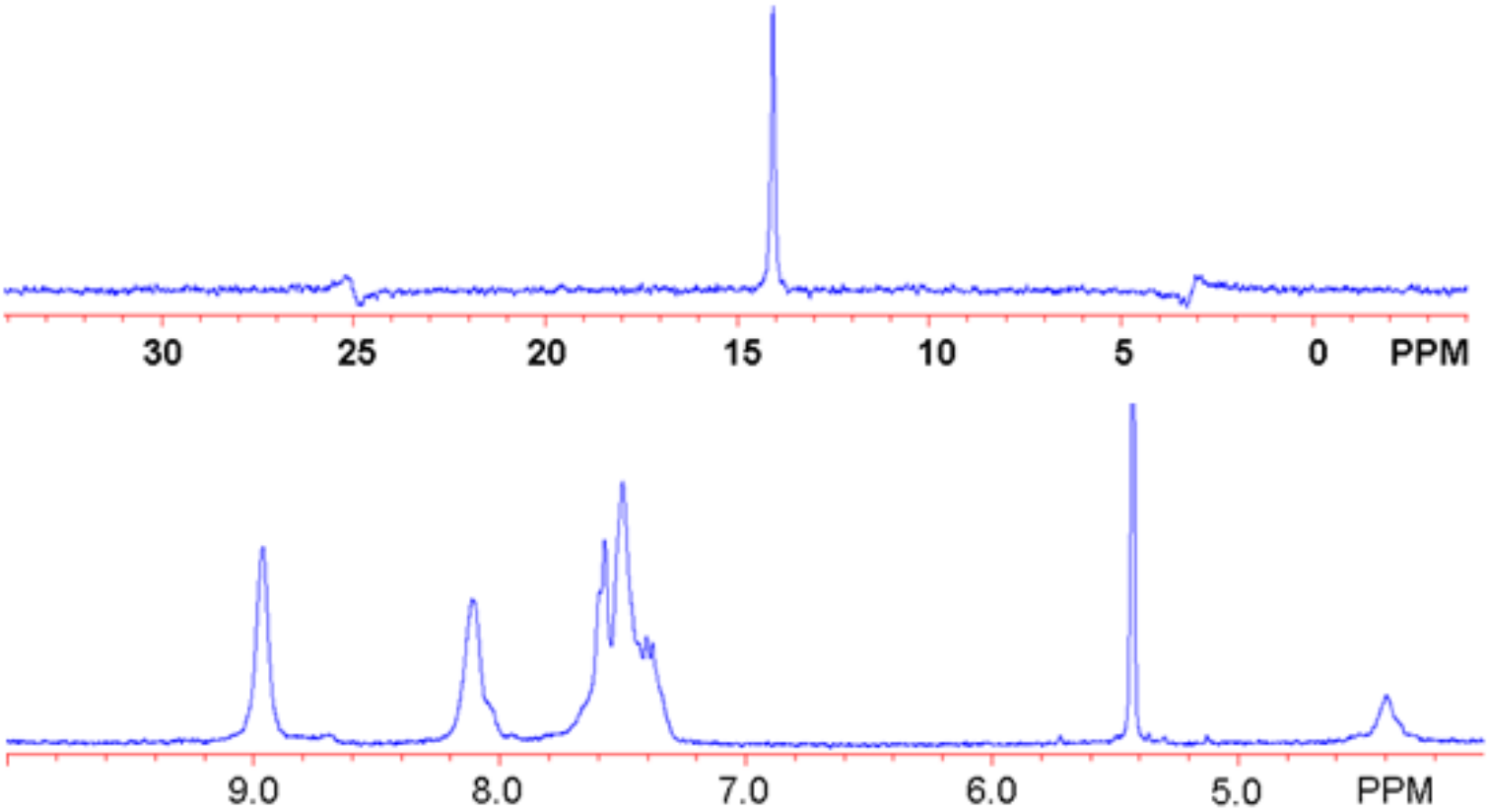

Figure A.90. $^{31}P\{^{1}H\}$ (top) and ^{1}H (bottom) (Acetone-d_6/CD_2Cl_2 1:1, 300MHz) NMR spectra of supramolecular dendrimer **6.3a**

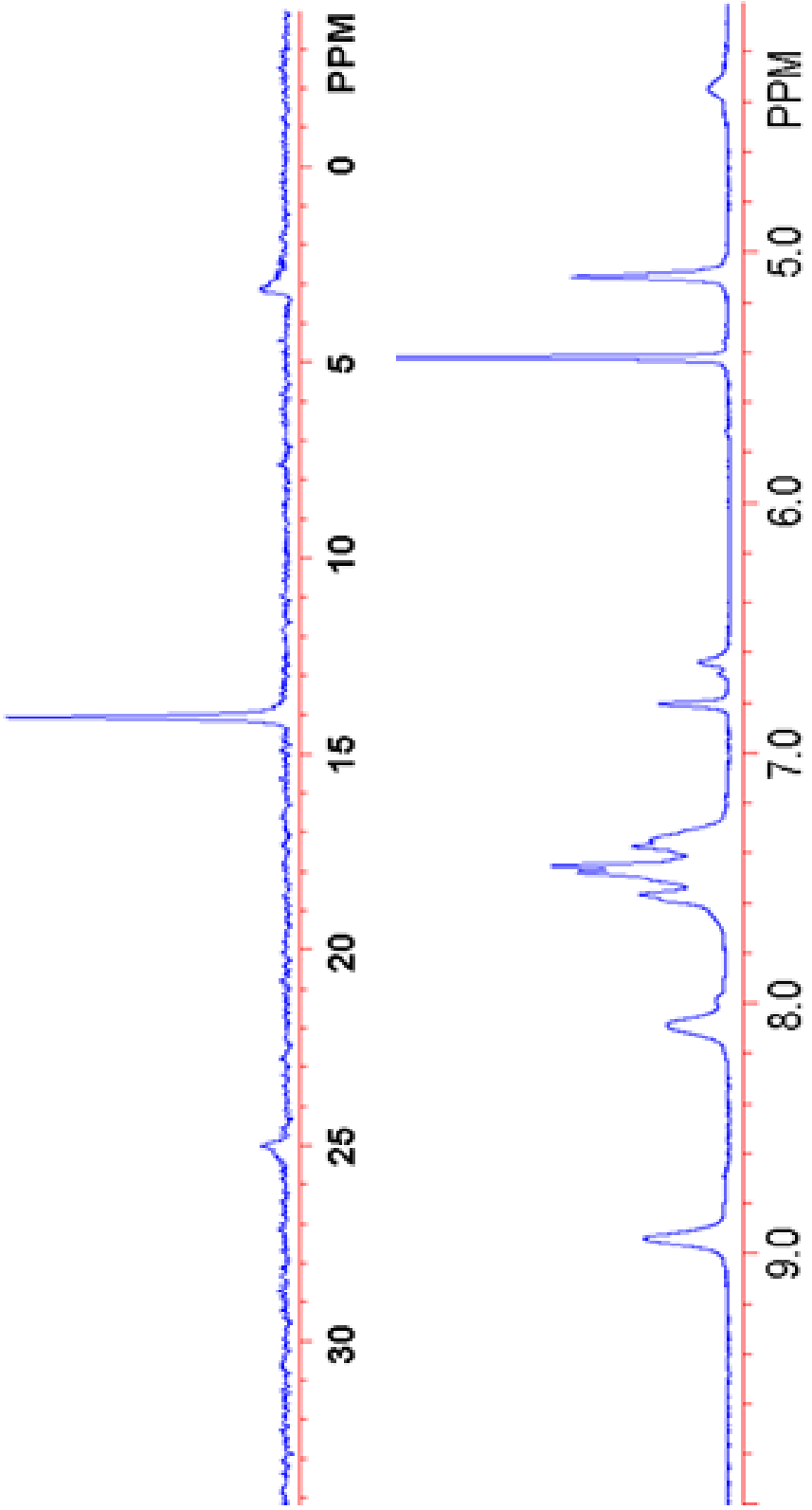

Figure A.91. $^{31}P\{^{1}H\}$ (top) and ^{1}H (bottom) (Acetone-d_6/CD_2Cl_2 1:1, 300MHz) NMR spectra of supramolecular dendrimer **6.3b**

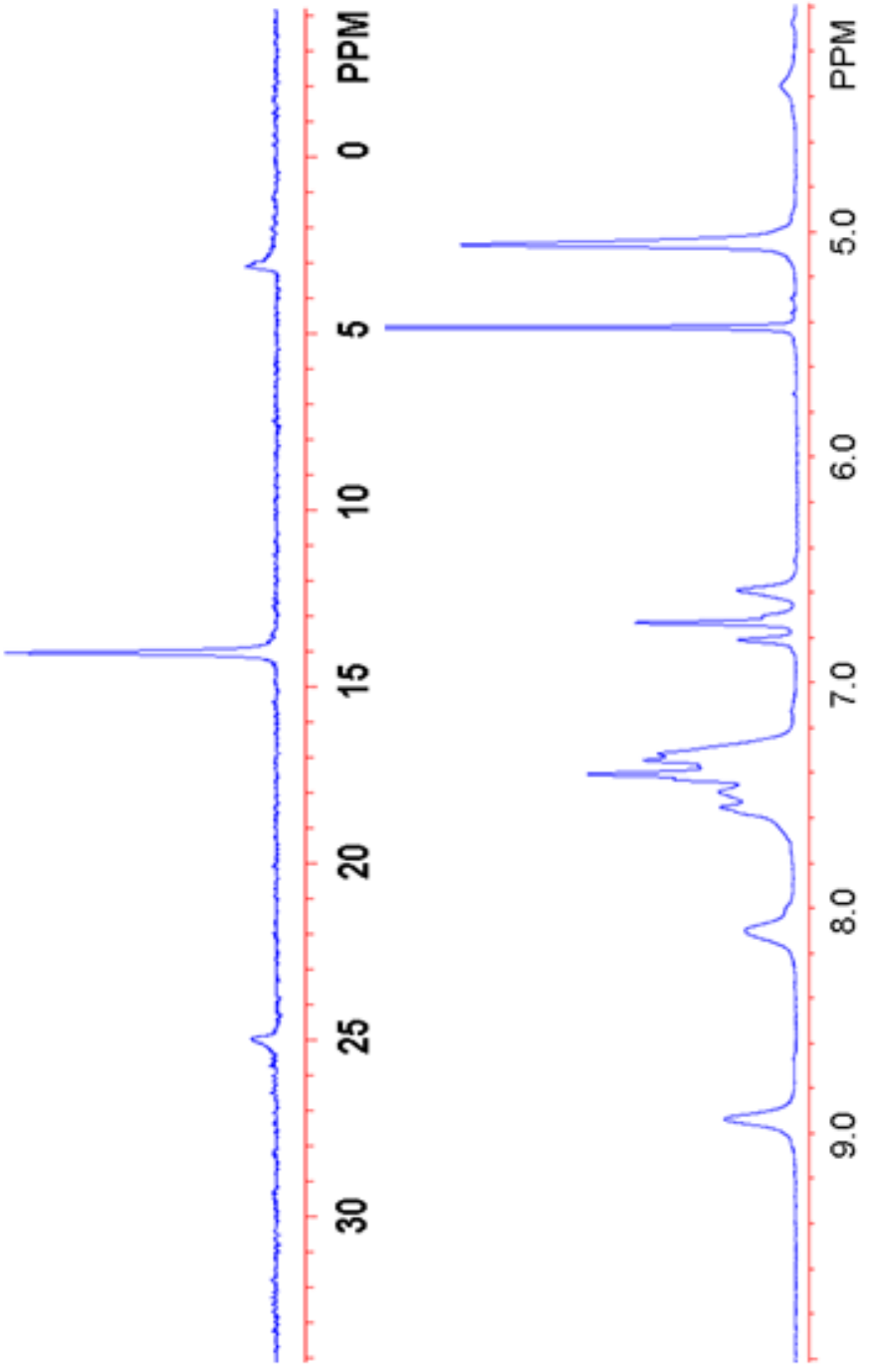

Figure A.92. $^{31}P\{^{1}H\}$ (top) and ^{1}H (bottom) (Acetone-d_6/CD_2Cl_2 1:1, 300MHz) NMR spectra of supramolecular dendrimer **6.3c**

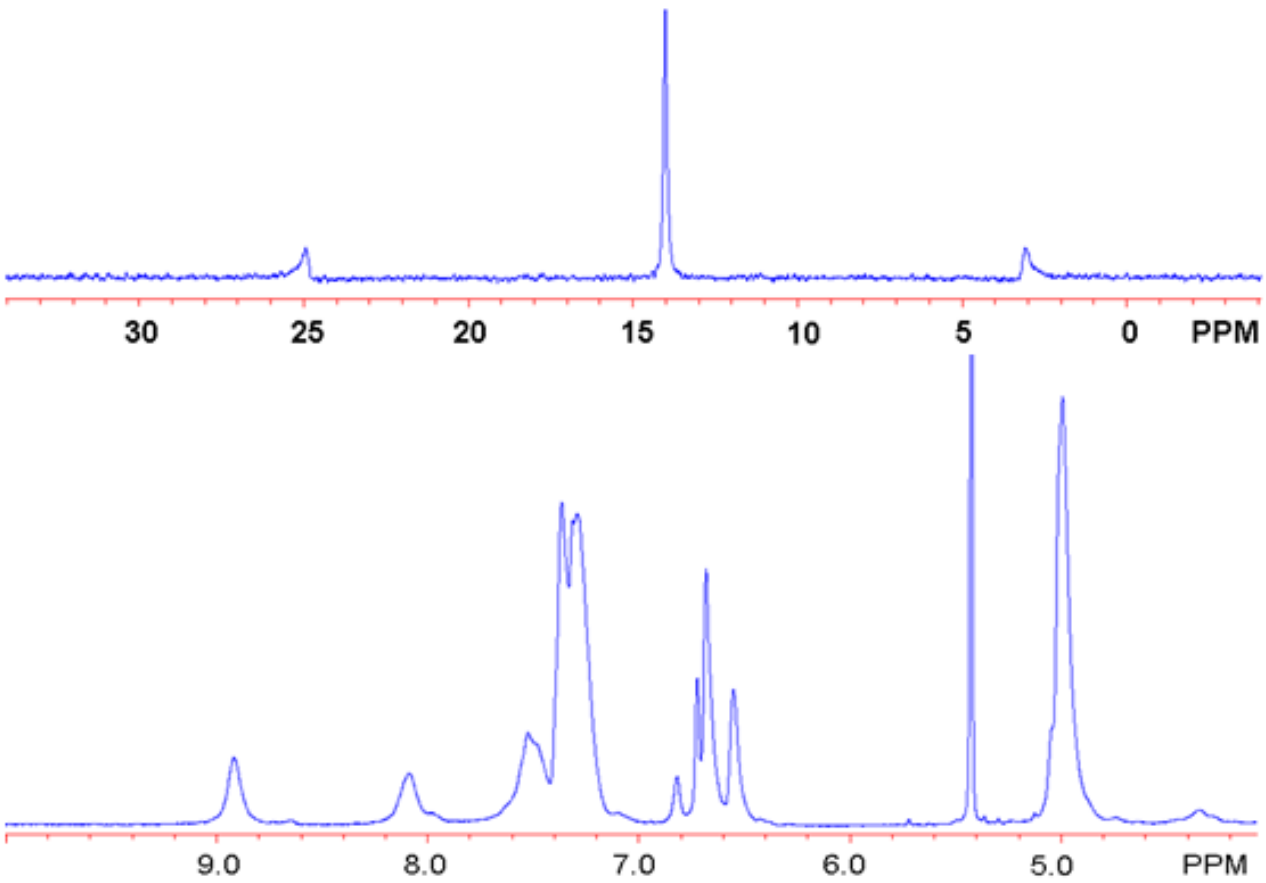

Figure A.93. $^{31}P\{^{1}H\}$ (top) and ^{1}H (bottom) (Acetone-d_6/CD_2Cl_2 1:1, 300MHz) NMR spectra of supramolecular dendrimer **6.3d**

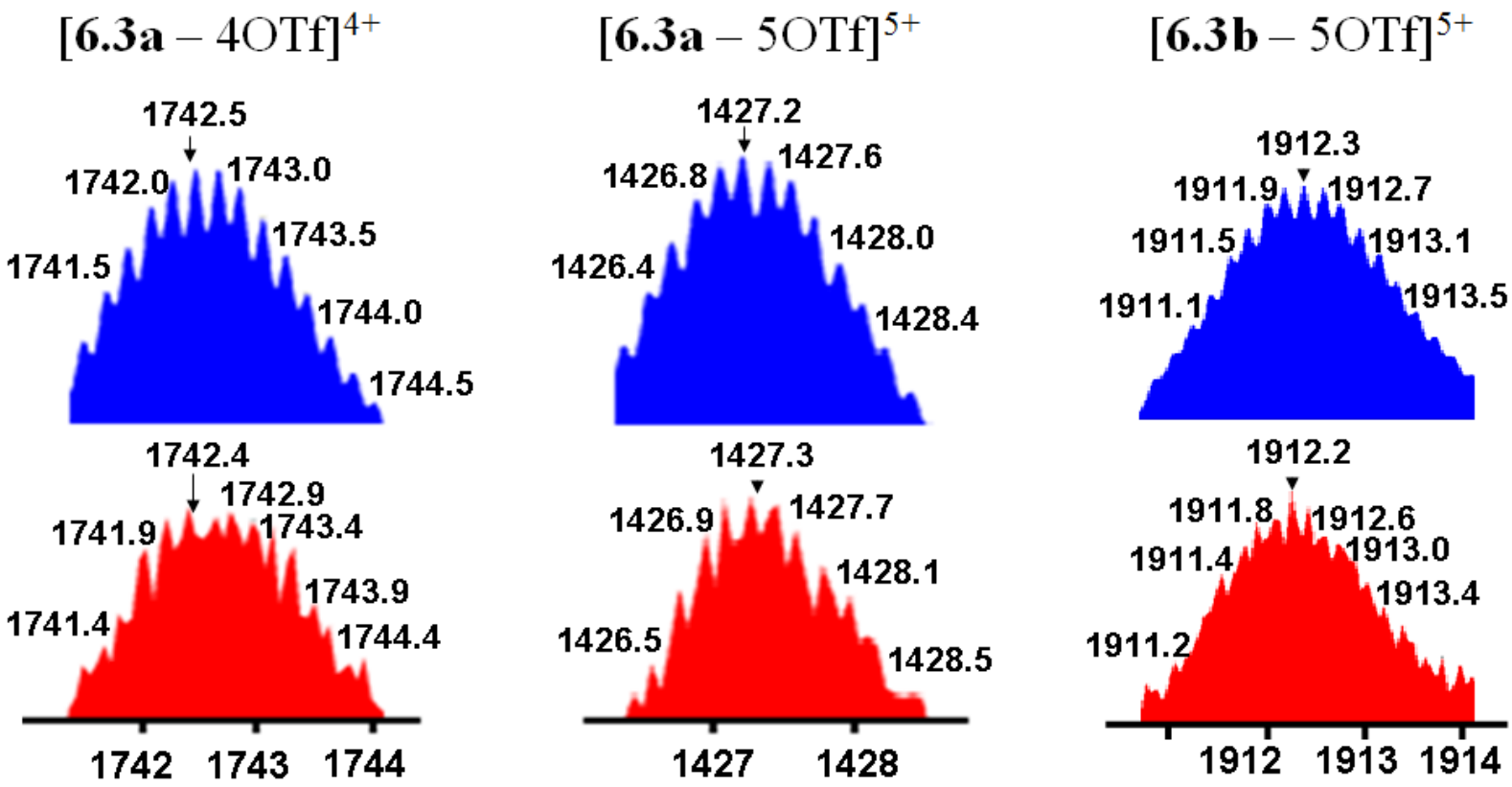

Figure A.94. Calculated (top) and experimental ESI-MS spectra of supramolecular dendrimer **6.3a** and **6.3b**